UNIVERSITAT DE BARCELONA

Expresión y funcionalidad de los heterómeros de GPCR en las enfermedades neurodegenerativas de Parkinson y Alzheimer

Rafael Rivas Santisteban

EXPRESIÓN Y FUNCIONALIDAD DE LOS HETERÓMEROS DE GPCR EN LAS ENFERMEDADES NEURODEGENERATIVAS DE PARKINSON Y ALZHEIMER

RAFAEL RIVAS SANTISTEBAN

UNIVERSITAT DE BARCELONA
FACULTAT DE BIOLOGIA
DEPARTAMENT DE BIOQUÍMICA I BIOMEDICINA MOLECULAR

Expresión y funcionalidad de los heterómeros de GPCR en las enfermedades neurodegenerativas de Parkinson y Alzheimer

Memoria presentada por el Graduado en Bioquímica
RAFAEL RIVAS SANTISTEBAN
para optar al grado de Doctor por la Universidad de Barcelona

Esta tesis se ha inscrito dentro del programa de doctorado de Biomedicina del Departamento de Bioquímica y Biomedicina Molecular de la Universidad de Barcelona

El trabajo experimental y la redacción de la presente memoria han sido realizados por Rafael Rivas Santisteban bajo la dirección del Dr. Rafael Franco Fernández y la Dra. Gemma Navarro Brugal

Dr. Rafael Franco Fernández
Director y tutor

Dra. Gemma Navarro Brugal
Directora

Rafael Rivas Santisteban

Barcelona, junio de 2021

Resumen

Los receptores acoplados a proteína G o GPCRs conforman la mayor familia de receptores de membrana celular en organismos eucariotas. En humanos se han descrito más de 800 GPCRs, gran parte de ellos descubiertos mediante ensayos de secuenciación en el proyecto Genoma Humano, que suponen aproximadamente un 5% del total del genoma (Craig Venter et al., 2001). Ostentan una gran relevancia en la actualidad, ya que más del 30% de los fármacos aprobados por la Administración de Medicamentos y Alimentos de los Estados Unidos tienen como diana terapéutica alguno de estos receptores (Garland, 2013; Shimada et al., 2019).

La caracterización y el estudio de GPCRs endógenos implicados en ciertas patologías parece clave para el descubrimiento de nuevas dianas terapéuticas más específicas y seguras (R. Santos et al., 2016). Entre 2015 y mediados del 2020 se han aprobado 41 fármacos que actúan sobre GPCRs por la "Food and Drug Administration" (FDA), administración de los Estados Unidos encargada de regular y aprobar nuevos medicamentos (Congreve et al., 2020).

Teniendo en cuenta los resultados obtenidos y presentados en esta Tesis doctoral se puede concluir el gran potencial terapéutico, actual y futuro, que poseen los GPCRs en el tratamiento de las enfermedades neurodegenerativas ya sea utilizando aproximaciones directas que potencien los efectos beneficiosos que promueven, como el AT_2R, o bien aproximaciones indirectas que busquen modular la acción de otros receptores clave, como el bloqueo de $A_{2A}R$ o CB_2R sobre la señalización perjudicial de NMDAR.

Abstract

G protein-coupled receptors (GPCRs) make up the largest family of cell membrane receptors in eukaryotic organisms. In humans, more than 800 GPCRs have been described, most of them discovered by sequencing assays in the Human Genome project, which account for approximately 5% of the total genome (Craig Venter et al., 2001). They are highly relevant today, since more than 30% of the drugs approved by the United States Food and Drug Administration have some of these receptors as therapeutic targets (Garland, 2013; Shimada et al., 2019).

The characterization and study of endogenous GPCRs involved in certain pathologies seems key to the discovery of new, more specific and safe therapeutic targets (R. Santos et al., 2016). Between 2015 and mid-2020, 41 drugs that act on GPCRs have been approved by the Food and Drug Administration (FDA), the United States administration in charge of regulating and approving new drugs (Congreve et al., 2020).

Taking into account the results obtained and sent in this doctoral Thesis, it is possible to conclude the great therapeutic potential, current and future, that GPCRs have in the treatment of neurodegenerative diseases either by using direct approaches that enhance the beneficial effects they promote, such as AT_2R, or indirect approaches that seek to modulate the action of other key receptors, such as the blockade of $A_{2A}R$ or CB_2R on harmful NMDAR signaling.

Agradecimientos

No podría empezar esta Tesis de otra forma más que agradeciendo a todas las personas que me han acompañado en el día a día durante estos años y es que, como me decían al comienzo, cuatro años dan para mucho, pero al mismo tiempo también pasan muy deprisa. Parece que fue ayer cuando vine por primera vez a Barcelona, sin saber realmente como serían los próximos años de mi vida, si me adaptaría bien o si no me sentiría solo estando tan lejos de casa… ¡Pero el que no arriesga no gana! Y sin duda ha merecido la pena por mucho, especialmente por las extraordinarias personas que he ido conociendo.

En primer lugar, quiero agradecer a mi familia, a mi madre Isabel y a mi padre Juan María, en todo momento he contado con su apoyo incondicional y me han animado a continuar en la carrera científica, incluso en los peores momentos. A mi hermano Juan, por su interés en nuestras investigaciones, ahora te toca a ti darle duro en tu nueva etapa. ¡Disfrútala mucho! A mi abueli Maribel y a mi abuelo Rafael, por preocuparse y desearme siempre lo mejor, espero que estéis orgullosos de mi.

También me gustaría agradecer a Rafa y a Gemma por acogerme y darme la oportunidad de poder formar parte de su equipo. Después de la mala experiencia que tuve en el pasado, llegar a un laboratorio como el vuestro dónde todo el mundo intenta echarse una mano y colaborar unos con otros fue lo mejor que me podía pasar. Gracias por ser capaces de velar por todos nosotros, por la paciencia que tenéis y, sobretodo, por mantenernos motivados y ayudarnos a ver las cosas con perspectiva cuando las cosas se tuercen. He aprendido muchísimo durante estos años y, en gran parte, os lo debo a vosotros.

Rafa, todo lo que ha llovido desde aquel café que nos tomamos cuando nos conocimos en persona. Después de tantos meses hablando por teléfono (ya sabemos lo "rápido" que van los temas administrativos) tenía bastante curiosidad por ver como sería el laboratorio. Gracias por ayudarme con todo el papeleo infernal del comienzo. Gracias por estar siempre disponible al mail para resolverme alguna duda, es algo que valoro mucho. Gracias por contar conmigo y escuchar mi opinión.

Al comienzo era "Rafa pequeño"/"el cordobés" (¡Esto es cosa tuya Rafa! Para evitar malentendidos quiero aclarar que realmente soy iliturgitano), quizá no fue la mejor época en la que podría haber entrado porque todo el mundo iba con prisas, a punto de finalizar su Tesis. Aún así, también la disfruté mucho. Gracias a David Aguinaga, por aquella primera semana que pasé en Barcelona en la que, sin conocerme todavía, me dejaste quedarme en tu casa hasta que pude mudarme. Espero que te vaya muy bien en el mundo de la fotografía; a Jas, fuiste la primera persona con la que tuve contacto del lab y probablemente todavía te sigas riendo de que no te tuteara desde el principio. A día de hoy la palabra "mordor" la sigo asociando más a tus riñas que al Señor de los Anillos. Irene gracias por todo lo que me enseñaste durante el tiempo que coincidimos, lo hiciste todo un poco más fácil para mí. ¡Para cuando defienda esta Tesis espero que ya estés de vuelta con nosotros! También quiero dar las gracias a Mar, a Edgar, a Patri y a Mireia "original" por tratarme como a uno más desde que nos conocimos.

No me olvido de ti Iñigo, que además de compañeros de trabajo, ser compañeros de piso y amigos es de las mejores cosas que me llevo de estos años. He estado cuidando el sitio que heredé de ti, de hecho, todavía conservo las escrituras. Gracias por esas partidas a la Switch al volver del lab. Gracias por esos juebirris con Javi y Gabri, que hacían mas cortas las semanas. ¡Tenemos que vernos pronto!

Gemma vuelves a salir aquí porque tengo mucho que agradecerte. Siempre intentas ponerte en nuestro lugar y… ¡Eso hace también que te sintamos mucho más cerca de nosotros! También admiro mucho la forma que tienes de afrontar los problemas, a ver si se me pega algo. Gracias Gemma por todo, tenemos muchísima suerte de poder contar contigo.

Poco a poco, por la gente que dejó el lab al leer la Tesis empezaron a ir viniendo personas nuevas que fueron ocupando su lugar hasta mantenernos en el grupo que somos ahora.

Jaume, nada de lo que escriba aquí será suficiente para agradecerte a ti. Aún así… gracias por estar a mi lado siempre; gracias a Alejandro el mejor personal trainer que he tenido, todavía me duelen las planchas que hacíamos en el EsportsUB. De las personas más fuertes que conozco, tanto por dentro como por fuera. El inventor de "Reifel", que tuvo la suficiente aceptación como para desplazar a "el cordobés" (¡Gracias!) ; gracias a Iu, también conocido como "maxinator", por estar dispuesto a echar un cable (y aunque a veces también le gusta cruzármelos, yo le quiero igual) ¡Gracias por tener tan buen corazón! ; a Claudia, la única persona a la que puedo acudir cuando para variar soy el que tiene un problema con la informática, muchas gracias por tu ayuda con los modelados; a Mireia 2.0, por conseguirme unas gafas nuevas en tiempo récord ; a Christopher por todo lo que nos ha ayudado estos años con el maravilloso y práctico "acuerdo marco UB" ¡Apañados estaríamos sin ti!; a Josema, por ser capaz de hacerte sacar una sonrisa cuando menos te lo esperas; a Wendy, porque a pesar del poco tiempo que pasamos juntos llegaste a confiar en mí, fuiste muy valiente al decidir tomar un nuevo rumbo; a Joana por esos pastelillos de Belém tan buenos que nos trajiste; a David Zafra, me alegró mucho saber que repetías con nosotros para hacer el TFM, eres buen tío aunque he de decirte que estás un poco loco… ¡Sigue así! Gracias a los "Joans" (1 y 2, os dejo elegir número que no quiero peleas) y a Nerea, que a pesar de haber llegado hace poco al lab os habéis hecho querer mucho. Los de las frases profundas sois vosotros, Geox el zapato que respira ¿Era así? Por muchos más Pinchiwoks, partidas de bolos, torneos de ping-pong y voleiplaya juntos.

También tengo que agradecer a todas las personas que he tenido la suerte de poder guiar en sus comienzos en el lab, porque enseñando también se aprende mucho. Para comenzar, muchas gracias a mi primera "alumna" Cati, que descubrió pronto que la vida es dura a golpe de BRETs y cual es el "truco" de como se tienen que levantar las células. Gracias por aguantarme los días que vengo más tonto de la cuenta, cuando leas tu Tesis te regalaré tu propio boli con punta de tungsteno; a Eva mi alemana favorita, ¡Quién nos iba a decir que nos íbamos a entender tan bien en inglés! Mira que me gusta la cerveza, pero tendré que practicar para seguirte el ritmo la próxima vez que nos veamos. ¡Te tomo la palabra y cuando menos te lo esperes iré a hacerte una visita! A Serranito, el último estudiante que llevaré de predoc, nunca vi a nadie comer sushi con tantas ganas. A Jordi,

aunque no te he enseñado yo directamente te considero mi "nieto" científico, sigo esperando mi copa del torneo de Mario Kart cuando quieras la revancha avisa.

Y como no, ¡Un buen párrafo para ti! que, aunque no te voy a contar nada que no sepas ya, te lo mereces. ¡Muchas gracias a mi mejor amiga Mari Carmen! Me acuerdo de la primera vez que quedamos en el Arenas cuando vine, todavía no me creía estar en Barcelona. Ya es casualidad que hayamos coincidido también para el doctorado y, además, viviendo en la misma calle, las típicas cosas que nos pasan. Gracias por todo lo que hemos vivido estos años. Ya estamos tardando en planificar el siguiente viaje.

Y finalmente, pero no por ello menos importantes, a mis amigos del pueblo; a Virginia, a Manolo, a Luis y a Blanca, por manteneros cerca de mí a pesar de haberme ido lejos. A ver cuando me dais una sorpresa y me mandáis otro jamón.

¡Gracias a todos! Sin vosotros estos años no hubieran sido lo mismo. Gracias por todo lo que me habéis ayudado y por todos los buenos momentos que hemos pasado (y seguiremos pasando) juntos. ¡Espero seguir contando con vosotros!

ABREVIATURAS

A
AC Adenilato ciclasa
ACE Enzima Convertidora de Angiotensina
ACE2 Enzima Convertidora de Angiotensina 2
AD *Alzheimer's Disease*
ADA Adenosina desaminasa
ADN Ácido desoxirribonucleico
ADP Adenosín difosfato
AEA Anandamida
Agt Angiotensinógeno
AMPA Ácido α-amino-3-hidroxi-5-metilo-4-isoxazolpropiónico
AMPc Adenosín monofosfato cíclico
Ang Angiotensina
APOE Apolipoproteína E
APP Proteína precursora amiloidea
ARBs *Angiotensin II Receptor Blocker*
Arg Arginasa
ARN Ácido ribonucleico
ARs Receptores de adenosina
AT_1R Receptor de Angiotensina II de tipo I
AT_2R Receptor de Angiotensina II de tipo II
ATP Adenosín trifosfato

B
BDA Dextrano amina biotinilada
BG Ganglios basales
BiFC *Bimolecular Fluorescence Complementation*
BRET *Bioluminiscence Resonance Energy Transfer*

C
Ca^{2+} Calcio
CB_1R Receptor de cannabinoides de tipo 1
CB_2R Receptor de cannabinoides de tipo 2
CBD Cannabidiol
CBG Cannabigerol
CBN Cannabinol
CNT Transportador de nucleósidos concentrativo
CoH *Coelenterazine-H*
COVID-19 Coronavirus 2019
CR Calretinina

D
Δ^9-THC Tetrahidrocannabinol
DAG Diacilglicerol
DIZE Aceturato de diminazeno
DMR *Dynamic mass redistribution*

E
EC_{50} Concentración efectiva media máxima
EGFR Receptor del factor de crecimiento epidérmico
ENT Transportador de nucleósidos equilibrador
ERK *Extracellular signal-regulated kinase*

F
FDA *Food and Drug Administration*
FRET *Förster Resonance Energy Transfer*

G
GDP Guanosín difosfato
GFP^2 *Green Fluorescent Protein 2*
GluR Receptores metabotrópicos de glutamato
GPCR *G-protein coupled receptor*
GP_e División externa del globo pálido
GP_i División interna del globo pálido
GRKs *G protein-coupled receptor kinases*
GTP Guanosín trifosfato

H
HEK-293T Células embrionarias de riñón humano
HTRF *Homogeneous Time Resolved Fluorescence*

I
IC_{50} Concentración inhibidora media máxima
IFN-γ Interferon gamma
IL Interleucina
iNOS Óxido nítrico sintasa
IP3 Inositol trifosfato

K
K^+ Potasio
KO *Knockout*

L
L-DOPA Levodopa
LPI Lisofosfatidilinositol
LPS Lipopolisacárido

M
MAPK *Mitogen-Activated Protein Kinases*
MD Dinámica molecular
Mg^{2+} Magnesio
MPTP 1-metil-4-fenil1,2,3,6-tetrahidropiridina
MrgE *Mas-related E*
Mrgprs *Mas-related G protein-coupled receptors*
MSN Neuronas espinosas medianas

N
Na^+ Sodio
NEP Neprilisina
nM Nanomolar
NMDA N-metil-D-Aspartato
NO Óxido nítrico

P
PD *Parkinson's Disease*
PET Tomografía de emisión de positrones
PI3K Fosfoinositol 3-quinasa
PKC Proteína Kinasa C
PLA *Proximity Ligation Assay*
PLC Fosfolipasa C
PP Proteína fosfatasa
PrNP Proteína priónica humana
PV Paralbúmina

R
R Receptor
RAS Sistema Renina-Angiotensina
RLuc *Renilla luciferasa*
RMN Resonancia magnética nuclear
ROS Especie reactiva de oxígeno

S
SARS-CoV-2 Coronavirus de tipo 2 causante del síndrome respiratorio agudo severo
SNC Sistema nervioso central
SNP *Single Nucleotide Polymorphism*
SRET BRET-FRET secuencial

T
TM Transmembrana

U
UCHL1 Ubiquitina carboxi-terminal hidrolasa L1

V
VIH Virus de la Inmunodeficiencia Humana
VTA Área tegmental ventral

W
WT *Wild-type*

Y
YFP *Yellow Fluorescence Protein*

OTROS
2-AG 2-araquidonilglicerol
5-HTR Receptor de serotonina
6-OHDA 6-hidroxidopamina
ß-AR Receptor adrenérgico
α-syn Alfa-sinucleína
µM Micromolar

INTRODUCCIÓN

1. Introducción

1.1 Receptores acoplados a proteína G

Los receptores acoplados a proteína G o GPCRs conforman la mayor familia de receptores de membrana celular en organismos eucariotas.

En humanos se han descrito más de 800 GPCRs, gran parte de ellos descubiertos mediante ensayos de secuenciación en el proyecto Genoma Humano, que suponen aproximadamente un 5% del total del genoma (Craig Venter et al., 2001). Ostentan una gran relevancia en la actualidad, ya que más del 30% de los fármacos aprobados por la Administración de Medicamentos y Alimentos de los Estados Unidos tienen como diana terapéutica alguno de estos receptores (Garland, 2013; Shimada et al., 2019).

Los GPCR se caracterizan por tener una estructura formada por siete dominios transmembrana (TM) de tipo α-hélice con 3 bucles extracelulares (E1, E2 y E3) y 3 bucles intracelulares (C1, C2 y C3). Así como un dominio n-terminal extracelular y un dominio c-terminal intracelular (Strotmann et al., 2011). La rodopsina ha sido el primer GPCR cuya estructura se ha detallado a nivel atómico, con una resolución de 2.8Å (Jastrzebska, 2015; Palczewski et al., 2000), lo que ha supuesto un importante avance en el conocimiento de esta familia de receptores. Recientemente, la estructura de la rodopsina unida a la proteína G heterotrimérica se ha conseguido estabilizar y resolver mediante criomicroscopía electrónica (Cryo-EM) (Kang et al., 2018). Dada la gran relevancia de esta familia de receptores, durante los últimos 20 años, muchas otras estructuras de GPCR se han analizado tanto en un estado conformacional inactivo (Y. Xu et al., 2019), como en un estado intermedio (Lebon et al., 2012) e incluso en su estado conformacional activo (Che et al., 2018).

Aunque los GPCR comparten una estructura terciaria de 7TM, existen diferencias en la secuencia de aminoácidos que los componen, así como diferencias en el tamaño de sus bucles intra y extracelulares y las colas amino- y carboxi- terminal. Estas diferencias han llevado a clasificar a los GPCR en 6 grandes familias, de las cuales únicamente 4 se encuentran presentes en humanos (Congreve et al., 2020):

- La familia A es la más numerosa, contando con un total de más de 700 receptores en humanos. Los receptores miembros de esta familia tienen una estructura similar al receptor de rodopsina, con una cola amino-terminal relativamente corta. La mayoría de estos receptores se encuentran implicados en la captación de estímulos olfativos o visuales.

- La familia B está formada por receptores con una estructura similar al receptor del glucagón y al receptor de la secretina, con 48 receptores descritos en humanos. Se caracterizan por una cola amino-terminal larga, con un dominio común formado por seis cisteínas.

- La familia C muestra una estructura similar al receptor metabotrópico de glutamato (mGluRs), con 22 receptores descritos en humanos. Se caracterizan por una cola

amino-terminal relativamente grande, con espacio suficiente para la unión del ligando.

- La familia F está formada por los receptores "frizzled/smoothened". En humanos se han descrito 11 receptores hasta la fecha que entran en esta clasificación. Su rasgo principal consiste en la activación por esteroides y pequeñas moléculas.

Existe una amplia variedad de moléculas que tienen afinidad e interactúan con GPCRs entre las que se incluyen desde aminas (cómo la dopamina o la serotonina), aminoácidos, péptidos (como la grelina o la angiotensina) y proteínas, hasta lípidos, nucleótidos y nucleósidos (como el ATP, el ADP o la adenosina) o iones de calcio (Marinissen & Gutkind, 2001). La unión de estos ligandos al GPCR implica cambios conformacionales que dan lugar al acoplamiento de la proteína G heterotrimérica, iniciando una cascada de señalización intracelular. Los GPCR se encuentran implicados en una gran diversidad de procesos fisiológicos de crítica importancia, como el metabolismo celular, la diferenciación y la muerte celular, las respuestas inmunológicas, la neurotransmisión o la captación de luz, olores y sabores. En este sentido, los GPCR constituyen importantes dianas terapéuticas para una gran variedad de procesos fisiológicos y patológicos, resultando, aproximadamente, un 35% de los fármacos aprobados y comercializados en la actualidad (Insel et al., 2019). La caracterización y el estudio de GPCRs endógenos implicados en ciertas patologías parece clave para el descubrimiento de nuevas dianas terapéuticas más específicas y seguras (R. Santos et al., 2016). Entre 2015 y mediados del 2020 se han aprobado 41 fármacos que actúan sobre GPCRs por la "Food and Drug Administration" (FDA), administración de los Estados Unidos encargada de regular y aprobar nuevos medicamentos (Congreve et al., 2020).

Los GPCR reconocen señales endógenas, desencadenando el acoplamiento a la proteína G heterotrimérica que resultará en la transmisión de señales al interior de la célula. Las proteínas G heterotriméricas fueron descubiertas por Alfred G. Gilman y Martin Rodbell, convirtiéndoles en merecedores del Premio Nobel de Medicina y Fisiología en el año 1994 (Ross et al., 1979). La proteína G está constituida por tres subunidades: la subunidad α ($G_{α,}$ 45 kDa), la subunidad ß ($G_{ß,}$ 37 kDa) y la subunidad γ ($G_{γ,}$ 9 kDa). La subunidad α posee una hendidura que le confiere la capacidad de unir los nucleótidos de guanina GTP y GDP, por otra parte, las subunidades ß y γ tienen gran afinidad entre ellas, formando el complejo $G_{ßγ}$ que se ancla en la membrana por el extremo c-terminal de la subunidad γ. Los GPCRs se acoplan a la proteína heterotrimérica G mediante la apertura del dominio transmembrana 6 y los bucles intracelulares C1, C2 y C3 (J. Wang et al., 2020).

En mamíferos se han descrito más de 20 subtipos de subunidad α. Entre ellas, cuatro subtipos muestran una mayor relevancia (McCudden et al., 2005; Shpakov, 2013):

1) $G\alpha_s$ o estimuladora. Su activación es capaz de estimular la adenilato ciclasa (AC), enzima liasa que cataliza la conversión de adenosín trifosfato (ATP) a adenosín monofosfato cíclico (AMPc), activando la proteína quinasa A (PKA).
2) $G\alpha_{i/o}$ o inhibidora. Su activación inhibe la AC, reduciendo los niveles intracelulares de AMPc. Es decir, con acción opuesta a la $G\alpha_s$.

3) $G\alpha_{q/11}$. Su activación estimula la fosfoinositida fosfolipasa C (PLC), generando inositol trifosfatos (IP3) y diacilglicerol (DAG), aumentando los niveles de calcio en el citosol.
4) $G\alpha_{12/13}$. Su activación puede estimular enzimas GTPasas de la familia Rho. Se ha descrito su implicación en procesos de regulación de la formación del citoesqueleto de la célula (Suzuki et al., 2009).

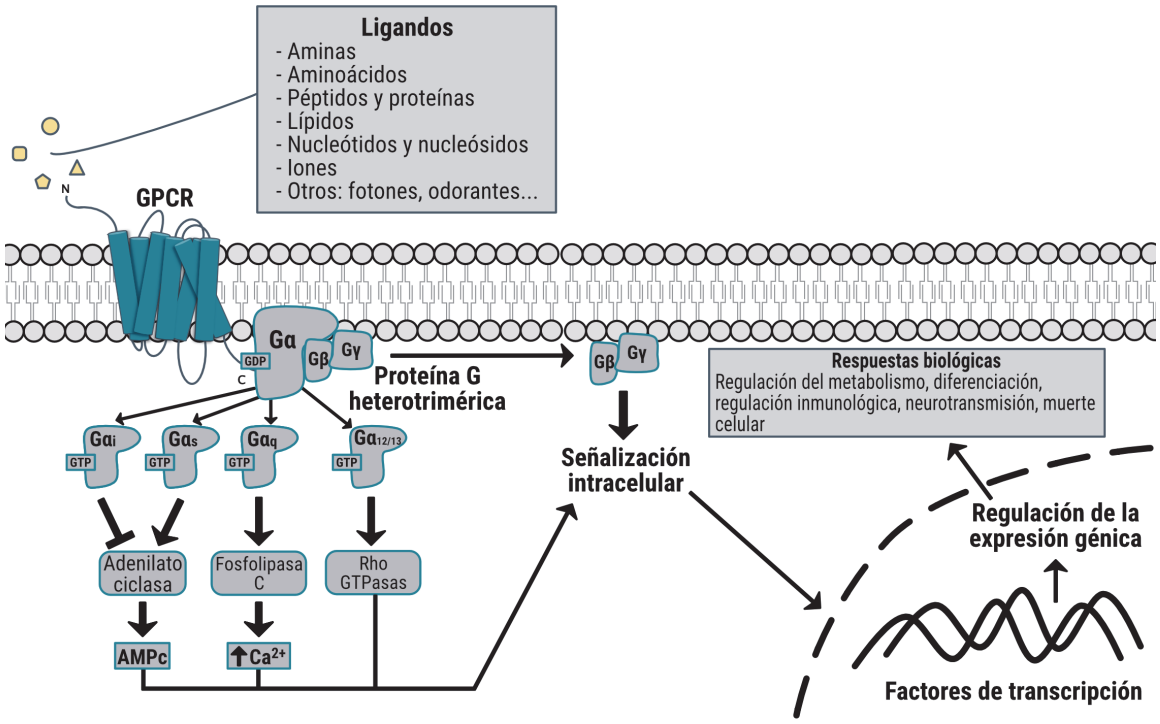

Figura 1: Diversidad de los ligandos capaces de activar GPCRs y la señalización mediada por las proteínas Gα más importantes.

Uno de los mensajeros secundarios más importantes en la activación de los GPCR es la fosforilación de las MAPK. Esta señal puede ser dependiente de proteínas G (fase temprana) o dependiente de ß-arrestinas (fase tardía). Es una respuesta que alcanza su pico máximo de activación a los pocos minutos y que persiste en el tiempo hasta un intervalo máximo de 30-60 minutos con señales ondulantes. La fosforilación de ERKs es una señal relacionada con la proliferación y supervivencia celular (Gurevich & Gurevich, 2020).

La visión clásica considera que los GPCR pueden tener únicamente dos estados conformacionales (activo e inactivo). Sin embargo, recientemente se ha descrito como realmente pueden adoptar un amplio abanico conformacional, desde un estado inactivo con el centro de unión a proteína heterotrimérica G enmascarado, pasando por una serie de estados intermedios en los que el ligando se encuentra unido al GPCR, pero no señaliza, hasta un estado completamente activo en el que el receptor es capaz de acoplar la proteína heterotrimérica G. La unión del ligando al receptor depende de la presencia de dominios ricos en leucina a nivel extracelular, aunque el mecanismo por el cual algunos GPCR son activados por iones u odorantes no se ha caracterizado (Manglik & Kruse, 2017).

Existe un control y una regulación homeostática mediante una serie de procesos en un delicado equilibrio, conocidos como mecanismos de desensibilización/resensibilización que regulan la señalización de los GPCR. Estos receptores pueden alcanzar un estado conformacional activo y acoplar proteína G incluso en ausencia de ligando, lo que se conoce como actividad basal (Gough, 2016; Miller et al., 2003). Uno de los principales mecanismos de los que dispone la célula para desensibilizar a los GPCR es su internalización mediada por las proteínas citosólicas ß-arrestinas, reduciendo la disponibilidad del receptor en la membrana plasmática para unir ligando y transducir señales (Ferguson et al., 1996). Para que este proceso tenga lugar, una vez el receptor ha sido activado por su correspondiente ligando, es fosforilado por las serina/treonina quinasas de los receptores acoplados a proteína G (GRKs). Esto permite la unión estable de las ß-arrestinas a los GPCR fosforilados y formar un complejo que abandona la membrana plasmática mediante endocitosis, penetrando en el interior de la célula (Cahill et al., 2017).

El receptor internalizado sigue dos posibles vías:

1) El receptor es marcado mediante ubiquitinación, para su transporte y degradación en los lisosomas mediante peptidasas, en su mayoría endopeptidasas de la familia de las catepsinas (Cottrell, 2013).

2) El receptor sufre un proceso de desfosforilación mediado por fosfatasas (principalmente PP1 y PP2) (Gupta et al., 2018) y un posterior reciclado a nivel de membrana plasmática, volviendo a ser un receptor funcional.

Los GPCR se clasifican en dos subtipos según la afinidad por las ß-arrestinas con la que forman complejos: los GPCRs tipo A se unen con menor afinidad, por lo que se desfosforilan y reciclan de forma más rápida y eficiente; por otro lado, los GPCRs tipo B muestran una mayor afinidad por las ß-arrestinas, con un proceso de resensibilización más lento (Luttrell, 2008)(Mohan et al., 2015).

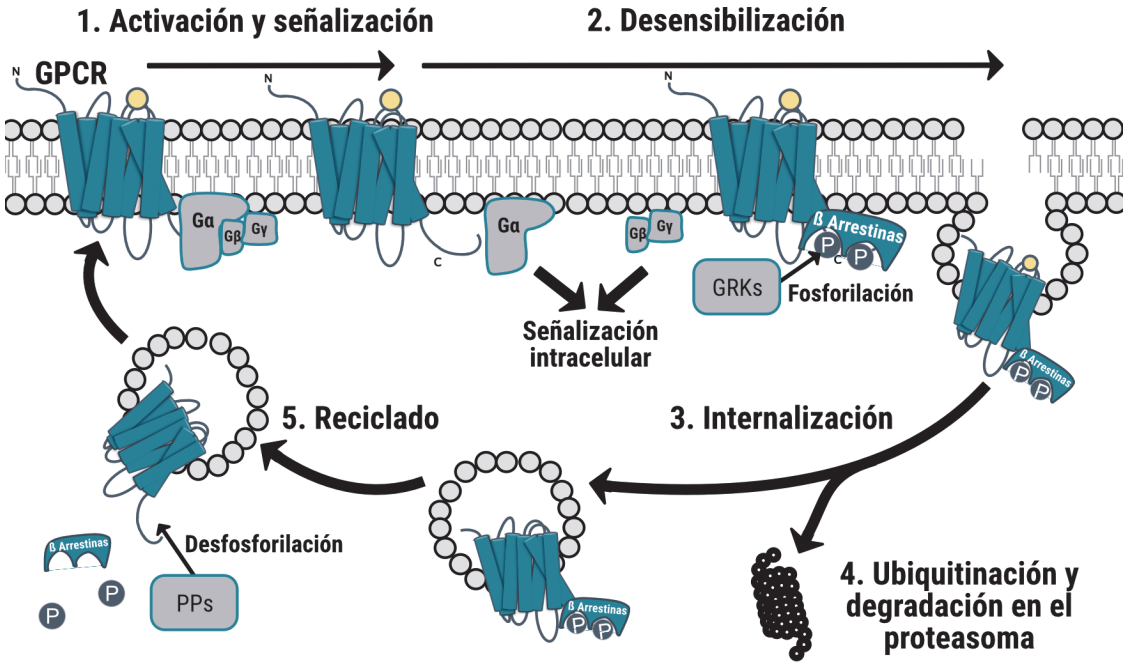

Figura 2: Esquema de los procesos de desensibilización de GPCRs mediante GRKs y ß-arrestinas, endocitosis y resensibilización en membrana celular.

La proteólisis mediada por peptidasas presentes en la membrana plasmática también tiene un papel relevante en la regulación de la actividad de los GPCR. Las peptidasas controlan la disponibilidad de péptidos bioactivos que pueden unirse a los GPCR y activar la señalización transducida. Un ejemplo es la angiotensina II, un péptido que ejerce su efecto al unirse al receptor GPCR de angiotensina II tipo 1 (AT_1R) y cuya disponibilidad está supeditada a la reacción de proteólisis mediada por la enzima convertidora de angiotensina (ACE), catalizando la conversión de angiotensina I en angiotensina II (Mogi et al., 2009).

1.1.1 Dímeros y oligómeros de orden superior

La membrana plasmática es la estructura celular encargada de delimitar el interior (citoplasma y orgánulos) del exterior celular. En ella se encuentran embebidos los receptores acoplados a proteína G junto con otras proteínas y lípidos, constituyendo lo que se conoce como mosaico fluido. La membrana plasmática es una estructura dinámica que contiene microdominios de entre 25 y 100 nm de diámetro llamados balsas de lípidos o "lipid rafts". Estos dominios se encuentran altamente organizados, con una composición rica en fosfolípidos, glicoesfingolípidos y colesterol. Tienen un papel muy relevante en el tráfico y señalización de los GPCR (Head et al., 2014) favoreciendo las interacciones proteína-proteína (Villar et al., 2016).

La asociación o interacción estrecha entre dos GPCR recibe el nombre de dímero, y el proceso por el que se forma dicho dímero se denomina dimerización (Rios et al., 2001), de

tal forma que estas estructuras actúan como una única unidad funcional. Los dímeros se pueden manifestar bien constituidos por dos receptores idénticos (homodímeros) o distintos (heterodímeros o heterómeros). En la actualidad existen más de 300 publicaciones en los últimos 5 años que reportan estas interacciones GPCR-GPCR (Wouters et al., 2019).

A su vez, se han descrito estructuras de GPCRs de orden superior, entre las que encontramos trímeros (Jiang et al., 2014), tetrámeros (Ferré, 2015) e incluso oligómeros (Barreto et al., 2020). El descubrimiento de los oligómeros de GPCRs ha llevado a replantear la manera en la que estos receptores median su señalización, puesto que en la membrana celular conviven la forma monomérica con otras estructuras de orden superior (Faron-Górecka et al., 2019).

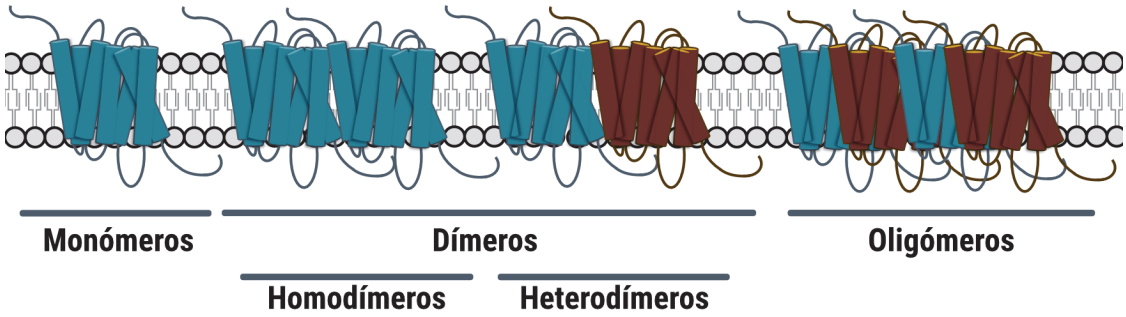

Figura 3: Interacciones entre los GPCRs.

La detección y posterior demostración de la interacción entre dos o más GPCR siempre ha estado ligada a la evolución y perfeccionamiento de numerosas técnicas experimentales (Barreto et al., 2020), entre las que se incluyen:

- Transferencia de Energía Resonante por Bioluminiscencia (BRET): esta técnica demuestra la interacción entre dos proteínas mediante la creación de proteínas de fusión. Una proteína actuará como dadora, fusionada a Renilla luciferasa y otra como aceptora fusionada a un fluorocromo (YFP o GFP). Si las proteínas de estudio se encuentran a una distancia inferior a 10 nm, se transferirá la energía de la proteína dadora a la aceptora que emitirá a una determinada longitud de onda, demostrando así la interacción física entre ambas (Bacart et al., 2008).

- Transferencia de Energía Resonante por Fluorescencia o Förster (FRET): Esta técnica mantiene la misma base molecular que el BRET. La principal diferencia consiste en que ambas proteínas dadora y aceptora son fluorocromos cuyos espectros de emisión y excitación se solapan (Chakraborty & Chattopadhyay, 2015).

- BRET-FRET secuencial (SRET): esta técnica permite la detección de heterómeros formados por tres proteínas diferentes mediante la combinación de las técnicas de BRET y FRET. La primera proteína se encuentra fusionada a una luciferasa y al catalizar la oxidación del sustrato coelenteracina H actúa como molécula dadora excitando al fluorocromo al que está fusionada la segunda proteína, que al excitarse emitirá a una determinada longitud de onda excitando al fluorocromo fusionado a la tercera proteína de estudio (Carriba et al., 2008).

- Transferencia de Energía Resonante por Fluorescencia Resuelta en Tiempo (TR-FRET): Esta técnica es una combinación del FRET con la fluorimetría a tiempo real (TRF). En esta técnica se marca la proteína dadora con europio o terbio y la proteína aceptora con fluorocromos de larga duración (Lin & Chen, 2018). El dador y el aceptor se pueden utilizar para marcar una amplia variedad de biomoléculas, en aplicaciones que incluyen epigenética, cuantificación de biomarcadores y señalización de GPCR entre otros.

- Complementación Bimolecular (BiFC): Esta técnica se basa en la fusión de las proteínas de análisis a dos hemiproteínas no fluorescentes de la proteína YFP. En el caso que las proteínas de estudio se encuentren interaccionando, las hemiproteínas se van a situar a una distancia inferior a 6 nm, siendo capaces de reconstituir a la proteína fluorescente YFP emitiendo fluorescencia de nuevo. En combinación con otras técnicas como el BRET o el FRET permite detectar oligómeros de GPCR de orden superior (Wouters et al., 2019).

- Ensayos de Ligación por Proximidad (PLA): Esta técnica es la única de las técnicas descritas que permite detectar interacciones físicas de proteínas en tejido. Se basa en el marcaje de las proteínas de interés con anticuerpos primarios específicos. Posteriormente, se usan anticuerpos secundarios conjugados con dos sondas de oligonucleótidos complementarias. Si los receptores se encuentran a una distancia inferior a 30 nm, y por lo tanto, interaccionando, tras una incubación con una ligasa y una polimerasa, las sondas de oligonucleótidos hibridan y se amplifica una señal que es fácilmente detectable como un clúster de coloración roja (Weibrecht et al., 2010).

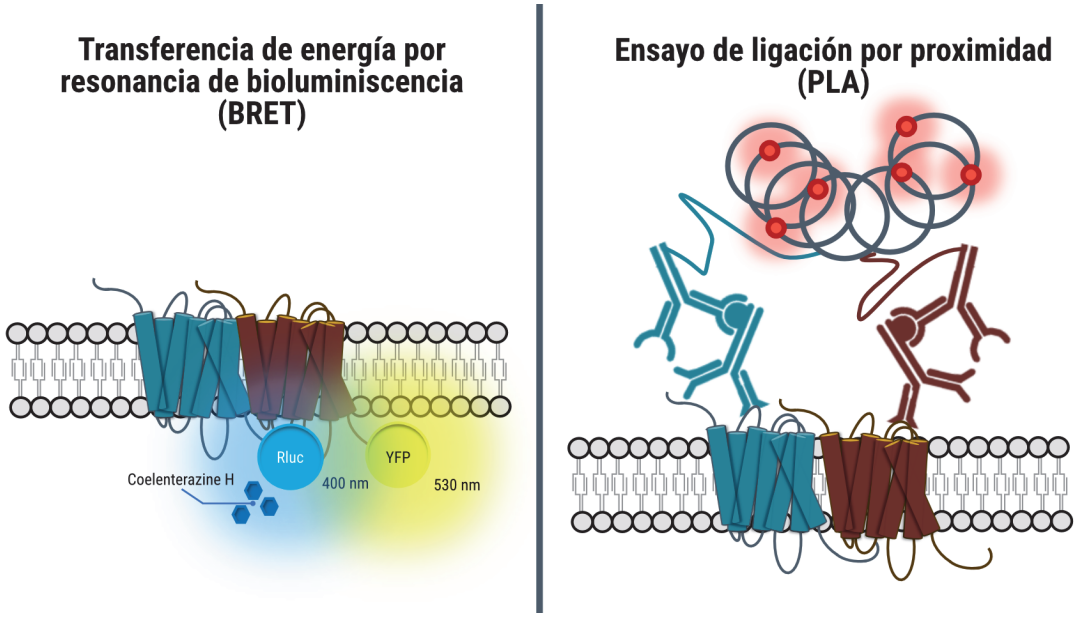

Figura 4: Dibujo esquemático de la técnica experimental de BRET (izquierda) y de la técnica de PLA (derecha).

Los dímeros y oligómeros de orden superior representan una nueva fase de complejidad en el campo de los GPCR. Aunque cada dímero de GPCR tiene características estructurales

propias, la evidencia científica sugiere que la unión de un ligando a un único miembro del dímero es suficiente para producir un cambio conformacional y permitir el acoplamiento a una proteína heterotrimérica G (Fuxe et al., 2012). Además, la dimerización entre GPCR puede dar lugar a una modulación alostérica directa, negativa o positiva. De esta forma, un receptor A puede disminuir o aumentar la afinidad del receptor B por su propio ligando cuando se encuentran formando un dímero. Otra posibilidad descrita es que la propia unión de un ligando al receptor A sea la causante de la internalización del segundo protómero del complejo o receptor B. Finalmente, también se ha descrito que la activación de un receptor en un complejo proteico puede afectar la transducción de señal y la funcionalidad del otro receptor del complejo (Pin et al., 2019).

Desde otro punto de vista, la oligomerización también pone sobre la mesa nuevas posibilidades para el uso de los GPCR como dianas terapéuticas. La detección de heterómeros implicados en determinadas patologías es un reto continuo y su utilización como dianas farmacológicas específicas puede potenciar los efectos beneficiosos de un determinado compuesto, disminuyendo los efectos adversos (Franco et al., 2013). Un ejemplo descrito es el heterómero formado por los receptores AT_1 y el receptor B_2 de bradicinina, que aumenta en estado de preeclamsia (AbdAlla, Lother, el Massiery, et al., 2001). Otro ejemplo descrito es el compuesto KW-6002, un antagonista específico de $A_{2A}R$ que, al contrario que sucede con otros antagonistas, no pierde afinidad por $A_{2A}R$ cuando este receptor se encuentra formando complejos heteroméricos lo que le confiere una gran capacidad terapéutica para combatir el Parkinson (Ferré et al., 2011).

Para recopilar las interacciones conocidas entre GPCRs existen bibliotecas virtuales de libre acceso como GPCR-HetNet (Borroto-Escuela et al., 2014) (http://www.gpcr-hetnet.com/)(Southan, 2016). Estas bases de datos indexan una red de receptores y reflejan sus interacciones apartando las referencias que las respaldan.

1.1.2 Selectividad funcional

Como se ha especificado en el *apartado 1.1*, existe una gran diversidad de compuestos capaces de interaccionar con los receptores acoplados a proteínas G. Estos compuestos se han clasificado atendiendo a su unión al centro ortostérico o principal del receptor o al centro alostérico o modulador (H. C. S. Chan et al., 2019).

La molécula capaz de unirse al sitio ortostérico activando al GPCR se llama agonista. En cambio, si el ligando tiene la cualidad de bloquear al receptor inhibiendo la acción del agonista se llama antagonista. Los agonistas pueden ser totales o parciales según su eficacia para promover una respuesta bioquímica en el receptor. Por otro lado, también se ha descrito el agonista inverso, que se une al centro ortostérico inhibiendo la respuesta basal del propio receptor en ausencia de ligandos. Por otra parte, si la molécula se une al centro alostérico hablamos de moduladores alostéricos positivos o negativos, aumentando o disminuyendo respectivamente, el efecto de un agonista sobre un receptor. También se han descrito compuestos capaces de unirse al sitio alostérico y no modificar la señalización del receptor, que se han denominado como moduladores alostéricos neutros (Neubig et al.,

2003). Hay que puntualizar que actualmente aun existen GPCR para los cuales no se conoce su propio ligando endógeno. Estos receptores se les describe como receptores huérfanos.

Guidetopharmacology (https://www.guidetopharmacology.org) se plantea como una gran herramienta para obtener información "curada" y referenciada sobre que compuestos actúan y con qué afinidad sobre un determinado GPCR.

Aunque el concepto fue introducido inicialmente por Kenakin (Kenakin, 1995), hasta años más recientes no se ha analizado en profundidad el fenómeno por el cual un ligando activa una señalización específica en un GPCR, que se ha denominado como agonismo sesgado ("biased-agonism") o selectividad funcional. El ligando que desencadena esta respuesta específica, estabilizando una conformación del receptor de las múltiples que puede estabilizar un ligando "balanceado", se denomina agonista sesgado (Gundry et al., 2017).

Aunque en la mayoría de la bibliografía se describe una selectividad funcional entre la señalización dependiente de proteína heterotrimérica G o dependiente de ß-arrestinas (C. H. Liu et al., 2017; N. Bohinc & Gesty-Palmer, 2012; Zhou et al., 2017), también existe selectividad funcional en cuanto al acoplamiento de los GPCR a diferentes proteínas heterotriméricas G puesto que algunos de estos receptores son capaces de acoplarse a más de un tipo de subunidad alfa (Navarro, Reyes-Resina, et al., 2018; Navarro, Varani, et al., 2018; Wisler et al., 2014).

Además de la selectividad funcional, también se ha reportado la existencia de un sesgo en la señalización dependiente del tiempo. Esto implica oscilaciones en algunas vías de señalización (Grundmann & Kostenis, 2017).

La selectividad funcional es un fenómeno que también se aplica a heterómeros de GPCR (Navarro, Reyes-Resina, et al., 2018). Un ejemplo, es el descrito por (Mustafa et al., 2012), donde el heterómero compuesto por el receptor adrenérgico α_{1A} y el receptor de quimiocina 2 (CXC2) demuestra tener una mayor facilidad para reclutar ß-arrestinas.

Este fenómeno del agonismo sesgado tiene una gran relevancia y está siendo utilizado en la actualidad para diseñar nuevos fármacos o incluso mejorar la eficacia de fármacos ya existentes y que muestren una reducción de los efectos secundarios indeseados, activando o bloqueando específicamente la vía de señalización terapéutica o causante de la patología (Franco et al., 2018). Es por ello que, desde un punto de vista farmacológico, un ligando sesgado es mucho más interesante que uno que active o bloquee de forma equilibrada todas las señalizaciones mediadas por un determinado receptor (Rominger et al., 2014).

Existen diferentes métodos para la cuantificación del sesgo de un ligando específico sobre un determinado receptor, pero el más conocido y utilizado es el "bias factor" (Gundry et al., 2017). Para su cálculo se requiere de dos valores: el valor de efecto máximo (r) y la K_A que se obtiene aplicando el antilogaritmo de la concentración efectiva media (EC_{50}) o de la concentración inhibitoria media (IC_{50}), según si el compuesto actúa potenciando o inhibiendo la vía de señalación estudiada. También se debe escoger un ligando y una vía de señalización de referencia, habitualmente se opta por el ligando endógeno y la vía de señalización principal del receptor de interés. Teniendo esta información, el bias factor se puede calcular

aplicando esta fórmula matemática, donde j_1 es la vía de señalización de interés y j_2 es la vía de señalización de referencia (Onaran et al., 2017):

$$\log bias = \Delta log(\mathrm{r}/K_A)_{\ j_1} \ - \ \Delta log(\mathrm{r}/K_A)_{\ j_2}$$

$$bias = 10^{\Delta\Delta\log\left(\frac{\tau}{K_A}\right)_{j_1 - j_2}}$$

Un bias factor superior a 1 indica que el ligando estudiado tiene una mayor preferencia a señalizar por una determinada vía de señalización que el ligando escogido como referencia, un valor inferior a 1 revela lo contrario.

En definitiva, la selectividad funcional y su adecuada cuantificación se proyectan como potentes herramientas a considerar en la caracterización de ligandos ya existentes o de nuevos compuestos, con el fin de evaluar de forma precisa la respuesta que desencadenan sobre un receptor en concreto.

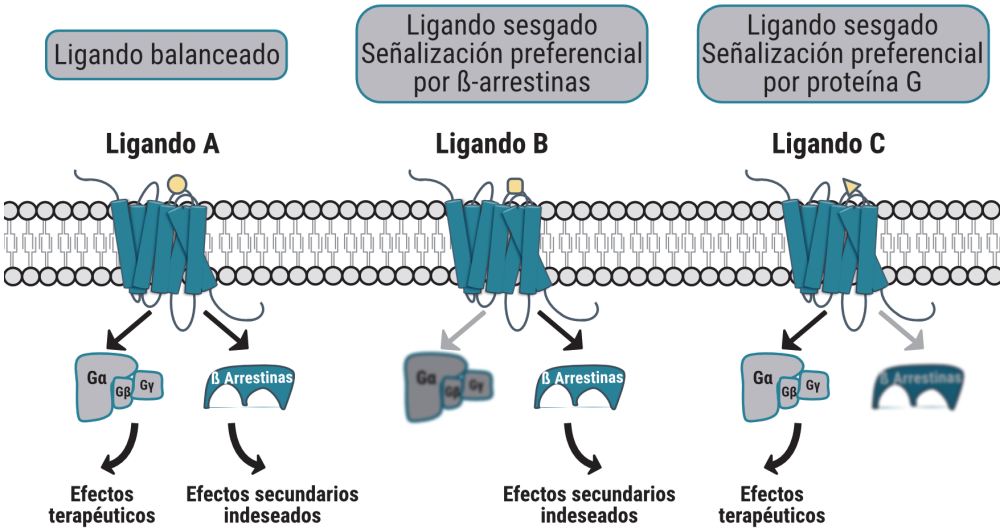

Figura 5: Diferencias entre el ligando balanceado y el ligando sesgado en la activación de los GPCRs y de la señalización mediada a través de ellos.

1.2 El sistema cannabinoide

Durante milenios, extractos de la planta *Cannabis sativa* se han utilizado como terapia para combatir diferentes patologías, utilizando sus propiedades analgésicas, antiinflamatorias y antioxidantes. A principios del siglo XIX, con el propósito de descubrir el principio activo que ofrecía propiedades medicinales a la planta *Cannabis sativa,* se aisló por primera vez un compuesto cannabinoide, el cannabinol (CBN) y, también, el Δ^9-tetrahidrocannabinol (Δ^9-THC) (Farag & Kayser, 2017). A partir de ahí y hasta la fecha, se han aislado más de 100 compuestos cannabinoides extraídos de *C. sativa* que pueden ser clasificados químicamente dentro de la categoría de terpenofenoles. (Amin M.R. & Ali DW., 2019).

El conjunto formado por los endocannabinoides, las enzimas responsables de su síntesis y degradación, los receptores y transportadores de cannabinoides recibe el nombre de sistema endocannabinoide. Los compuestos cannabinoides se caracterizan por sintetizarse en la membrana de la neurona postsináptica para unirse a los receptores de la neurona presináptica, por ello se considera al sistema cannabinoide con capacidad de señalización retrógada (Wilson & Nicoll, 2001).

Los compuestos cannabinoides se pueden clasificar según su origen en:

- Fitocannabinoides: son los cannabinoides extraídos de la planta *Cannabis sativa*. Entre ellos, el compuesto con efecto psicotrópico mayoritario es el Δ^9-THC, que representa aproximadamente el 17% del contenido total en compuestos cannabinoides de la planta. Por otra parte, el compuesto más abundante entre los no psicoactivos es el cannabidiol (CBD). Otros fitocannabinoides neutros relevantes son el cannabigerol (CBG) y el cannabinol (CBN). Los compuestos cannabinoides se encuentran en *C. sativa* de manera natural en su forma ácida (Δ^9-THCA, CBDA, CBGA), de la cual pueden aislarse su versión neutra (Δ^9-THC, CBD, CBG) y varínica (Δ^9-THCV, CBDV, CBGV) (Franco et al., 2020; Turner et al., 2017).

- Endocannabinoides: son los compuestos producidos de forma natural en el organismo. El primer endocannabinoide en ser descubierto fue la N-araquidonoetanolamina o anandamida (AEA) en 1992. Otro endocannabinoide de gran relevancia fisiológica, es el 2-araquidonilglicerol (2-AG), con una afinidad tanto por CB_1R como por CB_2R del orden de entre 50 a 500 veces más alta que la anandamida (Hanuš, 2009).

- Cannabinoides sintéticos: son un grupo heterogéneo de cannabinoides diseñados artificialmente en un laboratorio con la finalidad de obtener compuestos con propiedades terapéuticas y sin efectos secundarios no deseados. También se ha intentado potenciar su efecto psicotrópico, mediante modificaciones del Δ^9-THC, para su uso como droga recreativa (Karila et al., 2016; Martinotti et al., 2017).

En 1990 se clonó por primera vez el primer receptor cannabinoide, el receptor CB_1R (Matsuda et al., 1990) y tres años más tarde el segundo, el CB_2R (Munro et al., 1993). Ambos receptores pertenecen a la superfamilia de receptores acoplados a proteína G. Tanto CB_1R como CB_2R son receptores bastante conservados entre especies, mostrando una alta homología superior al 80% entre las secuencias de humano, ratón y rata (Abood et al., 1997)(Marcu et al., 2013). En cambio, CB_1 y CB_2 son receptores que tienen una identidad reducida entre sus secuencias con un aproximado del 44% (Howlett & Abood, 2017).

Años más tarde se encontró un nuevo receptor con capacidad de unir compuestos cannabinoides, el receptor GPR55. Inicialmente se consideró un receptor huérfano (Ryberg et al., 2007), después se teorizó como el tercer receptor de cannabinoides "CB_3R" (Moriconi et al., 2010). Sin embargo, nunca fue aceptado y sigue siendo un receptor poco caracterizado cuyo comportamiento farmacológico es atípico y con publicaciones contradictorias sobre su funcionalidad que dificultan la comprensión de su verdadero papel fisiológico (Kapur et al., 2009).

El sistema endocannabinoide se encuentra implicado en la modulación de una amplia variedad de procesos fisiológicos, entre los que encontramos el control de la ingesta de alimentos, la regulación del sistema inmune e incluso el desarrollo neuronal (D. Lu & Potter, 2017). Por este motivo, el sistema endocannabinoide se plantea como un claro objetivo de investigación para su aplicación en una gran diversidad de terapias y tratamientos entre los que se incluyen:

A) Tratamientos antiinflamatorios y calmantes del dolor. El uso de los cannabinoides para paliar el dolor se remonta a la antigua China (Roger G. Pertwee, 2006). Mientras que el receptor CB_1 se encuentra implicado en procesos complejos relacionados con el dolor (Woodhams et al., 2017), el receptor CB_2 se ha descrito con un papel antihiperalgésico y antiinflamatorio tanto en modelos de dolor agudo como crónico (Valenzano et al., 2005; L. Yang et al., 2014).

B) Trastornos metabólicos. Debido a la elevada expresión de CB_1R en tejido adiposo e hígado, así como la presencia de altas concentraciones de compuestos endocannabinoides en tejido adiposo de personas con obesidad (Kunos & Osei-Hyiaman, 2008). Un buen ejemplo es el rimonabant, un antagonista de CB_1R, utilizado como tratamiento para la obesidad (Burch et al., 2009).

C) Tratamientos neuroprotectores. Diferentes estudios *in vitro* han demostrado que ciertos compuestos cannabinoides (como Δ^9-THC o el cannabidiol) poseen propiedades neuroprotectoras, siendo algunos de ellos selectivos para un determinado receptor de cannabinoides, lo que facilita diseñar una terapia más específica (Fernández-Ruiz, 2019).

   El receptor cannabinoide CB_1 es el receptor más expresado a nivel de SNC. Además, existe una elevada expresión de los receptores cannabinoides en el sistema nervioso periférico. Por ello el sistema endocannabinoide es potencialmente útil para tratar la isquemia, la esclerosis múltiple, las lesiones de médula espinal, los desórdenes del movimiento como la enfermedad del Párkinson o el Huntington, la enfermedad de Alzhéimer y la epilepsia entre otras patologías relacionadas con el sistema nervioso (Pacher et al., 2006).

D) Tratamientos antieméticos. Se ha descrito como la activación de CB_1R mediante agonistas suprime las náuseas, así como el reflejo del vómito. También se ha reportado que el bloqueo de la señalización de CB_1R mediante antagonistas, como el rimonabant, provoca náuseas. Los mecanismos por los que este efecto tiene lugar no están perfectamente descritos y el estudio es complejo debido a que los modelos animales de rata o ratón son incapaces de vomitar (Parker et al., 2011).

E) Tratamientos anticancerígenos. Inicialmente, los cannabinoides se utilizaron como agentes paliativos en pacientes de cáncer con sintomatología grave. Años más tarde, se detectó un aumento significativo en su tasa de supervivencia (Aggarwal, 2016). Actualmente se ha visto que los receptores cannabinoides se encuentran sobreexpresados en numerosos tipos de cáncer, donde los niveles de endocannabinoides son más elevados. Así, se ha descrito que los cannabinoides

están implicados en procesos como la regulación de la proliferación celular y su supervivencia, por ello se están desarrollando terapias que inhiban la proliferación de las células cancerígenas y disminuyan su capacidad metastásica (Śledziński et al., 2018).

Entre los fármacos que contienen cannabinoides más utilizados se encuentran el Dronabinol® y el Cesamet®. En ambos casos su principio activo es el Δ^9-THC. Son compuestos aprobados para combatir las náuseas provocadas por la quimioterapia (Parker et al., 2011). También existen ensayos clínicos en los que se ha demostrado la eficacia del Dronabinol® para el tratamiento del dolor neuropático (Schimrigk et al., 2017). Otro fármaco regulado es el Sativex®, utilizado para combatir la sintomatología de la esclerosis múltiple y cuyos principios activos son el Δ^9-THC y el CBD a concentraciones equivalentes (Russo et al., 2017).

El sistema endocannabinoide tiene una gran plasticidad, es decir, una alta capacidad autorreguladora y homeostática. Algunos ejemplos incluyen la internalización de los receptores cannabinoides presentes en la membrana plasmática ante exposiciones prolongadas a cannabinoides o ciertas circunstancias como la ingesta de alimentos y la exposición a situaciones de estrés que son capaces de alterar la expresión de los componentes del sistema endocannabinoide (Castillo et al., 2012).

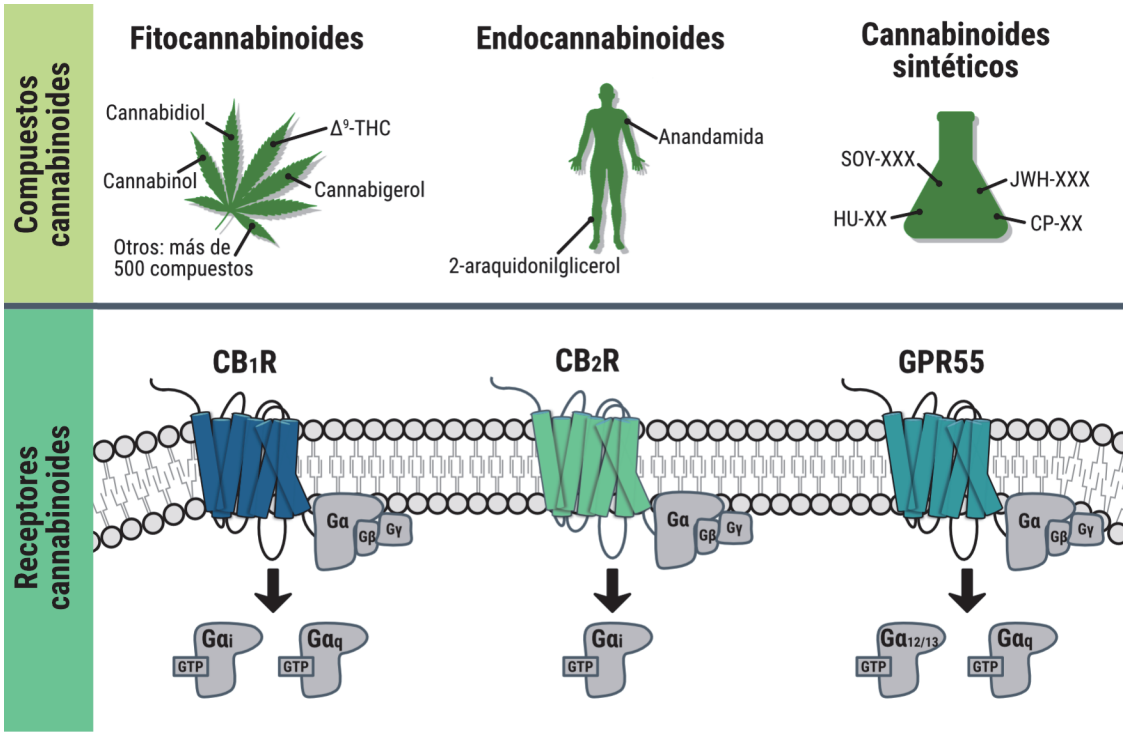

Figura 6: Clasificación de los compuestos cannabinoides y los receptores del sistema cannabiniode.

1.2.1 Receptor de cannabinoides de tipo 1 (CB_1R)

El receptor de cannabinoides de tipo 1 no sólo es el GPCR del sistema endocannabinoide mayoritario, sino que además es el GPCR de clase A más abundante y uno de los mejor caracterizados en la actualidad. Está compuesto por 473 aminoácidos y comparte las características estructurales de la familia de receptores de clase A. La unión de ligando al receptor desencadena un cambio estructural que abre la hélice transmembrana 6, permitiendo la interacción con la proteína $G\alpha_i$. El extremo N-terminal es de un tamaño inusualmente largo (117 aminoácidos) mientras que el extremo C-terminal tiene una longitud similar a otros GPCR (73 aminoácidos) y contiene 3 cisteínas y dominios ricos en serina y treonina susceptibles a ser fosforilados, con un papel relevante en la señalización del receptor (Stadel et al., 2011). La estructura de CB_1R se ha descrito detalladamente mediante cristales de alta resolución (Shao et al., 2016)

La activación de CB_1R al unir un ligando desencadena una señalización intracelular mediada mayoritariamente por el acoplamiento a proteína $G\alpha_{i/o}$, dando lugar a la inhibición de la adenilato ciclasa y disminuyendo los niveles de AMP cíclico intracelulares. Aunque también se ha descrito su unión a las subunidades $G\alpha_s$ y $G\alpha_{q/11}$ en condiciones excepcionales, como ocurre en la astroglía (Navarrete & Araque, 2008). Precisamente, mediante resonancia de plasmón por superficie se ha demostrado que los agonistas de CB_1R pueden estabilizar conformaciones estructurales diferentes, adquiriendo un acoplamiento preferencial a un tipo de proteína G u otro (Georgieva et al., 2008). Por otra parte, la activación de CB_1R también puede activar la fosforilación de proteínas MAPK tanto por la vía dependiente como independiente de proteína G, el reclutamiento de ß-arrestinas y la fosforilación de p38 o c-Jun (Al-Zoubi et al., 2019). Cabe destacar que se ha descrito que CB_1R muestra una alta actividad basal, controlada principalmente por una región reguladora en el extremo C-terminal del receptor (Hanlon & Vanderah, 2010).

La expresión del receptor CB_1 es ubicua en el organismo humano, con altos niveles en corazón, endotelio vascular, hígado, huesos, pulmones, sistema nervioso central y periférico y sistema reproductor, también se encuentra en órganos como el ojo, próstata, timo, amígdalas y médula ósea (Howlett & Abood, 2017). Hay que puntualizar que enfermedades como el Huntington o el Párkinson se han asociado a bajos niveles de expresión de CB_1R en el sistema nervioso central.

La activación de CB_1R desencadena en el organismo procesos que regulan la nocicepción, el aprendizaje, la memoria, la percepción sensorial y el metabolismo. Además, a través de CB_1R se producen los efectos psicotrópicos que promueven algunos compuestos cannabinoides como el Δ^9-THC. Existe una gran implicación del receptor CB_1 en procesos fisiológicos que controlan y regulan la depresión, la digestión, el dolor crónico, el hambre, la memoria y el miedo (Lutz et al., 2015; Schwitzer et al., 2016). La amplia variedad de efectos inducidos por los cannabinoides es uno de los motivos por los que el número de publicaciones relacionadas con este receptor se ha visto incrementado en la última década al orden de unas 500 publicaciones anuales (Pubmed, 2020).

El uso de antagonistas y agonistas inversos específicos dirigidos al sitio ortostérico del receptor CB_1 se ha investigado ampliamente como terapia farmacológica. Un claro ejemplo

es el rimonabant**,** un antagonista específico de CB_1R, que se ha descrito como efectivo para la reducción del apetito y para combatir la obesidad y que fue aprobado en 2006 (Carai et al., 2006). Dos años más tarde, fue retirado del mercado por sus efectos secundarios, que superaban los beneficios terapéuticos (Moreira & Crippa, 2009). Otro caso similar, es el agonista inverso de CB_1R taranabant, que no llegó a superar la fase III de los ensayos clínicos efectuados por Merck & Co. Inc (Proietto et al., 2010).

Como se ha descrito, a la hora de recurrir a compuestos que activan el receptor CB_1 mediante su unión al sitio ortostérico, existe un problema de aparición de efectos secundarios indeseados, especialmente los de carácter psicotrópico que pueden desencadenar conductas depresivas y ansiedad (Moreira & Crippa, 2009). Para evitar en la medida de lo posible este inconveniente se están buscando soluciones, las dos aproximaciones más prometedoras son las siguientes:

1) Modulación alostérica del receptor CB_1. Esta estrategia está despertando un gran interés entre la comunidad científica, cuyas publicaciones recientes están ampliando el conocimiento sobre los centros alostéricos del receptor CB_1 y sus compuestos selectivos. Entre los moduladores alostéricos positivos cabe destacar GAT-211, lipoxina A4, ORG27569, PSNCBAM-1 y RTI-371. Y entre los moduladores alostéricos negativos el cannabidiol, algunos péptidos endocannabinoides (pepcanos) y la pregnenolona (Hryhorowicz et al., 2019; Khurana et al., 2017).

2) Selectividad funcional. Existe un elevado número de compuestos cannabinoides que se comportan como agonistas sesgados. Entre los endocannabinoides, 2-AG y AEA señalizan a través de CB_1R preferentemente a través de $G\alpha_i$, mientras que la N-Araquidonoil dopamina (NADA) lo hace a través de $G\alpha_q$. Por otro lado, entre los fitocannabinoides, un claro ejemplo es el Δ^9-THC, que señaliza preferencialmente a través de ß-Arrestinas I y $G\alpha_q$. Sin embargo, debido a la amplia variedad de compuestos fitocannabinoides, aún quedan muchos por caracterizar. En último lugar, entre los cannabinoides sintéticos hay que resaltar que la selectividad funcional mostrada ante un determinado ligando sesgado puede depender de varios factores, como el tipo celular e incluso de la oligomerización de CB_1R con otros receptores (Al-Zoubi et al., 2019).

El receptor CB_1 se postula como uno de los transductores de señales más importantes en el organismo humano. La activación o bloqueo específico de la señalización mediada a través de CB_1R, evitando en la medida de lo posible efectos secundarios indeseados, puede ofrecer un amplio abanico de posibilidades en el tratamiento o atenuación de la sintomatología de un gran número de afecciones.

1.2.2 Receptor de cannabinoides de tipo 2 (CB_2R)

El receptor de cannabinoides tipo 2 (CB_2R) pertenece a la familia de GPCRs de clase A. En humanos, está constituido por un total de 360 aminoácidos. La longitud de su extremo C-terminal es algo más corta que el CB_1R, con 59 aminoácidos de extensión. Mediante la

técnica de resonancia magnética nuclear (RMN) se ha determinado con precisión la estructura del receptor CB_2 (Yeliseev, 2019; Yeliseev & Gawrisch, 2017).

Los polimorfismos o variantes genéticas de un determinado gen dentro de una especie son bastante frecuentes en la naturaleza. En el caso del receptor CB_2 existe un polimorfismo en seres humanos de una única base (SNP), este cambio en la secuencia de ADN resulta en una traducción a arginina en la posición 63 de la cadena polipeptídica, en lugar de una glutamina (Q63R). Este polimorfismo tiene relevancia fisiológica, relacionándose con pérdidas en el control de una correcta respuesta inmunitaria, con la aparición de procesos inflamatorios exacerbados (Rossi et al., 2011), una mayor predisposición a la obesidad (Bellini et al., 2015) y una mayor incidencia al alcoholismo (Ishiguro et al., 2007). Sin embargo, se ha descrito que su unión a compuestos cannabinoides es similar en ambas isoformas del CB_2R, aunque con una actividad reducida en el tiempo (Malfitano et al., 2014).

La distribución de CB_2R en el organismo es más limitada que CB_1R. CB_2R se expresa principalmente en células del sistema inmunitario, sistema hematopoyético (amígdala, bazo y timo) y sistema nervioso central (SNC). En SNC presenta bajos niveles de expresión en condiciones fisiológicas, aumentando significativamente en microglía activada. En el resto de tipos celulares del sistema nervioso central prevalece CB_1R (Howlett & Abood, 2017).

A nivel funcional, la activación de CB_2R al unirse a un agonista desencadena una señalización intracelular mediada mayoritariamente por el acoplamiento a la proteína $G\alpha_{i/o}$, dando lugar a la inhibición de la adenilato ciclasa y disminuyendo los niveles intracelulares de AMP cíclico. También promueve la fosforilación de MAP quinasas, así como el reclutamiento de ß-arrestinas I y II (Haspula & Clark, 2020). Esta señalización es muy parecida a la inducida por la activación de CB_1R, aunque no se ha descrito la capacidad del receptor CB_2 de acoplar proteína $G\alpha_s$ ni $G\alpha_q$.

El receptor CB_2 se encuentra implicado en procesos fisiológicos como el dolor, la inflamación, la regulación de la respuesta inmunitaria y distintos procesos metabólicos. Uno de los ejemplos mejor documentados es el papel de CB_2R en la microglía del sistema nervioso central, dónde en presencia de daño cerebral, aumenta su expresión y adquiere un papel clave en la migración de la microglía a zonas lesionadas, promoviendo la liberación de factores antiinflamatorios como las interleucinas 1 y 10 (IL-1 y IL-10), inhibiendo la liberación de factores proinflamatorios (especialmente IL-6) y desencadenando efectos neuroprotectores que promueven la supervivencia celular (Roche & Finn, 2010).

La implicación en tan diversas funciones fisiológicas convierte a CB_2R en una potencial diana terapéutica para una gran variedad de enfermedades en las que el control de la respuesta inmunitaria y la inflamación son especialmente relevantes. Generalmente, las estrategias terapéuticas que se han desarrollado intentan potenciar los efectos beneficiosos de CB_2R con agonistas selectivos, puesto que su activación no está acompañada de efectos psicoactivos (Aso et al., 2013; Parlar et al., 2018). Contrariamente, para CB_1R, se utilizan antagonistas selectivos del receptor.

Las principales investigaciones sobre las aplicaciones terapéuticas de CB_2R se centran en enfermedades del sistema nervioso (An et al., 2020) entre ellas encontramos:

1) La esclerosis múltiple es una enfermedad que se caracteriza por un sistema inmune desregulado que ataca a las vainas de mielina del sistema nervioso. Se han obtenido resultados prometedores utilizando como tratamiento el ß-cariofileno, un fitocannabonide que actúa como agonista específico de CB_2R, consiguiendo evitar el agravamiento de la esclerosis múltiple y mejorar su sintomatología en un modelo animal de la enfermedad (Alberti et al., 2017).

2) La isquemia cerebral es una enfermedad que aparece cuando hay un fallo en el suministro de sangre a alguna zona del cerebro. Se ha observado que en ratones modelo de isquemia el tratamiento con O-1966, agonista específico de CB_2R, reduce las zonas de tejido infartado (Ronca et al., 2015). Esta mejora puede atribuirse a las propiedades antiinflamatorias de CB_2R (Turcotte et al., 2016).

3) Enfermedades neurodegenerativas: En la enfermedad del Alzheimer se ha demostrado la capacidad de JWH-133, entre otros agonistas específicos de CB_2R, de modular la reactividad de la microglía frente a las placas de ß-amiloide, reduciendo los niveles de la citoquina proinflamatoria IL-6, así como mejorando el rendimiento cognitivo de roedores modelo de Alzheimer (Aso & Ferrer, 2016). En cuanto a la enfermedad de Parkinson, se ha determinado en modelos animales que el antagonista específico ß-cariofileno, puede ser potencialmente beneficioso para atenuar la neuroinflamación e inhibir la gliosis gracias al poder antioxidante y antiinflamatorio de la señalización mediada por CB_2R (Javed et al., 2016).

Desarrollar un compuesto cannabinoide específico para CB_2R entraña una gran dificultad debido a la gran similitud entre el centro de unión a ligando de CB_1R y CB_2R. Sin embargo, la obtención de ratones knockout para CB_1R o CB_2R ha producido un significativo avance en las investigaciones centradas en el desentrañar el papel de los receptores cannabinoides en diferentes procesos fisiológicos. Uno de los modelos más utilizados es el ratón *Cnr2*$^{-/-}$ que carece de la expresión de CB_2R (Sun et al., 2014). Este modelo ha sido utilizado en investigaciones contra la isquemia cerebral, donde la zona de necrosis y muerte celular es mucho más extensa en ratones *Cnr2*$^{-/-}$ en comparación con ratones *wt* (Haspula & Clark, 2020).

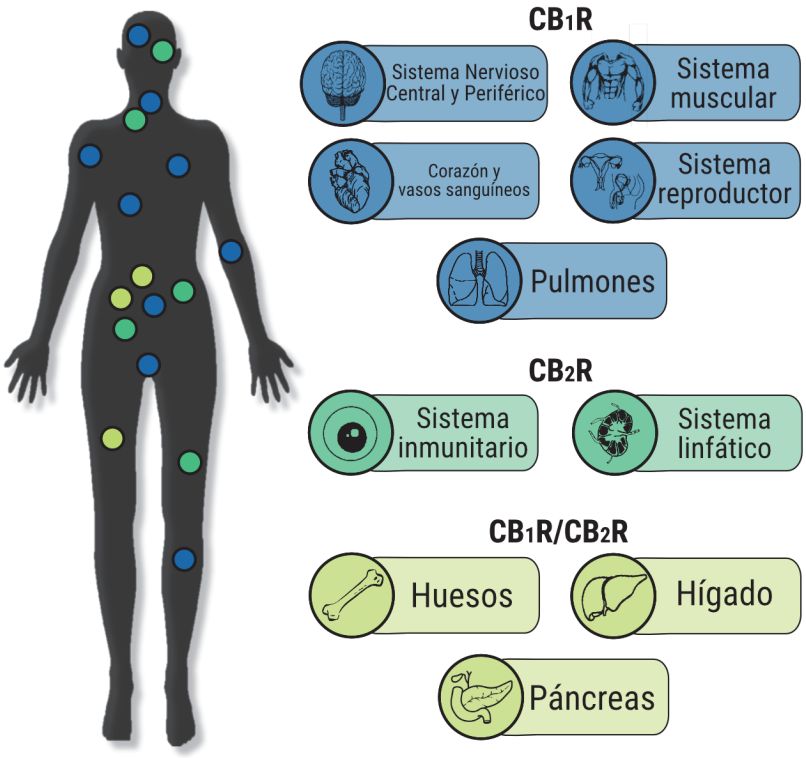

Figura 7: Expresión y distribución de los receptores cannabinoides mayoritarios en el organismo humano.

Recientemente, se ha descrito la capacidad de CB_2R para interaccionar con CB_1R formando complejos heterodiméricos. Este complejo funciona como una nueva unidad funcional, con un cross-talk negativo, donde la activación de un receptor en el heterómero bloquea la señal del otro receptor del complejo y un antagonismo cruzado en el que inactivar la señalización mediada por CB_1R con un antagonista específico también produce la inhibición de la señalización mediada a través de CB_2R y viceversa (Callén et al., 2012). Así, los receptores cannabinoides se bloquean entre si en condiciones fisiológicas.

1.2.3 Receptor GPR55

El receptor huérfano GPR55, pertenece a la familia de receptores acoplados a proteína G, concretamente a la clase A. Se identificó y clonó en 1999 (Sawzdargo et al., 1999) y poco después se le consideró como un posible receptor de cannabinoides tipo 3 (CB_3R) (R. G. Pertwee, 2007). Esta idea, aunque no ha sido completamente descartada, ha ido perdiendo impulso debido a la baja homología con los receptores cannabinoides, 13,5% de ellos con CB_1R y un 14,4% con CB_2R (Elbegdorj et al., 2013) y la falta de estudios *in vivo* que permitan confirmar la afinidad de algunos compuestos endocannabinoides por GPR55. En cambio, se ha identificado de forma clara como GPR55 responde frente a lípidos de la clasificación de los lisofosfatidilinositoles (Alhouayek et al., 2018). Actualmente, la Unión Internacional de Farmacología (IUPHAR) sigue considerando a GPR55 como un receptor huérfano.

GPR55 muestra una expresión importante en diferentes tejidos del organismo humano, entre ellos, sistema nervioso central tanto en neurona como en glía (predominantemente en las zonas del cuerpo estriado) (Sawzdargo et al., 1999), en diferentes tejidos del sistema gastrointestinal (Schicho & Storr, 2012), tejido óseo (tanto osteoblastos como osteoclastos) (Whyte et al., 2009) y también en tejido adiposo blanco (Imbernon et al., 2014).

La activación del receptor GPR55 supone el desencadenado de una cascada de señalización mediada, fundamentalmente, por el acoplamiento a la proteína $G\alpha_{12/13}$, promoviendo la activación de proteínas pequeñas con actividad enzimática GTPasa, incluyendo la proteína 42 de control de la división celular (Cdc42), Rac1 y RhoA y favoreciendo la liberación de calcio del retículo endoplasmático. El calcio actúa como segundo mensajero induciendo la fosforilación de proteínas MAPK y activando diferentes factores de transcripción nuclear entre los que se incluyen CREB, NFAT y NF-$\kappa\beta$. También se ha documentado la capacidad de GPR55 de acoplar la proteína $G\alpha_q$ para desencadenar, de manera alternativa a la proteína $G\alpha_{12/13}$, la liberación de calcio del retículo endoplasmático y la producción de DAG e IP3 (Lauckner et al., 2008). Al igual que otros muchos GPCR, GPR55 también puede reclutar ß-arrestinas (Southern et al., 2013).

También se reportado la capacidad de GPR55 de interaccionar y formar heterómeros funcionales con los receptores canónicos de cannabinoides. Por una parte, se ha descrito la existencia de heterómeros formados por GPR55 y CB_1R. En el heterómero se ha detectado una potenciación de la señalización mediada por CB_1R en presencia del receptor GPR55, centrada en un aumento de la fosforilación de MAPK inducida por la activación de CB_1R (Simcocks et al., 2014). Sin embargo, no se ha identificado un cambio en el patrón de internalización de estos receptores cuando constituyen el heterómero (Julia Kargl et al., 2012). Asimismo, se han descrito heterómeros GPR55-CB_2R, donde aparece un antagonismo cruzado en el que al bloquear CB_2R con un antagonista, los efectos mediados por GPR55 también son bloqueados (Balenga et al., 2014).

El receptor GPR55 se encuentra implicado en procesos fisiológicos como el control del peso, el desarrollo óseo, el control de eventos inflamatorios e incluso la regulación de la transmisión sináptica. Aunque actualmente, las investigaciones sobre el uso de GPR55 como diana terapéutica son menos concluyentes que las referentes a los receptores canónicos de cannabinoides CB_1R y CB_2R, no hay duda de su potencial terapéutico (Reggio & Shore, 2015).

Considerando la controversia entre las publicaciones que investigan la funcionalidad y potencial terapéutico del receptor GPR55, los resultados, aunque prometedores, son todavía poco concluyentes y prematuros. Una posible explicación sobre la controversia en la funcionalidad de GPR55 podría recaer en la existencia de un centro alostérico (Anavi-Goffer et al., 2012).

En este momento, las principales líneas de investigación abiertas con GPR55 como protagonistas consisten en tratar:

1) La obesidad: se ha reportado la implicación de GPR55 en la regulación de la motilidad intestinal y en los procesos que promueven su inflamación. Del mismo modo, se ha observado la capacidad de este receptor para aumentar la liberación de insulina y

regular la homeostasis de la glucosa en sangre. Además, se está investigando la posibilidad de emplear agonistas específicos de GPR55 para combatir la obesidad, debido a su capacidad para suprimir el apetito y, por tanto, la ingesta de alimento en ratones (Tudurí et al., 2017).

2) La osteoporosis: se ha descrito que la activación de GPR55 puede inducir la inhibición de la formación de los osteoclastos, aunque estimula la función de absorción ósea de los osteoclastos preexistentes (Whyte et al., 2009). La implicación de este receptor en la fisiología del hueso sigue sin esclarecerse y requiere de futuras investigaciones (Apostu et al., 2019).

3) Las enfermedades neurodegenerativas: la activación de GPR55 en células del sistema nervioso cursa generalmente con una reducción en la liberación del factor de crecimiento neuronal, así como un incremento de citoquinas proinflamatorias. Sin embargo, sorprendentemente se ha descrito un posible papel neuroprotector a nivel de hipocampo (Hill et al., 2019). Se ha descrito en cultivos primarios de microglía de rata que el uso de un antagonista sintético (KIT-17) para el receptor GPR55 puede producir efectos antiinflamatorios, lo que sugiere que el bloqueo de la señalización mediada por GPR55 podría ser una posible estrategia para el tratamiento de enfermedades neurodegenerativas (Saliba et al., 2018).

4) La terapia anticancerígena: se ha descrito que la activación mediante agonistas específicos de GPR55 contribuye a la proliferación de las masas tumorales (Hu et al., 2011), por ello se está investigando el antagonismo selectivo de este receptor como tratamiento para algunas modalidades de cáncer. Un ejemplo es el antagonista CID16020046 para tratar el cáncer de colon (J. Kargl et al., 2016). En la misma línea de razonamiento, se ha observado que los antagonistas de GPR55 pueden disminuir la tasa de migración en cáncer de páncreas (Singh et al., 2016).

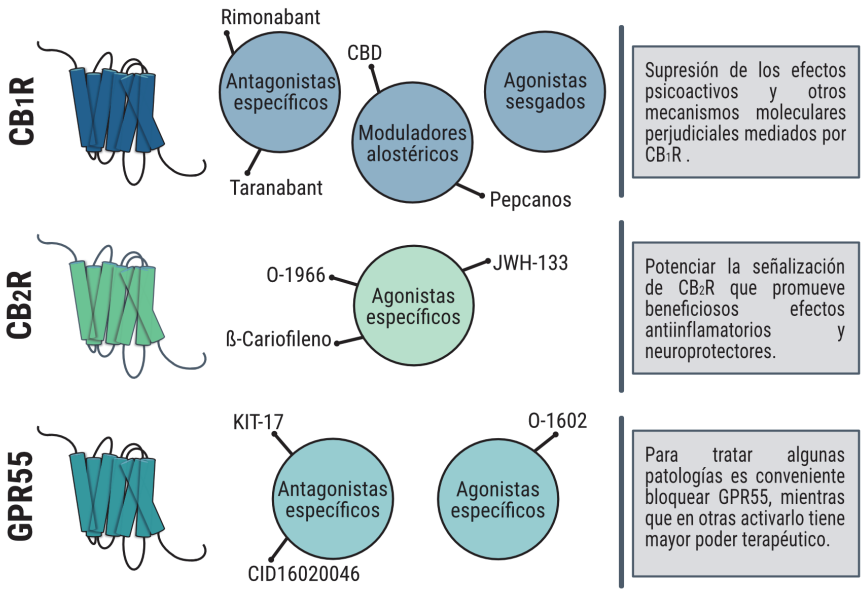

Figura 8: Estrategias terapéuticas principales de los receptores CB_1, CB_2 y GPR55.

1.3 El sistema renina-angiotensina

El descubrimiento del sistema renina-angiotensina (RAS) se remonta al año 1898, donde el fisiólogo Robert Tigerstedt y su equipo inyectaron suero salino extraído de riñón de conejo a conejos vivos y observaron como se producía un aumento paulatino en su presión arterial. Concluyeron que este aumento se produjo por una proteína a la que otorgaron el nombre de "renina" (Tigerstedt & Bergman, 1898). No sería hasta los años 70, con posteriores investigaciones, cuándo se termina de elucidar los principales integrantes del RAS (Wu et al., 2011).

Todos los componentes peptídicos del RAS son derivados de la degradación proteolítica de una glicoproteína que recibe el nombre de angiotensinógeno (Agt). Esta proteína pertenece a la familia de las serpinas, está constituida por 485 aminoácidos en seres humanos, con una región señal de 33 aminoácidos. El angiotensinógeno se sintetiza mayoritariamente en los lóbulos hepáticos, aunque también se genera en el epitelio renal, cerebro, corazón, tejido adrenal, endotelial e intestinal, posteriormente se libera al plasma sanguíneo donde se mantiene estable. La angiotensina I (Ang I) es un decapéptido (Asp-Arg-Val-Tyr-Ile-His-Pro-Phe-His-Leu) que se sintetiza biológicamente inactivo y se genera mediante la proteólisis del extremo N-terminal del angiotensinógeno catalizada por la enzima renina. Cabe destacar que la reacción catalizada por la renina discrimina entre especies. Un claro ejemplo es la renina de ratón que no puede degradar la Agt humana (Wu et al., 2011). En la reacción catalizada por la renina también se genera un fragmento que recibe el nombre de des(Ang I)Agt, que constituye el 98% de la proteína original, cuyo papel fisiológico permanece sin desvelar (H. Lu et al., 2016).

Tradicionalmente, el sistema renina-angiotensina se ha descrito como el encargado de regular la homeostasis en el riñón, sin embargo, también se encuentra distribuido en muchos otros órganos y tejidos del organismo humano donde realiza importantes funciones como la regulación de la presión arterial y mantener el adecuado equilibrio entre vasoconstricción y vasodilatación. Podemos encontrar miembros del RAS en el corazón y los vasos sanguíneos, el sistema nervioso, los órganos reproductores tanto masculinos como femeninos, la piel, los órganos encargados de la digestión (glándulas salivales, estómago, páncreas e intestino), el pulmón, el ojo, el tejido adiposo y el sistema linfático (Paul et al., 2006).

Recientemente se ha documentado la existencia de un RAS "local" en los riñones y en el cerebro, con una señalización autocrina/paracrina. Este sistema local estaría regulado positivamente por las vías de señalización mediadas por el receptor de pro-renina y por la vía Wnt/ß-Catenina (T. Yang & Xu, 2017).

Los componentes del sistema RAS se han clasificado en dos grandes cascadas de señalización: La vía clásica mediada a través de Ang II/ACE y la vía alternativa mediada por Ang (1-7)/ACE2 (Bitker & Burrell, 2019).

El conocimiento sobre los miembros del RAS y de sus interacciones está creciendo exponencialmente, revelando una visión más amplia de su complejidad.

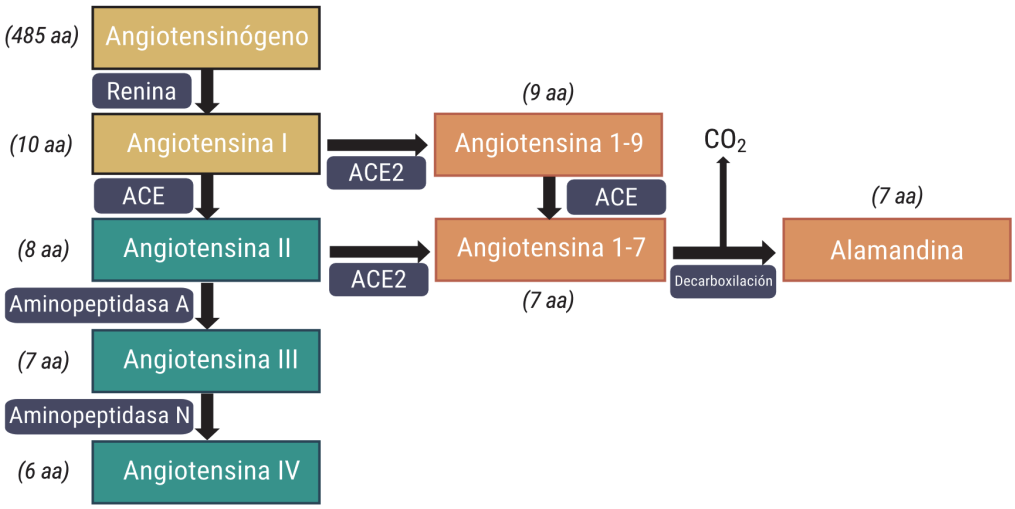

Figura 9: Péptidos del sistema renina-angiotensina clásico (verde), del sistema renina-angiotensina alternativo (naranja) y los precursores comunes a ambos (amarillo).

1.3.1 La vía clásica mediada por Ang II/ACE

La renina es una aspartil-proteasa que cataliza la formación de angiotensina I (Ang I) a partir del angiotensinógeno. Esta enzima se produce en los riñones y su liberación se encuentra altamente regulada, principalmente por cambios en la presión sanguínea (Sparks et al., 2014). La escisión de la Ang I mediante la enzima convertidora de angiotensina (ACE) produce el octapéptido angiotensina II (Ang II) (Harrison & Acharya, 2014). La Ang II es el péptido fundamental del RAS clásico y tiene potentes propiedades vasoconstrictoras (Moeller et al., 1998). Debido al exceso de angiotensinógeno en plasma humano, la producción de angiotensina II se encuentra limitada por la disponibilidad de renina, ya que es la encargada de generar el sustrato (Ang I) a partir del cual se genera Ang II.

ACE es una proteína integral de membrana cuya actividad enzimática dicarboxipeptidasa es dependiente de zinc. En mamíferos existen dos isoformas: la somática, con distribución ubicua en el organismo, que se caracteriza por sus dos dominios homólogos (uno N-terminal y otro C-terminal) cada uno con su propio centro catalítico y la isoforma testicular, con solo un único dominio en la región C-terminal de la proteína. El papel fisiológico principal de esta enzima es el incremento de la presión sanguínea, mediado tanto por la producción de Ang II como por la degradación del péptido bradicinina en fragmentos inactivos y, por tanto, suprimiendo sus propiedades vasodilatadoras (Harrison & Acharya, 2014).

La Ang II plasmática se degrada rápidamente a angiotensina III (Ang III), angiotensina IV (Ang IV) o angiotensina 1-7 (Ang (1-7)). El péptido Ang III es sintetizado por la enzima aminopeptidasa A, o por la escisión de la angiotensina 1-9 (Ang (1–9)) bajo la acción de ACE (Chiu et al., 1976). Al igual que Ang II aunque con efectos menos potentes, Ang III actúa como vasopresor, estimulante de la sed y el apetito, y activador de la secreción de aldosterona. A partir de Ang III, la enzima aminopeptidasa N puede generar el pentapéptido Ang IV. Ang IV se encarga de modular el flujo sanguíneo cerebral y la cognición, aumentar el flujo sanguíneo

renal y disminuir la reabsorción de agua y sodio en el epitelio renal mediante la unión y activación del receptor de angiotensina tipo 4 (AT_4R) (Nehme et al., 2019).

Los péptidos bioactivos del RAS clásico pueden activar diferentes receptores. Entre ellos, los más importantes de la vía clásica del RAS son el receptor de angiotensina tipo 1 (AT_1R) y el receptor de angiotensina tipo 2 (AT_2R).

La señalización producida a través de los componentes del RAS clásico circulante desencadena diversos efectos fisiológicos en el organismo entre los que se incluyen el control de la homeostasis renal (Regulación del flujo sanguíneo, la filtración glomerular, regulación de los niveles de sodio, regulación del pH), la regulación de la presión arterial debido a que por una parte Ang II induce la vasoconstricción mientras que el NO y la bradicinina inducen la vasodilatación, también la estimulación de la sed y el apetito a través de la acción mediada por Ang II en el cerebro y, además controlan la liberación hormonal de aldosterona, catecolaminas y vasopresina entre otras.

Debido a su capacidad para regular la presión arterial, la primera diana terapéutica que despertó el interés de las investigaciones por el RAS fueron los inhibidores de la enzima ACE para el tratamiento de la hipertensión. Estos compuestos evitaban la síntesis de Ang II y, por tanto, la subida de la presión arterial (Fyhrquist & Saijonmaa, 2008). Captopril fue el primero de los inhibidores de ACE efectivos a través de vía oral (Pitt, 1997; Reis et al., 2018). Si se compara la eficiencia de los inhibidores de ACE frente a inhibidores de receptores de angiotensina, se observa una tasa similar en cuanto a su baja mortalidad aunque una tasa de eficiencia ligeramente superior en inhibidores de los receptores de angiotensina (E. C. K. Li et al., 2014).

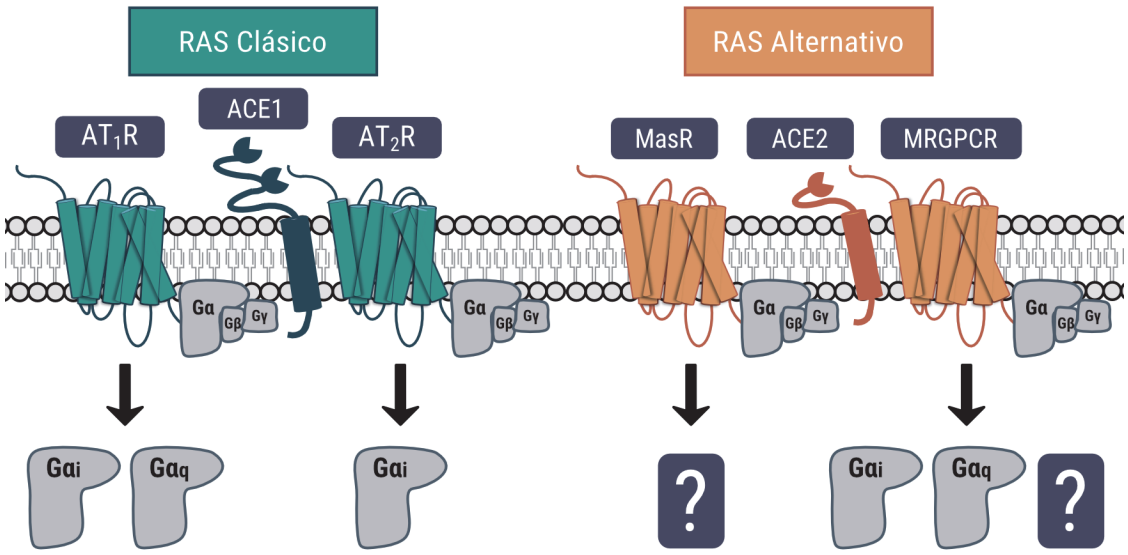

Figura 10: Los receptores y las enzimas convertidoras de angiotensina del sistema renina-angiotensina clásico (verde) y del sistema renina-angiotensina alternativo (naranja).

1.3.1.1 Receptor de angiotensina II de tipo 1

El receptor de angiotensina tipo 1 (AT_1R) se clonó por primera vez en 1991, aislándose de células glomerulares suprarrenales bovinas (Sasaki et al., 1991) y de células de tejido muscular liso (Murphy et al., 1991). Se encuentra clasificado dentro de la familia de GPCR de clase A, manteniendo sus características estructurales canónicas. Este receptor está constituido por 359 aminoácidos en humanos siendo uno de los más conservados entre mamíferos, con una homología de aproximadamente un 95% (Gosselin et al., 2000).

Se ha reportado la posibilidad de AT_1R de adquirir diferentes conformaciones activas estables, donde aparecen cambios estructurales en la orientación de los bucles intracelulares del receptor, donde el bucle intracelular 3 y la cola C-terminal juegan un papel protagonista. Cada una de estas conformaciones activa preferencialmente unas vías de señalización frente a otras (Devost et al., 2017).

La estimulación de AT_1R mediante Ang II, su agonista endógeno, induce el acoplamiento del receptor a proteína $G\alpha_{q/11}$, activando la fosfolipasa C y provocando el movimiento intracelular de iones de calcio. La liberación de calcio intracelular promueve la activación del receptor de crecimiento epidérmico (EGFR) que a su vez desencadenará la fosforilación de ERKs (Higuchi et al., 2007). AT_1R también puede acoplar $G\alpha_i$, inhibiendo la adenilato ciclasa y disminuyendo los niveles de AMPc intracelulares (Kawai et al., 2017). Del mismo modo, AT_1R también es capaz de mediar la activación de varias proteínas G pequeñas; principalmente Rac, Ras y Rho (Ohtsu et al., 2006).

La señalización mediada por AT_1R se traduce en un aumento de la tensión arterial y remodelación vascular. Por otro lado, las GTPasas pequeñas activadas por este receptor promueven procesos de contracción y remodelación vascular, así como la liberación de factores proinflamatorios y especies reactivas de oxígeno (ROS) (Ohtsu et al., 2006).

Es posible encontrar una expresión elevada de AT_1R en tejidos del cerebro (Benicky et al., 2011), corazón (Wackenfors et al., 2004), riñón (Zhuo et al., 1997), tejido adiposo (Boschmann et al., 2006) y glándulas adrenales (Sanchez-Lemus et al., 2008). Al tratarse de un receptor con una distribución tan ubicua en el organismo y con una amplia diversidad de funciones fisiológicas, su desregulación resulta un importante desencadenante de numerosas patologías. Esta es la causa de que AT_1 sea uno de los GPCR más estudiados.

1) Enfermedades cardíacas: la hiperactivación de AT_1R puede llevar a disfunción endotelial, lo que desencadena patologías como la hipertensión, la hipertrofia cardíaca, el infarto de miocardio y la arritmia cardíaca (J. Zhang & Crowley, 2013). Por ello, el uso de antagonistas o agonistas inversos que bloqueen la señalización de este receptor es una de las estrategias terapéuticas más utilizadas para combatir estas patologías (Michel et al., 2016). Actualmente, los bloqueadores de AT_1R (ARBs) son moléculas de bajo peso molecular con una alta especificidad por AT_1R y cuya función es competir con el péptido Ang II por su unión al receptor. Los ARBs más importantes son 8: azilsartan, eprosartan, telmisartan, candesartan, irbesartan, olmesartan, losartan y valsartan. De ellos, los 5 últimos comparten parte de su estructura química por lo que comúnmente se hace referencia a ellos como los ARBs

bifenilo tetrazoles (Takezako et al., 2017). Estos fármacos ya han sido aprobados para su comercialización.

Los ARBs, junto con los bloqueadores del receptor ß-adrenérgico (ß-AR), son los principales fármacos para tratar dolencias cardíacas. Así, el diseño de fármacos para tratar patologías cardíacas que actúen sobre AT_1R, se centra en encontrar un compuesto sesgado que bloqueé únicamente la señalización proteína G-dependiente del receptor debido a que la función mediada por ß-arrestinas promueve la supervivencia celular y, por tanto, es potencialmente beneficiosa (Grisanti et al., 2018).

2) Enfermedades renales: AT_1R es una atractiva diana terapéutica para prevenir e incluso tratar patologías con daño renal, debido a la elevada expresión del receptor en riñón, especialmente en las células tubulares y en los vasos sanguíneos (Gonçalves et al., 2004). Se ha determinado que el tratamiento con el ARB iosartan protege del estrés oxidativo y la inflamación previo a la isquemia renal, impidiendo que este estado degenere en una patología renal crónica (Rodríguez-Romo et al., 2016).

   El principal tratamiento utilizado para tratar la nefropatía diabética consiste en bloquear AT_1R (Ros-Ruiz et al., 2012), esto supone un problema a medio-largo plazo puesto que se produce un aumento de la síntesis de renina como mecanismo compensatorio y en consecuencia de la disponibilidad de Ang II. Para evitarlo, se ha investigado el tratamiento combinado de ARBs y vitamina D (con capacidad para suprimir la producción de renina) que ofrecen una sinergia positiva frente a esta patología (Y. Zhang et al., 2009; Z. Zhang et al., 2008).

   Una de las claves para evitar el rechazo inmunológico en pacientes que requieren de un trasplante de riñón consiste en monitorizar la presencia de anticuerpos dirigidos contra AT_1R, debido a que la interacción entre estos anticuerpos y AT_1R supone un riesgo elevado de rechazo. Se plantea una posible solución a este problema con el uso de ARBs para enmascarar el epítopo de AT_1R, evadiendo el rechazo (Sas-Strózik et al., 2020).

3) Enfermedades neurodegenerativas: Aunque la barrera hematoencefálica impide la entrada o salida de los componentes del RAS sistémico al cerebro, se ha observado que el péptido Ang II local del cerebro mejora los procesos de memoria y aprendizaje a corto plazo a través de AT_1R. En cambio, una hiperactivación del receptor desencadenaría estrés oxidativo y muerte neuronal (Mogi et al., 2012) (Wright et al., 2013).

   Nuevamente, se ha reportado como el bloqueo de AT_1R mediante ARBs produce una disminución de la neuroinflamación, de los niveles de estrés oxidativo y de la muerte neuronal tanto en modelos animales de Alzheimer y demencia como de la enfermedad del Parkinson (Saavedra, 2012a, 2012b).

Aunque AT_1R es activo de manera aislada, también se ha descrito su habilidad de interaccionar y formar complejos funcionales homoméricos (B. M. Young et al., 2017) como heteroméricos con otros miembros del sistema renina-angiotensina, como AT_2R (Ferrão et al., 2017) adquiriendo nuevas propiedades funcionales. No obstante, la señalización de AT_1R es aún más compleja, puesto que interacciona con receptores de otros sistemas fisiológicos, como el heterómero formado por AT_1R y CB_1R, de la familia de los cannabinoides (Rozenfeld et al., 2011) y el heterómero compuesto por AT_1R y $A_{2A}R$, de la familia de los receptores de adenosina (De Oliveira et al., 2017).

1.3.1.2 Receptor de angiotensina II de tipo 2

El receptor de angiotensina de tipo II (AT_2R) humano se clonó por primera vez en la década de los 90, aislado de una librería genómica de placenta. Su traducción a proteína se compone de 363 aminoácidos en humanos (Tsuzuki et al., 1994) y comparte una gran homología con rata y ratón, mayor al 90% (Hoe et al., 2003). Sin embargo, sólo hay una identidad de un 34% entre AT_1R y AT_2R humanos, siendo la secuencia de la región del tercer bucle intracelular, con un papel importante en la afinidad ligando-receptor y en la transducción de señales la secuencia con menor homología (Dittus et al., 1999; Hayashida et al., 1996).

Al igual que AT_1R, AT_2R se clasifica dentro de los GPCR de clase A. Como peculiaridad, mencionar que la octava alfa hélice de AT_2R se encuentra orientada de forma inusual. Originalmente se creyó que AT_2R no pertenecía a la familia de los GPCR, puesto que experimentalmente no se conseguía observar acoplamiento a proteínas G al estimular el receptor con Ang II (Bottari et al., 1991). Recientemente, se ha demostrado que aunque AT_2R puede unir el péptido Ang II, no es capaz de producir el cambio conformacional necesario para que este receptor pueda acoplar proteína G o pueda reclutar ß-arrestinas (Connolly et al., 2019), es por ello que la mayoría de los efectos fisiológicos inducidos por Ang II son mediados a través de AT_1R (Forrester et al., 2018).

La activación de AT_2R desencadena, principalmente, el acoplamiento a proteína $G\alpha_i$, disminuyendo los niveles de AMPc intracelular. Por otro lado, un aumento de los niveles de óxido nítrico (NO), promueve un incremento en la producción del segundo mensajero GMPc, y la activación de fosfatasas, suscitando la desfosforilación de las MAP quinasas (Kaschina & Unger, 2003; Porrello et al., 2009).

La expresión de AT_2R es muy elevada durante el desarrollo fetal y disminuye significativamente en la posnatalidad (Yoon et al., 2016). Su presencia se limita al sistema cardiovascular, las glándulas adrenales y el riñón, el sistema reproductor y las áreas cerebrales implicadas en la coordinación motora y la actividad sensorial (Bitker & Burrell, 2019). En adultos sanos, la expresión de AT_2R suele ser baja, aunque se ha determinado una sobreexpresión en ciertas condiciones patológicas entre las que se incluye el fallo renal, el infarto de miocardio y la isquemia cerebral (Padia & Carey, 2013).

Las principales funciones fisiológicas en las que está implicado AT_2R son la regulación del crecimiento tisular, la organogénesis y la reparación tisular y el desarrollo cerebral. Además, contribuye en la homeostasis de la liberación de catecolaminas (Danyel et al., 2013). Por lo

general, su activación tiene efectos antagónicos y opuestos a las señalización mediada por AT_1R, esto implica, entre otros: vasodilatación, efectos cardioprotectores, reducción del estrés oxidativo e inhibición de la proliferación celular (Henrion et al., 2001).

En la mayoría de las investigaciones se utiliza un agonista peptídico específico de AT_2R, el compuesto CGP-42112, para activar directamente los procesos fisiológicos beneficiosos y antagonizar los efectos indeseados de AT_1R de forma indirecta (Matavelli & Siragy, 2015). El potencial terapéutico de AT_2R, se centra fundamentalmente en afecciones renales, cardíacas y cerebrales:

1) Enfermedades cardíacas: AT_2R se encuentra sobreexpresado en diferentes patologías cardíacas como insuficiencia cardíaca o el infarto de miocardio (Jones et al., 2008). Así, se están investigando terapias combinadas de ARBs y CGP-42112, con el objetivo de potenciar el efecto anti-hipertensivo de los "sartanes", debido a las propiedades vasodilatadoras de AT_2R (Carey, 2017). Otros estudios utilizan el compuesto no-peptídico C21, un agonista altamente selectivo para AT_2R para mejorar la sintomatología de la fibrosis de miocardio debido a un efecto anti-inflamatorio y a una correcta regulación de la producción de colágeno (Y. Wang et al., 2017).

2) Enfermedades renales: AT_2R media la nefrogénesis durante el desarrollo embrionario y la excreción de sodio a través de la orina (natriuresis) (Danyel et al., 2013). Además, en la nefropatía diabética o hipertensiva se produce una sobreexpresión de este receptor con propiedades antiinflamatorias y antioxidantes. Por ello, la activación de AT_2R se traduce en una mejora en la progresión de estas enfermedades renales crónicas (Kaschina et al., 2017).

3) Enfermedades neurodegenerativas: se ha reportado que la expresión de AT_2R en el cerebro, especialmente en la *substantia nigra*, disminuye progresivamente con la edad. Desencadenando en un aumento de la expresión de AT_1R y de sus efectos pro-inflamatorios y pro-oxidativos, ligados a la aparición de enfermedades como el Alzheimer o el Parkinson (Rodriguez-Perez et al., 2020). Se ha descubierto que la expresión de AT_2R en microglía es baja respecto a la de AT_1R y se mantiene en esos niveles incluso en presencia de ang II. Sin embargo, el tratamiento con CGP-42112 produce un incremento significativo de AT_2R (Bhat et al., 2019). Este hecho abre el camino a utilizar AT_2R como diana terapéutica para tratar enfermedades neurodegenerativas y contrarrestar la hiperactivación de AT_1R (Ahmed & Ishrat, 2020).

Actualmente no hay compuestos que actúen como agonistas o antagonistas de AT_2R aprobados clínicamente. Por una parte, CGP-42112 tiene ciertas limitaciones debido a su baja selectividad para AT_2R a altas concentraciones. Además, no es conveniente su administración por vía oral (Whitebread et al., 1991). Así, se están estudiando nuevos compuestos sintéticos que se unan de forma altamente selectiva a AT_2R (Wallinder et al., 2019).

No obstante, gracias a las propiedades antiinflamatorias, cardio y neuroprotectoras mediadas por AT_2R y demostradas en numerosas publicaciones científicas (Juillerat-Jeanneret, 2020), la estimulación de este receptor se presenta como el principal mediador del "brazo protector" del RAS, con un gran potencial terapéutico en un futuro cercano.

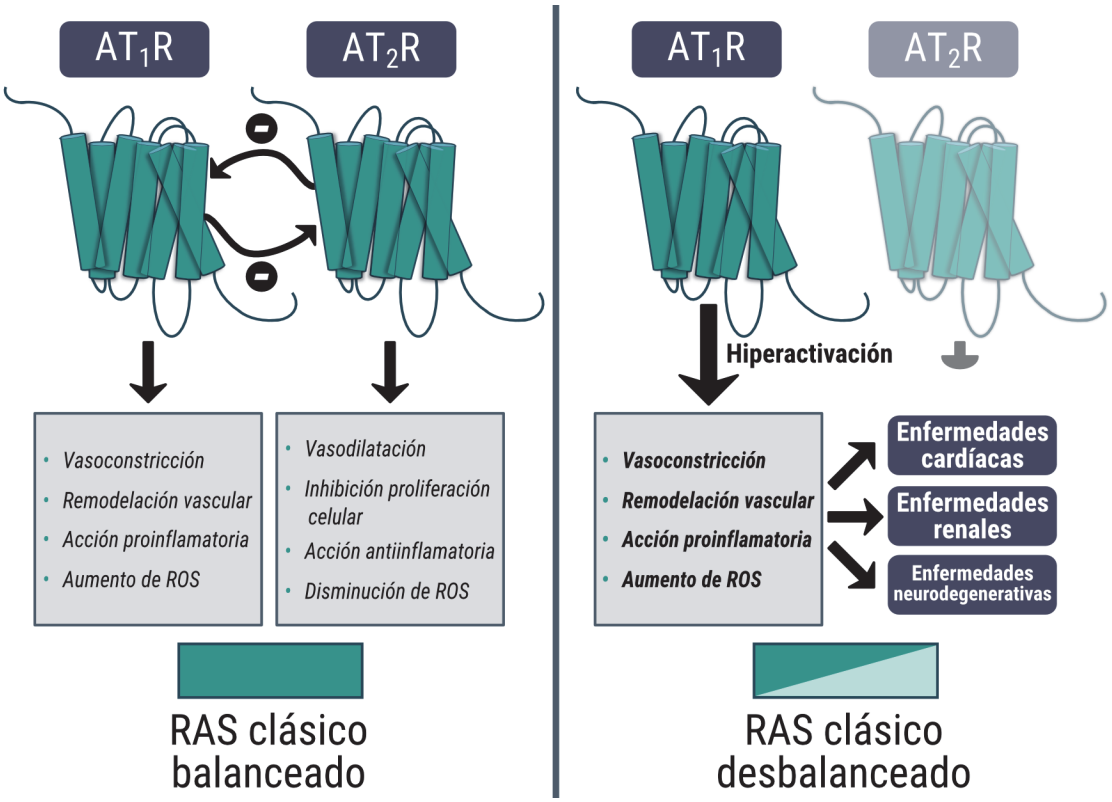

Figura 11: Efectos fisiológicos mediados por los receptores del sistema renina-angiotensina clásico (AT_1R y AT_2R). Balance (izquierda) y desregulación (derecha) entre los efectos mediados por AT_1R y AT_2R.

Se ha reportado como el receptor AT_2R actúa como antagonista natural de la señalización del receptor AT_1R de forma consensuada (AbdAlla, Lother, Abdel-tawab, et al., 2001; Duke et al., 2005; Horiuchi et al., 1999; Nakajima et al., 1995), e incluso con efectos opuestos cuando es activado por un agonista específico, como el compuesto CGP-42112 (Barber et al., 1999; McCarthy et al., 2009). Esta retroalimentación entre ambos receptores se debe, en parte, a su interacción cuando se encuentran, espontáneamente en la célula, formando el heterómero AT_1R/AT_2R (Ferrão et al., 2017).

De manera interesante, se ha descrito la capacidad de AT_2R de agregar entre sí y constituir complejos oligoméricos con la facultad de acoplar proteína $G\alpha_q$ (AbdAlla et al., 2009). También se ha reportado interacciones heterodiméricas entre AT_2R y B_2R (Abadir et al., 2006) y entre AT_2R y MasR (D. Villela et al., 2015) de la vía alternativa del RAS.

1.3.2 La vía alternativa mediada por Ang (1-7)/ACE2

El conocimiento sobre el RAS cambió radicalmente entre el 2000 y el 2010, período en el que se descubrieron y caracterizaron nuevos componentes del sistema RAS que formaban una vía completamente nueva, que se denominó como vía alternativa del RAS (Donoghue et al., 2000; Ferrario, 2011). La vía alternativa del RAS se caracteriza por mediar respuestas fisiológicas opuestas a la vía clásica. Los receptores de la vía alternativa son Mas (MasR) y Mas Related (Mas Related Receptors) y se caracterizan por unir el péptido Ang (1-7) (R. A. S. Santos et al., 2000) y derivados como la alamandina (Lautner et al., 2013).

Ang (1-7) es un heptapéptido con propiedades bioactivas que se encuentra principalmente en cerebro, riñón, corazón y vasos sanguíneos (Chappell et al., 1989). Este péptido puede ser generado en el organismo de distintas formas, entre ellas, la más común es la síntesis mediada por la enzima convertidora de angiotensina 2 (ACE2), una metaloproteasa dependiente de zinc con un único paso transmembrana. ACE2 es capaz de producir Ang (1-7) de forma muy eficiente mediante la degradación de Ang II (Burrell et al., 2004). También puede convertir Ang I en Ang (1-9), aunque esta enzima tiene una afinidad 500 veces inferior por Ang I que por Ang II (Chappell 2012). La Ang (1-7) también puede ser sintetizada mediante endopeptidasas. Una de ellas es la neprilisina (NEP) con capacidad para catalizar la conversión directa de Ang I o Ang (1-9) en Ang (1-7) (Domenig et al. 2016). Otro ejemplo es la prolil-oligopeptidasa (PEP) que media la catálisis directa de Ang I o Ang II en Ang (1-7) (Polgar and Szeltner 2008). Finalmente, también se ha descrito la síntesis de Ang (1-7) mediada por la actividad dicarboxipeptidasa de ACE con el sustrato Ang (1-9) (Kittana, 2018).

Las acciones fisiológicas principales mediadas por Ang (1-7) son la vasodilatación, aumentando la producción de NO, en el sistema cardiovascular (P. Li et al., 1997), el aumento del flujo sanguíneo renal y de la filtración glomerular asociado a mayor excreción de sodio y producción de orina (Handa et al., 1996) y el incremento del flujo sanguíneo cerebral (P. Xu et al., 2011). En conjunto, son efectos órgano-protectores y opuestos a los mediados por el eje ACE/Ang II.

A día de hoy se siguen investigando los componentes del RAS y sus interconexiones. Recientemente, se han descubierto nuevos péptidos bioactivos del RAS derivados de los más conocidos. Entre ellos se encuentra el heptapéptido Alamandina, generado a partir de una descarboxilación del extremo N-terminal de Ang (1-7) por una enzima que desconocida hasta el momento (Lautner et al., 2013). Sus principales efectos en el organismo son la vasodilatación y la antihipertensión. Ambos mediados a través del receptor Mas-Related D (MrgprD) (D. C. Villela et al., 2014).

Menos estudiado se encuentra el péptido Ang (1-9), generado por la acción catalítica de ACE2 sobre el sustrato Ang I. Sus efectos antihipertrófico y cardioprotector parecen ser mediados a través del receptor AT_2R (McKinney et al., 2014; Ocaranza et al., 2010).

El RAS alternativo se está estudiando en la actualidad activamente debido a su relevante implicación en la patofisiología de la enfermedad del Coronavirus 2019 (COVID-19) producida por el coronavirus de tipo 2 del síndrome respiratorio agudo severo (SARS-CoV-2), declarada pandemia mundial en los primeros meses de 2020 (Bedford et al., 2020). La

enzima ACE2 se expresa en las células endoteliales del tracto respiratorio y es la vía de entrada del SARS-CoV-2 a la célula (K. K. Chan et al., 2020). Otro factor a considerar es como el proceso infectivo del SARS-CoV-2 a través de ACE2 induce la internalización celular de la enzima, contribuyendo a la desregulación del RAS al producirse una disminución en la producción de Ang (1-7) y aumentando los niveles disponibles de Ang II (Ingraham et al., 2020).

En conclusión, existe una gran modulación entre el sistema renina-angiotensina convencional y alternativo, de forma que una activación crónica del RAS clásico se encuentra antagonizada por la señalización mediada por el RAS alternativo (Iwai & Horiuchi, 2009). Una disfunción en este balance es responsable del desarrollo de un numeroso abanico de patologías (Paz Ocaranza et al., 2020).

1.3.2.1 Receptor Mas

El gen *mas,* que codifica para el receptor Mas, se clonó por primera vez en la década de los 80, aislado a partir de una línea celular humana de carcinoma epidermoide (NIH3T3) (D. Young et al., 1986). En un inicio, se creyó que actuaba como un proto-oncogen, puesto que algunos estudios le atribuyeron propiedades tumorigénicas, sin embargo, ha sido desmentido años posteriores (Bader et al., 2014). MasR está compuesto por un total de 325 aminoácidos, dispuestos en una estructura clásica de GPCR de clase A (Iwai & Horiuchi, 2009).

MasR muestra una elevada expresión en cerebro (D. Young et al., 1988) y testículos (Alenina et al., 2002) y en niveles más bajos en corazón, riñón, pulmón, hígado, bazo, lengua y músculo esquelético (Alenina et al., 2008).

El ligando endógeno de MasR es el péptido Ang (1-7) (R. A. S. Santos et al., 2005). Al activarse, MasR desencadena un aumento en los niveles de NO (Sampaio et al., 2007) y una inhibición de la fosforilación de MAPK, promoviendo la activación de la vía PI3K/Akt (Muñoz et al., 2010). También se ha descrito como una activación prolongada induce la desensibilización e internalización celular de MasR (Gironacci et al., 2011). Asimismo, los efectos mediados por la acción de Ang (1-7) son bloqueados por la acción del antagonista selectivo sintético de MasR, la D-Alanina-Ang (1-7) (A-779) (Ambühl et al., 1994).

Existe cierta controversia alrededor de MasR, puesto que, a pesar de ser un GPCR, no se ha conseguido identificar su acoplamiento directo a proteína G al ser activado mediante Ang (1-7) (Shemesh et al., 2008). Sin embargo, si se ha descrito la capacidad de MasR para modular la actividad de otros receptores con los que interacciona, un ejemplo reportado es la potenciación de la señalización de AT_1R a través de $G\alpha_q$ cuando está formando el heterómero AT_1R/MasR (Canals et al., 2006). Actualmente, se requiere de una mejor caracterización de MasR, debido a que las evidencias publicadas hasta la fecha únicamente explican su señalización a través de mecanismos proteína G-independientes (Tirupula et al., 2014).

La activación de MasR induce principalmente efectos cardioprotectores en el organismo, pero también un papel neuroprotector en el SNC (Liao & Wu, 2020).

En la patología de Alzheimer, se ha evaluado la señalización de Ang (1-7)/MasR mediante aceturato de diminazeno (DIZE), capaz de potenciar la actividad enzimática de ACE2, reduciendo la actividad de AT_1R y potenciando la señalización de MasR. Los resultados han demostrado mejoras en la memoria y el aprendizaje gracias a una menor inflamación y una menor apoptosis neuronal (Kamel et al., 2018). Abriendo la puerta a utilizar MasR como diana terapéutica en la fisiopatología de Alzheimer.

También se ha reportado, en un modelo animal de la enfermedad de Parkinson, la acción neuroprotectora de MasR, que al ser activado, activa la vía PI3K/Akt estimulando la producción de tiroxina hidroxilasa y aumentando la disponibilidad de dopamina. Reduciendo así, la sintomatología en PD (Rabie et al., 2018).

1.3.2.2 Receptores Mas Related

La familia de receptores Mas Related (Mrgprs) está compuesta por más de 50 GPCRs de clase A que se encuentran relacionados con MasR guardando similitudes a nivel estructural. Los primeros en descubrirse fueron los receptores Mas-Related A (MrgA) y D (MrgD), que se describieron por primera vez en 2001 como receptores específicamente localizados en neuronas sensoriales, concretamente en aquellas de pequeño diámetro de los ganglios de la raíz dorsal y en los ganglios del trigémino (Q. Liu et al., 2001). En seres humanos, los receptores Mas Related se encuentran codificados en el cromosoma 11 (Dong et al., 2001). Posteriormente, se ha reportado la localización de los Mrgprs, con una baja expresión, en células de tejido adiposo blanco y pardo, arterias, cerebelo, cerebro, corazón, médula espinal, músculo esquelético, tracto gastrointestinal, globo ocular, peritoneo, próstata, pulmón, testículo, timo, tráquea, vejiga, vesícula seminal y útero (L. Zhang et al., 2005).

Esta familia de receptores tiene una clasificación compleja cuya última nomenclatura aprobada en (http://www.guidetopharmacology.org) los divide en: Mrgprs de clase A, B, C, D, E, F, G, H y X, siendo esta última exclusivo de organismos del orden de los primates (Burstein et al., 2006).

A pesar de la similitud estructural que los Mrgprs comparten con MasR, no se ha podido establecer un papel relevante de la mayoría de los integrantes de dicha familia en el sistema del RAS. Los Mrgprs son activados por una amplia variedad de ligandos endógenos que no forman parte del RAS (Steele & Han, 2020). Una excepción es MrgD, cuyo ligando endógeno es la Alamandina, componente del RAS alternativo (Etelvino et al., 2014). Además, también une Ang (1-7) (Tetzner et al., 2016).

La mayoría de Mrgprs señalizan a través de la proteína $G\alpha_q$, que desencadena la movilización de calcio del retículo endoplasmático y la activación de la proteína quinasa C (PKC) (Steele & Han, 2020). Aunque se han reportado casos de Mrgprs que acoplan a la proteína $G\alpha_i$ (D. Wang et al., 2013). Además, el receptor MrgprD, puede acoplar proteína $G\alpha_s$, promoviendo

un aumento en la disponibilidad celular de AMPc y la activación de la PKA (Bader et al., 2014; Shinohara et al., 2004).

Debido a su elevada expresión en neuronas sensoriales, las principales investigaciones de los Mrgprs se centran en la búsqueda de aplicaciones terapéuticas para tratar las sensaciones de dolor y picor crónicas (Meixiong & Dong, 2017). Se ha descubierto que los receptores MRGPRX1 y MRGPRX2 tienen un papel principal en la sensación de dolor, mientras MrgA en la sensación de picor, especialmente el MrgA3 (Green, 2021).

A pesar de su gran potencial terapéutico, es evidente que hay un gran desconocimiento y falta de caracterización de estos receptores en la actualidad por lo que se requiere un mayor número de estudios para poder comprender en su totalidad el funcionamiento y regulación de los Mrgprs.

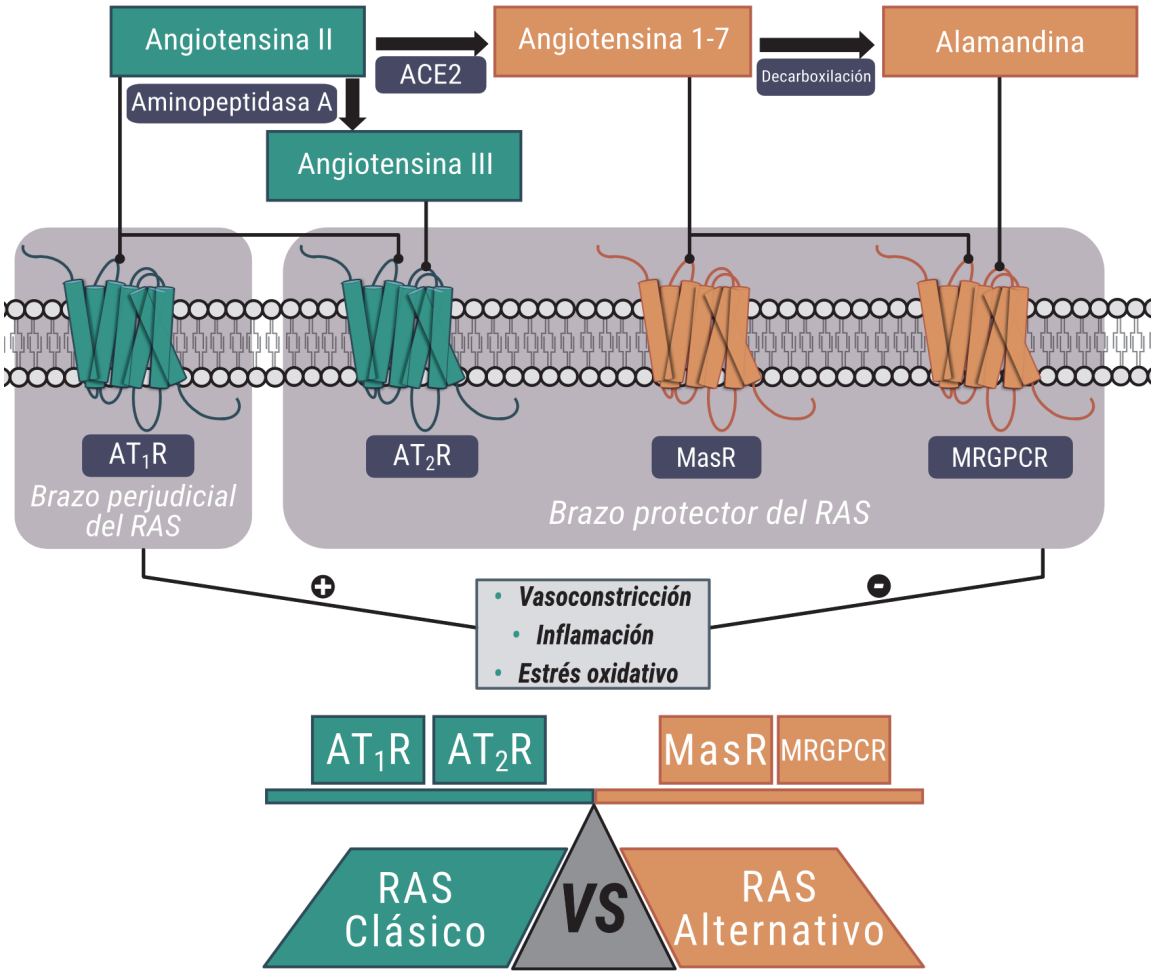

Figura 12: Balance entre el brazo perjudicial (AT_1R) y el brazo protector del RAS (AT_2R, MasR y MRGPCR). Equilibrio entre componentes del RAS clásico (verde) y componentes del RAS alternativo (naranja).

1.4 La familia de receptores de adenosina

Las purinas son los mensajeros químicos más extendidos y conservados a lo largo del tiempo en organismos del reino animal como del reino vegetal; siendo las más importantes la adenosina y el ATP (Schmidt, Lara, and Souza 2007; Zrenner et al. 2006).

La adenosina es un nucleósido de purina. Su papel fisiológico principal se describió en 1929 y consiste en la habilidad de modular el ritmo cardíaco (Drury and Szent-Györgyi 1929).

Se han descrito diferentes mecanismos que regulan la concentración de adenosina en el exterior como en el interior de la célula. A nivel extracelular, el principal mecanismo se basa en la actividad catalítica de la ectonucleotidasa CD39, que degrada el adenosín trifosfato (ATP) a adenosín difosfato (ADP) que a su vez es convertido en adenosina por la acción de la ectonucleotidasa CD73 (Ghiringhelli et al. 2012). Por otro lado, la adenosina no es permeable a la membrana plasmática, necesitando transportadores específicos. Los transportadores de adenosina pertenecen a la familia de transportadores de solutos (SLC) que se clasifican en transportadores de nucleósidos equilibradores (ENTs) y transportadores de nucleósidos concentrativos (CNTs). Mientras que los CNTs utilizan un gradiente de sodio para "concentrar" unidireccionalmente la adenosina en el interior celular, los ENTs tienen la capacidad de importar y exportar adenosina al exterior celular de manera bidireccional con concentraciones elevadas del nucleósido (Pastor-Anglada and Pérez-Torras 2018). También hay que tener en cuenta las enzimas que controlan la homeostasis de la adenosina en el interior celular, siendo las principales la adenosina quinasa, que sintetiza AMPc a partir de adenosina y la adenosina desaminasa que forma inosina mediante la desaminación de la adenosina (Boison 2013).

La ruta principal en la síntesis de adenosina es la generada por la hidrólisis del ATP mediante ectonucleotidasas en el espacio extracelular. Así, este nucleósido se expresa de manera ubicua en todos los fluidos corporales (Ghiringhelli et al. 2012). Esta amplia disponibilidad permite que pueda regular una gran variedad de funciones fisiológicas, jugando un papel especialmente relevante en la respuesta inmunológica a agentes patógenos (Haskó and Cronstein 2004), en la señalización neuronal (Snyder 1985), en la vasodilatación (Morgan et al. 1991) y en la atenuación de procesos inflamatorios (Haskó, Antonioli, and Cronstein 2018).

En condiciones fisiopatológicas de hipoxia y daño celular se ha descrito que la adenosina sufre una desregulación en su homeostasis, acumulándose en el espacio extracelular, fenómeno que se traduce en una hiperactivación de los receptores de adenosina (Grenz, Homann, and Eltzschig 2011).

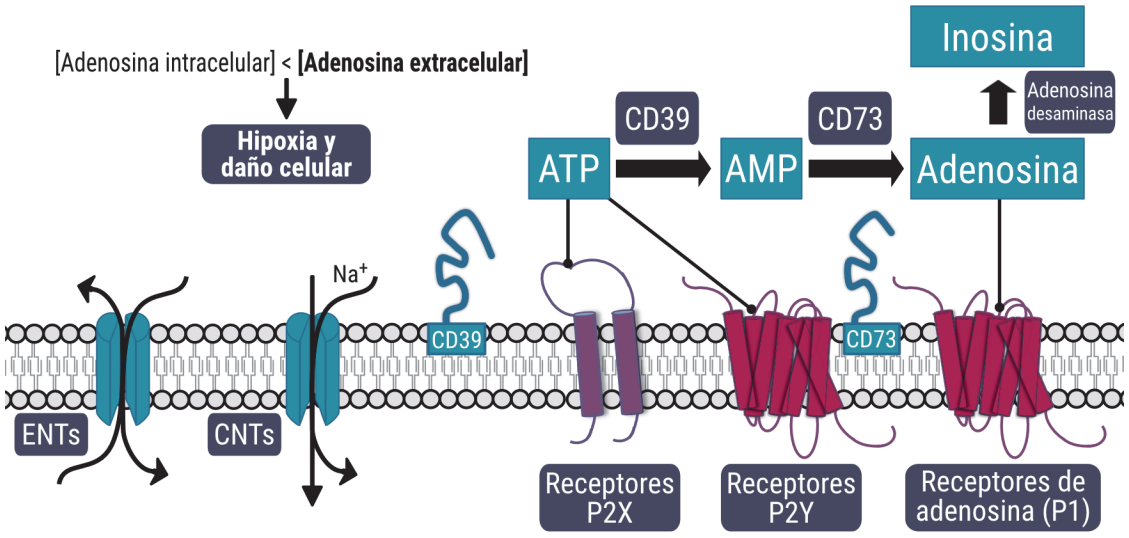

Figura 13: Metabolismo general de la adenosina. Transportadores ENTs y CNTs. Ectonucleotidasas y receptores de purinas (P1, P2X y P2Y).

Los receptores que unen purinas en el ser humano se agrupan en los GPCRs selectivos para adenosina, los receptores P1 y los receptores P2, dentro de los cuales encontramos los receptores P2X que son canales iónicos dependientes de unión a ligando y los GPCRs P2Y (Burnstock 2007). Los receptores P1 son los principales efectores que, al unir su ligando endógeno, adenosina, inducen la transducción de señal al interior de la célula, mediando un conjunto de funciones fisiológicas. Los receptores de adenosina se dividen en los receptores de alta afinidad, grupo compuesto por los receptores A_1 (70 nM) y A_{2A} (150 nM) y los receptores de baja afinidad que incluyen el A_{2B} y A_3. En concreto, A_{2B} tiene una baja afinidad por el nucleósido y requiere de concentraciones superiores a 10 µM para su unión, solamente encontradas en el organismo en condiciones de hipoxia o daño tisular. Esta afinidad diferencial es muy relevante, ya que también existe una concentración heterogénea de adenosina en el cerebro (entre 30 nM y 980 nM, según la zona) (Fried, Elliott, and Oshinsky 2017). Estos cuatro receptores comparten una elevada homología en su secuencia de aminoácidos de hasta un 60% en seres humanos (Palmer and Stiles 1995).

Los ARs se descubrieron en la década de los 80', aunque no se consiguieron clonar por primera vez hasta la década de los 90', debido a diversos problemas encontrados en su purificación que dificultaron obtener una secuenciación fiable (Alexander et al. 1996; Meng et al. 1994; Xie et al. 1994; Zhou et al. 1992). Todos ellos son GPCRs de clase A. A nivel estructural, se ha descrito que los 3 dominios extracelulares y los dominios TM3 y TM7 muy conservados en los cuatro ARs, son claves para la unión a ligando. (Fredholm et al. 2000).

La señalización canónica de los receptores A_1R y A_3R muestra su capacidad de acoplar proteína $G\alpha_i$, produciendo una disminución de los niveles de AMPc intracelulares al inhibir la actividad de la adenilato ciclasa (Linden 1994; Wise et al. 1999). Por otra parte, tanto A_{2A} como A_{2B} se reportan como receptores capaces de acoplar proteína $G\alpha_s$, aumentando la producción de AMPc intracelular al estimular la actividad de la adenilato ciclasa (Jacobson 2009). También se ha reportado la capacidad de $A_{2B}R$ y A_3R de señalizar mediante el

acoplamiento a proteína $G\alpha_q$, activando la proteína fosfolipasa C y favoreciendo la liberación de calcio intracelular (Kanno et al. 2012; Vecchio, White, and May 2019).

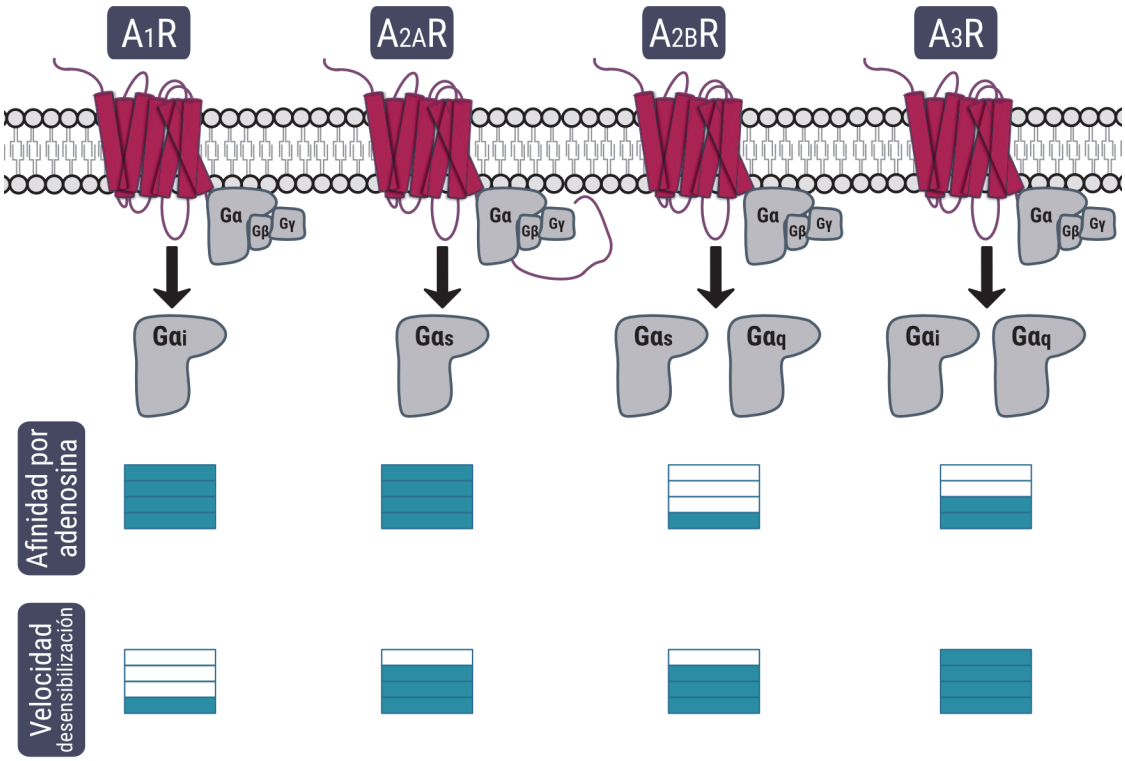

Figura 14: Receptores de adenosina: señalización, afinidad por adenosina y velocidad de desensibilización.

Se ha descrito que todos los ARs sufren un proceso de desensibilización tras períodos de activación prolongados. Este proceso es mediado, en la mayoría de los receptores, por la fosforilación a través de GRKs del extremo C-terminal del receptor; induciendo el reclutamiento de ß-arrestinas y la posterior internalización. Para A_1R, este proceso de internalización ocurre de manera lenta, para los receptores A_{2A} y A_{2B} es un proceso algo más eficiente, con una duración media inferior a la hora y, finalmente, el A_3R tiene la desensibilización más rápida, ocurriendo a los pocos minutos de su activación (Mundell and Kelly 2011).

La distribución de los ARs en el organismo es ubicua, se encuentran presentes en todos los órganos y tejidos del cuerpo humano, siendo una diana terapéutica interesante para el desarrollo de nuevos fármacos para el tratamiento de diversas patologías. Sin embargo, esta amplia distribución es un escollo por superar, ya que dificulta el descubrimiento de fármacos específicos que actúen únicamente sobre los órganos afectados por una patología concreta y no se produzcan efectos secundarios debido a su unión a ARs presentes en otras zonas del organismo. Como posible solución se está estudiando el uso de moduladores alostéricos positivos en lugar de aplicar un agonista que se dirija al sitio ortostérico, aprovechando el aumento natural en la concentración de adenosina en condiciones patológicas, y

potenciando la señalización de los ARs únicamente en las zonas afectadas (Miao et al. 2018; Vincenzi et al. 2016).

Los ARs juegan un papel principal en afecciones relacionadas con el cerebro y el sistema nervioso y las patologías cardíacas (Jacobson and Gao 2006). Por ello, la mayoría de las investigaciones se centran en aplicar el potencial de los ARs en enfermedades neurodegenerativas, en la sensación de dolor y en enfermedades cardíacas. A nivel de SNC, la adenosina ejerce una función neuromoduladora y reguladora de la homeostasis, pero también participa en los procesos de memoria y aprendizaje. Estos efectos son mediados esencialmente por A_1R y $A_{2A}R$ (Gomes et al. 2011). Las investigaciones que focalizan sus esfuerzos en los ARs como diana terapéutica se posicionan en como la activación de A_1R mediante agonistas específicos (Kong et al. 2020; Martire et al. 2019) o bien el bloqueo de $A_{2A}R$ mediante antagonistas (Franco and Navarro 2018) suponen una mejora en afecciones que cursan con un proceso de neurodegeneración, entre las que se incluyen la Enfermedad del Parkinson, la Enfermedad del Alzheimer y la demencia. El primer antagonista de $A_{2A}R$ aprobado en terapia, es el compuesto "istradefylline". Su uso se ha descrito beneficioso para potenciar la señalización dopaminérgica en la enfermedad de Parkinson (Casetta et al. 2014; Fredholm and Svenningsson 2020). En otros estudios se analiza la mejoría en la fisiopatología de enfermedades neurodegenerativas cuando se realiza un tratamiento con antagonistas de $A_{2A}R$, no selectivos de la familia de las xantinas al igual que la cafeína (Garcez et al. 2019) o selectivos (Jacobson, Gao, et al. 2020), obteniendo un efecto neuroprotector.

Por otro lado, se ha descrito ampliamente el papel de la cafeína, antagonista no selectivo de los ARs, para mitigar el dolor en migrañas y dolores de cabeza (Costenla, Cunha, and De Mendonça 2010; Lipton et al. 2017). El uso directo de adenosina para el tratamiento del dolor se ha probado, sin embargo, efectos secundarios entre los que se incluyen la vasodilatación o la activación de los P2Rs que median funciones proinflamatorias ha propiciado que se descarten como terapia (Habib et al. 2008; Jacobson, Giancotti, et al. 2020). En su lugar, se está investigado la posibilidad de utilizar agonistas parciales o moduladores alostérico positivos específicos para A_1R o A_3R, potenciando sus efectos antinociceptivos (Jacobson, Giancotti, et al. 2020; Zylka 2011).

En último lugar, a nivel de sistema cardiovascular, se ha observado, por una parte, que los receptores A_1 y A_3 contribuyen a la reducción del ritmo cardíaco mientras que el $A_{2A}R$ se encarga de incrementar las pulsaciones al ser activado. Además, todos los ARs juegan un papel determinante en la regulación de la angiogénesis y la vasculogénesis (Guieu et al. 2020). Así, los ARs resultan una diana farmacológica interesante para el tratamiento de ciertas patologías cardíacas como pueden ser la arritmia y la isquemia. En concreto, se ha descrito que la activación específica del A_1R muestra un efecto cardioprotector y antiinflamatorio (Headrick et al. 2013). Del mismo modo, también hay experimentos en los que se observa la efectividad de terapias cardioprotectoras que utilizan compuestos agonistas específicos que promueven la activación de A_1R y A_3R y esto a su vez un aumento de señalización de la vía PI3K/Akt y de ERKs1/2 con efectos anti-inflamatorios (Singh et al. 2018).

En conclusión, en la actualidad hay un número creciente de investigaciones que, a través del estudio de los ARs, pretenden mejorar la calidad de vida de millones de personas combatiendo las enfermedades neurodegenerativas, las enfermedades cardiovasculares y la sensación de dolor.

Al igual que ocurre con muchos otros GPCRs, los ARs también tienen la capacidad de interaccionar con otros receptores, formando complejos heteroméricos funcionales. En primer lugar, se describió la existencia de heterómeros entre miembros de los receptores de adenosina, como la interacción entre A_1 y $A_{2A}R$ (Sergi Ferre et al. 2008) o la homodimerización de $A_{2A}R$ (Canals et al. 2004). Y más adelante, se comprobó que los receptores de adenosina también pueden formar complejos heteroméricos interaccionando con los receptores P2Y (Jacobson et al. 2012; Yoshioka, Saitoh, and Nakata 2001), los receptores de dopamina (Ferré et al. 2004; Franco et al. 2007), los receptores de cannabinoides (Carriba et al. 2007) o los receptores de histamina (Márquez-Gómez et al. 2018). Cuando los receptores de adenosina se encuentran formando complejos con otros receptores, pueden cambiar sus propiedades a nivel de señalización. Un ejemplo es la modulación alostérica negativa que ejerce la activación de $A_{2A}R$ sobre D_2R, cuando se disponen constituyendo el oligómero $A_{2A}R$-D_2R (Borroto-Escuela et al. 2018).

1.4.1 Receptor de adenosina A_{2A}

En el ser humano, el receptor de adenosina A_{2A} se encuentra codificado en el cromosoma 22. Consta de una estructura con un total de 412 aminoácidos (Moreau and Huber 1999) y comparte una homología entre humano y ratón del 83% y entre rata y ratón del 95% (Fredholm, Cunha, and Svenningsson 2005).

Pertenece a la familia de GPCRs de clase A, al igual que el resto de los ARs, manteniendo características estructurales comunes como los 7 dominios α-hélice transmembrana. Pero se diferencia de ellos por una característica cola C-terminal inusualmente larga (Merighi, Gessi, and Borea 2018). La estructura del $A_{2A}R$ se ha descrito extensamente en estado inactivo, unido a ligando e incluso con el receptor acoplado a la proteína G heterotrimérica, mediante el uso de la técnica de cristalografía por difracción de rayos X (F. Xu et al. 2011) como, más recientemente, el uso de crio-microscopía (García-Nafría et al. 2018; Kang et al. 2018).

Se ha descrito que $A_{2A}R$ es capaz de interaccionar consigo mismo formando homómeros $A_{2A}R$-$A_{2A}R$ (Canals et al. 2004) y también con los otros miembros de la familia de los ARs constituyendo heterómeros A_1R-$A_{2A}R$ (Sergi Ferre et al. 2008; Lanznaster et al. 2019), $A_{2A}R$-$A_{2B}R$ (Hinz et al. 2018) y $A_{2A}R$-A_3R (Lillo et al. 2020). Del mismo modo, se ha documentado la habilidad de $A_{2A}R$ para establecer interacciones y modular la actividad de receptores de otras familias, la más importante descrita hasta el momento es el heterómero $A_{2A}R$-D_2R, donde existe un antagonismo cruzado entre ambos receptores (S. Ferre et al. 2008). También se ha descrito la capacidad de $A_{2A}R$ para interaccionar formando agregados funcionales de mayor orden como pueden ser heterotetrámeros A_1R-$A_{2A}R$ (Ferré et al. 2016; Ferré and Ciruela 2019).

La activación de $A_{2A}R$ mediada por la unión al sitio ortostérico de adenosina o agonistas específicos, estabiliza una conformación activa del receptor capaz de transmitir señales al interior de la célula (Carpenter and Lebon 2017). La señalización de $A_{2A}R$ se caracteriza, principalmente, por el acoplamiento a proteína $G\alpha_s$, activando la adenilato ciclasa, lo que se traduce en un aumento de los niveles de AMPc intracelulares (Fredholm et al. 2007) que activan la proteína kinasa A. De manera proteína G independiente, se produce una activación de la vía de las MAPK, favoreciendo la fosforilación de ERK1/2 (Oliveros et al. 2017). También se debe considerar la modulación alostérica de $A_{2A}R$, con capacidad de afectar significativamente a su señalización. Recientemente se está abordando el estudio de los posibles centros alostéricos de $A_{2A}R$ mediante espectroscopia de resonancia magnética nuclear (Eddy et al. 2018).

A través de su señalización, el $A_{2A}R$ se encarga de mediar diferentes procesos fisiológicos entre los que encontramos la vasodilatación (Shryock et al. 1998) y la regulación de los procesos inflamatorios (Awad et al. 2006) y a nivel de SNC, la regulación de la liberación de importantes neurotransmisores como el glutamato y la dopamina (Shen and Chen 2009).

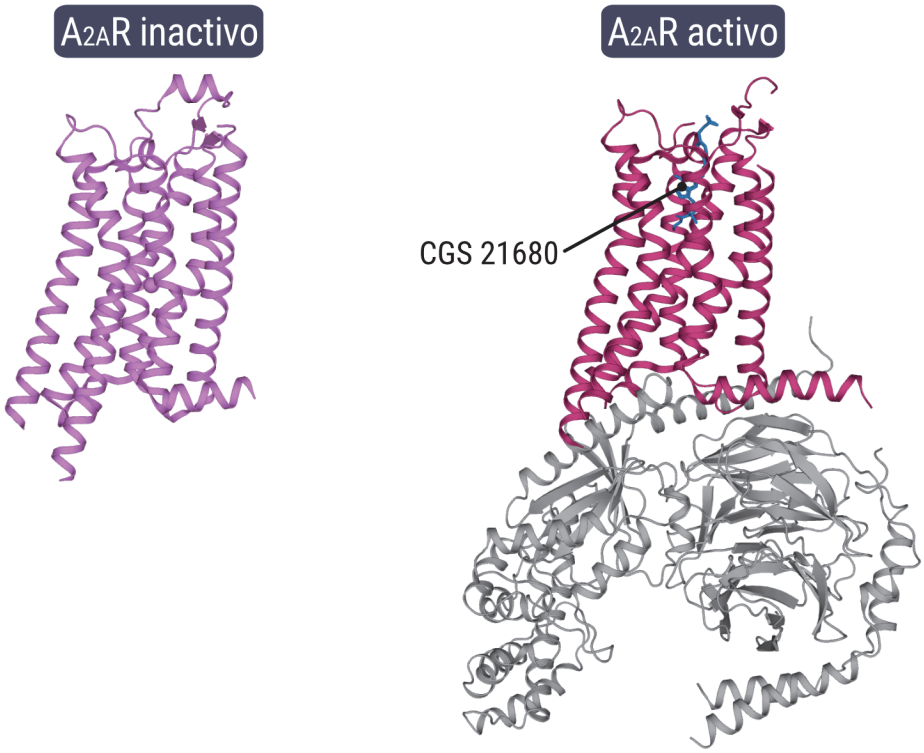

Figura 15: Estructura cristalizada en el estado inactivo del $A_{2A}R$ (rosa) y estructura cristalizada del $A_{2A}R$ en el estado activado (granate) por su agonista específico CGS 21680 (azul).

El receptor A_{2A} se encuentra altamente expresado en el cerebro, especialmente en el cuerpo estriado, en el bazo, el timo y las células del sistema inmune como los leucocitos. También se expresa, aunque en menor nivel, en otras regiones del cuerpo humano como el corazón, los vasos sanguíneos, o los pulmones (Peterfreund et al. 1996). La presencia de $A_{2A}R$ en

estos tejidos lo convierten en una diana terapéutica excepcional para mejorar la calidad de vida de pacientes con enfermedades neurodegenerativas, enfermedades cardíacas y trastornos del sistema inmunológico (de Lera Ruiz, Lim, and Zheng 2014).

Las aproximaciones terapéuticas que centradas en $A_{2A}R$ siguen dos estrategias: por un lado, encontramos aplicaciones terapéuticas que utilizan agonistas. El uso de adenosina se ha descartado en numerosas ocasiones debido su inespecificidad con el resto de miembros de ARs (Merighi et al. 2018). Por ello, se han estudiado compuestos que actúan de manera selectiva para $A_{2A}R$ (Lebon et al. 2015). Actualmente, estos compuestos se utilizan para tomar imágenes de perfusión miocárdica gracias a sus propiedades vasodilatadoras y, a dosis más bajas, para inhibir procesos inflamatorios en situaciones de asma y dolor neuropático (Al-Attraqchi et al. 2019).

Por otro lado, encontramos aplicaciones terapéuticas que utilizan antagonistas de $A_{2A}R$. En este sentido estos compuestos han demostrado ser seguros ejerciendo un papel neuroprotector en enfermedades neurodegenerativas como el Parkinson y el Alzheimer. Así, el uso de antagonistas específicos contra el $A_{2A}R$, altamente expresado en la sustancia nigra, potencia de manera indirecta la funcionalidad de D_2R mejorando la sintomatología de la patología del Parkinson, (Bara-Jimenez et al. 2003; Zheng, Zhang, and Zhen 2018), de hecho se está investigando el uso de compuestos bitópicos que actúan simultáneamente como antagonistas de $A_{2A}R$ y agonistas de D_2R (Shao et al. 2018).

También se ha observado experimentalmente que el tratamiento con cafeína, antagonista no selectivo de los ARs, o con antagonistas específicos para el $A_{2A}R$, protege de la toxicidad mediada por la agregación de la proteína ß-amiloide (Domenici et al. 2019), generando un efecto protector frente al deterioro cognitivo y de la memoria causado por la enfermedad de Alzheimer.

En conclusión, $A_{2A}R$ tiene un gran atractivo terapéutico. En los últimos 20 años se han conseguido sintetizar agonistas y antagonistas con una gran afinidad y especificidad por el receptor (Floris et al. 2012). En la actualidad se siguen investigando las interacciones de $A_{2A}R$ con otros receptores. Datos fundamentales para poder comprender, en mayor profundidad, la farmacología del receptor y poder desarrollar e implementar estrategias terapéuticas dirigidas.

1.5 Enfermedades neurodegenerativas

Hoy en día, existe un claro aumento de la esperanza de vida del ser humano, que se ha ampliado desde una media aproximada de 74,3 años para hombres y 80,9 años para mujeres en el año 2002, hasta 78,2 años en hombres y 83,7 años en mujeres en Europa en 2018, según datos publicados por la Oficina Europea de Estadística (Eurostat, 2020). Por desgracia, se está observando una separación cada vez mayor entre el aumento de la esperanza de vida y una buena calidad en la misma, en parte debido a que el envejecimiento poblacional se ha relacionado de forma indudable con una prevalencia cada vez mayor de enfermedades neurodegenerativas (Liotta et al. 2018). El envejecimiento se caracteriza por una progresiva pérdida en la regulación proteica y por el acortamiento de los telómeros, provocando la

inestabilidad genómica. Consecuentemente la edad avanzada constituye el factor de riesgo más importante en el desarrollo de las patologías neurodegenerativas (Hou et al. 2019).

No hay duda del gran impacto económico y social que tienen, en la actualidad, las enfermedades neurodegenerativas. Así, el descubrimiento de nuevos tratamientos que mejoren la calidad de vida de las personas que las padecen constituye uno de los retos más importantes de nuestra sociedad (Zahra et al. 2020).

Las enfermedades neurodegenerativas se desarrollan con una serie de procesos moleculares comunes que se desregulan de forma progresiva y acaban en muerte neuronal. Entre estos procesos se incluyen la desregulación del sistema del proteasoma, la agregación proteica, el aumento del estrés oxidativo, la neuroinflamación y, finalmente, muerte celular (Dugger and Dickson 2017; Forman, Trojanowski, and Lee 2004).

La pérdida de la regulación proteica o proteostasis, es un rasgo común en la mayoría de las enfermedades neurodegenerativas (Limanaqi et al. 2020). En un porcentaje minoritario de casos, se puede encontrar favorecida por herencia genética (Chiti et al. 2002). La proteostasis se encuentra regulada en la célula por el sistema de ubiquitinación-proteasoma y por la autofagia mediada por chaperonas (Kaushik and Cuervo 2015). Estos mecanismos moleculares se encargan de marcar y destruir las proteínas dañadas, mal plegadas o simplemente que ya no son necesarias, por lo que una desregulación en los mismos supone un importante condicionante para la paulatina acumulación y agregación de estas proteínas defectuosas (Thibaudeau, Anderson, and Smith 2018).

Los principales agregados de proteínas presentes en las enfermedades neurodegenerativas son los formados por tau, ß-amiloide (Aß), α-sinucleína o la proteína de respuesta transactiva conjugada a ADN (TDP-43) (Spires-Jones, Attems, and Thal 2017). La concentración de estos agregados no solo aumenta de forma progresiva con el transcurso de la enfermedad, aumentado la muerte neuronal y agravando la fisiopatología, sino que también se propaga a nuevas regiones cerebrales transmitiendo el mal plegamiento a otras proteínas, es decir, actuando de forma similar a la proteína priónica (Jucker and Walker 2013). En este proceso se suele desencadenar una sobreproducción y un mal plegamiento proteicos, que se escapa al sistema de regulación celular y, finalmente, una agregación de estas proteínas aberrantes, inicialmente solubles, en agregados macromoleculares insolubles que se depositan en el interior o en el exterior celular (Ross and Poirier 2004). Esta característica aparición de agregados proteicos en los trastornos neurodegenerativos es el motivo por el que también se conocen por el nombre de “proteinopatías” (Bayer 2015).

En las enfermedades neurodegenerativas la muerte neuronal, además de asociarse a la agregación proteica, también se atribuye a una activación crónica del sistema inmune en el SNC. En el cerebro, las principales células del sistema inmune son la microglía y los astrocitos, encargándose de importantes funciones como la defensa frente a infecciones, la reparación tisular y la eliminación de células apoptóticas y desechos celulares (Capuron and Miller 2011). Se han reportado dos fenotipos de microglía activada, el fenotipo clásico o proinflamatorio (M1), siendo el principal responsable en los procesos de neuroinflamación crónica de las enfermedades neurodegenerativas (Stephenson et al. 2018) y el fenotipo alternativo o antiinflamatorio (M2). Mientras que el fenotipo M1 se caracteriza por una

producción de citoquinas proinflamatorias y óxido nítrico, así como una sobreexpresión de la óxido nítrico sintasa (iNOS), en contraste, al fenotipo M2 se le atribuye la capacidad de producir citoquinas antiinflamatorias y diversos factores de crecimiento, así como una sobreexpresión de la arginasa (Arg), enzima que compite por su unión al sustrato L-arginina con la enzima iNOS (Orihuela, McPherson, and Harry 2016). A nivel de investigación, se puede inducir la polarización de la microglía al estado de activación M1 con un tratamiento con lipopolisacárido bacteriano (LPS) e inferterón-γ (IFN-γ) (Qin et al. 2015). Además, se ha descrito que el envejecimiento favorece un estado proinflamatorio de la microglía con un aumento importante en la liberación de citoquinas proinflamatorias, como IL-6 (Tha et al. 2000). La desregulación en la activación de la microglía supone una inflamación prolongada en el tiempo que se traslada a una situación de neurotoxicidad con capacidad de promover progresivamente la aparición de la patología neurodegenerativa (Gao and Hong 2008).

Un indudable problema que persiste hoy día es el diagnóstico temprano de la enfermedad neurodegenerativa, que permita un adecuado tratamiento personalizado puesto que una diagnosis precoz se asocia con una mejor evolución del cuadro clínico. Algunos de los estudios más prometedores se centran en el estudio de diversos biomarcadores en fluidos corporales que permitan detectar problemas en la sinapsis, daño axonal y procesos neuroinflamatorios, como son el péptido amiloide ß (Aß42) en fluido cerebroespinal, así como nuevos biomarcadores en la sangre (Mattsson-Carlgren et al. 2020; Simrén et al. 2020; Zetterberg 2017). También se está analizando la toma de fotografías cerebrales usando la técnica de tomografía de emisión de positrones (PET) que no solo ayudaría a un diagnóstico temprano sino que permitiría monitorear la severidad y la progresión de la enfermedad (Bischof et al. 2019; Shah and Catafau 2014). Para asegurar el diagnóstico definitivo de diversas enfermedades neurodegenerativas se realiza la autopsia *post-mortem*, en la que se confirma la atrofia de partes específicas del cerebro y la presencia de agregados proteicos (Burack et al. 2010; Kraybill et al. 2005).

Más del 90% del total de GPCRs no sensoriales expresados en seres humanos se encuentran en el cerebro, participando en la regulación de diferentes procesos neurológicos. Se ha descrito que la alteración de la señalización inducida por los GPCR en el sistema nervioso central es un factor desencadenante de numerosas enfermedades neurodegenerativas entre las cuales se incluyen las enfermedades de Alzheimer y Parkinson (Huang, Todd, and Thathiah 2017). Así, los GPCR constituyen dianas importantes para el estudio de los mecanismos moleculares que dan lugar al desarrollo de estas enfermedades así como para el descubrimiento de nuevas terapias (Azam et al. 2020). Algunos de los GPCR más estudiados para el tratamiento del Alzheimer son los receptores metabotrópicos de glutamato (GluR) y de serotonina (5-HTR) (Stahl 2018), mientras que en el tratamiento del Parkinson los receptores de dopamina juegan un papel crucial (Hisahara and Shimohama 2011).

La lucha contra las enfermedades neurodegenerativas ha llevado al diseño y creación de nuevos modelos experimentales que permitan entender el origen y desarrollo de estas patologías (Dawson, Golde, and Lagier-Tourenne 2018). Uno de los modelos más utilizados en Alzheimer son los ratones transgénicos que sobreexpresan el gen mutado de la proteína precursora amiloidea humana (App_{SW}) (Shen et al. 2018). Por otro lado, como modelo de Parkinson es ampliamente utilizada la rata con lesión nigroestriatal mediante la inyección de

6-hidroxidopamina (6-OHDA), compuesto neurotóxico (Romero-Sánchez et al. 2020). En ambos modelos se busca simular y replicar de forma precisa las condiciones fisiológicas que tienen lugar en el organismo cuando aparecen estos trastornos.

1.5.1 La Enfermedad de Alzheimer

La Enfermedad de Alzheimer (AD) se descubrió en el año 1907, cuando el psiquiatra y neurólogo alemán Alois Alzheimer se percató de unos depósitos de proteínas, ahora conocidos como placas seniles y ovillos neurofibrilares, en el cerebro de una mujer que padecía pérdidas de memoria y deterioro cognitivo. Este estudio se amplió con el caso de otro paciente en el año 1911 (Graeber 1998). Finalmente, la enfermedad denominó el mal de Alzheimer, en honor a su descubridor.

La demencia es la forma más severa con la que se presenta el deterioro cognitivo. De todos los tipos de demencia, el AD es la enfermedad prioritaria, supone entre el 50 y el 75% de los casos a nivel global, quedando lejos de la demencia vascular, que en la actualidad ocupa el segundo lugar (Rizzi, Rosset, and Roriz-Cruz 2014). Las estimaciones estadísticas consideran que en el año 2050 habrá un total de 130 millones de personas que sufrirán esta patología, con la consiguiente pérdida en su calidad de vida (Niu et al. 2017).

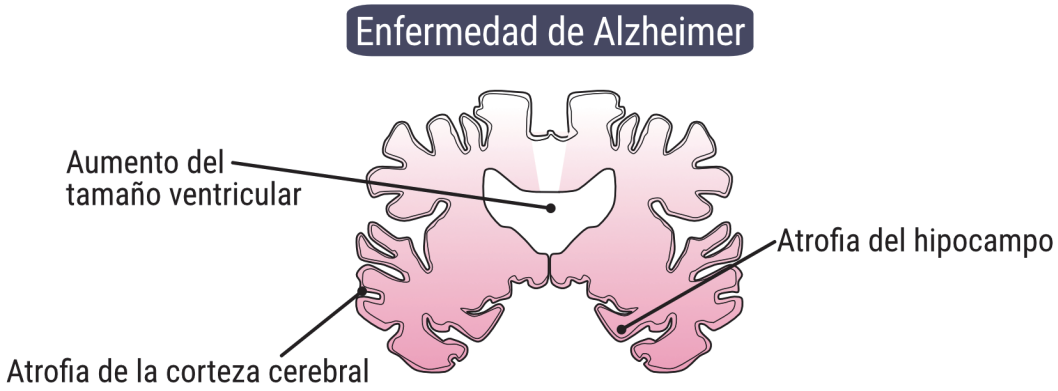

Figura 16: Principales zonas deterioradas del cerebro en la patología del Alzheimer.

La etiología del AD es compleja y multifactorial y, hoy en día, siguen existiendo muchas incógnitas, su causa permanece desconocida (Citron 2010). El envejecimiento es el factor desencadenante más importante. A partir de los 65 años, se dobla cada 5 años la probabilidad de padecer este trastorno (Alzheimer's Association Report 2019). La actividad física y social regular son factores que previenen o ralentizan el desarrollo de la patología (Dyer et al. 2020; Santos-Lozano et al. 2016), mientras que la hipertensión, la diabetes, la obesidad, una dieta no saludable o consumir tabaco y/o alcohol, así como la herencia de diversas mutaciones genéticas como la mutación de la apolipoproteína E (APOE) (Kivipelto, Mangialasche, and Ngandu 2018) favorecen su aparición. Estos procesos están relacionados entre sí y se retroalimentan, promoviendo la desregulación de varios procesos bioquímicos en el sistema nervioso central y finalmente la muerte neuronal (Kumar, Singh, and Ekavali

2015). Las principales consecuencias fisiopatológicas de la enfermedad de Alzheimer consisten en:

1) La deposición de agregados proteicos: La ruptura del equilibrio entre la eliminación de proteínas defectuosas y mal plegadas y su paulatina acumulación es un potente desencadenador de la agregación proteica en la AD, que resulta tóxica (Mawuenyega et al. 2010). En la AD aparecen placas Aß-amiloide, generalmente depositadas en el exterior celular (Kumar et al. 2011). Estas placas insolubles están constituidas mayoritariamente por $Aß_{42}$, sintetizada mediante la acción proteolítica de las enzimas ß y γ– secretasa (J. Wang et al. 2017).

   También es frecuente la aparición de otro tipo de agregados proteicos, los denominados ovillos neurofibrilares, que se depositan en el interior celular (Mandelkow 1999). Estos ovillo están constituidos por proteína tau hiperfosforilada. Esta proteína se expresa de forma habitual como unidad estructural de los microtúbulos en la neurona madura, dotándolos de estabilidad (Iqbal et al. 2010). Debido a una pérdida en la homeóstasis entre fosforilación y desfosforilación de esta proteína, se desplaza el equilibrio hacia una mayor fosforilación de tau, por lo que se produce una degradación microtubular y se forman filamentos helicoidales de proteína tau hiperfosforilada (Mandelkow and Mandelkow 2012).

2) Excitotoxicidad mediada por NMDAR: El receptor de NMDAR tiene un papel crucial en la plasticidad sináptica, participando también en la transmisión de la sinapsis (Cull-Candy and Leszkiewicz 2004). En AD se ha detectado una sobre estimulación de la señalización del neurotransmisor glutamato mediada por NMDAR extrasinápticos, produciendo una entrada incontrolada de calcio en la neurona y generando excitotoxicidad (Benarroch 2018; Wang and Reddy 2017).

3) Microglía proinflamatoria: La microglía forma parte del sistema inmune en el cerebro y se le atribuyen propiedades moduladoras de la función cognitiva así como la capacidad para eliminar sustancias de desecho y defender frente a agentes infecciosos (Cameron and Landreth 2010). La microglía se puede encontrar en diferentes estados formando un abanico que se mueve entre el estado de reposo/quiescencia hasta un estado activado que aparece frente la necesidad de responder a estímulos perjudiciales; entre ellos, la presencia de agregados proteicos típicos de la AD. Se ha reportado que la microglía activada favorece la degradación y eliminación de agregados de Aß-amiloide (Sarlus et al. 2017). En AD hay una clara pérdida del balance entre la microglía de tipo pro-inflamatoria, M1 y anti-inflamatoria, M2, siendo el fenotipo M1 el que prevalece y derivando en una secreción crónica de citoquinas proinflamatorias como IL-6 e IFN-γ (Wang et al. 2015).

4) Proteína priónica humana (PrNP): Aunque el PrNP se asocia de manera directa a las enfermedades priónicas como la enfermedad de Creutzfeldt–Jakob, también se ha descrito su posible implicación en la patogénesis del AD. Las más de 50 mutaciones descritas hasta la fecha en la proteína PrNP parecen ser un factor de

riesgo que condiciona el desarrollo de esta enfermedad (Bagyinszky et al. 2019; Zhang et al. 2016).

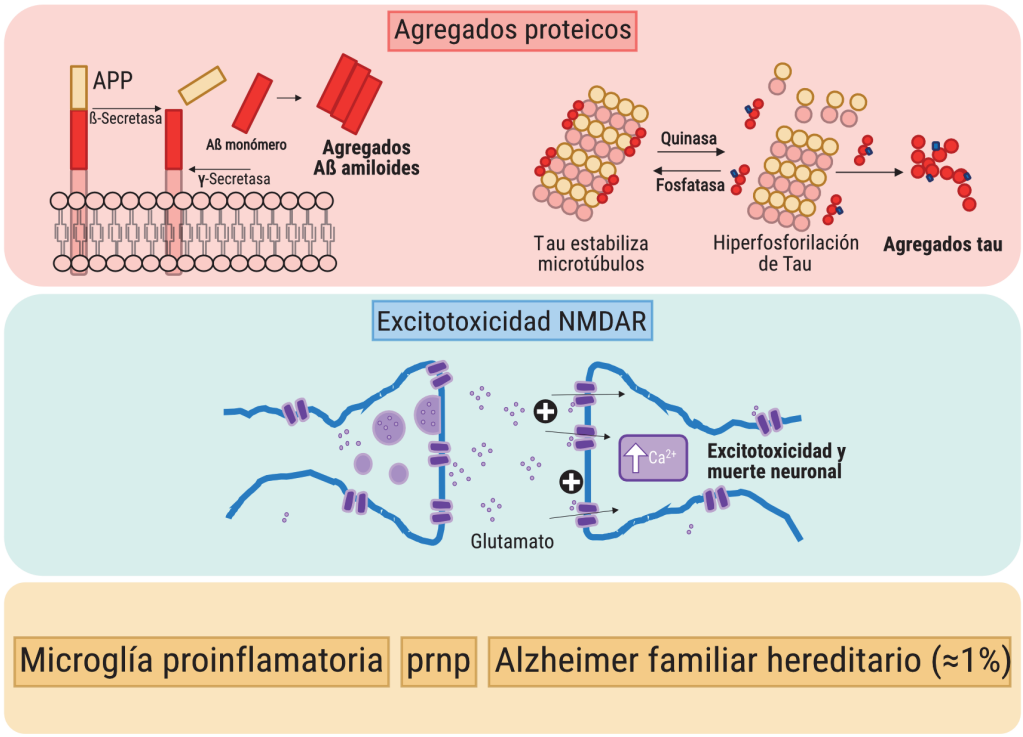

Figura 17: Mecanismos moleculares principales desencadenantes de la fisiopatología del Alzheimer.

El síntoma más frecuente que presentan los enfermos que padecen Alzheimer es la pérdida progresiva de las capacidades cognitivas. Especialmente, de la memoria a corto plazo en los estadios iniciales (Palmer et al. 2007). Otros síntomas habituales son la dificultad para articular palabras, los cambios en la personalidad y en el comportamiento (Kumar et al. 1988). Esta sintomatología es común en otras demencias, lo que dificulta un diagnóstico temprano y preciso de la enfermedad (Kalaria 2002; Lindau et al. 2000).

Los síntomas del Alzheimer son un reflejo de la degradación paulatina de importantes regiones cerebrales. Fundamentalmente, debido a la atrofia del hipocampo y de la corteza, así como a un aumento del tamaño ventricular cerebral (Frisoni et al. 1999).

Actualmente no existe un tratamiento efectivo para curar la patología del Alzheimer y por desgracia ha habido un gran número de ensayos clínicos fallidos (Anderson et al. 2017). Sin embargo, la FDA ha aprobado tratamientos sintomáticos. Entre ellos se encuentra la Memantina, que actúa como antagonista del receptor NMDA, regulando la excitotoxidad desencadenada por la liberación incontrolada de glutamato e inhibidores de la aceltilcolinesterasa, que intentan reforzar la señal mediada por la acetilcolina (Y.Y. Szeto and J.G. Lewis 2016). Desafortunadamente, estos fármacos tienen diversos efectos adversos y a pesar de que mejoran ciertos síntomas del AD potencian el desarrollo de otros nuevos.

1.5.1.1 Receptor de N-Metil-D-Aspartato

El glutamato se considera el neurotransmisor excitatorio más importante en el SNC (Wang and Reddy 2017). Los receptores que unen glutamato se clasifican en dos grandes categorías. Por un lado, se encuentran los receptores ionotrópicos, que se encuentran acoplados a canal iónico, con capacidad de transportar iones. Este grupo está formado por los receptores de N-Metil-D-Aspartato (NMDA) y de ácido α-amino-3-hidroxi-5-metilo-4-isoxazolpropiónico (AMPA). Por otro lado, el glutamato también se puede unir a los receptores metabotrópicos de glutamato (mGluRs), que pertenecen a la familia de GPCRs de clase C y que se caracterizan por un dominio N-terminal de gran tamaño (Koehl et al. 2019).

Los receptores NMDA tienen una estructura tetramérica formada por distintas subunidades que se integran con varias combinaciones. Se han descrito diferentes tipos de subunidades, dos del tipo NR1 (A-B), cuatro del tipo NR2 (A-D) y dos del tipo NR3 (A-B). Obligatoriamente, el tetrámero NMDA se debe componer por dos subunidades NR1 reguladoras, con un dominio de unión a glicina, cuya activación es necesaria para la señalización mediada por NMDA. Mientras que las otras dos subunidades, habitualmente de tipo NR2, van a tener un dominio de unión a glutamato (Flores-Soto et al. 2012).

El amplio abanico de combinaciones de subunidades que conforman NMDAR dotan a este receptor de una gran heterogeneidad en un mismo organismo. La prevalencia de una combinación de subunidades varía según el tipo de célula en el que se exprese, por ejemplo, neuronas, microglía, astrocitos u oligodendrocitos (Lee et al. 2010; Verkhratsky and Kirchhoff 2007). También se ha descrito una composición de subunidades en la estructura de NMDAR dependiente de su localización en la neurona (presináptica, extrasináptica o perisináptica) (Köhr 2006). Además, se ha descrito que la combinación tetramérica compuesta por dos subunidades NR1 y dos subunidades NR2B es la más frecuente en el desarrollo fetal y en NMDAR extrasináptico (Petralia et al. 2010).

La concentración media de glicina en el SNC, en la mayoría de las circunstancias, es suficiente para unirse a las subunidades reguladoras de NMDAR y permitir su activación ejerciendo como coagonista junto con el glutamato. Así, la unión de glutamato a NMDAR induce la liberación del bloqueo mediado por Mg^{2+}, fenómeno que suele estar favorecido por una despolarización de la membrana plasmática, y la entrada de Na^{+} y, especialmente, Ca^{2+} del exterior al interior celular. Puntualizar que bajo ciertas condiciones patológicas la concentración de glicina puede verse aumentada, favoreciendo la internalización de NMDAR (Nong et al. 2003).

La principal función fisiológica de NMDAR consiste en la regulación de la transmisión sináptica, propagando la despolarización de la membrana mediante la entrada de Ca^{2+} y favoreciendo la fosforilación de ERK1/2. También participa en la plasticidad y supervivencia neuronal (Dore et al. 2017) con una implicación directa en procesos como la memoria. De manera interesante, se ha descrito que mientras la activación de NMDAR en condiciones fisiológicas favorece la supervivencia neuronal, en situaciones patológicas una activación crónica del receptor puede desencadenar en excitotoxicidad y muerte neuronal (Papadia and Hardingham 2007). Así, el NMDAR tiene una gran implicación en la fisiopatología del Alzheimer, tal y como se describe en el *apartado 1.5*.

Actualmente, NMDAR se ha convertido en una de las dianas terapéuticas más prometedoras para desarrollar una terapia efectiva contra la enfermedad de Alzheimer. Se están realizando diversos estudios que tienen como estrategia bloquear el receptor NMDA mediante el uso de antagonistas específicos. Es cierto que inhibidores con gran afinidad por NMDAR como el MK-801 se han descartado como terapia por sus numerosos efectos secundarios indeseados (Chemistry 2007). Sin embargo, la Memantina es el único antagonista de NMDAR aprobado para el tratamiento de casos moderados o severos de AD, en los que los potenciales beneficios de la droga superan a sus efectos adversos (Robinson and Keating 2006). Recientemente, la estrategia principal se centra en la búsqueda de un antagonista selectivo para la subunidad NR2B de NMDAR, con el que se conseguiría una inhibición selectiva de los NMDAR extrasinápticos y, gracias a ello, se conservaría la señalización mediada por los tetrámeros de NMDAR que contuvieran la subunidad NR2A, favoreciendo la supervivencia neuronal (Liu et al. 2019).

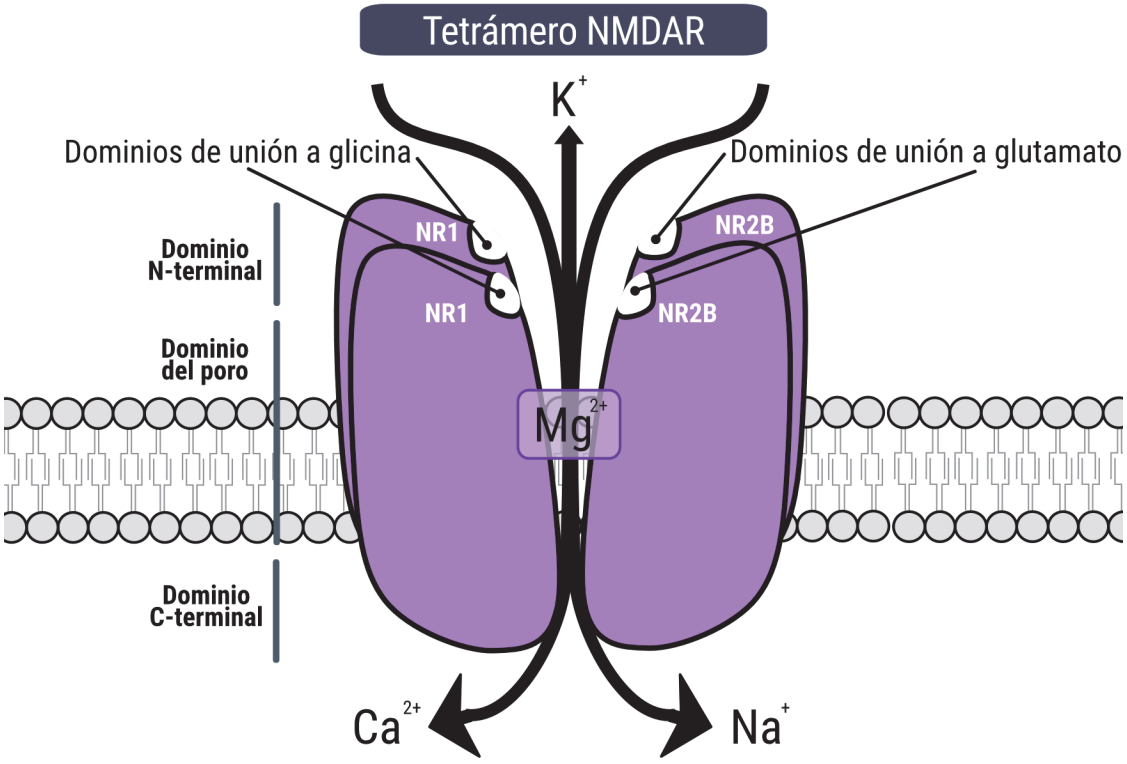

Figura 18: Estructura tetramérica y dominios del receptor NMDA.

1.5.2 La Enfermedad de Parkinson

El primer caso documentado de la Enfermedad de Parkinson (PD) se remonta al año 1817, cuando el doctor inglés James Parkinson se encargó de documentar los síntomas de un paciente. En 1872, Jean-Martin Charcot realizó su contribución, definiendo los principales síntomas del PD y separándolo de otros desórdenes como la esclerosis múltiple (Goetz 2011). No sería hasta el año 1912, cuando Friederich Lewy se encargaría de reportar una de las principales características que identifican la enfermedad de PD, la aparición de

agregados proteicos de α-syn que recibieron el nombre de cuerpos de Lewy en su honor (Scroll and For 2010). Además, se ha reportado una fuerte correlación entre el diagnóstico del PD y el desarrollo en años posteriores de un proceso de demencia (Setó-Salvia et al. 2011).

El Parkinson tiene una gran prevalencia, siendo el segundo desorden neurodegenerativo con mayor número de casos a nivel mundial. Varios estudios coinciden en una mayor predominancia de este trastorno en hombres que en mujeres, y como la probabilidad de desarrollarlo incrementa dramáticamente a partir de los 80 años (Muangpaisan et al. 2011). Desafortunadamente, existen proyecciones que prevén una tendencia al alza del número de casos de PD en las próximas décadas, en gran parte, debido a una mayor esperanza de vida (Savica et al. 2018).

A pesar de los esfuerzos de la comunidad científica por identificar los factores que influyen en la prevención y en la aparición del PD, no existe un consenso, probablemente, debido a las limitaciones en los estudios; como el escaso número de muestras con el que trabajar y la gran variabilidad que existe entre ellas (Belvisi et al. 2020). Sin embargo, si se han descrito los principales procesos bioquímicos característicos de esta enfermedad y que dan lugar a la muerte de las neuronas dopaminérgicas, generando un déficit de dopamina en el cuerpo estriado (Betarbet et al. 2002). Estos procesos consisten en:

1) Agregación proteica: Una de las características más importantes del PD es la aparición de agregados proteicos citoplasmáticos en las neuronas dopaminérgicas de la corteza cerebral y, especialmente, de la *Substantia nigra,* en la región de los ganglios basales. Estas inclusiones reciben el nombre de cuerpos de Lewy y están constituidos por varias proteínas, entre ellas, la α-sinucleína (α-syn) es la mayoritaria (Spillantini et al. 1997), aunque también se encuentran presentes la ubiquitina o la parkina (Dawson 2006). Defectos en el sistema de ubiquitinación y proteasoma de la célula se han asociado claramente a una mayor agregación proteica en el PD, propiciando la acumulación incontrolada de inclusiones citoplasmáticas (Tan, Wong, and Lim 2009). También se ha demostrado que la existencia de cuerpos de Lewy en la célula puede potenciar la agregación de proteína ß-amiloide (Gomperts et al. 2008).

2) Disfunción mitocondrial: Se ha descrito en varios estudios la posible implicación de la disfunción del complejo mitocondrial (Greenamyre et al. 1999). Este defecto sería el causante de la producción de especies reactivas de oxígeno (ROS) capaces de dañar al ADN, proteínas y lípidos en la célula (Xie, Wan, and Chung 2010). Otra consecuencia consiste en una progresiva disminución de los niveles de ATP celulares que llevan a una peor eficiencia de la bomba ATPasa Na^+/K^+, exponiendo la célula a una situación excitotóxica mediada por NMDAR (Xiong et al. 2012).

Se han propuesto mutaciones que podrían propiciar la agregación proteica y la disfunción mitocondrial y, debido a ello, favorecer el desarrollo del PD familiar. Entre ellas, son especialmente relevantes la mutaciones puntuales A53T y A30P que se producen en el gen que codifica la α-syn (Kilpeläinen et al. 2019), favoreciendo la formación de cuerpos de Lewy. También son determinantes los genes que codifican para componentes clave en el sistema

de ubiquitinación y proteasoma como la parkina (Kitada et al. 1998; Lücking et al. 2000) o la ubiquitina carboxi-terminal hidrolasa L1 (UCHL1) (Rydning et al. 2017).

En las fases iniciales del PD, en las que todavía no hay síntomas apreciables, los cuerpos de Lewy se encuentran limitados al bulbo raquídeo y al bulbo olfatorio. Sin embargo, estas inclusiones se propagan con la evolución de la patología hasta la *substantia nigra* y otros núcleos del mesencéfalo, donde se observan las primeras alteraciones motoras. Finalmente, en estadios más avanzados, los agregados proteicos se pueden extender hasta el neocórtex (Sveinbjornsdottir 2016).

La propagación de los cuerpos de Lewy supone, en líneas generales, la degeneración de la vía dopaminérgica nigroestriatal, favoreciendo la aparición de la sintomatología asociada al PD. Estos síntomas se suelen clasificar en dos grandes categorías; síntomas motores, que incluyen la bradiquinesia, la rigidez muscular, la inestabilidad postural, la distonía y la disquinesia y, por otra parte, síntomas no-motores, entre los que se encuentran la apatía, la dificultad para conciliar el sueño, la pérdidas de memoria, la depresión y la ansiedad (Aarsland et al. 2007; Heisters 2011).

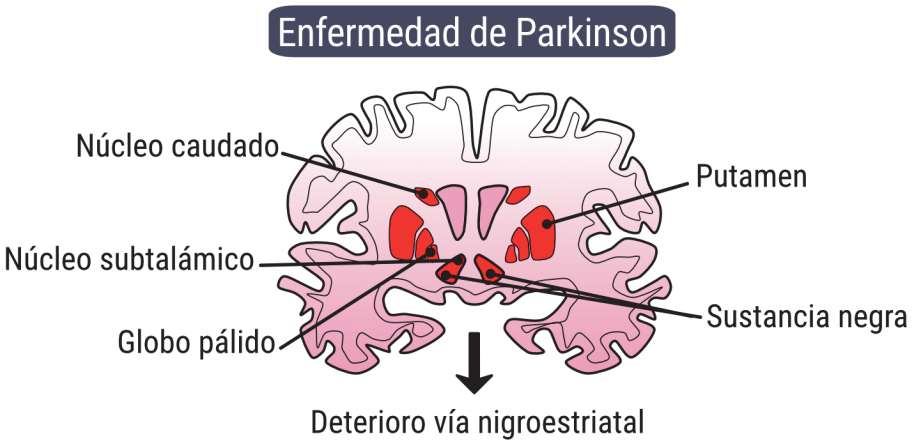

Figura 19: Principales zonas deterioradas del cerebro en la patología del Parkinson.

Actualmente, la terapia farmacológica que nos ofrece una mayor tasa de éxito para el tratamiento del PD es la levodopa (L-DOPA). El hecho de ser un precursor natural de la dopamina, le ofrece una gran biodisponibilidad y absorción en el intestino al ser administrada mediante vía oral. También se caracteriza por su capacidad para atravesar con éxito la barrera hematoencefálica y reestablecer parcialmente una adecuada señalización dopaminérgica, resultando en un excelente tratamiento para el Parkinson que consigue paliar en gran medida su sintomatología (Lewitt 2015). Desgraciadamente, la terapia continuada con L-DOPA en pacientes con Parkinson suele venir acompañada de la generación de resistencia a dicho tratamiento a medio-largo plazo. Hecho que se traduce en una pérdida de efectividad, requiriéndose dosis cada vez mayores de este compuesto, y en el retorno de ciertos síntomas como las disquinesias (Aquino and Fox 2015).

A pesar de los inconvenientes de la L-DOPA, sigue siendo el tratamiento más utilizado para combatir la sintomatología del Parkinson, junto con o alternativamente a otros agonistas de

los receptores de dopamina como el ropinirol o la rotigotina (Latt et al. 2019). Otro tratamiento en auge es la estimulación cerebral profunda, que permite solventar de forma efectiva los síntomas motores del Parkinson, aunque tiene escaso efecto sobre los síntomas no motores (Hartmann et al. 2019). Los estudios más innovadores se centran en la tecnología del ARN de interferencia para intentar reducir la producción de α-syn del organismo o potenciar su eliminación, ambas estrategias buscan evitar la formación de cuerpos de Lewy (Stoker, Torsney, and Barker 2018).

A pesar de estos avances, se necesita de nuevas investigaciones para conseguir un tratamiento no solamente útil para mejorar la sintomatología durante los primeros estadios, si no que permita una cura efectiva que devuelva la calidad de vida a los enfermos con la patología de Parkinson.

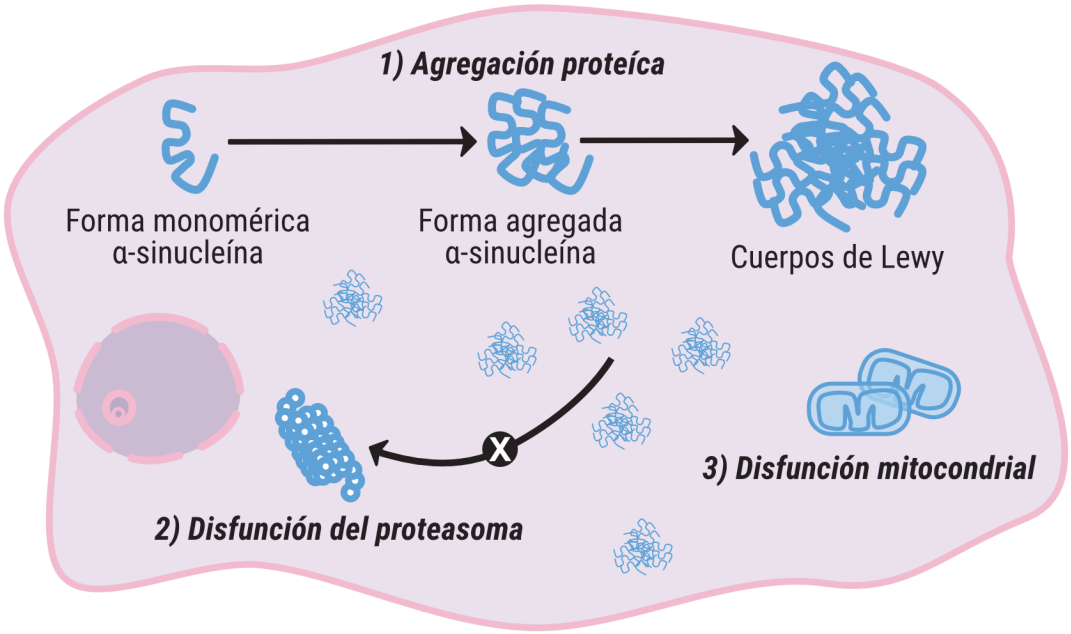

Figura 20: Mecanismos moleculares principales desencadenantes de la fisiopatología del Parkinson.

OBJETIVOS

2. Objetivos

Objetivo 1. Caracterizar la selectividad funcional de una librería de compuestos cannabinoides en ausencia y presencia de CBD sobre los receptores de cannabinoides CB_1, CB_2 y el heterómero de receptores CB_1-CB_2.

Objetivo 2. Caracterizar la afinidad y la funcionalidad inducida por el fitocannabinoide CBG sobre los receptores de cannabinoides CB_1, CB_2 y el heterómero de receptores CB_1-CB_2.

Objetivo 3. Detectar cambios en la expresión de los complejos heteroméricos CB_1R-GPR55 y CB_2R-GPR55 en un modelo de primate de la enfermedad de Parkinson.

Objetivo 4. Determinar si existe una interacción específica entre los receptores AT_1 y AT_2 a nivel de membrana plasmática y estudiar como afecta a su funcionalidad en células transfectadas y cultivos primarios de ratón. Detectar cambios de expresión de los heterómeros AT_1R-AT_2R en secciones de cerebro de un modelo animal de la enfermedad de Parkinson.

Objetivo 5. Determinar si existe una interacción específica entre los receptores de angiotensina AT_1 y/o AT_2 y Mas a nivel de membrana plasmática y estudiar las características funcionales de los nuevos complejos descritos en células HEK-293T transfectadas y en cultivos primarios neuronales y gliales. Determinar si existe una interacción trimérica entre los receptores AT_1, AT_2 y Mas. Detectar cambios de expresión de los heterómeros AT_1R-MasR y AT_2R-MasR en secciones de cerebro de un modelo animal de la enfermedad de Parkinson.

Objetivo 6. Determinar si existe una interacción específica entre la enzima ACE2 y los receptores AT_1, AT_2 y Mas a nivel de membrana plasmática y estudiar como afecta a su funcionalidad y a su expresión en membrana. Detectar cambios de expresión de los complejos ACE2-AT_1R, ACE2-AT_2R y ACE2-MasR en tejido pulmonar de fetos de ratón y de ratón adulto.

Objetivo 7. Determinar la implicación del eje ACE2/Ang (1-7)/Alamandina/MrgE mitocondrial en la regulación de las especies reactivas de oxígeno.

Objetivo 8. Determinar si la cola C-terminal del receptor de adenosina A_{2A}, inusualmente larga para un GPCR, tiene un implicación funcional relevante en la transmisión de señales del receptor.

Objetivo 9. Determinar si existe una interacción específica entre los receptores NMDA y A_{2A} o CB_2 a nivel de membrana plasmática y describir la funcionalidad de las nuevas unidades estructurales. Detectar cambios significativos en la expresión de los heterómeros A_{2A}R-NMDAR y CB_2R-NMDAR en cultivos primarios de un modelo animal de la enfermedad de Alzheimer (ratón $App_{Sw/Ind}$).

RESULTADOS

Rafael Franco Fernández y Gemma Navarro Brugal
Grupo de Neurobiología Molecular
Departamento de Bioquímica y Biomedicina Molecular
Av. Diagonal, 643
Edificio Prevosti, Planta -2 08028 Barcelona

La tesis doctoral de Rafael Rivas Santisteban titulada "***Expresión y funcionalidad de los heterómeros de GPCR en las enfermedades neurodegenerativas de Parkinson y Alzheimer***" se presenta como un compendio de publicaciones.

El manuscrito **"Cannabidiol skews biased agonism at cannabinoid CB_1 and CB_2 receptors with smaller effect in CB1-CB2 heteroreceptor complexes"** ha sido publicado en *Biochemical Pharmacology* que tiene un factor de impacto en el año de publicación (2018) de 4,825. El manuscrito "**Cannabigerol Action at Cannabinoid CB_1 and CB_2 Receptors and at CB_1–CB_2 Heteroreceptor Complexes**" ha sido publicado en *Frontiers in Pharmacology* que tiene un factor de impacto en el año de publicación (2018) de 3,845. El manuscrito **"Expression of cannabinoid CB_1R–GPR55 heteromers in neuronal subtypes of the *Macaca fascicularis* striatum"** ha sido publicado en *Annals of the New York Academy of Sciences* que tiene un factor de impacto en el año de publicación (2020) de 4,718. El manuscrito **"Expression of GPR55 and either cannabinoid CB_1 or CB_2 heteroreceptor complexes in the caudate, putamen, and accumbens nuclei of control, parkinsonian, and dyskinetic non-human primates"** ha sido publicado en *Brain Structure and Function* que tiene un factor de impacto en el año de publicación (2020) de 3,298. El manuscrito "**Angiotensin AT_1 and AT_2 receptor heteromer expression in the hemilesioned rat model of Parkinson's disease that increases with levodopa-induced dyskinesia"** ha sido publicado en *Journal of Neuroinflammation* que tiene un factor de impacto en el año de publicación (2020) de 5,793. El manuscrito **"Novel Interactions Involving the Mas Receptor Show Potential of the Renin–Angiotensin system in the Regulation of Microglia Activation: Altered Expression in Parkinsonism and Dyskinesia"** ha sido publicado en *Neurotherapeutics* que tiene un factor de impacto en el año de publicación (2020) de 6,035. El manuscrito **"Functional Complexes of Angiotensin-Converting Enzyme 2 and Renin-Angiotensin System Receptors: Expression in Adult but Not Fetal Lung Tissue"** ha sido publicado en *International Journal of Molecular Sciences* que tiene un factor de impacto en el año de publicación (2020) de 4,556. El manuscrito **"An ACE2/Mas-related receptor MrgE axis in dopaminergic neuron mitochondria"** ha sido publicado en Redox Biology que tiene un factor de impacto en el año de publicación (2021) de 11,799. El manuscrito **"SARS-CoV-2 as a Factor to Disbalance the Renin-Angiotensin System: A Suspect in the Case of Exacerbated IL-6 Production"** ha sido publicado en *The Journal of Immunology* que tiene un factor de impacto en el año de publicación (2020) de 4,886. El manuscrito **"Experimental and computational analysis of biased agonism on full-length and a C-terminally truncated adenosine A_{2A} receptor"** ha sido publicado en *Computational and Structural Biotechnology Journal* que tiene un factor de impacto en el año de publicación (2020) de 6,018. El manuscrito **"Adenosine A_{2A} Receptor Antagonists Affects NMDA Glutamate Receptor Function. Potential to Address Neurodegeneration in Alzheimer's Disease"** ha sido publicado en *Cells* que tiene un factor de impacto en el año de publicación (2020) de 4,366. El manuscrito **"N-Methyl-D-Aspartate (NMDA) and cannabinoid CB_2 receptors form functional complexes in neural cells. Insights into the therapeutic potential of NMDA receptors in neurons and microglia"** ha sido enviado para su consideración en *Brain, Behavior and Immunity* que tiene un factor de impacto en 2021 de 6,633.

En el estudio "**Cannabidiol skews biased agonism at cannabinoid CB_1 and CB_2 receptors with smaller effect in CB1-CB2 heteroreceptor complexes"** el doctorando Rafael Rivas Santisteban participó en el tratamiento de datos, elaborando los "radar plots" para la cuantificación del agonismo sesgado de los compuestos cannabinoides ensayados, así como en la realización del mapa de calor del efecto máximo y EC/IC_{50} de dichos compuestos. En el estudio "**Cannabigerol Action at Cannabinoid CB_1 and CB_2 Receptors and at CB_1–CB_2 Heteroreceptor Complexes**" el doctorando Rafael Rivas Santisteban participó en el análisis y tratamiento de datos. En los estudios **"Expression of cannabinoid CB_1R–GPR55 heteromers in neuronal subtypes of the *Macaca fascicularis* striatum"** y **"Expression of GPR55 and either cannabinoid CB_1 or CB_2 heteroreceptor complexes in the caudate, putamen, and accumbens nuclei of control, parkinsonian, and dyskinetic non-human primates"** el doctorando Rafael Rivas Santisteban, junto a Jaume Lillo, llevó a cabo la cuantificación de la expresión de los complejos heteroméricos CB_1R-GPR55 y CB_2R-GPR55 de las fotografías obtenidas de los ensayos de PLA mediante la extensión de software "Andy's Algorithms" para FIJI. En el estudio **"Angiotensin AT_1 and AT_2 receptor heteromer expression in the hemilesioned rat model of Parkinson's disease that increases with levodopa-induced dyskinesia"** el doctorando Rafael Rivas Santisteban llevó a cabo el clonaje de las construcciones del receptor AT_2 fusionado a la proteína YFP y RLuc, los ensayos de BRET para determinar la interacción entre AT_1R y AT_2R, los ensayos de funcionalidad en HEK-293T transfectadas, en neuronas estriatales y en microglía, así como los ensayos de PLA en cortes de cerebro de un modelo animal de la PD. En el estudio **"Novel Interactions Involving the Mas Receptor Show Potential of the Renin–Angiotensin system in the Regulation of Microglia Activation: Altered Expression in Parkinsonism and Dyskinesia"** el doctorando Rafael Rivas Santisteban llevó a cabo el clonaje de las construcciones del receptor Mas fusionado a la proteína YFP y RLuc, los ensayos de BRET y de SRET para determinar la interacción entre AT_1R, AT_2R y MasR, los ensayos de funcionalidad en HEK-293T transfectadas, en neuronas estriatales y en microglía, así como los ensayos de PLA en cortes de cerebro de un modelo animal de la PD. En el estudio **"Functional Complexes of Angiotensin-Converting Enzyme 2 and Renin-Angiotensin System Receptors: Expression in Adult but Not Fetal Lung Tissue"** el doctorando Rafael Rivas Santisteban participó en la preparación de las muestras de tejido de pulmón fetal y adulto de ratón y en la realización de los ensayos de PLA que permitieron detectar la expresión de los complejos AT_1R-ACE2, AT_2R-ACE2 y MasR-ACE2. En el estudio **"An ACE2/Mas-related receptor MrgE axis in dopaminergic neuron mitochondria"** el doctorando Rafael Rivas Santisteban realizó los experimentos de "*binding*" no radiactivo con Fluoresceína (FAM)-Alamandina para detectar la unión de varios compuestos al receptor MrgE. En la publicación "**SARS-CoV-2 as a Factor to Disbalance the Renin-Angiotensin System: A Suspect in the Case of Exacerbated IL-6 Production"** el doctorando Rafael Rivas Santisteban contribuyó a la recopilación de información y en la elaboración de las figuras del artículo. En la publicación **"Experimental and computational analysis of biased agonism on full-length and a C-terminally truncated adenosine A_{2A} receptor"** el doctorando Rafael Rivas Santisteban participó en el tratamiento de datos, elaborando los "radar plots" para la cuantificación del agonismo sesgado de los compuestos ensayados. En la publicación **"Adenosine A_{2A} Receptor Antagonists Affects NMDA Glutamate Receptor Function. Potential to Address Neurodegeneration in Alzheimer's Disease"** el doctorando Rafael Rivas Santisteban participó en la realización y en la toma de imágenes en el confocal de las PLAs y los marcadores de microglía iNOS y Arginasa. En el estudio **"N-Methyl-D-Aspartate (NMDA) and cannabinoid CB_2 receptors form functional complexes in neural cells. Insights into the therapeutic potential of NMDA receptors in neurons and microglia"** el doctorando Rafael Rivas Santisteban realizó

el ensayo de inmunocitoquímica, los ensayos de BRET para determinar la interacción entre CB_2R y NMDAR, los ensayos de funcionalidad en HEK-293T transfectadas, en microglía y en neuronas de hipocampo de animales control y animales modelo de la AD, así como los ensayos de PLA.

Barcelona, a 2 de Julio de 2021

Dr. Rafael Franco Fernández
Director y tutor

Dra. Gemma Navarro Brugal
Directora

Los resultados de la presente Tesis Doctoral están reflejados en los siguientes manuscritos:

3.1 Gemma Navarro, Irene Reyes-Resina, **Rafael Rivas-Santisteban**, Verónica Sánchez de Medina, Paula Morales, Salvatore Casano, Carlos Ferreiro-Vera, Alejandro Lillo, David Aguinaga, Nadine Jagerovic, Xavier Nadal y Rafael Franco. **Cannabidiol skews biased agonism at cannabinoid CB_1 and CB_2 receptors with smaller effect in CB1-CB2 heteroreceptor complexes.**

Manuscrito publicado en Biochemical Pharmacology.

3.2 Gemma Navarro, Katia Varani, Irene Reyes-Resina, Verónica Sánchez de Medina, **Rafael Rivas-Santisteban**, Carolina Sánchez Carnerero Callado, Fabrizio Vincenzi, Salvatore Casano, Carlos Ferreiro-Vera, Enric I. Canela, Pier Andrea Borea, Xavier Nadal y Rafael Franco. **Cannabigerol Action at Cannabinoid CB_1 and CB_2 Receptors and at CB_1–CB_2 Heteroreceptor Complexes**.

Manuscrito publicado en Frontiers in Pharmacology.

3.3 Eva Martínez-Pinilla, Alberto J. Rico, **Rafael Rivas-Santisteban**, Jaume Lillo, Elvira Roda, Gemma Navarro, Gemma, Rafael Franco, Rafael y José Luis Lanciego. **Expression of cannabinoid CB_1R–GPR55 heteromers in neuronal subtypes of the Macaca fascicularis striatum**.

Manuscrito publicado en Annals of the New York Academy of Sciences.

3.4 Eva Martínez-Pinilla, Alberto J. Rico, **Rafael Rivas-Santisteban**, Jaume Lillo, Elvira Roda, Gemma Navarro, Rafael Franco y José Luis Lanciego. **Expression of GPR55 and either cannabinoid CB_1 or CB_2 heteroreceptor complexes in the caudate, putamen, and accumbens nuclei of control, parkinsonian, and dyskinetic non-human primates**.

Manuscrito publicado en Brain Structure and Function.

3.5 **Rafael Rivas-Santisteban**, Ana I. Rodriguez-Perez, Ana Muñoz, Irene Reyes-Resina, José Luis Labandeira-García, Gemma Navarro y Rafael Franco. **Angiotensin AT_1 and AT_2 receptor heteromer expression in the hemilesioned rat model of Parkinson's disease that increases with levodopa-induced dyskinesia.**

Manuscrito publicado en Journal of Neuroinflammation.

3.6 **Rafael Rivas-Santisteban**, Jaume Lillo, Ana Muñoz, Ana I. Rodríguez-Pérez, José Luís Labandeira-García, Gemma Navarro y Rafael Franco. **Novel Interactions Involving the Mas Receptor Show Potential of the Renin–Angiotensin system in the Regulation of Microglia Activation: Altered Expression in Parkinsonism and Dyskinesia**.

Manuscrito publicado en Neurotherapeutics.

3.7 Rafael Franco, Alejandro Lillo, **Rafael Rivas-Santisteban**, Ana I. Rodríguez-Pérez, Irene Reyes-Resina, Irene, José L. Labandeira-García y Gemma Navarro. **Functional Complexes of Angiotensin-Converting Enzyme 2 and Renin-Angiotensin System Receptors: Expression in Adult but Not Fetal Lung Tissue**.

Manuscrito publicado en International Journal of Molecular Sciences.

3.8 Rita Valenzuela, Ana I. Rodriguez-Perez, Maria A. Costa-Besada, Araceli Piñeiro, **Rafael Rivas-Santisteban**, Pablo Garrido-Gil, Andrea Lopez-Lopez, Gemma Navarro, Jose L. Lanciego, Rafael

Franco, Jose L. Labandeira-Garcia. **An ACE2/Mas-related receptor MrgE axis in dopaminergic neuron mitochondria.**

Manuscrito publicado en Redox Biology.

3.9 Rafael Franco, **Rafael Rivas-Santisteban**, Joan Serrano-Marín, Ana I. Rodríguez-Pérez, José L. Labandeira-García, Gemma Navarro. **SARS-CoV-2 as a Factor to Disbalance the Renin-Angiotensin System: A Suspect in the Case of Exacerbated IL-6 Production**.

Manuscrito publicado en The Journal of Immunology.

3.10 Gemma Navarro, Ángel Gonzalez, Stefano Campanacci, **Rafael Rivas-Santisteban**, Irene Reyes-Resina, Nil Casajuana-Martin, Arnau Cordomí, Leonardo Pardo y Rafael Franco. **Experimental and computational analysis of biased agonism on full-length and a C-terminally truncated adenosine A_{2A} receptor**.

Manuscrito publicado en Computational and Structural Biotechnology Journal.

3.11 Rafael Franco, **Rafael Rivas-Santisteban**, Mireia Casanovas, Alejandro Lillo, Carlos A Saura, Gemma Navarro. **Adenosine A_{2A} Receptor Antagonists Affects NMDA Glutamate Receptor Function. Potential to Address Neurodegeneration in Alzheimer's Disease**.

Manuscrito publicado en Cells.

3.12 **Rafael Rivas-Santisteban**, Alejandro Lillo, Jaume Lillo, Anna Del-Ser, Carles Saura, Rafael Franco*, Gemma Navarro*. **N-Methyl-D-Aspartate (NMDA) and cannabinoid CB_2 receptors form functional complexes in neural cells. Insights into the therapeutic potential of NMDA receptors in neurons and microglia.**

Manuscrito enviado para su consideración en Brain, Behavior and Immunity.

3.1 Cannabidiol skews biased agonism at cannabinoid CB_1 and CB_2 receptors with smaller effect in CB_1-CB_2 heteroreceptor complexes.

Gemma Navarro, Irene Reyes-Resina, **Rafael Rivas-Santisteban**, Verónica Sánchez de Medina, Paula Morales, Salvatore Casano, Carlos Ferreiro-Vera, Alejandro Lillo, David Aguinaga, Nadine Jagerovic, Xavier Nadal y Rafael Franco.

Manuscrito publicado en *Biochemical Pharmacology*, Septiembre 2018; 157: 148-158.

Hoy en día, el estudio del agonismo sesgado es una de las aproximaciones terapéuticas más novedosas para el desarrollo de nuevos compuestos con propiedades terapéuticas. La información que se obtiene mediante la investigación del agonismo sesgado permite seleccionar aquellos compuestos que tienen una señalización beneficiosa y descartar aquellos compuestos con una funcionalidad que desencadena efectos secundarios indeseados. En nuestra investigación analizamos la funcionalidad de una serie de compuestos cannabinoides, en presencia o no de cannabidiol (CBD), mediante el estudio de la señalización que promueven regulando los niveles de AMP intracelular, la fosforilación de quinasas (ERK1/2), el reclutamiento de ß-arrestina y la redistribución dinámica de masas (DMR) en células HEK-293T transfectadas con el receptor CB_1, el receptor CB_2 o el complejo heterómerico formado por los receptores CB_1-CB_2. La concentración que se aplicó de CBD (100 nM) no permite su unión de forma significativa al sitio ortostérico a ninguno de los receptores cannabinoides. Es destacable como los dos compuestos cannabinoides (Δ^9-THC y CP-55940) con capacidad de producir efectos psicoactivos en el organismo mostraron un sesgo similar en CB_1R y, además, el Δ^9-THC al actuar sobre CB_2R no fue capaz de activar la proteína $G\alpha_i$. De manera interesante, el fenómeno del agonismo sesgado se ve reducido en células que expresan el complejo heteromérico de receptores CB_1-CB_2. También se observa como el cotratamiento con CBD modifica, probablemente uniéndose al sitio alostérico de los receptores cannabinoides, la funcionalidad de los compuestos cannabinoides ensayados. Además, de forma novedosa, se caracteriza en un contexto heteromérico el agonismo sesgado de los GPCR.

Biochemical Pharmacology 157 (2018) 148–158

Contents lists available at ScienceDirect

Biochemical Pharmacology

journal homepage: www.elsevier.com/locate/biochempharm

Cannabidiol skews biased agonism at cannabinoid CB_1 and CB_2 receptors with smaller effect in CB_1-CB_2 heteroreceptor complexes

Gemma Navarro[a,b], Irene Reyes-Resina[b,c], Rafael Rivas-Santisteban[b,c], Verónica Sánchez de Medina[d], Paula Morales[e], Salvatore Casano[d], Carlos Ferreiro-Vera[d], Alejandro Lillo[c], David Aguinaga[c], Nadine Jagerovic[e], Xavier Nadal[d,*], Rafael Franco[b,c,*]

[a] Molecular Neurobiology Laboratory, Department of Biochemistry and Physiology, Universitat de Barcelona, Barcelona, Spain
[b] Centro de Investigación en Red, Enfermedades Neurodegenerativas (CIBERNED), Instituto de Salud Carlos III, Madrid, Spain
[c] Molecular Neurobiology Laboratory, Department of Biochemistry and Molecular Biomedicine, Universitat de Barcelona, Barcelona, Spain
[d] Phytoplant Research S.L., Córdoba, Spain
[e] Instituto de Química Médica, Consejo Superior de Investigaciones Científicas, Madrid, Spain

ARTICLE INFO

Keywords:
BRET
CNS
Drug discovery
Endocannabinoids
G-protein-coupled receptor
Phytocannabinoids

ABSTRACT

Currently, biased agonism is at the center stage of drug development approaches. We analyzed effects of a battery of cannabinoids plus/minus cannabidiol (CBD) in four functional parameters (cAMP levels, phosphorylation of extracellular signal–regulated kinases (ERK1/2), β-arrestin recruitment and label-free/DMR) in HEK-293T cells expressing cannabinoid receptors, CB_1 or CB_2, or CB_1-CB_2 heteroreceptor complexes. In all cases two natural agonists plus two selective synthetic agonists were used. Furthermore, the effect of cannabidiol, at a dose (100 nM) that does not allow significant binding to the orthosteric center of either receptor, was measured. From the huge amount of generated data, we would like to highlight that the two psychotropic molecules (Δ^9-tetrahydrocannabinol/THC and CP-55940) showed similar bias in CB_1R and that the bias of THC was particularly relevant toward MAPK pathway. Furthermore, THC did not activate the G_i protein coupled to CB_2R. Interestingly, the biased agonism was reduced when assays were performed in cells expressing the two receptors, thus suggesting that the heteromer allows less functional selectivity. In terms of cannabidiol action, the phytocannabinoid altered the functional responses, likely by allosteric means, and modified potency, agonist IC_{50}/EC_{50} values and biased agonism in qualitative and/or quantitative different ways depending on the agonist. The effect of cannabidiol on anandamide actions on both cannabinoid receptors was particularly noteworthy as was significantly different from that of other compounds. Results are a compendium of data on biased agonism on cannabinoid receptors in the absence and presence of cannabidiol. In addition, for the first time, GPCR biased agonism is characterized in an heteromeric context.

1. Introduction

Endocannabinoid function is mediated by the two main endocannabinoids, anandamide and 2-arachidonoylglycerol (2-AG), and the cannabinoid CB_1 and CB_2 receptors, which also respond to phytocannabinoids derived from *Cannabis sativa* L.. CB_1 and CB_2 are class A rhodopsin-like members of the superfamily of G-protein-coupled receptors (GPCR) and their cognate protein is G_i, i.e. their activation by cannabinoids leads to the inhibition of adenylate cyclase activity and the decrease of intracellular cAMP levels. The hydrophobic nature of the endogenous agonists, 2-AG and anandamide, is an important issue to understand cannabinoid receptor pharmacology. The binding mode of receptor agonists seemingly contrasts with that of many of class A GPCRs, whose orthosteric site is formed by a cavity located within the seven transmembrane helix barrel and, therefore, is open wide to the extracellular milieu [1,2]. The elucidation of the structure of the CB_1 receptor, recently achieved in two different laboratories, confirmed the hydrophobicity hypothesis but adds a new element, namely that the orthosteric site is hidden by the N-terminal end of the receptor that acts as a lid. Accordingly, it is now hypothesized that agonists enter to the

* Corresponding authors at: The Science and Technology Park of Córdoba-Rabanales 21, Astrónoma Cecilia Payne Street, Centauro Building, B-1, 14014 Córdoba, Spain (X. Nadal). Dept. Biochemistry and Molecular Biomedicine, School of Biology, University of Barcelona, Avda. Diagonal 643, Prevosti Building, 08028 Barcelona, Spain (R. Franco).
E-mail addresses: x.nadal@phytoplant.es (X. Nadal), rfranco@ub.edu (R. Franco).

https://doi.org/10.1016/j.bcp.2018.08.046
Received 31 May 2018; Accepted 31 August 2018
Available online 06 September 2018

orthosteric site laterally, via narrow openings within close transmembrane helical domains [3–5].

Among the phytocannabinoids extracted from *Cannabis sativa* L., cannabidiol (CBD) has attracted similar interest to that of the main psychoactive component in the plant, delta-9-tetrahydrocannabinol (THC). Whereas THC is a well-known non-selective cannabinoid receptor agonist acting in the orthosteric site, CBD's action was first attributed to cannabinoid receptors but, later on, experimental evidence suggested agonism at, among others, 5-hydroxytryptamine receptors, transient receptor potential (TRP)-like channels and peroxisome proliferator-activated γ (PPAR γ) receptors [6,7]. Nanomolar-ranged high affinity binding of CBD to the orthosteric site of cannabinoid or other receptors has never been reported [8–12]. Recently, two laboratories have reported modulation by CBD of CB_1 [13] and CB_2 [14] receptor function, likely by binding to an allosteric site. The results in those two reports point to a negative effect of CBD on cannabinoid receptor activation.

Functional selectivity is now one of the elements to consider in the GPCR field. In fact, functional selectivity consists of differential qualitative engagement of cytocrin signaling pathways [15]. The most straightforward way to approach the issue is to look for biased agonism; Kenakin defines biased agonists as those that "*select which signaling pathways become activated upon binding to the receptor*" [16]. In other words, two biased agonists for a given (e.g. cannabinoid) receptor are able to preferentially engage two different responses [17]. This paper provides insights into cannabinoid functional selectivity by means of two approaches. First, the biased signaling of two natural and two synthetic selective agonists for each receptor was tested in cells expressing CB_1, CB_2 or CB_1 and CB_2 receptors. The compounds used were: THC and anandamide as natural cannabinoids, and CP-55940, ACEA, JWH-133 and PM224 as synthetic cannabinoids. Secondly, we checked whether a low CBD concentration (100 nM), that does not allow significant binding to the orthosteric center, may affect biased agonism at both cannabinoid receptor types and/or heteroreceptor complexes. Calculation of the bias factor in the presence and absence of CBD gives novel insights into the pharmacology and signaling of cannabinoid receptors. A heat map of the CBD effect on both maximum effects and agonist IC_{50}/EC_{50} values also provides relevant information. THC bias properties seem important to understand its psychotropic and physiological activities; remarkably we found that THC engages G_i in CB_1- but not CB_2-receptor expressing cells.

2. Methods and materials

2.1. Reagents

ACEA, CP-55940, JWH-133, CGS-21680, LUF-5834 and anandamide (AEA) were purchased from Tocris Bioscience (Bristol, UK), CBD and THC analytical standard solutions were purchased from Cerilliant (Texas, US) and CB_2R agonist, 3-[[4-[2-*tert*-butyl-1-(tetrahydropyran-4-ylmethyl)benzimidazol-5-yl]sulfonyl-2-pyridyl]oxy]propan-1-amine (PM224), was developed as described elsewhere [18]. HEPES, pertussis and cholera toxins were purchased from SigmaAldrich (St. Louis, MO, US).

Compounds were handled using glass vials and tests were performed to check for actual concentration of compounds. In our assay conditions, the measure of concentrations after serial dilutions indicated that the actual concentration of compounds was > 95% in the 1–500 nM range (100% being the theoretical concentration assuming the initial compound was pure). Silanization of glass containers did not led to significant differences and, therefore, silanization was omitted.

2.2. Cannabinoid isolation, purification and analysis

CBD was purified from the Cannabis variety SARA (CPVO Application number 2015/0098; granted with decision N° EU 50007 of 16 July 2018) by crystallization, THC from the variety MONIEK (CPVO Application number 2016/0114; granted with decision N° EU 50008 of 16 July 2018) by liquid-liquid chromatography. Both compounds were purified following a previously described method [19] that provides compounds with > 95% purity. An Agilent liquid chromatography setup (Model 1260, Pittsburgh, PA, US) consisting of a binary pump, a vacuum degasser, a column oven, an autosampler and a diode array detector (DAD) equipped with a 150 mm length × 2.1 mm internal diameter, 2.7 µm pore size Poroshell 120 EC-C18 column was used for the quality control of the purified cannabinoids. The analysis was performed using water and acetonitrile both containing ammonium formate 50 mM as mobile phases. Flow-rate was 0.2 mL/min and the injection volume was 3 µL. Chromatographic peaks were recorded at 210 nm. All determinations were carried out at 35 °C. All samples were analyzed in duplicate. The results of each cannabinoid (CBD 98.5%, THC 95.3%) were calculated as weight (%) versus a commercial standard from Cerilliant (CBD batch n° FE01271601 and THC batch n° FE04231406).

2.3. Cell culture and transfection

Human embryonic kidney 293T (HEK-293T) cells were grown in DMEM supplemented with 2 mM L-glutamine, 1 mM sodium pyruvate, 100 units/mL penicillin/streptomycin, and 5% (v/v) FBS [all supplements were from Invitrogen, (Paisley, Scotland, UK)]. Cells were maintained at 37 °C in a humidified atmosphere of 5% CO_2 and were passaged, with enzyme-free cell dissociation buffer (13151-014, Gibco®, Thermo Fisher, Waltham, MA, US), when they were 80–90% confluent, i.e. approximately twice a week. Cells were transiently transfected with the PEI (Polyethylenimine, SigmaAldrich, St. Louis, MO, US) method as previously described [20,21]. Unless otherwise stated, the sequences of the cDNA used were those coding for the human receptors. *Ad hoc* experiments using cDNAs for receptors fused to YFP indicated similar levels of expression of receptors. Taking CB_1R-YFP as reference we found that the levels of CB_2R-YFP were similar and that the levels of the two receptors in co-transfected cells varied between a narrow range (90–110% of the values obtained in single-transfected cells). It should be noted that within a given experimental session, for instance of determination of cAMP levels, all agonists (plus/minus CBD when indicated) were tested in the same batch of transfected cells.

2.4. Bioluminescence resonance energy transfer (BRET) assays

HEK-293T cells were transiently cotransfected with a constant amount of cDNA encoding for CB_1-RLuc and with increasing amounts of cDNA corresponding to CB_2-YFP or D_1-YFP. 48 h after transfection cells were adjusted to 20 µg of protein using a Bradford assay kit (Bio-Rad, Munich, Germany) and bovine serum albumin for standardization. To quantify protein-YFP expression, fluorescence was read in a Mithras LB 940 (Berthold, Bad Wildbad, Germany) equipped with a high-energy xenon flash lamp, using a 30-nm bandwidth excitation and emission filters at 485 and 530 nm, respectively. For BRET measurements, readings were collected 1 min after addition of 5 µM coelenterazine H (Molecular Probes, Eugene, OR, US) using a Mithras LB 940, which allows the integration of the signals detected in the short-wavelength filter at 485 nm and the long-wavelength filter at 530 nm. To quantify protein-RLuc expression, luminescence readings were performed 10 min after 5 µM coelenterazine H addition using a Mithras LB 940. The net BRET is defined as [(long-wavelength emission)/(short-wavelength emission)] − C_f, where C_f corresponds to [(long-wavelength emission)/(short-wavelength emission)] for the donor construct expressed alone in the same experiment. GraphPad Prism software (San Diego, CA, US) was used to fit data. BRET is expressed as milli BRET units, mBU (net BRET × 1000) [22,23].

2.5. In situ proximity ligation assays (PLA)

HEK-293T cells grown on glass coverslips were fixed in 4% paraformaldehyde for 15 min, washed with PBS containing 20 mM glycine to quench the aldehyde groups and permeabilized with the same buffer containing 0.05% Triton X-100 (5 min treatment). Fixed cells were incubated for 1 h at 37° with blocking solution (from PLA kit, see below) and subsequently treated with specific antibodies against CB_1 (sc-293419 raised in mouse; 1/100) and CB_2 (sc-10073 raised in goat; 1/100) receptors (both from Santa Cruz Biotechnology, Dallas, TX, US) and processed using the PLA probes detecting mouse and goat antibodies [Duolink II PLA probe anti-Mouse plus and Duolink II PLA probe anti-Goat minus (SigmaAldrich, St. Louis, MO, US)]. Specificity of antibodies was tested in untransfected HEK-293T cells (data not shown). Duolink II in situ PLA detection kit [Duolink® In Situ Detection Reagents Red, DUO92008, developed by Olink Bioscience, Uppsala, Sweden; and now distributed by SigmaAldrich (St. Louis, MO, US) as Duolink® using PLA® Technology] was used to detect the presence/absence of receptor clusters in the samples, which were incubated with the ligation solution for 1 h, washed and subsequently incubated with the amplification solution for 100 min (both steps at 37 °C in a humid chamber). Nuclei were stained with Hoechst (1/100; SigmaAldrich, St. Louis, MO, US). Mounting was performed using 30% Mowiol (Merck, Darmstadt, Germany). Negative controls were performed by omitting the primary antibodies. Samples were observed in a Leica SP2 confocal microscope (Leica Microsystems, Mannheim, Germany) equipped with an apochromatic 63× oil-immersion objective (N.A. 1.4), and 405 nm and 561 nm laser lines. For each field of view a stack of two channels (one per staining) and 5 Z stacks with a step size of 1 μm were acquired.

2.6. cAMP determination

Two hours before initiating the experiment, HEK-293T cell-culture medium was replaced by serum-starved DMEM medium. Then, cells were detached, suspended in growing medium containing 50 μM zardaverine, a dual-selective PDE3/4 phosphodiesterase inhibitor used to prevent cAMP to AMP conversion [24], and placed in 384-well microplates (2500 cells/well). Cells were pretreated (15 min) with CBD-or vehicle- and stimulated with agonists (15 min) before adding 0.5 μM forskolin or vehicle (15 min). Readings were performed after one hour incubation at 25 °C. Homogeneous time-resolved fluorescence energy transfer (HTRF) measures were performed using the Lance Ultra cAMP kit (PerkinElmer, Waltham, MA, US). Fluorescence at 665 nm was analyzed in a PHERAstar Flagship microplate reader equipped with an HTRF optical module (BMG Lab technologies, Offenburg, Germany). None of the cannabinoid agonists used exert any significant effect in cells not expressing cannabinoid receptors. When using toxins, pertussis toxin was incubated for 24 h before the experiment, and cholera toxin was incubated for 30 min before the experiment. Positive control was obtained using the A_{2A} receptor, which is G_s-coupled and whose activation with a selective compound, CGS-21680 (100 nM), led to an increase in cAMP levels of approximately 250% over basal values.

2.7. ERK phosphorylation assays

To determine ERK1/2 phosphorylation, 50,000 HEK-293T cells/well were plated in transparent Deltalab 96-well microplates and kept at the incubator for 24 h. 4 h before the experiment, the medium was substituted by serum-starved DMEM medium. Then, cells were pretreated at 25 °C for 10 min with vehicle or CBD in serum-starved DMEM medium and stimulated for an additional 7 min with agonists. Cells were then washed twice with cold PBS before addition of lysis buffer (20 min treatment). 10 μL of each supernatant were placed in white ProxiPlate 384-well microplates and ERK1/2 phosphorylation was determined using AlphaScreen®SureFire® kit (Perkin Elmer, Waltham, MA, US) following the instructions of the supplier and using an EnSpire® Multimode Plate Reader (PerkinElmer, Waltham, MA, US). None of the cannabinoid agonists used exert any significant effect in cells not expressing cannabinoid receptors. Positive control was obtained using the A_{2A} receptor, which is G_s-coupled and whose activation with a selective compound, CGS-21680 (100 nM), led to an increase in pERK levels of approximately 220% over basal values.

2.8. Dynamic mass redistribution assays (DMR)

Cell mass redistribution induced upon receptor activation was detected by illuminating the underside of a biosensor with polychromatic light and measuring the changes in the wavelength of the reflected monochromatic light. The magnitude of this wavelength shift (in picometers) is directly proportional to the amount of DMR. HEK-293T cells were seeded in 384-well sensor microplates to obtain 70–80% confluent monolayers constituted by approximately 10,000 cells per well. Previous to the assay, cells were washed twice with assay buffer (HBSS with 20 mM HEPES, pH 7.15 and 1% BSA (SigmaAldrich, St. Louis, MO, US) and incubated for 2 h with assay-buffer containing 0.1% DMSO (24°, 30 μL/well). Hereafter, the sensor plate was scanned and a baseline optical signature was recorded for 10 min before adding 10 μL of CBD for 30 min followed by the addition of 10 μL of the agonist preparation; all test compounds were dissolved in assay buffer. The cell signaling signature was determined using an EnSpire® Multimode Plate Reader (PerkinElmer, Waltham, MA, US) by a label-free technology. Then, DMR responses were monitored for at least 5000 s. Results were analyzed using EnSpire Workstation Software v 4.10 and (in all cases) measures at 500 s were used for analysis.

2.9. β-arrestin 2 recruitment

Arrestin recruitment was determined as previously described [20,21]. Briefly, BRET experiments were performed in HEK-293T cells 48 h after transfection with the cDNAs corresponding to the CB_2R-YFP, CB_1R-YFP or CB_2R-YFP and CB_1R and 1 μg cDNA corresponding to β-arrestin 2-Rluc. Cells (20 μg protein) were distributed in 96-well microplates (Corning 3600, white plates with white bottom) and were incubated with CBD for 15 min and stimulated with the agonist for 10 min prior the addition of 5 μM coelenterazine H. After 10 min of adding coelenterazine H, BRET between β-arrestin 2-Rluc and receptor-YFP was determined and quantified. The readings were collected using a Mithras LB-940 (Berthold Technologies, Bad Wildbad, Germany) that allows the integration of the signals detected in the short-wavelength filter at 485 nm and the long-wavelength filter at 530 nm. To quantify protein-RLuc expression luminescence readings were also performed 10 min of adding 5 μM coelenterazine H. A (negative) control was obtained using a deletion mutant (lacking part of the C-terminal domain) of the adenosine A_{2A} receptor, that upon activation with LUF-5834 is unable to significantly recruit β-arrestin 2.

2.10. Calculation of bias factor

Using the operational model [25] and according to Rajagopal et al. [26], the bias factor "*quantifies the relative stabilization of one signaling state over another compared with a selected reference agonist*". The formulas and definitions are all taken from [26]. The formula to calculate bias factor "bias" is:

$$bias = 10^{\Delta\Delta \log\left(\frac{\tau}{K_A}\right) j_1 - j_2}$$

$$\log bias = \Delta \log(\tau/K_A) j_1$$

In which j_i denotes one of the analyzed pathways/responses (here j_1, j_2, j_3 and j_4, as four different responses were measured). The pathway of reference was the canonical for G_i, i.e. j_1 refers to cAMP level determinations. τ denotes the maximum value in each response and K_A is

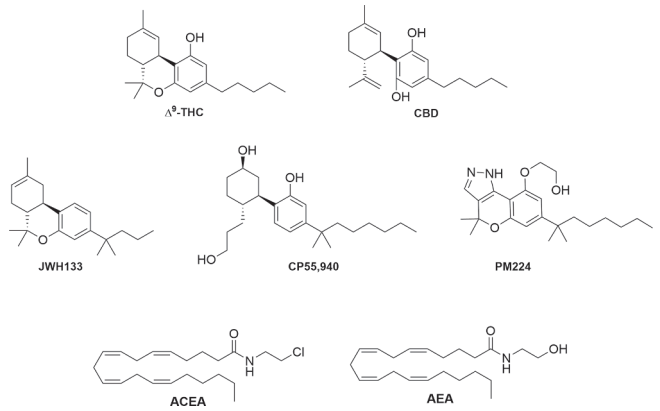

Fig. 1. Chemical structure of compounds used in the study.

the antilogarithm of half maximal effective concentration: EC_{50} if the agonist provides a direct response or IC_{50} if the agonist provides a reduction of the response provided by another reagent (for instance forskolin in cAMP level determination assays).

2.11. Statistical analysis

Data are the mean ± S.E.M. Comparisons were performed using one-way ANOVA followed by *post-hoc* Bonferroni's test. $P < 0.05$ was considered as significant.

3. Results

3.1. Biased agonism in CB_1 receptors

Four different functional readouts were analyzed for CB_1 receptor activation: cAMP, ERK1/2 phosphorylation, β-arrestin 2 recruitment and dynamic mass redistribution (DMR) assays in transiently expressed receptors activated using different natural or synthetic cannabinoids (Fig. 1). In the case of CB_1 receptor (CB_1R) ACEA was the agonist of reference, as it is considered a full agonist with consistent inter-assay results. The functional response used as reference to calculate the bias factor was the canonically linked to G_i, i.e. the effect on forskolin-induced intracellular cAMP levels in the presence of zardaverine, a dual-selective PDE3/4 phosphodiesterase inhibitor used to prevent cAMP to AMP conversion [24]. Fig. 2A shows the effect of ACEA in forskolin-induced cAMP levels in CB_1R-expressing cells. The effects of THC and ACEA were similar, i.e. the two compounds behaved as full agonists, but the EC_{50} of ACEA was lower. In ERK1/2 phosphorylation, ACEA effect was higher and the EC_{50} was lower than that of THC. Fig. 2B shows the effect of ACEA and THC in MAP kinase pathway engagement. When normalized to G_i-mediated signal of ACEA, the bias factor of THC for ERK1/2 phosphorylation was 45.3. Similar experiments were performed for β-arrestin 2 recruitment (Fig. 2C) and for DMR, a label-free technique that has provided relevant information on GPCR research (see [27,28] for review). The radar plot showing bias factors for four agonists, ACEA, anandamide, THC and CP-55940 and for the four signaling responses (cAMP, ERK1/2 phosphorylation, β-arrestin 2 recruitment and DMR) taking cAMP and ACEA as reference is shown in Fig. 2D. From these results, a number of features may be highlighted. We observed similar behavior of ACEA and anandamide with the

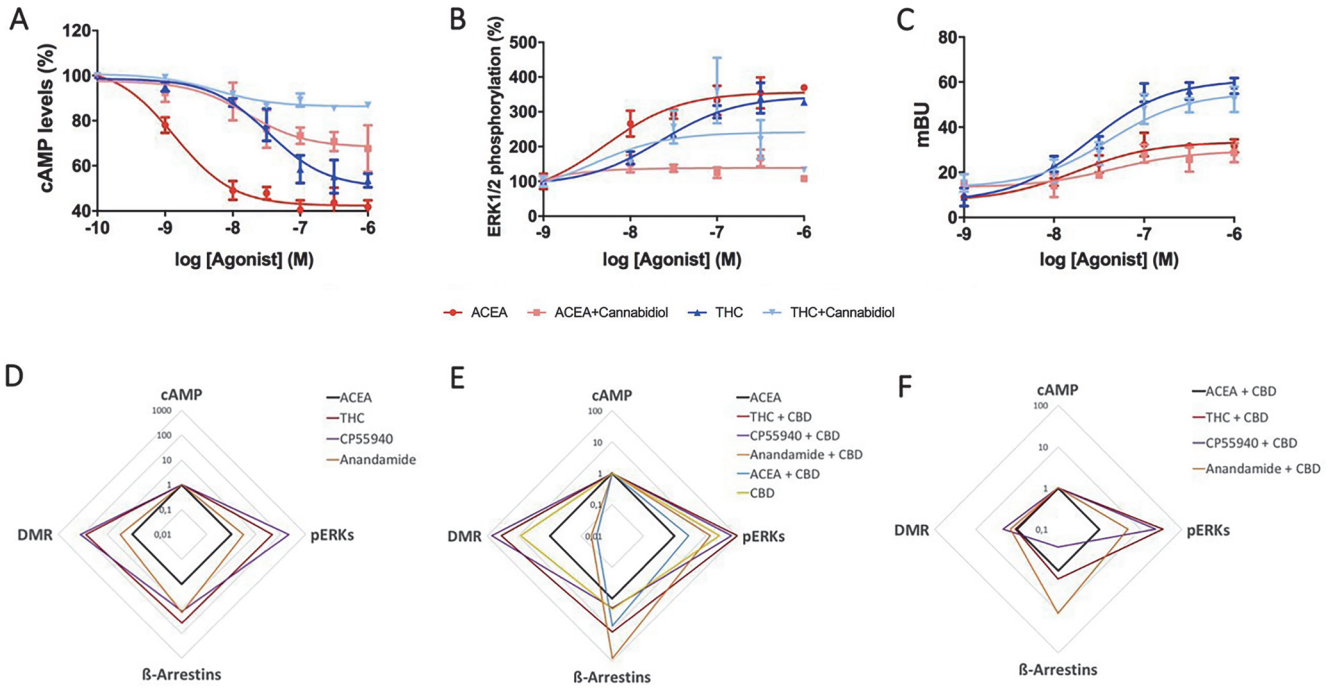

Fig. 2. Signaling and biased agonism on CB_1 receptors. Panels A and B: HEK-293T cells expressing human CB_1R (0.7 μg cDNA) and treated with the indicated cannabinoids in the presence (weak color) or absence (intense color) of 100 nM CBD. The effect of compounds on 500 nM forskolin-induced cAMP levels (100%) was determined as described in Methods, and data are expressed as % of reduction (A). ERK1/2 phosphorylation data are expressed as % respect to basal levels (B). Panel C: HEK-293T were transfected with cDNAs corresponding to β-arrestin 2-RLuc and CB_1R-YFP. Cells (20 μg protein) were distributed in 96-well microplates and BRET assays were initiated by the addition of coelenterazine H; BRET was determined 10 min after substrate addition and data are given in milli BRET units (mBU; see further details in Methods). Data represent the mean ± SEM of 6 different experiments performed with 3 replicates. Panels D–F. Radar plots showing the bias factors of the different compounds in the different functional outcomes in the absence (D) or presence of 100 nM CBD (E, F). In D and E, the compound of reference was ACEA and the response of reference was forskolin-induced cAMP. In E, the plot of bias due to CBD is included; it should be noted that this plot is constructed using CBD at different concentrations (in the absence of any other cannabinoid) and, therefore, is due to binding to the orthosteric center (and requires micromolar concentrations of CBD). In F, the treatment of reference was ACEA + CBD.

Table 1
CBD-induced modification of potency and maximum effect in cells expressing CB_1 (top), CB_2 (middle) or CB_1 and CB_2 (botom) receptors.

	EC50[a]				Maximum effect[b]			
	HEK-293T – CB_1R							
	cAMP	ERKs	β-Arrestins	DMR	cAMP	ERKs	β-Arrestins	DMR
ACEA + CBD	12.02*	0.55	2.99*	0.15*	−44.9	−85.3	−11.9	−33.0
THC + CBD	0.16	0.28*	0.18*	0.54	−72.3	−46.4	−9.3	−26.9
CP55940 + CBD	1.14	0.20*	1.14	0.30*	−80.1	−70.2	14.3	−34.6
Anandamide + CBD	8.9r2*	0.85	1.40	0.38*	−15.4	−61.9	−15.3	−49.1
	HEK-293T – CB_2R							
	cAMP	ERKs	β-Arrestins	DMR	cAMP	ERKs	β-Arrestins	DMR
JWH133 + CBD	4.79*	0.72	1.43	1.05	−2.5	−35.5	−6.2	−27.2
THC + CBD	NC[c]	0.33*	1.88	1.09	NC[c]	−22.0	−13.6	−40.9
PM224 + CBD	NC[c]	1.80	2.69*	0.98	NC[c]	−5.9	0.9	−35.1
Anandamide + CBD	17.24*	NC[c]	1.61	0.27*	−33.8	NC[c]	−10.2	−69.5
	HEK-293T – CB_1R-CB_2R							
	cAMP	ERKs	β-Arrestins	DMR	cAMP	ERKs	β-Arrestins	DMR
ACEA + CBD	2.86*	0.83	0.10*	0.59	−16.6	−41.2	10.3	−29.3
THC + CBD	NC[c]	1.34	0.46*	0.63	NC[c]	−36.8	−10.6	−22.5
CP55940 + CBD	0.92	0.94	0.92	0.61	−5.9	−39.0	−4.6	−17.1
Anandamide + CBD	2.78*	0.69	1.40	0.48*	−31.4	−52.0	−13.1	−23.3
JWH133 + CBD	1.27	0.57	0.24*	0.69	−43.3	−30.8	−20.4	−18.2
PM224 + CBD	6.52*	0.98	0.29*	0.61	−1.9	−39.3	−0.4	−33.7

[a] In-fold versus parameter values in the absence of CBD.
[b] Values in percentage (100% being the value in the absence of CBD).
[c] NC: It was not possible to calculate the value because of the uncertainty in values related to cannabinoid agonist effect on tested assay (either in CB2- or CB1 and CB2-receptor expressing cells).
* $p < 0.05$.

exception of anandamide being more biased to β-arrestin recruitment than ACEA. Also interesting is the finding of a similar bias to MAPK and β-arrestin when CB_1R was activated with the two known psychotropic compounds, the phytocannabinoid ligand THC, and the synthetic cannabinoid CP-55940.

Similar experiments were performed in the presence of 100 nM CBD. The results from cAMP levels, ERK1/2 phosphorylation and β-arrestin assays in response to ACEA and THC are shown in Fig. 2A–C and in Table 1. Remarkably, the aforementioned concentration of CBD markedly decreased the signaling of compounds as structurally different as ACEA and THC (Fig. 1). The radar plot showing bias factors for the four agonists and their corresponding responses in the presence of CBD is shown in Fig. 2E. First of all, this radar plot shows that the biased effect of CBD on ACEA was similar to that of anandamide. Secondly, although CP-55940 and THC behaved, again, similarly, CBD was able to virtually abrogate the β-arrestin bias of the synthetic compound, but not of the natural compound, THC. Table 1 shows that CBD is reducing the effect of almost all the agonists, being remarkable the abolishment of the DMR signal produced by ACEA. The effect of single treatments with 100 nM CBD were < 10% of the maximal ones obtained by either ACEA or THC; therefore, they were considered as negligible in both calculations and data interpretation. Fig. 2E includes the radar plot for CBD, i.e. performing the dose-response assays and using the EC_{50}/IC_{50} values due to binding to the orthosteric center (i.e. EC_{50}/IC_{50} values were in the micromolar range). When data are re-interpreted taking as a reference cAMP and ACEA + CBD, the radar plots show that the other three tested agonists showed a marked bias except for DMR (Fig. 2F). It should be also noted that CBD by itself is able to produce a label-free signal but at high concentrations (EC_{50} = 9.7 μM). In the case of THC, the effect of CBD is almost opposite to that exerted on ACEA as the effect on [cAMP] is almost abolished but the MAPK signaling is only reduced (Fig. 2A and B). Overall, CBD exerted potent regulation of CB_1R-mediated effects and the bias trend depended on the agonist used, i.e. CBD effect on bias was different depending on the particular bias displayed by each agonist.

3.2. Biased agonism in CB_2 receptors

The same four different functional responses were analyzed for CB_2 receptor activation, being JWH-133 the agonist of reference for similar reasons as those used to select ACEA in the case of CB_1R, i.e. a full agonist with consistent inter-assay results. Also, the functional readout of reference to calculate the bias factor was that related to G_i. Fig. 3A shows the full agonism of JWH-133 in forskolin-induced cAMP levels in cells expressing the CB_2R. The same figure shows the lack of effect of THC; actually, if any, THC leads to small increases of cAMP levels. As demonstrated by the use of cholera toxin (see below) THC did not engage Gs proteins, a possibility that was first suggested in 1997 [29]. Fig. 3B shows the effect of JWH-133 and THC in MAP kinase pathway engagement. ERK1/2 phosphorylation produced by JWH-133 treatment was lower than the effect produced by THC. When normalized to JWH-133 and the G_i-mediated signal, the bias factor of THC for ERK1/2 phosphorylation was 1.7. Fig. 3D shows the radar plot for four agonists, JWH-133, anandamide, THC and PM224 [18] and four signaling responses (cAMP, ERK1/2 phosphorylation, β-arrestin recruitment – Fig. 3C- and DMR) taking cAMP and JWH-133 as reference. As in the case of CB_1R, the radar plot showing results for CB_2R-mediated effects, provides relevant information. On the one hand, THC showed a moderate bias towards β-arrestin recruitment and DMR. On the other hand, anandamide provided the largest deviation because it did not show preference for DMR but, mainly, because the bias factor to MAPK signaling was unexpectedly small. Despite differences in chemical structures, PM224 showed no special bias when JWH-133 and cAMP were taken as references.

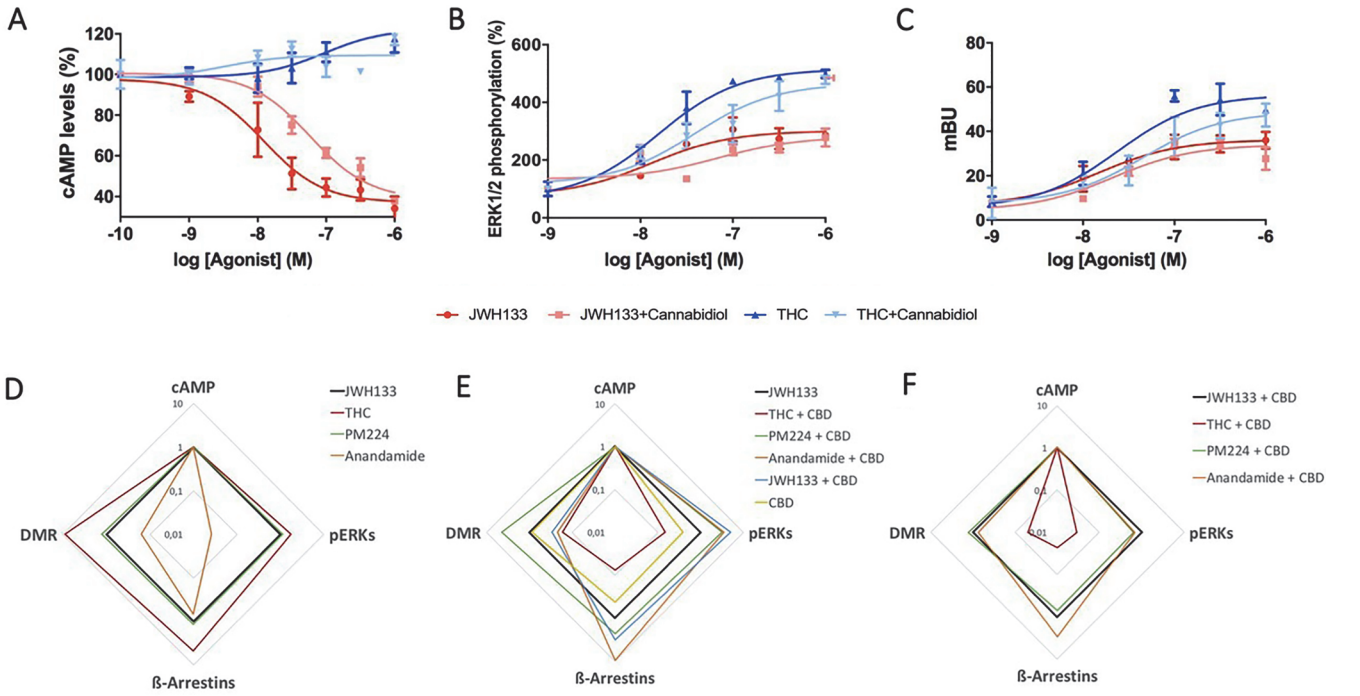

Fig. 3. Signaling and biased agonism on CB_2 receptors. Panels A and B: HEK-293T cells expressing human CB_2R (0.5 µg cDNA) and treated with the indicated cannabinoids in the presence (weak color) or absence (intense color) of 100 nM CBD. The effect of compounds on 500 nM forskolin-induced cAMP levels (100%) was determined as described in methods, and data are expressed as % of reduction (A). ERK1/2 phosphorylation data are expressed as % respect to basal levels (B). Panel C: HEK-293T cells were transfected with cDNAs corresponding to β-arrestin 2-RLuc and CB_2R-YFP. Cells (20 µg protein) were distributed in 96-well microplates and BRET assays were initiated by the addition of coelenterazine H; BRET was determined 10 min after substrate addition and data are given in milli BRET units (mBU; see further details in Methods). Data represent the mean ± SEM of 6 different experiments performed with 3 replicates. Panels D-F. Radar plots showing the bias factors of the different compounds in the different functional outcomes in the absence (D) or presence of 100 nM CBD (E, F). In D and E, the compound of reference was JWH-133 and the response of reference was forskolin-induced cAMP. In E, the plot of bias due to CBD is included; it should be noted that this plot is constructed using CBD at different concentrations (in the absence of any other cannabinoid) and, therefore, is due to binding to the orthosteric center (and requires micromolar concentrations of CBD). In F, the treatment of reference was JWH-133 + CBD.

Similar experiments performed in the presence of 100 nM CBD showed a marked modification of biased agonism, much more significant than in the case of the CB_1 receptor (Table 1). One relevant finding was the increased bias of PM224 when compared with the reference compound (JWH-133). It should be noted that CBD-induced reduction of G_i engagement due to JWH-133 is significant but quantitatively modest [14]. Bias factors for THC were fairly different than in the absence of CBD (Fig. 3E and F). Except in cAMP assays, the effect of single treatments with 100 nM CBD were < 10% of the maximal ones in JWH-133 or THC; therefore, they were considered as negligible in both calculations and data interpretation. The effect of 100 nM CBD in cAMP assays was approximately a 25% of that obtained by JWH-133. Fig. 3E includes the radar plot for CBD, i.e. performing the dose-response assays and using the EC_{50}/IC_{50} values due to binding to the orthosteric center (i.e. EC_{50}/IC_{50} values were in the micromolar range). Finally, CBD exerted less effect on anandamide than on other agonists. The latter result is probably of physiological relevance as it seems that anandamide displays more balanced actions on CB_2R in the presence of nanomolar concentrations of CBD. In summary, CBD significantly modified CB_2R agonism; notably, CBD profoundly affected the agonist effect of anandamide.

3.3. Biased agonism in CB_1-CB_2 receptors heteromers (CB_1-CB_2-Hets)

The next aim of the study was to perform signaling assays in cells co-expressing the two receptors and, likely, expressing CB_1-CB_2-Hets [30,31]. A direct interaction was obtained in biophysical BRET experiments using cells co-expressing CB_1-RLuc and CB_2-YFP, which provides a saturation curve indicative of a specific interaction between the two receptors, while the (negative) control performed in cells expressing CB_1-RLuc and the dopamine D_1 receptor fused to YFP gave an unspecific linear signal (Fig. 4A). We also undertook PLA, which is a tool to detect heteromers even in natural sources. The results in co-transfected cells provided red clusters, which correspond to heteromer expression, that were surrounding Hoechst-stained nuclei (Fig. 4B). Subsequently we wanted to address whether the heteromer was G_i-coupled as when the receptors are individually expressed. Accordingly, we performed similar experiments of cAMP determination in CB_1-, CB_2- or CB_1-CB_2-Het-expressing cells preincubated with either pertussis toxin, which affects G_i-mediated signaling, or cholera toxin, which affects G_s-mediated signaling. The results displayed in Fig. 4 C, indicate that G_i-coupling in CB_1-expressing cells treated with ACEA was abolished using pertussis but not cholera toxin. Similar results were obtained in CB_2-expressing cells treated with JWH-133 and CB_1-CB_2-Het-expressing cells with ACEA or with JWH-133, thus showing that the heteromer is coupled to G_i protein. In order to test whether THC may engage receptors eventually coupled to G_s, we performed parallel assays using THC. The results show that THC does not engage any G_s-mediated signaling, although it is confirmed that the phytocannabinoid does engage G_i in CB_1-expressing cells (Fig. 4C).

The four different functional responses were analyzed in cells co-expressing the two receptors and the main differential results respect to cells expressing only one receptor were i) the lack of G_i-coupling when receptors are activated by THC in a heteromeric context and ii) the reduced potency of JWH-133 on engaging the MAPK pathway if compared with THC or ACEA. As for individual receptors, 100 nM CBD produced reductions in the effect of agonists on heteroreceptor complexes (Fig. 5A–C). The results related to biased agonism were analyzed using ACEA as reference compound. The pathway of reference to calculate the bias factor was not changed, i.e. it was the G_i-mediated

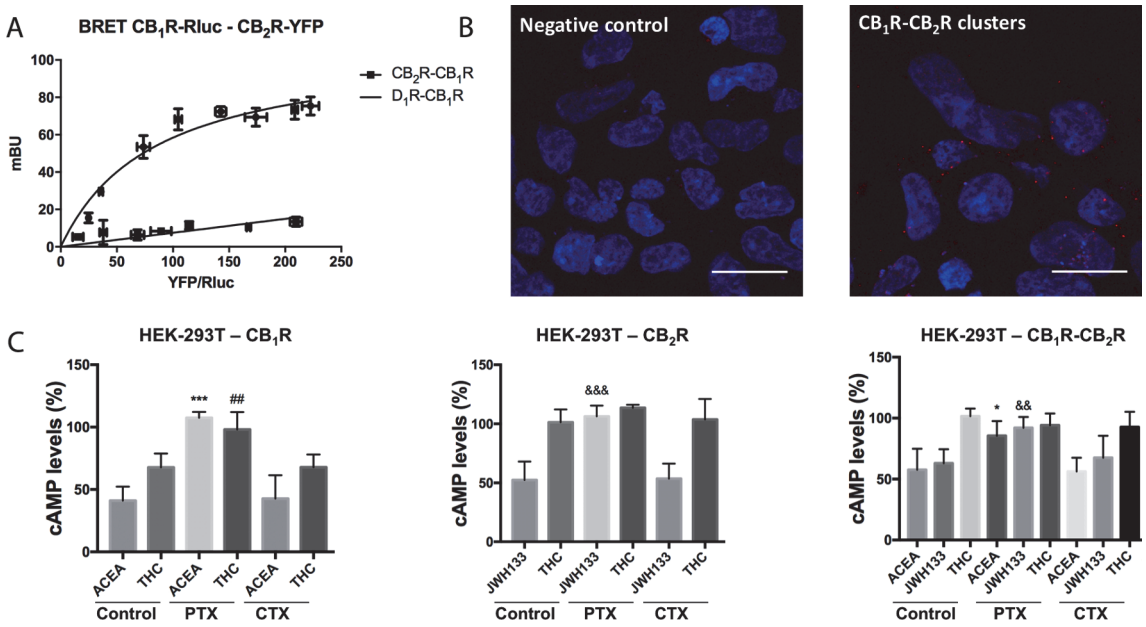

Fig. 4. Effect of toxins in CB_1- and/or CB_2- receptor expressing cells. Panel A: BRET assays were performed in HEK-293T cells transfected with a constant amount of cDNA for CB_1R-RLuc (0.7 μg) and increasing amounts of cDNA for CB_2R-YFP (0.2–1 μg). As negative control, HEK-293T cells were transfected with a constant amount of CB_1R-RLuc (0.7 μg) and increasing amounts of cDNA coding for the dopamine D_1 receptor fused to YFP (0.3–1.5 μg). Values are ± S.E.M. of 8 different experiments. Panel B: Representative confocal microscopy images (five superimposed sections) of an in situ proximity ligation assays (PLA) in cells coexpressing CB_1 and CB_2 receptors. CB_1R-CB_2R heteroreceptor complexes appear as red spots. Cell nuclei were stained with Hoechst (blue). As negative control, PLA was performed in the absence of one primary antibody. Scale bars = 20 μm. Panel C: HEK-293T cells were transfected with cDNA for CB_1R (left), for CB_2R (middle) or both (right). Cells were treated with selective agonists (100 nM ACEA for CB_1 receptors; 100 nM JWH-133 for CB_2 receptors) or with 100 nM THC in both absence (control) or presence of either 10 ng/ml pertussis toxin (PTX) or 100 ng/ml cholera toxin (CTX). cAMP accumulation was detected by TR-FRET (see Methods) in cells pretreated with 0.5 μM forskolin. Values are mean ± S.E.M. of 5 different experiments performed in triplicates. In all cAMP accumulation assays, one-way ANOVA followed by Bonferroni's multiple comparison post hoc test were used for statistical analysis. ($^{*}p < 0.05$, $^{***}p < 0.001$; versus ACEA). ($^{\#\#}p < 0.01$; versus THC). ($^{\&\&}p < 0.01$, $^{\&\&\&}p < 0.001$; versus JWH-133.)

inhibition of adenylate cyclase. Remarkably, the biased agonism (in the absence of CBD) virtually disappeared as indicated in the radar plots in Fig. 5D. The exception was JWH-133 that, within the heteromeric context, lost its ability to engage the MAPK pathway. Similar assays performed in the presence of CBD showed that the phytocannabinoid was able to modify the bias but to a less extent than in cells expressing individual receptors (Fig. 5). It should be however noted that CBD affected more the bias of natural than of synthetic cannabinoids (Table 1). On the one hand, the selective CB_2R agonist, JWH-133 showed similar bias in the absence and in the presence of CBD. On the other hand, anandamide signaling towards the MAPK pathway was markedly decreased while its responses were slightly reduced in DMR and β-arrestin recruitment. Finally, CBD increased by two orders of magnitude the THC functional activity towards MAPK, β-arrestin and DMR. In summary, CB_1-CB_2-Hets displayed less functional sensitivity than individual receptors, and CBD altered the bias of natural cannabinoids acting on cannabinoid receptor heteromers (Fig. 5E and F).

3.4. Differential bias in CB_1-, CB_2- and CB_1-CB_2-Het-expressing cells

Data collected from all the experiments performed in the three cell types have been comparatively analyzed using a heat map approach; the results are displayed in Fig. 6. In terms of CBD effects on efficacy (maximum responses), the results are qualitatively similar in all assayed cells. CBD reduced the maximum effect of any agonist of any of the receptors. The magnitude was strong in CB_1-receptor expressing cells whereas it was very mild in CB_2-receptor-expressing cells. The results in cotransfected cells were also moderate, more similar to those in CB_2- than to those in CB_1-expressing cells. Occasionally, CBD led to increases in maximum effect but of very small magnitude (around 10%, pale rose color in Fig. 6).

The differences due to CBD in EC_{50}/IC_{50} values were significant, specially in cells expressing the CB_1 receptor and in cotransfected cells (Fig. 6). Quite often in these cells CBD led to decrease in the potency of the agonists. Then, in the majority of cases CBD led to reduce maximum effect and agonist potency. In some cases, however, CBD led to an increase in potency while decreasing the maximum effect. For instance, this occurred in the case of cAMP read-outs in response to ACEA acting on CB_1-expressing cells and, with a lower intensity in cotransfected cells. The pattern in CB_2 receptor-expressing cells is different and the effect on the concentration given a 50% of the response was usually positive, i.e. decreasing EC_{50} or IC_{50} values. Thus, in these cells CBD was lowering maximal effects but increasing the potency; quantitatively however the changes were moderate. Interestingly, the most significant effect was found for the phytocannabinoid THC, as CBD decreased (moderately) maximal effects and the potency (significantly) of THC when MAPK activation was measured. Overall, these results confirm that the effect of CBD is meaningful and varied depending on the cannabinoid receptor, the agonist and the occurrence or not of cannabinoid receptor heteromers.

4. Discussion

GPCR receptor action may be modulated in different ways depending on the cellular context. GPCR-mediated signaling not only depends on the coupled G protein, but on other molecules able to interact with the receptor and/or with the signaling machinery [32–37]. Biased agonism, one of the recent and promising approaches for drug discovery, is particularly relevant for cannabinoid receptors whose pharmacological development is hampered by both the hydrophobic nature of agonists and the particular structure of receptors, solved for CB_1R [3–5] and assumed to be similar for CB_2R [38].

This paper focused first on comparing biased agonism in CB_1R and CB_2R using synthetic agonists as reference and using an

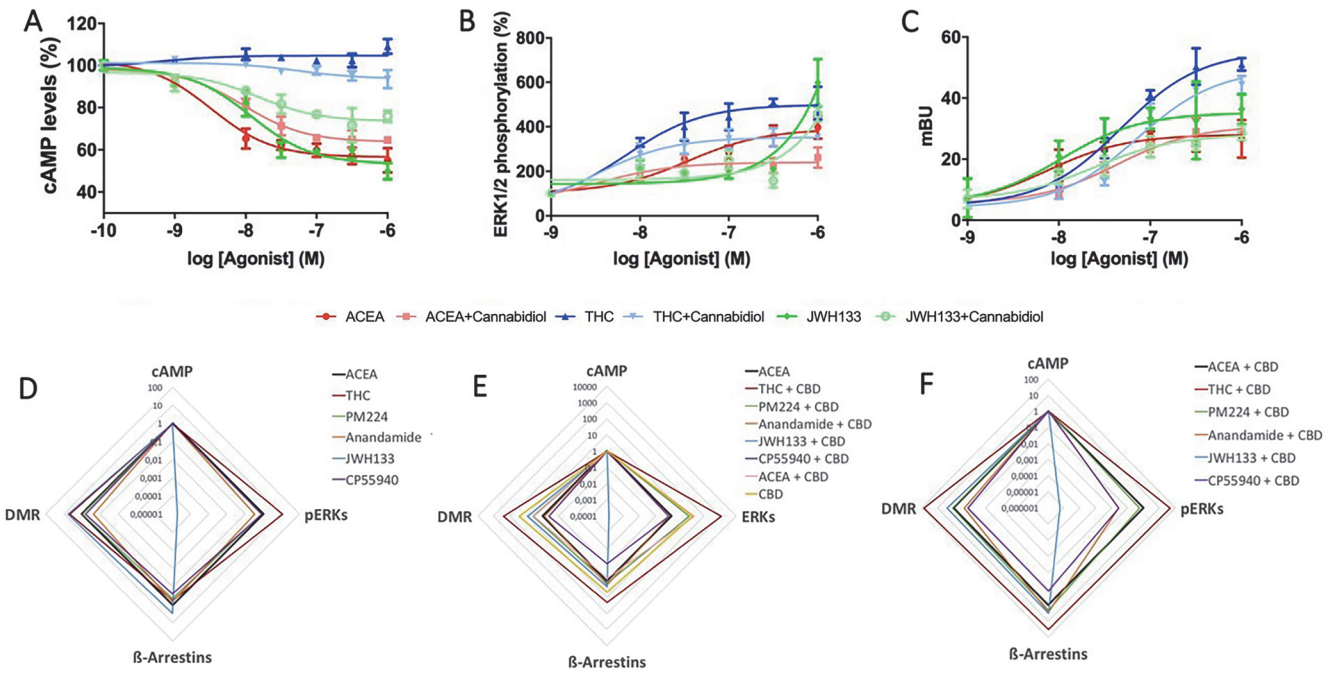

Fig. 5. Signaling and biased agonism on CB_1/CB_2 heteroreceptor complexes. Panels A and B: HEK-293T cells expressing human CB_1R (0.5 μg cDNA) and CB_2R (0.4 μg cDNA) and treated with the indicated cannabinoids in the presence (weak color) or absence (intense color) of 100 nM CBD. The effect of compounds on 500 nM forskolin-induced cAMP levels (100%) was determined as described in methods, and data are expressed as % of reduction (A). ERK1/2 phosphorylation data are expressed as % respect to basal levels (B). Panel C: HEK-293T were transfected with cDNAs corresponding to β-arrestin 2-RLuc, CB_2R-YFP and CB_1R. Cells (20 μg protein) were distributed in 96-well microplates and BRET assays were initiated by the addition of coelenterazine H; BRET was determined 10 min after substrate addition and data are given in milli BRET units (mBU; see further details in Methods). Data represent the mean ± SEM of 6 different experiments performed with 3 replicates. Panels D–F. Radar plots showing the bias factors of the different compounds in the different functional outcomes in the absence (D) or presence of 100 nM CBD (E, F). In D and E, the compound of reference was ACEA and the response of reference was forskolin-induced cAMP. In E, the plot of bias due to CBD is included; it should be noted that this plot is constructed using CBD at different concentrations (in the absence of any other cannabinoid) and, therefore, is likely due to binding to the orthosteric center (and that requires micromolar concentrations of CBD). In F, the treatment of reference was ACEA + CBD.

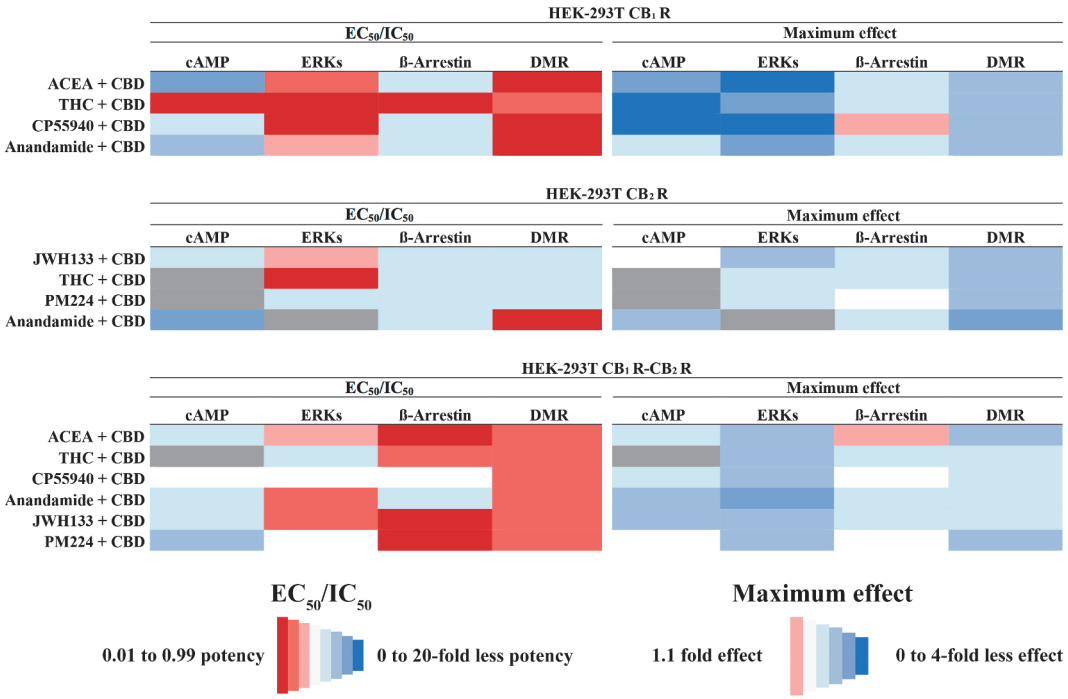

Fig. 6. Heat maps of the differential effect of CBD on maximal and IC_{50}/EC_{50} values obtained in cells expressing CB_1 and/or CB_2 receptors. Values of maximal IC_{50}/EC_{50} corresponding to the different signaling pathways were computed and independently compared in the three cell types. Color code is designed in such a way that red indicates higher maximal effect or maximal differences in IC_{50}/EC_{50} values (always comparing with values obtained in the absence of CBD). Indication of the magnitude of the changes is shown in the scheme at the bottom. White color indicates negligible differences (within a ± 5% range). Grey color indicates that the comparison could not be properly done, for instance when data values were small and, therefore, giving rise to unreliable results.

endocannabinoid, anandamide, and the psychoactive component of *Cannabis sativa* L., THC. Taking into account all agonists except THC, biased agonism is more marked for CB_1 than for CB_2 receptors. Anandamide for instance is a little biased in CB_2R while it is markedly biased towards β-arrestin recruitment in CB_1R. The results concerning THC were unexpected. On the one hand, bias in CB_1R was similar to that of another psychoactive compound, CP-55940. On the other hand, THC action on CB_2R appears as markedly biased towards ERK1/2 phosphorylation, β-arrestin recruitment and DMR. Interestingly, such trend in cells expressing CB_2R correlated with an apparent failure to couple to G_i when activated by THC. In fact, THC robustly engaged G_i-mediated coupling in CB_1R but not in CB_2R. There is controversy surrounding THC action on CB_2R, in some studies THC reportedly engages G_i via CB_2R [39–43] meanwhile in some other studies, in agreement with our findings, THC failed to engage G_i via CB_2R [44–47]. In CB_2R-expressing CHO cells THC displays an IC_{50} of 42 nM for inhibition of forskolin-stimulated cAMP levels [39]. Above this concentration and up to 1 μM, THC was able to reduce forskolin-stimulated cAMP levels in mouse CB_2R CHO transfected cells but was unable to produce a significant reduction of forskolin-stimulated cAMP levels in CHO cells expressing the human CB_2R [42]. In contrast, THC at concentrations from 10 nM to 1 μM was not able to inhibit forskolin-stimulated cAMP levels in COS-7 and CHO hCB_2R transfected cells [44,45]. Possibilities to explain discrepancies are, among others, i) G_i-coupled signaling could be due to THC acting on CB_1R and not on CB_2R, ii) there is another receptor that is responding to THC via G_i or iii) the high concentrations used (e.g. 10–50 μM [40,42,43,48]) are providing unspecific/off-site effects that result in decreases in forskolin-induced cAMP levels. Overlooking the discrepancies, we observe that THC in concentrations below 1 μM is not able to reduce the cAMP in a variety of cell types expressing the human CB_2R. Therefore, our findings are in agreement with the literature and permit us to infer that THC activated CB_2R is not able to engage the coupled G_i protein or is interacting with a conformation of the receptor that is not coupled to G_i. Coupling to G_s has been discarded by the results with toxins reported in Fig. 4. Therefore, it is suggested that THC binds to a part of the orthosteric site that is not connected to G_i activation mechanisms. As phospholipase Cβ3 activation may occur by THC acting on CB_1R, we cannot exclude that the compound can promote the activation of a G_q protein [17]. Other possibilities such as off-target actions leading to blockade of G_i activation cannot be ruled out. In our opinion, one of the advantages of performing these studies in parallel is to show that the coupling to the cognate protein of cannabinoid receptors does not occur in the case of CB_2R but occurs in the case of CB_1R, in which THC behaves as a potent full agonist able to decrease forskolin-induced cAMP levels.

Biased allosteric modulation, i.e. biased agonism in the presence of an allosteric modulator of the CB_1R was studied by Khajehali et al., [49]. Their results showed that the small molecule modulator, Org27569, mainly blocked G_i-mediated effects, i.e. the decrease of forskolin-induced cAMP levels by agonists was abolished. In contrast, Org27569 did not affect ERK phosphorylation induced by some of the CB_1R agonists. These results are different from those described here for CBD biased allosteric/non-orthosteric modulation, thus suggesting that the mode of regulation of Org27569 and CBD on CB_1R action is different.

Our results concerning biased agonism of THC and anandamide on CB_2R are similar to those in a recent paper on biased signaling using a variety of selective and non-selective compounds [50]. The study does not report any effect of THC on forskolin-induced cAMP levels and shows a bias to the MAPK pathway.

In cells expressing receptor heteromers THC is also unable to significantly modify the forskolin-induced cAMP levels. All together these results are important as there is a link between G_i-mediated signaling and MAPK activation [51], which may be engaged by THC acting on CB_1R but not on CB_2R or on CB_1/CB_2 heteroreceptor complexes. The link of GPCR to the MAPK signaling pathway has remained controversial in the field in what concerned (heterotrimeric) G protein mediation. Although cross-talk between different pathways is always considered, the direct link of GPCR to MAPK activation was considered either totally independent or partially dependent of coupled G proteins [52–55]. In addition, these results might be cell-type and functional readout specific. Accordingly, further studies with diverse GPCRs should be done in order to fully understand the intricacies of G-protein-dependent and G-protein-independent signaling pathways.

A recent report in cells lacking active G proteins demonstrates that for most G_i-coupled class A GPCRs, the pERK signal is exclusively triggered by G proteins and not by β-arrestins [56]. Our results concerning THC, that is not able to activate G_i but triggers phosphorylation of ERK, suggest that the G_i-coupled CB_2R may be an exception or that it may be coupled to other G proteins able to mediate activation of ERK phosphorylation, e.g. Gq as reported for the CB_1R [17].

Besides information obtained upon comparison of biased signaling of two natural cannabinoids, anandamide and THC, at CB_1 and at CB_2 receptors, the results also highlight the important role of CBD on regulating cannabinoid signaling. Apart from CBD potential off-side effects, recent studies have shown that CBD is affecting CB_1R- [13] and CB_2R- [14] mediated signaling, likely by binding to an allosteric site. From the data in those two papers it was unlikely that the putative allosteric site was located in equivalent places in the two receptors. In fact, the putative allosteric site in CB_1R is not present in CB_2R. Our results here show that CBD affects biased signaling in a different way in the two receptors, thus reinforcing the idea that the potential allosteric site is different in the two receptors. It is tempting to speculate that CBD may be affecting CB_1, CB_2 and eventually other GPCRs ("off-side"), by interacting with lipid-receptor interfaces. This hypothesis could explain the myriad of effects reported for CBD and mediation by different GPCRs; in all cases the binding to the orthosteric site occurs at micromolar concentrations, i.e. too high to be of physiological relevance. It should be noted that the concentration here used to provide such significant results was 100 nM.

Remarkably, our findings show that functional selectivity displayed by agonists is reduced when cannabinoid receptors are forming heteromeric complexes. The results suggest that the heteroreceptor complex is tightly coupled to the signaling machinery with less chance for biased signaling. Also relevant was the finding of increased functionality when cells co-expressing the two receptors were pretreated with CBD. These findings may explain some of the controversial results concerning whether the phytocannabinoid interacts or not with cannabinoid receptors. The actions of CBD may be consequence of binding to allosteric sites in the two receptors, as suggested in the two aforementioned papers [13,14]. The effect of cannabidiol on anandamide actions on both cannabinoid receptors was particularly noteworthy as was significantly different from that of other compounds. Cannabinoid drug discovery may take advantage of functional selectivity regulation by CBD.

Acknowledgements

This work was partially supported by grants from the Spanish Ministry of Economy and Competitiveness (Ref. no. BFU2015-64405-R and SAF2017-84117-R; they may include FEDER funds) and by grant 201413-30 from: *Fundació la Marató de TV3*.

Conflict of interests

Authors declare that this research was undertaken in collaboration with Phytoplant Research S.L. Co-authors working in the Spanish University of Barcelona do not receive honoraria from the company and do not have any participation in the company (stock shares or similar).

References

[1] V.-P. Jaakola, M.T. Griffith, M.A. Hanson, V. Cherezov, E.Y.T. Chien, J.R. Lane, A.P. Ijzerman, R.C. Stevens, The 2.6 angstrom crystal structure of a human A2A adenosine receptor bound to an antagonist, Science 322 (2008) 1211–1217, https://doi.org/10.1126/science.1164772.

[2] M.R. Whorton, M.P. Bokoch, S.G.F. Rasmussen, B. Huang, R.N. Zare, B. Kobilka, R.K. Sunahara, J. Huang, S. Chen, J.J. Zhang, X.-Y. Huang, Crystal structure of oligomeric β1-adrenergic G protein-coupled receptors in ligand-free basal state, Nat. Struct. Mol. Biol. 20 (2013) 419–425, https://doi.org/10.1038/nsmb.2504.

[3] T. Hua, K. Vemuri, M. Pu, L. Qu, G.W. Han, Y. Wu, S. Zhao, W. Shui, S. Li, A. Korde, R.B. Laprairie, E.L. Stahl, J.H. Ho, N. Zvonok, H. Zhou, I. Kufareva, B. Wu, Q. Zhao, M.A. Hanson, L.M. Bohn, A. Makriyannis, R.C. Stevens, Z.J. Liu, Crystal structure of the human cannabinoid receptor CB1, Cell 167 (2016) 750–762.e14, https://doi.org/10.1016/j.cell.2016.10.004.

[4] T. Hua, K. Vemuri, S.P. Nikas, R.B. Laprairie, Y. Wu, L. Qu, M. Pu, A. Korde, S. Jiang, J.H. Ho, G.W. Han, K. Ding, X. Li, H. Liu, M.A. Hanson, S. Zhao, L.M. Bohn, A. Makriyannis, R.C. Stevens, Z.J. Liu, Crystal structures of agonist-bound human cannabinoid receptor CB1, Nature 547 (2017) 468–471, https://doi.org/10.1038/nature23272.

[5] Z. Shao, J. Yin, K. Chapman, M. Grzemska, L. Clark, J. Wang, D.M. Rosenbaum, High-resolution crystal structure of the human CB1 cannabinoid receptor, Nature 540 (2016) 602–606, https://doi.org/10.1038/nature20613.

[6] P.S. Fasinu, S. Phillips, M.A. ElSohly, L.A. Walker, Current status and prospects for cannabidiol preparations as new therapeutic agents, Pharmacotherapy 36 (2016) 781–796, https://doi.org/10.1002/phar.1780.

[7] P. Morales, P.H. Reggio, N. Jagerovic, An overview on medicinal chemistry of synthetic and natural derivatives of cannabidiol, Front. Pharmacol. 8 (2017) 422, https://doi.org/10.3389/fphar.2017.00422.

[8] E.B. Russo, A. Burnett, B. Hall, K.K. Parker, Agonistic properties of cannabidiol at 5-HT1a receptors, Neurochem. Res. 30 (2005) 1037–1043, https://doi.org/10.1007/s11064-005-6978-1.

[9] L. Hanus, S. Tchilibon, D.E. Ponde, A. Breuer, E. Fride, R. Mechoulam, Enantiomeric cannabidiol derivatives: synthesis and binding to cannabinoid receptors, Org. Biomol. Chem. 3 (2005) 1116, https://doi.org/10.1039/b416943c.

[10] R.G. Pertwee, The diverse CB 1 and CB 2 receptor pharmacology of three plant cannabinoids: Δ 9-tetrahydrocannabinol, cannabidiol and Δ 9-tetrahydrocannabivarin, Br. J. Pharmacol. 153 (2008) 199–215, https://doi.org/10.1038/sj.bjp.0707442.

[11] J.M. McPartland, M. Duncan, V. Di Marzo, R.G. Pertwee, Are cannabidiol and Δ9-tetrahydrocannabivarin negative modulators of the endocannabinoid system? A systematic review, Br. J. Pharmacol. 172 (2015) 737–753, https://doi.org/10.1111/bph.12944.

[12] J.M. McPartland, M. Glass, R.G. Pertwee, Meta-analysis of cannabinoid ligand binding affinity and receptor distribution: interspecies differences, Br. J. Pharmacol. 152 (2007) 583–593, https://doi.org/10.1038/sj.bjp.0707399.

[13] R.B. Laprairie, A.M. Bagher, M.E.M. Kelly, E.M. Denovan-Wright, Cannabidiol is a negative allosteric modulator of the cannabinoid CB1 receptor, Br. J. Pharmacol. 172 (2015) 4790–4805, https://doi.org/10.1111/bph.13250.

[14] E. Martínez-Pinilla, K. Varani, I. Reyes-Resina, E. Angelats, F. Vincenzi, C. Ferreiro-Vera, J. Oyarzabal, E.I. Canela, J.L. Lanciego, X. Nadal, G. Navarro, P.A. Borea, R. Franco, Binding and signaling studies disclose a potential allosteric site for cannabidiol in cannabinoid CB2receptors, Front. Pharmacol. 8 (2017) 744, https://doi.org/10.3389/fphar.2017.00744.

[15] G. Navarro, N. Franco, E. Martínez-Pinilla, R. Franco, The epigenetic cytocrin pathway to the nucleus. Epigenetic factors, epigenetic mediators, and epigenetic traits. A biochemist perspective, Front. Genet. 8 (179) (2017) 1–6, https://doi.org/10.3389/fgene.2017.00179.

[16] T. Kenakin, Biased agonism, F1000 Biol. Rep. 1 (2009) 87, https://doi.org/10.3410/B1-87.

[17] R.B. Laprairie, A.M. Bagher, E.M. Denovan-Wright, Cannabinoid receptor ligand bias: implications in the central nervous system, Curr. Opin. Pharmacol. 32 (2017) 32–43, https://doi.org/10.1016/j.coph.2016.10.005.

[18] P. Morales, M. Gómez-Cañas, G. Navarro, D.P. Hurst, F.J. Carrillo-Salinas, L. Lagartera, R. Pazos, P. Goya, P.H. Reggio, C. Guaza, R. Franco, J. Fernández-Ruiz, N. Jagerovic, Chromenopyrazole, a versatile cannabinoid scaffold with in vivo activity in a model of multiple sclerosis, J. Med. Chem. 59 (2016) 6753–6771, https://doi.org/10.1021/acs.jmedchem.6b00397.

[19] X. Nadal, Methods of Purifying Cannabinoids, Compositions and Kits Thereof, US9765000 B2 and WO2016116628A1, 2016.

[20] M. Medrano, D. Aguinaga, I. Reyes-Resina, E.I. Canela, J. Mallol, G. Navarro, R. Franco, Orexin A/hypocretin modulates leptin receptor-mediated signaling by allosteric modulations mediated by the ghrelin GHS-R1A receptor in hypothalamic neurons, Mol. Neurobiol. (2017) 1–13, https://doi.org/10.1007/s12035-017-0670-8.

[21] G. Navarro, A. Cordomí, M. Brugarolas, E. Moreno, D. Aguinaga, L. Pérez-Benito, S. Ferre, A. Cortés, V. Casadó, J. Mallol, E. Canela, C. Lluís, L. Pardo, P. McCormick, R. Franco, Cross-communication between Gi and Gs in a G-protein-coupled receptor heterotetramer guided by a receptor C-terminal domain, BMC Biol. 16 (24) (2018) 1–15, https://doi.org/10.1186/s12915-018-0491-x.

[22] S. Hinz, G. Navarro, D. Borroto-Escuela, B.F. Seibt, C. Ammon, E. De Filippo, A. Danish, S.K. Lacher, B. Červinková, M. Rafehi, K. Fuxe, A.C. Schiedel, R. Franco, C.E. Müller, Adenosine A2A receptor ligand recognition and signaling is blocked by A2B receptors, Oncotarget 9 (2018) 13593–13611, https://doi.org/10.18632/oncotarget.24423.

[23] G. Navarro, A. Cordomí, M. Brugarolas, E. Moreno, D. Aguinaga, L. Pérez-Benito, S. Ferre, A. Cortés, V. Casadó, J. Mallol, E.I. Canela, C. Lluís, L. Pardo, P.J. McCormick, R. Franco, Cross-communication between Gi and Gs in a G-protein-coupled receptor heterotetramer guided by a receptor C-terminal domain, BMC Biol. 16 (2018) 24, https://doi.org/10.1186/s12915-018-0491-x.

[24] A.E. Kümmerle, M. Schmitt, S.V.S. Cardozo, C. Lugnier, P. Villa, A.B. Lopes, N.C. Romeiro, H. Justiniano, M.A. Martins, C.A.M. Fraga, J.J. Bourguignon, E.J. Barreiro, Design, synthesis, and pharmacological evaluation of N-acylhydrazones and novel conformationally constrained compounds as selective and potent orally active phosphodiesterase-4 inhibitors, J. Med. Chem. 55 (2012) 7525–7545, https://doi.org/10.1021/jm300514y.

[25] J.W. Black, P. Leff, Operational models of pharmacological agonism, Proc. R. Soc. London. Ser. B, Biol. Sci. 220 (1983) 141–162 (accessed May 23, 2018), http://www.ncbi.nlm.nih.gov/pubmed/6141562.

[26] S. Rajagopal, S. Ahn, D.H. Rominger, W. Gowen-MacDonald, C.M. Lam, S.M. DeWire, J.D. Violin, R.J. Lefkowitz, Quantifying ligand bias at seven-transmembrane receptors, Mol. Pharmacol. 80 (2011) 367–377, https://doi.org/10.1124/mol.111.072801.

[27] A. Kebig, E. Kostenis, K. Mohr, M. Mohr-Andrä, An optical dynamic mass redistribution assay reveals biased signaling of dualsteric GPCR activators, J. Receptor Signal Transduct. 29 (2009) 140–145, https://doi.org/10.1080/10799890903047437.

[28] M. Grundmann, E. Kostenis, Label-free biosensor assays in GPCR screening, G Protein-Coupled Recept. Screen. Assays Methods Protoc. 2015, pp. 199–213, , https://doi.org/10.1007/978-1-4939-2336-6_14.

[29] M. Glass, C.C. Felder, Concurrent stimulation of cannabinoid CB1 and dopamine D2 receptors augments cAMP accumulation in striatal neurons: evidence for a Gs linkage to the CB1 receptor, J. Neurosci. 17 (1997) 5327–5333, https://doi.org/10.1523/JNEUROSCI.17-14-05327.1997.

[30] L. Callén, E. Moreno, P. Barroso-Chinea, D. Moreno-Delgado, A. Cortés, J. Mallol, V. Casadó, J.L. Lanciego, R. Franco, C. Lluis, E.I. Canela, P.J. McCormick, Cannabinoid receptors CB1 and CB2 form functional heteromers in brain, J. Biol. Chem. 287 (2012) 20851–20865, https://doi.org/10.1074/jbc.M111.335273.

[31] G. Navarro, D. Borroto-Escuela, E. Angelats, Í. Etayo, I. Reyes-Resina, M. Pulido-Salgado, A.I. Rodríguez-Pérez, E.I. Canela, J. Saura, J.L. Lanciego, J.L. Labandeira-García, C.A. Saura, K. Fuxe, R. Franco, A.I. Rodriguez-Perez, E.I. Canela, J. Saura, J.L. Lanciego, J.L. Labandeira-García, C.A. Saura, K. Fuxe, R. Franco, Receptor-heteromer mediated regulation of endocannabinoid signaling in activated microglia. Role of CB1 and CB2 receptors and relevance for Alzheimer's disease and levodopa-induced dyskinesia, Brain. Behav. Immun. 67 (2018) 139–151, https://doi.org/10.1016/j.bbi.2017.08.015.

[32] A.E. Brady, L.E. Limbird, G protein-coupled receptor interacting proteins: emerging roles in localization and signal transduction, Cell. Signal. 14 (2002) 297–309 (accessed August 7, 2018), http://www.ncbi.nlm.nih.gov/pubmed/11858937.

[33] Q. Wang, L.E. Limbird, Regulation of α2AR trafficking and signaling by interacting proteins, Biochem. Pharmacol. 73 (2007) 1135–1145, https://doi.org/10.1016/j.bcp.2006.12.024.

[34] J. Tao, H.Y. Wang, C.C. Malbon, AKAR2-AKAP12 fusion protein "biosenses" dynamic phosphorylation and localization of a GPCR-based scaffold, J. Mol. Signal. 5 (2010) 3, https://doi.org/10.1186/1750-2187-5-3.

[35] C.C. Malbon, J. Tao, H. Wang, AKAPs (A-kinase anchoring proteins) and molecules that compose their G-protein-coupled receptor signalling complexes, Biochem. J. 379 (2004) 1–9, https://doi.org/10.1042/BJ20031648.

[36] S. Maudsley, B. Martin, L.M. Luttrell, G protein-coupled receptor signaling complexity in neuronal tissue: implications for novel therapeutics, Curr. Alzheimer Res. 4 (2007) 3–19 (accessed August 7, 2018), http://www.ncbi.nlm.nih.gov/pubmed/17316162.

[37] G. Romero, M. von Zastrow, P.A. Friedman, Role of PDZ proteins in regulating trafficking, signaling, and function of GPCRs: means, motif, and opportunity, Adv. Pharmacol. (2011) 279–314, https://doi.org/10.1016/B978-0-12-385952-5.00003-8.

[38] G. Navarro, P. Morales, C. Rodríguez-Cueto, J. Fernández-Ruiz, N. Jagerovic, R. Franco, Targeting cannabinoid CB2 receptors in the central nervous system. medicinal chemistry approaches with focus on neurodegenerative disorders, Front. Neurosci 10 (2016), https://doi.org/10.3389/fnins.2016.00406.

[39] C.C. Felder, K.E. Joyce, E.M. Briley, J. Mansouri, K. Mackie, O. Blond, Y. Lai, A.L. Ma, R.L. Mitchell, Comparison of the pharmacology and signal transduction of the human cannabinoid CB1 and CB2 receptors, Mol. Pharmacol. 48 (1995) 443–450 (accessed March 14, 2018), http://www.ncbi.nlm.nih.gov/pubmed/7565624.

[40] B.C. Paria, S.K. Das, S.K. Dey, The preimplantation mouse embryo is a target for cannabinoid ligand-receptor signaling, Proc. Natl. Acad. Sci. U.S.A. 92 (1995) 9460–9464, https://doi.org/10.1073/pnas.92.21.9460.

[41] H.J. Jeong, R.J. Vandenberg, C.W. Vaughan, N-arachidonyl-glycine modulates synaptic transmission in superficial dorsal horn, Br. J. Pharmacol. 161 (2010) 925–935, https://doi.org/10.1111/j.1476-5381.2010.00935.x.

[42] H. Iwamura, H. Suzuki, Y. Ueda, T. Kaya, T. Inaba, In vitro and in vivo pharmacological characterization of JTE-907, a novel selective ligand for cannabinoid CB2 receptor, J. Pharmacol. Exp. Ther. 296 (2001) 420–425 (accessed March 14, 2018), http://www.ncbi.nlm.nih.gov/pubmed/11160626.

[43] R. Condie, A. Herring, W.S. Koh, M. Lee, N.E. Kaminski, Cannabinoid inhibition of adenylate cyclase-mediated signal transduction and interleukin 2 (IL-2) expression in the murine T-cell line, EL4.IL-2, J. Biol. Chem. 271 (1996) 13175–13183, https://doi.org/10.1074/jbc.271.22.13175.

[44] M. Bayewitch, T. Avidor-Reiss, R. Levy, J. Barg, R. Mechoulam, Z. Vogel, The peripheral cannabinoid receptor: adenylate cyclase inhibition and G protein

coupling, FEBS Lett. 375 (1995) 143–147, https://doi.org/10.1016/0014-5793(95)01207-U.
[45] M. Bayewitch, M.H. Rhee, T. Avidor-Reiss, A. Breuer, R. Mechoulam, Z. Vogel, (−)-Delta9-tetrahydrocannabinol antagonizes the peripheral cannabinoid receptor-mediated inhibition of adenylyl cyclase, J. Biol. Chem. 271 (1996) 9902–9905 (accessed August 7, 2018), http://www.ncbi.nlm.nih.gov/pubmed/8626625.
[46] D.M. Slipetz, G.P. O'Neill, L. Favreau, C. Dufresne, M. Gallant, Y. Gareau, D. Guay, M. Labelle, K.M. Metters, Activation of the human peripheral cannabinoid receptor results in inhibition of adenylyl cyclase, Mol. Pharmacol. 48 (1995) 352–361 (accessed August 7, 2018), http://www.ncbi.nlm.nih.gov/pubmed/7651369.
[47] A.A. Makda, M.A. Elmore, M.E. Hill, A. Stamps, S. Tejura, M.J. Finnen, Differential effects of CB1 and CB2 agonists on cAMP levels and MAP kinase activation in human peripheral blood mononuclear cells, Biochem. Soc. Trans. 25 (1997) 217S (accessed March 14, 2018).
[48] Y.J. Jeon, K.H. Yang, J.T. Pulaski, N.E. Kaminski, Attenuation of inducible nitric oxide synthase gene expression by Δ9-tetrahydrocannabinol is mediated through the inhibition of nuclear factor-kappa B/Rel activation, Mol. Pharmacol. 50 (1996) 334–341 (accessed March 14, 2018), http://www.ncbi.nlm.nih.gov/pubmed/8700141.
[49] E. Khajehali, D.T. Malone, M. Glass, P.M. Sexton, A. Christopoulos, K. Leach, Biased agonism and biased allosteric modulation at the CB1 cannabinoid receptor, Mol. Pharmacol. 88 (2015) 368–379, https://doi.org/10.1124/mol.115.099192.
[50] M. Soethoudt, U. Grether, J. Fingerle, T.W. Grim, F. Fezza, L. De Petrocellis, C. Ullmer, B. Rothenhäusler, C. Perret, N. Van Gils, D. Finlay, C. Macdonald, A. Chicca, M.D. Gens, J. Stuart, H. De Vries, N. Mastrangelo, L. Xia, G. Alachouzos, M.P. Baggelaar, A. Martella, E.D. Mock, H. Deng, L.H. Heitman, M. Connor, V. Di Marzo, J. Gertsch, A.H. Lichtman, M. Maccarrone, P. Pacher, M. Glass, M. Van Der Stelt, Cannabinoid CB2 receptor ligand profiling reveals biased signalling and off-target activity, Nat. Commun. 8 (2017) 13958, https://doi.org/10.1038/ncomms13958.
[51] Z.G. Goldsmith, D.N. Dhanasekaran, G Protein regulation of MAPK networks, Oncogene 26 (2007) 3122–3142, https://doi.org/10.1038/sj.onc.1210407.
[52] C. Liebmann, Bradykinin signalling to MAP kinase: cell-specific connections versus principle mitogenic pathways, Biol. Chem. 382 (2001) 49–55, https://doi.org/10.1515/BC.2001.008.
[53] G. Schulte, B.B. Fredholm, Signalling from adenosine receptors to mitogen-activated protein kinases, Cell. Signal. 15 (2003) 813–827 (accessed August 1, 2018), http://www.ncbi.nlm.nih.gov/pubmed/12834807.
[54] R. Wetzker, F.-D. Böhmer, Transactivation joins multiple tracks to the ERK/MAPK cascade, Nat. Rev. Mol. Cell Biol. 4 (2003) 651–657, https://doi.org/10.1038/nrm1173.
[55] G. Turu, L. Hunyady, Signal transduction of the CB1 cannabinoid receptor, J. Mol. Endocrinol. 44 (2010) 75–85, https://doi.org/10.1677/JME-08-0190.
[56] M. Grundmann, N. Merten, D. Malfacini, A. Inoue, P. Preis, K. Simon, N. Rüttiger, N. Ziegler, T. Benkel, N.K. Schmitt, S. Ishida, I. Müller, R. Reher, K. Kawakami, A. Inoue, U. Rick, T. Kühl, D. Imhof, J. Aoki, G.M. König, C. Hoffmann, J. Gomeza, J. Wess, E. Kostenis, Lack of beta-arrestin signaling in the absence of active G proteins, Nat. Commun. 9 (2018) 341, https://doi.org/10.1038/s41467-017-02661-3.

3.2 Cannabigerol Action at Cannabinoid CB_1 and CB_2 Receptors and at CB_1–CB_2 Heteroreceptor Complexes.

Gemma Navarro, Katia Varani, Irene Reyes-Resina, Verónica Sánchez de Medina, **Rafael Rivas-Santisteban**, Carolina Sánchez Carnerero Callado, Fabrizio Vincenzi, Salvatore Casano, Carlos Ferreiro-Vera, Enric I. Canela, Pier Andrea Borea, Xavier Nadal y Rafael Franco.

Manuscrito publicado en *Frontiers in Pharmacology*, Junio 2018; 9: 632.

A partir de la planta *Cannabis sativa* se han conseguido identificar más de 500 compuestos cannabinoides, que reciben el nombre de compuestos fitocannabinoides. Dentro de esta categoría de compuestos, el cannabigerol (CBG) es uno de los que tienen un mayor protagonismo y que está adquiriendo la atención de la industria farmacológica al no producir efectos psicoactivos y encontrarse a gran concentración en algunas variedades del cáñamo. En este estudio se caracterizaron los efectos del CBG al actuar sobre los receptores cannabinoides CB_1, CB_2 y en complejos heteroméricos formados por los receptores CB_1-CB_2 y la modulación que CBG ejerce en la funcionalidad de estos receptores al ser activados por un agonista específico. Usando [3H]-CP-55940, CBG compitió con valores bajos de K_i micromolar para la unión a CB_1R y CB_2R. También es interesante puntualizar que CBG compitió por la unión de [3H]-WIN-55,212-2 a CB_2R, pero no a CB_1R (K_i: 2,7 μM frente a > 30 μM). Se realizaron ensayos de determinación de los niveles de AMP intracelular, la fosforilación de quinasas (ERK1/2), el reclutamiento de ß-arrestinas y la redistribución dinámica de masas (DMR), observándose como CBG actúa como un agonista parcial de CB_2R. Los resultados obtenidos en nuestros experimentos indican que el CBG es eficaz como modulador de la señalización endocannabinoide.

frontiers in Pharmacology

ORIGINAL RESEARCH
published: 21 June 2018
doi: 10.3389/fphar.2018.00632

Cannabigerol Action at Cannabinoid CB_1 and CB_2 Receptors and at CB_1–CB_2 Heteroreceptor Complexes

Gemma Navarro[1,2], Katia Varani[3], Irene Reyes-Resina[2,4], Verónica Sánchez de Medina[5], Rafael Rivas-Santisteban[2,4], Carolina Sánchez-Carnerero Callado[6], Fabrizio Vincenzi[3], Salvatore Casano[7], Carlos Ferreiro-Vera[6], Enric I. Canela[2,4], Pier Andrea Borea[3], Xavier Nadal[5†] and Rafael Franco[2,4*†]*

[1] Department of Biochemistry and Physiology, Faculty of Pharmacy, University of Barcelona, Barcelona, Spain, [2] Centro de Investigación Biomédica en Red, Enfermedades Neurodegenerativas (CIBERNED), Instituto de Salud Carlos III, Madrid, Spain, [3] Department of Medical Sciences, Institute of Pharmacology, University of Ferrara, Ferrara, Italy, [4] Molecular Neurobiology Laboratory, Department of Biochemistry and Molecular Biomedicine, University of Barcelona, Barcelona, Spain, [5] Department of R&D – Extraction, Phytoplant Research S.L., Córdoba, Spain, [6] Department of Analytical Chemistry, Phytoplant Research S.L., Córdoba, Spain, [7] Department of Breeding and Cultivation, Phytoplant Research S.L., Córdoba, Spain

OPEN ACCESS

Edited by:
Fabricio A. Pamplona, Entourage Phytolab, Brazil

Reviewed by:
Steven R. Laviolette, University of Western Ontario, Canada
Attila Köfalvi, Universidade de Coimbra, Portugal

****Correspondence:***
Xavier Nadal
x.nadal@phytoplant.es
Rafael Franco
rfranco123@gmail.com

† These authors have contributed equally to this work.

Specialty section:
This article was submitted to Neuropharmacology, a section of the journal Frontiers in Pharmacology

Received: *22 February 2018*
Accepted: *25 May 2018*
Published: *21 June 2018*

Citation:
Navarro G, Varani K, Reyes-Resina I, Sánchez de Medina V, Rivas-Santisteban R, Sánchez-Carnerero Callado C, Vincenzi F, Casano S, Ferreiro-Vera C, Canela EI, Borea PA, Nadal X and Franco R (2018) Cannabigerol Action at Cannabinoid CB_1 and CB_2 Receptors and at CB_1–CB_2 Heteroreceptor Complexes. Front. Pharmacol. 9:632. doi: 10.3389/fphar.2018.00632

Cannabigerol (CBG) is one of the major phytocannabinoids present in *Cannabis sativa* L. that is attracting pharmacological interest because it is non-psychotropic and is abundant in some industrial hemp varieties. The aim of this work was to investigate in parallel the binding properties of CBG to cannabinoid CB_1 (CB_1R) and CB_2 (CB_2R) receptors and the effects of the compound on agonist activation of those receptors and of CB_1–CB_2 heteroreceptor complexes. Using [^{3}H]-CP-55940, CBG competed with low micromolar K_i values the binding to CB_1R and CB_2R. Homogeneous binding in living cells, which is only technically possible for the CB_2R, provided a 152 nM K_i value. Also interesting, CBG competed the binding of [^{3}H]-WIN-55,212-2 to CB_2R but not to CB_1R (K_i: 2.7 versus >30 μM). The phytocannabinoid modulated signaling mediated by receptors and receptor heteromers even at low concentrations of 0.1–1 μM. cAMP, pERK, β-arrestin recruitment and label-free assays in HEK-293T cells expressing the receptors and treated with endocannabinoids or selective agonists proved that CBG is a partial agonist of CB_2R. The action on cells expressing heteromers was similar to that obtained in cells expressing the CB_2R. The effect of CBG on CB_1R was measurable but the underlying molecular mechanisms remain uncertain. The results indicate that CBG is indeed effective as regulator of endocannabinoid signaling.

Keywords: cannabinoid receptor, cannabigerol, G-protein-coupled receptor, phytocannabinoid, TR-FRET, partial agonist

Abbreviations: Δ^8-THC, Δ^8-tetrahydrocannabinol; Δ^9-THC, Δ^9-tetrahydrocannabinol; Δ^9-THCA, Δ^9- tetrahy drocannabinolic acid; Δ^9-THCV, Δ^9-tetrahydrocannabivarin; 2-AG, 2-arachidonoyl glicerol; AEA, anandamide; CB_1R, cannabinoid receptor 1; CB_2R, cannabinoid receptor 2; CBC, cannabichromene; CBD, cannabidiol; CBDA, cannabidiolic acid; CBDV, cannabidivarin; CBG, cannabigerol; CBGA, cannabigerolic acid; CBN, cannabinol; CNS, central nervous system; DMR, dynamic mass redistribution; HEK, human embryonic kidney; HTRF, homogeneous time-resolved fluorescence; SNAP, protein used as a tag; it contains circa 180 amino acids and may be covalently labeled with different probes; Tb, terbium; TLB, Tag-lite labeling medium.

INTRODUCTION

Cannabinoid compounds bind and activate cannabinoid CB_1 (CB_1R) and CB_2 (CB_2R) receptors, which belong to the superfamily of G-protein-coupled receptors. There are many ways to classify them, but the most used distinguishes between endogenous molecules (endocannabinoids), phytocannabinoids and synthetic cannabinoids. Endocannabinoids and one of the most studied phytocannabinoids, Δ^9-tetrahydrocannabinol (Δ^9-THC), are agonists with more or less CB_1R/CB_2R selectivity. Furthermore, synthetic cannabinoids mainly act (as agonists or antagonists) by binding to the orthosteric site of receptors (Mechoulam, 2016). Indeed, there is a limited number of molecules, either synthetic or phytocannabinoids, that behave as allosteric modulators of cannabinoid receptor function.

Anandamide and 2-arachidonoyl glycerol (2-AG) are the two main endocannabinoids, being synthesized from membrane lipids and having an alkyl-amide chemical structure. They are retrograde effectors being produced in the post-synaptic neuron to act in the pre-synaptic neuron where they regulate the release of neurotransmitters (Diana and Marty, 2004).

Phytocannabinoids are phenolic terpenes biosynthesized in nature nearly exclusively in the *Cannabis sativa* L. plant. In the *Cannabis* plant, all cannabinoids are biosynthesized in the acid form, mainly Δ^9-THCA, CBDA, etc. CBGA is the first molecule formed in the biosynthetic pathway and the substrate of Δ^9-tetrahydrocannabinol-synthase and CBD-synthase (Fellermeier and Zenk, 1998). The pharmacologic effects of *Cannabis* components, traditionally consumed through inhalation, are attributed to the decarboxylated neutral products of above mentioned acids: Δ^9-THC, CBD, and CBG.

Synthetic cannabinoids are very different in chemical structure. For instance, they may be indoles like WIN-55,212-2, AM-1241 or JWH-018, or phenolic, phenols lacking the pyrene ring, like CP-55,940 or HU-308. All these compounds have been used in cannabinoid research and have helped to unveil pharmacological aspects of the endocannabinoid system. It should be noted that some of these compounds have recently arrived at the streets sold as *legal highs*, thus raising Public Health concerns (Adams et al., 2017; Weinstein et al., 2017).

The endocannabinoid system is constituted by the endogenous cannabinoids, the enzymes that produce and degrade them, and by the receptors that mediate their actions. Whereas endocannabinoids consist of molecules with aliphatic structure, AEA and 2-AG, the structure of natural cannabinoids, derived from *C. sativa* L., is fairly different [see (Lu and Mackie, 2016) and references therein]. Although it is well established that one of the main active components of the plant and one of the few that are psychoactive, namely Δ^9-THC, acts via cannabinoid receptors, there is controversy on whether these receptors mediate the action of phytocannabinoids such as CBN, CBD or CBG. As happened the last years for CBD, a new research and revision of the cannabinoid receptor pharmacology must be done with the rest of phytocannabinoids as CBG. A further phenomenon that may be considered to understand the action of molecules from *C. sativa* L. and its extracts is the fact that cannabinoid receptors may form heteromers, namely CB_1–CB_2 heteroreceptors, which display particular functional properties (Callén et al., 2012). It should be noted that in CNS those heteromers are mainly expressed in pallidal neurons (Lanciego et al., 2011; Sierra et al., 2015) and in activated microglia (Navarro et al., 2018a).

Cannabigerol was isolated, characterized and synthetized by the same researchers than reported the structure of the main psychotropic agent of *Cannabis*, Δ^9-THC (Gaoni and Mechoulan, 1964). Few years later *in vivo* assays showed that CBG was non-psychoactive (Grunfeld and Edery, 1969; Mechoulam et al., 1970). The lower concentration and the lack of psychoactivity was probably the cause that CBG was shadowed by Δ^9-THC. In fact, CBG has attracted less attention than Δ^9-THC and even than CBD, but nowadays is gaining interest among the scientific community. Some commercial hemp varieties have CBG and CBGA as main cannabinoids and, therefore, CBG is another of the phytocannabinoids to be considered by the unregulated market of hemp oils and derivatives. As recently pointed out, the increased therapeutic potential of *C. sativa* L. components requires a more in deep understanding of the pharmacology of phytocannabinoids other than Δ^9-THC, namely CBD, CBG, CBN, Δ^9-THCV, Δ^8-THC, CBC and CBDV (Turner et al., 2017).

Preliminary results using membranes from mice brain or from CHO cells expressing the human CB_2R led to postulate that CBG could be a partial agonist at both CB_1R and CB_2R with K_i values in the 300–500 nM range (Gauson et al., 2007; Pertwee, 2008). The first published data on the binding of CBG to human CB_1R and CB_2R were provided by (Rosenthaler et al., 2014) working with [^{3}H]CP-55,940 as radioligand and with preparations from Sf9 cells co-expressing one receptor and the Gαi3β1γ2 protein. The K_i values obtained in competition assays are 897 and 153 nM for CB_1R and CB_2R, respectively. CBG may modulate the activity of transient receptor potential channels of ankyrin type-1; however, the EC_{50} values lie in the micromolar range (De Petrocellis et al., 2008). It has been reported that CBG binds to CB_1R (K_i = 381 nM) from mouse brain membranes and CB_2R (K_i = 2.6 μM) from CHO cells expressing the human receptor; CBG at high concentrations (10 μM) antagonized [^{35}S]GTPγS binding in mouse brain membranes treated with AEA or CP-55940 (Cascio et al., 2010). Authors also reported CBG as α_2-adrenoceptor agonist at nanomolar levels (EC_{50} = 0.2 nM), and being also able to antagonize [^{35}S]GTPγS binding upon stimulation of the $5HT_{1A}$ receptor by 1 μM 8-OH-DPAT (Cascio et al., 2010). Other findings indicate that CBG can act as (i) agonist/desensitizer of TRPA1 (EC_{50} = 700 nM), (ii) agonist of TRPV1 (EC_{50} = 1.3 μM) (iii) agonist of TRPV2 (EC_{50} = 1.7 μM), (iv) antagonist of TRPM8 channels (IC_{50} = 160 nM) and v) inhibitor of AEA cell uptake (K_i = 11.3 μM) (De Petrocellis et al., 2011). More recently, the PPARγ has been reported as target of the phytocannabinoid CBG (K_i = 11.7 μM) that at high concentrations, in the 10–25 μM range, may enhance the PPARγ transcriptional activity (Granja

et al., 2012; Nadal et al., 2017). A recent review substantiates the complexity of the field and highlights that other players, GPR55 for instance, are also targeted by cannabinoids (Solymosi and Kofalvi, 2017).

The aim of this work was to characterize CBG pharmacology on the cannabinoid receptors using binding and measurement of different signal transduction mechanisms in living HEK-293T cells expressing human CB_1R, CB_2R, or CB_1–CB_2 heteroreceptor complexes. The results indicate that, in our experimental conditions, CBG mainly acts on CB_2R and behaves as a partial agonist.

MATERIALS AND METHODS

Reagents

ACEA, JWH133, and AEA were purchased from Tocris Bioscience (Bristol, United Kingdom), CBD and CBG analytical standard solutions were purchased from THCpharm (Frankfurt, DE). Concentrated (10 mM) stock solutions prepared in ethanol (CBG, ACEA, and AEA) or DMSO (JWH133 and CM-157) were stored at −20°C. In each experimental session, aliquots of concentrated solutions of compounds were thawed and conveniently diluted in the appropriate experimental solution. For non-radioactive binding assays, TLB was obtained from Cisbio Bioassays (LABMED; Codolet, France). The Tb derivative of O6-benzylguanine was synthesized by Cisbio Bioassays and is commercialized as SNAP-Lumi4-Tb (SSNPTBC; Cisbio Assays). The plasmid encoding for the SNAP-tagged human CB_2R used for transient transfection was obtained from Cisbio Bioassays (PSNAP-CB2). CB_2R agonist 3-[[4-[2-tert-butyl-1-(tetrahydropyran-4-ylmethyl)benzimidazol-5-yl]sulfonyl-2-pyridyl]oxy]propan-1-amine (CM-157) conjugated to a fluorescent probe was developed in collaboration with Cisbio Bioassays (Martínez-Pinilla et al., 2016).

Cannabinoid Isolation, Purification and Analysis

Cannabidiol was purified from dried leaves and inflorescences of the *Cannabis* variety SARA (CPVO file number: 20150098), CBG from the variety AIDA (CPVO file number: 20160167) following a previously described method (Nadal, 2016) that provides compounds with >95% purity. An Agilent liquid chromatography set-up (Model 1260, Pittsburgh, PA, United States) consisting of a binary pump, a vacuum degasser, a column oven, an autosampler and a diode array detector (DAD) equipped with a 150 mm length × 2.1 mm internal diameter, 2.7 μm pore size Poroshell 120 EC-C18 column was used for the quality control of the purified cannabinoids. The analysis was performed using water and acetonitrile both containing ammonium formate 50 mM as mobile phases. Flow-rate was 0.2 mL/min and the injection volume was 3 μL. Chromatographic peaks were recorded at 210 nm. All determinations were carried out at 35°C. All samples were analyzed in duplicate. The results of each cannabinoid purity, 96.04% for CBD and 99.9% for CBG, were calculated as weight (%) versus a commercial standard from THCpharm (CBD batch n° L01258-M-1.0; CBG batch n° L01260-M-1.0).

Radioligand Binding Assays

Cell Culture and Membrane Preparation

For radioligand binding experiments CHO cells, stably transfected with cDNA for human CB_1 or CB_2 cannabinoid receptors, were grown adherently and maintained in Ham's F12 containing 10% fetal bovine serum, penicillin (100 U/mL), streptomycin (100 μg/mL) and geneticin (G418, 0.4 mg/mL) at 37°C in a humid atmosphere of 5% CO_2. Membranes were prepared from cells washed with PBS and scraped off plates in ice-cold hypotonic buffer (5 mM Tris HCl, 2 mM EDTA, pH 7.4). The cell suspension was homogenized with a Polytron and then centrifuged for 30 min at 40,000 × *g*.

Saturation Binding Experiments

[^{3}H]-CP-55940 saturation binding experiments (specific activity 169 Ci/mmol, Perkin Elmer) were performed incubating different concentrations of the radioligand (0.03 – 10 nM) in binding buffer (50 mM Tris-HCl, pH 7.4, 2.5 mM EDTA, 5 mM $MgCl_2$ for CB_1R or 50 mM Tris-HCl, pH 7.4, 1 mM EDTA, 5 mM $MgCl_2$ for CB_2R) using CHO membranes expressing the human versions of CB_1R or CB_2R (10 μg protein/sample) at 30°C. Non-specific binding was determined in the presence of 1 μM WIN-55,212-2. At the end of the incubation period (90 min for CB_1R or 60 min for CB_2R) bound and free radioactivity were separated in a cell harvester (Brandel Instruments) by filtering the assay mixture through Whatman GF/B glass fiber filters. The filter-bound radioactivity was counted in a 2810 TR liquid scintillation counter (Perkin Elmer).

[^{3}H]-WIN-55,212-2 saturation binding experiments (specific activity 48 Ci/mmol, Perkin Elmer) were performed incubating different concentrations of the radioligand (0.5–100 nM for CB_1R or 0.2–40 nM for CB_2R) in binding buffer (50 mM Tris-HCl, pH 7.4, 1 mM EDTA, 5 mM $MgCl_2$) with CB_1R- or CB_2R-containing CHO cell membranes (10 μg protein/sample) at 30°C. Non-specific binding was determined in the presence of 1 μM WIN-55,212-2. At the end of the incubation period (60 min) bound and free radioactivity were separated in a cell harvester (Brandel Instruments) by filtering the assay mixture through Whatman GF/B glass fiber filters. The filter-bound radioactivity was counted in a 2810 TR liquid scintillation counter (Perkin Elmer).

Competition Binding Experiments

[^{3}H]-CP-55940 competition binding experiments were performed incubating 0.3 nM of radioligand and different concentrations of the tested compounds with membranes obtained from CHO cells expressing human CB_1 or CB_2 receptors (10 μg protein/sample) for 90 min (CB_1R) or 60 min (CB_2R) at 30°C. Non-specific binding was determined in the presence of 1 μM WIN-55,212-2. Bound and free radioactivity were separated by filtering the assay mixture as above indicated. The filter bound radioactivity was counted using a Packard Tri Carb 2810 TR scintillation counter (Perkin Elmer).

Competition binding experiments were also performed incubating 3 nM [^{3}H]-WIN-55,212-2 and different concentrations of the tested compounds with membranes obtained from CHO cells transfected with human CB_1 or CB_2 receptors (10 μg protein/sample) for 60 min at 30°C. Non-specific binding was determined in the presence of 1 μM WIN-55,212-2. Bound and free radioactivity were separated by filtering the assay mixture as above indicated. The filter bound radioactivity was counted using a Packard Tri Carb 2810 TR scintillation counter (Perkin Elmer).

Homogeneous Binding Assays in Living Cells

Expression Vector

cDNAs for the human version of cannabinoid CB_2R without their stop codon were obtained by PCR and subcloned to SNAP-containing vector (PSNAP; Cisbio Bioassays) using sense and antisense primers harboring unique restriction sites for HindIII and BamHI generating the SNAP tagged CB_2R (CB_2R-SNAP).

Cell Culture and Transfection

For HTRF assays, HEK-293T cells were used. HEK 293T (HEK-293T) cells were grown in DMEM supplemented with 2 mM L-glutamine, 1 mM sodium pyruvate, 100 units/mL penicillin/streptomycin, and 5% (v/v) FBS [all supplements were from Invitrogen, (Paisley, Scotland, United Kingdom)]. Cells were maintained at 37°C in a humidified atmosphere of 5% CO_2 and were passaged, with enzyme-free cell dissociation buffer (13151-014, Gibco®, Thermo Fisher, Waltham, MA, United States), when they were 80–90% confluent, i.e., approximately twice a week. Cells were transiently transfected with the PEI (Polyethylenimine, Sigma, St. Louis, MO, United States) method as previously described (Medrano et al., 2017; Navarro et al., 2018b). Experiments were carried out in cells expressing SNAP-tagged CB_2R in the presence or in the absence of CB_1R.

Labeling of Cells Expressing SNAP-Tagged CB_2R

Cell culture medium was removed from the 25-cm^2 flask and 100 nM SNAP-Lumi4-Tb, previously diluted in 3 mL of TLB 1X, was added to the flask and incubated for 1 h at 37°C under 5% CO_2 atmosphere in a cell incubator. Cells were then washed four times with 2 mL of TLB 1X to remove the excess of SNAP-Lumi4-Tb, detached with enzyme-free cell dissociation buffer, centrifuged 5 min at 1,500 rpm and collected in 1 mL of TLB 1X. Tag-lite-based binding assays were performed 24 h after transfection. Densities in the 2,500–3,000 cells/well range were used to carry out binding assays in white opaque 384-well plates.

Non-radioactive Competition Binding Assays

For competition binding assays, the fluorophore-conjugated CB_2R ligand (labeled CM-157), unconjugated CM-157 and CBG were diluted in TLB 1X. HEK-293T cells transiently expressing Tb-labeled SNAP-CB_2R with or without CB_1R were incubated with 20 nM fluorophore-conjugated CB_2R ligand, in the presence of increasing concentrations (0–10 μM range) of CBG or CM-157. Plates contained 10 μL of labeled cells, and 5 μL of TLB 1X or 5 μL of CBG or 5 μL CM-157 were added prior to the addition of 5 μL of the fluorescent ligand. Plates were then incubated for at least 2 h at room temperature before signal detection. Detailed description of the HTRF assay is found in Martínez-Pinilla et al. (2016).

Signal was detected using an EnVision microplate reader (PerkinElmer, Waltham, MA, United States) equipped with a FRET optic module allowing donor excitation at 337 nm and signal collection at both 665 and 620 nm. A frequency of 10 flashes/well was selected for the xenon flash lamp excitation. The signal was collected at both 665 and 620 nm using the following time-resolved settings: delay, 150 μs; integration time, 500 μs. HTRF® ratios were obtained by dividing the acceptor (665 nm) by the donor (620 nm) signals and multiplying by 10,000. The 10,000-multiplying factor is used solely for the purpose of easier data handling.

Functional Assays

Cell Culture and Transient Transfection

HEK-293T cells were grown in DMEM medium (Gibco, Paisley, Scotland, United Kingdom) supplemented with 2 mM L-glutamine, 100 U/mL penicillin/streptomycin, MEM Non-Essential Amino Acids Solution (1/100) and 5% (v/v) heat inactivated Foetal Bovine Serum (FBS) (Invitrogen, Paisley, Scotland, United Kingdom). Cells were maintained in a humid atmosphere of 5% CO_2 at 37°C. Cells were transiently transfected with the PEI (Polyethylenimine, Sigma, St. Louis, MO, United States) method as previously described (Medrano et al., 2017; Navarro et al., 2018b) and used for functional assays 48 h later (unless otherwise stated).

cAMP Determination

Signaling experiments have been performed as previously described (Navarro et al., 2010, 2016, 2018b; Hinz et al., 2018). Two hours before initiating the experiment, HEK-293T cell-culture medium was replaced by serum-starved DMEM medium. Then, cells were detached, resuspended in growing medium containing 50 μM zardaverine and placed in 384-well microplates (2,500 cells/well). Cells were pretreated (15 min) with CBG -or vehicle- and stimulated with agonists (15 min) before adding 0.5 μM forskolin or vehicle. Readings were performed after 15 min incubation at 25°C. HTRF energy transfer measures were performed using the Lance Ultra cAMP kit (PerkinElmer, Waltham, MA, United States). Fluorescence at 665 nm was analyzed in a PHERAstar Flagship microplate reader equipped with an HTRF optical module (BMG Lab Technologies, Offenburg, Germany).

ERK Phosphorylation Assays

To determine ERK1/2 phosphorylation, 50,000 HEK-293T cells/well were plated in transparent Deltalab 96-well microplates and kept at the incubator for 24 h. 2 to 4 h before the experiment, the medium was substituted by serum-starved DMEM medium. Then, cells were pre-treated at 25°C for 10 min with vehicle or CBG in serum-starved DMEM medium and stimulated for an additional 7 min with the specific agonists. Cells were then washed twice with cold PBS before addition of lysis

buffer (20 min treatment). 10 μL of each supernatant were placed in white ProxiPlate 384-well microplates and ERK 1/2 phosphorylation was determined using AlphaScreen®SureFire® kit (Perkin Elmer) following the instructions of the supplier and using an EnSpire® Multimode Plate Reader (PerkinElmer, Waltham, MA, United States).

Dynamic Mass Redistribution Assays (DMR)

Cell mass redistribution induced upon receptor activation was detected by illuminating the underside of a biosensor with polychromatic light and measuring the changes in the wavelength of the reflected monochromatic light. The magnitude of this wavelength shift (in picometers) is directly proportional to the amount of DMR. HEK-293T cells were seeded in 384-well sensor microplates to obtain 70–80% confluent monolayers constituted by approximately 10,000 cells per well. Previous to the assay, cells were washed twice with assay buffer (HBSS with 20 mM HEPES, pH 7.15) and incubated for 2 h with assay-buffer containing 0.1% DMSO (24°C, 30 μL/well). Hereafter, the sensor plate was scanned and a baseline optical signature was recorded for 10 min before adding 10 μL of CBG for 30 min followed by the addition of 10 μL of specific agonists; all test compounds were dissolved in assay buffer. The cell signaling signature was determined using an EnSpire® Multimode Plate Reader (PerkinElmer, Waltham, MA, United States) by a label-free technology. Then, DMR responses were monitored for at least 5,000 s. Results were analyzed using EnSpire Workstation Software v 4.10.

β-Arrestin 2 Recruitment

Arrestin recruitment was determined as previously described (Medrano et al., 2017; Navarro et al., 2018b). Briefly, BRET experiments were performed in HEK-293T cells 48 h after transfection with the cDNA corresponding to the CB_2R-YFP or CB_1R-YFP and 1 μg cDNA corresponding to β-arrestin 2-Rluc. Cells (20 μg protein) were distributed in 96-well microplates (Corning 3600, white plates with white bottom) and were incubated with CBG for 15 min and stimulated with the agonist for 10 min prior the addition of 5 μM coelenterazine H (Molecular Probes, Eugene, OR, United States). After 1 min of adding coelenterazine H, BRET between β-arrestin 2-Rluc and receptor-YFP was determined and quantified. The readings were collected using a Mithras LB 940 (Berthold Technologies, Bad Wildbad, Germany) that allows the integration of the signals detected in the short-wavelength filter at 485 nm and the long-wavelength filter at 530 nm. To quantify protein-RLuc expression luminescence readings were also performed 10 min of adding 5 μM coelenterazine H.

Data Handling and Statistical Analysis

Affinity values (Ki) were calculated from the IC_{50} obtained in competition radioligand binding assays according to the Cheng and Prusoff equation: $K_i = IC_{50}/(1 + [C]/K_D)$, where $[C]$ is the free concentration of the radioligand and K_D its dissociation constant (Cheng, 2001).

Data from homogeneous binding assays were analyzed using Prism 6 (GraphPad Software, Inc., San Diego, CA, United States). K_i values were determined according to the Cheng and Prusoff equation with K_D = 21 nM for CM-157 (Cheng, 2001). Signal-to-background (S/B ratio) calculations were performed by dividing the mean of the maximum value (μ_{max}) by that of the minimum value (μ_{min}) obtained from the sigmoid fits.

The data are shown as the mean ± SEM. Statistical analysis was performed with SPSS 18.0 software. The test of Kolmogorov–Smirnov with the correction of Lilliefors was used to evaluate normal distribution and the test of Levene to evaluate the homogeneity of variance. Significance was analyzed by one-way ANOVA, followed by Bonferroni's multiple comparison *post hoc* test. Significant differences were considered when $p < 0.05$.

RESULTS

Saturation and Competition Radioligand-Based Assays in Membranes Expressing CB_1R or CB_2R

The effect of CBG on radioligand binding to CB_1R or CB_2R was first tested using the classical radioligand-binding assay in membranes isolated from CHO cells expressing human CB_1R or CB_2R and incubated with radioligands: [^{3}H]-CP-55940 or [^{3}H]-WIN-55,212-2. Data obtained from binding isotherms using increasing [^{3}H]-CP-55940 or [^{3}H]-WIN-55,212-2 concentrations lead to a monophasic saturation curve. Saturation curves, receptor density (B_{max} values) and affinity (K_D values) are shown in **Figures 1A–D**. The affinity of the two radioligands was in the nanomolar range for both CB_1R and CB_2R. K_D for [^{3}H]-CP-55940 to CB_1R and CB_2R was similar with values around 0.3 nM. K_D values for WIN-55,212-2 were 9.4 and 3.2 nM for CB_1R and CB_2R, respectively (**Figures 1C,D**). Overall the results agree with previously reported data (McPartland et al., 2007; Merighi et al., 2010).

Competition binding assays of WIN-55,212-2 showed similar K_i values using the two radioligands to CB_1R and CB_2R and agreed with the K_D values for [^{3}H]-WIN-55,212-2 binding (**Table 1** and **Figures 1E,F**). **Table 1** reports the affinity values of CBG. K_i values of CBG obtained using [^{3}H]-CP-55940 as radioligand were in the low micromolar range in both CB_1R and CB_2R. The affinity value of CBG obtained using [^{3}H]-WIN-55,212-2 for CB_2R was 2.7 μM, about twofold higher than that obtained using [^{3}H]-CP-55940. Using [^{3}H]-WIN-55,212-2 in competition binding experiments on CB_1R, CBG was not able to displace the radioligand (**Figures 2A,B**). In summary, CBG displayed K_i values in the low micromolar range when competing for the binding to the CB_2R. Surprisingly, significant competition in the binding to the CB_1R was only observed when using [^{3}H]-CP-55940 as radioligand.

CBG Binds to the Orthosteric Site of Cannabinoid CB_2R at Nanomolar Concentrations

Competition experiments were performed using 20 nM of a fluorophore-conjugated selective CB_2R agonist (CM-157) and

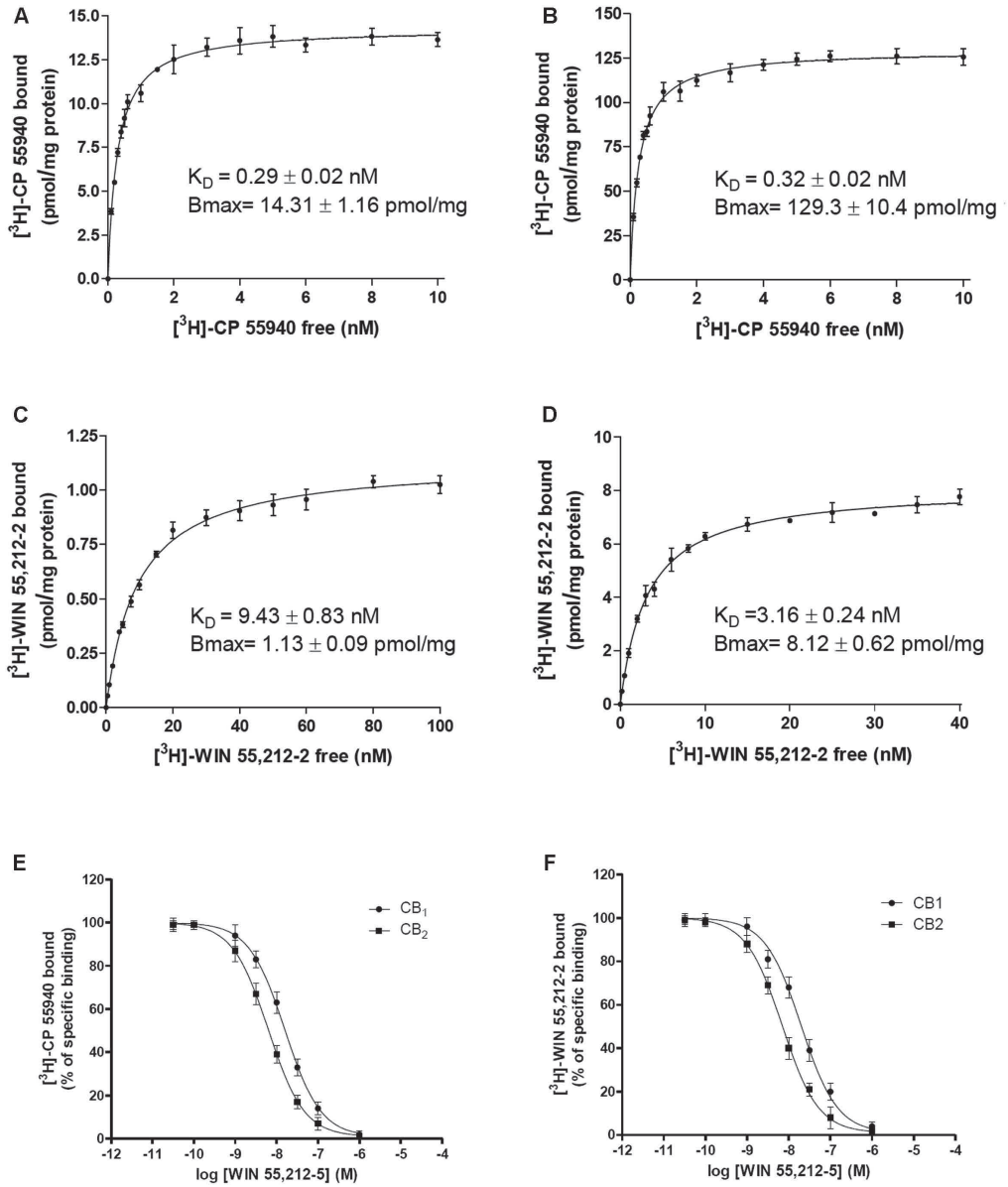

FIGURE 1 | Radioligand binding assays to CB_1R and CB_2R. **(A–D)** Saturation curves of either [^{3}H]-CP-55940 or [^{3}H]-WIN-55,212-2 binding on membranes from CHO cells stably expressing human CB_1R **(A,C)** or CB_2R **(B,D)**. **(E,F)** Competition curves for WIN-55,212-2 in radioligand-based assays using either [^{3}H]-CP-55940 **(E)** or [^{3}H]-WIN-55,212-2 **(F)** binding on membranes from CHO cells stably expressing human CB_1R or CB_2R. Data are expressed as the mean ± SEM of five independent experiments performed in duplicate. K_D (obtained from saturation isotherms) are shown in **Table 1**.

a homogeneous non-radioactive method performed in living cells expressing SNAP-CB_2R (details in Martínez-Pinilla et al., 2016; **Figure 2C**). Unfortunately, the equivalent fluorophore-conjugated selective CB_1R ligand is not available to perform HTRF assays in SNAP-CB_1R-expressing living cells. Competition assays were performed in HEK-293T cells expressing Lumi4-Tb-labeled CB_2R fused to the SNAP protein and incubated with a fixed amount of the fluorophore-conjugated agonist and different CBG concentrations. As observed in **Figure 2**, both the unlabelled selective agonist (CM-157) and CBG decreased the binding to SNAP-CB_2R in monophasic fashion and with K_i values in the nanomolar range (16 nM for CM-157 and of 152 nM for CBG; **Figures 2D,E**). The K_i obtained for CM-157 matches with previously reported dissociation constant K_D values (Martínez-Pinilla et al., 2016). These results indicate that CBG can significantly bind to the orthosteric site of cannabinoid CB_2R at nanomolar concentrations.

Similar experiments were carried out in HEK-293T cells expressing SNAP-CB_2R fusion protein and a similar amount of CB_1R, i.e., in cells that express CB_2R in a CB_1–CB_2 receptor heteromer context. In the presence of cannabinoid CB_1R the K_i for CM-157 was 19 nM (**Figure 2F**) and K_i for CBG was reduced

TABLE 1 | Affinity values of CB compounds obtained from radioligand binding assays.

	[^{3}H]-CP-55940 competition binding experiments		[^{3}H]-WIN-55,212-2 competition binding experiments	
	CB_1 – K_D (nM)	**CB_2 – K_D (nM)**	**CB_1 – K_D (nM)**	**CB_2 – K_D (nM)**
	0.29 ± 0.02	0.32 ± 0.02	9.43 ± 0.83	3.16 ± 0.24
	CB_1 – K_i (nM)	**CB_2 – K_i (nM)**	**CB_1 – K_i (nM)**	**CB_2 – K_i (nM)**
WIN-55,212-2	8.08 ± 0.65	3.22 ± 0.31	9.86 ± 0.84	3.48 ± 0.27
CBG	1,045 ± 74	1,225 ± 85	>30,000	2,656 ± 130
CBD	1,690 ± 110	1,714 ± 70	>30,000	4,019 ± 342

K_D values were obtained from saturation isotherms and K_i from data in competition assays using the indicated radiolabelled compounds ([^{3}H]-CP-55940 or [^{3}H]-WIN-55,212-2).

(56 nM, **Figure 2G**). These results indicate that in cells expressing both cannabinoid receptors, CB_1 and CB_2, CBG shows higher affinity for cannabinoid CB_2R.

CBG Effects on Cannabinoid Receptor-Agonist-Induced Effects

Previous reports Gauson et al. (2007), Cascio et al. (2010) suggest that CBG may be a partial agonist of cannabinoid receptors. To investigate this possibility, HEK-293T cells expressing CB_1R or CB_2R were treated with increasing concentrations of CBG (1 nM to 10 μM) and cAMP, MAPK, β-arrestin recruitment and dynamic mass cell redistribution (DMR) assays were developed. Interestingly, it was observed that in cells expressing CB_1R (**Figure 3**, blue curves), CBG induced a small decrease in forskolin induced cAMP levels and a small increase in β-arrestin recruitment (**Figures 3A,C**), while having no significant action on MAPK phosphorylation assay (**Figure 3B**). Consequently, CBG in label-free assays induced a slight effect in the DMR signal (**Figure 3D**) that is consistent with a G protein-dependent action on cAMP levels; label-free signal is based on optical detection of DMR following receptor activation and mainly reflects G-protein-coupling (Kebig et al., 2009; Schröder et al., 2009; Hamamoto et al., 2015). On the other hand, in HEK-293T cells expressing CB_2R (**Figure 3**, red curves), the action on forskolin-induced cAMP levels and on the DMR signal was small and similar to that exerted in CB_1R-expressing cells (**Figure 3A**). On the contrary, the activation of the MAP kinase pathway was notable (**Figure 3B**). Also noteworthy was the CBG-induced β-arrestin recruitment (**Figure 3C**). Taken together these data suggest that CBG is a poor agonist of CB_1R, whereas it acts as a partial agonist in some of the signaling pathways analyzed in cells expressing CB_2R.

To further examine the CBG effect over CB_1R, HEK-293T cells expressing CB_1R were treated with the endocannabinoid agonist, AEA, or with ACEA in the presence or in the absence of 100 nM or 1 μM CBG. In forskolin-induced cAMP assays we found that 100 nM or 1 μM CBG pretreatment induced a significant decrease in both, AEA and ACEA induced effects (**Figure 4A**). In contrast, CBG (100 nM or 1 μM) was unable to modify the agonist-induced MAPK phosphorylation and β-arrestin recruitment (**Figures 4B,C**). In label-free DMR assays the results were similar to those obtained in cAMP determination assays, i.e., CBG reduced the effect of the agonists (**Figure 4D**).

Cannabigerol (100 nM or 1 μM) was also tested in HEK-293T cells expressing CB_2R and using AEA and a receptor selective agonist, JWH133. Pretreatment with CBG reduced the effects of AEA and JWH133 in experiments of forskolin-induced cAMP levels, ERK1/2 phosphorylation and in label-free DMR read-outs (**Figure 4**). In contrast, CBG did not affect the recruitment of β-arrestin induced by agonists (**Figure 4G**). This last result may be due to the low sensitivity of the assay as β-arrestin recruitment BRET signal was virtually negligible. Energy transfer techniques completely depend on the correct orientation of the fusion proteins and the reduced signal may be due to poor recruitment of β-arrestin and/or to a high distance between BRET donor/acceptor in the putative β-arrestin-Rluc/CB_2R-YFP complex. Thus, CBG in cells activated by endocannabinoids or by selective agonists behaves as a partial agonist of the CB_2R.

CBG Effect in HEK-293T Cells Expressing CB_1R and CB_2R

Experiments were finally performed in cells co-expressing the two cannabinoid receptors, which are able to form heteromeric complexes. A CB_1–CB_2 receptor heteromer print consists of a negative cross-talk observed in Akt phosphorylation and neurite outgrowth; i.e., activation of one receptor reduces the signaling originated upon partner receptor activation (Callén et al., 2012). To characterize the CBG effect, experiments were performed in HEK-293T cells expressing the two cannabinoid receptors. Dose-effect curves were provided for cAMP level and ERK1/2 phosphorylation determination, and for label-free DMR signal and β-arresting recruitment. Interestingly, the effect on cAMP level determination and DMR assays was additive (**Figure 5**), i.e., the presence of CBG blunted the negative cross-talk in these signaling pathways. However, the negative cross-talk was still evident in both ERK1/2 phosphorylation and β-arrestin recruitment experiments (**Figures 5B,C**).

Finally, the effect of 100 nM CBG (100 nM) on AEA, ACEA and/or JWH133 actions was investigated in cells co-expressing CB_1R and CB_2R. CBG pretreatment led to significant effects, always reducing the effect of the agonists, in cAMP-related assays (**Figure 5E**). However, the effect in the other assay types was

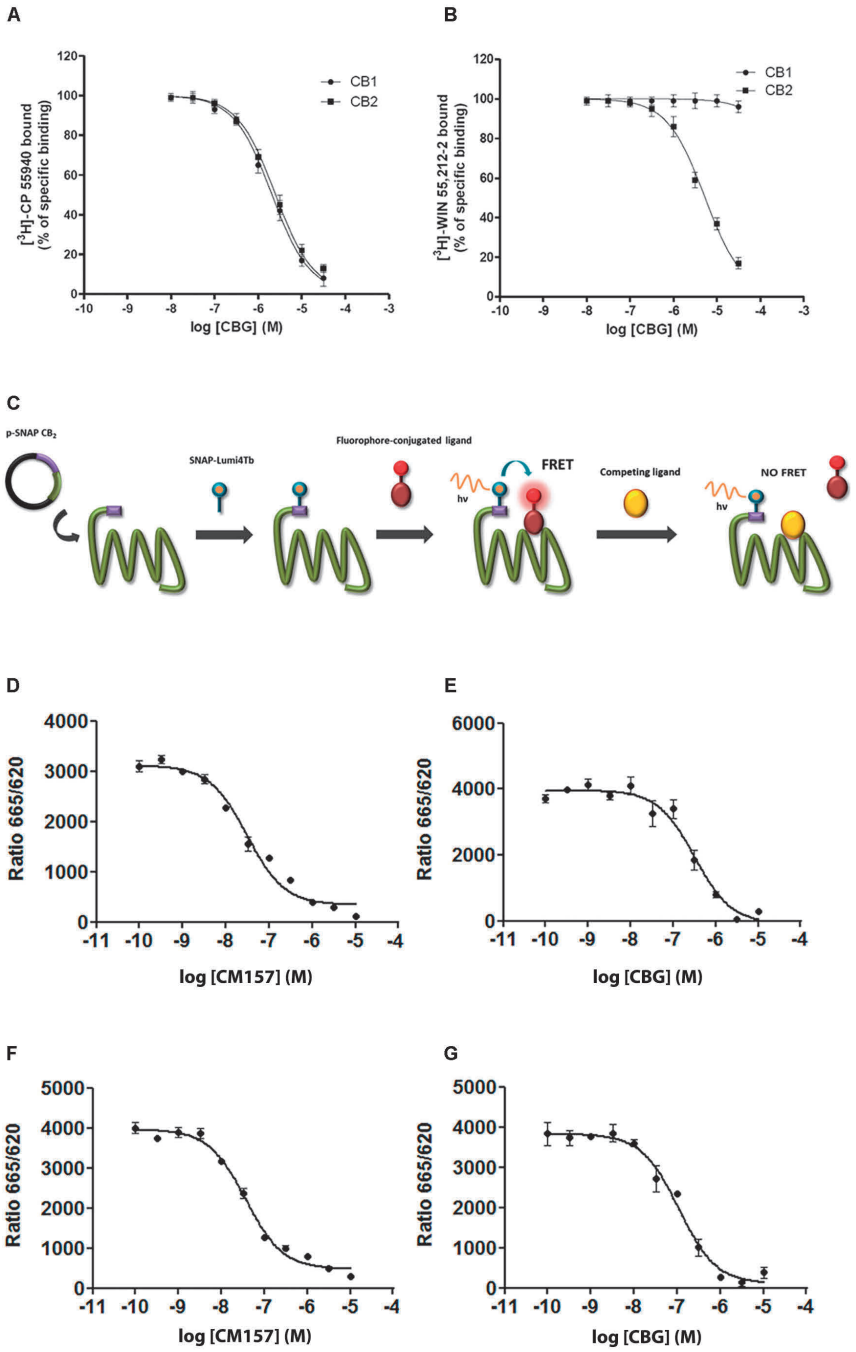

FIGURE 2 | Competition by CBG of agonist binding to CB_1R and/or CB_2R. **(A,B)** Competition curves for CBG in radioligand-based assays using either [^{3}H]-CP-55940 **(A)** or [^{3}H]-WIN-55,212-2 **(B)** binding on membranes from CHO cells stably expressing human CB_1R or CB_2R. **(C)** Scheme of the HTRF-based competitive binding assay. The GPCR of interest with the SNAP-tagged enzyme fused to its N-terminal domain is expressed at the cell surface. SNAP is a commercially available tag consisting of circa 180 amino acids, that can be labeled with fluorophores or other probes in a covalent fashion. The GPCR–SNAP-tagged cells are subsequently labeled with a Tb-containing probe (SNAP-Lumi4-Tb) through a covalent bond between the Tb and the reactive side of the SNAP enzyme. The Tb acts as FRET donor of an acceptor covalently linked to a selective CB2 receptor ligand. Thus, upon binding of a fluorophore-conjugated ligand (FRET acceptor) on the donor-labeled SNAP-tagged/GPCR fusion protein, an HTRF signal from the sensitized acceptor can be detected since the energy transfer can occur only when the donor and the acceptor are in close proximity. In competition binding assays using CM-157, the unlabelled specific ligand competes for receptor binding site with the fluorophore-conjugated ligand, leading to a decrease in the HTRF signal detected. **(D–G)** HEK-293T were transiently transfected with 1 μg cDNA for SNAP-CB_2R in the absence **(D,E)** or presence of 0.5 μg cDNA for CB_1R **(F,G)**. Competition curves of specific binding of 20 nM fluorophore-conjugated CM-157 using CM-157 (0–10 μM) **(D,F)** or of CBG (0–10 μM) **(E,G)** as competitors are shown. Data represent the mean ± SEM of five experiments in triplicates.

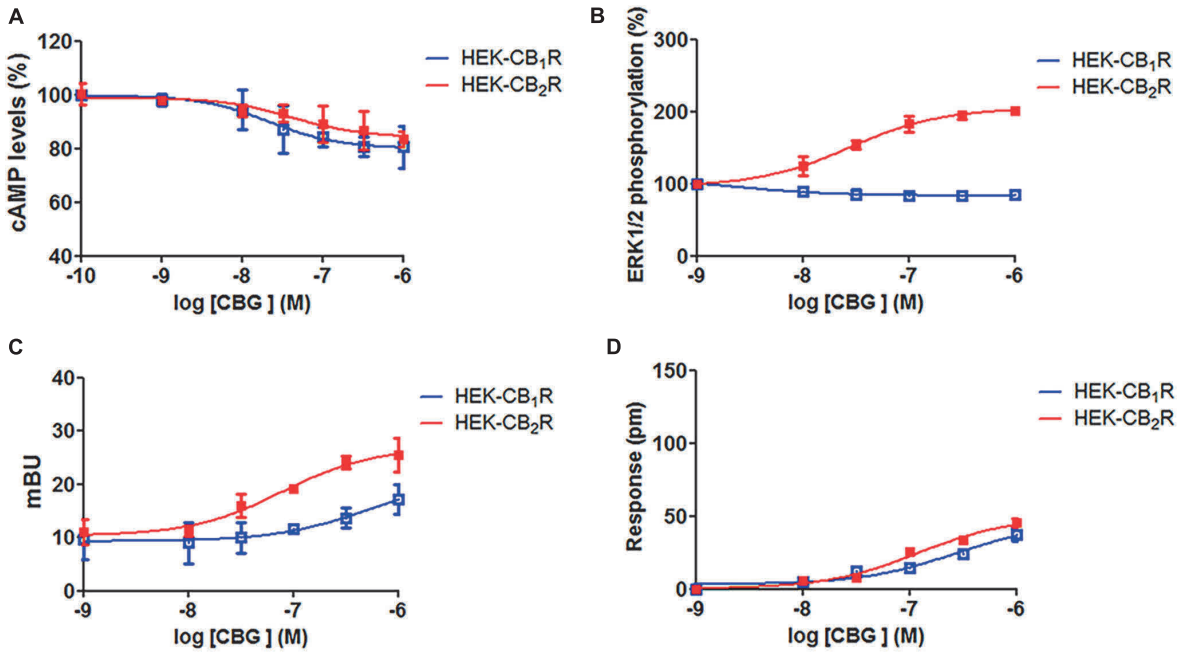

FIGURE 3 | Cannabigerol action in cells expressing CB_1R or CB_2R. HEK-293T cells were transfected with 0.75 μg cDNA for CB_1R (red line) or 1 μg cDNA for CB_2R (blue line). Dose–effect curves for cAMP production are expressed as % of levels obtained by 0.5 μM forskolin treatment **(A)**. Dose-effect curves for ERK1/2 phosphorylation are expressed as % respect to basal levels **(B)**. Dose-effect curves for β-arrestin recruitment **(C)** and label-free **(D)** assays are expressed, respectively, in mBRET units and pm. In β-arrestin-2 recruitment assays cells were transfected with 1 μg cDNA for β-arrestin-Rluc and either 0.75 μg cDNA for CB_1R-YFP or 1 μg cDNA for CB_2R-YFP. Data are the mean ± SEM of a representative experiment in triplicates (n = 6).

negligible except for the negative modulation of the ACEA effect on ERK1/2 phosphorylation and DMR, and of the AEA effect on DMR read-outs (**Figures 5F–H**). Therefore, CBG either blunted the cAMP-dependent signaling or did not significantly alter the negative cross-talk when other CB_1/CB_2-mediated signaling read-outs were determined (see **Figures 5B,C**). It should be noted that cross-talk at the intracellular signaling level, cannot be ruled out to partly explain some of the findings (Bayewitch et al., 1995; Wartmann et al., 1995; Mcguinness et al., 2009; Peters and Scott, 2009; Van Der Lee et al., 2009).

DISCUSSION

The aim of this paper was to comparatively address CBG pharmacology and effects on CB_1 and CB_2 receptors, and on CB_1–CB_2 heteroreceptor complexes. The binding experiments using radiolabelled- and non-radiolabelled-based approaches have provided relevant results. The results on CB_2R are clear an indicate that CBG acts as a competitive partial agonist ligand. There is, however, an interesting observation as the K_i values for competing both [^{3}H]-CP-55940 and [^{3}H]-WIN-55,212-2 are in the low micromolar range (**Table 1**), whereas displaying a value of 152 nM in HTRF-based assays. As pointed out in previous reports, the conditions of the approach using a fluorescent-conjugated CM-157 allows identification of different states of the receptor. Irrespective of the molecular mechanism, the marked differences in affinity constants suggest different ways to accommodate the ligand within the orthosteric center. To our knowledge this is the first report performed in parallel binding assays using three different ligands that reportedly bind to the orthosteric center of the CB_2R ([^{3}H]-CP-55940, [^{3}H]-WIN-55,212-2 and fluorescence-conjugated-CM-157). In summary, the most reasonable assumption is that CBG binds to the orthosteric center of CB_2R but with marked differences in affinity depending on the assay. It should be noted that differences in affinity may result from the fact that HTRF binding is performed in living cells whereas radioligand binding assays are performed in isolated membranes. The already existing data concerning CBG affinity for CB_1 and CB_2 receptors, all performed using [^{3}H]-CP-55940 also indicate that the affinity may vary depending on the context of the receptor, by *inter alia* the constraints of the membrane, heteromerization or interaction with G-proteins. Comparing our results with similar data using [^{3}H]-CP-55940, the affinity is higher for receptors expressed in HEK-293 cells or in brain membranes (Gauson et al., 2007; Pertwee, 2008; Pollastro et al., 2011) that in receptors expressed in CHO cells (**Table 1**). In competition assays of radioligand binding to CB_1R or to CB_2R, affinity for CBG is similar to that previously published (Gauson et al., 2007; Pertwee, 2008), except in the case of Sf9 cells (K_i: 897 and 153 nM for, respectively, CB_1R and CB_2R). This piece of data would indicate conformational changes induced by third molecules that affect the binding of the radioligand and/or of CBG. In fact, Sf9 are insect cells that do not express the cognate G_i protein and, therefore, Gαi3β1γ2 was heterologously expressed to perform the

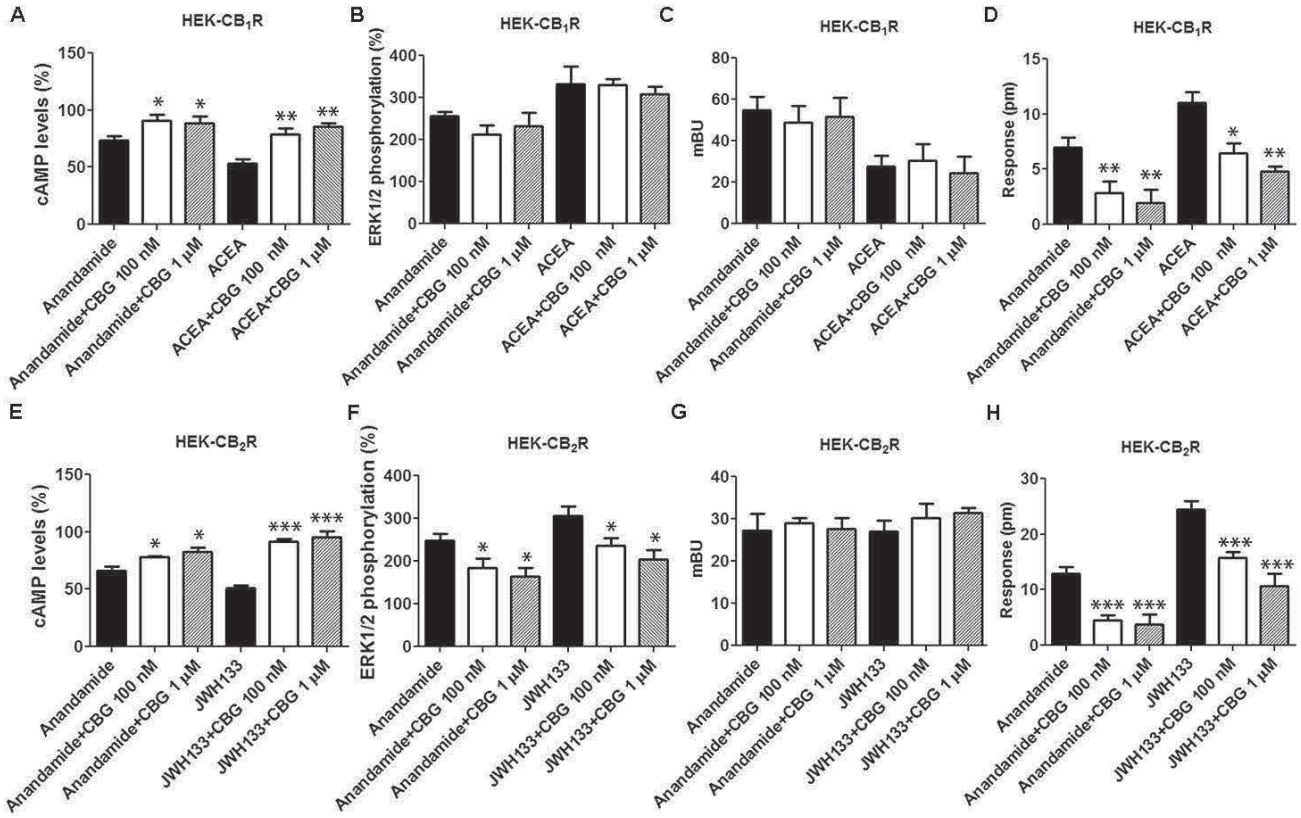

FIGURE 4 | Effect of CBG on the action of CB_1R and CB_2R agonists. **(A–D)** HEK-293T cells were transfected with 0.75 μg cDNA for CB_1R and treated with 100 nM AEA or a selective CB_1R ligand (100 nM ACEA) in the absence (black bars) or presence of 100 nM (white bars) or 1 μM (gray bars) CBG. **(E–H)** HEK-293T cells were transfected with 1 μg cDNA for CB_2R and treated with 100 nM AEA or a selective CB_2R ligand (100 nM JWH133) in the absence (black bars) or presence of 100 nM (white bars) or 1 μM (gray bars) CBG. cAMP production **(A,E)** is expressed as % of levels obtained by 0.5 μM forskolin. ERK1/2 phosphorylation data are expressed as % respect to basal levels **(B,F)**. In β-arrestin-2 recruitment assays cells were transfected with 1 μg cDNA for β-arrestin-Rluc and either 0.75 μg cDNA for CB_1R-YFP or 1 μg cDNA for CB_2R-YFP. Data for β-arrestin recruitment **(C,G)** and label-free **(D,H)** assays are expressed, respectively, in mBRET units and pm. Data represent the mean ± SEM of six different experiments performed with six replicates. One-way ANOVA and Bonferroni's multiple comparison *post hoc* test were used for statistical analysis (*$p < 0.05$, **$p < 0.01$, ***$p < 0.001$; versus treatment with AEA, ACEA, or JWH133 alone).

binding assays that led to different affinities for CBG (897 and 153 nM for, respectively, CB_1R and CB_2R) (Rosenthaler et al., 2014).

The results from binding to the CB_1R are not very robust and more difficult to interpret. Unfortunately, there are no ligands available to perform HTRF binding to SNAP-CB_1R-expressing living cells, whereas the data from competition assays using [^{3}H]-CP-55940 or [^{3}H]-WIN-55,212-2 were contradictory. On the one hand, the K_i for binding to the CB_1R using [^{3}H]-CP-55940 was in the low micromolar range, as it occurred with data from radioligand binding to the CB_2R. However, CBG was unable to compete [^{3}H]-WIN-55,212-2 binding to the CB_1R. Taking into account that recognition sites for CP-55940 and WIN-55,212-2 are not identical in the CB_1R, one possibility is that CBG binds to the orthosteric center but displaying different equilibrium binding parameters depending on the radioligand. It was early observed that Lys^{192} in the CB_1R third transmembrane domain (TM3) was crucial for binding of CP-55940 and AEA but not for WIN-55,212-2 (Bonner et al., 1996; Chin et al., 1998). Later, *in silico* models pointed to an hydrophobic pocket for CP-55940 binding that involved residues in different transmembrane domains (not only in TM3) and in the second extracellular loop (Shim et al., 2003). Those models showed that WIN-55,212-2 not only binds to the hydrophobic pocket described for CP-55940 but to another hydrophobic region involving residues in TM2 and TM3 (Shim and Howlett, 2006). The structure of CBG is more similar to CP-55940 than to WIN-55,212,2, bearing an OH in the A ring that may interact with the TM3 Lys^{192} residue. In brief, CBG binds to the orthosteric center of CB_1R as indicated by the fact that CBG affects CP-55940 binding without affecting the binding of [^{3}H]-WIN-55,212-2. In other words, CBG was able to distinguish between two subregions of the CB_1R orthosteric center. We therefore suggest that pharmacological studies concerning the CB_1R should be run in parallel using radiolabelled CP-55940 and WIN-55,212-2. Interestingly CP-55940 and WIN-55,212-2 are able to fix the CB_1R in two different conformations (Georgieva et al., 2008) and, therefore, CBG would affect more the conformation and signaling arising from occupation of the CP-55940 binding site. Other possibilities cannot be ruled out and, in this respect,

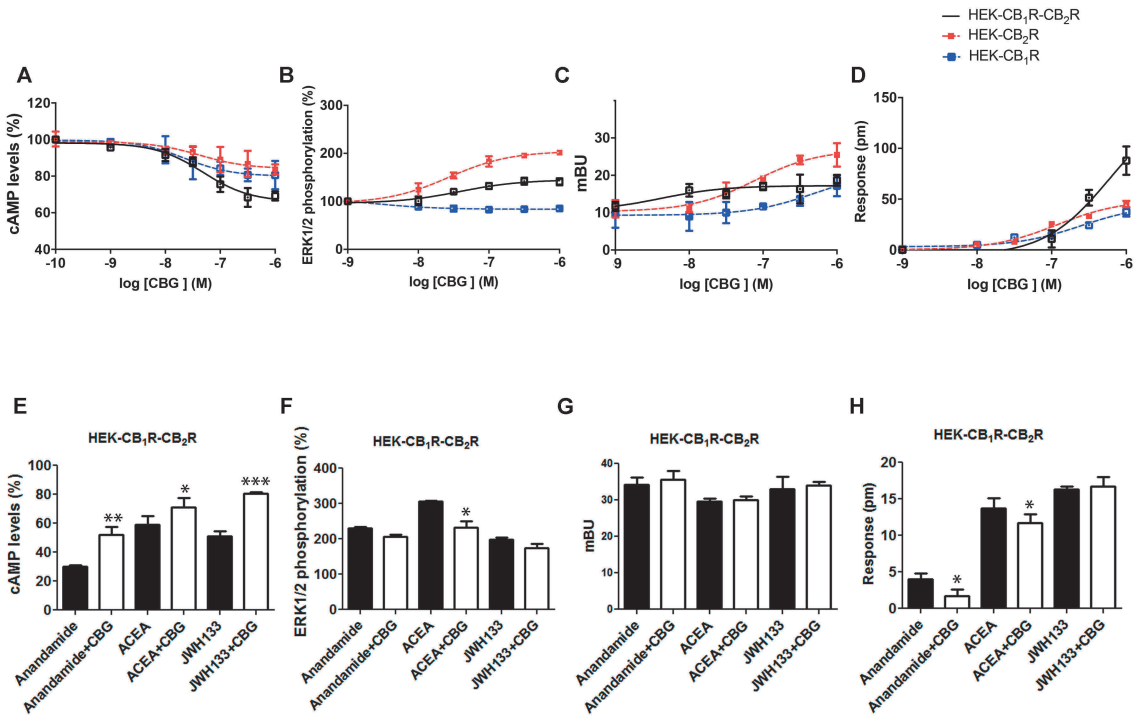

FIGURE 5 | Effect of CBG in cells expressing CB_1 and CB_2 receptors. **(A–D)** Effect of CBG in HEK-293T cells transfected with 0.75 μg cDNA for CB_1R and 1 μg cDNA for CB_2R **(A,B,D)** or 1 μg cDNA for β-arrestin-Rluc, 0.75 μg cDNA for CB_1R and 1 μg cDNA for CB_2R-YFP **(C)**. Dose–effect curves for cAMP production are expressed as % of levels obtained by 0.5 μM forskolin treatment **(A)**. Dose-effect curves for ERK1/2 phosphorylation are expressed as % respect of basal levels **(B)**. Dose-effect curves for β-arrestin recruitment **(C)** and label-free **(D)** assays are expressed, respectively, in mBRET units and pm. Dotted lines (red and blue) are the same than those shown in **Figure 3** and serve as a reference for differential effects in cells coexpressing both receptors. Data are the mean ± SEM of a representative experiment in triplicates ($n = 6$). **(E–H)** HEK-293T cells transfected with 0.75 μg cDNA for CB_1R and 1 μg cDNA for CB_2R **(E,F,H)** or 1 μg cDNA for β-arrestin-Rluc, 0.75 μg cDNA for CB_1R and 1 μg cDNA for CB_2R-YFP **(G)** were treated with 100 nM AEA or a selective CB_2R ligand (100 nM JWH133) in the absence (black bars) or presence (white bars) of 100 nM CBG. cAMP production **(E)** is expressed as % of levels obtained by 0.5 μM forskolin. ERK1/2 phosphorylation data are expressed as % respect of basal levels **(F)**. Data for β-arrestin recruitment **(G)** and label-free **(H)** assays are expressed, respectively, in mBRET units and pm. Data represent the mean ± SEM of six different experiments performed with three replicates. One-way ANOVA and Bonferroni's multiple comparison *post hoc* test were used for statistical analysis (*$p < 0.05$, **$p < 0.01$, ***$p < 0.001$; versus treatment with AEA, ACEA, or JWH133 alone).

we assayed CBD in competition assays and obtained similar results than those obtained using CBG (**Table 1**). Accordingly, CBG could act on CB_1R (but not on CB_2R) as non-competitive (allosteric) modulator, as described for CBD (Laprairie et al., 2015).

When one compound binds to the orthosteric center and affects several signaling pathways with different potency as in the case of CBG in cells expressing CB_1R, the phenomenon is known as functional selectivity or biased agonism. In cells expressing CB_1R, CBG effect is skewed toward the G_i-mediated signaling pathway. This is in agreement with our finding of significant effect in label-free assays; often DMR signals correlate with effect on cAMP levels in the case of receptors coupled to G_i or G_s proteins (Grundmann and Kostenis, 2015a,b; Hamamoto et al., 2015). It is, however, intriguing that CBG was unable to displace the binding of [^{3}H]-WIN-55,212-2 to the CB_1R. Therefore, an action of CBG on a particular state of the receptor, which, in the case of CB_2R may be disclosed by HTRF binding in living cells (Martínez-Pinilla et al., 2016), cannot be ruled out. Taking together all results, an allosteric action of CBG on the CB_1R would not explain why it is able to engage G_i –mediating signaling. Another possibility, which was suggested for AM630, a previously considered CB_2R antagonist (Bolognini et al., 2012), is that CBG is a protean agonist displaying biased agonism.

Data from CB_2R-mediated functional assays were easier to interpret. First of all, the efficacy was lower compared to selective synthetic agonists and endocannabinoids. Also, CBG led to biased agonism as the effect on cAMP levels was small while being quite marked in ERK phosphorylation and β-arrestin recruitment. Therefore, CBG acted as a partial agonist and, as such, it was able to reduce the effects of other cannabinoid agonists. At 1 μM the effect of CBG on receptor activation by other agonists was similar to that exerted by 100 nM (**Figure 4**) thus suggesting that the *effective* affinity in living cells is that obtained in HTRF non-radioactive-based assays.

Due to the complex pharmacology of cannabinoids this research was undertaken to investigate whether CBG could be exerting a differential action on the CB_1–CB_2 receptor heteromers. Previous data have shown that the interplay between the two receptors in an heteromeric context is also complex. Whereas Callén et al. (2012) showed a negative cross-talk in

a heterologous expression system, the allosteric interaction in the CB_1–CB_2 heteroreceptor complex is synergistic in primary cultures of activated microglia activated with LPS and interferon gamma and in primary cultures of microglia from a transgenic model of Alzheimer's disease (Navarro et al., 2018a). Dose-effect experiments here undertaken in the HEK-293T-based heterologous expression system showed that CBG treatment in the absence of any other agonist, led to additive/synergistic effects on cAMP and label-free read-outs. In contrast, in ERK phosphorylation and β-arrestin recruitment, we found the negative cross-talk already described for this heteromer when full agonists are used to activate the receptors (Callén et al., 2012). These results suggest that partial agonism on the CB_2R is regulated by the presence of CB_1R; however, more complex alternative scenarios cannot be ruled out as CBG may act on the orthosteric site of the CB_2R protomer and as protean agonist of the CB_1R protomer. In cells expressing the two receptors, the overall effect of 100 nM CBG on agonist-induced activation is more consistent with acting on CB_2R than on CB_1R. In fact, the results in co-expressing cells, which likely express heteromers, are similar to those encountered in CB_2R-expressing cells. In summary, CBG significantly modulates CB_2R- or CB_1R/CB_2R-mediated endocannabinoid action, while the effects are weak in CB_1R-expressing cells. Our findings demonstrating the action of CBG on the cannabinoid receptors are in complete agreement and may explain the *in vitro* results, reporting the protection of macrophages against oxidative stress (Giacoppo et al., 2017), and the beneficial *in vivo* effects in a model of inflammatory bowel disease (Borrelli et al., 2013). In the first of these two studies CBG-mediated protection is blocked by AM630, a selective CB_2R ligand, whereas the CB_1R antagonist, SR141716A, had no effect on CBG action (Giacoppo et al., 2017). The second study reported that CBG may both reduce the histological and molecular changes of experimental colitis and nitrite release from macrophages after LPS stimulation; again these effects were seemingly mediated by CB_2R (Borrelli et al., 2013). These results can be explained by our findings; CBG acting as a partial agonist and exerting actions via CB_2R in macrophages (Giacoppo et al., 2017) or "antagonizing" the effects of endogenous or synthetic cannabinoids, as in LPS-stimulated macrophages (Borrelli et al., 2013). In conclusion, the results presented in this study reveal that the non-psychotropic phytocannabinoid, CBG, may exert beneficial actions with therapeutic potential via cannabinoid receptors.

AUTHOR CONTRIBUTIONS

XN and RF had the original idea, designed and coordinated actions in the different participating institutions, and wrote the initial manuscript. GN performed non-radiolabelled-based homogeneous binding assays, participated in the signaling experiments, and significantly contributed to manuscript preparation. IR-R participated in the signaling experiments and in writing methods. RR-S actively participated in data analysis and parameter calculation. EC supervised data analysis, provided pharmacological expertise, and insight into data interpretation. FV performed the radioligand binding experiments. KV and PB performed the radioligand binding data analysis and interpretation. SC selected the *Cannabis* varieties and supervised the production of the vegetal raw material used for the isolation and purification of cannabinoids. VSM performed the isolation and purification of cannabinoids. CS-CC and CF-V performed the analytical quality control to the purified cannabinoids. All co-authors critically revised, contributed to the editing, and approved the manuscript.

FUNDING

This work was partially supported by grants from the Spanish Ministry of Economy and Competitiveness (Ref. No. BFU2015-64405-R and SAF2017-84117-R; they may include FEDER funds) and by a grant 201413-30 from: *Fundació la Marató de TV3*.

REFERENCES

Adams, A. J., Banister, S. D., Irizarry, L., Trecki, J., Schwartz, M., and Gerona, R. (2017). Zombie" outbreak caused by the synthetic cannabinoid AMB-FUBINACA in New York. *N. Engl. J. Med.* 376, 235–242. doi: 10.1056/NEJMoa1610300

Bayewitch, M., Avidor-Reiss, T., Levy, R., Barg, J., Mechoulam, R., and Vogel, Z. (1995). The peripheral cannabinoid receptor: adenylate cyclase inhibition and G protein coupling. *FEBS Lett.* 375, 143–147. doi: 10.1016/0014-5793(95)01207-U

Bolognini, D., Grazia, A., Parolaro, D., and Pertwee, R. G. (2012). AM630 behaves as a protean ligand at the human cannabinoid CB2 receptor. *Br. J. Pharmacol.* 165, 2561–2574. doi: 10.1111/j.1476-5381.2011.01503.x

Bonner, I., Song, Z. H., and Bonner, T. I. (1996). A lysine residue of the cannabinoid receptor is critical for receptor recognition by several agonists but not WIN55212-2. *Mol. Pharmacol.* 49, 891–896.

Borrelli, F., Fasolino, I., Romano, B., Capasso, R., Maiello, F., Coppola, D., et al. (2013). Beneficial effect of the non-psychotropic plant cannabinoid cannabigerol on experimental inflammatory bowel disease. *Biochem. Pharmacol.* 85, 1306–1316. doi: 10.1016/j.bcp.2013.01.017

Callén, L., Moreno, E., Barroso-Chinea, P., Moreno-Delgado, D., Cortés, A., Mallol, J., et al. (2012). Cannabinoid receptors CB1 and CB2 form functional heteromers in brain. *J. Biol. Chem.* 287, 20851–20865. doi: 10.1074/jbc.M111.335273

Cascio, M. G., Gauson, L. A., Stevenson, L. A., Ross, R. A., and Pertwee, R. G. (2010). Evidence that the plant cannabinoid cannabigerol is a highly potent α 2-adrenoceptor agonist and moderately potent 5HT 1A receptor antagonist. *Br. J. Pharmacol.* 159, 129–141. doi: 10.1111/j.1476-5381.2009.00515.x

Cheng, H. C. (2001). The power issue: determination of KB or Ki from IC50 - A closer look at the Cheng-Prusoff equation, the Schild plot and related power equations. *J. Pharmacol. Toxicol. Methods* 46, 61–71. doi: 10.1016/S1056-8719(02)00166-1

Chin, C. N., Lucas-Lenard, J., Abadji, V., and Kendall, D. A. (1998). Ligand binding and modulation of cyclic AMP levels depend on the chemical nature of residue 192 of the human cannabinoid receptor 1. *J. Neurochem.* 70, 366–373.

De Petrocellis, L., Ligresti, A., Moriello, A. S., Allarà, M., Bisogno, T., Petrosino, S., et al. (2011). Effects of cannabinoids and cannabinoid-enriched *Cannabis* extracts on TRP channels and endocannabinoid metabolic enzymes. *Br. J. Pharmacol.* 163, 1479–1494. doi: 10.1111/j.1476-5381.2010.01166.x

De Petrocellis, L., Vellani, V., Schiano-Moriello, A., Marini, P., Magherini, P. C., Orlando, P., et al. (2008). Plant-derived cannabinoids modulate the activity of transient receptor potential channels of ankyrin type-1 and melastatin type-8. *J. Pharmacol. Exp. Ther.* 325, 1007–1015. doi: 10.1124/jpet.107.134809

Diana, M. A., and Marty, A. (2004). Endocannabinoid-mediated short-term synaptic plasticity: depolarization-induced suppression of inhibition (DSI) and depolarization- induced suppression of excitation (DSE). *Br. J. Pharmacol.* 142, 9–19. doi: 10.1038/sj.bjp.0705726

Fellermeier, M., and Zenk, M. H. (1998). Prenylation of olivetolate by a hemp transferase yields cannabigerolic acid, the precursor of tetrahydrocannabinol. *FEBS Lett.* 427, 283–285. doi: 10.1016/S0014-5793(98)00450-5

Gaoni, Y., and Mechoulan, R. (1964). Structure synthesis of cannabigerol new hashish constituent. *Proc. Chem. Soc. Lond.* 82, 2189–2192.

Gauson, L. A., Stevenson, L. A., Thomas, A., Baillie, G. L., Ross, R. A., and Pertwee, R. G. (2007). "Cannabigerol behaves as a partial agonist at both CB1 and CB2 receptors," in *Proceedings of the 17th Annual Symposium on the Cannabinoids*, (Burlington, VT: International Cannabinoid Research Society), 206.

Georgieva, T., Devanathan, S., Stropova, D., Park, C. K., Salamon, Z., Tollin, G., et al. (2008). Unique agonist-bound cannabinoid CB1 receptor conformations indicate agonist specificity in signaling. *Eur. J. Pharmacol.* 581, 19–29. doi: 10.1016/j.ejphar.2007.11.053

Giacoppo, S., Gugliandolo, A., Trubiani, O., Pollastro, F., Grassi, G., Bramanti, P., et al. (2017). Cannabinoid CB2 receptors are involved in the protection of RAW264.7 macrophages against the oxidative stress: An in vitro study. *Eur. J. Histochem.* 61, 1–13. doi: 10.4081/ejh.2017.2749

Granja, A. G., Carrillo-Salinas, F., Pagani, A., Gómez-Cañas, M., Negri, R., Navarrete, C., et al. (2012). A cannabigerol quinone alleviates neuroinflammation in a chronic model of multiple sclerosis. *J. Neuroimmune Pharmacol.* 7, 1002–1016. doi: 10.1007/s11481-012-9399-3

Grundmann, M., and Kostenis, E. (2015a). Holistic methods for the analysis of cNMP effects. *Handb. Exp. Pharmacol.* 238, 339–357. doi: 10.1007/164_2015_42

Grundmann, M., and Kostenis, E. (2015b). Label-free biosensor assays in GPCR screening. *Methods Mol. Biol.* 1272, 199–213. doi: 10.1007/978-1-4939-2336-6_14

Grunfeld, Y., and Edery, H. (1969). Psychopharmacological activity of the active constituents of hashish and some related cannabinoids. *Psychopharmacologia* 14, 200–210. doi: 10.1007/BF00404218

Hamamoto, A., Kobayashi, Y., and Saito, Y. (2015). Identification of amino acids that are selectively involved in Gi/o activation by rat melanin-concentrating hormone receptor 1. *Cell. Signal.* 27, 818–827. doi: 10.1016/j.cellsig.2015.01.008

Hinz, S., Navarro, G., Borroto-Escuela, D., Seibt, B. F., Ammon, C., de Filippo, E., et al. (2018). Adenosine A2A receptor ligand recognition and signaling is blocked by A2B receptors. *Oncotarget* 9, 13593–13611. doi: 10.18632/oncotarget.24423

Kebig, A., Kostenis, E., Mohr, K., and Mohr-Andrä, M. (2009). An optical dynamic mass redistribution assay reveals biased signaling of dualsteric GPCR activators. *J. Recept. Signal Transduct.* 29, 140–145. doi: 10.1080/10799890903047437

Lanciego, J. L., Barroso-Chinea, P., Rico, A. J., Conte-Perales, L., Callén, L., Roda, E., et al. (2011). Expression of the mRNA coding the cannabinoid receptor 2 in the pallidal complex of *Macaca fascicularis*. *J. Psychopharmacol.* 25, 97–104. doi: 10.1177/0269881110367732

Laprairie, R. B., Bagher, A. M., Kelly, M. E. M., and Denovan-Wright, E. M. (2015). Cannabidiol is a negative allosteric modulator of the cannabinoid CB1 receptor. *Br. J. Pharmacol.* 172, 4790–4805. doi: 10.1111/bph.13250

Lu, H.-C. C., and Mackie, K. (2016). an introduction to the endogenous cannabinoid system. *Biol. Psychiatry* 79, 516–525. doi: 10.1016/j.biopsych.2015.07.028

Martínez-Pinilla, E., Rabal, O., Reyes-Resina, I., Zamarbide, M., Navarro, G., Sanchez-Arias, J. A., et al. (2016). Two affinity sites of the cannabinoid subtype 2 receptor identified by a novel homogeneous binding assay. *J. Pharmacol. Exp. Ther.* 358, 580–587. doi: 10.1124/jpet.116.234948

Mcguinness, D., Malikzay, A., Visconti, R., Lin, K., Bayne, M., Monsma, F., et al. (2009). Characterizing cannabinoid CB2 receptor ligands using DiscoveRx PathHunter^{TM} β-arrestin assay. *J. Biomol. Screen.* 14, 49–58. doi: 10.1177/1087057108327329

McPartland, J. M., Glass, M., and Pertwee, R. G. (2007). Meta-analysis of cannabinoid ligand binding affinity and receptor distribution: Interspecies differences. *Br. J. Pharmacol.* 152, 583–593. doi: 10.1038/sj.bjp.0707399

Mechoulam, R. (2016). Cannabis - The Israeli perspective. *J. Basic Clin. Physiol. Pharmacol.* 27, 181–187. doi: 10.1515/jbcpp-2015-0091

Mechoulam, R., Shani, A., Edery, H., and Grunfeld, Y. (1970). Chemical basis of hashish activity. *Science* 169, 611–612. doi: 10.1126/science.169.3945.611

Medrano, M., Aguinaga, D., Reyes-Resina, I., Canela, E. I., Mallol, J., Navarro, G., et al. (2017). Orexin A/Hypocretin modulates leptin receptor-mediated signaling by allosteric modulations mediated by the Ghrelin GHS-R1A receptor in hypothalamic neurons. *Mol. Neurobiol.* 55, 4718–4730. doi: 10.1007/s12035-017-0670-8

Merighi, S., Simioni, C., Gessi, S., Varani, K., and Borea, P. A. (2010). Binding thermodynamics at the human cannabinoid CB1 and CB2 receptors. *Biochem. Pharmacol.* 79, 471–477. doi: 10.1016/j.bcp.2009.09.009

Nadal, X. (2016). Methods of purifying cannabinoids, compositions and kits thereof. U.S. Patent No 9,765,000. Washington, DC: U.S. Patent and Trademark Office.

Nadal, X., del Río, C., Casano, S., Palomares, B., Ferreiro-Vera, C., Navarrete, C., et al. (2017). Tetrahydrocannabinolic acid is a potent PPARγ agonist with neuroprotective activity. *Br. J. Pharmacol.* 174, 4263–4276. doi: 10.1111/bph.14019

Navarro, G., Borroto-Escuela, D., Angelats, E., Etayo, Í., Reyes-Resina, I., Pulido-Salgado, M., et al. (2018a). Receptor-heteromer mediated regulation of endocannabinoid signaling in activated microglia. Role of CB1 and CB2 receptors and relevance for Alzheimer's disease and levodopa-induced dyskinesia. *Brain Behav. Immun.* 67, 139–151. doi: 10.1016/j.bbi.2017.08.015

Navarro, G., Cordomí, A., Brugarolas, M., Moreno, E., Aguinaga, D., Pérez-Benito, L., et al. (2018b). Cross-communication between Gi and Gs in a G-protein-coupled receptor heterotetramer guided by a receptor C-terminal domain. *BMC Biol.* 16:24. doi: 10.1186/s12915-018-0491-x

Navarro, G., Cordomí, A., Zelman-Femiak, M., Brugarolas, M., Moreno, E., Aguinaga, D., et al. (2016). Quaternary structure of a G-protein-coupled receptor heterotetramer in complex with Gi and Gs. *BMC Biol.* 14:26. doi: 10.1186/s12915-016-0247-4

Navarro, G., Ferré, S., Cordomi, A., Moreno, E., Mallol, J., Casadó, V., et al. (2010). Interactions between intracellular domains as key determinants of the quaternary structure and function of receptor heteromers. *J. Biol. Chem.* 285, 27346–27359. doi: 10.1074/jbc.M110.115634

Pertwee, R. G. (2008). The diverse CB 1 and CB 2 receptor pharmacology of three plant cannabinoids: Δ 9-tetrahydrocannabinol, cannabidiol and Δ 9-tetrahydrocannabivarin. *Br. J. Pharmacol.* 153, 199–215. doi: 10.1038/sj.bjp.0707442

Peters, M. F., and Scott, C. W. (2009). Evaluating cellular impedance assays for detection of GPCR pleiotropic signaling and functional selectivity. *J. Biomol. Screen.* 14, 246–255. doi: 10.1177/1087057108330115

Pollastro, F., Taglialatela-Scafati, O., Allarà, M., Muñoz, E., Di Marzo, V., De Petrocellis, L., et al. (2011). Bioactive prenylogous cannabinoid from fiber hemp (*Cannabis sativa*). *J. Nat. Prod.* 74, 2019–2022. doi: 10.1021/np200500p

Rosenthaler, S., Pöhn, B., Kolmanz, C., Nguyen Huu, C., Krewenka, C., Huber, A., et al. (2014). Differences in receptor binding affinity of several phytocannabinoids do not explain their effects on neural cell cultures. *Neurotoxicol. Teratol.* 46, 49–56. doi: 10.1016/j.ntt.2014.09.003

Schröder, R., Merten, N., Mathiesen, J. M., Martini, L., Kruljac-Letunic, A., Krop, F., et al. (2009). The C-terminal tail of CRTH2 is a key molecular determinant that constrains Gαi and downstream signaling cascade activation. *J. Biol. Chem.* 284, 1324–1336. doi: 10.1074/jbc.M806867200

Shim, J. Y., and Howlett, A. C. (2006). WIN55212-2 docking to the CB 1 cannabinoid receptor and multiple pathways for conformational induction. *J. Chem. Inf. Model.* 46, 1286–1300. doi: 10.1021/ci0504824

Shim, J. Y., Welsh, W. J., and Howlett, A. C. (2003). Homology model of the CB1 cannabinoid receptor: sites critical for nonclassical cannabinoid agonist interaction. *Biopolym. Pept. Sci. Sect.* 71, 169–189. doi: 10.1002/bip.10424

Sierra, S., Luquin, N., Rico, A. J., Gómez-Bautista, V., Roda, E., Dopeso-Reyes, I. G., et al. (2015). Detection of cannabinoid receptors CB1 and CB2 within basal ganglia output neurons in macaques: changes following experimental parkinsonism. *Brain Struct. Funct.* 220, 2721–2738. doi: 10.1007/s00429-014-0823-8

Solymosi, K., and Kofalvi, A. (2017). Cannabis: a treasure trove or pandora's box? *Mini Rev. Med. Chem.* 17, 1223–1291. doi: 10.2174/1389557516666161004162133

Turner, S. E., Williams, C. M., Iversen, L., and Whalley, B. J. (2017). Molecular pharmacology of phytocannabinoids. *Prog. Chem. Org. Nat. Prod.* 103, 61–101. doi: 10.1007/978-3-319-45541-9_3

Van Der Lee, M. M. C., Blomenröhr, M., Van Der Doelen, A. A., Wat, J. W. Y., Smits, N., Hanson, B. J., et al. (2009). Pharmacological characterization of receptor redistribution and β-arrestin recruitment assays for the cannabinoid receptor 1. *J. Biomol. Screen.* 14, 811–823. doi: 10.1177/1087057109337937

Wartmann, M., Campbell, D., Subramanian, A., Burstein, S. H., and Davis, R. J. (1995). The MAP kinase signal transduction pathway is activated by the endogenous cannabinoid anandamide. *FEBS Lett.* 359, 133–136. doi: 10.1016/0014-5793(95)00027-7

Weinstein, A. M., Rosca, P., Fattore, L., and London, E. D. (2017). Synthetic cathinone and cannabinoid designer drugs pose a major risk for public health. *Front. Psychiatry* 8:156. doi: 10.3389/fpsyt.2017.00156

Conflict of Interest Statement: Authors declare that this research was undertaken in collaboration with Phytoplant Research S.L. Co-authors working in the Spanish and Italian public institutions do not receive honoraria from the company and do not have any participation in the company (stock shares or similar).

3.3 Expression of cannabinoid CB_1R–GPR55 heteromers in neuronal subtypes of the *Macaca fascicularis* striatum.

Eva Martínez-Pinilla, Alberto J. Rico, **Rafael Rivas-Santisteban**, Jaume Lillo, Elvira Roda, Gemma Navarro, Gemma, Rafael Franco, Rafael y José Luis Lanciego.

Manuscrito publicado en *Annals of the New York Academy of Sciences*, Septiembre 2020; 1475(1):34-42.

El receptor cannabinoide CB_1 es el receptor mayoritario del sistema endocannabinoide y, además, es el receptor acoplado a proteína G más expresado en el sistema nervioso central, lo que le permite ejercer una función neuromoduladora. Se ha caracterizado la expresión de complejos heteroméricos compuestos por los receptores CB_1 y GPR55 en el cuerpo estriado. El objetivo de nuestro estudio consiste en la caracterización de la expresión de los heterómeros CB_1R-GPR55 en los ganglios basales de los primates *Macaca fascicularis* tanto en las neuronas de proyección del estriado como en las interneuronas, empleando la técnica de ensayo de ligación por proximidad *in situ* (PLA). Para la identificación de la población de neuronas que proyectan el estriado se utilizó un trazador neuroanatómico retrógrado, la amina de dextrano biotinilada (BDA), inyectado en las subdivisiones externas o internas del globo pálido. Se pudieron detectar 1) neuronas marcadas con BDA, 2) heterómeros CB_1R-GPR55 mediante PLA y 3) interneuronas estriales positivas para colina acetiltransferasa, parvalbúmina, calretinina u óxido nítrico sintasa. Se detectaron heterómeros CB_1R-GPR55 en ambos tipos de neuronas de proyección, así como en todas las interneuronas, con la excepción de las neuronas colinérgicas. Serán requeridos estudios posteriores para determinar la capacidad terapéutica de los heterómeros CB_1R-GPR55 en enfermedades que guardan relación con los desequilibrios del control motor, como la enfermedad de Parkinson.

Ann. N.Y. Acad. Sci. ISSN 0077-8923

ANNALS OF THE NEW YORK ACADEMY OF SCIENCES
Special Issue: Annals *Reports*

Concise Original Report

Expression of cannabinoid CB_1R–GPR55 heteromers in neuronal subtypes of the *Macaca fascicularis* striatum

Eva Martínez-Pinilla,[1,2,3,a] Alberto J. Rico,[4,5,6,a] Rafael Rivas-Santisteban,[6,7,8] Jaume Lillo,[6,7,8] Elvira Roda,[4,5,6] Gemma Navarro,[6,8,9] Rafael Franco,[6,7,8,a] and José Luis Lanciego[4,5,6,a]

[1]Department of Morphology and Cell Biology, Faculty of Medicine, the University of Oviedo, Oviedo, Asturias, Spain. [2]Instituto de Neurociencias del Principado de Asturias (INEUROPA), Asturias, Spain. [3]Instituto de Investigación Sanitaria del Principado de Asturias (ISPA), Asturias, Spain. [4]Neurosciences Division, Centre for Applied Medical Research (CIMA), the University of Navarra, Pamplona, Spain. [5]Instituto de Investigaciones Sanitarias de Navarra (IdiSNA), Pamplona, Spain. [6]Centro de Investigación Biomédica en Red Enfermedades Neurodegenerativas (CIBERNED), Madrid, Spain. [7]Molecular Neurobiology Laboratory, Department of Biochemistry and Molecular Biomedicine, the University of Barcelona, Barcelona, Spain. [8]Institut de Biomedicina de la Universitat de Barcelona (IBUB), Barcelona, Spain. [9]Department of Biochemistry and Physiology, School of Pharmacy and Food Science, University of Barcelona, Barcelona, Spain

Addresses for correspondence: Eva Martínez-Pinilla (martinezpinillaeva@gmail.com), José Luis Lanciego (jlanciego@unav.es), Gemma Navarro (g.navarro@ub.edu), and Rafael Franco (rfranco123@gmail.com, rfranco@ub.edu)

The cannabinoid CB_1 receptor (CB_1R) is the most abundant G protein–coupled receptor in the central nervous system, consistent with the important role of endocannabinoids as neuromodulators. Cannabinoids also modulate the function of G protein–coupled receptor 55 (GPR55), which forms heteroreceptor complexes with the CB_1R in the striatum. The aim was to characterize cannabinoid CB_1R–GPR55 heteromers (CB_1R/GPR55Hets) in the basal ganglia input nuclei of nonhuman primates, *Macaca fascicularis*, both in projection neurons and interneurons, by the *in situ* proximity ligation assay. Striatal projecting neurons were identified by the retrograde neuroanatomical tracer, biotinylated dextran amine (BDA), injected into external or internal subdivisions of the globus pallidus. Triple immunofluorescent stains were carried out to visualize (1) BDA-labeled neurons, (2) CB_1R/GPR55Hets, and (3) striatal interneurons positive for choline acetyltransferase, parvalbumin, calretinin, or nitric oxide synthase. CB_1R/GPR55Hets were identified within both types of projection neurons as well as all interneurons except those that are cholinergic. Moreover, CB_1R/GPR55Hets were found specifically in the neuronal cell surface, and also in intracellular membranes. Further research efforts will be needed to confirm the intracellular occurrence of heteromers and their potential as therapeutic targets in diseases related to motor control imbalances, particularly within a parkinsonian context (with or without levodopa-induced dyskinesia).

Keywords: G protein–coupled receptor (GPCR); heteromer; biotinylated dextran amine; projection neurons; interneurons; cannabinoid receptor; CB_1

Introduction

Endocannabinoids acting on cannabinoid CB_1 and CB_2 receptors regulate neurotransmission and synaptic plasticity in the basal ganglia (BG) (see Giuffrida and Seillier for review, Ref. 1). The cannabinoid CB_1 receptor (CB_1R), which is a member of the G protein–coupled receptor (GPCR) superfamily, is considered the most abundant GPCR in neurons of the mammalian central nervous system (CNS) and, therefore, drugs that activate or block receptor function do have functional

[a]These authors contributed equally to this manuscript.

doi: 10.1111/nyas.14413

consequences in the CNS.[2–5] Consequently, natural and synthetic cannabinoids have been proposed as medicines targeting neurodegenerative diseases engaging, among others, motor control–related brain areas.[6,7]

GPR55 (G protein–coupled receptor 55) was first considered a third cannabinoid receptor because its signaling is modulated by cannabinoids and there was a significant degree of amino acid sequence similarity around the ligand-binding site.[8] Later, it was discovered that cannabinoid action may occur via an allosteric center, while the orthosteric center may accommodate an endogenous compound, lysophosphatidylinositol.[9] GPR55 is widely expressed in both CNS neurons and glial cells. Specifically, mRNA transcripts have been detected in neurons of human caudate and putamen nuclei, and of the hippocampus, thalamic nuclei, and midbrain regions of rodent brains.[10,11] Although GPR55 function is still poorly characterized, knockout mice for GPR55 show impaired motor coordination, thus suggesting an important role of this receptor in controlling events taking place within BG neural networks.[12] Relevant for the present study is the fact that mapping GPR55 expression in the primate brain still remains to be addressed.

Heteromerization of GPCRs on the cell surface has opened a new field of research since GPCR heteromers are known to constitute novel functional units, that is, their functionality is different from that of each receptor when considered separately.[13,14] In particular, G protein coupling and further cytocrin signaling pathways are affected by the activation of receptors in a heteromeric context.[15] We have previously demonstrated that the CB_1R may heteromerize with GPR55 and that heteromerization affects receptor functionality in rodent models.[16,17] Taking advantage of our atlas of the *Macaca fascicularis* brain[18] and our experience in dealing with neuroanatomical tracers,[19,20] here, we aimed to adequately characterize the expression of CB_1R–GPR55 heteromers (CB_1R/GPR55Hets) within the identified subtypes of striatal neurons comprising both projection neurons and interneurons.

Materials and methods

To the best of our knowledge, this manuscript adheres to the guidelines detailed elsewhere.[21] Studies were designed to generate groups of equal sizes, using randomization and blinded analysis. Immunological-based assays were conducted in full keeping with guidelines detailed in Ref. 22.

Animals

A total of six naive young adult male *M. fascicularis* primates (body weight 3.5–4.7 kg) were used in this study. Animal handling was conducted at all times in accordance with the European Council Directive 2010/63/UE as well as in keeping with current Spanish legislation (RD53/2013). The experimental design was reviewed and approved by the Ethical Committee for Animal Testing of the University of Navarra (protocol ref: 009/12). All animals were captive-bred and supplied by R.C. Hartelust (Leiden, the Netherlands).

Ventriculography-assisted stereotaxic surgery for tracer delivery

The stereotaxic atlas of Lanciego and Vázquez[18] was used to allocate proper coordinates of tracer injection into the internal and external divisions of the globus pallidus (GPi and GPe, respectively). Target selection was assisted by ventriculography, ensuring appropriate targeting of either the GPi or GPe. Coordinates for the GPi nucleus were 3.5 mm caudal to the anterior commissure (ac), 1.5 mm ventral to the bicommisural plane (ac-pc plane), and 6 mm lateral to the midline. Coordinates for the GPe nucleus were 3.5 mm caudal to ac, 1.5 mm dorsal to the ac-pc plane, and 8.5 mm lateral to the midline. Animals received a single pressure injection of 1 μL of biotinylated dextran amine (BDA; 10 kDa, lysine fixable; D-1956, Molecular Probes, Invitrogen) through a Hamilton® syringe (5 mg/mL in 0.01 M phosphate buffer (PB) at neutral pH) in either the GPi or the GPe nuclei. Tracer delivery was carried out in pulses of 0.1 μL/2 min and once completed, the microsyringe was left in place for 15 min before withdrawal to minimize tracer reflux through the injection tract.

The survival time should be adapted to the length of the pathway being studied. There is little information available on the detectability of BDA as a function of the survival time, but it seems that it has a wide range.[23–28] The BDA's longest reported survival time is 7 weeks for squirrel monkeys. In our case, 2 weeks were enough to obtain consistent staining.

Tissue processing

Two weeks postinjection, animals were anesthetized with an overdose of anesthesia and perfused transcardially. The perfusates were made of a saline Ringer's solution followed by 3000 mL of a fixative solution containing 4% paraformaldehyde and 0.1% glutaraldehyde in 0.125 M PB at neutral pH. Perfusion was continued with 1000 mL of a cryoprotectant solution made of 10% glycerin and 1% of dimethyl sulfoxide (DMSO) in 0.125 M PB, pH 7.4. Once perfusion was completed, the brain was removed and stored in a cryoprotective solution containing 20% glycerin and 2% DMSO for 48–72 hours. Finally, 10 series of frozen coronal adjacent sections (40-μm thick) were obtained in a sliding microtome. These series were used for (1) the *in situ* proximity ligation assay (PLA) counterstained with TO-PRO® -3; (2) histochemical detection of transported BDA counterstained with the Nissl method; (3) fluorescent detection of transported BDA combined with the PLA-mediated detection of CB_1R/GPR55Hets; (4) immunofluorescent detection of neurons positive for choline acetyltransferase (ChAT), combined with BDA tracing and PLA detection of CB_1R/GPR55Hets; (5) immunofluorescent detection of neurons positive for parvalbumin (PV), combined with BDA tracing and PLA detection of CB_1R/GPR55Hets; (6) immunofluorescent detection of neurons positive for calretinin (CR), combined with BDA tracing and PLA detection of CB_1R/GPR55Hets; (7) immunofluorescent detection of neurons positive for nitric oxide synthase (nNOS), combined with BDA tracing and PLA detection of CB_1R/GPR55Hets; and (8) control stains assessing the specificity of the PLA method for the detection of CB_1R/GPR55Hets. The remaining two series of sections were stored at −80 °C as backup materials for further processing, if needed.

Detection of transported BDA was carried out by 90 min of incubation in HRP-conjugated streptavidin (1:5000; Sigma) and finally visualized with a nickel-enhanced solution of DBA (Sigma). Sections were mounted on gelatin-coated slides, air-dried, counterstained with the Nissl method, and finally coverslipped with Entellan® (Merck).

The PLA method

Proximity probes consisted of affinity-purified antibodies modified by covalent attachment of the 5′ end of various nucleotides to each primary antibody. PLA probes were prepared by conjugating a rabbit anti-CB_1R antibody (ref: PA1-745, Thermo Scientific, Rockford, IL) raised against the first 77-amino acid (extracellular) sequence of the rat receptor with a PLUS oligonucleotide (Duolink® In Situ Probemaker PLUS; DUO92009, Sigma) and a rabbit anti-GPR55 antibody (10224, Cayman Chemical) raised against the human 207–219 sequence (internal cytoplasmic region) with a MINUS oligonucleotide (Duolink In Situ Probemaker MINUS; DUO92010, Sigma) according to the manufacturer's guidelines. Using a heterologous expression system in which the human version of the receptors was expressed, we have previously shown that the anti-CB_1R antibody does not recognize GPR55 and vice versa (the *M. fascicularis* DNA sequence of GPCR genes is almost undisguisable from the human sequence).[17,29] In Figure 1, another anti-CB_1R antibody was also used, a polyclonal antibody raised against a C-terminal region (461–472 amino acid sequence) of the human receptor (ab23703, Abcam).

Tissue sections containing the caudate and putamen nuclei were used for the detection of CB_1R/GPR55Hets with the PLA technique. Briefly, free-floating sections were incubated for 1 h at 37 °C with the blocking solution, followed by overnight incubation at 4 °C with the PLA probe–linked antibodies (at a final concentration of 75 μg/mL). After washing with buffer A (wash buffer A, DUO82047; Sigma), samples were immersed for 1 h in a 1:400 solution of TO-PRO-3 (T3605; Molecular Probes-Invitrogen). GPCR heteromers were detected using the Duolink *II* In Situ PLA detection kit (Duolink In Situ Detection Reagents Red; DUO92008, Sigma). Sections were washed with buffer A and incubated with the ligation solution for 1 h at 37 °C in a humidity chamber. After washing with buffer A, sections were incubated with the amplification solution for 100 min at 37 °C and then washed with buffer B (wash buffer B; DUO82048; Sigma). Sections were finally mounted using an aqueous mounting medium. Appropriate negative control assays in which one of the antibodies was missing were carried out to ensure that there was a lack of nonspecific labeling and amplification; similar negative controls have been previously reported using the same antibodies (see Fig. 2 in Ref. 17 and Fig. 5 in Ref. 29).

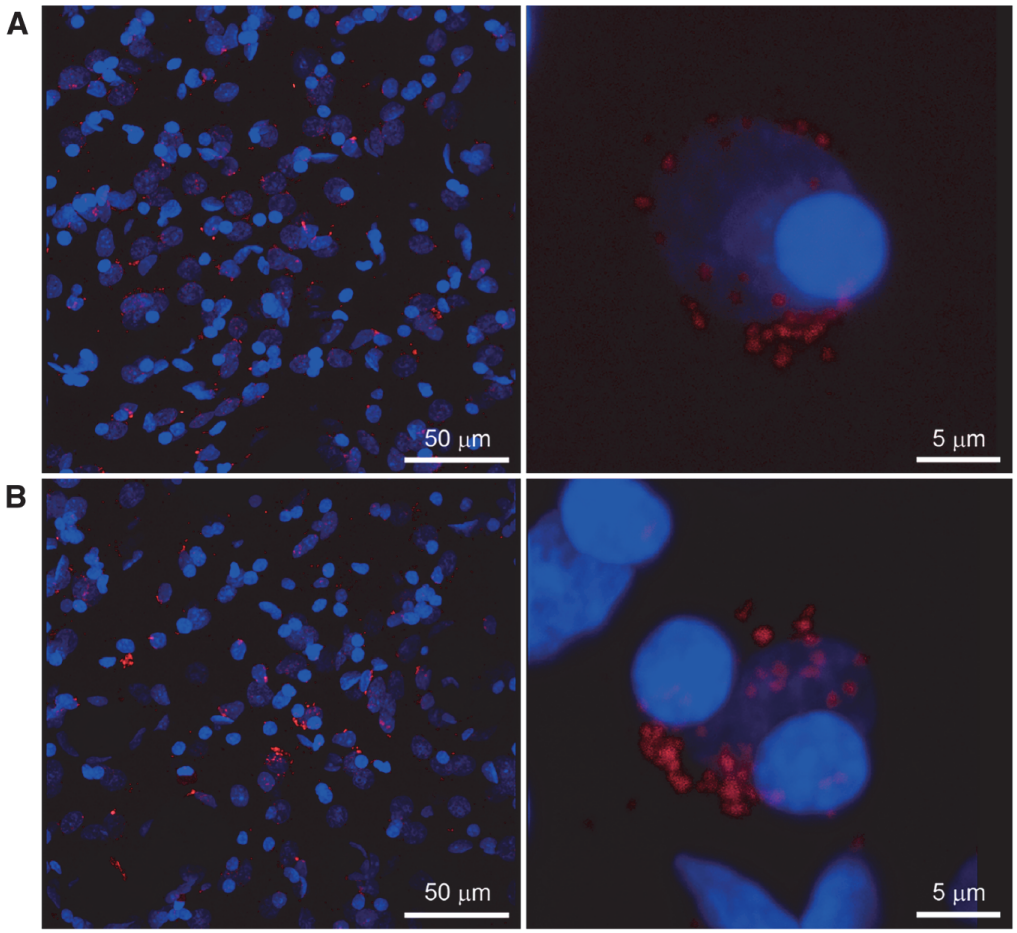

Figure 1. **Validation of antibodies for PLAs. Expression of heteromers in striatal sections using two different anti-CB_1R antibodies. (A) Striatal neurons showing PLA label for CB_1R/GPR55Hets using a rabbit antibody raised against the N-terminus of the CB_1R and with a rabbit anti-GPR55 antibody. (B) Striatal neurons showing PLA label for CB_1R/GPR55Hets detected using a rabbit anti-GPR55 antibody and a goat antibody raised against the C-terminal domain of the CB_1R. Nuclei are labeled with TO-PRO-3. Scale bar 50 μm.**

The PLA method combined with the detection of neuronal markers

The identity of striatal neuron subtypes (projection neurons and interneurons) expressing CB_1R/GPR55Hets was carried out by combining the PLA technique with both BDA histochemistry and the immunofluorescent detection using specific markers for striatal interneurons. The PLA technique was conducted first, followed by the fluorescent detection of BDA and then by stains for different interneuron subtypes. Cholinergic interneurons were detected with a goat anti-ChAT primary antibody (1:1000; AB144P, Millipore) followed by an Alexa Fluor® 633–tagged donkey anti-goat IgG (1:200; A-21082, Thermo Scientific). For PV detection, a rabbit anti-PV antibody was used first (1:250; AB15736, Millipore), followed by an Alexa Fluor 647–coupled donkey anti-rabbit IgG (1:200; A-31573, Thermo Scientific). CR-positive neurons were detected with a goat anti-CR primary antibody (1:500; AB1550, Millipore) followed by an Alexa Fluor 633–coupled donkey anti-goat IgG (1:200; A-21082, Thermo Scientific). Finally, nNOS-positive neurons were visualized by incubation with a rabbit anti-nNOS primary antibody (1:500; AB5380, Millipore) and then with an Alexa Fluor 647–coupled donkey anti-rabbit IgG (1:200; A-31573, Thermo Scientific). Striatal projection neurons retrogradely labeled with BDA were visualized with an Alexa Fluor 488–coupled streptavidin (1:100; S32354, Molecular Probes, Invitrogen).

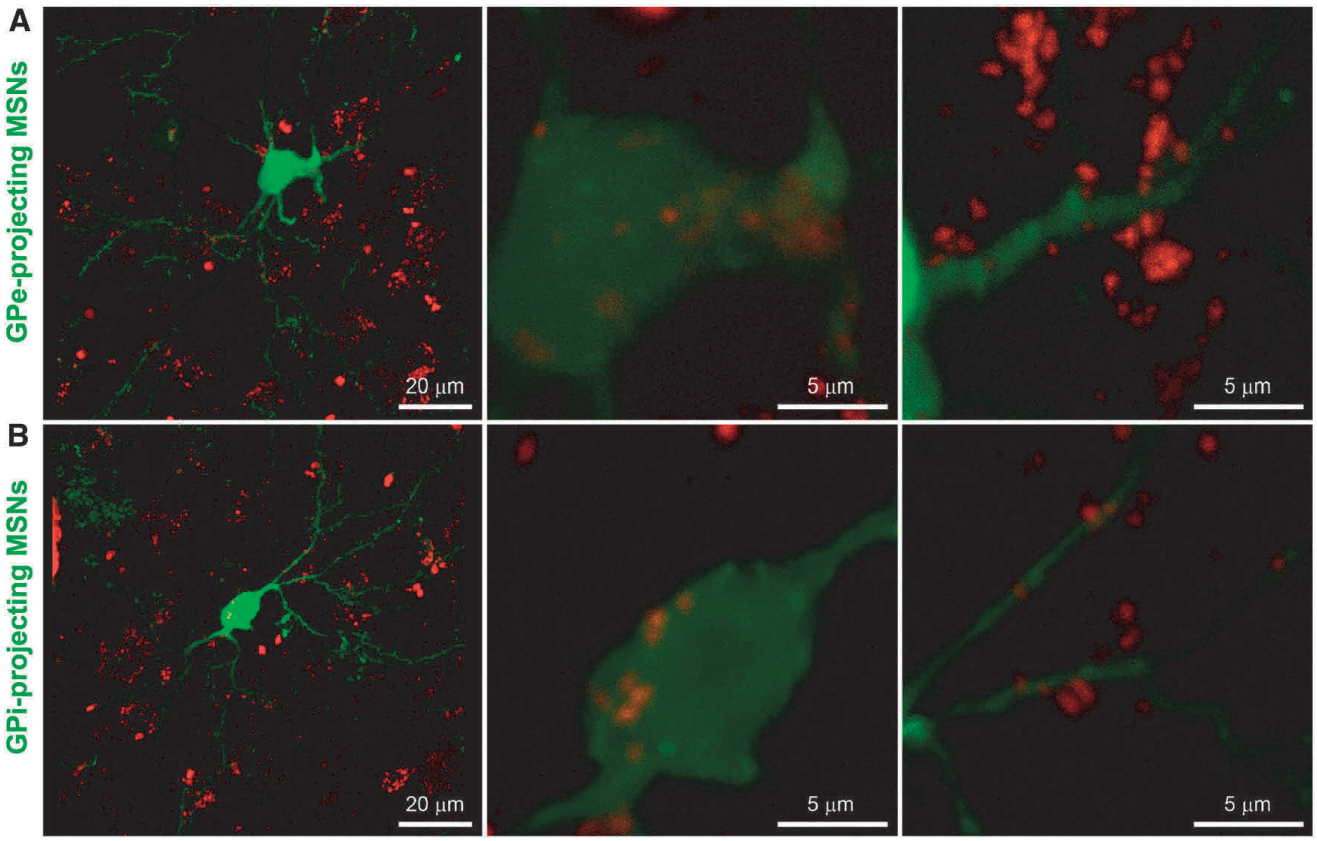

Figure 2. **Expression of CB_1R-GPR55 heteromers within striatal projecting neurons. CB_1R/GPR55Hets within a striatal neuron innervating the GPe nucleus (A) and within a striatal neuron projecting to the GPi nucleus (B). Heteromers were only found in the cell soma, and not in proximal and/or distal dendrites.**

Results

Expression of CB_1R–GPR55 heteromers in striatal projecting neurons and striatal interneurons

The experimental approach was designed to identify neuronal types that express CB_1R/GPR55Hets. While the *in situ* PLA was used to detect the presence of receptor heteromeric complexes, interneurons were visualized by means of immunohistochemical procedures and striatal medium-sized spiny neurons (MSNs) were identified by the retrograde transport of the neuroanatomical tracer BDA.

The *in situ* PLA is instrumental to detect receptor–receptor interactions in a natural system. Thus, red clusters in PLA assays proved the occurrence of CB_1R/GPR55Hets in a significant number of striatal neurons. The specificity of the signal was addressed by using a negative control (lack of one of the primary antibodies, not shown) and by using two different anti-CB_1R antibodies recognizing two different domains of the receptor. As shown in Figure 1, the results obtained using each of the two antibodies were similar. For further experiments, the antibody raised against the first 77-amino acid (extracellular) sequence of the rat receptor was selected (versus the antibody recognizing an intracellular region (see the Materials and methods section)). On the one hand, the selected antibody is the same used in previous studies in which CB_1R-containing heteromers were detected.[17,29] On the other hand, we reasoned that specificity would be maximized by using antibodies against two different regions of the assayed GPCR, namely, an extracellular domain in the case of the CB_1R and an intracellular domain in the case of GPR55.

We next addressed the expression of CB_1R/GPR55Hets by injecting BDA into either the GPe or the GPi nuclei. Analysis of the expression of CB_1R/GPR55Hets within striatal neurons, retrogradely labeled with BDA, showed that heteromers were expressed in the cell soma of neurons labeled by the tracer, without being found in dendrites (Fig. 2).

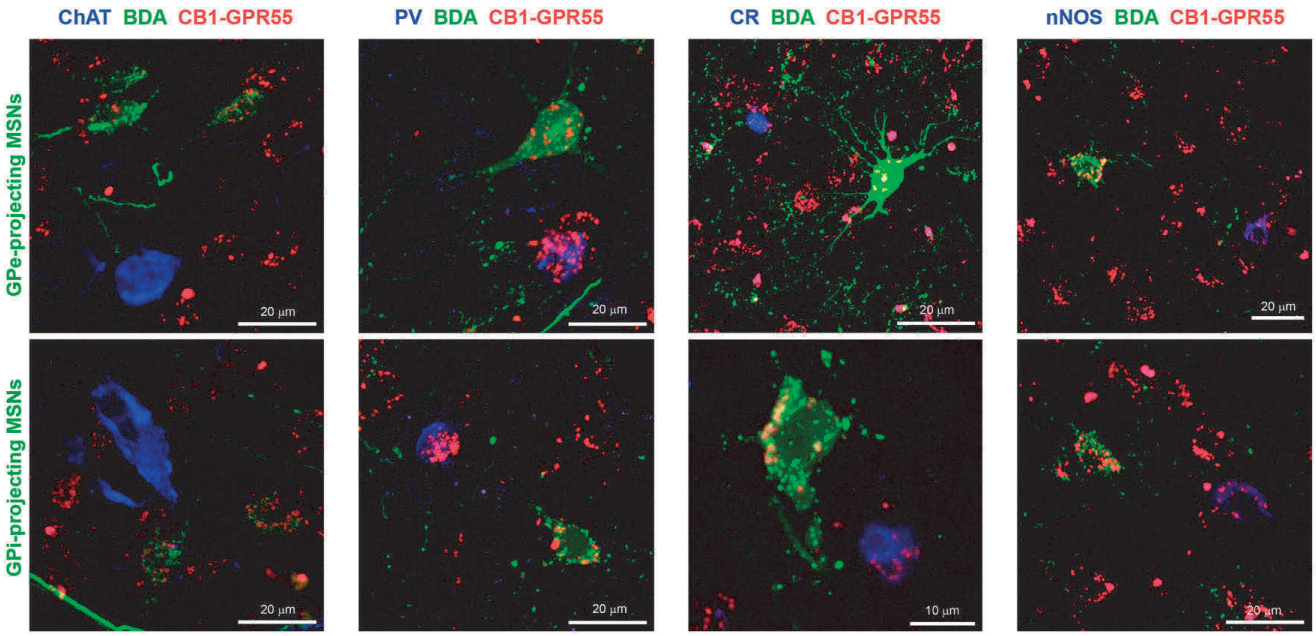

Figure 3. **Expression of CB_1R-GPR55 heteromeric complexes in different subtypes of striatal projection neurons and interneurons. Triple immunofluorescent stains were performed to detect CB_1R/GPR55Hets (by PLA), BDA-labeled neurons, and striatal interneurons positive for either ChAT, PV, CR, or nNOS. PV^+ neurons are by far the striatal neuron subtype containing the highest amount of heteromers.**

Besides MSNs, the striatum contains up to four main types of interneurons, namely, cholinergic ($ChAT^+$), PV-positive (PV^+), CR-positive (CR^+), and nNOS-positive ($nNOS^+$). Accordingly, we identified CB_1R/GPR55Hets–expressing interneurons by the PLA technique followed by an immunofluorescent stain using reagents that label the different neuronal subtypes. In short, triple immunofluorescent stains were carried out to visualize (1) BDA-labeled neurons, (2) CB_1R/GPR55Hets, and (3) striatal interneurons positive for ChAT, PV, CR, or nNOS. CB_1R/GPR55Hets were found in interneurons positive for PV, CR, and nNOS, whereas $ChAT^+$ interneurons lacked CB_1R/GPR55Het expression (Fig. 3). Furthermore, when compared with any other striatal neuron subtype (either projection neurons and interneurons), it is worth noting that PV^+ neurons were found to be the ones showing the highest density of CB_1R/GPR55Hets.

In summary, CB_1R/GPR55Hets were found in the projecting MSNs, as well as in most of the identified subtypes of striatal interneurons (those expressing PV, CR, or nNOS), with the only exception of $ChAT^+$ interneurons.

Discussion

Mapping ionotropic and metabotropic receptors across the CNS was one of the seminal achievements to know the molecular basis governing neurotransmission and brain circuitry. Similarly, mapping dopaminergic receptors and dopamine-producing neurons allowed to propose a first model of motor control, basically constituted by dopaminergic neurons in the substantia nigra, BG pathways, and the BG output neurons that project to the thalamus.[30] Input information (mainly arising from glutamatergic corticostriatal and thalamostriatal projections) is processed at the level of the striatum through both GABAergic MSNs and striatal interneurons.[31–33]

The simplest model of motor control considers two striatal pathways, known as direct and indirect. The first contains dopamine D_1 receptor–expressing neurons projecting "directly" to GPi, and the second contains dopamine D_2 receptor–expressing neurons projecting "indirectly" to the GPe. However, it should be noted that in nonhuman primates, both striatofugal pathways are known to be highly collateralized, as reported by Lévesque and Parent.[34] The model was also

challenged by the discovery of projecting neurons containing both D_1 and D_2 receptors that may interact to form D_1–D_2 receptor heteromers in rodents and primates.[35–37] Differential expression of these heteromers, depending on the gender, results in significant changes in protein kinase B/glycogen synthase kinase 3/β-catenin and brain-derived neurotrophic factor/tyrosine receptor kinase B signaling pathways, making female more predisposed than male rats to anxiety and depression-like behavior.[38] As one might expect, the BG motor control circuitry is more complex in primates than in rodents. Single-axon tracing studies in squirrel monkeys showed that most of the neurons from the putamen and caudate nuclei were projecting to both GPi and GPe.[34] In other words, virtually all striatofugal neurons in nonhuman primates project into the GPe and, in fact, there are no neurons that exclusively innervate the GPi or substantia nigra pars reticulata or both. This means that compared with rodents, primates do not have a pathway that can be considered as "direct." In humans, dysregulation of the whole system by the lack of dopamine production, owing to the progressive death of nigral dopaminergic neurons, results in the appearance of cardinal motor symptoms that typically characterize Parkinson's disease (PD).

Cumulative evidence during the past two decades using animal models of PD sustained the therapeutic potential of cannabinoids as drugs to combat PD symptoms and, eventually, to delay disease progression,[6,7] since (1) cannabinoids target neuronal cannabinoid CB_1R and regulate GPR55 function, and (2) these two GPCRs may interact to form novel functional units. By taking advantage of the PLA technique in combination with retrograde tract-tracing and the immunofluorescent detection of striatal interneurons, the expression of CB_1R/GPR55Hets was here addressed in the different neuronal types existing in the striatum of the nonhuman primate, an experimental animal often considered as the gold standard in the field of animal models of PD. Accordingly, once the presence of CB_1R/GPR55Hets complexes was assessed within different subtypes of striatal neurons, further research effort is needed to ascertain potential changes, if any, in their expression when considering parkinsonian animals (with or without levodopa-induced dyskinesia).

Our results show that CB_1R/GPR55Hets are expressed in all neuronal cell types, except in $ChAT^+$ interneurons. The occurrence of CB_1R/GPR55Hets in BDA-labeled projecting neurons indicates that they are expressed in MSNs projecting to the GPi and/or to the GPe. In projection neurons, CB_1R/GPR55Hets were found in the cell soma, and not in dendrites. Striatal interneurons positive for PV, CR, and nNOS also contain CB_1R/GPR55Hets. The highest amount of these heteromers was found in PV^+ interneurons, followed by CR^+ interneurons, and then $nNOS^+$ interneurons.

The result concerning the widespread expression of the CB_1R was expected as it is considered the GPCR with the highest occurrence in the CNS neurons. However, the findings about GPR55 are novel as its mapping at the individual level had not been previously attempted. Interestingly, CB_1R/GPR55Hets were identified in both neuronal cell surface and intracellular locations. Although there are a few studies related to the occurrence of GPCRs in positions other than the cell surface, the CB_1R has been identified in mitochondria, where it regulates energy metabolism.[39–42] Despite technical challenges with detecting intracellular heteromers, the subcellular location of heteroreceptor complexes needs to be further investigated. These cellular/subcellular locations suggest a functional role for CB_1R/GPR55Hets independent of the cannabinoid receptor–mediated control of neurotransmitter release at axon terminals.

Acknowledgments

This work was supported by grants from Spanish Ministerio de Economía y Competitividad (MINECO) (#BFU2012-37907, #SAF2008-03118-E, and #SAF2012-39875-C02-01; they may include EU FEDER funds), Eranet-Neuron (Heteropark), CIBERNED (CB06/05/006), Fundació La Marató de TV3 (20141330 to R.F. and 20141331 to J.L.L.), and by the Departamento de Salud del Gobierno de Navarra.

Competing interests

The authors declare no competing interests.

References

1. Giuffrida, A. & A. Seillier. 2012. New insights on endocannabinoid transmission in psychomotor disorders. *Prog. Neuropsychopharmacol. Biol. Psychiatry* **38:** 51–58.
2. Mendiguren, A., E. Aostri & J. Pineda. 2018. Regulation of noradrenergic and serotonergic systems by cannabinoids: relevance to cannabinoid-induced effects. *Life Sci.* **192:** 115–127.
3. Aymerich, M.S., E. Aso, M.A. Abellanas, *et al.* 2018. Cannabinoid pharmacology/therapeutics in chronic degenerative disorders affecting the central nervous system. *Biochem. Pharmacol.* **157:** 67–84.
4. Covey, D.P., Y. Mateo, D. Sulzer, *et al.* 2017. Endocannabinoid modulation of dopamine neurotransmission. *Neuropharmacology* **124:** 52–61.
5. Wang, Z.J., S.S.J. Hu, H.B. Bradshaw, *et al.* 2019. Cannabinoid receptor-mediated modulation of inhibitory inputs to mitral cells in the main olfactory bulb. *J. Neurophysiol.* **122:** 749–759.
6. Fernández-Ruiz, J., M.A. Moro & J. Martínez-Orgado. 2015. Cannabinoids in neurodegenerative disorders and stroke/brain trauma: from preclinical models to clinical applications. *Neurotherapeutics* **12:** 793–806.
7. Sagredo, O., M. García-Arencibia, E. de Lago, *et al.* 2007. Cannabinoids and neuroprotection in basal ganglia disorders. *Mol. Neurobiol.* **36:** 82–91.
8. Baker, D., G. Pryce, W.L. Davies, *et al.* 2006. *In silico* patent searching reveals a new cannabinoid receptor. *Trends Pharmacol. Sci.* **27:** 1–4.
9. Oka, S., K. Nakajima, A. Yamashita, *et al.* 2007. Identification of GPR55 as a lysophosphatidylinositol receptor. *Biochem. Biophys. Res. Commun.* **362:** 928–934.
10. Sawzdargo, M., T. Nguyen, D.K. Lee, *et al.* 1999. Identification and cloning of three novel human G protein-coupled receptor genes GPR52, ΨGPR53 and GPR55: gPR55 is extensively expressed in human brain. *Mol. Brain Res.* **64:** 193–198.
11. Wu, C.-S., J. Zhu, J. Wager-Miller, *et al.* 2010. Requirement of cannabinoid CB(1) receptors in cortical pyramidal neurons for appropriate development of corticothalamic and thalamocortical projections. *Eur. J. Neurosci.* **32:** 693–706.
12. Wu, C.-S., H. Chen, H. Sun, *et al.* 2013. GPR55, a G-protein coupled receptor for lysophosphatidylinositol, plays a role in motor coordination. *PLoS One* **8:** e60314.
13. Ferré, S., R. Baler, M. Bouvier, *et al.* 2009. Building a new conceptual framework for receptor heteromers. *Nat. Chem. Biol.* **5:** 131–134.
14. Franco, R., E. Martínez-Pinilla, J.L. Lanciego, *et al.* 2016. Basic pharmacological and structural evidence for class A G-protein-coupled receptor heteromerization. *Front. Pharmacol.* **7:** 76.
15. Franco, R., D. Aguinaga, J. Jiménez, *et al.* 2018. Biased receptor functionality versus biased agonism in G-protein-coupled receptors. *Biomol. Concepts* **9:** 143–154.
16. Balenga, N.A., E. Martínez-Pinilla, J. Kargl, *et al.* 2014. Heteromerization of GPR55 and cannabinoid CB2 receptors modulates signalling. *Br. J. Pharmacol.* **171:** 1–64.
17. Martínez-Pinilla, E., I. Reyes-Resina, A. Oñatibia-Astibia, *et al.* 2014. CB1 and GPR55 receptors are co-expressed and form heteromers in rat and monkey striatum. *Exp. Neurol.* **261:** 44–52.
18. Lanciego, J.L. & A. Vázquez. 2012. The basal ganglia and thalamus of the long-tailed macaque in stereotaxic coordinates. A template atlas based on coronal, sagittal and horizontal brain sections. *Brain Struct. Funct.* **217:** 613–666.
19. Lanciego, J.L., M.R. Luquin, J. Guillén, *et al.* 1998. Multiple neuroanatomical tracing in primates. *Brain Res. Brain Res. Protoc.* **2:** 323–332.
20. López, I.P., P. Salin, P. Kachidian, *et al.* 2010. The added value of rabies virus as a retrograde tracer when combined with dual anterograde tract-tracing. *J. Neurosci. Methods* **194:** 21–27.
21. Curtis, M.J., S. Alexander, G. Cirino, *et al.* 2018. Experimental design and analysis and their reporting II: updated and simplified guidance for authors and peer reviewers. *Br. J. Pharmacol.* **175:** 987–993.
22. Alexander, S.P.H., R.E. Roberts, B.R.S. Broughton, *et al.* 2018. Goals and practicalities of immunoblotting and immunohistochemistry: a guide for submission to the British Journal of Pharmacology. *Br. J. Pharmacol.* **175:** 407–411.
23. Brandt, H.M. & A.V. Apkarian. 1992. Biotin-dextran: a sensitive anterograde tracer for neuroanatomic studies in rat and monkey. *J. Neurosci. Methods* **45:** 35–40.
24. Lanciego, J. & F. Wouterlood. 1994. Dual anterograde axonal tracing with *Phaseolus vulgaris* leucoagglutinin (PHA-L) and biotinylated dextran amine (BDA). *Neurosci. Protoc.* 94-050-06.
25. Lanciego, J.L., F.G. Wouterlood, E. Erro, *et al.* 1998. Multiple axonal tracing: simultaneous detection of three tracers in the same section. *Histochem. Cell Biol.* **110:** 509–515.
26. Rajakumar, N., K. Elisevich & B.A. Flumerfelt. 1993. Biotinylated dextran: a versatile anterograde and retrograde neuronal tracer. *Brain Res.* **607:** 47–53.
27. Veenman, C.L., A. Reiner & M.G. Honig. 1992. Biotinylated dextran amine as an anterograde tracer for single- and double-labeling studies. *J. Neurosci. Methods* **41:** 239–254.
28. Wouterlood, F.G. & B. Jorritsma-Byham. 1993. The anterograde neuroanatomical tracer biotinylated dextran-amine: comparison with the tracer *Phaseolus vulgaris*-leucoagglutinin in preparations for electron microscopy. *J. Neurosci. Methods* **48:** 75–87.
29. Martínez-Pinilla, E., D. Aguinaga, G. Navarro, *et al.* 2019. Targeting CB1 and GPR55 endocannabinoid receptors as a potential neuroprotective approach for Parkinson's disease. *Mol. Neurobiol.* **56:** 5900–5910.
30. Wooten, G.F., L.J. Currie, J.P. Bennett, *et al.* 1997. Maternal inheritance in Parkinson's disease. *Ann. Neurol.* **41:** 265–268.
31. Chang, H.T. & H. Kita. 1992. Interneurons in the rat striatum: relationships between parvalbumin neurons and cholinergic neurons. *Brain Res.* **574:** 307–311.
32. Kita, H., T. Kosaka & C.W. Heizmann. 1990. Parvalbumin-immunoreactive neurons in the rat neostriatum: a light and electron microscopic study. *Brain Res.* **536:** 1–15.
33. Kaneko, T., R. Shigemoto, S. Nakanishi, *et al.* 1993. Substance P receptor-immunoreactive neurons in the rat neostriatum are segregated into somatostatinergic and cholinergic aspiny neurons. *Brain Res.* **631:** 297–303.

34. Lévesque, M. & A. Parent. 2005. The striatofugal fiber system in primates: a reevaluation of its organization based on single-axon tracing studies. *Proc. Natl. Acad. Sci. USA* **102:** 11888–11893.
35. Hasbi, A., T. Fan, M. Alijaniaram, *et al*. 2009. Calcium signaling cascade links dopamine D1–D2 receptor heteromer to striatal BDNF production and neuronal growth. *Proc. Natl. Acad. Sci. USA* **106:** 21377–21382.
36. Perreault, M.L., A. Hasbi, M.Y.F. Shen, *et al*. 2016. Disruption of a dopamine receptor complex amplifies the actions of cocaine. *Eur. Neuropsychopharmacol.* **26:** 1366–1377.
37. Rico, A.J., I.G. Dopeso-Reyes, E. Martínez-Pinilla, *et al*. 2016. Neurochemical evidence supporting dopamine D1–D2 receptor heteromers in the striatum of the long-tailed macaque: changes following dopaminergic manipulation. *Brain Struct. Funct.* **222:** 1–18.
38. Hasbi, A., T. Nguyen, H. Rahal, *et al*. 2020. Sex difference in dopamine D1–D2 receptor complex expression and signaling affects depression- and anxiety-like behaviors. *Biol. Sex Differ.* **11:** 8.
39. Hebert-Chatelain, E., L. Reguero, N. Puente, *et al*. 2014. Cannabinoid control of brain bioenergetics: exploring the subcellular localization of the CB1 receptor. *Mol. Metab.* **3:** 495–504.
40. Bénard, G., F. Massa, N. Puente, *et al*. 2012. Mitochondrial CB1 receptors regulate neuronal energy metabolism. *Nat. Neurosci.* **15:** 558–564.
41. Gutiérrez-Rodríguez, A., I. Bonilla-Del Río, N. Puente, *et al*. 2018. Localization of the cannabinoid type-1 receptor in subcellular astrocyte compartments of mutant mouse hippocampus. *Glia* **66:** 1417–1431.
42. Melser, S., A.C.P. Zottola, R. Serrat, *et al*. 2017. Functional analysis of mitochondrial CB1 cannabinoid receptors (mtCB1) in the brain. *Methods Enzymol.* **593:** 143–174.

3.4 Expression of GPR55 and either cannabinoid CB_1 or CB_2 heteroreceptor complexes in the caudate, putamen, and accumbens nuclei of control, parkinsonian, and dyskinetic non-human primates.

Eva Martínez-Pinilla, Alberto J. Rico, **Rafael Rivas-Santisteban**, Jaume Lillo, Elvira Roda, Gemma Navarro, Rafael Franco y José Luis Lanciego.

Manuscrito publicado en *Brain Structure and Function*, Julio 2020; 225(7):2153-2164.

Los endocannabinoides son compuestos con propiedades neuromoduladoras que actúan sobre los receptores acoplados a proteínas G (GPCR) del sistema cannabinoide (CB_1R y CB_2R), que representan atractivas dianas terapéuticas para las enfermedades neurodegenerativas. Del mismo modo, los cannabinoides también son capaces de regular la actividad del GPCR GPR55, que a su vez es un receptor capaz de interaccionar con los receptores CB_1 y CB_2. La hipótesis de este estudio es que los heterómeros formados por los receptores cannabinoides pueden ofrecer beneficios terapéuticos para la enfermedad de Parkinson. En nuestra investigación detectamos la presencia de los heterómeros CB_1R-GPR55 y CB_2R-GPR55 en el cuerpo estriado de muestras de tejido de macacos control y parkinsonianos (con y sin presencia de disquinesia inducida por el tratamiento de levodopa) mediante el ensayo de ligación por proximidad (PLA). Para generar el modelo animal de Parkinson se realizó el tratamiento mediante inyección con MPTP. Para el posterior análisis de la imágenes se utilizó el software informático FIJI junto a la extensión de código abierto "*Andy's Algorithms*" que permite la cuantificación de los puntos/célula que se corresponden con la expresión de los heterómeros CB_1R-GPR55 y CB_2R-GPR55. Nuestros resultados demuestran que hay un aumento en la expresión del heterómero CB_1R-GPR55 en los ganglios basales en ratas modelo de la enfermedad de Parkinson respecto a los animales control y que estos vuelven a sus valores iniciales con el tratamiento crónico con levodopa en animales que presentan los movimientos discinéticos. En cuanto a la expresión del heterómero CB_2R-GPR55, se obtuvieron resultados similares con un nivel de expresión similar entre animales control y animales parkinsonianos que presentan las disquinesias, así como un aumento significativo en los animales inyectados con MPTP pero que no presentaban las disquinesias. Estos resultados, en su conjunto, apuntan a los heterómeros CB_1R-GPR55 y CB_2R-GPR55 como buenos blancos moleculares no dopaminérgicos para mejorar la fisiopatología del Parkinson.

Brain Structure and Function
https://doi.org/10.1007/s00429-020-02116-4

ORIGINAL ARTICLE

Expression of GPR55 and either cannabinoid CB_1 or CB_2 heteroreceptor complexes in the caudate, putamen, and accumbens nuclei of control, parkinsonian, and dyskinetic non-human primates

Eva Martínez-Pinilla[1,2,3] · Alberto J. Rico[4,5,6] · Rafael Rivas-Santisteban[6,7] · Jaume Lillo[6,7] · Elvira Roda[4,5,6] · Gemma Navarro[6,8] · José Luis Lanciego[4,5,6] · Rafael Franco[6,7]

Received: 27 March 2020 / Accepted: 9 July 2020

Abstract

Endocannabinoids are neuromodulators acting on specific cannabinoid CB_1 and CB_2 G-protein-coupled receptors (GPCRs), representing potential therapeutic targets for neurodegenerative diseases. Cannabinoids also regulate the activity of GPR55, a recently "deorphanized" GPCR that directly interacts with CB_1 and with CB_2 receptors. Our hypothesis is that these heteromers may be taken as potential targets for Parkinson's disease (PD). This work aims at assessing the expression of heteromers made of GPR55 and CB_1/CB_2 receptors in the striatum of control and parkinsonian macaques (with and without levodopa-induced dyskinesia). For this purpose, double blind in situ proximity ligation assays, enabling the detection of GPCR heteromers in tissue samples, were performed in striatal sections of control, MPTP-treated and MPTP-treated animals rendered dyskinetic by chronic treatment with levodopa. Image analysis and statistical assessment were performed using dedicated software. We have previously demonstrated the formation of heteromers between GPR55 and CB_1 receptor (CB_1-GPR55_Hets), which is highly expressed in the central nervous system (CNS), but also with the CB_2 receptor (CB_2-GPR55_Hets). Compared to the baseline expression of CB_1-GPR55_Hets in control animals, our results showed increased expression levels in basal ganglia input nuclei of MPTP-treated animals. These observed increases in CB_1-GPR55_Hets returned back to baseline levels upon chronic treatment with levodopa in dyskinetic animals. Obtained data regarding CB_2-GPR55_Hets were quite similar, with somehow equivalent amounts in control and dyskinetic animals, and with increased expression levels in MPTP animals. Taken together, the detected increased expression of GPR55-endocannabinoid heteromers appoints these GPCR complexes as potential non-dopaminergic targets for PD therapy.

Keywords G-protein coupled receptor (GPCR) heteromer · Levodopa · Parkinson's disease · Proximity ligation assay (PLA) · Striatum

Eva Martínez-Pinilla, Alberto J. Rico, Gemma Navarro, José Luis Lanciego and Rafael Franco contributed equally to this work.

✉ Eva Martínez-Pinilla
martinezpinillaeva@gmail.com

✉ José Luis Lanciego
jlanciego@unav.es

✉ Rafael Franco
rfranco@ub.edu; rfranco123@gmail.com

[1] Department of Morphology and Cell Biology, Faculty of Medicine, University of Oviedo, Julián Clavería s/n, 33006 Asturias, Spain

[2] Instituto de Neurociencias del Principado de Asturias (INEUROPA), Asturias, Spain

[3] Instituto de Investigación Sanitaria del Principado de Asturias (ISPA), Asturias, Spain

[4] Neurosciences Division, Centre for Applied Medical Research, CIMA, University of Navarra, Avenida Pío XII, 55, 31008 Pamplona, Spain

[5] Instituto de Investigaciones Sanitarias de Navarra (IdiSNA), Pamplona, Spain

[6] Centro de Investigación Biomédica en Red Enfermedades Neurodegenerativas (CIBERNED), Madrid, Spain

[7] Molecular Neurobiology Laboratory, Department of Biochemistry and Molecular Biomedicine, School of Chemistry, Universitat de Barcelona, Diagonal 643, 08028 Barcelona, Spain

[8] Department of Biochemistry and Physiology, Faculty of Pharmacy and Food Science, University of Barcelona, Barcelona, Spain

Published online: 20 July 2020

Abbreviations

CB_1-GPR55_Hets	Complexes formed by CB_1 and GPR55 receptors
CB_1R	CB_1 receptors
CB_2-GPR55_Hets	Complexes formed by CB_2 and GPR55 receptors
CB_2R	CB_2 receptors
CLAHE	Contrast Limited Adaptive Histogram Equalization
CNS	Central nervous system
GPCRs	G-protein-coupled receptors
LPI	Lysophosphatidylinositol
PD	Parkinson's disease
PLA	In situ proximity ligation assay
SN	Substantia nigra

Introduction

Endocannabinoids and their specific G-protein-coupled receptors (GPCRs), CB_1 and CB_2, are known to regulate neurotransmission and synaptic plasticity in the basal ganglia [see (Giuffrida and Seillier 2012) for review]. Consequently, synthetic or natural (e.g. Sativex® or Epidiolex®) cannabinoids have been proposed as novel drug compounds for Parkinson's disease (PD) treatment. Neuroprotective and/or anti-symptomatic mechanisms of cannabinoids may result from activation/blockade of CB_1 receptors (CB_1R, mainly expressed in neurons), of CB_2 receptors (CB_2R, expressed in microglia and in some neuronal populations (Onaivi 2006; Onaivi et al. 2006; Brusco et al. 2008; Lanciego et al. 2011)), or be receptor-independent [see (Fernández-Ruiz et al. 2011) for review].

Despite lack of consensus, GPR55 was deorphanized to be preliminarily considered as a receptor for lysophosphatidylinositol (LPI) (Oka et al. 2007). GPR55 is widely expressed in the central nervous system (CNS). Thus, mRNA transcripts were found by Northern blot in human caudate and putamen nuclei, and by in situ hybridization in hippocampus, thalamic nuclei and midbrain regions of rodent brains (Sawzdargo et al. 1999; Wu et al. 2010). Moreover, it is also expressed in microglia (Pietr et al. 2009), similarly to CB_2R (Núñez et al. 2004). GPR55 is still poorly characterized due to a variety of factors. Firstly identified as a putative cannabinoid receptor because of similar amino acid sequence in the binding region (Baker et al. 2006), extensive characterization at GlaxoSmithKline and AstraZeneca pharmaceutical companies led to propose that the receptor was responsible for the blood pressure lowering properties of cannabinoids. However, whereas GPR55 seems to be activated by endogenous or exogenous (plant and synthetic) cannabinoids, research studies using GPR55 knockout mice showed that the receptor does not mediate vasodilator effects (Johns et al. 2009). Interestingly, phenotypic characterization of these animals guided to the discovery of receptor involvement in motor control (Wu et al. 2013). In fact, the knockout mouse showed impaired motor coordination providing the basis of a relevant role of the receptor in basal ganglia neural circuits.

$G_{i/o}$ are the cognate heterotrimeric proteins of cannabinoid receptors (Alexander et al. 2017) (https://www.guidetopharmacology.org/). In the case of GPR55, these proteins are of the G_q/G_{11} and G_{12}/G_{13} families (Alexander et al. 2017) (https://www.guidetopharmacology.org/) leading to a quite complex pharmacology. In this sense, not only cytosolic calcium increases resulting from receptor activation are slower than for other G_q-coupled receptors but it has been reported that the receptor activation may engage multiple signaling pathways (Henstridge et al. 2010). Among the mechanisms underlying such pleiotropic actions, receptor heteromerization is included. Dimer/oligomerization is now considered a general phenomenon for practically all cell surface receptors. Noteworthy, we have previously demonstrated that CB_1R and CB_2R may heteromerize with GPR55 and that heteromerization affects receptor functionality (Balenga et al. 2014; Martínez-Pinilla et al. 2014). Indeed, as a general rule, GPCR heteromers are currently considered as novel molecular entities, with signaling and ligand characteristics different than those for each GPCR when considered individually (Ferré et al. 2009; Franco et al. 2016, 2018).

The aim of this study was to assess, from a cell biology and anatomical perspective, whether the striatal expression of GPR55-containing heteromers is altered in Parkinsonism and in levodopa-induced dyskinesia. For this purpose, in situ proximity ligation (PLA), a technique instrumental for detecting receptor-receptor interactions and their precise anatomical localization, was used in samples from the MPTP monkey PD model. The results obtained showed that whereas both heteroreceptor complexes increase in caudate, putamen and accumbens nuclei of parkinsonian animals, chronic levodopa treatment tuned down these increases back to normal expression levels.

Material and methods

This manuscript adheres to the guidelines detailed in (Curtis et al. 2018). Studies were designed to generate groups of equal sizes, using randomization and blinded analysis. Immunological based assays were conducted according to the guidelines detailed in (Alexander et al. 2018).

Generation of parkinsonian animals and levodopa treatment

A total of 9 naïve young adults male *Macaca fascicularis* primates (body weight 3.5–4.7 kg) were used in this study.

Animal handling was conducted at all times in accordance with the European Council Directive 2010/63/UE as well as in keeping with current Spanish legislation (RD53/2013). The experimental design was reviewed and approved by the Ethical Committee for Animal Testing of the University of Navarra (Protocol Ref: 009/12). All animals were captive-bred and supplied by R. C. Hartelust (Leiden, The Netherlands).

To induce a bilateral parkinsonian syndrome, 6 monkeys were systemically administered 1-methyl-4-phenyl-1,2,3,6-tetrahydropyridine (MPTP, Sigma Aldrich, St. Louis, USA) (Rico et al. 2010). Animals received a weekly injection of MPTP (0.2 mg/kg i/v; accumulated doses ranging from 5 to 7 mg/kg) until reaching a non-reversible, stable parkinsonian syndrome. The severity of the MPTP-induced Parkinsonism was evaluated using a clinical rating scale (Kurlan et al. 1991). This scale rates parkinsonian motor symptoms such as resting tremor (0–3), action or intention tremor (0–3), facial expression (0–3), posture (0–2), balance coordination (0–3), gait (0–3), bradykinesia (0–4), defense reaction (0–2), and gross motor skills of the upper (0–3) or lower limb (0–3); using this scale the highest severity corresponds to the maximal score, 29. Once primates reached a score of at least 21 points, the treatment was discontinued for a wash-out period of 2 months before performing any further assay. At the end of the stabilization period, the PD scores were in the 21–24 range. Dyskinesia was induced in 3 animals scoring 21, 22 and 24 points in the Kurlan's scale through oral chronic administration of levodopa/benserazide (200:50 Roche) at a dose of 25 mg/kg daily. Levodopa effects were monitored by motor scoring (Kurlan et al. 1991) and by assessing the "off/on" states and the duration of the "on" response (Lanciego et al. 2008). Dyskinesias were evaluated using the scale included in the "Core Assessment Program for Intracerebral Transplantation for Parkinson's disease" (Langston et al. 1992), subsequently modified and validated for the assessment of dyskinesias in patients (Goetz et al. 1994). Accordingly, they were rated as severe when dyskinesias were continuous, generalized and perturbing motor behavior; moderate if were presented during most of the "on" period without interfering with voluntary movements; and mild, when happened only under a stress challenge. By the time of sacrifice, all 3 monkeys treated with levodopa showed severe dyskinesia. These primates entered in the "on" state 30 min post-levodopa oral delivery and the duration of the "on" period was maintained for 2.5–3 h. A mild dyskinetic syndrome was displayed by the end of the first month of treatment, whereas severe dyskinetic symptoms appeared later and remained stable until sacrifice. Levodopa-treated animals were euthanized in the "on" state (peak-of-dose dyskinesia).

Tissue processing

Animals were anesthetized with an overdose of 10% chloral hydrate and perfused transcardially. The perfusate was made of a saline Ringer solution followed by 3000 mL of fixative solution containing 4% paraformaldehyde and 0.1% glutaraldehyde in 0.125 M phosphate buffer (PB) at neutral pH. Perfusion was continued with 1000 mL of a cryoprotective solution made of 10% glycerin and 1% of dimethyl sulfoxide (DMSO) in 0.125 M PB, pH 7.4. Once perfusion was completed, the brain was removed and stored in a cryoprotective solution containing 20% glycerin and 2% DMSO for 48–72 h. Finally, 10 series of frozen coronal adjacent sections (40 µm-thick) were obtained in a sliding microtome. These series were used for (1) in situ PLA for CB_1-GPR55_Hets counterstained with Topro-3, (2) in situ PLA for CB_2-GPR55_Hets counterstained with Topro-3, (3) immunohistochemical detection of tyrosine hydroxylase, and (4) control stains assessing the specificity of the PLA method for the detection of CB_1-GPR55_Hets. The remaining 6 series of sections were stored at − 80 ºC as backup materials for further processing, if needed. Areas of interest for PLA stains (pre-and post-commissural caudate, putamen and accumbens nuclei), were selected according to the stereotaxic atlas of (Lanciego and Vázquez 2012).

In situ proximity ligation assays (PLA)

PLA allows the ex vivo detection of molecular interactions between two endogenous proteins. Assays were performed in samples from 3 monkeys per group (control, parkinsonian and dyskinetic). Proximity probes consisted of affinity-purified antibodies modified by covalent attachment of 5′ end of various nucleotides to each primary antibody. PLA probes were prepared by conjugating a rabbit anti-CB_1 antibody (Ref: PA1-745, Thermo Scientific, Rockford, USA) with a PLUS oligonucleotide (Duolink In Situ Probemaker PLUS ref: DUO92009; Sigma) and a rabbit anti-GPR55 antibody (Ref: 10224; Cayman Chemicals; Ann Arbor, MI, USA), raised against the human 207–219 sequence, with a MINUS oligonucleotide (Duolink In Situ Probemaker MINUS Ref: DUO92010; Sigma) according to manufacturer's guidelines. For CB_2-GPR55_Hets detection, a rabbit anti-CB_2 antibody (Ref: 1001012; Cayman Chemicals) was conjugated with a PLUS oligonucleotide, whereas the rabbit anti-GPR55 antibody was conjugated as described above. Tissue sections containing the caudate and putamen nuclei were used for the detection of either CB_1-GPR55_Hets or CB_2-GPR55_Hets with the PLA technique. Briefly, free-floating sections were incubated for 1 h at 37 ºC with the blocking solution, followed by overnight incubation at 4 ºC with the PLA probe-linked antibodies described above (at a final concentration

of 75 µg/mL). After washing with buffer A (wash buffer A, ref: DUO82047; Sigma), samples were immersed for 1 h in a 1:400 solution of Topro-3 (ref: T3605; Molecular Probes-Invitrogen). GPCR heteromers were detected using the Duolink II in situ PLA detection kit (Duolink In Situ Detection Reagents Red ref: DUO92008; Sigma). Sections were washed with buffer A and incubated with the ligation solution for 1 h at 37 ºC in a humidity chamber. After washing with buffer A again, sections were incubated with the amplification solution for 100 min at 37 ºC and then washed with buffer B (Wash buffer B, Ref: DUO82048; Sigma). Sections were finally mounted using an aqueous mounting medium. Appropriate negative control assays were carried out to ensure that there was a lack of non-specific labeling and amplification.

Statistical analysis on the receptor heteromer densities were conducted using dedicated software (Duolink Image Tool, Ref: DUO90806; Sigma-Olink). This software has been developed for quantification of PLA signals and cell nuclei in images generated from fluorescent confocal microscopy. Regarding selected regions of interest (ROIs), and for each field of view, a stack of two channels (one per staining) and 9–15 Z stacks with a step size of 1 µm were acquired. A quantification of cells containing one or more red spots *versus* total cells (blue nucleus), and the ratio *r* (number of red spots/cell) in cells containing spots were determined considering a total of 300–400 cells from six different fields within basal ganglia from three different animals per group using the Andy's algorithm and the procedure detailed elsewhere (Law et al. 2017). Nuclei and red spots were counted on the maximum projections of each image stack. After getting the projection, each channel was processed individually. The nuclei were segmented by filtering with a median filter, subtracting the background, enhancing the contrast with the Contrast Limited Adaptive Histogram Equalization (CLAHE) plug-in and finally applying a threshold to obtain the binary image and the ROI around each nucleus. Red spots images were also filtered and thresholded to obtain the binary images. Red spots were counted in each of the ROI obtained in the nuclei images.

It should be noted that the experiments were achieved in a blind basis; the experimenter was not aware of the label and the conditions (control, parkinsonian or dyskinetic) when images were taken. Moreover, the experimenter who made the analysis did not know the exact nature of the analyzed samples.

Data analysis

Data collected in samples from 3 animals per group (control, parkinsonian and dyskinetic) were the mean ± SEM. One- or two-way ANOVA followed by Bonferroni's post hoc multiple comparison tests were used to compare the values (% of positive cells or *r* spots/cell) obtained for each pair of receptors in different disease states or in different striatal regions. The normality of populations and homogeneity of variances were tested prior to ANOVA. Differences were considered significant when $p \leq 0.05$. Statistical analysis were carried out with GraphPad Prism software version 5 (San Diego, CA, USA). Outlier tests were not used; all data points were used for analysis.

Results

Expression of CB_1R-GPR55 heteromers in control, parkinsonian and dyskinetic macaques

The PLA technique enables the detection of receptor-receptor interactions in a native system. Red clusters detected in PLA assays proved the occurrence of complexes formed by CB_1 and GPR55 receptors (CB_1-GPR55_Hets) in all samples analyzed. PLA data was collected from different fields in samples of pre- and post-commissural basal ganglia input nuclei, which included caudate, putamen and accumbens. The areas that were considered in the study are delineated in Fig. 1 and the color code was used in subsequent figures.

A representative image of results of CB_1-GPR55_Het expression in all analyzed areas is given in Fig. 2, where the increase in the amount of red signal in samples from parkinsonian animals is already noticed. Analysis using the Andy's algorithm (see "Materials and methods") confirmed that the number of red dots per cell was significantly higher in the parkinsonian conditions. Remarkably, the level of expression in dyskinetic animals was similar to that found in control animals (Fig. 3a). These quantitative findings (higher density of CB_1-GPR55_Het clusters) in parkinsonian conditions were similar in post- and pre-commissural areas (Fig. 3b). Also relevant was that all regions showed significant increase of CB_1-GPR55_Het expression in samples from the PD animal model (Fig. 3c).

Expression of CB_2R-GPR55 heteromers in control, parkinsonian and dyskinetic macaques

Analogous analysis performed in the same regions but addressing CB_2-GPR55_Het expression led to similar findings. Under the blind-like conditions of the experiments we discovered that in every animal in a given group the expression was similar in all analyzed regions, and that there was an increase in samples from parkinsonian animals that returned to "normal" after levodopa-induced dyskinesia (Figs. 4 and 5). The results were similar in pre- and post-commissural areas, and all regions showed significant increase of CB_2-GPR55_Het expression in samples from the PD animal model (Fig. 5b, c). A difference was the higher

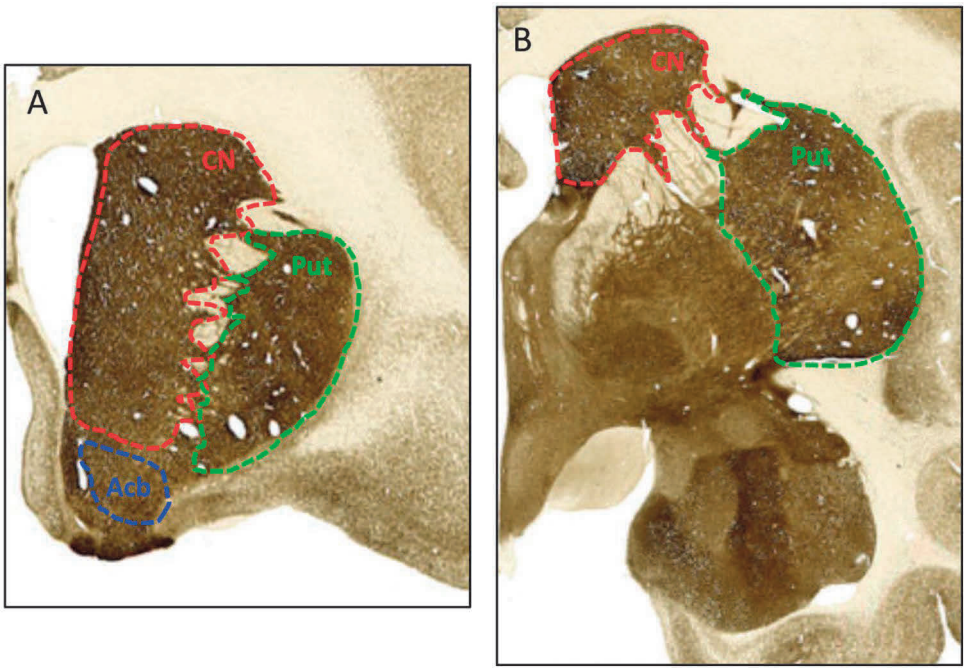

Fig. 1 Delineation of pre- (**a**) and postcommissural (**b**) areas of interest in the *Macaca fascicularis* brain. Caudate (CN, red), putamen (Put, green) and accumbens (Acb, blue) are indicated in a color code that will be used in Figs. 3c and 5c

number of red clusters per cell if compared with the results concerning the CB_1-GPR55_Het.

Discussion

The present study was aimed at knowing whether Parkinsonism correlates with altered expression of CB_1-GPR55_Hets and/or CB_2-GPR55_Hets. The results here reported are quite clear in showing that the expression of both heteromers was significantly higher in MPTP-treated monkeys in all analyzed nuclei (caudate, putamen and accumbens). Increases of striatal expression in PD models have been similarly demonstrated for other heteromers (Rodríguez-Ruiz et al. 2017). Also interesting is the disruption of heteromers here shown when parkinsonian animals are rendered dyskinetic after chronic levodopa treatment; a similar alteration has been demonstrated for adenosine A_{2A}/dopamine D_2/cannabinoid CB_1 heteroreceptor complexes (Armentero et al. 2011; Pinna et al. 2014; Bonaventura et al. 2014). Disorganization of dopamine receptor heteromers has been associated to differential effects exerted by cocaine action (Perreault et al. 2016). The trend is not unspecific as there are cases of increased heteromer expression in dyskinesia. One relevant example, due to the possibility of alleviate dyskinesias by dopamine D_3 receptor blockade, is the increase of striatal expression of the D_3 receptor itself and of dopamine D_1–D_3 receptor heteromers in dyskinetic macaques (Marcellino et al. 2008; Fuxe et al. 2015; Farré et al. 2015).

In a recent report, we have addressed the expression of CB_1-GPR55_Hets in the basal ganglia input nuclei both in interneurons and in projection neurons in samples from naïve *Macaca fascicularis*. By using a tracer, delivered to the internal or to the external subdivisions of the globus pallidus, and immunohistochemical techniques we showed that heteromers are expressed in both striatofugal projection neuron types. CB_1-GPR55_Hets were not found in dendrites but in the cell somata. Triple immunofluorescent stains identified heteromers in parvalbumin, calretinin and nitric oxide positive interneurons. In contrast, cholinergic interneurons lacked heteromer expression (Martínez-Pinilla et al. 2020).

For drug development, the CB_1R was first considered as better alternative than CB_2R due to its higher expression in neurons. However, potential psychotropic effects of drugs acting on the CB_1R have led to focus more on the CB_2R. Our results would indicate that, to counteract the increase in receptor expression associated to PD, the most appropriate intervention would be the use of CB_1R and/or GPR55 antagonists. While GPR55 has been poorly addressed in drug discovery, the serious side effects of rimonabant, a CB_1R antagonist, led to regulatory bodies to withdrawn this anti-obesity drug (Christensen et al. 2007). Alternatively, the benefits of targeting CB_2R are mainly based on the upregulation of the receptor in activated glial cells that is concomitant with dopaminergic neurodegeneration (Price et al. 2009; Palomo-Garo et al. 2016; Navarro et al. 2016). Our results open perspectives for the non-dopaminergic management of PD patients.

As indicated in the introduction, the presence of CB_2R in neurons is scarce. Although the receptor is significantly expressed in some pallidal, cerebellar and cortical neurons, striatal ones have negligible levels. Consistent with

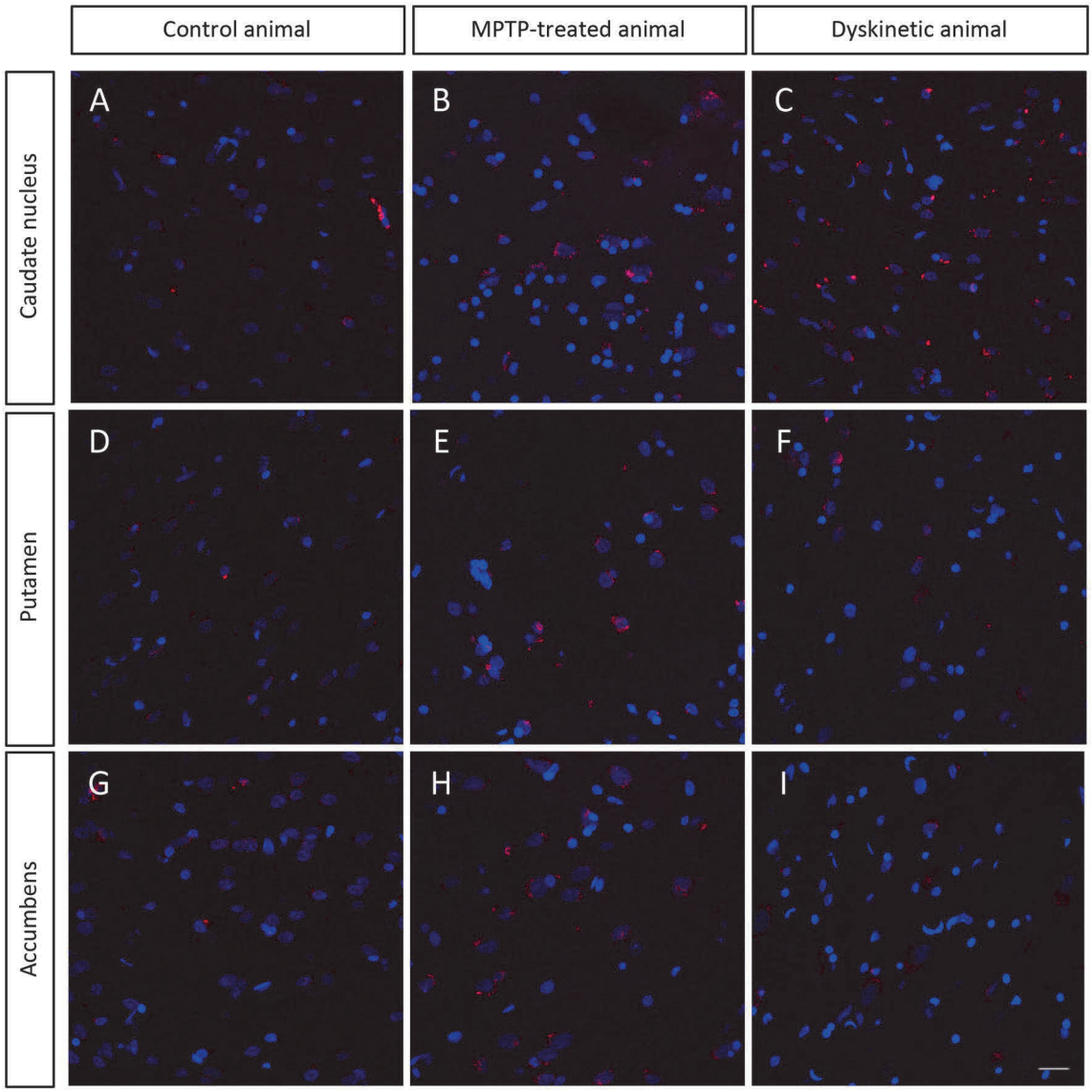

Fig. 2 CB_1-GPR55_Hets detected by the in situ proximity ligation assay (PLA) in striatal regions of the monkey brain. Representative images showing PLA label for CB_1-GPR55_Hets in the regions of interest: caudate, putamen and accumbens (see Fig. 1 legend). Experiments were performed in samples from the 3 animal groups namely control, parkinsonian (MPTP-treated) and dyskinetic. Quantification of red dots/cell is shown in the bar graphs displayed in Fig. 3

neuroinflammation occurring in PD and with upregulation of the receptor in microglia, it is likely that the increase in CB_2-GPR55_Hets in parkinsonian animals is due to activated (reactive) microglia. Cannabinoids are important regulators of neuroinflammation associated with neurodegenerative diseases (Palazuelos et al. 2009; Stella 2010; Kong et al. 2014; Janssen et al. 2016, 2018; Tao et al. 2016; Attili et al. 2019). Approaches to skew the phenotype of microglial cells from the M1 proinflammatory to the M2 neuroprotective (Franco and Fernández-Suárez 2015) are being actively sought. In this sense, there is the possibility for cannabinoids to regulate the M1/M2 balance (Galve-Roperh et al. 2008; Stella 2009; Aso and Ferrer 2014; Mecha et al. 2015, 2016; Tao et al. 2016). Interestingly, there are already data showing that GPR55 may be a non-dopaminergic therapeutic target in PD (Wu et al. 2013; Celorrio et al. 2017).

The above-commented study of identification of neurons expressing CB_1-GPR55_Hets in the striatum of naïve animals also concluded that the heteromers are not only expressed on cell surface but in intracellular structures (Martínez-Pinilla et al. 2020). In this regard, it has been reported that the CB_1R may be present in mitochondria and may mediate regulation of mitochondrial function by cannabinoids (Bénard et al. 2012; Hebert-Chatelain et al. 2014; Melser et al. 2017; Gutiérrez-Rodríguez et al. 2018). There are huge technical challenges to detect heteromers, either CB_1-GPR55_Hets

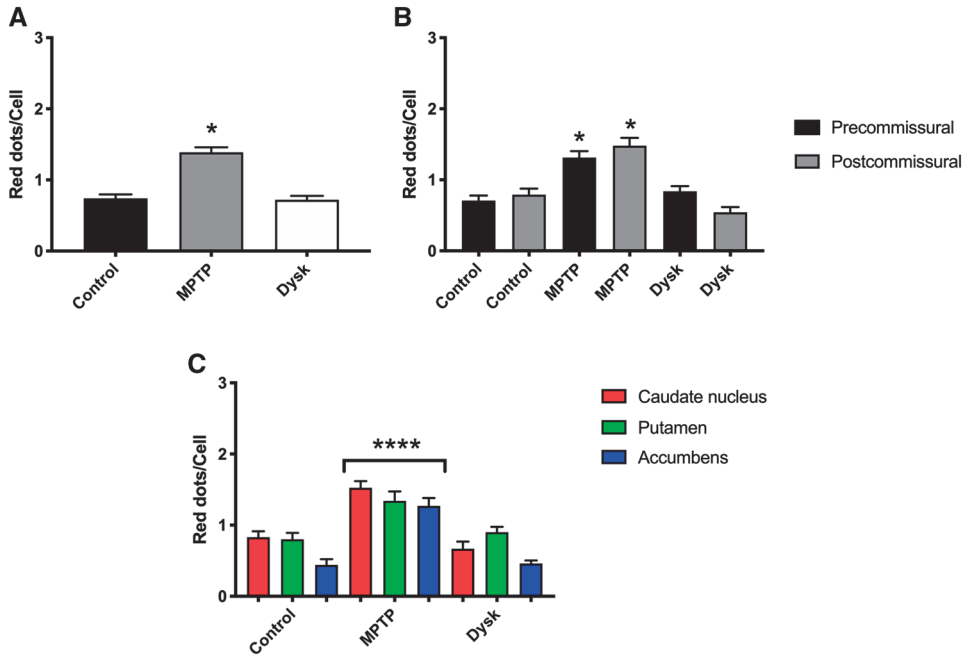

Fig. 3 Quantitation of CB_1-GPR55_Hets performed according to the Andy's algorithm (see "Materials and methods") in all striatal areas (caudate, putamen and accumbens nuclei) and in samples from control, MPTP-treated and dyskinetic animals. **a** Quantitation adding up the PLA label in all regions and both in pre- and post-commissural locations. **b** Quantitation in pre- *versus* quantitation in post-commissural areas. **c** Quantitation in each area (caudate, putamen and accumbens nuclei) following the color code indicated in Fig. 1. Data are the mean ± SEM (150 data points from 3 sections, 6 fields and $n = 3$ per group). Significant differences were analyzed by a one- or two-way ANOVA followed by post-hoc Bonferroni's test. *$p < 0.05$ compared with control; in **c**: ****$p < 0.0001$: every region in MPTP-treated animals *versus* both control and dyskinetic

or CB_2-GPR55_Hets, but it is worth knowing whether cannabinoids may affect neural cell energy production via these GPR55-containing receptor complexes and whether expression alterations during PD correlate with changes in the expression of heteromers at the mitochondrial level. Indeed, altered mitochondrial functionality is raising as a culprit in sporadic PD cases (Macdonald et al. 2018; Ben-Shachar 2019). Therefore, targeting intracellular receptors by plasma-membrane-permeant cannabinoids could be a good possibility to revert mitochondrial malfunctioning and prevent neuronal death.

The physiological role of the interactions, i.e. the properties of the heteromers in terms of signaling, must be taken into account in order to design the most effective approach. In this sense, CB_2R agonists or allosteric modulators such as cannabidiol, a very safe compound, may be useful (Fernández-Ruiz et al. 2011; Pertwee 2012; Noel 2017; Martínez-Pinilla et al. 2017; Navarro et al. 2018; Fraguas-Sánchez and Torres-Suárez 2018). In contrast, more experimental effort is needed to know the most convenient way to approach GPR55 targeting, apart from doubts on which is mechanistically the best option, i.e. to measure the efficacy of agonists, antagonists or allosteric modulators in PD models. The safety of GPR55 ligands must be also tested.

With regard to GPR55, it is important to note that the affinity, the potency and the selectivity of different natural and synthetic cannabinoids are inconsistent across studies. For instance, whereas Kapur et al. (2009) and Yin et al. (2009) reported agonist activity of rimonabant using a β-arrestin reporter assay, Lauckner et al. (2008) showed that the drug behaved as GPR55 antagonist in intracellular Ca^{2+} mobilization assays. GPR55 shows the most unique features as it seems to act primarily through the $G_{\alpha 12}$-family of proteins and RhoA (Ryberg et al. 2007; Henstridge et al. 2010; Obara et al. 2011), but it may also couple to G_q (Lauckner et al. 2008; Waldeck-Weiermair et al. 2008). In a careful study by Henstridge et al. (2010), it appears that GPR55 is linked to a range of downstream signaling events and that the activity of GPR55 ligands is influenced by the functional assay employed, with notable differences in potency and efficacy (Henstridge et al. 2010). Among these factors, the most investigated are ERK1/2 (Oka et al. 2007; Ryberg et al. 2007; Lauckner et al. 2008; Waldeck-Weiermair et al. 2008; Pietr et al. 2009; Kapur et al. 2009; Andradas et al. 2011; Piñeiro et al. 2011), and p38 MAPK (Oka et al. 2010). Importantly, it has been demonstrated that LPI-induced ERK1/2 phosphorylation is controlled, at least in part, by GPR55 coupling to $G_{\alpha 12/13}$ which indicates a crosstalk between MAPK and Rho GTPases signaling (Andradas et al. 2011; Anavi-Goffer et al. 2012). Using a variety of homogenous assays, Anavi-Goffer et al. (2012)

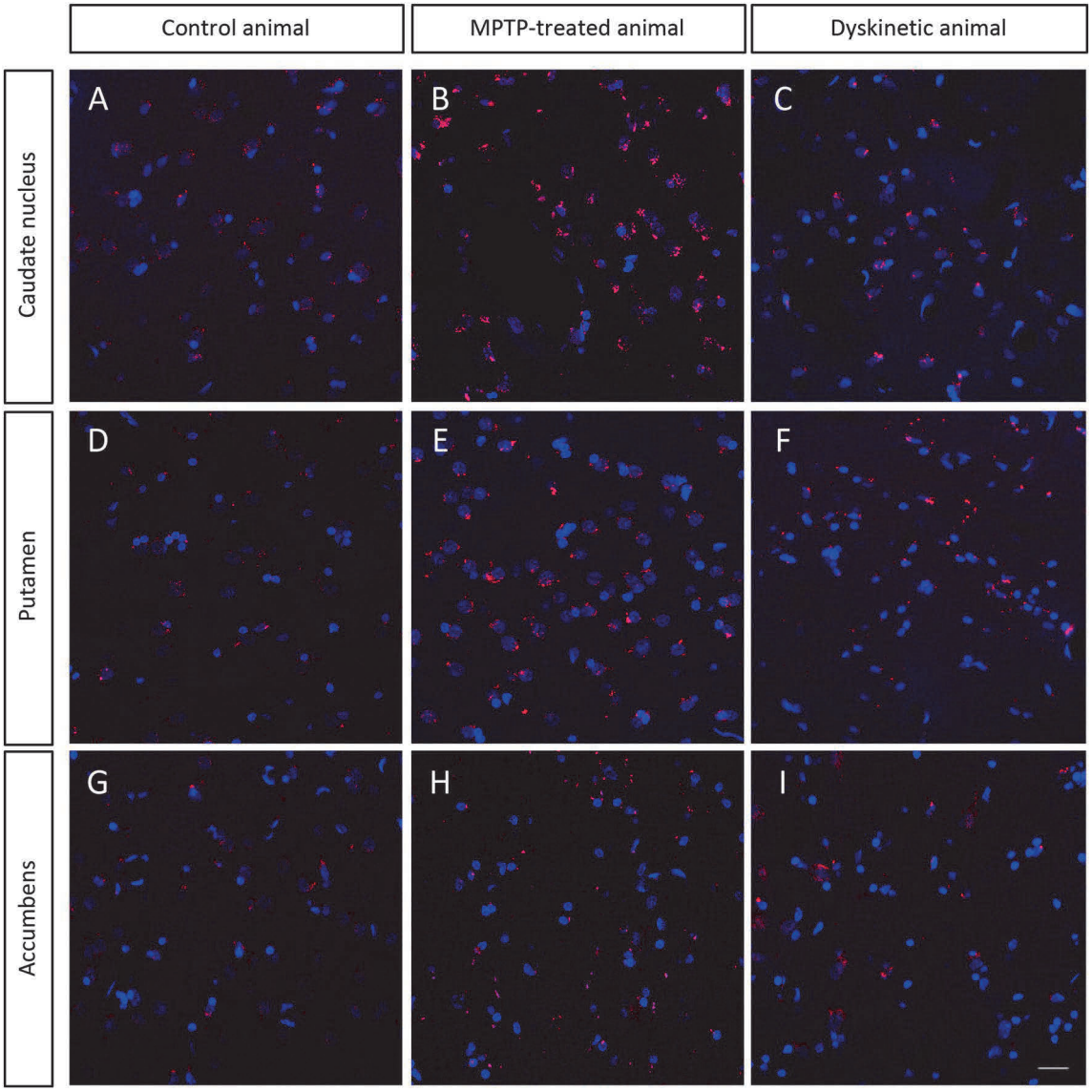

Fig. 4 CB_2-GPR55_Hets detected by the in situ proximity ligation assay (PLA) in striatal regions of the monkey brain. Representative images showing PLA label for CB_2-GPR55_Hets in the regions of interest: caudate, putamen and accumbens nuclei (see Fig. 1 legend). Experiments were performed in samples from the 3 animal groups namely control, parkinsonian (MPTP-treated) and dyskinetic. Quantification of red dots/cell is shown in the bar graphs displayed in Fig. 5

reported that certain cannabinoids can both activate GPR55 and attenuate LPI-mediated ERK1/2 phosphorylation concluding that "*cannabinoid ligands have complex interactions with the LPI/GPR55 signalling system*" (Anavi-Goffer et al. 2012). Some of the results may be attributed to CB_2-GPR55 receptor heteromerization. In fact, GPR55-mediated regulation of cannabinoid effects on CB_2R was first suggested in human neutrophils (Balenga et al. 2011; Irving 2011). Concerning CB_2-GPR55_Hets, we have previously shown that signaling by agonists of either receptor in cell models "*was governed (i) by the presence or absence of the partner receptors (with the consequent formation of heteromers) and (ii) by the activation state of the partner receptor*" (Balenga et al. 2014).

The atypical pharmacology often reported (including the above-described phenotypic profiles for antagonists) for CB_1R and CB_2R but even more extreme for GPR55 makes these receptors excellent candidates to show, as a proof-of-concept, that heteromerization influences pharmacology and the coupling to signaling pathways. In this context, additional forms of functional selectivity still need to be examined. For example, ligand-directed selectivity in G-protein-independent signaling pathways, which has been demonstrated with β-arrestin biased ligands for the β_2-adrenergic

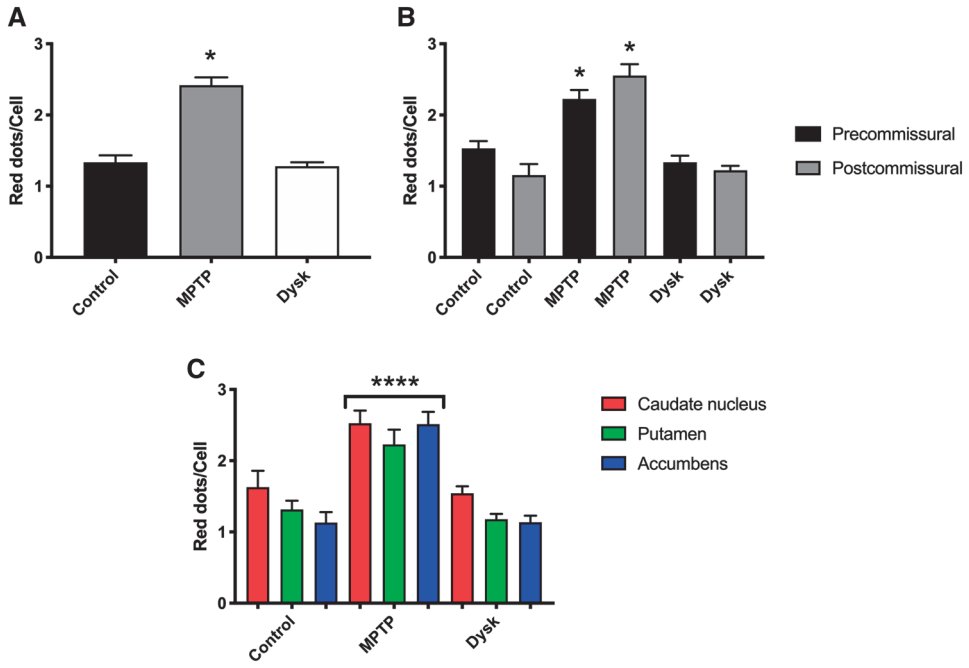

Fig. 5 Quantitation of CB_2-GPR55_Hets performed according to the Andy's algorithm (see "Materials and methods") in all striatal areas (caudate, putamen and accumbens nuclei) and in samples from control, MPTP-treated and dyskinetic animals. **a** Quantitation adding up the PLA label in all regions and both in pre- and post-commissural locations. **b** Quantitation in pre- *versus* quantitation in post-commissural areas. **c** Quantitation in each area (caudate, putamen and accumbens nuclei) following the color code indicated in Fig. 1. Data are the mean ± SEM (150 data points from 3 sections, 6 fields and $n = 3$ per group). Significant differences were analyzed by a one- or two-way ANOVA followed by post-hoc Bonferroni's test. $^*p < 0.05$ compared with control; in **c**: $^{****}p < 0.0001$: every region in MPTP-treated animals *versus* both control and dyskinetic

receptors (Drake et al. 2008), has not been examined in full detail for CB_1R, CB_2R or GPR55.

Acknowledgements This work was supported by grants from Spanish Ministerio de Economía y Competitividad (MINECO) (#BFU2012-37907, #SAF2008-03118-E and #SAF2012-39875-C02-01; they may include EU FEDER funds), Eranet-Neuron (Heteropark), CIBERNED (CB06/05/006), Fundació La Marató de TV3 [20141330 to RF, and 20141331 to JLL] and by Departamento de Salud del Gobierno de Navarra.

Author contributions JLL, GN and RF participated in the design of the project and analyzed the results; it is considered that their contribution was similar. EMP and AJR performed the majority of the experiments and took care of animals and measured ad hoc scores; it is considered that their contribution was similar. ER participated in a significant number of experiments. RRS and JL incorporated the software to analyze the PLA results, and actively participated in the PLA data analysis and in providing data for final Figures. JLL did many of the imaging assays in the confocal microscope, took images and participated in data analysis. EMP, JLL and RF wrote the first draft of the manuscript that was further edited by all co-authors, who agreed with submission.

Compliance with ethical standards

Conflict of interest The authors declare no conflict of interest.

Ethical approval All experiments have been performed with approved protocols and under the regional supervision, i.e. strictly following all national and EU regulations.

References

Alexander SP, Christopoulos A, Davenport AP et al (2017) The concise guide to pharmacology 2017/18: G protein-coupled receptors. Br J Pharmacol 174:S17–S129. https://doi.org/10.1111/bph.13878

Alexander SPH, Roberts RE, Broughton BRS et al (2018) Goals and practicalities of immunoblotting and immunohistochemistry: A guide for submission to the British Journal of Pharmacology. Br J Pharmacol 175:407–411

Anavi-Goffer S, Baillie G, Irving AJ et al (2012) Modulation of L-α-lysophosphatidylinositol/GPR55 mitogen-activated protein kinase (MAPK) signaling by cannabinoids. J Biol Chem 287:91–104. https://doi.org/10.1074/jbc.M111.296020

Andradas C, Caffarel MM, Pérez-Gómez E et al (2011) The orphan G protein-coupled receptor GPR55 promotes cancer cell proliferation via ERK. Oncogene 30:245–252. https://doi.org/10.1038/onc.2010.402

Armentero MT, Pinna A, Ferré S et al (2011) Past, present and future of A2A adenosine receptor antagonists in the therapy of Parkinson's disease. Pharmacol Ther 132:280–299. https://doi.org/10.1016/j.pharmthera.2011.07.004

Aso E, Ferrer I (2014) Cannabinoids for treatment of Alzheimer's disease: moving toward the clinic. Front Pharmacol 5:37. https://doi.org/10.3389/fphar.2014.00037

Attili B, Celen S, Ahamed M et al (2019) Preclinical evaluation of [18 F]MA3: a CB 2 receptor agonist radiotracer for PET. Br J Pharmacol 176:1481–1491. https://doi.org/10.1111/bph.14564

Baker D, Pryce G, Davies WL, Hiley CR (2006) ScienceDirect—trends in pharmacological sciences: in silico patent searching reveals a new cannabinoid receptor. Trends Pharmacol Sci 27:1–4. https://doi.org/10.1016/j.tips.2005.11.003

Balenga NAB, Aflaki E, Kargl J et al (2011) GPR55 regulates cannabinoid 2 receptor-mediated responses in human neutrophils. Cell Res 21:1452–1469. https://doi.org/10.1038/cr.2011.60

Balenga NA, Martínez-Pinilla E, Kargl J et al (2014) Heteromerization of GPR55 and cannabinoid CB2 receptors modulates signalling. Br J Pharmacol 171:1–64. https://doi.org/10.1111/bph.12850

Bénard G, Massa F, Puente N et al (2012) Mitochondrial CB1 receptors regulate neuronal energy metabolism. Nat Neurosci 15:558–564. https://doi.org/10.1038/nn.3053

Ben-Shachar D (2019) The bimodal mechanism of interaction between dopamine and mitochondria as reflected in Parkinson's disease and in schizophrenia. J. Neural Transm 127:159–168

Bonaventura J, Rico AJ, Moreno E et al (2014) L-DOPA-treatment in primates disrupts the expression of A(2A) adenosine-CB(1) cannabinoid-D(2) dopamine receptor heteromers in the caudate nucleus. Neuropharmacology 79:90–100. https://doi.org/10.1016/j.neuropharm.2013.10.036

Brusco A, Tagliaferro PA, Saez T, Onaivi ES (2008) Ultrastructural localization of neuronal brain CB2 cannabinoid receptors. Ann N Y Acad Sci 1139:450–457. https://doi.org/10.1196/annals.1432.037

Celorrio M, Rojo-Bustamante E, Fernández-Suárez D et al (2017) GPR55: a therapeutic target for Parkinson's disease? Neuropharmacology 125:319–332. https://doi.org/10.1016/j.neuropharm.2017.08.017

Christensen R, Kristensen PK, Bartels EM et al (2007) Efficacy and safety of the weight-loss drug rimonabant: a meta-analysis of randomised trials. Lancet (London, Engl) 370:1706–1713. https://doi.org/10.1016/S0140-6736(07)61721-8

Curtis MJ, Alexander S, Cirino G et al (2018) Experimental design and analysis and their reporting II: updated and simplified guidance for authors and peer reviewers. Br J Pharmacol 175:987–993. https://doi.org/10.1111/bph.14153

Drake MT, Violin JD, Whalen EJ et al (2008) β-arrestin-biased agonism at the β2-adrenergic receptor. J Biol Chem 283:5669–5676. https://doi.org/10.1074/jbc.M708118200

Farré D, Muñoz A, Moreno E et al (2015) Stronger dopamine D1 receptor-mediated neurotransmission in dyskinesia. Mol Neurobiol 52:1408–1420. https://doi.org/10.1007/s12035-014-8936-x

Fernández-Ruiz J, Moreno-Martet M, Rodríguez-Cueto C et al (2011) Prospects for cannabinoid therapies in basal ganglia disorders. Br J Pharmacol 163:1365–1378. https://doi.org/10.1111/j.1476-5381.2011.01365.x

Ferré S, Baler R, Bouvier M et al (2009) Building a new conceptual framework for receptor heteromers. Nat Chem Biol 5:131–134. https://doi.org/10.1038/nchembio0309-131

Fraguas-Sánchez AI, Torres-Suárez AI (2018) Medical use of cannabinoids. Drugs 78:1665–1703. https://doi.org/10.1007/s40265-018-0996-1

Franco R, Fernández-Suárez D (2015) Alternatively activated microglia and macrophages in the central nervous system. Prog Neurobiol 131:65–86. https://doi.org/10.1016/j.pneurobio.2015.05.003

Franco R, Martínez-Pinilla E, Lanciego JLJLJL, Navarro G (2016) Basic pharmacological and structural evidence for class A G-protein-coupled receptor heteromerization. Front Pharmacol 7:76. https://doi.org/10.3389/fphar.2016.00076

Franco R, Aguinaga D, Jiménez J et al (2018) Biased receptor functionality versus biased agonism in G-protein-coupled receptors. Biomol Concepts 9:143–154. https://doi.org/10.1515/bmc-2018-0013

Fuxe K, Guidolin D, Agnati LF, Borroto-Escuela DO (2015) Dopamine heteroreceptor complexes as therapeutic targets in Parkinson's disease. Expert Opin Ther Targets 19:377–398. https://doi.org/10.1517/14728222.2014.981529

Galve-Roperh I, Aguado T, Palazuelos J, Guzmán M (2008) Mechanisms of control of neuron survival by the endocannabinoid system. Curr Pharm Des 14:2279–2288. https://doi.org/10.2174/138161208785740117

Giuffrida A, Seillier A (2012) New insights on endocannabinoid transmission in psychomotor disorders. Prog Neuro-Psychopharmacol Biol Psychiatry 38:51–58

Goetz CG, Stebbins GT, Shale HM et al (1994) Utility of an objective dyskinesia rating scale for Parkinson's disease: Inter- and intrarater reliability assessment. Mov Disord 9:390–394. https://doi.org/10.1002/mds.870090403

Gutiérrez-Rodríguez A, Bonilla-Del Río I, Puente N et al (2018) Localization of the cannabinoid type-1 receptor in subcellular astrocyte compartments of mutant mouse hippocampus. Glia 66:1417–1431. https://doi.org/10.1002/glia.23314

Hebert-Chatelain E, Reguero L, Puente N et al (2014) Cannabinoid control of brain bioenergetics: exploring the subcellular localization of the CB1 receptor. Mol Metab 3:495–504. https://doi.org/10.1016/j.molmet.2014.03.007

Henstridge CM, Balenga NA, Schröder R et al (2010) GPR55 ligands promote receptor coupling to multiple signalling pathways. Br J Pharmacol 160:604–614. https://doi.org/10.1111/j.1476-5381.2009.00625.x

Irving A (2011) New blood brothers: the GPR55 and CB 2 partnership. Cell Res 21:1391–1392

Janssen B, Vugts DJ, Funke U et al (2016) Imaging of neuroinflammation in Alzheimer's disease, multiple sclerosis and stroke: Recent developments in positron emission tomography. Biochim Biophys Acta Mol Basis Dis 1862:425–441. https://doi.org/10.1016/j.bbadis.2015.11.011

Janssen B, Vugts D, Windhorst A, Mach R (2018) PET imaging of microglial activation—beyond targeting TSPO. Molecules 23:607. https://doi.org/10.3390/molecules23030607

Johns DG, Behm DJ, Walker DJ et al (2009) The novel endocannabinoid receptor GPR55 is activated by atypical cannabinoids but does not mediate their vasodilator effects. Br J Pharmacol 152:825–831. https://doi.org/10.1038/sj.bjp.0707419

Kapur A, Zhao P, Sharir H et al (2009) Atypical responsiveness of the orphan receptor GPR55 to cannabinoid ligands. J Biol Chem 284:29817–29827. https://doi.org/10.1074/jbc.M109.050187

Kong W, Li H, Tuma RF, Ganea D (2014) Selective CB2 receptor activation ameliorates EAE by reducing Th17 differentiation and immune cell accumulation in the CNS. Cell Immunol 287:1–17. https://doi.org/10.1016/j.cellimm.2013.11.002

Kurlan R, Kim MH, Gash DM (1991) Oral levodopa dose-response study in MPTP-induced hemiparkinsonian monkeys: assessment with a new rating scale for monkey Parkinsonism. Mov Disord 6:111–118. https://doi.org/10.1002/mds.870060205

Lanciego JL, Vázquez A (2012) The basal ganglia and thalamus of the long-tailed macaque in stereotaxic coordinates. A template atlas based on coronal, sagittal and horizontal brain sections. Brain Struct Funct 217:613–666. https://doi.org/10.1007/s00429-011-0370-5

Lanciego JL, Rodríguez-Oroz MC, Blesa FJ et al (2008) Lesion of the centromedian thalamic nucleus in MPTP-treated monkeys. Mov Disord 23:708–715. https://doi.org/10.1002/mds.21906

Lanciego JL, Barroso-Chinea P, Rico AJ et al (2011) Expression of the mRNA coding the cannabinoid receptor 2 in the pallidal

complex of Macaca fascicularis. J Psychopharmacol. https://doi.org/10.1177/0269881110367732
Langston JW, Widner H, Goetz CG et al (1992) Core assessment program for intracerebral transplantations (CAPIT). Mov Disord 7:2–13. https://doi.org/10.1002/mds.870070103
Lauckner JE, Jensen JB, Chen H-Y et al (2008) GPR55 is a cannabinoid receptor that increases intracellular calcium and inhibits M current. Proc Natl Acad Sci U S A 105:2699–2704. https://doi.org/10.1073/pnas.0711278105
Law AMK, Yin JXM, Castillo L et al (2017) Andy's Algorithms: new automated digital image analysis pipelines for FIJI. Sci Rep 7:15717. https://doi.org/10.1038/s41598-017-15885-6
Macdonald R, Barnes K, Hastings C, Mortiboys H (2018) Mitochondrial abnormalities in Parkinson's disease and Alzheimer's disease: can mitochondria be targeted therapeutically? Biochem Soc Trans 46:891–909
Marcellino D, Ferré S, Casadó V et al (2008) Identification of dopamine D1–D3 receptor heteromers: Indications for a role of synergistic D1–D3 receptor interactions in the striatum. J Biol Chem 283:26016–26025. https://doi.org/10.1074/jbc.M710349200
Martínez-Pinilla E, Reyes-Resina I, Oñatibia-Astibia A et al (2014) CB1 and GPR55 receptors are co-expressed and form heteromers in rat and monkey striatum. Exp Neurol 261:44–52. https://doi.org/10.1016/j.expneurol.2014.06.017
Martínez-Pinilla E, Varani K, Reyes-Resina I et al (2017) Binding and signaling studies disclose a potential allosteric site for cannabidiol in cannabinoid CB2receptors. Front Pharmacol 8:744. https://doi.org/10.3389/fphar.2017.00744
Martínez-Pinilla E, Rico AJ, Rivas-Santisteban R et al (2020) Expression of cannabinoid CB 1 R-GPR55 heteromers in neuronal subtypes of the *Macaca fascicularis* striatum. Ann N Y Acad Sci. https://doi.org/10.1111/nyas.14413
Mecha M, Feliú A, Carrillo-Salinas FJ et al (2015) Endocannabinoids drive the acquisition of an alternative phenotype in microglia. Brain Behav Immun 49:233–245. https://doi.org/10.1016/j.bbi.2015.06.002
Mecha M, Carrillo-Salinas FJ, Feliú A et al (2016) Microglia activation states and cannabinoid system: therapeutic implications. Pharmacol Ther 166:40–55. https://doi.org/10.1016/j.pharmthera.2016.06.011
Melser S, Zottola ACP, Serrat R et al (2017) Functional analysis of mitochondrial CB1 cannabinoid receptors (mtCB1) in the brain. Methods Enzymol 593:143–174. https://doi.org/10.1016/bs.mie.2017.06.023
Navarro G, Morales P, Rodríguez-Cueto C et al (2016) Targeting cannabinoid CB2 receptors in the central nervous system. Medicinal chemistry approaches with focus on neurodegenerative disorders. Front Neurosci. https://doi.org/10.3389/fnins.2016.00406
Navarro G, Reyes-Resina I, Rivas-Santisteban R et al (2018) Cannabidiol skews biased agonism at cannabinoid CB1 and CB2 receptors with smaller effect in CB1–CB2 heteroreceptor complexes. Biochem Pharmacol 157:148–158. https://doi.org/10.1016/j.bcp.2018.08.046
Noel C (2017) Evidence for the use of "medical marijuana" in psychiatric and neurologic disorders. Ment Heal Clin 7:29–38. https://doi.org/10.9740/mhc.2017.01.029
Núñez E, Benito C, Pazos MR et al (2004) Cannabinoid CB2 receptors are expressed by perivascular microglial cells in the human brain: an Immunohistochemical Study. Synapse 53:208–213. https://doi.org/10.1002/syn.20050
Obara Y, Ueno S, Yanagihata Y, Nakahata N (2011) Lysophosphatidylinositol causes neurite retraction via GPR55, G13 and RhoA in PC12 cells. PLoS ONE 6:e24284. https://doi.org/10.1371/journal.pone.0024284
Oka S, Nakajima K, Yamashita A et al (2007) Identification of GPR55 as a lysophosphatidylinositol receptor. Biochem Biophys Res Commun 362:928–934. https://doi.org/10.1016/j.bbrc.2007.08.078
Oka S, Kimura S, Toshida T et al (2010) Lysophosphatidylinositol induces rapid phosphorylation of p38 mitogen-activated protein kinase and activating transcription factor 2 in HEK293 cells expressing GPR55 and IM-9 lymphoblastoid cells. J Biochem 147:671–678. https://doi.org/10.1093/jb/mvp208
Onaivi ES (2006) Neuropsychobiological evidence for the functional presence and expression of cannabinoid CB2 receptors in the brain. Neuropsychobiology 54:231–246. https://doi.org/10.1159/000100778
Onaivi ES, Ishiguro H, Gong J-P et al (2006) Discovery of the presence and functional expression of cannabinoid CB2 receptors in brain. Ann N Y Acad Sci 1074:514–536. https://doi.org/10.1196/annals.1369.052
Palazuelos J, Aguado T, Pazos MR et al (2009) Microglial CB2cannabinoid receptors are neuroprotective in Huntington's disease excitotoxicity. Brain 132:3152–3164. https://doi.org/10.1093/brain/awp239
Palomo-Garo C, Gómez-Gálvez Y, García C, Fernández-Ruiz J (2016) Targeting the cannabinoid CB 2 receptor to attenuate the progression of motor deficits in LRRK2-transgenic mice. Pharmacol Res 110:181–192. https://doi.org/10.1016/j.phrs.2016.04.004
Perreault ML, Hasbi A, Shen MYFFMYF et al (2016) Disruption of a dopamine receptor complex amplifies the actions of cocaine. Eur Neuropsychopharmacol 26:1366–1377. https://doi.org/10.1016/j.euroneuro.2016.07.008
Pertwee RG (2012) Targeting the endocannabinoid system with cannabinoid receptor agonists: pharmacological strategies and therapeutic possibilities. Philos Trans R Soc B Biol Sci 367:3353–3363. https://doi.org/10.1098/rstb.2011.0381
Pietr M, Kozela E, Levy R et al (2009) Differential changes in GPR55 during microglial cell activation. FEBS Lett 583:2071–2076. https://doi.org/10.1016/j.febslet.2009.05.028
Piñeiro R, Maffucci T, Falasca M (2011) The putative cannabinoid receptor GPR55 defines a novel autocrine loop in cancer cell proliferation. Oncogene 30:142–152. https://doi.org/10.1038/onc.2010.417
Pinna A, Bonaventura J, Farré D et al (2014) L-DOPA disrupts adenosine A(2A)-cannabinoid CB(1)-dopamine D(2) receptor heteromer cross-talk in the striatum of hemiparkinsonian rats: biochemical and behavioral studies. Exp Neurol 253:180–191. https://doi.org/10.1016/j.expneurol.2013.12.021
Price DA, Martinez AA, Seillier A et al (2009) WIN55,212–2, a cannabinoid receptor agonist, protects against nigrostriatal cell loss in the 1-methyl-4-phenyl-1,2,3,6-tetrahydropyridine mouse model of Parkinson's disease. Eur J Neurosci 29:2177–2186. https://doi.org/10.1111/j.1460-9568.2009.06764.x
Rico AJ, Barroso-Chinea P, Conte-Perales L et al (2010) A direct projection from the subthalamic nucleus to the ventral thalamus in monkeys. Neurobiol Dis 39:381–392. https://doi.org/10.1016/j.nbd.2010.05.004
Rodríguez-Ruiz M, Moreno E, Moreno-Delgado D et al (2017) Heteroreceptor complexes formed by dopamine D1, histamine H3, and *N*-methyl-D-aspartate glutamate receptors as targets to prevent neuronal death in Alzheimer's disease. Mol Neurobiol 54:4537–4550. https://doi.org/10.1007/s12035-016-9995-y
Ryberg E, Larsson N, Sjögren S et al (2007) The orphan receptor GPR55 is a novel cannabinoid receptor. Br J Pharmacol 152:1092–1101. https://doi.org/10.1038/sj.bjp.0707460
Sawzdargo M, Nguyen T, Lee DK et al (1999) Identification and cloning of three novel human G protein-coupled receptor genes GPR52, ΨGPR53 and GPR55: GPR55 is extensively expressed in human brain. Mol Brain Res 64:193–198. https://doi.org/10.1016/S0169-328X(98)00277-0

Stella N (2009) Endocannabinoid signaling in microglial cells. Neuropharmacology 56:244–253. https://doi.org/10.1016/j.neuropharm.2008.07.037

Stella N (2010) Endocannabinoid signaling in microglial cells. Glia 58(Suppl 1):244–253. https://doi.org/10.1002/glia.20983

Tao Y, Li L, Jiang B et al (2016) Cannabinoid receptor-2 stimulation suppresses neuroinflammation by regulating microglial M1/M2 polarization through the cAMP/PKA pathway in an experimental GMH rat model. Brain Behav Immun 58:118–129. https://doi.org/10.1016/j.bbi.2016.05.020

Waldeck-Weiermair M, Zoratti C, Osibow K et al (2008) Integrin clustering enables anandamide-induced Ca2+ signaling in endothelial cells via GPR55 by protection against CB1-receptor-triggered repression. J Cell Sci 121:1704–1717. https://doi.org/10.1242/jcs.020958

Wu C-S, Zhu J, Wager-Miller J et al (2010) Requirement of cannabinoid CB(1) receptors in cortical pyramidal neurons for appropriate development of corticothalamic and thalamocortical projections. Eur J Neurosci 32:693–706. https://doi.org/10.1111/j.1460-9568.2010.07337.x

Wu C-S, Chen H, Sun H et al (2013) GPR55, a G-protein coupled receptor for lysophosphatidylinositol, plays a role in motor coordination. PLoS ONE 8:e60314. https://doi.org/10.1371/journal.pone.0060314

Yin H, Chu A, Li W et al (2009) Lipid G protein-coupled receptor ligand identification using β-arrestin PathHunter assay. J Biol Chem 284:12328–12338. https://doi.org/10.1074/jbc.M806516200

3.5 Angiotensin AT_1 and AT_2 receptor heteromer expression in the hemilesioned rat model of Parkinson's disease that increases with levodopa-induced dyskinesia.

Rafael Rivas-Santisteban, Ana I. Rodriguez-Perez, Ana Muñoz, Irene Reyes-Resina, José Luis Labandeira-García, Gemma Navarro y Rafael Franco.

Manuscrito publicado en *Journal of Neuroinflammation*, Agosto 2020; 17:243.

El sistema renina-angiotensina (RAS) se encuentra alterado en la enfermedad de Parkinson (PD), una enfermedad que aparece debido a una neurodegeneración de la *substantia nigra* del cerebro. En la actualidad, la terapia principal consiste en reestablecer los niveles de dopamina, utilizando el precursor levodopa, que conduce a medio-largo plazo a una resistencia al tratamiento y a efectos secundarios indeseados como las discinesias. Los receptores de angiotensina AT_1 y AT_2 son los efectores clásicos del RAS, y aunque son conocidos principalmente por su papel en la regulación de la homeostasis del agua y la presión arterial, también se expresan en el sistema nervioso central. En este estudio determinamos la capacidad de AT_1R y AT_2R de interaccionar de forma estrecha formando heterómeros AT_1R-AT_2R. Se realizaron determinaciones de calcio y cAMP intracelulares, activación de MAPK y ensayos de redistribución dinámica de masas (DMR) para caracterizar la señalización en sistemas homólogos y heterólogos. Se utilizaron ensayos de ligación por proximidad (PLA) para cuantificar la expresión del receptor en cultivos primarios de neurona estriatal y de microglía de ratón y en secciones del cuerpo estriado de rata. Nuestros resultados demuestran la existencia de heterómeros AT_1R-AT_2R que se expresan en células del sistema nervioso central y que actúan como unidades funcionales novedosas. Es importante destacar que la coactivación de los dos receptores en el heterómero se traduce en un cross-talk negativo y como se produce una potenciación en la señalización mediada por la activación de AT_2R inducida por el bloqueo de AT_1R con candesartan, su antagonista específico. Finalmente, se observó un aumento de la expresión del heterómero AT_1R-AT_2R en animales modelo de Parkinson respecto a los animales control, siendo este aumento más significativo en animales modelo de Parkinson que fueron tratados con levodopa. En su conjunto, los resultados apuntan como posible estrategia terapéutica en la PD el bloqueo del receptor AT_1R para promover la acción neuroprotectora mediada a través del AT_2R.

Rivas-Santisteban et al. Journal of Neuroinflammation (2020) 17:243
https://doi.org/10.1186/s12974-020-01908-z

Journal of Neuroinflammation

RESEARCH Open Access

Angiotensin AT_1 and AT_2 receptor heteromer expression in the hemilesioned rat model of Parkinson's disease that increases with levodopa-induced dyskinesia

Rafael Rivas-Santisteban[1,2], Ana I. Rodriguez-Perez[2,3], Ana Muñoz[2,3], Irene Reyes-Resina[1,2,4], José Luis Labandeira-García[2,3], Gemma Navarro[2,5*†] and Rafael Franco[2,6*†]

Abstract

Background/aims: The renin-angiotensin system (RAS) is altered in Parkinson's disease (PD), a disease due to substantia nigra neurodegeneration and whose dopamine-replacement therapy, using the precursor levodopa, leads to dyskinesias as the main side effect. Angiotensin AT_1 and AT_2 receptors, mainly known for their role in regulating water homeostasis and blood pressure and able to form heterodimers ($AT_{1/2}$Hets), are present in the central nervous system. We assessed the functionality and expression of $AT_{1/2}$Hets in Parkinson disease (PD).

Methods: Immunocytochemistry was used to analyze the colocalization between angiotensin receptors; bioluminescence resonance energy transfer was used to detect $AT_{1/2}$Hets. Calcium and cAMP determination, MAPK activation, and label-free assays were performed to characterize signaling in homologous and heterologous systems. Proximity ligation assays were used to quantify receptor expression in mouse primary cultures and in rat striatal sections.

Results: We confirmed that AT_1 and AT_2 receptors form $AT_{1/2}$Hets that are expressed in cells of the central nervous system. $AT_{1/2}$Hets are novel functional units with particular signaling properties. Importantly, the coactivation of the two receptors in the heteromer reduces the signaling output of angiotensin. Remarkably, $AT_{1/2}$Hets that are expressed in both striatal neurons and microglia make possible that candesartan, the antagonist of AT_1, increases the effect of AT_2 receptor agonists. In addition, the level of striatal expression increased in the unilateral 6-OH-dopamine lesioned rat PD model and was markedly higher in parkinsonian-like animals that did not become dyskinetic upon levodopa chronic administration if compared with expression in those that became dyskinetic.

Conclusion: The results indicate that boosting the action of neuroprotective AT_2 receptors using an AT_1 receptor antagonist constitutes a promising therapeutic strategy in PD.

Keywords: Neuroinflammation, Heteromer, G-protein-coupled receptor (GPCR), Dyskinesia, Levodopa

* Correspondence: g.navarro@ub.edu; rfranco123@gmail.com
†Gemma Navarro and Rafael Franco contributed equally to this work.
[2]Centro de Investigación en Red, enfermedades Neurodegenerativas, CiberNed, Instituto de Salud Carlos III, Madrid, Spain
Full list of author information is available at the end of the article

Introduction

The renin angiotensin system (RAS) is composed of enzymes that produce angiotensin (Ang) peptides and of cell surface receptors that convey cytocrin signals to achieve specific cell responses. There are two angiotensin receptors (AT_1R and AT_2R) that belong to the superfamily of G-protein-coupled receptors. RAS has been abundantly studied in the periphery, mainly in relation with the control of arterial blood pressure. However, different laboratories have provided solid evidence of the relevant role of RAS in the central nervous system (CNS). Ang is an important regulator of motor control, and AT_1R and AT_2R have been suggested as targets to combat Parkinson's disease (PD) and related conditions such as levodopa (L-DOPA)-induced dyskinesias [38, 45].

Age is a main risk factor for sporadic PD, which is characterized by dysregulation of the dopaminergic function due to the death of dopaminergic neurons of the *substantia nigra* (SN). A local RAS has been reported in the SN [20, 61], in which overactivity of AT_1R correlates with aging-related alterations, neuronal death [22, 31], and neuroinflammation (Labandeira-Garcia et al., [29, 30, 52]). Microglial cells are the main mediators of neuroinflammation and despite once activated they are considered as detrimental, it is now known that they may undertake the pro-inflammatory (M1) or the neuroprotective (M2) phenotype. The search for pharmacological tools targeting G-protein-coupled receptors to convert M1 into M2 phenotype is an active field of research. The role of AT_2R and the interplay between the two receptors in the above-mentioned changes due to Ang action in the aged or in the pathological brain is still unclear.

The cognate proteins for coupling to AT_1R and AT_2R are, respectively, Gq (also Gi) and Gi. Accordingly, agonists of AT_1R may mobilize calcium ion from intracellular stores, whereas agonists of AT_2R decrease the activity of adenylyl cyclase thus depressing the cAMP/PKA signaling (https://www.guidetopharmacology.org). Interestingly, the two receptors may interact, leading to the formation of receptor heteromers with particular properties: pharmacological, functional, or both [15, 48]. On the one hand, heteromerization modifies receptor trafficking and ß-arrestin recruitment [48]. On the other hand, Ang II induces the formation of heteromers of the two receptors ($AT_{1/2}$Hets) in luminal membranes of kidney tubular epithelial LLC-PK1 cells. In these cells, the peptide activates a calcium channel, sarco/endoplasmic reticulum Ca^{2+}-ATPase (SERCA), that in kidney cells participates in the control of blood pressure [14].

The main target for pharmacological anti-parkinsonian interventions is the striatum that receives the SN dopaminergic input needed for motor control. What is important is to know whether AT_1 and AT_2 receptors interact in the CNS, which is their physiological function and how their expression alters the course of a neurodegenerative disease. Accordingly, the aims of this paper were to (i) get further insight into the properties of $AT_{1/2}$Hets in a heterologous expression system; (ii) investigate the expression and function of AT_1R, AT_2R, and $AT_{1/2}$Hets in striatal neurons; and (iii) investigate the expression and function of AT_1R, AT_2R, and $AT_{1/2}$Hets in striatal microglia in resting and activated states. The results show that AT_2R are expressed in neurons and in activated microglia where they interact with AT_1R to form $AT_{1/2}$Hets. Accordingly, a final aim was to discover differential expression of $AT_{1/2}$Hets in striatal samples from parkinsonian and dyskinetic animals.

Materials and methods

Reagents

Lipopolysaccharide (LPS), interferon-γ (IFN-γ), and forskolin, Angiotensin II (Ang II), CGP-42112A (CGP), Candesartan (CAN) and PD123319 (PD) were purchased from Sigma-Aldrich (St Louis, MO).

HEK-293T cells and primary cultures

Human embryonic kidney (HEK-293T) cells were grown in Dulbecco's modified Eagle's medium (DMEM) (Gibco) supplemented with 2 mM L-glutamine, 100 μg/mL sodium pyruvate, 100 U/mL penicillin/streptomycin, MEM non-essential amino acids solution (1/100), and 5% (v/v) heat-inactivated fetal bovine serum (FBS) (all supplements were from Invitrogen, Paisley, Scotland, UK).

To prepare mouse striatal primary microglial cultures, brain was removed from C57BL/6 mice of 2–4 days of age. Microglial cells were isolated following protocols described elsewhere [40, 49, 56] and grown in DMEM medium supplemented with 2 mM L-glutamine, 100 U/mL penicillin/streptomycin, MEM non-essential amino acids preparation (1/100), and 5% (v/v) heat-inactivated FBS (Invitrogen, Paisley, Scotland, UK). Briefly, striatum tissue was dissected, carefully stripped of its meninges, and digested with 0.25% trypsin for 20 min at 37 °C. The action of the proteolytic enzyme was stopped by adding an equal volume of culture medium (Dulbecco's modified Eagle medium-F-12 nutrient mixture, fetal bovine serum 10%, penicillin 100 U/mL, streptomycin 100 μg/mL, and amphotericin B 0.5 μg/mL) with 160 μg/mL deoxyribonuclease I (all reagents from Invitrogen). Cells were brought to a single cell suspension by repeated pipetting followed by passage through a 100 μm-pore mesh and pelleted (7 min, 200×*g*). Glial cells were resuspended in medium and seeded at a density of 3.5×10^5 cells/mL in 6-well plates for cyclic adenylic acid (cAMP) assays, in 12-well plates with coverslips for in situ proximity ligation assays (PLA), and in 96-well plates for mitogen-activated protein kinase (MAPK) activation experiments. Cultures were maintained at 37 °C in humidified 5%

CO_2 atmosphere and medium was replaced at DIV 2 and then once a week. At DIV 19-21 cells were treated with diluted trypsin [56] to obtain > 98% pure microglial cultures.

For neuronal primary cultures, the striatum from mouse embryos (E19) was removed and the neurons were isolated as described by [25] and plated at a density of circa 120, 000 cells/cm^2. The cells were grown in a neurobasal medium supplemented with 2 mM L-glutamine, 100 U/mL penicillin/streptomycin, and 2% (v/v) B27 supplement (Gibco) in a 6-, 12-, or 96-well plate for 19–21 days. Cultures were maintained at 37 °C in humidified 5% CO_2 atmosphere and medium was replaced every 4–5 days.

Immunodetection of specific markers (NeuN for neurons and CD-11b for microglia) showed that neuronal preparations contained > 98% neurons and microglia preparations contained, at least, 98% microglial cells [39].

Parkinson's disease model generation, levodopa treatment, and dyskinesia assessment

All experiments were carried out in accordance with EU directives (2010/63/EU and 86/609/CEE) and were approved by the Ethical committee of the University of Santiago de Compostela. Similar to the approach elsewhere described [13], an experimental design using male Wistar rats was aimed at obtaining four group of animals as described below. Animals were 8-week-old at the beginning of the experimental procedure.

Details of model generation, protocol of drug administration, and behavioral analysis, performed by a blinded investigator, are given elsewhere [38, 47]. Surgery was performed on rats anesthetized with ketamine/xylazine (1% ketamine—75 mg/kg, and 2% xylazine—10 mg/kg). Lesions were produced in the right medial forebrain bundle to achieve complete lesion of the nigrostriatal pathway. The rats were injected with 12 μg of 6-OH-DA (to provide 8 μg of 6-hydroxy-DA free base; Sigma-Aldrich) in 4 μL of sterile saline containing 0.2% ascorbic acid. These were considered "lesioned" animals. Injection of vehicle lead to generation of naïve (or non-lesioned) animals.

The 6-OH-dopamine hemilesioned rat is considered a PD model. Amphetamine-induced rotation was tested in a bank of eight automated rotometer bowls (Rota-count 8, Columbus Instruments, Columbus, OH, USA) by monitoring full (360°) body turns in either direction. Right and left full body turns were recorded over 90 min following an injection of D-amphetamine (2.5 mg/kg i.p.) dissolved in saline. Rats that displayed more than six full body turns/min ipsilateral to the lesion were included in the study (this rate would correspond to more than 90% depletion of dopamine fibers in the striatum) [65].

Spontaneous use of forelimb can be measured by the cylinder test [28, 57]. Rats were placed individually in a glass cylinder (20 cm in diameter), and the number of left or right forepaw contacts were scored by an observer blinded to the animals' identity and presented as left (impaired) touches in percentage of total touches. A control animal would thus receive an unbiased score of 50%, whereas lesion usually reduces performance of the impaired paw to less than 20% of total wall contacts.

Of the lesioned animals displaying parkinsonism-like behavior according to the above described tests (18 in total), 12 were chronically treated with L-DOPA daily for 3 weeks. A mixture of L-DOPA methyl ester (6 mg/kg) plus benserazide (10 mg/kg) was subcutaneously administered. The treatment reliably induces dyskinetic movements in some rats. As described in a previous report [13], abnormal involuntary movements (AIMs) were evaluated according to the rat dyskinesia scale described in detail elsewhere [5, 12, 33, 36, 47]. The severity of each AIM subtype (limb, orolingual, and axial) was assessed using scores from 0 to 4 (1, occasional, i.e., present < 50% of the time; 2, frequent, i.e., present > 50% of the time; 3, continuous, but interrupted by strong sensory stimuli; 4, continuous, not interrupted by strong sensory stimuli). Rats were classified as "dyskinetic" if they displayed a ≥ 2 score per monitoring period on at least two AIM subtypes. Animals classified as "non-dyskinetic" exhibited either no L-DOPA-induced abnormal involuntary movements or very mild/occasional ones [41]. Animals with low scores, i.e., either non-dyskinetic or dyskinetic, were discarded. In summary, four groups of animals were obtained: (i) non-lesioned, (ii) lesioned treated with vehicle, (iii) lesioned L-DOPA-treated becoming dyskinetic, and (iv) lesioned that upon L-DOPA treatment did not become dyskinetic. In every animal, tyrosine hydroxylase immunostaining was performed in sections taken post-mortem [19, 38]; selected animals undergoing 6-OH-dopamine treatment showed in the lesioned hemisphere a > 95% nigral dopaminergic denervation. Overall, 4 animals, those with better scores, were selected in each of following 4 groups: naïve, lesioned, lesioned/L-DOPA dyskinetic, and lesioned/L-DOPA non dyskinetic. PLA analysis (see below) was performed in different fields of striatal sections from each of the 16 finally selected animals. The striatum was delimited in sections using a bright field and images were captured within delimitation coordinates.

Fusion proteins

Human cDNAs for AT_1, AT_2, and σ_1 receptors cloned into pcDNA3.1 were amplified without their stop codons using sense and antisense primers harboring either BamHI and HindIII restriction sites to amplify AT_1R and AT_2R or BamHI and EcoRI restriction sites to amplify σ_1 receptor. Amplified fragments were then subcloned to be in frame with an enhanced yellow

fluorescent protein (pEYFP-N1; Clontech, Heidelberg, Germany) or a Rluc (pRluc-N1; PerkinElmer, Wellesley, MA) on the C-terminal end of the receptor to produce AT_1R-YFP, AT_2R-RLuc, AT_2R-YFP, and σ_1R-RLuc fusion proteins.

Cell transfection

HEK-293T cells were transiently transfected with the corresponding cDNA by the polyethylenimine (PEI, Sigma-Aldrich, St. Louis, MO) method [18, 23]. Briefly, the corresponding cDNA diluted in 150 mM NaCl was mixed with PEI (5.5 mM in nitrogen residues) also prepared in 150 mM NaCl for 10 min. The cDNA-PEI complexes were transferred to HEK-293T cells and were incubated for 4 h in a serum-starved medium. Then, the medium was replaced by fresh supplemented culture medium and cells were maintained at 37 °C in a humid atmosphere of 5% CO_2. Forty-eight hours after transfection, cells were washed, detached, and resuspended in the assay buffer.

Immunocytochemistry

HEK-293T cells were seeded on glass coverslips in 12-well plates. On DIV 2, cells were transfected with AT_1R-YFP cDNA (1 μg), AT_2R-Rluc cDNA (1 μg), or both. On DIV 4, cells were fixed in 4% paraformaldehyde for 15 min and washed twice with PBS containing 20 mM glycine before permeabilization with PBS-glycine containing 0.2% Triton X-100 (5-min incubation). Cells were blocked during 1 h with PBS containing 1% bovine serum albumin. HEK-293T cells were labeled with a mouse anti-Rluc antibody (1/100; Millipore, Darmstadt, Germany) and subsequently treated with Cy3 conjugated anti-mouse (1/200; Jackson ImmunoResearch (red)) IgG (1 h each). The AT_1R-YFP expression was detected by YFP's own fluorescence. Controls using untransfected cells and cells incubated without the primary antibody are shown in Supplementary Figure S1. Samples were washed several times and mounted with 30% Mowiol (Calbiochem). Images were obtained in a Leica SP2 confocal microscope (Leica Microsystems) with the × 63 oil objective.

Bioluminescence resonance energy transfer assays

For bioluminescence resonance energy transfer (BRET) assays, HEK-293T cells were transiently cotransfected with a constant amount of cDNA encoding for AT_2R-RLuc (0.9 μg) and with increasing amounts of cDNA corresponding to AT_1R-YFP (0.5 to 4 μg). For negative control, HEK-293T cells were transiently cotransfected with a constant amount of cDNA encoding for σ_1-RLuc (0.75 μg) and with increasing amounts of cDNA corresponding to AT_2R-YFP (0.1 to 4 μg). To control the cell number, sample protein concentration was determined using a Bradford assay kit (Bio-Rad, Munich, Germany) using bovine serum albumin (BSA) dilutions to prepare the standard absorbance versus concentration relationship. To quantify fluorescent proteins, cells (20 μg protein) were distributed in 96-well microplates (black plates with a transparent bottom) and fluorescence was read in a Fluostar Optima Fluorimeter (BMG Labtech, Offenburg, Germany) equipped with a high-energy xenon flash lamp, using a 10 nm bandwidth excitation filter at 485 nm. For BRET measurements, the equivalent of 20 μg of cell suspension was distributed in 96-well white microplates with white bottom (Corning 3600, Corning, NY) and 5 μM coelenterazine H (Molecular Probes, Eugene, OR) was added. One minute after adding coelenterazine H, BRET was determined using a Mithras LB 940 reader (Berthold Technologies, DLReady, Germany), which allows the integration of the signals detected in the short-wavelength filter at 485 nm and the long-wavelength filter at 530 nm. To quantify AT_2R-RLuc expression, luminescence readings were performed 10 min after the addition of 5 μM coelenterazine H. MilliBRET units (mBU) are defined as:

$$\mathrm{mBU} = \left[\frac{\lambda_{530}(\text{long} - \text{wavelength emission})}{\lambda_{485}(\text{short} - \text{wavelength emission})} - C_f \right] \text{x } 1000$$

where C_f corresponds to [(long-wavelength emission)/(short-wavelength emission)] for the RLuc construct expressed alone in the same experiment.

Detection of cytoplasmic calcium ion

HEK-293T cells were cotransfected with the cDNA for the Ang receptors AT_1 (1 μg) and/or AT_2 (1 μg) and the GCaMP6 calcium sensor (1 μg) [11] by the use of PEI method (Section "Cell Transfection"). Forty-eight hours post-transfection, HEK-293T cells plated in 6-well black, clear bottom plates, were incubated with Mg^{2+}-free Locke's buffer (154 mM NaCl, 5.6 mM KCl, 3.6 mM $NaHCO_3$, 2.3 mM $CaCl_2$, 5.6 mM glucose, 5 mM HEPES, pH 7.4) supplemented with 10 μM glycine. Receptor antagonists were added only 15 min before readings to allow efficient binding to receptors while avoiding unspecific or long-term noxious events. Receptor agonists were added right before readings as calcium level increase when mediated by Gq-coupled receptors is very quick. Fluorescence emission intensity of GCaMP6 was recorded at 515 nm upon excitation at 488 nm on the EnSpire® Multimode Plate Reader for 150 s every 5 s at 100 flashes per well.

cAMP level determination

The analysis of cAMP levels was performed in HEK-293T cells transfected with cDNA for AT_1 (1 μg) and/or AT_2 (1 μg) receptors in primary cultures of striatal neurons or glia using the Lance Ultra cAMP kit

(PerkinElmer). The optimal cell density to obtain an appropriate fluorescent signal was first established by measuring the TR-FRET signal as a function of forskolin concentration using different cell densities. Forskolin dose-response curves were related to the cAMP standard curve in order to establish which cell density provides a response that covers most of the dynamic range of cAMP standard curve. Two hours before the experiment, the medium was substituted by serum-starved DMEM medium. Cells (2000 HEK-293T cells, 4000 striatal neurons, or glial cells by well in 384-well microplates) growing in medium containing 50 μM zardaverine were pre-treated with the AT_1R or AT_2R antagonists (Candesartan and PD123319 respectively) or the corresponding vehicle at 24 °C for 15 min, and stimulated with the AT_1R and/or AT_2R agonists (Ang II and CGP-42112A respectively) for 15 min before adding 0.5 μM forskolin or vehicle, and incubating for an additional 15-min period. After 1 h, fluorescence at 665 nm was analyzed on a PHERAstar Flagship microplate reader equipped with an HTRF optical module (BMG Labtech). A standard curve for cAMP was obtained in each experiment.

Extracellular signal-regulated kinases 1/2 phosphorylation

To determine extracellular signal-regulated kinases 1/2 (ERK1/2) phosphorylation, 40,000 HEK-293T cells transfected with cDNA for AT_1R (1 μg) and/or AT_2R (1 μg) or 50,000 striatal neurons or glial cells primary cultures were plated in each well of transparent Deltalab 96-well microplates. Two hours before the experiment, the medium was substituted by serum-starved DMEM medium. Then, cells were treated or not for 15 min with the selective antagonists Candesartan or PD123319 in serum starved DMEM medium followed by 7-min treatment with the selective agonists Ang II and/or CGP-42112A. Cells were then washed twice with cold PBS before the addition of lysis buffer (15-min treatment). Ten microliters of each supernatant were placed in white ProxiPlate 384-well microplates and ERK1/2 phosphorylation was determined using AlphaScreen®SureFire® kit (Perkin Elmer) following the instructions of the supplier and using an EnSpire® Multimode Plate Reader (PerkinElmer, Waltham, MA, USA).

Dynamic mass-redistribution label-free assays

Cell signaling was explored using an EnSpire® Multimode Plate Reader (PerkinElmer, Waltham, MA, USA) by a label-free technology. Cellular cytoskeleton redistribution movement induced upon receptor activation were detected by illuminating the underside of the plate with polychromatic light and measured as changes in wavelength of the reflected monochromatic light that is a sensitive function of the index of refraction. The magnitude of this wavelength shift (in picometers) is directly proportional to the amount of dynamic mass redistribution (DMR). To determine the label free-DMR signal, 10,000 HEK-293T cells transfected with cDNA for AT_1R (1 μg) and/or AT_2R (1 μg) receptors or 10,000 striatal neurons or glial cells primary cultures were plated on each well of transparent 384-well fibronectin-coated microplates to obtain 70–80% confluent monolayers, and kept in the incubator for 24 h. Previous to the assay, cells were washed twice with assay buffer (HBSS with 20 mM HEPES, pH 7.15, 0.1% DMSO) and incubated in the reader for 2 h in 30 μL/well of assay buffer at 24 °C. Hereafter, the sensor plate was scanned and a baseline optical signature was recorded for 10 min before adding 10 μL of antagonists (Candesartan or PD123319) dissolved in assay buffer, followed by the addition, 30 min later of 10 μL of selective agonists (Ang II and/or CGP-42112A) also dissolved in assay buffer. DMR responses induced by the agonist were monitored for a minimum of 3600 s.

Proximity ligation assay

Detection in natural sources of clusters formed by AT_1 and AT_2 receptors was addressed in primary cultures of glial cells and rat brain sections.

Rats were processed for histological analysis as it follows. Animals were injected an overdose of chloral hydrate and transcardial perfusion fixation quickly undertaken using cold 4% paraformaldehyde in 0.1 M phosphate buffer (PB), pH 7.4. Brains were removed, washed, and cryoprotected in the same buffer containing 20% sucrose. Serial 40-μm-thick coronal sections were then cut with a freezing microtome and those containing the striatum were collected in cryoprotectant solution.

Cells were grown on glass coverslips, fixed in 4% paraformaldehyde for 15 min, washed with PBS containing 20 mM glycine to quench the aldehyde groups, permeabilized with the same buffer containing 0.05% Triton X-100 for 5 to 15 min, and washed with PBS.

Cells and sections were then similarly processed. After 1-h incubation at 37 °C with the blocking solution in a pre-heated humidity chamber, samples were incubated overnight at 4 °C with a mixture of a mouse monoclonal anti-AT_1R antibody (1/100, sc-515884, Santa Cruz Biotechnology, Texas, USA), a rabbit monoclonal anti-AT_2R antibody (1/100, ab92445, Abcam, Cambridge, UK), and Hoechst (1/100 from stock 1 mg/mL; Sigma-Aldrich) to stain the nuclei. The antibodies were validated following the method in the technical brochure of the vendor with fairly similar results and also by immunofluorescence in HEK-293T cells (transfected versus untransfected). Samples from KO animals were not available for validation.

Cells or brain sections were further processed using the proximity ligation assays (PLA) probes detecting

primary antibodies (Duolink In Situ PLA probe Anti-Mouse plus and Duolink In Situ PLA probe Anti-Rabbit minus) (1/5 v:v for 1-hour at 37 °C). Ligation and amplification were done as indicated by the supplier (Sigma-Aldrich) and cells were mounted using the mounting medium 30% Mowiol (Calbiochem). To detect red dots corresponding to $AT_{1/2}$Hets, samples were observed in a Leica SP2 confocal microscope (Leica Microsystems, Mannheim, Germany) equipped with an apochromatic × 63 oil-immersion objective (N.A. 1.4), and a 405 nm and 561 nm laser lines. For each field of view, a stack of two channels (one per staining) and 3 Z-planes with a step size of 1 μm were acquired. The Andy's Algorithm [32], a specific ImageJ macro for reproducible and high-throughput quantification of the total PLA foci dots and total nuclei, was used for data analysis.

Statistical analysis

The data in graphs are the mean ± SEM. GraphPad Prism software version 7 (San Diego, CA, USA) was used for data fitting and statistical analysis. The test of Kolmogorov-Smirnov with the correction of Lilliefors was used to evaluate normal distribution and the test of Levene to evaluate the homogeneity of variance. The Student's t test and one-way ANOVA were used for comparing, respectively, two or > 2 means. When indicated, Bonferroni's method was used as a post-hoc test for multiple comparisons. Significant differences were considered when the p value was < 0.05.

Results

Functionality of $AT_{1/2}$Hets in a heterologous expression system

Interactions between AT_1 and AT_2 receptors have been previously reported [14, 48]. Hence, we first investigated whether in HEK-293T cells and in our assay conditions AT_1 and AT_2 receptors may form heteromers. We analyzed the colocalization of angiotensin receptors at the plasma membrane by using HEK-293T cells coexpressing AT_1R and AT_2R fused to, respectively, the yellow fluorescent protein (YFP) and Renilla luciferase (Rluc). The proper traffic of fusion proteins to the cell membrane was confirmed by immunocytochemical analysis (Fig. 1a, b). The high degree of colocalization between AT_1R-YFP and AT_2R-Rluc in the plasma membrane and in the cytosol is shown in yellow (Fig. 1c). To know whether a direct interaction between AT_1 and AT_2 receptors is possible, BRET assays were performed in HEK-293T cells expressing a constant amount of a fusion protein consisting of AT_2R and Renilla Luciferase (AT_2R-Rluc) and increasing amounts of AT_1R fused to YFP (AT_1R-YFP). The saturation curve in Fig. 1d indicates close proximity between the two Ang receptors. The $BRET_{max}$ and $BRET_{50}$ values were 42 ± 1 mBU and 6 ± 2, respectively. When HEK-293T cells were transfected with a constant amount of cDNA for σ1-Rluc and increasing amounts of cDNA for AT_1R-YFP, a linear response was observed indicating a nonspecific interaction of this negative control (Fig. 1d). These results confirm that the two Ang receptors may form heteromers in living HEK-293T cells. The proper functionality of fusion proteins was confirmed by cAMP assays (data not shown). A schematic representation of the technique is shown in Fig. 1e.

To characterize the $AT_{1/2}$Het functionality, signaling assays were performed in single-transfected HEK-293T cells and in cotransfected $AT_{1/2}$Hets-expressing cells. Cytosolic calcium levels, cAMP determination, ERK1/2 phosphorylation, and label-free DMR assays were performed after treatment with AT_1R and/or AT_2R ligands. Consistent with Gq coupling of AT_1R, treatment of AT_1R-expressing cells with Ang II led to a marked increase in cytosolic calcium levels. The effect was receptor-mediated, as it was blocked by candesartan, the AT_1R antagonist (Fig. 2a). In AT_2R expressing cells, the AT_2R agonist CGP-42112A did not induce mobilization of the ion. These results agree with AT_2R not engaging Gq proteins. In cotransfected cells, CGP-42112A did not produce any effect but reduced the response peak produced by Ang II. Hence, within the $AT_{1/2}$Het, AT_2R stimulation inhibits the AT_1 receptor signaling. Unlike the selective AT_1R antagonist, candesartan, which blunted the agonist effect, the selective AT_2R antagonist, PD123319, potentiated the AT_1R-mediated effect (Fig. 2c).

Consistent with AT_2R coupling to Gi, CGP-42112A reduced the forskolin-induced cAMP cytosolic levels in AT_2R single transfected cells. Interestingly, in AT_1R-expressing cells, Ang II treatment also reduced the forskolin-induced cAMP levels. These effects can be explained by AT_1R coupling not only to Gq, but also to Gi proteins. These effects were receptor-mediated and specific as they were blocked by the corresponding antagonist (Fig. 2d, e). Analysis of cAMP-PKA signaling in cotransfected cells is more complex. On the one hand, all agonists reduced forskolin-induced [cAMP] and each antagonist blocked the effect of the corresponding agonist. Simultaneous administration of Ang II and CGP-42112A did not result in an additive effect. On the other hand, the antagonist of the AT_2R enhanced the effect induced by the AT_1R agonist and vice-versa, the antagonist of the AT_1R enhanced the effect of the AT_2R agonist (Fig. 2e). These latter results fit with data from calcium release experiments assays where the antagonist of the AT_2R potentiated the action of Ang II. Then, it seems that both angiotensin receptors regulate one another via heteromerization. The negative regulation can be reversed and the antagonist of one receptor can even reinforce the output due to activation of the partner receptor.

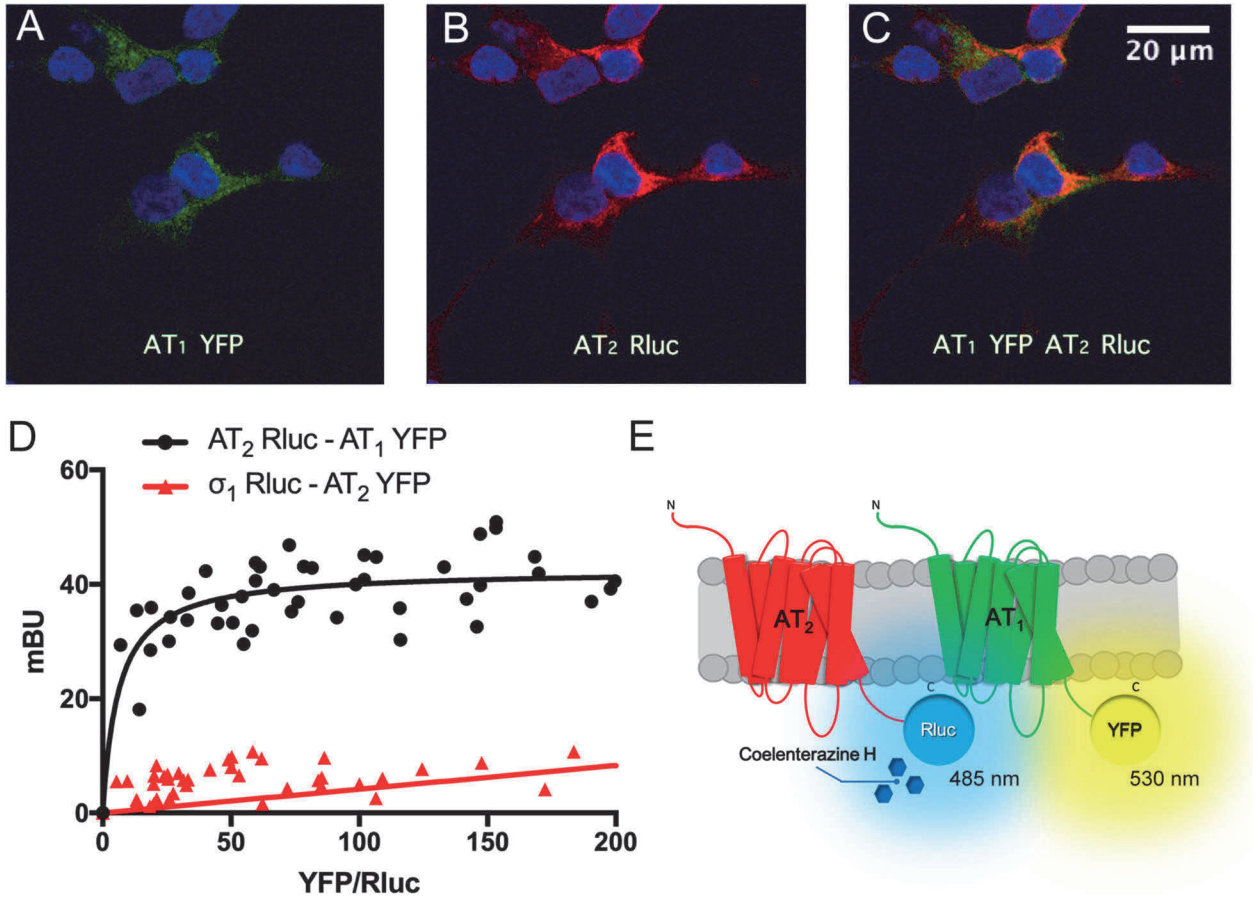

Fig. 1 Human AT_1 and AT_2 receptors interact in a heterologous expression system. **a**–**c** Immunocytochemistry assays were performed in HEK-293T cells expressing AT_1R-YFP (1 μg cDNA), which was detected by its own yellow fluorescence (green), and AT_2R-Rluc (1 μg cDNA), which was detected by a mouse anti-Rluc antibody and a secondary Cy3 anti-mouse antibody (red). Colocalization is shown in yellow. Cell nuclei were stained with Hoechst (blue). Scale bar: 20 μm. **d** BRET assays were performed in HEK-293T cells transfected with a constant amount of cDNA for AT_2R-Rluc (0.9 μg) or σ_1R-Rluc (0.75 μg) (as negative control) and increasing amounts of cDNA for AT_1R-YFP (0.5 to 4 μg) or AT_2R-YFP (0.1 to 4 μg) (as negative control). Values are the mean ± S.E.M. of 8 independent experiments performed in duplicates. **e** Schematic representation of BRET assay: the occurrence of energy transfer depends on the distance between the BRET donor (Rluc) and the BRET acceptor (YFP)

In AT_1R-expressing cells, a marked increase in agonist-induced ERK1/2 phosphorylation that was blocked by candesartan was observed, while in AT_2R-expressing cells, a mild non-significant effect was obtained by treatment with the agonist, CGP-42112A (Fig. 3a, b). Remarkably, $AT_{1/2}$Hets expression in cotransfected cells led to a significant increase in ERK1/2 phosphorylation upon Ang II treatment. The selective AT_2R agonist was still unable to produce any significant effect but, in combined treatments, it markedly reduced the effect induced by Ang II (Fig. 3c). Therefore, these results are in the same line with that observed in calcium release and cAMP accumulation, indicating that both receptors inhibit one another in the $AT_{1/2}$Het.

DMR was modified by agonists in both types of single-transfected cells. In AT_1R-expressing cells, the antagonist could not revert totally the effect of the agonist, indicating that part of the output signal is due to off-site action of Ang II (Fig. 3d). In contrast, the effect of CGP-42112A on AT_2R-expressing was totally blocked by PD123319 (Fig. 3e). In cotransfected cells, the results indicate that both angiotensin receptors show a characteristic signal that is blocked by selective antagonists. However, coactivation in these cells produced an important decrease in the signal. This effect is named negative crosstalk and it is similar to that observed in MAPK phosphorylation assays (Fig. 3e). The enhancement by candesartan of the effect of CGP-42112A, the AT_2R agonist, was also noticed.

In summary, these results indicate a particular functionality of the $AT_{1/2}$Het, namely Ang is able to engage two different signaling pathways. This dual effect is regulated by activation of the partner receptor within the $AT_{1/2}$Het as (i) activation of AT_1R blocks AT_2R agonist induced effect and vice-versa and (ii) AT_1R antagonist releases the inhibition exerted by AT_2R over AT_1R and vice-versa.

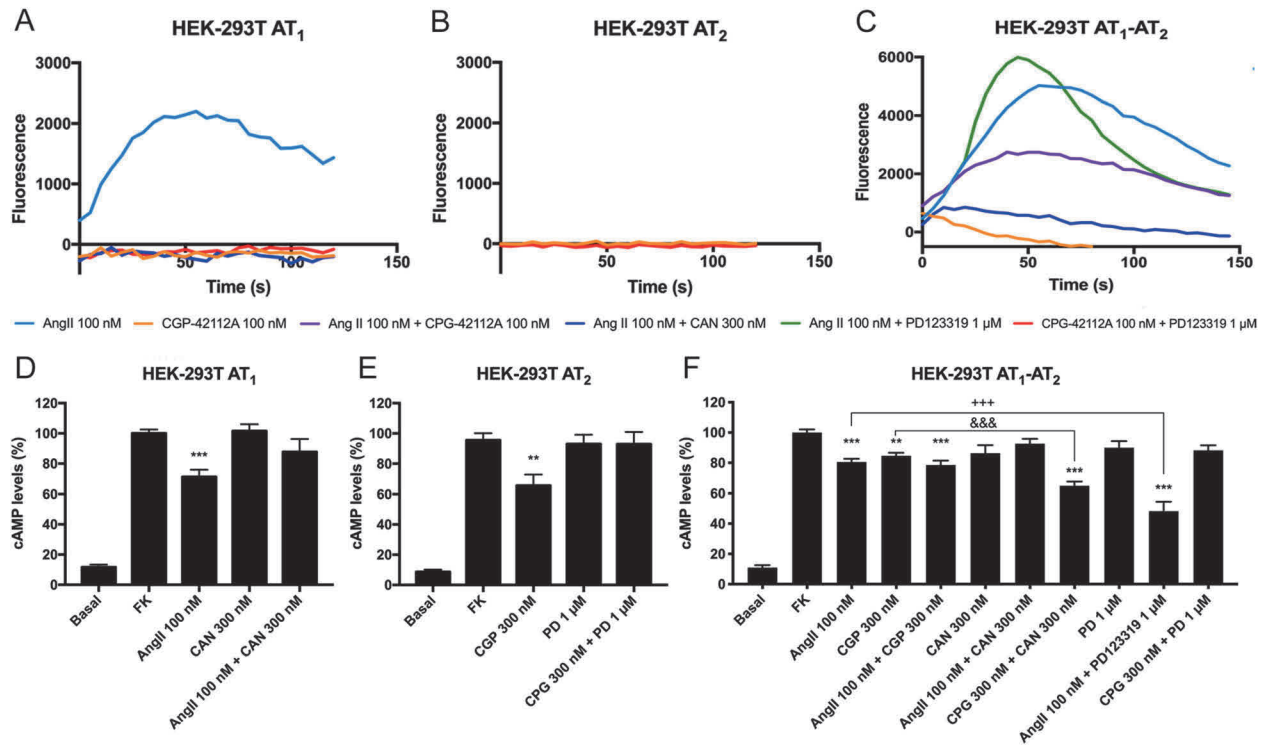

Fig. 2 Functional characterization in HEK-293T cells expressing the AT_1R-AT_2R heteromer. HEK-293T cells were pretreated with selective receptor antagonists (300 nM candesartan for AT_1R or 1 μM PD123319 for AT_2R) and subsequently treated with selective agonists (100 nM angiotensin II for AT_1R and 300 nM CGP-42112A for AT_2R) **a–c** Cytosolic calcium detection assay were performed in HEK-293T cells transfected with the cDNAs for an engineered calcium sensor, 6GCaMP (1 μg), AT_1R (1 μg), and/or AT_2R (1 μg). Values are the mean ± S.E.M. of 5 independent experiments performed in duplicates. **d–f** Intracellular cAMP levels were determined by TR-FRET as described in Methods. HEK-293T cells were transfected with cDNAs for AT_1R (1 μg) and/or AT_2R (1 μg). When G_i coupling was assessed, decreases in [cAMP] were determined using 0.5 μM forskolin added 15 min after the agonists stimulation. Values are the mean ± S.E.M. of 6 independent experiments performed in triplicates. In cAMP one-way ANOVA followed by Bonferroni's multiple comparison post-hoc test were used for statistical analysis. Signaling output was the dependent variable and the different treatments were the independent variables. (*$p < 0.05$, **$p < 0.01$, ***$p < 0.001$ versus forskolin treatment; +++$p < 0.001$ versus Ang II treatment; &&&$p < 0.001$ versus CGP-42112A treatment)

Functionality of AT_1R and AT_2R in primary cultures of striatal neurons

On the basis of the above-described relevance of Ang receptors in motor control and as potential targets to combat PD, we investigated Ang receptor-mediated signaling in primary cultures of neurons isolated from mouse striatum. Reduction of forskolin-induced [cAMP] was obtained using Ang II, while no sign of Gi-coupled AT_2R was detectable (Fig. 4a). Interestingly, in simultaneous treatment with agonists, the lower decrease of forskolin-induced [cAMP] indicated the presence of AT_2R whose activation reduced AT_2R-mediated signaling. In the presence of the AT_1R antagonist, candesartan, the AT_2R agonist, CGP-42112A, induced a significant decrease in forskolin-induced cAMP levels (& in Fig. 4a). These results indicate that in the $AT_{1/2}$Het, the AT_2R signal is inhibited by AT_1R expression and this effect is counteracted by AT_1R antagonists. Similar results were confirmed in experiments of ERK1/2 phosphorylation determination in cultured striatal neurons, where cells responded (moderately) to Ang II and non-significantly to CGP-42112A (Fig. 4b). However, candesartan pretreatment potentiated AT_2R signal. In agreement with the results in HEK-293T cells, cotreatment with agonists induced a lower signal to that induced by angiotensin II, indicating a negative crosstalk effect in both cAMP and MAPK phosphorylation signaling pathways. Overall, these cells express $AT_{1/2}$Hets with similar functional characteristics to that observed in cotransfected HEK-293T cells.

Functionality of AT_1R and AT_2R in primary cultures of striatal microglia: expression of $AT_{1/2}$Hets

Before assessing the functionality of Ang receptors in resting and LPS + IFN-γ activated microglia isolated from striatum, we used in situ PLA to assess the expression of $AT_{1/2}$Hets; PLA is instrumental to detect clusters of interacting proteins in natural sources. Figure 5b shows that resting cells have a few number of red dots due to $AT_{1/2}$Hets, while the negative control show a negligible number of red dots (Fig. 5a). Interestingly, the

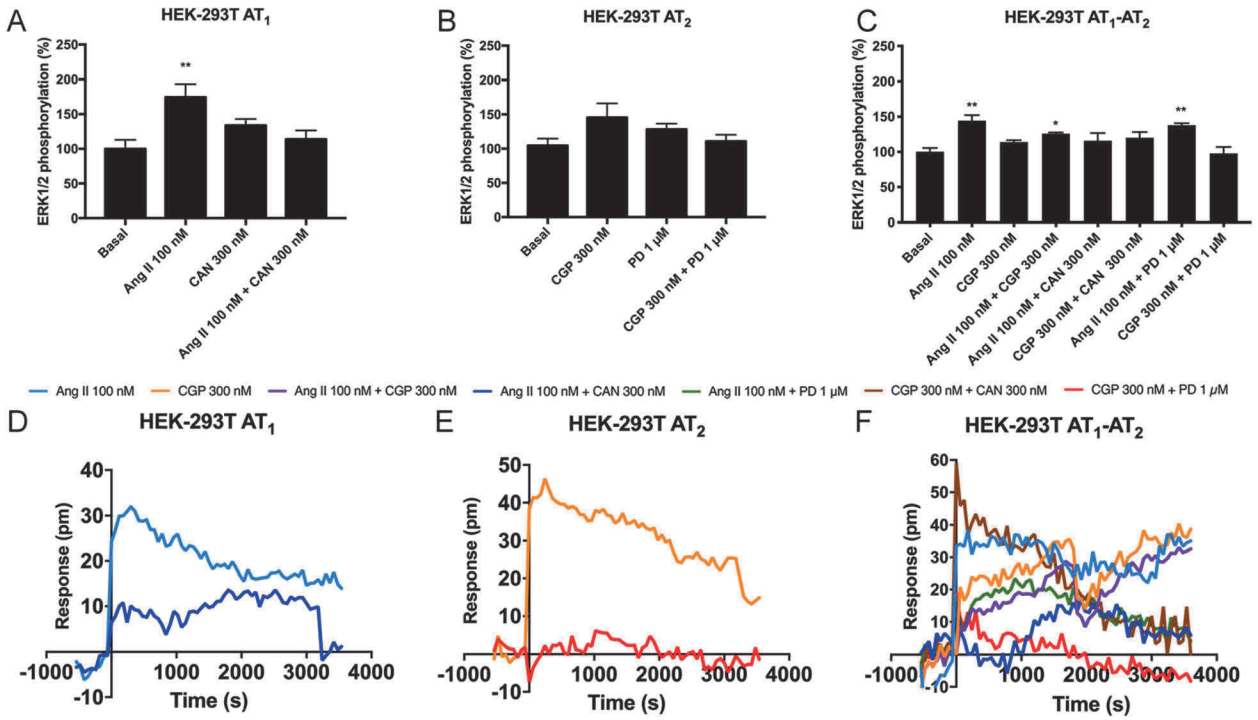

Fig. 3 Functional characterization of AT_1R-AT_2R heteromer in HEK-293T cells. HEK-293T cells were transfected with cDNAs for AT_1R (1 μg) and/or AT_2R (1 μg). Cells were pretreated (15 min) with selective receptor antagonists (300 nM candesartan for AT_1R or 1 μM PD123319 for AT_2R receptors) and subsequently treated with selective agonists (100 nM angiotensin II for AT_1R and 300 nM CGP-42112A for AT_2R receptors). **a–c** ERK1/2 phosphorylation was analyzed using an AlphaScreen®SureFire® kit (Perkin Elmer). Values are the mean ± S.E.M. of 5 independent experiments performed in duplicates. One-way ANOVA followed by Bonferroni's multiple comparison post-hoc test were used for statistical analysis. Signaling output was the dependent variable and the different treatments were the independent variables (*$p < 0.05$, **$p < 0.01$, ***$p < 0.001$; versus vehicle treatment (basal)). **d–f** DMR tracings represent the picometer-shifts of reflected light wavelength over time. Values are the mean ± S.E.M. 8 independent experiments performed in triplicates

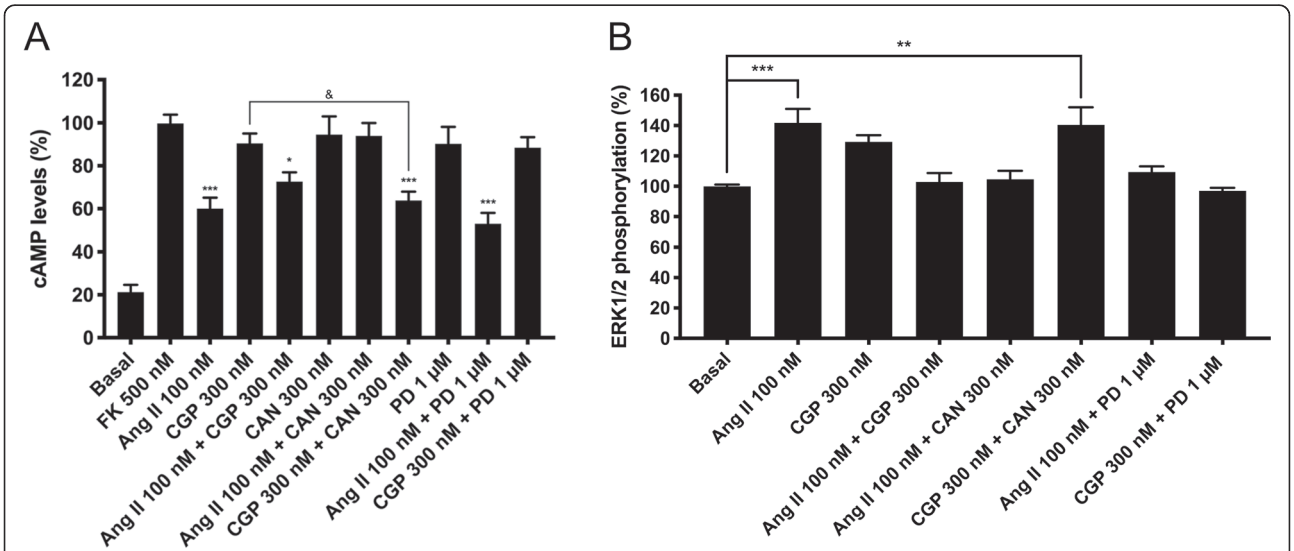

Fig. 4 AT_1R-AT_2R heteromer functionality in primary cultures of striatal neurons. For cAMP (**a**) or ERK1/2 phosphorylation (**b**), cells were pretreated (15 min) with selective receptor antagonists (300 nM candesartan for AT_1R or 1 μM PD123319 for AT_2R) and subsequently treated with selective agonists (100 nM angiotensin II for AT_1R and/or 300 nM CGP-42112A for AT_2R). Values are the mean ± S.E.M. of 5 independent experiments performed in triplicates. One-way ANOVA followed by Bonferroni's multiple comparison post-hoc test were used for statistical analysis. Signaling output was the dependent variable and the different treatments were the independent variables. (&$p < 0.05$ versus CGP-42112A treatment; *$p < 0.05$, **$p < 0.01$, ***$p < 0.001$ versus forskolin treatment in cAMP determinations or versus vehicle treatment (basal) in pERK determinations)

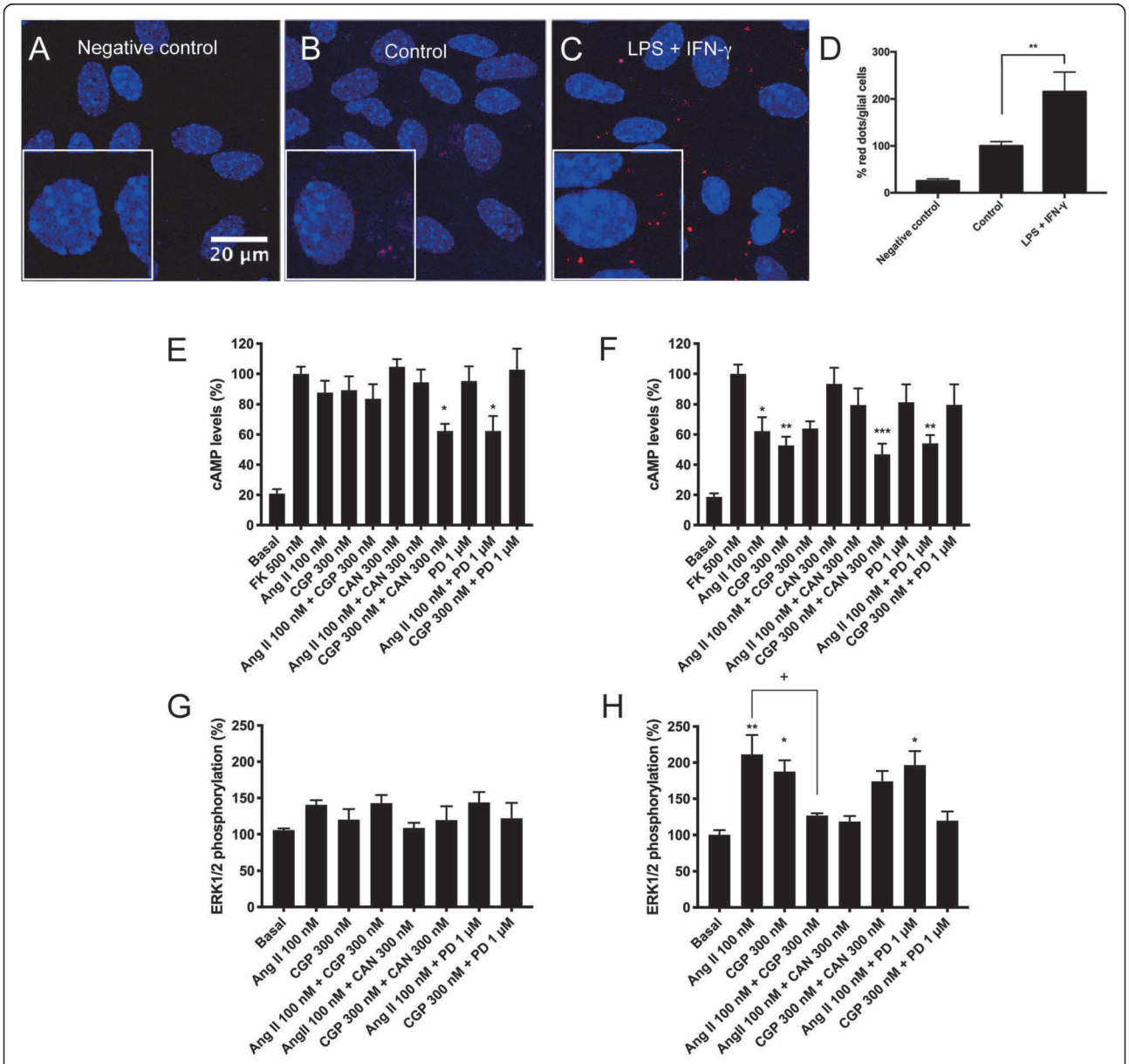

Fig. 5 AT_1R-AT_2R heteromer functionality in microglial primary cultures treated with LPS and IFN-γ. **a**–**c** Expression of AT_1R/AT_2R heteromers in primary microglial cultures were determined by PLA, which was performed using specific primary antibodies against AT_1 and AT_2 receptors (confocal microscopy images (stacks of 3 consecutive planes) show heteroreceptor complexes as red clusters and Hoechst-stained nuclei (blue)). Scale bar: 20 μm. **d** Bar graph showing the percentage of red dots/cell respect non-treated cells; mean ± S.E.M of counts in 5–7 different fields (n = 5; $^{**}p < 0.01$; Student's t test versus the control condition). **e, f** Microglial cultures were incubated for 48 h in the absence (left) or in the presence (right) of 1 μM LPS and 200 U/mL IFN-γ. Microglial cells were pretreated (15 min) with selective receptor antagonists (300 nM candesartan for AT_1R or 1 μM PD123319 for AT_2R receptors) and subsequently with the specific agonists (100 nM angiotensin II for AT_1R and 300 nM CGP-42112A for AT_2R receptors). cAMP (**e**-**f**) and ERK1/2 phosphorylation (**g**-**h**) were subsequently measured. Values are the mean ± S.E.M. of 5 independent experiments performed in triplicates. One-way ANOVA followed by Bonferroni's multiple comparison post-hoc test were used for statistical analysis. Signaling output was the dependent variable and the different treatments were the independent variables. ($+p < 0.05$ versus Ang II treatment in pERK determinations; and $^{*}p < 0.05$, $^{**}p < 0.01$, $^{***}p < 0.001$; versus forskolin treatment in cAMP measurements or versus vehicle treatment (basal) in pERK measurements)

red label was markedly increased in activated cells, as shown in Fig. 5c and in the bar graph of Fig. 5d indicating that $AT_{1/2}$Hets expression increases in activated microglia. We then performed cAMP level determination and ERK1/2 phosphorylation assays in resting and activated microglial cells. The functionality of AT_1R, AT_2R, and/or $AT_{1/2}$Hets in resting cells was very low. But in cAMP assays, pretreatment with candesartan potentiated AT_2R

induced signaling, and PD123319 potentiated AT_1R functionality (Fig. 5e, g). In contrast, the angiotensin-receptor-mediated signaling was more robust in LPS + IFN-γ activated cells (Fig. 5f, h). In cAMP assays, the agonist of the two receptors reduced the forskolin-induced levels of this second messenger, although receptor costimulation did not lead to any additive effect. As it occurred in HEK-293T cells and neuronal primary cultures, antagonist pretreatments potentiated the partner receptor signal. On the other hand, the agonist of any of the two receptors activated the MAPK signaling pathway, while simultaneous stimulation completely blunted the ERK1/2 phosphorylation effect in activated microglia. In this signaling pathway, antagonists blocked the cognate receptor and did not potentiate the activation of the partner receptor in the heteromer. Taken together, these results indicate that $AT_{1/2}$Hets are significantly expressed in activated microglia showing the same properties than those displayed in heterologous system.

Expression $AT_{1/2}$Hets in the striatum of parkinsonian and dyskinetic rats

Striatal sections of naïve and of 6-OH-dopamine hemilesioned rats, treated or not with L-DOPA and divided into L-DOPA/dyskinetic or resistant to L-DOPA-induced dyskinesia were prepared as described in methods. PLA assays were performed simultaneously and in identical conditions to detect the occurrence and the amount of $AT_{1/2}$Hets. A representative image of each of the conditions is shown in Fig. 6a–d, while quantitation is shown in the form of bar graph in Fig. 6e. Whereas the amount of $AT_{1/2}$Hets was negligible in the non-lesioned striatum, the lesioned one displayed more receptor clusters. L-DOPA/dyskinetic animals showed a two-fold increase if compared with the ipsilateral hemisphere of lesioned rats. Remarkably, animals resistant to L-DOPA-induced dyskinesia had a circa 10-fold increase in the amount of $AT_{1/2}$Hets (compared to control, non-lesioned hemisphere). These results show that, in this specific PD

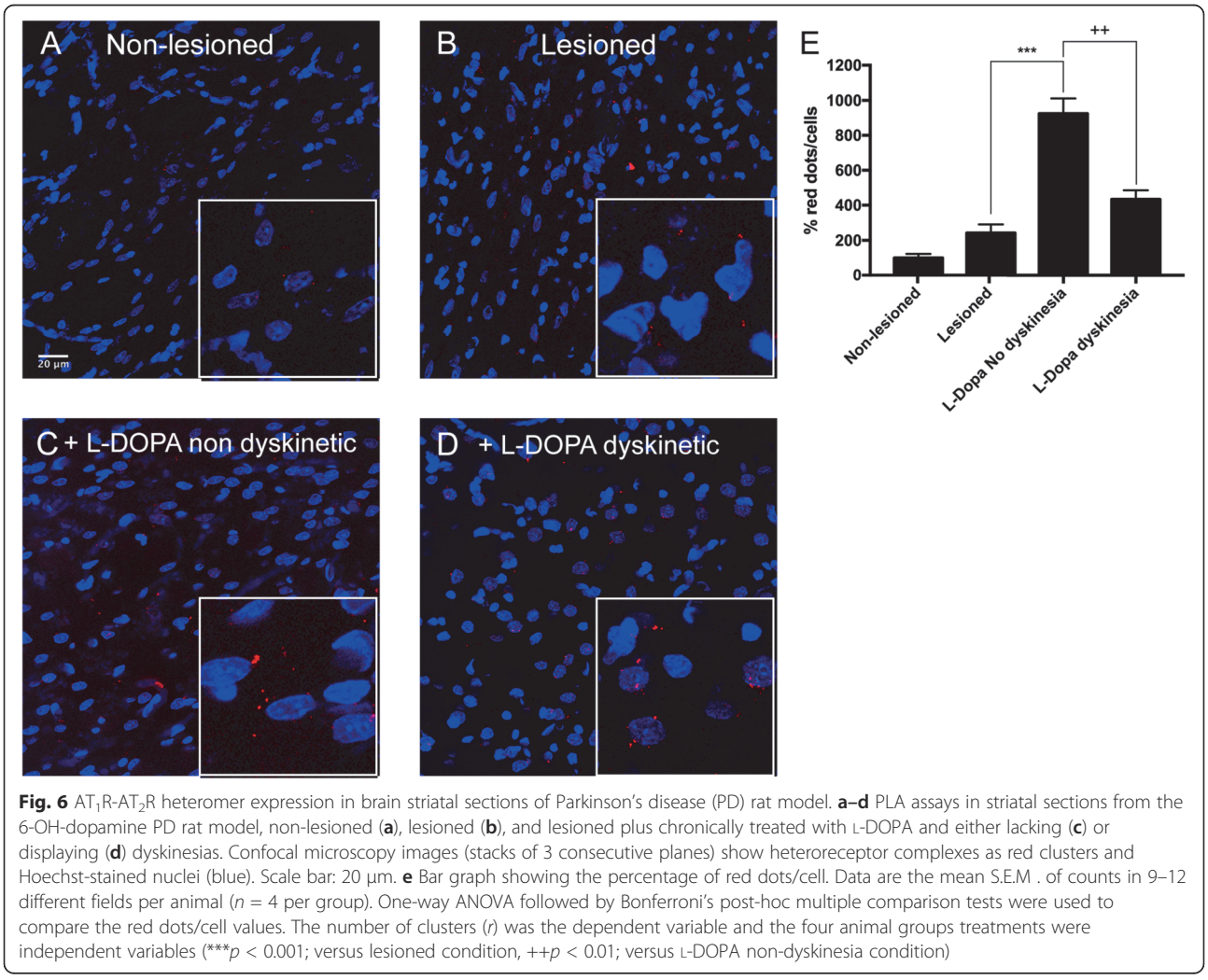

Fig. 6 AT_1R-AT_2R heteromer expression in brain striatal sections of Parkinson's disease (PD) rat model. **a–d** PLA assays in striatal sections from the 6-OH-dopamine PD rat model, non-lesioned (**a**), lesioned (**b**), and lesioned plus chronically treated with L-DOPA and either lacking (**c**) or displaying (**d**) dyskinesias. Confocal microscopy images (stacks of 3 consecutive planes) show heteroreceptor complexes as red clusters and Hoechst-stained nuclei (blue). Scale bar: 20 µm. **e** Bar graph showing the percentage of red dots/cell. Data are the mean S.E.M . of counts in 9–12 different fields per animal ($n = 4$ per group). One-way ANOVA followed by Bonferroni's post-hoc multiple comparison tests were used to compare the red dots/cell values. The number of clusters (r) was the dependent variable and the four animal groups treatments were independent variables (***$p < 0.001$; versus lesioned condition, ++$p < 0.01$; versus L-DOPA non-dyskinesia condition)

model, of maximal dopaminergic denervation similar to that observed in advanced stages of the disease, there is striatal expression of the heteromer that is increased upon L-DOPA administration. Remarkably, a much higher increase in expression was found in L-DOPA-treated animals that did not become dyskinetic.

Discussion

Details of peripheral RAS have been instrumental to develop a successful therapy to combat hypertension. The knowledge of RAS in the CNS is still fragmentary but with repercussions in dopaminergic neurotransmission and potential in PD and/or PD therapy-related dyskinesias. One of the added values of any future PD intervention based in central RAS is the safety of angiotensin receptor antagonists that have been used for decades in hypertensive patients. While no double-blind placebo controlled clinical trials have been designed, epidemiological studies addressing the risk of hypertensive patients taking angiotensin receptor antagonists have been performed. The fact that not all the drugs are able to cross the blood-brain barrier complicates data analysis. Anyhow, some of the reported results appear promising and using ß-blockers as a control and 65,001 hypertensive patients for > 4 years [34] showed that the use of certain antihypertensives (angiotensin receptor blockers included) associates with reduced PD risk. The still unsolved question is whether such drugs may be of benefit in improving symptoms, avoiding L-DOPA-induced dyskinesias and/or in delaying the progression of the disease.

First of all, it has been described that the global effects of angiotensin on AT_1 and AT_2 receptors are opposite. In several tissues, overactivity of the AT_1 receptor has been linked to aging-related pro-inflammatory changes ([16]; Labandeira-Garcia et al., [29, 30]). Different mechanisms have been proposed to explain counteracting effects of AT_2R on AT_1R signaling (see [43, 44], and [59] for review). Although the issue is complex, the expression of AT_2R in brain suggests a relevant role in the regulation of neuroinflammation. On the one hand, as earlier indicated, the two angiotensin receptors may interact leading to receptor heteromers with particular properties such as regulating SERCA activity [14, 48]. On the other hand, several heteromers formed by angiotensin receptors have been described. Among other examples [58], it has been reported that apelin and AT_1 receptors interact and that the resulting heteromers mediate the apelin inhibition of AT_1R-mediated actions. MAS protooncogene, the novel player in RAS research, rescues a defective AT_1R, likely by forming heterodimers [55]. The discovery of interaction between AT_1R and the most abundant receptor in the CNS, namely the cannabinoid CB_1 receptor, has led to hypothesize that these functional units may lead to pathogenic actions when Ang II is produced. However, the potential toxicity was studied in hepatic cells in relation to ethanol consumption but it was not assayed in neuronal cell models [53]. The AT_1R may form complexes with a variety of adrenergic receptors [4, 21], although their relevance to CNS physiology seems scarce. Less data are available for the AT_2R receptor that may interact (in the periphery) with MAS and with bradykinin B2 receptors [1, 35, 44, 63]. In addition, $AT_{1/2}$Hets may form dimers that may eventually interact with MAS or with bradykinin B2 receptors in cells in which three of these receptors are expressed together [10, 54]. One of the relevant results in this study is the demonstration in a rat model of microglial $AT_{1/2}$Hets expression and its upregulation correlating with PD and with ulterior treatment with L-DOPA, the most extended therapeutic agent in PD [9, 24, 42].

What is relevant for PD pathophysiology and disease progression is to delay the death of the approximately 30% nigral dopaminergic neurons that are left at the time of PD diagnosis. Glia in general, and microglia in what concerns to neuroinflammation, are key to preserve neurons from death. AT_1Rs have been proposed as targets to reduce chronic neuroinflammation [26, 27, 50] as that occurring in PD. The general idea is that activation of the AT_1R is detrimental, for instance by a microglia-mediated enhancement of neuronal loss in status epilepticus induced in rats [60]. In a previous study performed in the SN of rats we showed that angiotensin-induced Rho-kinase activation was involved in NADPH-oxidase activation, which, in turn, was involved in angiotensin-induced Rho-kinase activation [51]. In addition, a prevention of astrocyte activation and promotion of hippocampal neurogenesis has been attributed to AT_1R blockade and subsequent prevention of NFκB and MAP kinase signaling and activation of Wnt/β-catenin signaling [7]. In our experimental conditions performed with already activated striatal microglia, MAP kinase signaling is suppressed by combined treatment with AT_1 and AT_2 receptor agonists. In the retina, AT_1R activation results in regulating microglial activation thus suggesting that Ang II may have important implications in diabetic retinopathy [46]. To our knowledge, the expression of $AT_{1/2}$Hets in retinal cells has not been addressed yet. In agreement with the occurrence of a RAS opposite arm consisting of AT_2R (also of Mas receptor) (Labandeira-Garcia et al., [29, 30]), AT_2R activation attenuates microglial activation in an autoimmune encephalomyelitis rodent model [62]. Activation of the receptor is neuroprotective in a model of ischemia induced in conscious rats [37]. Similarly, the report by Bennion et al. [6] proves that AT_2R activation in neurons and glial cells affords long-term neuroprotection in stroke, by both direct and indirect mechanisms. Recent studies show that the receptor prevents/attenuates pro-inflammatory microglial activity

via protein phosphatase 2A-mediated inhibition of protein kinase C [8].

To our knowledge, the AT_1-bradikinin B2 heteroreceptor complex was the first to be associated to a peripheral-affecting disease. In fact, the expression of the heteromer was increased thus mediating a higher Ang responsiveness in preeclampsia, a disease that markedly alters blood pressure in pregnancy [2]. The heteromer physiological function involves diverse signaling pathways and a variety of cells events such as phosphorylation of c-Jun terminal kinase and enhanced production of nitric oxide and a second messenger, cGMP [1]. An unbalanced proportion of AT_1-bradikinin B2 receptor heteromers alters activation of cognate G-proteins and receptor desensitization [3, 64]. We have collected data on differential expression of dopamine-receptor-containing heteromers in PD and the conclusion is that very often the expression of heteromers is altered in one or different stages of the disease. Usually, the expression of those heteromers in dyskinesia is lower than in PD animals treated with L-DOPA but not displaying dyskinesias. Hence, this is the first example in which the already enhanced expression of heteromers in parkinsonian conditions is further increased in animals that were not rendered dyskinetic by L-DOPA treatment. These results are relevant as antagonists of angiotensin are considered as having potential to both improve PD symptoms and minimize L-DOPA-induced dyskinesias.

As in any other study focused on a neurodegenerative disease, there are a number of limitations. Among them we are extrapolating to "adult" cells using primary cells obtained from fetuses of neonates. Although this is a common procedure because the procedure of isolation of primary neural cells from adult animals is not optimized, a note of caution is needed. Another limitation of our study is the variety of neural cell types. It is a challenge to know the relative expression of receptors in projection neurons, in choline acetyltransferase (ChAT), parvalbumin (PV), calretinin (CR), or nitric oxide synthase interneurons and in astroglia and microglia, which may be at different degrees of activation depending on the disease status. Furthermore, receptor functionality in response to a given receptor ligand may vary from cell to cell [17] and at onset of disease when comparing naïve versus L-DOPA-treated individuals.

But in any case, pharmacological manipulation of RAS components presents potential in PD (Labandeira-Garcia et al., [29, 30]). One of the relevant findings in this paper is the insensitivity of AT_2R to agonist treatment of striatal neurons. Indeed, those neurons express both Ang receptor types as previously demonstrated [19]. However, it is more remarkable that it becomes functional in the presence of candesartan. There are few examples of similar findings and a recent one consists of progressive decrease of adenosine A_{2A} receptor functionality upon coexpression of another adenosine receptor, A_{2B}, and formation of A_{2A}/A_{2B} heteroreceptor complexes. This phenomenon is due to allosteric interprotomer interactions in the heteromer, i.e., the presence of one receptor blocks the signaling of the partner receptor in the complex [23]. Interestingly, the presence of an antagonist could make, as in the case of Ang receptor heteromers in striatal neurons, appear AT_2R functionality back. Therefore, AT_1R antagonists in these neurons may achieve two benefits, which are repressing the detrimental actions mediated by the AT_1R while making that the AT_2R becomes functional and provides the benefits associated to its activation. Furthermore, in terms of looking for interventions to prevent PD disease progression, there is enough information to agree that microglial cells may be key if there is a way to skew the physiology to acquire the M2 neuroprotective phenotype. On the one hand, neuronal alpha-synuclein produces an upregulation of AT_1R while increasing in microglia the proportion of pro-inflammatory M1 versus neuroprotective M2 markers; accordingly, it is suggested that antagonists already used in hypertension and able to cross the blood-brain barrier may be repurposed for the therapy of PD [52]. On the other hand, microglial AT_2Rs, constituent in $AT_{1/2}Hets$, show promise as (i) they are upregulated in both parkinsonian conditions and in L-DOPA-induced dyskinesias and (ii) their activation is seemingly neuroprotective. Remarkably, $AT_{1/2}Hets$ do not show cross-antagonism, a property displayed by many heteromers and that would lead to a therapeutic dead end in terms of neuroprotection; instead, the antagonist of one receptor releases the brake on activation of the partner receptor. Taken together, the opposite action of AT_1 and AT_2 receptors, their expression in microglia, and the marked upregulation of $AT_{1/2}Hets$ lacking cross-antagonism but displaying antagonist-mediated cross-potentiation suggest that interventions aimed at antagonizing central AT_1Rs to potentiate AT_2R-mediated actions may be beneficial in PD. Further experimental effort is required to identify the cell types expressing the heteromer in the different parkinsonian conditions and to prove the functionality of the heteromer in in vivo conditions, something that at present is technically challenging.

Conclusions

Main conclusions

The present study demonstrates that AT_1 and AT_2 receptors form $AT_1/_2Hets$ that are expressed in cells of the central nervous system. $AT_1/_2Hets$ are novel functional units with particular signaling properties. Importantly, the coactivation of the two receptors in the heteromer reduces the signaling output of angiotensin. Remarkably, $AT_1/_2Hets$, which are expressed in both striatal neurons and microglia, show a cross-potentiation, i.e., candesartan, the antagonist of AT_1 increases the effect of AT_2 receptor agonists. In

addition, the level of expression in the unilateral 6-OH-dopamine lesioned rat PD model increases upon L-DOPA treatment and is maximal in those animals that do not become dyskinetic.

Importance and relevance of the study reported

These findings reported are potentially important because they indicate that boosting the action of neuroprotective AT_2 receptors using an AT_1 receptor antagonist constitutes a promising therapeutic strategy in PD. The strategy may consist of designing AT_1R receptor antagonists able to readily cross the blood-brain barrier and effective in releasing the brake on the AT_2 receptor. The fact that SARS-CoV-2 uses angiotensin-converting enzyme 2 (ACE2) as receptor, that ACE2 interacts with angiotensin receptors, that some COVID-19 patients with severe symptoms display a "cytokine storm" driven by macrophages and/or suffer neurological alterations, adds interest to the present work on the RAS system in microglia.

Supplementary information

Supplementary information accompanies this paper at https://doi.org/10.1186/s12974-020-01908-z.

Additional file 1.

Abbreviations

6-hydroxy-DA: 6-Hydroxydopamine; AIMS: Abnormal involuntary movements; Ang: Angiotensin; Ang II: Angiotensin II; $AT_{1/2}$Hets: AT1-AT2 Heterodimers; BRET: Bioluminescence resonance energy transfer; BSA: Bovine Serum Albumin; cAMP: Cyclic adenylic acid; CAN: Candesartan; CGP: CGP-42112A; ChAT: Choline acetyltransferase; CNS: Central nervous system; CR: Calretinin; Cy3: Cyano 3; DA: Dopamine; DIV: Days in vitro; DMEM: Dulbecco's modified Eagle's medium; DMR: Dynamic mass redistribution; DMSO: Dimethyl sulfoxide; FBS: Fetal bovine serum; FK: Forskolin; HBSS: Hanks' balanced salt solution; HTRF: Homogeneous time resolved fluorescence; IFN-γ: Interferon-γ; L-DOPA: Levodopa; LPS: Lipopolysaccharide; MAPK: Mitogen-activated protein kinase; mBU: Milli bioluminescence resonance energy transfer units; NaCl: Sodium chloride; PBS: Phosphate-buffered saline; PD: Parkinson's disease; PEI: Polyethylenimine; PKA: Protein kinase A; PLA: Proximity ligation assays; PV: Parvalbumin; RAS: Renin-angiotensin system; Rluc: Renilla luciferase; SERCA: Sarco/endoplasmic reticulum Ca^{2+}-ATPase; SN: Substantia nigra; TR-FRET: Time-resolved fluorescence energy transfer; YFP: Yellow fluorescent protein

Acknowledgements

We acknowledge the excellent technical/logistic help provided by Jasmina Jiménez.

Authors' contributions

RF, GN, and JLL designed, supervised the work in the different laboratories, and validated the data in the manuscript. RRS and IRR performed biophysical, signaling, and immunohistochemical assays. RRS analyzed proximity ligation assay data. AM and AIRP did the lesions, characterized the different animal groups, and prepared brain sections. RF wrote the first draft that was edited first by GN and JLL and, subsequently, by all co-authors. The author(s) read and approved the final manuscript.

Funding

This work was supported by grants of the Spanish Ministry of Health (PI17/00828 and CIBERNED) and from the Spanish Ministry of Science, Innovation and Universities (RTI2018-098830-B-I00 and RTI2018-094204-B-I00; they include EU FEDER funds).

Availability of data and materials

All data are available upon request to the corresponding author(s).

Ethics approval and consent to participate

All animal experiments were carried out in accordance with EU directives (2010/63/EU and 86/609/CEE) and were approved by the Ethical committee of the University of Santiago de Compostela (#2016/0345) whose resolutions are supervised by regional and National regulatory bodies.

Consent for publication

Co-authors have acknowledged reception of the final version of the manuscript and concur with the submission.

Competing interests

The authors declare that they have no competing interests.

Author details

[1]Department of Biochemistry and Molecular Biomedicine, School of Biology, Universitat de Barcelona, Barcelona, Spain. [2]Centro de Investigación en Red, enfermedades Neurodegenerativas, CiberNed, Instituto de Salud Carlos III, Madrid, Spain. [3]Laboratory of Cellular and Molecular Neurobiology of Parkinson's disease, Research Center for Molecular Medicine and Chronic Diseases (CIMUS), Department of Morphological Sciences, IDIS, University of Santiago de Compostela, Santiago de Compostela, Spain. [4]Current adress: RG Neuroplasticity, Leibniz Institute for Neurobiology, 39118 Magdeburg, Germany. [5]Department of Biochemistry and Physiology, School of Pharmacy and Food Sciences, Universitat de Barcelona, Barcelona, Spain. [6]School of Chemistry, Universitat de Barcelona, Barcelona, Spain.

Received: 25 March 2020 Accepted: 21 July 2020
Published online: 17 August 2020

References

1. Abadir PM, Periasamy A, Carey RM, Siragy HM. Angiotensin II type 2 receptor–bradykinin B $_2$ receptor functional heterodimerization. Hypertension. 2006;48:316–22. https://doi.org/10.1161/01.HYP.0000228997.88162.a8.
2. AbdAlla S, Lother H, el Massiery A, Quitterer U. Increased AT1 receptor heterodimers in preeclampsia mediate enhanced angiotensin II responsiveness. Nat Med. 2001;7:1003–9. https://doi.org/10.1038/nm0901-1003.
3. AbdAlla S, Lother H, Quitterer U. AT1-receptor heterodimers show enhanced G-protein activation and altered receptor sequestration. Nature. 2000;407:94–8. https://doi.org/10.1038/35024095.
4. Barki-Harrington L, Luttrell LM, Rockman HA. Dual inhibition of β-adrenergic and angiotensin II receptors by a single antagonist. Circulation. 2003;108:1611–8. https://doi.org/10.1161/01.CIR.0000092166.30360.78.
5. Benito C, Núñez E, Tolón RM, Carrier EJ, Rábano A, Hillard CJ, Romero J. Cannabinoid CB2 receptors and fatty acid amide hydrolase are selectively overexpressed in neuritic plaque-associated glia in Alzheimer's disease brains. J Neurosci. 2003;23:11136–41.
6. Bennion DM, Isenberg JD, Harmel AT, DeMars K, Dang AN, Jones CH, Pignataro ME, Graham JT, Steckelings UM, Alexander JC, Febo M, Krause EG, de Kloet AD, Candelario-Jalil E, Sumners C. Post-stroke angiotensin II type 2 receptor activation provides long-term neuroprotection in aged rats. PLoS One. 2017;12:e0180738. https://doi.org/10.1371/journal.pone.0180738.
7. Bhat SA, Goel R, Shukla S, Shukla R, Hanif K. Angiotensin receptor blockade by inhibiting glial activation promotes hippocampal neurogenesis via activation of Wnt/β-catenin signaling in hypertension. Mol Neurobiol. 2018;55:5282–98. https://doi.org/10.1007/s12035-017-0754-5.
8. Bhat SA, Sood A, Shukla R, Hanif K. AT2R activation prevents microglia pro-inflammatory activation in a NOX-dependent manner: inhibition of PKC activation and p47 phox phosphorylation by PP2A. Mol Neurobiol. 2019;56:3005–23. https://doi.org/10.1007/s12035-018-1272-9.
9. Birkmayer W, Hornykiewicz O. Additional experimental studies on L-DOPA in Parkinson's syndrome and reserpine parkinsonism. Arch Psychiatr Nervenkr. 1964;206:367–81.
10. Cerrato BD, Carretero OA, Janic B, Grecco HE, Gironacci MM. Heteromerization between the bradykinin B2 receptor and the angiotensin-(1-7) mas receptor: functional consequences. Hypertens (Dallas, Tex. 1979). 2016;68:1039–48. https://doi.org/10.1161/HYPERTENSIONAHA.116.07874.

11. Chen T-W, Wardill TJ, Sun Y, Pulver SR, Renninger SL, Baohan A, Schreiter ER, Kerr RA, Orger MB, Jayaraman V, Looger LL, Svoboda K, Kim DS. Ultrasensitive fluorescent proteins for imaging neuronal activity. Nature. 2013;499:295–300. https://doi.org/10.1038/nature12354.
12. De Filippis D, Steardo A, D'Amico A, Scuderi C, Cipriano M, Esposito G, Iuvone T. Differential cannabinoid receptor expression during reactive gliosis: a possible implication for a nonpsychotropic neuroprotection. Sci World J. 2009;9:229–35. https://doi.org/10.1100/tsw.2009.31.
13. Farré D, Muñoz A, Moreno E, Reyes-Resina I, Canet-Pons J, Dopeso-Reyes IG, Rico AJ, Lluís C, Mallol J, Navarro G, Canela EI, Cortés A, Labandeira-García JL, Casadó V, Lanciego JL, Franco R. Stronger dopamine D1 receptor-mediated neurotransmission in dyskinesia. Mol Neurobiol. 2015;52:1408–20. https://doi.org/10.1007/s12035-014-8936-x.
14. Ferrão FM, Lara LS, Axelband F, Dias J, Carmona AK, Reis RI, Costa-Neto CM, Vieyra A, Lowe J. Exposure of luminal membranes of LLC-PK $_1$ cells to ANG II induces dimerization of AT $_1$ /AT $_2$ receptors to activate SERCA and to promote Ca $^{2+}$ mobilization. Am J Physiol Physiol. 2012;302:F875–83. https://doi.org/10.1152/ajprenal.00381.2011.
15. Ferré S, Baler R, Bouvier M, Caron MG, Devi LA, Durroux T, Fuxe K, George SR, Javitch JA, Lohse MJ, Mackie K, Milligan G, Pfleger KDG, Pin J-P, Volkow ND, Waldhoer M, Woods AS, Franco R. Building a new conceptual framework for receptor heteromers. Nat Chem Biol. 2009;5:131–4. https://doi.org/10.1038/nchembio0309-131.
16. Franceschi C, Bonafe M, Valensin S, Olivieri F, De Luca M, Ottaviani E, De Benedictis G. Inflamm-aging: an evolutionary perspective on immunosenescence. Ann N Y Acad Sci. 2006;908:244–54. https://doi.org/10.1111/j.1749-6632.2000.tb06651.x.
17. Franco R, Aguinaga D, Jiménez J, Lillo J, Martínez-Pinilla E, Navarro G. Biased receptor functionality versus biased agonism in G-protein-coupled receptors. Biomol Concepts. 2018;9:143–54. https://doi.org/10.1515/bmc-2018-0013.
18. Franco, R., Navarro, G., Rivas Santisteban, R., Awad Alkozi, H., 2019. Potency of melatonin at G-protein-coupled MT1 and MT2 receptors. Available at: osf.io/w7qxh.
19. Garrido-Gil P, Rodriguez-Perez AI, Fernandez-Rodriguez P, Lanciego JL, Labandeira-Garcia JL. Expression of angiotensinogen and receptors for angiotensin and prorenin in the rat and monkey striatal neurons and glial cells. Brain Struct Funct. 2017;222:2559–71. https://doi.org/10.1007/s00429-016-1357-z.
20. Garrido-Gil P, Valenzuela R, Villar-Cheda B, Lanciego JL, Labandeira-Garcia JL. Expression of angiotensinogen and receptors for angiotensin and prorenin in the monkey and human substantia nigra: an intracellular renin-angiotensin system in the nigra. Brain Struct Funct. 2013;218:373–88. https://doi.org/10.1007/s00429-012-0402-9.
21. González-Hernández MDL, Godínez-Hernández D, Bobadilla-Lugo RA, López-Sánchez P. Angiotensin-II type 1 receptor (AT1R) and alpha-1D adrenoceptor form a heterodimer during pregnancy-induced hypertension. Auton Autacoid Pharmacol. 2010;30:167–72. https://doi.org/10.1111/j.1474-8673.2009.00446.x.
22. Grammatopoulos TN, Jones SM, Ahmadi FA, Hoover BR, Snell LD, Skoch J, Jhaveri VV, Poczobutt AM, Weyhenmeyer JA, Zawada WM. Angiotensin type 1 receptor antagonist losartan, reduces MPTP-induced degeneration of dopaminergic neurons in substantia nigra. Mol Neurodegener. 2007;2:1. https://doi.org/10.1186/1750-1326-2-1.
23. Hinz S, Navarro G, Borroto-Escuela D, Seibt BF, Ammon C, De Filippo E, Danish A, Lacher SK, Červinková B, Rafehi M, Fuxe K, Schiedel AC, Franco R, Müller CE, Ammon YC, de Filippo E, Danish A, Lacher SK, Červinková B, Rafehi M, Fuxe K, Schiedel AC, Franco R, Müller CE, Ammon C, De Filippo E, Danish A, Lacher SK, Červinková B, Rafehi M, Fuxe K, Schiedel AC, Franco R, Müller CE. Adenosine A2A receptor ligand recognition and signaling is blocked by A2B receptors. Oncotarget. 2018;9:13593–611. https://doi.org/10.18632/oncotarget.24423.
24. Hornykiewicz O. The discovery of dopamine deficiency in the parkinsonian brain. J Neural Transm Suppl. 2006;70:9–15. https://doi.org/10.1007/978-3-211-45295-0_3.
25. Hradsky J, Mikhaylova M, Karpova A, Kreutz MR, Zuschratter W. Super-resolution microscopy of the neuronal calcium-binding proteins Calneuron-1 and Caldendrin. Methods Mol Biol. 2013;963:147–69. https://doi.org/10.1007/978-1-62703-230-8_10.
26. Jarrott B, Williams SJ. Chronic Brain Inflammation: The Neurochemical Basis for Drugs to Reduce Inflammation. Neurochem Res. 2016;41:523–33. https://doi.org/10.1007/s11064-015-1661-7.
27. Joglar B, Rodriguez-Pallares J, Rodriguez-Perez AI, Rey P, Guerra MJ, Labandeira-Garcia JL. The inflammatory response in the MPTP model of Parkinson's disease is mediated by brain angiotensin: relevance to progression of the disease. J Neurochem. 2009;109:656–69. https://doi.org/10.1111/j.1471-4159.2009.05999.x.
28. Kirik D, Winkler C, Björklund A. Growth and functional efficacy of intrastriatal nigral transplants depend on the extent of nigrostriatal degeneration. J Neurosci. 2001;21:2889–96.
29. Labandeira-Garcia JL, Rodríguez-Perez A, Garrido-Gil P, Rodriguez-Pallares J, Lanciego J, Guerra MJ. Brain Renin-Angiotensin System and Microglial Polarization: Implications for Aging and Neurodegeneration. Front Aging Neurosci. 2017b;9:129. https://doi.org/10.3389/fnagi.2017.00129.
30. Labandeira-Garcia JL, Costa-Besada MA, Labandeira CM, Villar-Cheda B, Rodríguez-Perez AI. Insulin-Like Growth Factor-1 and Neuroinflammation. Front Aging Neurosci. 2017a;9:365. https://doi.org/10.3389/fnagi.2017.00365.
31. Labandeira-Garcia JL, Rodriguez-Pallares J, Dominguez-Meijide A, Valenzuela R, Villar-Cheda B, Rodríguez-Perez AI. Dopamine-angiotensin interactions in the basal ganglia and their relevance for Parkinson's disease. Mov Disord. 2013;28:1337–42. https://doi.org/10.1002/mds.25614.
32. Law AMK, Yin JXM, Castillo L, Young AIJ, Piggin C, Rogers S, Caldon CE, Burgess A, Millar EKA, O'Toole SA, Gallego-Ortega D, Ormandy CJ, Oakes SR. Andy's Algorithms: new automated digital image analysis pipelines for FIJI. Sci Rep. 2017;7:15717. https://doi.org/10.1038/s41598-017-15885-6.
33. Lee CS, Cenci MA, Schulzer M, Björklund A. Embryonic ventral mesencephalic grafts improve levodopa-induced dyskinesia in a rat model of Parkinson's disease. Brain. 2000;123(Pt 7):1365–79. https://doi.org/10.1093/brain/123.7.1365.
34. Lee YC, Lin CH, Wu RM, Lin JW, Chang CH, Lai MS. Antihypertensive agents and risk of Parkinson's disease: A nationwide cohort study. PLoS One. 2014;9:e98961. https://doi.org/10.1371/journal.pone.0098961.
35. Leonhardt J, Villela DC, Teichmann A, Münter L-M, Mayer MC, Mardahl M, Kirsch S, Namsolleck P, Lucht K, Benz V, Alenina N, Daniell N, Horiuchi M, Iwai M, Multhaup G, Schülein R, Bader M, Santos RA, Unger T, Steckelings UM. Evidence for Heterodimerization and Functional Interaction of the Angiotensin Type 2 Receptor and the Receptor MASNovelty and Significance. Hypertension. 2017;69:1128–35. https://doi.org/10.1161/HYPERTENSIONAHA.116.08814.
36. Lundblad M, Andersson M, Winkler C, Kirik D, Wierup N, Cenci Nilsson MA. Pharmacological validation of behavioural measures of akinesia and dyskinesia in a rat model of Parkinson's disease. Eur J Neurosci. 2002;15:120–32. https://doi.org/10.1046/j.0953-816x.2001.01843.x.
37. McCarthy CA, Vinh A, Miller AA, Hallberg A, Alterman M, Callaway JK, Widdop RE. Direct angiotensin AT2 receptor stimulation using a novel AT2 receptor agonist, compound 21, evokes neuroprotection in conscious hypertensive rats. PLoS One. 2014;9:e95762. https://doi.org/10.1371/journal.pone.0095762.
38. Muñoz A, Garrido-Gil P, Dominguez-Meijide A, Labandeira-Garcia JL. Angiotensin type 1 receptor blockage reduces l-dopa-induced dyskinesia in the 6-OHDA model of Parkinson's disease. Involvement of vascular endothelial growth factor and interleukin-1?? Exp Neurol. 2014;261:720–32. https://doi.org/10.1016/j.expneurol.2014.08.019.
39. Navarro G, Borroto-Escuela D, Angelats E, Etayo I, Reyes-Resina I, Pulido-Salgado M, Rodríguez-Pérez AAI, Canela EIE, Saura J, Lanciego JJL, Labandeira-García JLJ, Saura CA, Fuxe K, Franco R. Receptor-heteromer mediated regulation of endocannabinoid signaling in activated microglia. Relevance for Alzheimer's disease and levo-dopa-induced dyskinesia. Brain Behav Immun. 2018;67:139–51. https://doi.org/10.1016/j.bbi.2017.08.015.
40. Newell EA, Exo JL, Verrier JD, Jackson TC, Gillespie DG, Janesko-Feldman K, Kochanek PM, Jackson EK. 2′,3′-cAMP, 3′-AMP, 2′-AMP and adenosine inhibit TNF-α and CXCL10 production from activated primary murine microglia via A2A receptors. Brain Res. 2015;1594:27–35. https://doi.org/10.1016/j.brainres.2014.10.059.
41. Ohlin KE, Sebastianutto I, Adkins CE, Lundblad C, Lockman PR, Cenci MA. Impact of L-DOPA treatment on regional cerebral blood flow and metabolism in the basal ganglia in a rat model of Parkinson's disease. Neuroimage. 2012;61:228–39. https://doi.org/10.1016/j.neuroimage.2012.02.066.
42. Olanow CW, Agid Y, Mizuno Y, Albanese A, Bonuccelli U, Bonucelli U, Damier P, De Yebenes J, Gershanik O, Guttman M, Grandas F, Hallett M, Hornykiewicz O, Jenner P, Katzenschlager R, Langston WJ, LeWitt P, Melamed E, Mena MA, Michel PP, Mytilineou C, Obeso JA, Poewe W, Quinn N, Raisman-Vozari R, Rajput AH, Rascol O, Sampaio C, Stocchi F. Levodopa in

the treatment of Parkinson's disease: current controversies. Mov Disord. 2004;19:997–1005. https://doi.org/10.1002/mds.20243.
43. Padia SH, Carey RM. AT2 receptors: beneficial counter-regulatory role in cardiovascular and renal function. Pflugers Arch. 2013;465:99–110. https://doi.org/10.1007/s00424-012-1146-3.
44. Patel S, Hussain T. Dimerization of AT2 and mas receptors in control of blood pressure. Curr Hypertens Rep. 2018;20:1–9. https://doi.org/10.1007/s11906-018-0845-3.
45. Perez-Lloret S, Otero-Losada M, Toblli JE, Capani F. Renin-angiotensin system as a potential target for new therapeutic approaches in Parkinson's disease. Expert Opin Investig Drugs. 2017;26:1163–73. https://doi.org/10.1080/13543784.2017.1371133.
46. Phipps JA, Vessey KA, Brandli A, Nag N, Tran MX, Jobling AI, Fletcher EL. The Role of Angiotensin II/AT1 Receptor Signaling in Regulating Retinal Microglial Activation. Investig Opthalmology Vis Sci. 2018;59:487. https://doi.org/10.1167/iovs.17-22416.
47. Pinna A, Bonaventura J, Farré D, Sánchez M, Simola N, Mallol J, Lluís C, Costa G, Baqi Y, Müller CE, Cortés A, McCormick P, Canela EI, Martínez-Pinilla E, Lanciego JL, Casadó V, Armentero M-TT, Franco R. l-DOPA disrupts adenosine A2A–cannabinoid CB1–dopamine D2 receptor heteromer cross-talk in the striatum of hemiparkinsonian rats: Biochemical and behavioral studies. Exp Neurol. 2014;253:180–91. https://doi.org/10.1016/j.expneurol.2013.12.021.
48. Porrello ER, Pfleger KDG, Seeber RM, Qian H, Oro C, Abogadie F, Delbridge LMD, Thomas WG. Heteromerization of angiotensin receptors changes trafficking and arrestin recruitment profiles. Cell Signal. 2011;23:1767–76. https://doi.org/10.1016/j.cellsig.2011.06.011.
49. Pulido-Salgado M, Vidal-Taboada JM, Garcia Diaz-Barriga G, Serratosa J, Valente T, Castillo P, Matalonga J, Straccia M, Canals JM, Valledor A, Solà C, Saura J. Myeloid C/EBPβ deficiency reshapes microglial gene expression and is protective in experimental autoimmune encephalomyelitis. J Neuroinflammation. 2017;14:54. https://doi.org/10.1186/s12974-017-0834-5.
50. Rodriguez-Pallares J, Rey P, Parga JA, Muñoz A, Guerra MJ, Labandeira-Garcia JL. Brain angiotensin enhances dopaminergic cell death via microglial activation and NADPH-derived ROS. Neurobiol Dis. 2008;31:58–73. https://doi.org/10.1016/j.nbd.2008.03.003.
51. Rodriguez-Perez AI, Borrajo A, Rodriguez-Pallares J, Guerra MJ, Labandeira-Garcia JL. Interaction between NADPH-oxidase and Rho-kinase in angiotensin II-induced microglial activation. Glia. 2015;63:466–82. https://doi.org/10.1002/glia.22765.
52. Rodriguez-Perez AI, Sucunza D, Pedrosa MA, Garrido-Gil P, Kulisevsky J, Lanciego JL, Labandeira-Garcia JL. Angiotensin Type 1 Receptor antagonists protect against alpha-synuclein-induced neuroinflammation and dopaminergic neuron death. Neurotherapeutics. 2018;15:1063–81. https://doi.org/10.1007/s13311-018-0646-z.
53. Rozenfeld R, Gupta A, Gagnidze K, Lim MP, Gomes I, Lee-Ramos D, Nieto N, Devi LA. AT1R-CB1 R heteromerization reveals a new mechanism for the pathogenic properties of angiotensin II. EMBO J. 2011;30:2350–63. https://doi.org/10.1038/emboj.2011.139.
54. Rubio-Ruíz ME, Del Valle-Mondragón L, Castrejón-Tellez V, Carreón-Torres E, Díaz-Díaz E, Guarner-Lans V. Angiotensin II and 1-7 during aging in Metabolic Syndrome rats. Expression of AT1, AT2 and Mas receptors in abdominal white adipose tissue. Peptides. 2014;57:101–8. https://doi.org/10.1016/j.peptides.2014.04.021.
55. Santos EL, Reis RI, Silva RG, Shimuta SI, Pecher C, Bascands JL, Schanstra JP, Oliveira L, Bader M, Paiva ACMM, Costa-Neto CM, Pesquero JB. Functional rescue of a defective angiotensin II AT1 receptor mutant by the Mas protooncogene. Regul Pept. 2007;141:159–67. https://doi.org/10.1016/j.regpep.2006.12.030.
56. Saura J, Tusell JM, Serratosa J. High-Yield Isolation of Murine Microglia by Mild Trypsinization. Glia. 2003;44:183–9. https://doi.org/10.1002/glia.10274.
57. Schallert T, Kozlowski DA, Humm JL, Cocke R. Use-dependent structural events in recovery of function. Adv Neurol. 1997;73:229–38.
58. Siddiquee K, Hampton J, McAnally D, May L, Smith L. The apelin receptor inhibits the angiotensin II type 1 receptor via allosteric trans-inhibition. Br J Pharmacol. 2013;168:1104–17. https://doi.org/10.1111/j.1476-5381.2012.02192.x.
59. Steckelings UM, Kaschina E, Unger T. The AT2 receptor--a matter of love and hate. Peptides. 2005;26:1401–9. https://doi.org/10.1016/j.peptides.2005.03.010.
60. Sun H, Wu H, Yu X, Zhang G, Zhang R, Zhan S, Wang H, Bu N, Ma X, Li Y. Angiotensin II and its receptor in activated microglia enhanced neuronal loss and cognitive impairment following pilocarpine-induced status epilepticus. Mol Cell Neurosci. 2015;65:58–67. https://doi.org/10.1016/j.mcn.2015.02.014.
61. Valenzuela R, Barroso-Chinea P, Villar-Cheda B, Joglar B, Muñoz A, Lanciego JL, Labandeira-Garcia JL. Location of prorenin receptors in primate substantia nigra: effects on dopaminergic cell death. J Neuropathol Exp Neurol. 2010;69:1130–42. https://doi.org/10.1097/NEN.0b013e3181fa0308.
62. Valero-Esquitino V, Lucht K, Namsolleck P, Monnet-Tschudi F, Stubbe T, Lucht F, Liu M, Ebner F, Brandt C, Danyel LA, Villela DC, Paulis L, Thoene-Reineke C, Dahlöf B, Hallberg A, Unger T, Sumners C, Steckelings UM. Direct angiotensin type 2 receptor (AT_2R) stimulation attenuates T-cell and microglia activation and prevents demyelination in experimental autoimmune encephalomyelitis in mice. Clin Sci. 2015;128:95–109. https://doi.org/10.1042/CS20130601.
63. Villela D, Leonhardt J, Patel N, Joseph J, Kirsch S, Hallberg A, Unger T, Bader M, Santos RA, Sumners C, Steckelings UM. Angiotensin type 2 receptor (AT 2 R) and receptor Mas: a complex liaison. Clin Sci. 2015;128:227–34. https://doi.org/10.1042/CS20130515.
64. Wilson PC, Lee M-H, Appleton KM, El-Shewy HM, Morinelli TA, Peterson YK, Luttrell LM, Jaffa AA. The arrestin-selective angiotensin AT_1 receptor agonist [Sar^1,Ile^4,Ile^8]-AngII negatively regulates bradykinin B_2 receptor signaling via AT_1-B_2 receptor heterodimers. J Biol Chem. 2013;288:18872–84. https://doi.org/10.1074/jbc.M113.472381.
65. Winkler C, Kirik D, Björklund A, Cenci MA. L-DOPA-induced dyskinesia in the intrastriatal 6-hydroxydopamine model of parkinson's disease: relation to motor and cellular parameters of nigrostriatal function. Neurobiol Dis. 2002;10:165–86. https://doi.org/10.1006/nbdi.2002.0499.

Publisher's Note

3.6 Novel Interactions Involving the Mas Receptor Show Potential of the Renin–Angiotensin system in the Regulation of Microglia Activation: Altered Expression in Parkinsonism and Dyskinesia.

Rafael Rivas-Santisteban, Jaume Lillo, Ana Muñoz, Ana I. Rodríguez-Pérez, José Luís Labandeira-García, Gemma Navarro y Rafael Franco.

Manuscrito publicado en *Neurotherapeutics*, Diciembre 2020; 20;1-19.

El sistema renina-angiotensina (RAS) no solo juega un papel importante en el control de la presión arterial, sino que también participa en casi todos los procesos para mantener la homeostasis en los mamíferos. La expresión de los componentes del RAS en los ganglios basales es un indicio que sugiere que la modulación mediada por el RAS puede mejorar la terapia de enfermedades neurodegenerativas. Los datos relacionados con el RAS llevaron a la hipótesis de que los receptores que componen este sistema pueden interactuar entre sí. El objetivo de este trabajo fue encontrar heterómeros formados por el receptor Mas y receptores de angiotensina y abordar su funcionalidad en neuronas y microglía de ratón. Se han descubierto nuevas interacciones heteroméricas entre AT_1R-MasR y AT_2R-MasR mediante el uso de técnicas de transferencia de energía por resonancia (BRET). La funcionalidad de los receptores individuales y formando complejos heteroméricos de receptores se ensayó detectando los niveles de los segundos mensajeros intracelulares AMPc y Ca^{2+} en células renales embrionarias humanas transfectadas (HEK-293T) y cultivos primarios de células estriatales de ratón. La expresión de los complejos heteroméricos AT_1R-MasR y AT_2R-MasR se analizó mediante los ensayos de ligación por proximidad (PLA) en secciones de cerebro de ratas parksonianas y discinéticas. La funcionalidad y expresión se ensayaron en paralelo en los cultivos primarios de microglía tratados o no con el lipopolisacárido y el interferón-γ (IFN-γ). Hemos demostrado que los tres receptores, MasR, AT_1R y AT_2R, pueden interactuar entre ellos para formar complejos heterotriméricos en un sistema heterólogo. Además, se observó que la expresión de los dímeros de receptores (AT_1R-MasR y AT_2R-MasR) es mayor en la microglía que en las neuronas y se ve afectada de manera diferencial por la activación de la microglía con lipopolisacárido e IFN-γ. En todos los casos, la señalización inducida por agonistas se redujo con la coactivación de ambos receptores y, en algunos casos, solo con la formación del complejo dimérico. Además, a menudo se observó que el tratamiento con el antagonista selectivo de uno de los receptores induce el bloqueo de la señalización de los dos receptores en un complejo, suceso que recibe el nombre de antagonismo cruzado. Los resultados obtenidos en esta investigación arrojan una nueva perspectiva de cómo se regulan entre sí los receptores del RAS. Además, los componentes de RAS en la microglía activada merecen atención de cara al desarrollo de fármacos para combatir la neurodegeneración.

Neurotherapeutics
https://doi.org/10.1007/s13311-020-00986-4

ORIGINAL ARTICLE

Novel Interactions Involving the Mas Receptor Show Potential of the Renin–Angiotensin system in the Regulation of Microglia Activation: Altered Expression in Parkinsonism and Dyskinesia

Rafael Rivas-Santisteban[1,2] · Jaume Lillo[1,2] · Ana Muñoz[2,3] · Ana I. Rodríguez-Pérez[2,3] · José Luís Labandeira-García[2,3] · Gemma Navarro[2,4] · Rafael Franco[1]

Accepted: 2 December 2020

Abstract

The renin–angiotensin system (RAS) not only plays an important role in controlling blood pressure but also participates in almost every process to maintain homeostasis in mammals. Interest has recently increased because SARS viruses use one RAS component (ACE2) as a target-cell receptor. The occurrence of RAS in the basal ganglia suggests that the system may be targeted to improve the therapy of neurodegenerative diseases. RAS-related data led to the hypothesis that RAS receptors may interact with each other. The aim of this paper was to find heteromers formed by Mas and angiotensin receptors and to address their functionality in neurons and microglia. Novel interactions were discovered by using resonance energy transfer techniques. The functionality of individual and interacting receptors was assayed by measuring levels of the second messengers cAMP and Ca^{2+} in transfected human embryonic kidney cells (HEK-293T) and primary cultures of striatal cells. Receptor complex expression was assayed by *in situ* proximity ligation assay. Functionality and expression were assayed in parallel in primary cultures of microglia treated or not with lipopolysaccharide and interferon-γ (IFN-γ). The proximity ligation assay was used to assess heteromer expression in parkinsonian and dyskinetic conditions. Complexes formed by Mas and the angiotensin AT_1 or AT_2 receptors were identified in both a heterologous expression system and in neural primary cultures. In the heterologous system, we showed that the three receptors—MasR, AT_1R, and AT_2R—can interact to form heterotrimers. The expression of receptor dimers (AT_1R-MasR or AT_2R-MasR) was higher in microglia than in neurons and was differentially affected upon microglial activation with lipopolysaccharide and IFN-γ. In all cases, agonist-induced signaling was reduced upon coactivation, and in some cases just by coexpression. Also, the blockade of signaling of two receptors in a complex by the action of a given (selective) receptor antagonist (cross-antagonism) was often observed. Differential expression of the complexes was observed in the striatum under parkinsonian conditions and especially in animals rendered dyskinetic by levodopa treatment. The negative modulation of calcium mobilization (mediated by AT_1R activation), the multiplicity of possibilities on RAS affecting the MAPK pathway, and the disbalanced expression of heteromers in dyskinesia yield new insight into the operation of the RAS system, how it becomes unbalanced, and how a disbalanced RAS can be rebalanced. Furthermore, RAS components in activated microglia warrant attention in drug-development approaches to address neurodegeneration.

Gemma Navarro and Rafael Franco contributed equally to this work.

✉ Rafael Franco
rfranco123@gmail.com; rfranco@ub.edu

[1] Department Biochemistry and Molecular Biomedicine, School of Biology, University of Barcelona, Diagonal 643, Barcelona, Catalonia 08028, Spain

[2] Centro de Investigación en Red, Enfermedades Neurodegenerativas (CIberNed), Instituto de Salud Carlos III, Valderrebollo 5, Madrid, Madrid 28031, Spain

[3] Laboratory of Cellular and Molecular Neurobiology of Parkinson's disease, Research Center for Molecular Medicine and Chronic Diseases (CIMUS), Department of Morphological Sciences, IDIS, University of Santiago de Compostela, Santiago de Compostela 15782, Spain

[4] Department of Biochemistry and Physiology, School of Pharmacy and Food Science, University of Barcelona, Barcelona, Catalonia 08028, Spain

Published online: 20 January 2021

Key Words Parkinson · microglia · Mas receptor · GPCR · angiotensin · angiotensin AT_1 receptor · angiotensin AT_2 receptor

Introduction

The renin–angiotensin system (RAS) has been widely studied for its role in controlling blood pressure. Protein components of RAS are angiotensin-converting enzyme 1 (ACE1), which produces angiotensin II (Ang II); angiotensin-converting enzyme 2 (ACE2), which converts Ang II to angiotensin 1–7 (Ang(1-7)); the Ang II receptors AT_1R and AT_2R; and the Ang(1-7) receptor Mas. For several decades, the balance between the prooxidative, proinflammatory, and the antioxidative, anti-inflammatory RAS arms was thought to be centered in the functional equilibrium of AT_1R and AT_2R. Now, the role of the ACE2/Mas receptor function has been revealed as a crucial element of RAS balance and RAS function. The Mas receptor (MasR) was identified as a product of an oncogene and, because of its resemblance to the mitochondrial assembly gene from *Saccharomyces cerevisiae*, it was first known as Mas-related proto-oncogene. All RAS receptors belong to the superfamily of G protein-coupled receptors (GPCRs). A novel family of RAS-related receptors are named Mas-related GPCRs (Mrgprs); they respond to Ang (1-7) but their endogenous agonist is one of the newest members of the RAS system, alamandine [1–5]. ACE2 is considered the canonical cell surface receptor for SARS-CoV-2, the virus that causes COVID-19. In fact, ACE2 was serendipitously identified as the receptor for viruses of the SARS family [6–10].

RAS has a relevant role in controlling neurotransmission in both the central and peripheral nervous systems. Identification of Ang II receptors in neural cells of the substantia nigra and other regions within the basal ganglia has uncovered novel therapeutic approaches to address neurodegeneration in Parkinson's disease (PD) and other synucleinopathies [11–18]. For obvious reasons, we must consider the brain RAS to understand the neurological manifestations of some patients infected with SARS-CoV-2. In fact, some cases of COVID-19 have neurological symptoms as diverse as encephalitis and seizures [19–21]. In some cases, the basal ganglia have been identified as mediating virus-induced central nervous system (CNS) alterations [13, 22, 23].

Although angiotensin I has little biological activity, ACE1 converts it into Ang II, the principal RAS effector, which activates AT_1R and AT_2R, whose actions in CNS development have been clearly delineated. However, in adults, the scenario is quite complex because AT_1R and AT_2R seemingly mediate opposite actions, whereas AT_1R activation usually leads to production of reactive oxygen species, activation of AT_2R counterbalances this noxious effect. In macrophages and microglia, AT_1R is thought to contribute to inflammation, whereas AT_2R attenuates inflammation and contributes to neuroprotection. These data reinforce the hypothesis that RAS balance is important in illnesses such as PD, which involves glial activation and neuroinflammation [14, 24–27]. MasR, whose endogenous agonist is Ang (1-7), adds complexity by mediating antioxidant and anti-inflammatory effects of AT_2R [24, 28]. In summary, RAS action in a given cell or brain circuit depends on peptide production by ACE1 and ACE2 and the expression of RAS receptors. Overall, the mechanisms underlying RAS balance in healthy conditions and RAS unbalance in aging [14] or disease remain unknown.

The physiological action of GPCRs is often mediated by heteromers; that is, by complexes having more than one receptor. Consensus is that receptor heteromers are novel functional units—their properties are different from those of the individually expressed receptors [29–31]. The first reported heteromer consisted of two GPCRs with the same endogenous agonist; namely, the μ-δ opioid receptor heteromer [32]. Further examples of heteromers formed by two receptors for the same endogenous ligand are adenosine A_1-A_{2A} and adenosine A_{2A}-A_{2B} receptors. In these cases, the presence and/or activation of one of the receptors blunts the response arising in the partner receptor, and structural information can explain how the trans blockade may happen [33–38]. Importantly, it has been reported that AT_1R and AT_2R and MasR and AT_2R form heteromers [39–41]. The aim of this study was to demonstrate the presence of Mas and AT_1/AT_2 receptor heterodimerization in neurons and microglia. The function of the MasR-AT_1R/AT_2R complexes in resting and activated microglia was investigated to complement our recent findings on AT_1R-AT_2R heteromer function in neural cells [42]. Importantly, we assessed the expression of heteroreceptor complexes in animal models of parkinsonian and dyskinesia. We focused on the striatum because of its relevance in PD. Our results provide a holistic model to understand RAS action, especially under conditions in which microglia become activated.

Materials and Methods

Reagents

Lipopolysaccharide (LPS), interferon-γ (IFN-γ), Ang II, CGP-42112A, Ang [1–7], candesartan, PD123319, and A779 were purchased from Sigma-Aldrich (St. Louis, MO, USA). Forskolin was purchased from Tocris (Bristol, UK). The concentrations of ligands used for signaling assays were selected on the basis of the dose–response experiments shown in Supplementary Figure S1.

Cell Culture

Human embryonic kidney (HEK-293T) cells were grown in Dulbecco's modified Eagle's medium (DMEM; Gibco/Thermo Fisher Scientific, Paisley, UK) supplemented with 2 mM L-glutamine, 100 μg/mL sodium pyruvate, 100 U/mL penicillin/streptomycin, MEM Non-Essential Amino Acids Solution (1/100) and 5% (v/v) heat-inactivated fetal bovine serum (FBS) (all supplements were from Invitrogen/Thermo Fisher Scientific, Paisley, UK). Cells were maintained at 37 °C in a humid atmosphere of 5% CO_2.

As mentioned in the "Introduction," in this study, we focused on brain striatum. To prepare mice striatal primary microglial cultures, the brain was removed from C57BL/6 mice at 2 to 4 days of age. Microglial cells were isolated as described in [43] and grown in DMEM supplemented with 2 mM L-glutamine, 100 U/mL penicillin/streptomycin, MEM non-essential amino acids preparation (1/100), and 5% (*v*/v) heat-inactivated FBS. Briefly, striatum tissue was dissected, carefully stripped of its meninges, and digested with 0.25% trypsin for 20 min at 37 °C. Digestion was stopped by washing the tissue. A cell suspension was prepared by passing the cells through a 100-μm pore mesh. Glial cells were resuspended in medium and seeded at a density of 1×10^6 cells/mL in 6-well plates for cyclic adenylic acid (cAMP) assays, in 12-well plates with coverslips for *in situ* proximity ligation assays (PLA), and in 96-well plates for mitogen-activated protein kinase (MAPK) experiments. Cultures were maintained at 37 °C in a humidified 5% CO_2 atmosphere, and unless otherwise stated, the medium was replaced once a week.

For neuronal primary cultures, the striatum from mouse embryos (E19) was removed and the neurons were isolated, as described by [44], and plated at a density of approximately 120,000 cells/cm^2. The cells were grown in a neurobasal medium supplemented with 2 mM L-glutamine, 100 U/mL penicillin/streptomycin, and 2% (v/v) B27 supplement (Gibco) in a 6-, 12-, or 96-well plate for 19 to 21 days. Cultures were maintained at 37 °C in a humidified 5% CO_2 atmosphere, and the medium was replaced every 4 to 5 days.

Immunodetection of specific markers (NeuN for neurons and CD-11b for microglia) showed that neuronal preparations contained > 98% neurons and that microglia preparations contained at least 98% microglial cells [45, 46]. Contamination by astrocytes was negligible; in our hands, the passage of the suspension through a syringe disrupts astroglial cells, and in addition, the culture medium used does not favor astrocyte survival (checked in every culture).

PD Model Generation, Levodopa Treatment, and Dyskinesia Assessment

All experiments were carried out in accordance with EU directives (2010/63/EU and 86/609/CEE) and were approved by the ethical committee of the University of Santiago de Compostela. Similar to the approach elsewhere described [47], our experimental design using male Wistar rats aimed to obtain four groups of animals as described below. Animals were 8 weeks old at the beginning of the experimental procedure.

Details of model generation and the protocol of drug administration and behavioral analysis, performed by a blinded investigator, are given elsewhere [48, 49]. Surgery was performed on rats anesthetized with ketamine/xylazine (1% ketamine, 75 mg/kg, and 2% xylazine, 10 mg/kg). Lesions were produced in the right medial forebrain bundle to achieve a complete degeneration of the nigrostriatal pathway. The rats were injected with 12 μg of 6-hydroxydopamine (6-OH-DA) (to provide 8 μg of 6-hydroxy-DA free base; Sigma-Aldrich) in 4 μL of sterile saline containing 0.2% ascorbic acid. These were considered "lesioned" animals. Injection of the vehicle led to the generation of naïve (or non-lesioned) animals.

The 6-OH-DA hemilesioned rat is considered a PD model. Amphetamine-induced rotation was tested in a bank of 8 automated rotometer bowls (Rota-count 8, Columbus Instruments, Columbus, OH, USA) by monitoring full (360°) body turns in either direction. Right and left full body turns were recorded over 90 min following an injection of D-amphetamine (2.5 mg/kg i.p.) dissolved in saline. Rats that displayed more than 6 full body turns/min ipsilateral to the lesion were included in the study (this rate would correspond to > 90% depletion of dopamine fibers in the striatum [50]).

Spontaneous use of forelimb can be measured by the cylinder test [51, 52]. Rats were placed individually in a glass cylinder (20 cm in diameter) and the number of left or right forepaw contacts was scored by an observer blinded to the animals' identity and presented as left (impaired) touches as a percentage of total touches. A control animal would thus receive an unbiased score of 50%, whereas the lesion usually reduces the performance of the impaired paw to less than 20% of total wall contacts.

Of the lesioned animals displaying parkinsonism-like behavior according to the above described tests (18 in total), 12 were chronically treated with L-DOPA daily for 3 weeks. A mixture of L-DOPA methyl ester (6 mg/kg) plus benserazide (10 mg/kg) was administered subcutaneously. The treatment reliably induces dyskinetic movements in some rats. As described in a previous report [47], abnormal involuntary movements were evaluated according to the rat dyskinesia scale described in detail elsewhere [48, 53–56]. The severity of each abnormal involuntary movement (AIM) subtype (limb, orolingual, and axial) was assessed using scores from 0 to 4 (1 = occasional, present < 50% of the time; 2 = frequent, present > 50% of the time; 3 = continuous but interrupted by strong sensory stimuli; 4 = continuous, not interrupted by strong sensory stimuli). Rats were classified as "dyskinetic" if

they displayed a score ≥2 per monitoring period on at least two AIM subtypes. Animals classified as "non-dyskinetic" exhibited either no L-DOPA-induced abnormal involuntary movements or very mild/occasional ones [57]. Animals with low scores, either non-dyskinetic or dyskinetic, were excluded. In summary, four groups of animals were obtained: [1] non-lesioned; [2] lesioned, treated with vehicle; [3] lesioned and became dyskinetic when treated with L-DOPA; and [4] lesioned and did not become dyskinetic upon L-DOPA treatment. Tyrosine hydroxylase immunostaining was performed in every animal from sections taken postmortem [18, 49]; selected animals undergoing 6-OH-DA treatment showed, in the lesioned hemisphere, >95% nigral dopaminergic denervation. Overall, 4 animals (those with better scores) were selected in each of the following 4 groups: naïve, lesioned, lesioned/L-DOPA dyskinetic, and lesioned/L-DOPA non-dyskinetic. The PLA analysis (see below) was performed in different fields of striatal sections from each of the 16 selected animals. The striatum was delimited in sections using a bright field, and images were captured within delimitation coordinates.

Fusion proteins

Human cDNAs for AT_1, AT_2, Mas, and σ_1 receptors cloned into pcDNA3.1 were amplified without their stop codons using sense and antisense primers harboring either BamHI and HindIII restriction sites to amplify AT_1R and AT_2R or with BamHI and EcoRI restriction sites to amplify Mas and σ_1 receptors. Amplified fragments were then subcloned to be in frame with an enhanced yellow fluorescent protein (pEYFP-N1; Clontech, Heidelberg, Germany) or a Rluc (pRluc-N1; PerkinElmer, Wellesley, MA) on the C-terminal end of the receptor to produce AT_1R-YFP, AT_1R-Rluc, AT_2R-YFP, Mas-YFP, Mas-Rluc, and σ_1R-Rluc fusion proteins.

Cell Transfection

HEK-293T cells were transiently transfected with the corresponding cDNA by means of the poly-ethylenimine (PEI; Sigma-Aldrich) method, as previously described [58]. Briefly, the corresponding cDNA diluted in 150 mM NaCl was mixed with PEI (5.5 mM in nitrogen residues) also prepared in 150 mM NaCl for 10 min. The cDNA-PEI complexes were transferred to HEK-293T cells, which were incubated for 4 h in serum-starved medium. Then, the medium was replaced by fresh supplemented culture medium and cells were maintained at 37 °C in a humid atmosphere of 5% CO_2. Forty-eight hours after transfection, cells were washed, detached, and resuspended in the assay buffer.

Immunocytochemistry

HEK-293T cells were seeded on glass coverslips in 12-well plates. After 24 h of culture, cells were transfected with AT_1R-YFP cDNA (1 μg) and Mas-Rluc cDNA (1 μg) or with AT_2R-Rluc cDNA (1 μg) and Mas-Rluc cDNA (1 μg). Forty-eight hours later, cells were fixed in 4% paraformaldehyde for 15 min and washed twice with PBS containing 20 mM glycine before permeabilization with PBS-glycine containing 0.2% Triton X-100 (5 min incubation). A blocking solution consisting of PBS containing 1% bovine serum albumin was added (1 h). HEK-293T cells were then labeled with a mouse anti-Rluc antibody (1/100; Millipore, Darmstadt, Germany) and subsequently treated with Cy3-conjugated anti-mouse (1/200; Jackson ImmunoResearch, West Grove, PA, USA; red) antibody (1 h each). The expression of Mas-YFP and AT_2R-YFP was detected by their YFP fluorescence. Nuclei were stained with Hoechst (1/100 from 1 mg/mL stock; Sigma-Aldrich). Samples were washed several times and mounted with 30% Mowiol (Calbiochem, Merck, Darmstadt, Germany). Images were obtained in a Zeiss LSM 880 confocal microscope (Zeiss, Jena, Germany) with a × 63 oil objective.

Bioluminescence Resonance Energy Transfer Assay

HEK-293T cells were transiently cotransfected with a constant amount of cDNA encoding Mas-Rluc (0.75 μg) and with increasing amounts of cDNAs corresponding to AT_1R-YFP (0.5 to 2.5 μg) or AT_2R-YFP (0.5 to 3 μg). When indicated cDNA coding for AT_1R fused to Rluc was used. For negative control, HEK-293T cells were transiently cotransfected with a constant amount of cDNA encoding σ_1-Rluc (0.75 μg) and with increasing amounts of cDNA corresponding to AT_2R-YFP (0.5 to 3 μg). To control the cell number, sample protein concentration was determined using a Bradford assay kit (Bio-Rad, Munich, Germany) using bovine serum albumin (BSA) dilutions as standards. To quantify fluorescent proteins, cells (20 μg of total protein) were distributed in 96-well microplates (black plates with transparent bottoms) and fluorescence was read in a Fluostar Optima Fluorimeter (BMG Labtech, Offenburg, Germany) equipped with a high-energy xenon flash lamp, using a 10-nm bandwidth excitation filter at 485 nm. For bioluminescence resonance energy transfer (BRET) measurements, the equivalent of 20 μg of total protein cell suspension was distributed in 96-well white microplates with white bottoms (Corning 3600; Corning Inc., Corning, NY, USA). BRET was determined 1 min after adding coelenterazine H (Molecular Probes, Eugene, OR), using a Mithras LB 940 reader (DLReady, Berthold Technologies, Bad Wildbad, Germany), which allows the integration of the signals detected in the short-wavelength filter at 485 nm and the long-wavelength filter at 530 nm. To quantify Mas-Rluc expression, luminescence readings were

obtained 10 min after the addition of 5 μM coelenterazine H. MilliBRET units (mBU) are defined as follows:

$$\mathrm{mBU} = \left[\frac{\lambda_{530}(\text{long-wavelength emission})}{\lambda_{485}(\text{short-wavelength emission})} - C_f\right] \times 1000$$

in which C_f corresponds to [(long-wavelength emission)/(short-wavelength emission)] for the Rluc construct expressed alone in the same experiment.

Sequential BRET-FRET Assay

HEK-293T cells were transiently cotransfected with a constant amount of cDNA for MasR-Rluc (0.6 μg) and for AT_1R-GFP^2 (1 μg) and increasing amounts of cDNA for AT_2R-YFP (0.5 to 4.1 μg). For the negative control, HEK-293T cells were transiently cotransfected with a constant amount of σ_1R-Rluc (0.3 μg) and AT_1R-GFP^2 (1 μg) and increasing amounts of cDNA for AT_2R-YFP (0.5 to 4.1 μg). To control the cell number, sample protein concentration was determined using a Bradford assay kit (Bio-Rad) using BSA dilutions as standards and adjusted to 0.2 mg/mL. To quantify fluorescent proteins, cells (20 μg of total protein) were distributed in 96-well microplates (black plates with transparent bottoms) and fluorescence was read in a Fluostar Optima Fluorimeter (BMG Labtech) equipped with a high-energy xenon flash lamp, using a 10-nm bandwidth excitation filter with a 485-nm excitation filter for YFP or 410-nm excitation filter for GFP^2. For SRET measurements, the equivalent of 20 μg of total protein cell suspension was distributed in 96-well white microplates (Corning 3600). SRET was determined 30 s after the addition of Deepblue C (5 μM) (Molecular Probes), using a Mithras LB 940 reader (Berthold Technologies), which allows the integration of the signals detected in the short-wavelength filter at 400 nm and the long-wavelength filter at 530 nm. To quantify MasR-Rluc or σ_1R-Rluc expression, luminescence readings were obtained 10 min after the addition of 5 μM coelenterazine H.

Assessment of Cytoplasmic Calcium Ion Levels

HEK-293T cells were cotransfected with the cDNAs for AT_1 (1 μg) and/or AT_2 (1 μg), and/or MasR (1 μg) and/or the GCaMP6 calcium sensor (1 μg) [59] by the use of PEI method, as described above. Forty-eight hours after transfection, HEK-293T cells plated in 6-well plates (black, clear-bottomed) were incubated with Mg^{2+}-free Locke's buffer (154 mM NaCl, 5.6 mM KCl, 3.6 mM $NaHCO_3$, 2.3 mM $CaCl_2$, 5.6 mM glucose, 5 mM HEPES, 10 μM glycine, pH 7.4). Receptor antagonists were added 10 min before readings and receptor agonists were added a few seconds before readings. Fluorescence emission intensity of GCaMP6 was recorded at 515 nm upon excitation at 488 nm on an EnSpire Multimode Plate Reader (PerkinElmer, Waltham, MA, USA) for 150 s every 5 s at 100 flashes per well.

Determination of cAMP Level

The analysis of cAMP levels in primary neural cells or in transfected HEK-293T was performed using the Lance® Ultra cAMP kit (PerkinElmer). Two hours before the experiment, cells were placed in serum-starved DMEM. Cells growing in the medium containing 50 μM zardaverine were distributed in 384-well microplates (2000 HEK-293T cells or 4000 striatal neurons or microglial cells per well) and pretreated with the AT_1R, AT_2R, and MasR antagonists candesartan, PD123319, and A779, respectively, or with the vehicle at room temperature for 15 min, and then stimulated with the AT_1R, AT_2R, and MasR agonists Ang II, CGP-42112A, and Ang(1-7), respectively, for 15 min before adding 0.5 μM forskolin or vehicle for an additional 15 min. Homogeneous time-resolved fluorescence energy transfer (HTRF) measures were performed using the Lance® Ultra cAMP kit (PerkinElmer). Fluorescence at 665 nm was measured on a PHERAstar Flagship microplate reader equipped with an HTRF optical module (BMG Labtech). A standard curve for (cAMP) was obtained in each experiment.

Extracellular Signal-Regulated Kinases 1/2 Phosphorylation

To determine ERK1/2 phosphorylation, 40,000 HEK-293T cells expressing MasR and either AT_1R or AT_2R, or 50,000 striatal neurons, or microglial primary cultures were plated in transparent Deltalab 96-well microplates. Two hours before the experiment, the medium was substituted with serum-starved DMEM. Cells were treated or not for 10 min with the selective antagonists (300 nM candesartan, 1 μM PD123319, or 500 nM A779) followed by 7-min treatment with the selective agonists (Ang II, CGP-42112A, or Ang(1-7). Cells were then washed twice with cold PBS before the addition of lysis buffer (15-min treatment). Ten microliters of each supernatant was placed in white ProxiPlate 384-well microplates, and ERK1/2 phosphorylation was determined using an AlphaScreen SureFire kit (PerkinElmer) following the instructions of the supplier and using an EnSpire Multimode Plate Reader (PerkinElmer).

Dynamic Mass-Redistribution Label-Free Assays

Cell signaling was explored using an EnSpire Multimode Plate Reader (PerkinElmer) by using label-free technology. Cellular cytoskeleton redistribution movement induced upon receptor activation was detected by illuminating the underside of the plate with polychromatic light and measured as changes in the wavelength of the reflected monochromatic light, which

is a sensitive function of the index of refraction. The magnitude of this wavelength shift (in picometers) is directly proportional to the amount of dynamic mass-redistribution (DMR). To determine the label-free DMR signal, 10,000 HEK-293T cells cotransfected with cDNAs for AT_1R (1 μg) or AT_2R (1 μg) and MasR or 10,000 striatal neuronal or microglial primary cultures cells were plated on transparent 384-well fibronectin-coated microplates to obtain 70 to 80% confluent monolayers, and kept in the incubator for 24 h. Before the assay, cells were washed twice with assay buffer (Hanks' balanced salt solution with 20 mM HEPES, pH 7.15, 0.1% dimethyl sulfoxide) and incubated in the reader for 2 h in 30 μL/well of assay buffer at 24 °C. Then, the sensor plate was scanned and a baseline optical signature was recorded for 10 min before adding 10 μL of test antagonist (candesartan, PD123319, or A779) dissolved in assay buffer, followed by the addition of 10 μL of selective agonist (Ang II, CGP-42112A, or Ang(1-7)) also dissolved in assay buffer. The DMR responses induced by the agonist were monitored for a minimum of 3600 s.

Proximity Ligation Assay

Detection in natural sources of clusters formed by AT_1 and Mas receptors or AT_2 and Mas receptors was addressed in primary cultures of microglia or striatal neurons and in brain sections. Cells grown on glass coverslips were fixed in 4% paraformaldehyde for 15 min, washed twice with PBS containing 20 mM glycine to quench the aldehyde groups, permeabilized with the same buffer containing 0.05% Triton X-100 for 5 to 15 min, and washed with PBS. After a 1-h incubation at 37 °C with the blocking solution in a preheated humidity chamber, samples were incubated overnight at 4 °C with a mixture of a rabbit monoclonal anti-AT_1R antibody (1/100, ab124734, Abcam, Cambridge, UK) and a mouse monoclonal anti-MasR antibody (1/100, sc-390453, Santa Cruz Biotechnology, Santa Cruz, CA, USA) or a mixture of a rabbit monoclonal anti-AT_2R antibody (1/100, ab92445, Abcam) and the mouse monoclonal anti-MasR antibody (1/100, sc-390453, Santa Cruz Biotechnology). Nuclei were stained with Hoechst (1/100 from 1 mg/mL stock; Sigma-Aldrich). The antibodies were validated following the method in the technical brochure of the vendor and also by immunofluorescence in HEK-293T cells (transfected *vs* non-transfected). Cells were further processed using PLA probes detecting primary antibodies (Duolink In Situ PLA probe anti-mouse plus and Duolink In Situ PLA probe Anti-Rabbit minus; all probes from Sigma-Aldrich) (1/5 v:v for 1 h at 37 °C). Ligation and amplification were done as indicated by the supplier (Sigma-Aldrich), and cells were mounted using the mounting medium 30% Mowiol (Calbiochem, Merck). To detect red dots corresponding to AT_1-MasHets or AT_2-MasHets, samples were observed in a Zeiss LSM 880 confocal microscope equipped with an apochromatic 63× oil-immersion objective, and 405- and 561-nm laser lines. For each field of view, a stack of 2 channels (one per staining) and 3 *Z*-planes with a step size of 1 μm were acquired. Andy's algorithm, a specific ImageJ (National Institutes of Health, Bethesda, MD, USA) macro for reproducible and high-throughput quantification of the total PLA foci dots and total nuclei, was used for data analysis [60].

The specificity of antibodies against angiotensin receptors has been questioned, even though different laboratories have reported excellent performance of different antibodies see [58–61]. All antibodies used in this study were monoclonal; however, to check the specificity of the antibodies used, we performed experiments in HEK-293T cells, either non-transfected or expressing AT_1R or AT_2R. Signal was negligible in AT_2R-expressing cells and non-transfected cells when the anti-AT_1R antibody was used and negligible in AT_1R-expressing cells and non-transfected cells when the anti-AT_2R antibody was used (Supplementary Figure S2). These results confirm the antibody specificity as previously reported [62].

Data Analysis

All data were obtained from at least five independent experiments and are expressed as the mean ± standard error of the mean (SEM). GraphPad Prism 8 software (GraphPad Inc., San Diego, CA, USA) was used for data fitting and statistical analysis. One-way ANOVA and post hoc Bonferroni's test were used when comparing multiple values. When a pair of values was compared, Student's *t* test was used. Significant differences were considered when the p value was < 0.05.

Results

The Mas Receptor Physically Interacts with AT_1 or AT_2 Receptors

Colocalization of MasR with AT_1R or AT_2R was first addressed using a heterologous expression system. Immunocytochemical assays performed in HEK-293T cells transfected with cDNAs encoding MasR fused to YFP and AT_1 fused to Rluc (Fig. 1A–C) indicated a marked degree of colocalization (yellow in Fig. 1C). A lower degree of colocalization was observed after immunocytochemical assays performed in HEK-293T cells transfected with cDNAs encoding MasR fused to Rluc and AT_2R fused to YFP (Fig. 1D–F). In those experiments, red fluorescence was due to a secondary Cy3-conjugated antibody, whereas green fluorescence was due to YFP (see "Materials and Methods"); colocalization can be observed by yellow in the merged image. It should be noted that the images are taken near the glass

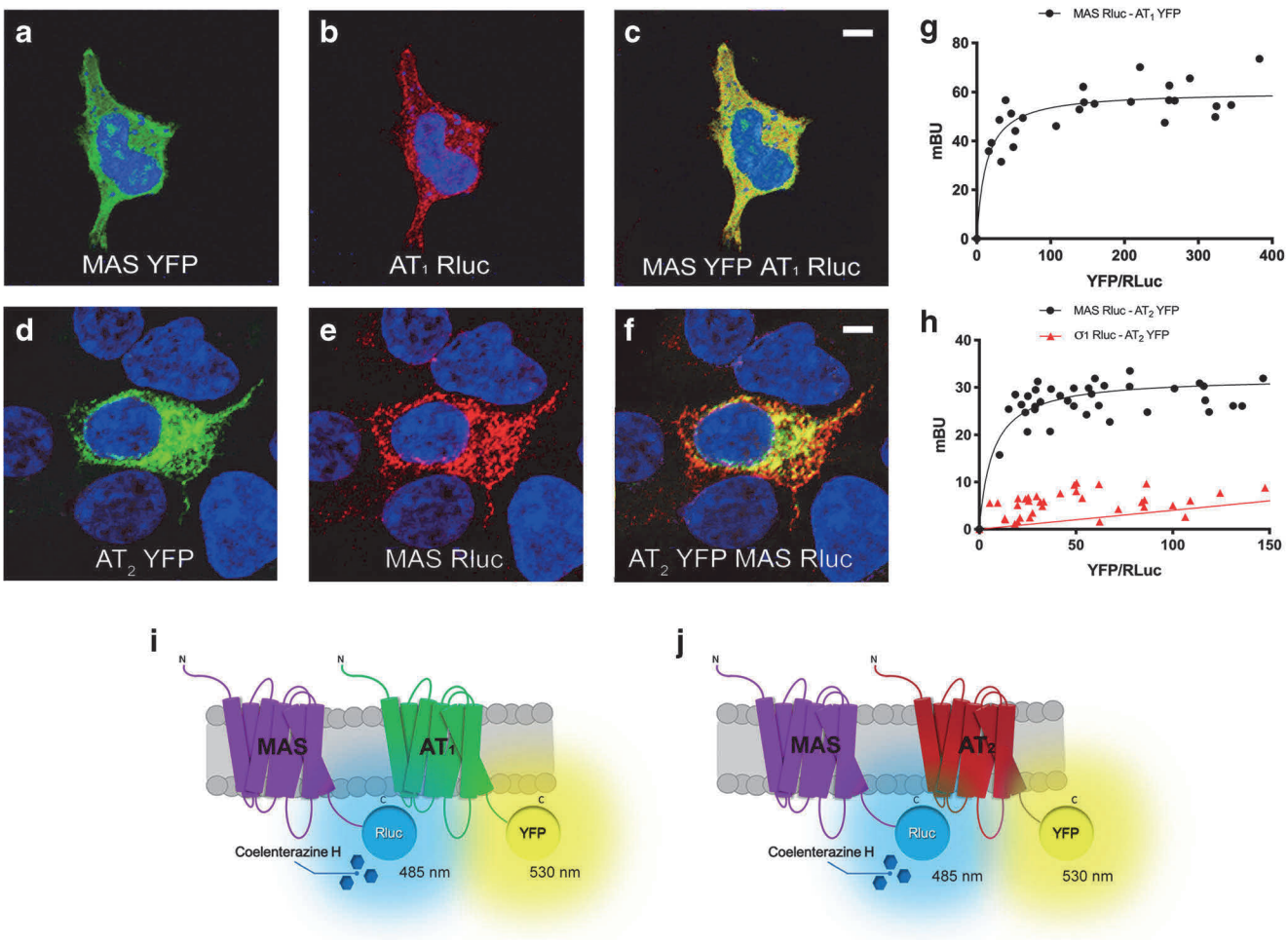

Fig. 1 Human AT_1 and AT_2 receptors interact with Mas receptor (MasR) in transfected HEK-293T cells. Immunocytochemistry assays were performed in HEK-293T cells expressing Mas-YFP and AT_1-Rluc receptors (1 μg of cDNA each) (**A**–**C**), or Mas-Rluc and AT_2R-YFP (1 μg of cDNA each) (**D**–**F**). Images were taken using a Zeiss 880 confocal microscope. Receptors fused to YFP were detected by yellow fluorescence (green), and receptors fused to Rluc were detected by a mouse anti-Rluc antibody and a secondary Cy3 anti-mouse antibody (red). Colocalization is shown in yellow. Cell nuclei were stained with Hoechst (blue). Scale bar: 2 μm. **G**, **H** BRET assays were performed in HEK-293T cells transfected with a constant amount of cDNA for Mas-Rluc (0.75 μg) or σ_1R-Rluc (0.75 μg) (as negative control) and increasing amounts of cDNA for AT_1R-YFP (0.5 to 2.5 μg) or AT_2R-YFP (0.5 to 3 μg). Values are the mean ± SEM of 8 independent experiments performed in duplicates. **I**, **J** Schematic representation of BRET assays: energy transfer and fluorescence emission at 530 nM only occurs if the BRET donor (Rluc) and the BRET acceptor (YFP) are close

surface, that is, most of the labeling was due to proteins in the cell membrane proximal to the slide.

Immunocytochemistry assays do not demonstrate physical interactions because they occur within distances of 200 nm. Thus, we addressed potential interactions using BRET in HEK-293T cells expressing a constant amount of MasR-Rluc and increasing amounts of AT_1R-YFP. The saturable BRET curve ($BRET_{max}$ 60 ± 2 mBU; $BRET_{50}$ 13 ± 4 mBU) indicates specific interactions between Mas and AT_1 receptors (Fig. 1G). A saturable curve was obtained when a similar experiment was carried out in HEK-293T cells expressing a constant amount of MasR-Rluc and increasing amounts of AT_2R-YFP ($BRET_{max}$ 32 ± 1; $BRET_{50}$ 7 ± 2), indicating that the two receptors do physically interact in living cells (Fig. 1H), confirming the results previously reported in HEK-293T cells using fluorescence resonance energy transfer and cross-correlation spectroscopy [40]. In contrast, experiments in cells coexpressing σ_1R-Rluc and AT_2-YFP showed a linear non-specific signal (negative control in Fig. 1H).

We addressed the potential formation of trimers by taking advantage of the sequential resonance energy transfer (SRET; [63]) technique using cells expressing MasR-Rluc, AT_1R-GFP^2, and AT_2R-YFP. The saturable curve, which was not detected in the negative control (σ_1R-Rluc, AT_1R-GFP^2, and AT_2R-YFP), indicated that the three RAS receptors interacted in a heterologous system, forming trimers (Fig. 2A). Trimer formation led to a structural rearrangement; in fact, increased expression of MasR led to a higher BRET signal due to the AT_1R-Rluc and AT_2R-YFP pair. These results are consistent with the reduced distance between Rluc fused to AT_1R and

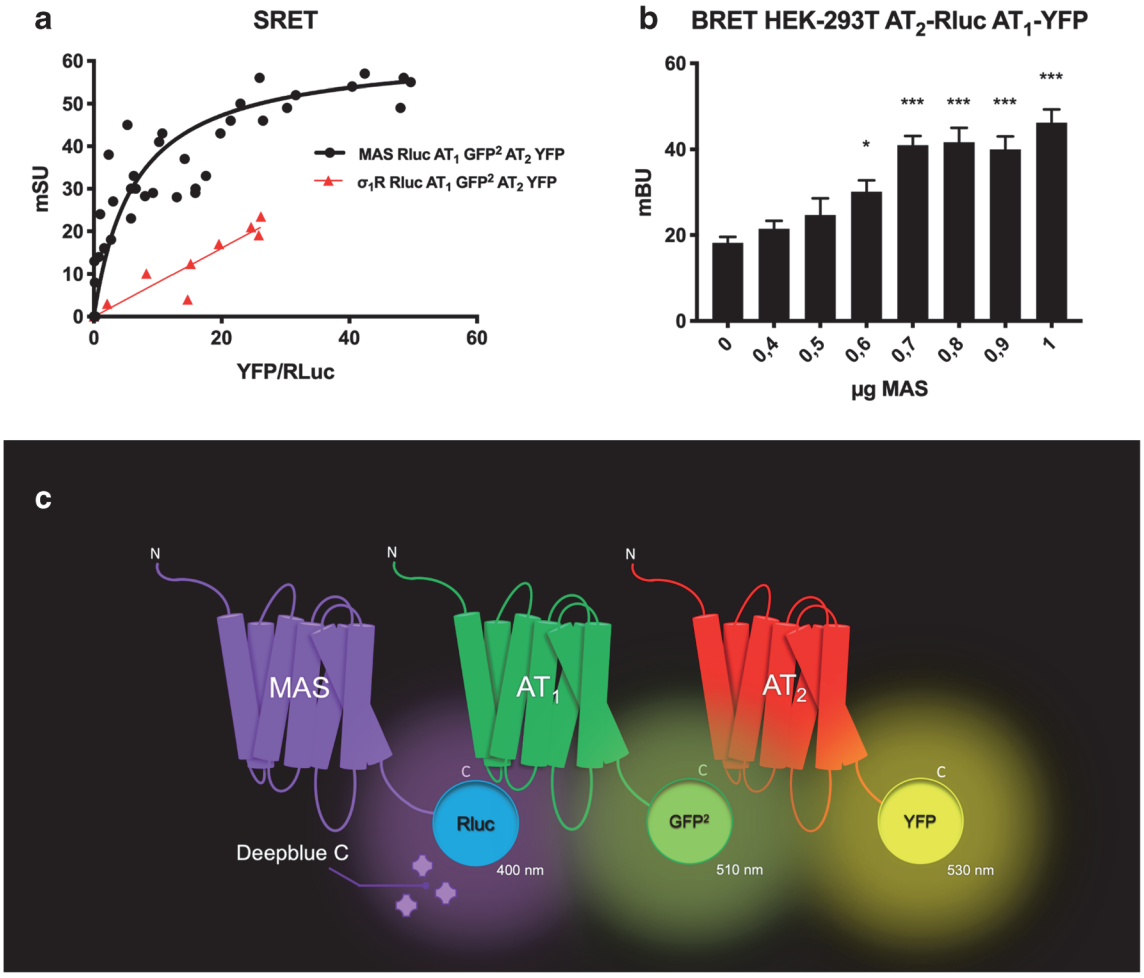

Fig. 2 All three RAS receptors interact in transfected HEK-293T cells. **A** Sequential resonance energy transfer ($SRET^2$) assays were performed in HEK-293T cells transfected with a constant amount of cDNA for MasR-Rluc (0.6 µg) or σ_1R-Rluc (0.3 µg) (as negative control), a constant amount of cDNA for AT_1R-GFP^2 (1 µg), and increasing amounts of cDNA for AT_2R-YFP (0.5 to 4.1 µg). Values are the mean ± SEM of 8 independent experiments performed in duplicate. **B** BRET assays were performed in HEK-293T cells transfected with a constant amount of cDNA for AT_2R-Rluc (0.5 µg), a constant amount of cDNA for AT_1R-YFP (3 µg), and increasing amounts of cDNA for MasR (0 to 1 µg). Values are the mean ± SEM of 5 independent experiments performed in triplicate. One-way ANOVA followed by Bonferroni's multiple comparison post hoc tests were used for statistical analysis. **C**: Schematic representation of the $SRET^2$ assay. *$p < 0.05$, ***$p < 0.0001$ *versus* absence of MasR

YFP fused to AT_2R when forming receptor heterotrimers with MasR (Fig. 2B).

Functional Characterization of AT_1R-MasR Heteromeric Complexes in HEK-293T Cells

Upon identification of AT_1-MasHets and AT_2-MasHets in cotransfected HEK-293T cells, we characterized the functionality of these complexes. It is well established that the AT_1 receptor couples to G_q proteins, increasing inositol trisphosphate (IP_3) and diacylglycerol (DAG) levels by breaking phosphatidylinositol 4,5-bisphosphate (PIP_2) and subsequently releasing calcium (II) ion from endoplasmic reticulum channels, but it also couples to G_i proteins, inhibiting adenylate cyclase and decreasing cAMP levels. In contrast, the MasR signal transduction pathway has not yet been fully characterized. Calcium measurements were first addressed in HEK-293T cells transfected with cDNAs

Fig. 3 Functional analysis of AT_1R-MasR and AT_2R-MasR complexes in HEK-293T cells. HEK-293T cells were transfected with the cDNAs for MasR (1 µg) and for either AT_1R (1 µg) or AT_2R (1 µg) and, in assays of Ca^{2+} determination, with the cDNA for an engineered calcium sensor, GCaMP6 (1 µg). Transfected cells were pretreated with the selective antagonists (300 nM candesartan for AT_1R, 1 µM PD123319 for AT_2R, and 500 nM A779 for MasR) and subsequently treated with selective agonists (100 nM Ang II for AT_1R, 300 nM CGP-42112A for AT_2R, and 500 nM Ang [1–7] for MasR). Thereafter, cytosolic calcium increases (**A**, **B**), intracellular cAMP levels (**C**, **D**), ERK1/2 phosphorylation (**E**, **F**), and the time-dependent DMR signal (**G**, **H**) were determined. Values are the mean ± SEM of 6 independent experiments performed in triplicate. One-way ANOVA followed by Bonferroni's multiple comparison post hoc test were used for statistical analysis. *$p < 0.05$, **$p < 0.01$, ***$p < 0.001$ *versus* forskolin treatment in cAMP determinations or *versus* vehicle in pERK and DMR assays

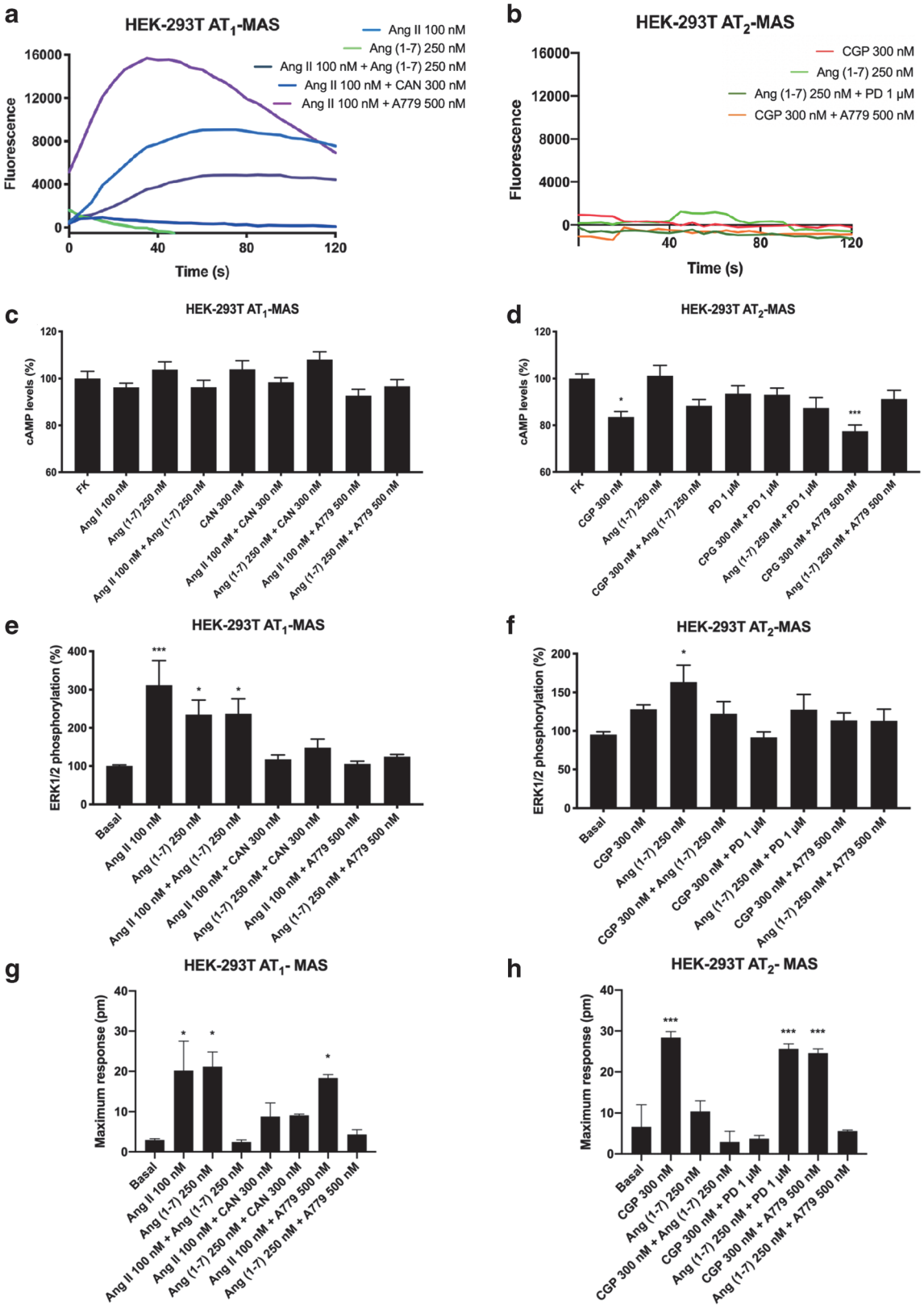

for AT_1 and Mas receptors (1 µg of cDNA each) and with the cDNA for the GCaMP6 calcium sensor (1 µg of cDNA). After treating cells with the AT_1R agonist Ang II (100 nM), a characteristic curve of cytoplasmic transient [Ca^{2+}] increase was recorded. This ion mobilization was completely blocked in cells pretreated with the AT_1R

antagonist candesartan (300 nM; Fig. 3A). Interestingly, when cells were pretreated with the MasR antagonist A779 (500 nM) followed by Ang II stimulation, we observed a marked increase in the calcium mobilization signal. Thus, MasR blockade potentiated AT_1R-mediated signaling in the AT_1-MasHet context. The MasR agonist Ang(1-7) (250 nM) induced no effect, indicating that the MasR receptor does not couple with G_q.

Because of the controversy existing around the pathways engaged by MasR activation, we assayed whether the receptor agonist could affect the cytoplasmic levels of cAMP. As can be observed in Fig. 3C, activation of MasR in HEK-293T cells coexpressing AT_1 and Mas receptors (1 μg of cDNA each) did not have any effect on either basal or forskolin-induced cAMP levels, indicating that MasR does not couple with either G_s or G_i. Similar results were obtained in cells only expressing MasR (Supplementary Figure S3). Furthermore, Ang II stimulation induced no effect in cells expressing AT_1-MasHets (Fig. 3C).

We next addressed activation of the MAPK pathway, which is linked to the action of many GPCRs. When HEK-293T cells expressing AT_1-MasHets were treated with Ang II or Ang(1-7), observed an increase in ERK1/2 phosphorylation. However, when cells were simultaneously stimulated with both agonists, the signal was reduced (Fig. 3E). This phenomenon—in which the signal in a combined treatment is lower than the sum of individual activation—is known as negative cross-talk and it can be used to detect AT_1-MasHets in native tissues. Furthermore, when cells were pretreated with selective antagonists, we observed that A779 treatment blocked not only the MasR-induced signal but also the AT_1R-induced signal. Similarly, candesartan blocked both AT_1R-induced and MasR-induced signals (Fig. 3E). This phenomenon—by which the antagonist of one receptor in the heteromer blocks the signaling of the other protomer in the complex—is known as cross-antagonism and is a common print found for different GPCR heteromers.

Finally, when AT_1-MasR complex signaling was assayed by using label-free DMR, a technique that detects cytoskeletal rearrangements upon receptor activation, negative cross-talk was detected when cells were costimulated; cross-antagonism was unidirectional because it was only detected with candesartan (Fig. 3G).

Functional Characterization of AT_2R-MasR Heteromeric Complexes in HEK-293T Cells

After confirming that MasR and AT_1R arrange into a functional unit with novel properties, we proceeded to analyze the possibility of a similar scenario for AT_2R. The assays were similar to those described in the previous section. On the one hand, HEK-293T cells expressing AT_2-MasHet and the GCaMP6 calcium sensor did not respond to the MasR agonist Ang [1–7] (250 nM) or to the AT_2R agonist CGP-42112A (300 nM). These results fit with a lack of G_q coupling (Fig. 3B). On the other hand, assays to determine cAMP levels showed that CGP-42112A decreased the forskolin-induced effect by approximately 20%, whereas Ang [1–7] produced no effect (Fig. 3D). Similar results were obtained in cells expressing either AT_2R (CGP-42112A) or MasR (Ang [1–7]) (Supplementary Figure S3). However, MasR activation partially blocked the AT_2R signal. Interestingly, when HEK-293T cells expressing AT_2-MasHets were pretreated with the MasR antagonist A779 followed by AT_2R activation, potentiation of AT_2R-mediated signaling was detected. Thus, these results show that MasR stimulation blocked AT_2R-induced signaling, whereas, remarkably, MasR blockade potentiated AT_2R functionality. To further characterize signaling in AT_1-MasHet-expressing cells, ERK1/2 phosphorylation and DMR were determined. Equivalent results were found in both assays, namely negative cross-talk when receptors were simultaneously activated (Fig. 3F, H) and partial cross-antagonism in MAPK phosphorylation when cells were pretreated with selective antagonists. This partial cross-antagonism was not detectable in DMR assays (Fig. 3H). MasR blockade did not potentiate AT_2R functionality in MAPK activation or DMR assays.

AT_1R-MasR and AT_2R-MasR Heteromeric Complexes in Neuronal Primary cultures

Parkinson's disease is characterized by neuronal death and neuroinflammation, mainly affecting the indirect pathway of the basal ganglia, where angiotensin receptors are expressed. Thus, we isolated primary cultures of brain striatum to look for expression of angiotensin and Mas receptor complexes.

We first identified AT_1-MasHets and AT_2-MasHets in primary neurons by *in situ* PLA. Clusters of receptor pairs were identifiable as red fluorescent dots (Fig. 4A–D); 1.44 red dots/cell were counted using primary antibodies against AT_1R and MasR, and 0.63 red dots/cell were counted using primary antibodies against AT_2R and MasR. The non-specific signal was equivalent to 0.17 red dots/cell in the negative control.

Once expression of heteromers was demonstrated, we addressed their functionality in striatal neurons. Receptors in primary cultures of striatal neurons were treated with selective antagonists (candesartan for AT_1R, PD123319 for AT_2R, and A779 for MasR) and activated with agonists (Ang II for AT_1R, CGP-42112A for AT_2R, and Ang(1-7) for MasR), and cAMP levels and MAPK activation were analyzed.

In the cAMP assays, we observed that only AT_2R activation produced a significant decrease in forskolin-induced cAMP levels (Fig. 4E–G). This effect was partially counteracted by MasR activation and thus congruent with the data obtained in the heterologous expression system. In addition, pretreatment with MasR antagonist potentiated AT_2R signaling.

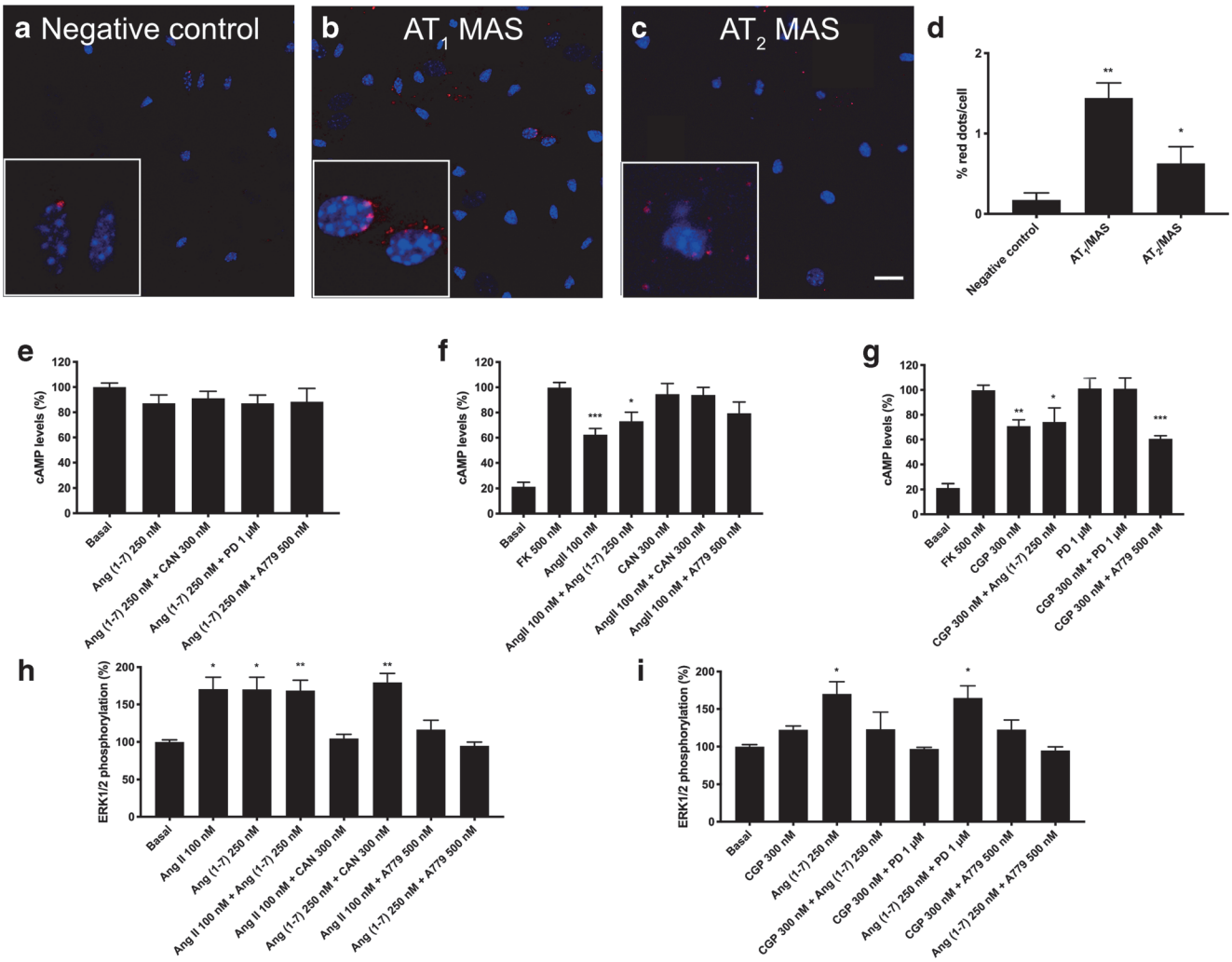

Fig. 4 AT_1-MasHet and AT_2-MasHet expression and function in primary cultures of striatal neurons. **A**–**C** Expression of AT_1-MasHets and AT_2-MasHets heteromers was determined by proximity ligation assay (PLA), which was performed using specific primary antibodies against AT_1, AT_2, and Mas receptors. Confocal microscopy images (stacks of 4 consecutive planes) show heteroreceptor complexes; nuclei are Hoechst-stained (blue). Scale bar: 20 µm. **D** Bar graph showing the percentage of AT_1R-MasR and AT_2R-MasR clusters as red dots/cell compared with the negative control (*$p < 0.05$, **$p < 0.01$; Student's *t* test *vs* the negative control condition). For cAMP (**E**–**G**) or ERK1/2 phosphorylation (**H**, **I**), cells were pretreated with selective receptor antagonists (300 nM candesartan for AT_1R, 1 µM PD123319 for AT_2R, and 500 nM A779 for MasR) and subsequently treated with selective agonists (100 nM Ang II for AT_1R, 300 nM CGP-42112A for AT_2R, and 250 nM Ang(1-7) for MasR). Values are the mean ± SEM of 5 independent experiments performed in triplicate. One-way ANOVA followed by Bonferroni's multiple comparison post hoc tests were used for statistical analysis. *$p < 0.05$, **$p < 0.01$, ***$p < 0.001$ *versus* forskolin treatment in cAMP determinations or *versus* vehicle treatment (basal) in pERK determinations

Finally, except for AT_2R in cells expressing AT_2-MasHets, individual activation of receptors led to ERK1/2 phosphorylation. Furthermore, AT_2R activation blunted the effect of MasR activation. Antagonists allowed us to identify unidirectional cross-antagonism, that is, the MasR antagonist blocked the AT_1R-induced but not the AT_2R-induced effect, whereas angiotensin receptor antagonists did not affect the link of MasR and the MAPK pathway (Fig. 4H, I). Compared with results in transfected HEK-293T cells, the cross-antagonism of AT_1 and AT_2 receptors over MasR was not observed in neurons.

AT_2R-MasR Heteromeric Complex Expression in Microglia Treated or Not with LPS and IFN-γ

In pathological conditions, microglia migrate to the injury site, releasing pro- and anti-inflammatory factors, and becoming key actors in regulating the neurodegenerative/neuroprotective balance [64]. First, expression of the AT_1R-MasR and AT_2R-MasR heteromeric complexes was detected by PLA in primary microglia, both resting and activated. Microglia were activated by treating the cells for 48 h with 1 µM LPS and 200 U/mL IFN-γ. As can be observed in Fig. 5, 3.8 and 4.4 red dots/cell were

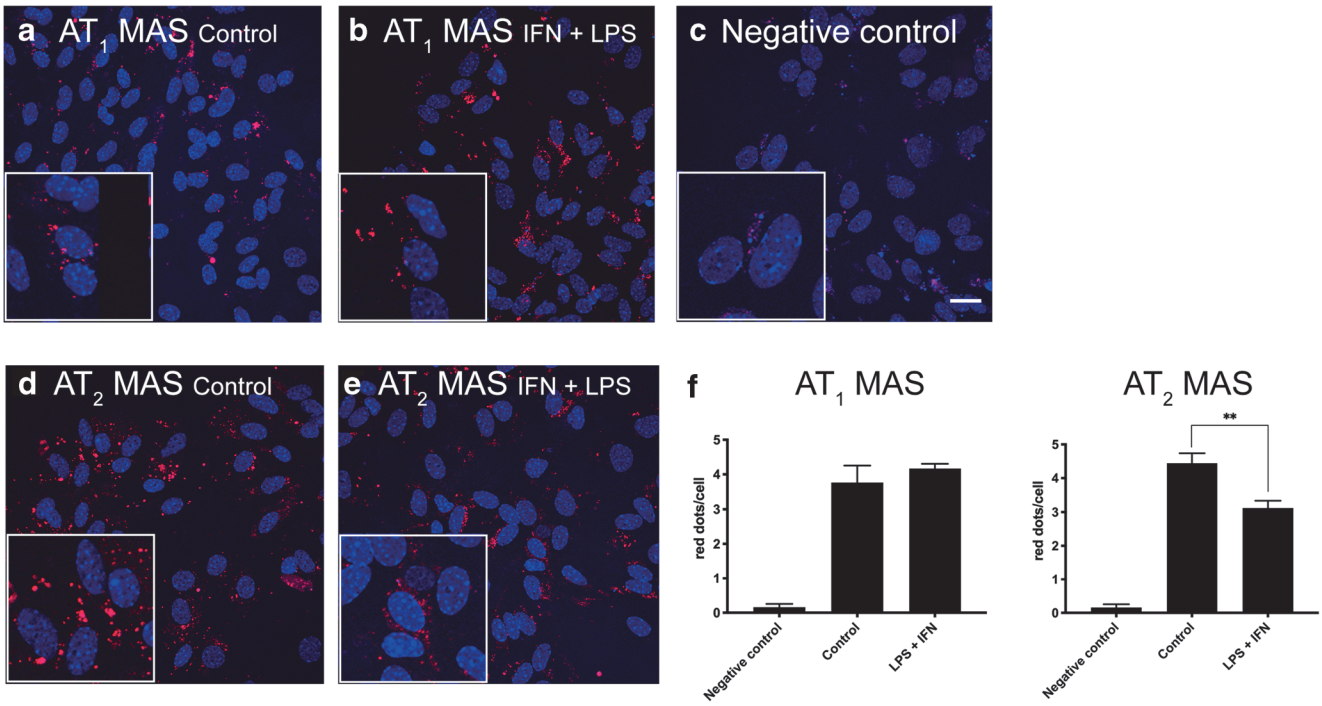

Fig. 5 AT_1-MasHet and AT_2-MasHet expression in microglial primary cultures treated with LPS and IFN-γ. **A**–**E** Expression of AT_1R-MasR and AT_2R-MasR heteromers in primary microglial cultures was determined by proximity ligation assay (PLA), which was performed using specific primary antibodies against AT_1, AT_2, and Mas receptors. Confocal microscopy images (stacks of 4 consecutive planes) show heteroreceptor complexes; nuclei are Hoechst-stained (blue). Microglial cultures were incubated for 48 h in the absence (**A**, **C**, **D**) or in the presence (**B**, **E**) of 1 μM LPS and 200 U/mL IFN-γ. Scale bar: 20 μm. **F**: Bar graph showing the percentage of AT_1R-MasR and AT_2R-MasR clusters as red dots/cell. $^{**}p < 0.01$; Student's *t* test *versus* resting cells

counted for AT_1-MasHets (Fig. 5A) and AT_2-MasHets (Fig. 5D), respectively, in resting microglia; in the negative control using the MasR primary antibody, only 0.2 red dots/cells were counted (Fig. 5C). These results indicate an expression level of AT_1-MasHets and AT_2-MasHets that seems markedly higher in resting microglia than in striatal neurons (see previous section). Interestingly, when the same experiment was performed in activated microglia, a significant decrease was observed in expression of the AT_2R-MasR complex (3.1 red dots/cell) (Fig. 5E) but not in expression of the AT_1R-MasR complex (4.2 red dots/cell) (Fig. 5B).

AT_1R-MasR Complexes Show Negative Cross-talk in cAMP and MAPK Signaling Pathways in Microglia Treated or Not with LPS and IFN-γ

Signaling outputs were used to look for any differential functionality of heteromers in resting *versus* activated microglial cells. As observed in Fig. 6A, B, neither AT_1R nor MasR activation resulted in any cAMP level alteration in resting microglia. Also, activation of each receptor led to MAPK activation (Fig. 6C). Moreover, simultaneous coactivation of resting microglia with the two agonists induced negative cross-talk, whereas experiments with antagonists showed cross-antagonism. Interestingly, when primary cultures were treated for 48 h with 1 mM LPS and 200 U/mL IFN-γ, Ang II led to a significant G_i-mediated effect, indicating that the blockade of AT_1R that occurred when forming complexes with MasR disappeared in activated microglia. This effect was potentiated when receptors were coactivated and cross-antagonism was not detected (Fig. 6D). By analyzing ERK1/2 phosphorylation data, we observed a similar effect of the MasR agonist in both resting and activated microglia. However, as in resting microglia, negative cross-talk and cross-antagonism were observed (Fig. 6E). To summarize, in activated microglia, the AT_1-MasHets seem to undergo structural reorganization favoring the action of Ang II on G_i-coupled AT_1R.

AT_2R-MasR Complexes Show Negative Cross-talk in cAMP and MAPK Signaling Pathways in microglia Treated or Not with LPS and IFN-γ

As in the previous section, we observed differential effects in resting and activated microglia when the AT_2R-MasR couple was analyzed with a functional perspective. The cAMP data indicated a non-significant effect upon AT_2R or MasR activation in resting cells (Fig. 7A). Again, in resting microglia, a blockade of G_i-mediated AT_2R function was detected when AT_2R was coexpressed with MasR. In resting cells, only MasR was linked to MAPK pathway activation but with

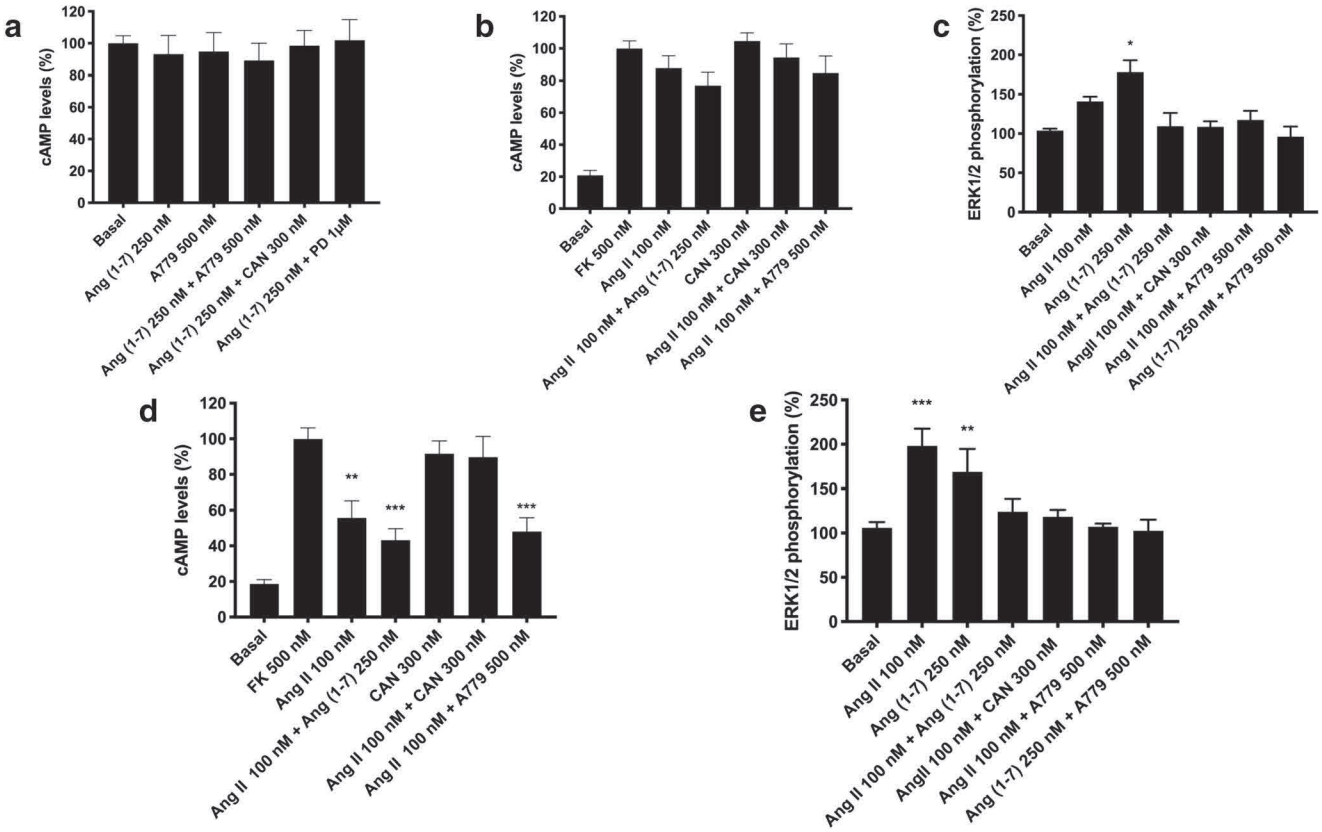

Fig. 6 AT_1-MasHet function in primary cultures of microglia. **A**–**E** Microglia in primary cultures were incubated for 48 h with 1 μM LPS and 200 U/mL IFN-γ (**D**, **E**) or vehicle (**A**–**C**). Then, cultures were pretreated with selective receptor antagonists (300 nM candesartan for AT_1R, 1 μM PD123319 for AT_2R, and 500 nM A779 for MasR) and subsequently treated with selective agonists (100 nM Ang II for AT_1R, 300 nM CGP-42112A for AT_2R, and 250 nM Ang [1–7] for MasR). Cytosolic cAMP levels (**A**, **B**, **D**) and ERK1/2 phosphorylation (**C**, **E**) were subsequently determined. Values are the mean ± SEM of 5 independent experiments performed in triplicate. One-way ANOVA followed by Bonferroni's multiple comparison post hoc test were used for statistical analysis. $*p < 0.05$, $**p < 0.01$, $***p < 0.001$ *versus* basal treatment (**A**) or forskolin treatment (**B**, **D**) in cAMP measurements or *versus* vehicle in pERK measurements (**C**, **E**)

marked negative cross-talk when the AT_2R agonist was present and with a cross-antagonism effect (Fig. 7B). These results are similar to those obtained in the heterologous expression system.

In microglia activated for 48 h with 1 mM LPS and 200 U/mL IFN-γ, we observed that the AT_2R agonist CGP-42112A induced a significant decrease in forskolin-induced cAMP levels (Fig. 7C). Activation of microglia provoked structural alterations in AT_2-MasHets because cross-antagonism and negative cross-talk were not found; that is, there was no blockade by MasR over AT_2R. In terms of ERK1/2 phosphorylation, the results were similar to those found in resting cells: only MasR was linked to MAPK pathway activation, with marked negative cross-talk and cross-antagonism (Fig. 7D).

Expression of Heteroreceptor Complexes in Parkinsonian and Dyskinetic Animals

In situ PLA is instrumental in detecting receptor heteromer clusters in natural sources. We performed PLA in striatal sections from the 6-OH-dopamine-based PD model. Assays were performed in sections from non-lesioned and lesioned hemispheres in three animal groups (see "Materials and Methods"): untreated, levodopa-treated non-dyskinetic, and levodopa-treated dyskinetic. Both AT_1R-MasR and AT_2R-MasR clusters were expressed but at relatively low levels (Fig. 8) and their expression was markedly enhanced in the lesioned hemisphere (Fig. 8). Levodopa treatment per se did not lead to significant modification of expression in parkinsonian animals; however, in dyskinetic animals (i.e., animals that developed dyskinesias upon treatment with the drug), expression was modified. Importantly, the expression in dyskinetic animals (with respect to non-dyskinetic animals) was lower in the case of the AT_2R-MasR heteromer but significantly higher in the case of AT_1R-MasR (Fig. 8).

Discussion

At the beginning of the twenty-first century, research on GPCRs uncovered a novel property resulting from the

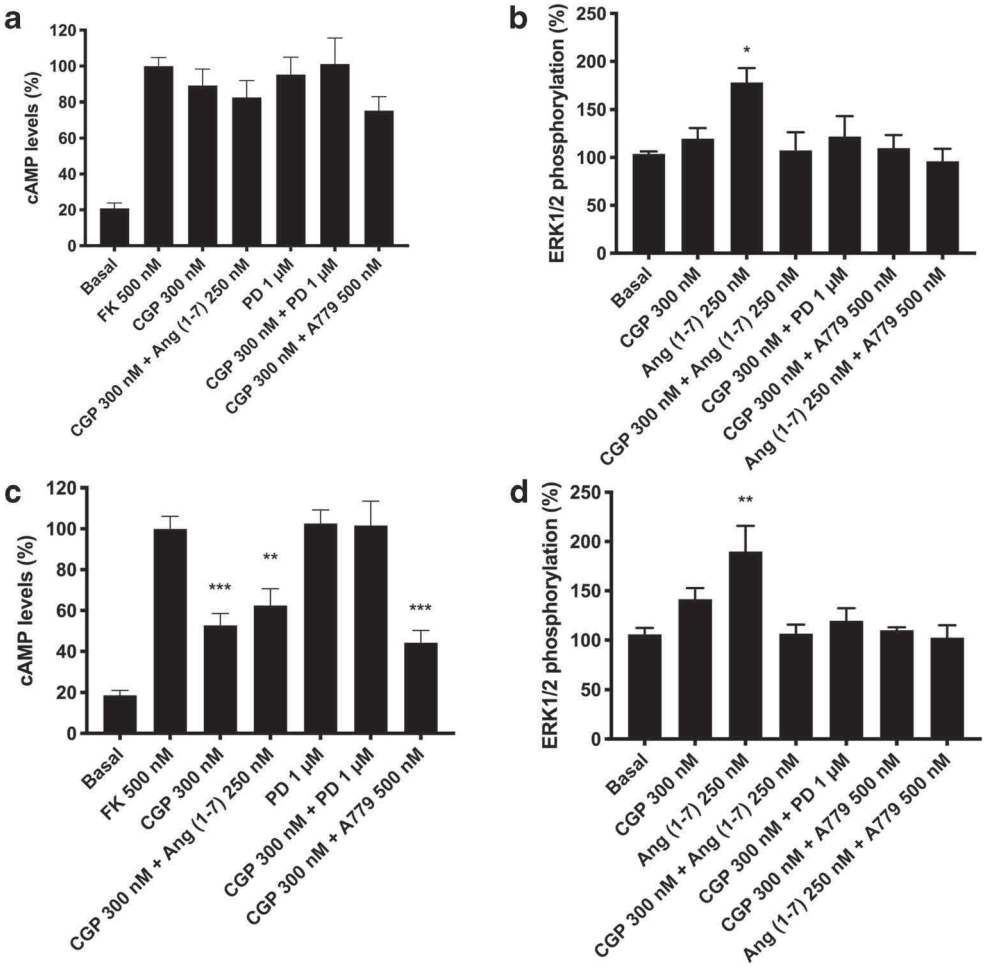

Fig. 7 AT_2-MasHet functionality in primary cultures of microglia. **A**–**D** Microglia in primary cultures were incubated for 48 h with 1 μM LPS and 200 U/mL IFN-γ (**C**, **D**) or vehicle (**A**, **B**). Microglial cells were pretreated with selective receptor antagonists (300 nM candesartan for AT_1R, 1 μM PD123319 for AT_2R, and 500 nM A779 for MasR) and subsequently treated with selective agonists (100 nM Ang II for AT_1R, 300 nM CGP-42112A for AT_2R, and 250 nM Ang [1–7] for MasR). Cytosolic cAMP levels (**A**, **C**) and ERK1/2 phosphorylation (**B**, **D**) were subsequently determined. Values are the mean ± SEM of 5 independent experiments performed in triplicate. One-way ANOVA followed by Bonferroni's multiple comparison post hoc test were used for statistical analysis. $^*p < 0.05$, $^{**}p < 0.01$, $^{***}p < 0.001$ *versus* forskolin treatment in cAMP measurements (**A**, **C**) or *versus* vehicle in pERK assays (**B**, **D**)

formation of heteroreceptor complexes. Receptor–receptor interactions lead to new functional units whose properties are different from those displayed by the individually acting receptors. Interestingly, consideration of receptor heteromers was first suggested for neurodegenerative conditions such as those occurring in PD. Heteromers containing adenosine and cannabinoid receptors are among those relevant to striatal function [65–71]. The occurrence of angiotensin receptors in

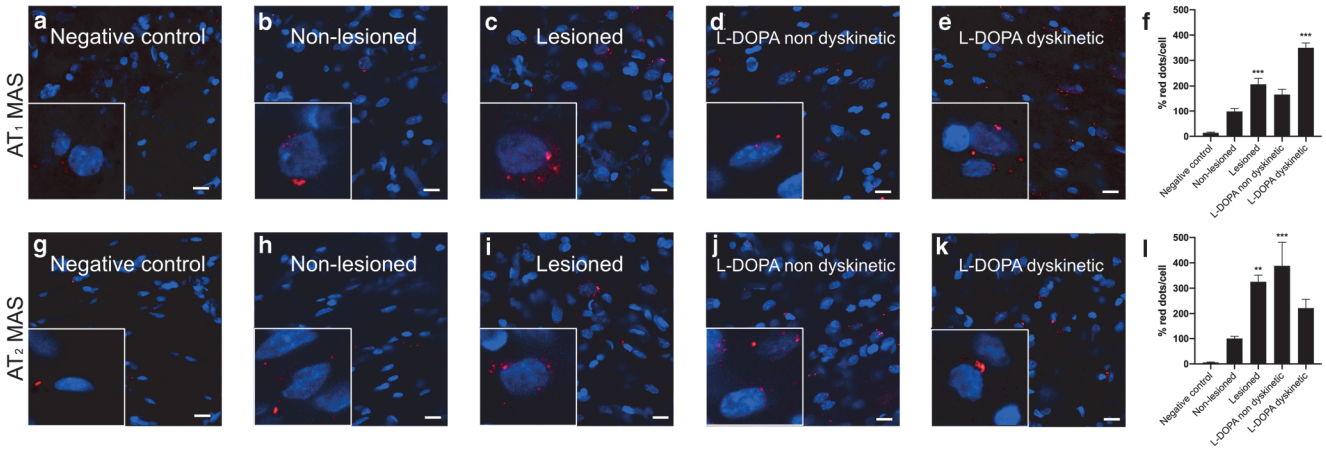

Fig. 8 AT_1-MasHet and AT_2-MasHet complex expression in the striatum of lesioned and levodopa-treated animals. Heteroreceptor expression was assessed by the *in situ* proximity ligation assay (PLA) in the striatum of the different groups of animals treated as described in Methods. Graphs in the right represent the quantification of the red labeling in the different groups calculated using Andy's algorithm. $^*p < 0.05$, $^{**}p < 0.01$, $^{***}p < 0.001$ *versus* non-lesioned animals

the nigra and the striatum was followed by the identification of complexes formed by AT_1R and AT_2R [39, 42]. In this paper, we showed that the Mas receptor forms heteroreceptor complexes with AT_1R and AT_2R and that such complexes are relevant for better understanding the role of RAS in neuroinflammation.

The RAS imbalance has been well studied in relation to blood pressure alterations, which are exacerbated by aging [14, 72, 73]. However, alterations in RAS balance upon aging affects almost any physiological process. RAS regulates functions in the kidneys, lungs, and brain and thus is key for maintaining homeostasis both in the periphery and in the CNS. Unbalanced RAS upon aging is seen as an opportunity to intervene using ligands of RAS receptors to combat neurological diseases whose main risk factor is age. Parkinson's and Alzheimer's diseases are the most prevalent aging-related diseases affecting the CNS [74–76]. It is tempting to speculate that RAS is center stage in understanding the greater severity of COVID-19 in older patients and the variety of symptoms ranging from asymptomatic to serious lung, kidney, immunological, and/or neurological manifestations [19, 21, 22, 77].

A review in 2009 questioned whether results associated with the RAS system were due to cross-talk or to heteromerization [78]. Both AT_1R-AT_2R [39, 79] and AT_2R-MasR interactions had previously been reported [4, 40]. In 2018, it was suggested that MasR and AT_2R were "joining forces" to counteract deleterious actions on blood pressure mediated by AT_1R and that AT_2-MasHets could help explain the functionality of AT_1R [41]. A scenario of RAS receptors interacting with each other raised numerous questions, particularly to understand why receptors mediating opposing effects would "join forces." To approach the issue, two lines of inquiry are necessary: [1] assessing the expression levels of the different components of the system in targeted cells/tissues, heteromers included; and [2] deciphering the properties of the units resulting from receptor–receptor interactions. The functionality studies reported here show differential behaviors depending on the signaling pathway and inter-receptor interactions that lead to negative cross-talk, even reaching full blockade and cross-antagonism. Such counterbalancing effects occurred for both AT_1-MasHets and AT_2-MasHets. Cross-antagonism was reported for AT_2-MasHet expressed in mouse astrocytes using the mRNA level of the CX3C chemokine receptor-1 as a read-out [40]. Apart from cross-antagonism, which is often a characteristic of heteromer expression, a novel feature that is also explained by inter-receptor interaction is that the antagonist of MasR increased the calcium peak elicited by the AT_1R agonist [31, 80, 81]. The properties of these heteromers must be considered to understand the efficacy of antihypertensive medication targeting RAS and for repurposing such approved drugs.

Unbalanced RAS associated with Parkinson's and Alzheimer's diseases opens new therapeutic perspectives. Pharmacological manipulation of RAS components has potential in PD [82]; it is suggested that antagonists already used to treat hypertension and able to cross the blood–brain barrier may be repurposed to treat PD [83]. On the one hand, the system has been extensively characterized in relation to nigral neurodegeneration [27, 72, 83–85]. On the other hand, there are confounding factors in assessing the risk of PD in individuals taking antihypertensive medication. This is due to the multiplicity of therapeutic choices but also to the fact that some drugs targeting RAS enter the brain (e.g., candesartan) [86], whereas others cannot cross the blood–brain barrier. Therefore, we cannot assess with certainty whether chronic administration of RAS-related antihypertensives is neuroprotective or whether they can delay neurodegeneration once the disease shows clinical symptoms. Selecting the most appropriate cell to be targeted is also important. It is feasible to target activated microglia to prevent neurodegeneration if the disease has a neuroinflammatory component. In addition, MasR is key for microglia-driven development of the retinal vasculature [87]. The results presented here and those related to expression of AT_1R-AT_2R heteromers in striatal cells [42] suggest that MasR-related therapies to delay progression of PD should consider RAS components in microglia, with the ultimate goal of attenuating inflammation or skewing microglia toward the M2 neuroprotective phenotype [64]. RAS is well positioned to be targeted to polarization of microglia activated upon neuroinflammation [82]. In contrast to results in transfected HEK-293T cells and activated microglia, we did not observe cross-antagonism of AT_1 and AT_2 receptors over MasR in neurons. This, together with the lesser expression of MasR-containing heteromers, suggests that MasR functionality in neurons is not efficiently regulated by Ang II acting on AT_1 or AT_2 receptors.

Further parameters to consider are the expression of ACE1 and ACE2 and the possibility that these enzymes also interact with RAS receptors, thus affecting the local concentration of agonists of RAS receptors. In relation to COVID-19 management, it has been demonstrated that ACE2 interacts with AT_1R [88]. Combining these results with the results presented here, we cannot rule out the occurrence of a functional unit constituted by an enzyme, two receptors, and the corresponding G-coupled proteins. The functionality of equivalent macromolecular complexes and the 3-dimensional structure underlying the particular functional features has been demonstrated for adenosine A_1-A_{2A} and A_{2A}-A_{2B} receptors ([33–38] and data in preparation). Both the allosteric modulation of ACE2 activity that results from the interaction with SARS-CoV viruses and the effect of viral infection on the surface expression of RAS components, heteromers included, need to be addressed.

Mechanistically, the two most relevant findings are the MasR-mediated regulation of cytosolic calcium mobilization triggered by AT_1R agonists and the differential link between RAS and MAPK activation, depending on which heteromers are expressed in a given cell type and which

agonist(s) is (are) affecting RAS receptors. Very few mechanisms lead to radical changes in the activation of the MAPK pathway. However, we present here data that show that one of the properties of RAS receptor heteromers is the possibility to engage or not this relevant pathway, depending on the overall RAS balance. Several years ago, we reported that histamine H_3 receptor activation could not lead to ERK phosphorylation unless it formed a heteromer with the dopamine D_1 receptor. D_1-H_3 receptor heteromers are unique devices directing histaminergic and dopaminergic signaling toward the MAPK pathway in a G_i-dependent but G_s-independent manner [89]. Remarkably, MasR in activated microglia is linked to MAPK pathway activation with marked negative cross-talk and cross-antagonism. In a complementary recent study, we showed that AT_1-AT_2 receptor heteromers are expressed in microglia where [1] they are upregulated in both parkinsonian conditions and in L-DOPA-induced dyskinesias, and [2] their activation is seemingly neuroprotective. The data shown in Fig. 8 suggest that expression of heteroreceptor complexes formed by MasR and either AT_1R or AT_2R is higher in the striatum of the lesioned hemisphere in the rat 6-OH-DA-based PD model. The marked increase in the case of AT_1R-MasR heteromers in dyskinetic animals open new therapeutic avenues for the assessment of this well-known side effect of antiparkinsonian medication. In microglia, a differential pharmacological trend, when Ang II receptor heteromers are compared with AT_1-MasHets or AT_2-MasHets, is cross-antagonism, which is not found in the former but in the latter. This is promising from a therapeutic point of view, because cross-antagonism in AT_1R-AT_2R heteromers would lead to a dead end in terms of neuroprotection; instead, the antagonist of one Ang II receptor releases the brake on activation of the partner Ang II receptor within the AT_1R-AT_2R heteromer [42].

Supplementary Information The online version contains supplementary material available at https://doi.org/10.1007/s13311-020-00986-4.

Required Author Forms Disclosure forms provided by the authors are available with the online version of this article.

Funding This work was partially supported by grants from the Spanish Ministry of Science and Innovation (MICINN) and/or Science, Innovation, and Universities; they may include EU FEDER funds (BFU2015-64405-R, SAF2016-77830-R, AARFD-17-503612, SAF2017-84117-R, RTI2018-094204-B-I00, and RTI2018-098830-B-I00). The laboratory of the University of Barcelona is considered of excellence by the Regional Catalonian Government (*grup consolidat* #2017 SGR 1497), which does not provide any specific funding for personnel, equipment, and reagents or for payment of services.

Data Availability The data that support the findings of this study are available from the corresponding author upon reasonable request.

Compliance with Ethical Standards

Conflict of Interest The authors declare that they have no conflict of interest.

Statement of Ethics Under the current legislation, obtaining protocol approval is not needed if animals are sacrificed to obtain a specific tissue. Animal handling, sacrifice and further experiments were conducted according to the guidelines set in Directive 2010/63/EU of the European Parliament and the Council of the European Union that is enforced in Spain by National and Regional organisms; also the 3R rule (replace, refine, reduce) for animal experimentation was taken into account.

References

1. Villela DC, Passos-Silva DG, Santos RAS. Alamandine: A new member of the angiotensin family. Vol. 23, Current Opinion in Nephrology and Hypertension. Curr Opin Nephrol Hypertens; 2014. p. 130–4.
2. Souza LL, Duchene J, Todiras M, Azevedo LCP, Costa-Neto CM, Alenina N, et al. Receptor mas protects mice against hypothermia and mortality induced by endotoxemia. Shock. 2014;41(4):331–6.
3. Santos RAS, Simoes e Silva AC, Maric C, Silva DMR, Machado RP, de Buhr I, et al. Angiotensin-(1-7) is an endogenous ligand for the G protein-coupled receptor Mas. Proc Natl Acad Sci U S A [Internet]. 2003;100(14):8258–63. Available from: http://www.pnas.org/content/100/14/8258.full
4. Villela D, Leonhardt J, Patel N, Joseph J, Kirsch S, Hallberg A, et al. Angiotensin type 2 receptor (AT 2 R) and receptor Mas: a complex liaison. Clin Sci [Internet]. 2015;128(4):227–34. Available from: http://www.clinsci.org/content/128/4/227.abstract%5Cn, http://clinsci.org/lookup/10.1042/CS20130515
5. De Carvalho Santuchi M, Dutra MF, Vago JP, Lima KM, Galvão I, De Souza-Neto FP, et al. Angiotensin-(1-7) and Alamandine Promote Anti-inflammatory Response in Macrophages in Vitro and in Vivo. Mediators Inflamm [Internet]. 2019 [cited 2020 Apr 29];2019(1):2401081. Available from: https://doi.org/10.1155/2019/2401081
6. Clarke NE, Turner AJ. Angiotensin-Converting Enzyme 2: The First Decade. Int J Hypertens [Internet]. 2012;2012:1–12. Available from: http://www.hindawi.com/journals/ijhy/2012/307315/
7. Wan Y, Shang J, Graham R, Baric RS, Li F. Receptor Recognition by the Novel Coronavirus from Wuhan: an Analysis Based on Decade-Long Structural Studies of SARS Coronavirus. J Virol. 2020 Jan 29;94(7).
8. Shang J, Ye G, Shi K, Wan Y, Luo C, Aihara H, et al. Structural basis of receptor recognition by SARS-CoV-2. Nature. 2020 Mar 30;581(7807):221–4.
9. Kuhn JH, Li W, Choe H, Farzan M. Angiotensin-converting enzyme 2: A functional receptor for SARS coronavirus [Internet]. Vol. 61, Cellular and Molecular Life Sciences. 2004 [cited 2020 May 26]. p. 2738–43. Available from: https://www.nature.com/articles/nature02145
10. Li W, Moore MJ, Vasllieva N, Sui J, Wong SK, Berne MA, et al. Angiotensin-converting enzyme 2 is a functional receptor for the SARS coronavirus. Nature. 2003 Nov 27;426(6965):450–4.
11. Valenzuela R, Barroso-Chinea P, Villar-Cheda B, Joglar B, Muñoz A, Lanciego JL, et al. Location of Prorenin Receptors in Primate Substantia Nigra: Effects on Dopaminergic Cell Death. J Neuropathol Exp Neurol [Internet]. 2010 Nov [cited 2019 Sep 1];69(11):1130–42. Available from: http://www.ncbi.nlm.nih.gov/pubmed/20940627
12. Jarrott B, Williams SJ. Chronic Brain Inflammation: The Neurochemical Basis for Drugs to Reduce Inflammation. Neurochem Res [Internet]. 2016 Mar 16 [cited 2019 Oct 4];41(3):523–33. Available from: http://www.ncbi.nlm.nih.gov/pubmed/26177578

13. Perez-Lloret S, Otero-Losada M, Toblli JE, Capani F. Renin-angiotensin system as a potential target for new therapeutic approaches in Parkinson's disease. Expert Opin Investig Drugs [Internet]. 2017 Oct 3 [cited 2019 Oct 15];26(10):1163–73. Available from: https://www.tandfonline.com/full/10.1080/13543784.2017.1371133
14. Villar-Cheda B, Dominguez-Meijide A, Valenzuela R, Granado N, Moratalla R, Labandeira-Garcia JL. Aging-related dysregulation of dopamine and angiotensin receptor interaction. Neurobiol Aging [Internet]. 2014 Jul [cited 2019 Sep 1];35(7):1726–38. Available from: http://www.ncbi.nlm.nih.gov/pubmed/24529758
15. Rabie MA, Abd El Fattah MA, Nassar NN, Abdallah DM, El-Abhar HS. Correlation between angiotensin 1–7-mediated Mas receptor expression with motor improvement, activated STAT3/SOCS3 cascade, and suppressed HMGB-1/RAGE/NF-κB signaling in 6-hydroxydopamine hemiparkinsonian rats. Biochem Pharmacol. 2020 Jan 1;171.
16. Mccarthy CA, Widdop RE, Deliyanti D, Wilkinson-Berka JL. Brain and retinal microglia in health and disease: An unrecognized target of the renin-angiotensin system. Vol. 40, Clinical and Experimental Pharmacology and Physiology. 2013. p. 571–9.
17. Gironacci MM, Vicario A, Cerezo G, Silva MG. The depressor axis of the renin-angiotensin system and brain disorders: A translational approach. Vol. 132, Clinical Science. Portland Press Ltd; 2018. p. 1021–38.
18. Garrido-Gil P, Rodriguez-Perez AI, Fernandez-Rodriguez P, Lanciego JL, Labandeira-Garcia JL. Expression of angiotensinogen and receptors for angiotensin and prorenin in the rat and monkey striatal neurons and glial cells. Brain Struct Funct [Internet]. 2017 Aug 4 [cited 2019 Oct 8];222(6):2559–71. Available from: http://www.ncbi.nlm.nih.gov/pubmed/28161727
19. Haddadi K, Ghasemian R, Shafizad M. Basal Ganglia Involvement and Altered Mental Status: A Unique Neurological Manifestation of Coronavirus Disease 2019. Cureus. 2020 Apr 28;12(4).
20. Lahiri D, Ardila A. COVID-19 Pandemic: A Neurological Perspective. Cureus. 2020 Apr 29;12(4).
21. Baig AM, Sanders EC. Potential Neuroinvasive Pathways of SARS-CoV-2: Deciphering the Spectrum of Neurological Deficit Seen in Coronavirus Disease 2019 (COVID-19). J Med Virol [Internet]. 2020 Jun 3 [cited 2020 Jun 6]; Available from: http://www.ncbi.nlm.nih.gov/pubmed/32492193
22. Brun G, Hak JF, Coze S, Kaphan E, Carvelli J, Girard N, et al. COVID-19-White matter and globus pallidum lesions: Demyelination or small-vessel vasculitis? Neurol Neuroimmunol neuroinflammation. 2020 Jul 1;7(4).
23. Dixon L, Varley J, Gontsarova A, Mallon D, Tona F, Muir D, et al. COVID-19-related acute necrotizing encephalopathy with brain stem involvement in a patient with aplastic anemia. Neurol Neuroimmunol neuroinflammation [Internet]. 2020 Sep 3 [cited 2020 Jun 6];7(5). Available from: http://www.ncbi.nlm.nih.gov/pubmed/32457227
24. Rodriguez-Perez AI, Garrido-Gil P, Pedrosa MA, Garcia-Garrote M, Valenzuela R, Navarro G, et al. Angiotensin type 2 receptors: Role in aging and neuroinflammation in the substantia nigra. Brain Behav Immun [Internet]. 2019 [cited 2020 Jun 6]; Available from: https://pubmed.ncbi.nlm.nih.gov/31863823/
25. Dominguez-Meijide A, Rodriguez-Perez AI, Diaz-Ruiz C, Guerra MJ, Labandeira-Garcia JL. Dopamine modulates astroglial and microglial activity via glial renin-angiotensin system in cultures. Brain Behav Immun [Internet]. 2017 May [cited 2019 Oct 4];62:277–90. Available from: http://www.ncbi.nlm.nih.gov/pubmed/28232171
26. Labandeira-Garcia JL, Rodriguez-Pallares J, Dominguez-Meijide A, Valenzuela R, Villar-Cheda B, Rodríguez-Perez AI. Dopamine-angiotensin interactions in the basal ganglia and their relevance for Parkinson's disease. Mov Disord [Internet]. 2013 Sep [cited 2019 Sep 1];28(10):1337–42. Available from: http://doi.wiley.com/10.1002/mds.25614
27. Costa-Besada MA, Valenzuela R, Garrido-Gil P, Villar-Cheda B, Parga JA, Lanciego JL, et al. Paracrine and Intracrine Angiotensin 1-7/Mas Receptor Axis in the Substantia Nigra of Rodents, Monkeys, and Humans. Mol Neurobiol [Internet]. 2018 Jul 30 [cited 2019 Aug 30];55(7):5847–67. Available from: http://www.ncbi.nlm.nih.gov/pubmed/29086247
28. Jiang M, Huang W, Wang Z, Ren F, Luo L, Zhou J, et al. Anti-inflammatory effects of Ang-(1–7) via TLR4-mediated inhibition of the JNK/FoxO1 pathway in lipopolysaccharide-stimulated RAW264.7 cells. Dev Comp Immunol. 2019 Mar 1;92:291–8.
29. Ferré S, Baler R, Bouvier M, Caron MG, Devi LA, Durroux T, et al. Building a new conceptual framework for receptor heteromers. Nat Chem Biol [Internet]. 2009 Mar [cited 2020 May 11];5(3):131–4. Available from: http://www.ncbi.nlm.nih.gov/pubmed/19219011
30. Franco R, Martínez-Pinilla E, Lanciego JLJLJL, Navarro G. Basic Pharmacological and Structural Evidence for Class A G-Protein-Coupled Receptor Heteromerization. Front Pharmacol [Internet]. 2016 Jan 31 [cited 2016 Apr 12];7(MAR):76. Available from: http://www.ncbi.nlm.nih.gov/pubmed/27065866
31. Franco N, Franco R. Understanding the added value of g-protein-coupled receptor heteromers. Scientifica (Cairo) [Internet]. 2014;2014:362937. Available from: http://www.pubmedcentral.nih.gov/articlerender.fcgi?artid=4017843&tool=pmcentrez&rendertype=abstract
32. Gupta A, Mulder J, Gomes I, Rozenfeld R, Bushlin I, Ong E, et al. Increased abundance of opioid receptor heteromers after chronic morphine administration. Sci Signal [Internet]. 2010 Jan [cited 2016 Feb 23];3(131):ra54. Available from: http://www.pubmedcentral.nih.gov/articlerender.fcgi?artid=3125674&tool=pmcentrez&rendertype=abstract
33. Ciruela F, Casadó V, Rodrigues R, Luján R, Burgueño J, Canals M, et al. Presynaptic Control of Striatal Glutamatergic Neurotransmission by Adenosine A1-A2A Receptor Heteromers. J Neurosci [Internet]. 2006 Feb 15 [cited 2015 Mar 21];26(7):2080–7. Available from: http://www.jneurosci.org/cgi/10.1523/JNEUROSCI.3574-05.2006
34. Ciruela F, Ferré S, Casadó V, Cortés A, Cunha R, Lluis C, et al. Heterodimeric adenosine receptors: A device to regulate neurotransmitter release. Cell Mol Life Sci. 2006;63(21):2427–31.
35. Cristóvão-Ferreira S, Navarro G, Brugarolas M, Pérez-Capote K, Vaz SH, Fattorini G, et al. A1R-A2AR heteromers coupled to Gs and G i/o proteins modulate GABA transport into astrocytes. Purinergic Signal [Internet]. 2013 Sep [cited 2015 Dec 14];9(3):433–49. Available from: http://www.pubmedcentral.nih.gov/articlerender.fcgi?artid=3757138&tool=pmcentrez&rendertype=abstract
36. Navarro G, Cordomí A, Brugarolas M, Moreno E, Aguinaga D, Pérez-Benito L, et al. Cross-communication between Gi and Gs in a G-protein-coupled receptor heterotetramer guided by a receptor C-terminal domain. BMC Biol [Internet]. 2018;16:24(1):1–15. Available from: https://bmcbiol.biomedcentral.com/articles/10.1186/s12915-018-0491-x
37. Navarro G, Cordomí A, Zelman-Femiak M, Brugarolas M, Moreno E, Aguinaga D, et al. Quaternary structure of a G-protein-coupled receptor heterotetramer in complex with Gi and Gs. BMC Biol [Internet]. 2016 Jan 5 [cited 2016 Apr 8];14(1):26. Available from: http://bmcbiol.biomedcentral.com/articles/10.1186/s12915-016-0247-4
38. Hinz S, Navarro G, Borroto-Escuela D, Seibt BF, Ammon C, Filippo E De, et al. Adenosine A2A receptor ligand recognition and signaling is blocked by A2B receptors. Oncotarget [Internet]. 2018 Mar 2 [cited 2018 Apr 5];9(17):13593–611. Available from: http://www.ncbi.nlm.nih.gov/pubmed/29568380
39. Porrello ER, Pfleger KDG, Seeber RM, Qian H, Oro C, Abogadie F, et al. Heteromerization of angiotensin receptors changes trafficking and arrestin recruitment profiles. Cell Signal [Internet]. 2011

Nov [cited 2019 Aug 30];23(11):1767–76. Available from: http://www.ncbi.nlm.nih.gov/pubmed/21740964
40. Leonhardt J, Villela DC, Teichmann A, Münter L-M, Mayer MC, Mardahl M, et al. Evidence for Heterodimerization and Functional Interaction of the Angiotensin Type 2 Receptor and the Receptor MASNovelty and Significance. Hypertension [Internet]. 2017 Jun [cited 2019 Aug 30];69(6):1128–35. Available from: http://hyper.ahajournals.org/lookup/10.1161/HYPERTENSIONAHA.116.08814
41. Patel S, Hussain T. Dimerization of AT2 and Mas Receptors in Control of Blood Pressure. Curr Hypertens Rep [Internet]. 2018 May 1 [cited 2018 May 6];20(5):1–9. Available from: http://www.ncbi.nlm.nih.gov/pubmed/29717388
42. Rivas-Santisteban R, Rodriguez-Perez AI, Muñoz A, Reyes-Resina I, Labandeira-García JL, Navarro G, et al. Angiotensin AT1and AT2receptor heteromer expression in the hemilesioned rat model of Parkinson's disease that increases with levodopa-induced dyskinesia. J Neuroinflammation. 2020 May 29;17(1).
43. Newell EA, Exo JL, Verrier JD, Jackson TC, Gillespie DG, Janesko-Feldman K, et al. 2′,3′-cAMP, 3′-AMP, 2′-AMP and adenosine inhibit TNF-α and CXCL10 production from activated primary murine microglia via A2A receptors. Brain Res. 2015 Jan;1594:27–35.
44. Hradsky J, Mikhaylova M, Karpova A, Kreutz MR, Zuschratter W. Super-resolution microscopy of the neuronal calcium-binding proteins Calneuron-1 and Caldendrin. Methods Mol Biol [Internet]. 2013 [cited 2017 Jun 4];963:147–69. Available from: http://link.springer.com/10.1007/978-1-62703-230-8_10
45. Reyes-Resina I, Navarro G, Aguinaga D, Canela EI, Schoeder CT, Załuski M, et al. Molecular and functional interaction between GPR18 and cannabinoid CB2G-protein-coupled receptors. Relevance in neurodegenerative diseases. Biochemical Pharmacology [Internet]. 2018 Jun [cited 2018 Jun 26];In the Press. Available from: http://linkinghub.elsevier.com/retrieve/pii/S0006295218302090
46. Navarro G, Borroto-Escuela D, Angelats E, Etayo I, Reyes-Resina I, Pulido-Salgado M, et al. Receptor-heteromer mediated regulation of endocannabinoid signaling in activated microglia. Role of CB1 and CB2 receptors and relevance for Alzheimer's disease and levodopa-induced dyskinesia. Brain Behav Immun [Internet]. 2018 Aug [cited 2018 Feb 3];67:139–51. Available from: http://linkinghub.elsevier.com/retrieve/pii/S0889159117304038
47. Farré D, Muñoz A, Moreno E, Reyes-Resina I, Canet-Pons J, Dopeso-Reyes IG, et al. Stronger Dopamine D1 Receptor-Mediated Neurotransmission in Dyskinesia. Mol Neurobiol [Internet]. 2015 Oct 26 [cited 2014 Oct 29];52(3):1408–20. Available from: http://www.ncbi.nlm.nih.gov/pubmed/25344317
48. Pinna A, Bonaventura J, Farré D, Sánchez M, Simola N, Mallol J, et al. l-DOPA disrupts adenosine A2A–cannabinoid CB1–dopamine D2 receptor heteromer cross-talk in the striatum of hemiparkinsonian rats: Biochemical and behavioral studies. Exp Neurol [Internet]. 2014 Mar [cited 2015 Mar 17];253:180–91. Available from: http://www.ncbi.nlm.nih.gov/pubmed/24412491
49. Muñoz A, Garrido-Gil P, Dominguez-Meijide A, Labandeira-Garcia JL. Angiotensin type 1 receptor blockage reduces l-dopa-induced dyskinesia in the 6-OHDA model of Parkinson's disease. Involvement of vascular endothelial growth factor and interleukin-1ß. Exp Neurol [Internet]. 2014 Nov [cited 2017 Aug 2];261:720–32. Available from: https://doi.org/10.1016/j.expneurol.2014.08.019
50. Winkler C, Kirik D, Björklund A, Cenci MA. L-DOPA-induced dyskinesia in the intrastriatal 6-hydroxydopamine model of parkinson's disease: relation to motor and cellular parameters of nigrostriatal function. Neurobiol Dis. 2002;10(2):165–86.
51. Schallert T, Kozlowski DA, Humm JL CR. Use-dependent structural events in recovery of function. Adv Neurol. 1997;73(1):229–38.
52. Kirik D, Winkler C, Björklund A. Growth and functional efficacy of intrastriatal nigral transplants depend on the extent of nigrostriatal degeneration. J Neurosci [Internet]. 2001 Apr 15 [cited 2016 Dec 7];21(8):2889–96. Available from: http://www.ncbi.nlm.nih.gov/pubmed/11306640
53. Lee CS, Cenci MA, Schulzer M, Björklund A. Embryonic ventral mesencephalic grafts improve levodopa-induced dyskinesia in a rat model of Parkinson's disease. Brain [Internet]. 2000 Jul [cited 2016 Dec 7];123 (Pt 7:1365–79. Available from: http://www.ncbi.nlm.nih.gov/pubmed/10869049
54. Lundblad M, Andersson M, Winkler C, Kirik D, Wierup N, Cenci Nilsson MA. Pharmacological validation of behavioural measures of akinesia and dyskinesia in a rat model of Parkinson's disease. Eur J Neurosci [Internet]. 2002 Jan [cited 2016 Dec 7];15(1):120–32. Available from: http://www.ncbi.nlm.nih.gov/pubmed/11860512
55. Benito C, Núñez E, Tolón RM, Carrier EJ, Rábano A, Hillard CJ, et al. Cannabinoid CB2 receptors and fatty acid amide hydrolase are selectively overexpressed in neuritic plaque-associated glia in Alzheimer's disease brains. J Neurosci [Internet]. 2003 Dec 3 [cited 2016 Feb 18];23(35):11136–41. Available from: http://www.ncbi.nlm.nih.gov/pubmed/14657172
56. De Filippis D, Steardo A, D'Amico A, Scuderi C, Cipriano M, Esposito G, et al. Differential Cannabinoid Receptor Expression during Reactive Gliosis: a Possible Implication for a Nonpsychotropic Neuroprotection. Sci World J [Internet]. 2009 Mar 31 [cited 2016 Dec 7];9:229–35. Available from: http://www.ncbi.nlm.nih.gov/pubmed/19347234
57. Ohlin KE, Sebastianutto I, Adkins CE, Lundblad C, Lockman PR, Cenci MA. Impact of L-DOPA treatment on regional cerebral blood flow and metabolism in the basal ganglia in a rat model of Parkinson's disease. Neuroimage [Internet]. 2012 May 15 [cited 2016 Dec 7];61(1):228–39. Available from: http://linkinghub.elsevier.com/retrieve/pii/S1053811912002510
58. Navarro G, Hradsky J, Lluís C, Casadó V, McCormick PJ, Kreutz MR, et al. NCS-1 associates with adenosine A(2A) receptors and modulates receptor function. Front Mol Neurosci [Internet]. 2012 Apr;5(April):53. Available from: http://www.pubmedcentral.nih.gov/articlerender.fcgi?artid=3328853&tool=pmcentrez&rendertype=abstract
59. Chen T-W, Wardill TJ, Sun Y, Pulver SR, Renninger SL, Baohan A, et al. Ultrasensitive fluorescent proteins for imaging neuronal activity. Nature [Internet]. 2013 Jul 17 [cited 2017 Jun 4];499(7458):295–300. Available from: http://www.ncbi.nlm.nih.gov/pubmed/23868258
60. Law AMK, Yin JXM, Castillo L, Young AIJ, Piggin C, Rogers S, et al. Andy's Algorithms: new automated digital image analysis pipelines for FIJI. Sci Rep [Internet]. 2017 Dec 16 [cited 2019 Aug 26];7(1):15717. Available from: http://www.nature.com/articles/s41598-017-15885-6
61. Giles ME, Fernley RT, Nakamura Y, Moeller I, Aldred GP, Ferraro T, et al. Characterization of a specific antibody to the rat angiotensin II AT1 receptor. J Histochem Cytochem [Internet]. 1999 [cited 2020 Oct 25];47(4):507–15. Available from: https://pubmed.ncbi.nlm.nih.gov/10082752/
62. Valenzuela R, Costa-Besada MAMA, Iglesias-Gonzalez J, Perez-Costas E, Villar-Cheda B, Garrido-Gil P, et al. Mitochondrial angiotensin receptors in dopaminergic neurons. Role in cell protection and aging-related vulnerability to neurodegeneration. Cell Death Dis [Internet]. 2016 Oct 20 [cited 2019 Sep 1];7(10):e2427. Available from: https://doi.org/10.1038/cddis.2016.327%5Cnhttp://www.ncbi.nlm.nih.gov/pubmed/27763643
63. Carriba P, Navarro G, Ciruela F, Ferré S, Casadó V, Agnati L, et al. Detection of heteromerization of more than two proteins by sequential BRET-FRET. Nat Methods [Internet]. 2008 Aug [cited 2015 Nov 22];5(8):727–33. Available from: http://www.ncbi.nlm.nih.gov/pubmed/18587404
64. Franco R, Fernández-Suárez D. Alternatively activated microglia and macrophages in the central nervous system. Prog Neurobiol

[Internet]. 2015 Jun 8 [cited 2015 Jun 14];131:65–86. Available from: http://www.ncbi.nlm.nih.gov/pubmed/26067058
65. Ferré S, Goldberg SR, Lluis C, Franco R. Looking for the role of cannabinoid receptor heteromers in striatal function. Neuropharmacology [Internet]. 2009 Jan [cited 2017 Dec 27];56(SUPPL. 1):226–34. Available from: http://www.ncbi.nlm.nih.gov/pubmed/18691604
66. Martínez-Pinilla E, Rico AJ, Rivas-Santisteban R, Lillo J, Roda E, Navarro G, et al. Expression of GPR55 and either cannabinoid CB1 or CB2 heteroreceptor complexes in the caudate, putamen, and accumbens nuclei of control, parkinsonian, and dyskinetic non-human primates. Brain Struct Funct [Internet]. 2020 Sep 1 [cited 2020 Oct 28];225(7):2153–64. Available from: https://pubmed.ncbi.nlm.nih.gov/32691218/
67. Tebano MT, Martire A, Popoli P. Adenosine A2A-cannabinoid CB1 receptor interaction: An integrative mechanism in striatal glutamatergic neurotransmission [Internet]. Vol. 1476, Brain Research. Brain Res; 2012 [cited 2020 Sep 24]. p. 108–18. Available from: https://pubmed.ncbi.nlm.nih.gov/22565012/
68. Ferré S, Agnati LF, Ciruela F, Lluis C, Woods AS, Fuxe K, et al. Neurotransmitter receptor heteromers and their integrative role in "local modules": The striatal spine module. Brain Res Rev [Internet]. 2007 Aug [cited 2017 Dec 27];55(1):55–67. Available from: http://www.ncbi.nlm.nih.gov/pubmed/17408563
69. Ferré S, Ciruela F, Quiroz C, Luján R, Popoli P, Cunha RARA, et al. Adenosine receptor heteromers and their integrative role in striatal function. ScientificWorldJournal [Internet]. 2007 Jan 2 [cited 2016 Feb 15];7(SUPPL. 2):74–85. Available from: https://pubmed.ncbi.nlm.nih.gov/17982579/
70. Franco R, Lluis C, Canela EI, Mallol J, Agnati L, Casadó V, et al. Receptor-receptor interactions involving adenosine A1 or dopamine D1 receptors and accessory proteins. J Neural Transm [Internet]. 2007 Jan 9 [cited 2018 Dec 30];114(1):93–104. Available from: http://www.ncbi.nlm.nih.gov/pubmed/17024327
71. Martínez-Pinilla E, Rodríguez-Pérez AII, Navarro G, Aguinaga D, Moreno E, Lanciego JLL, et al. Dopamine D2 and angiotensin II type 1 receptors form functional heteromers in rat striatum. Biochem Pharmacol [Internet]. 2015 Jul 15 [cited 2015 Dec 6];96(2):131–42. Available from: http://linkinghub.elsevier.com/retrieve/pii/S000629521500252X
72. Villar-Cheda B, Valenzuela R, Rodriguez-Perez AI, Guerra MJ, Labandeira-Garcia JL. Aging-related changes in the nigral angiotensin system enhances proinflammatory and pro-oxidative markers and 6-OHDA-induced dopaminergic degeneration. Neurobiol Aging [Internet]. 2012 Jan [cited 2019 Sep 1];33(1):204.e1-11. Available from: https://linkinghub.elsevier.com/retrieve/pii/S0197458010003544
73. Arnold AC, Gallagher PE, Diz DI. Brain renin-angiotensin system in the nexus of hypertension and aging. Vol. 36, Hypertension Research. Hypertens Res; 2013. p. 5–13.
74. Oertel WH. Parkinson's disease: epidemiology, (differential) diagnosis, therapy, relation to dementia. Arzneimittelforschung [Internet]. 1995 Mar [cited 2020 Jun 7];45(3A):386–9. Available from: http://www.ncbi.nlm.nih.gov/pubmed/7763330
75. Rocca W. Frequency, distribution, and risk factors for Alzheimer's disease. Nurs Clin North Am [Internet]. 1994 [cited 2020 Jun 7];29(1):101–11. Available from: https://europepmc.org/abstract/med/8121814
76. Hornykiewicz O. The discovery of dopamine deficiency in the parkinsonian brain. J Neural Transm Suppl [Internet]. 2006;70:9–15. Available from: http://www.ncbi.nlm.nih.gov/pubmed/17017502
77. Tang D, Comish P, Kang R. The hallmarks of COVID-19 disease. PLoS Pathog [Internet]. 2020 [cited 2020 Jun 7];16(5):e1008536. Available from: http://www.ncbi.nlm.nih.gov/pubmed/32442210
78. Lyngsø C, Erikstrup N, Hansen JL. Functional interactions between 7TM receptors in the Renin-Angiotensin System-Dimerization or crosstalk? Vol. 302, Molecular and Cellular Endocrinology. 2009. p. 203–12.
79. Ferrão FM, Lara LS, Axelband F, Dias J, Carmona AK, Reis RI, et al. Exposure of luminal membranes of LLC-PK $_1$ cells to ANG II induces dimerization of AT $_1$ /AT $_2$ receptors to activate SERCA and to promote Ca^{2+} mobilization. Am J Physiol Physiol [Internet]. 2012 Apr 1 [cited 2019 Aug 30];302(7):F875–83. Available from: http://www.ncbi.nlm.nih.gov/pubmed/22218590
80. Franco R, Aguinaga D, Jiménez J, Lillo J, Martínez-Pinilla E, Navarro G. Biased receptor functionality versus biased agonism in G-protein-coupled receptors. Biomol Concepts [Internet]. 2018 Dec 26 [cited 2019 Jul 26];9(1):143–54. Available from: http://www.ncbi.nlm.nih.gov/pubmed/30864350
81. Franco R, Casadó V, Cortés A, Ferrada C, Mallol J, Woods A, et al. Basic concepts in G-protein-coupled receptor homo- and heterodimerization. ScientificWorldJournal. 2007;7(SUPPL. 2).
82. Labandeira-Garcia J, Rodríguez-Perez A, Garrido-Gil P, Rodriguez-Pallares J, Lanciego J, Guerra M. Brain renin-angiotensin system and microglial polarization: Implications for aging and neurodegeneration. Front Aging Neurosci [Internet]. 2017 May 3 [cited 2019 Oct 4];9(MAY):129. Available from: http://www.ncbi.nlm.nih.gov/pubmed/28515690
83. Rodriguez-Perez AI, Sucunza D, Pedrosa MA, Garrido-Gil P, Kulisevsky J, Lanciego JL, et al. Angiotensin Type 1 Receptor Antagonists Protect Against Alpha-Synuclein-Induced Neuroinflammation and Dopaminergic Neuron Death. Neurotherapeutics [Internet]. 2018 Oct 9 [cited 2019 Sep 1];15(4):1063–81. Available from: http://www.ncbi.nlm.nih.gov/pubmed/29987762
84. Rodriguez-Pallares J, Rey P, Parga JA, Muñoz A, Guerra MJ, Labandeira-Garcia JL. Brain angiotensin enhances dopaminergic cell death via microglial activation and NADPH-derived ROS. Neurobiol Dis [Internet]. 2008 Jul [cited 2019 Oct 14];31(1):58–73. Available from: https://linkinghub.elsevier.com/retrieve/pii/S0969996108000533
85. Saavedra JM. Beneficial effects of Angiotensin II receptor blockers in brain disorders. Vol. 125, Pharmacological Research. Academic Press; 2017. p. 91–103.
86. Pelisch N, Hosomi N, Ueno M, Masugata H, Murao K, Hitomi H, et al. Systemic candesartan reduces brain angiotensin II via down-regulation of brain renin-angiotensin system. Hypertens Res [Internet]. 2010 Feb 27 [cited 2020 Jul 6];33(2):161–4. Available from: www.nature.com/hr
87. Foulquier S, Caolo V, Swennen G, Milanova I, Reinhold S, Recarti C, et al. The role of receptor MAS in microglia-driven retinal vascular development. Angiogenesis [Internet]. 2019 Nov 1 [cited 2020 Oct 23];22(4):481–9. Available from: https://pubmed.ncbi.nlm.nih.gov/31240418/
88. Deshotels MR, Xia H, Sriramula S, Lazartigues E, Filipeanu CM. Angiotensin II mediates angiotensin converting enzyme type 2 internalization and degradation through an Angiotensin II type I receptor-dependent mechanism. Hypertension. 2014;64(6):1368–75.
89. Ferrada C, Moreno E, Casadó V, Bongers G, Cortés A, Mallol J, et al. Marked changes in signal transduction upon heteromerization of dopamine D1 and histamine H3 receptors. Br J Pharmacol [Internet]. 2009 May 8 [cited 2016 May 16];157(1):64–75. Available from: http://www.ncbi.nlm.nih.gov/pubmed/19413572

3.7 Functional Complexes of Angiotensin-Converting Enzyme 2 and Renin-Angiotensin System Receptors: Expression in Adult but Not Fetal Lung Tissue.

Rafael Franco, Alejandro Lillo, **Rafael Rivas-Santisteban**, Ana I. Rodríguez-Pérez, Irene Reyes-Resina, Irene, José L. Labandeira-García y Gemma Navarro.

Manuscrito publicado en *International Journal of Molecular Sciences*, Diciembre 2020; 21, 9602.

La enzima convertidora de angiotensina 2 (ACE2) es una peptidasa de membrana y un componente clave del sistema renina-angiotensina (RAS) capaz de catalizar la reacción que degrada la angiotensina II (Ang II) a angiotensina 1-7 (Ang 1-7). ACE2 se expresa en las células de todos los órganos, incluidos los pulmones. En la actualidad está adquiriendo una gran importancia, ya que se ha descrito como la entrada principal por la que el SARS-CoV-2 puede penetrar a la célula. Años atrás ya se identificó la enzima ACE2 como el receptor que utilizan los coronavirus del síndrome respiratorio agudo severo (SARS). Sin embargo, el mecanismo subyacente a la entrada celular sigue siendo desconocido. Planteamos la hipótesis de que ACE2 también podría ser capaz de establecer interacciones estrechas con receptores acoplados a proteína G (GPCR) asociados al RAS. Usando ensayos de transferencia de energía por resonancia y ensayos de determinación de AMPc intracelular y proteína quinasa activada por mitógenos (MAPK), encontramos que el ACE2 humano interactúa con receptores del RAS, en concreto, tanto con el receptor de angiotensina II tipo 1 (AT_1R), como con el receptor de angiotensina II tipo 2 (AT_2R) y el receptor del protooncogén MAS1 (MasR). Aunque estas interacciones conducen a alteraciones menores de la transducción de señal, hemos observado como las células que expresan niveles más altos de AT_2R son más propensas a facilitar la adhesión del SARS-CoV-2 debido a los niveles más altos de expresión de ACE2 en membrana. Los ensayos de ligación por proximidad (PLA) realizados revelaron complejos macromoleculares compuestos por ACE2 y AT_1R, AT_2R o MasR en tejido pulmonar de ratón adulto, pero no fetal. Estos hallazgos destacan la relevancia del RAS en la infección por SARS-CoV-2 y el papel de los complejos que contienen ACE2 como posibles dianas terapéuticas.

International Journal of
Molecular Sciences

MDPI

Article

Functional Complexes of Angiotensin-Converting Enzyme 2 and Renin-Angiotensin System Receptors: Expression in Adult but Not Fetal Lung Tissue

Rafael Franco [1,2,*], Alejandro Lillo [1], Rafael Rivas-Santisteban [1,2], Ana I. Rodríguez-Pérez [2,3], Irene Reyes-Resina [1,4], José L. Labandeira-García [2,3] and Gemma Navarro [2,5,*]

1 Laboratory of Molecular Neurobiology, Department Biochemistry and Molecular Biomedicine, School of Biology, University of Barcelona, 08007 Barcelona, Spain; alilloma55@gmail.com (A.L.); rrivasbioq@gmail.com (R.R.-S.); ire-reyes@hotmail.com (I.R.-R.)
2 Network Center, Neurodegenerative Diseases (CiberNed), Spanish National Health Institute Carlos III, Valderrebollo 5, 28031 Madrid, Spain; anai.rodriguez@usc.es (A.I.R.-P.); joseluis.labandeira@usc.es (J.L.L.-G.)
3 Laboratory of Cellular and Molecular Neurobiology of Parkinson's Disease, Research Center for Molecular Medicine and Chronic Diseases (CIMUS), Department of Morphological Sciences, IDIS, University of Santiago de Compostela, 15705 Santiago de Compostela, Spain
4 RG Neuroplasticity, Leibniz Institute for Neurobiology, 39118 Magdeburg, Germany
5 Department of Biochemistry and Physiology, School of Pharmacy and Food Science, University of Barcelona, 08007 Barcelona, Spain
* Correspondence: rfranco123@gmail.com or rfranco@ub.edu (R.F.); g.navarro@ub.edu or dimartts@hotmail.com (G.N.); Tel.: +34-934-021-208 (R.F.); +34-934-034-500 (G.N.)

Received: 14 November 2020; Accepted: 11 December 2020; Published: 16 December 2020

Abstract: Angiotensin-converting enzyme 2 (ACE2) is a membrane peptidase and a component of the renin-angiotensin system (RAS) that has been found in cells of all organs, including the lungs. While ACE2 has been identified as the receptor for severe acute respiratory syndrome (SARS) coronaviruses, the mechanism underlying cell entry remains unknown. Human immunodeficiency virus infects target cells via CXC chemokine receptor 4 (CXCR4)-mediated endocytosis. Furthermore, CXCR4 interacts with dipeptidyl peptidase-4 (CD26/DPPIV), an enzyme that cleaves CXCL12/SDF-1, which is the chemokine that activates this receptor. By analogy, we hypothesized that ACE2 might also be capable of interactions with RAS-associated G-protein coupled receptors. Using resonance energy transfer and cAMP and mitogen-activated protein kinase signaling assays, we found that human ACE2 interacts with RAS-related receptors, namely the angiotensin II type 1 receptor (AT_1R), the angiotensin II type 2 receptor (AT_2R), and the MAS1 oncogene receptor (MasR). Although these interactions lead to minor alterations of signal transduction, ligand binding to AT_1R and AT_2R, but not to MasR, resulted in the upregulation of ACE2 cell surface expression. Proximity ligation assays performed in situ revealed macromolecular complexes containing ACE2 and AT_1R, AT_2R or MasR in adult but not fetal mouse lung tissue. These findings highlight the relevance of RAS in SARS-CoV-2 infection and the role of ACE2-containing complexes as potential therapeutic targets.

Keywords: COVID-19; SARS-CoV-2 receptor; RAS; ACE2; angiotensin receptor; Mas receptor; lung

1. Introduction

The current coronavirus disease-2019 (COVID-19) pandemic is the result of widespread infection with the severe acute respiratory syndrome-coronavirus-2 (SARS-CoV-2) pathogen. The main cell surface receptor for SARS-CoV-2 is angiotensin-converting enzyme 2 (ACE2), which is an enzyme that catalyzes the conversion of angiotensin II (Ang II) into angiotensin 1-7 (Ang 1-7). The link between ACE2 and SARS coronaviruses was discovered serendipitously [1–5]. ACE2 is a component of the renin-angiotensin system (RAS), which has been characterized extensively in the kidney and serves as the target of efficacious antihypertensive drugs. In addition to enzymes that process renin and angiotensin, components of the RAS include members of the G-protein-coupled receptor (GPCR) superfamily. Receptors for Ang II type 1 (AT_1Rs) and Ang II type 2 (AT_2Rs) share Ang II as an endogenous ligand. As noted, Ang II is also a substrate for enzymatic processing by ACE2 [6]. By contrast, the Mas1 oncogene receptor (MasR) interacts with Ang 1-7. Mas1, also known as the Mas-related proto-oncogene, is related to a putative ancestor gene identified in *Saccharomyces cerevisiae* that encodes mitochondrial assembly protein-1 [7]. Additional RAS receptors, the Mas-related GPCRs (Mrgprs), are also responsive to Ang 1-7 [8–10] and to another endogenous agonist that is an Ang 1-7 derivative, alamandine [6].

Coronaviruses and the human immunodeficiency virus (HIV), the latter pathogen recognized as the causative agent of acquired immunodeficiency syndrome (AIDS), have several common characteristics. Both RNA viruses contain nucleic acids enveloped within a membrane that contains host components and viral proteins that facilitate interactions with surface receptors on target cells. The most studied of the HIV subtypes, HIV-1, interacts with target cell surface receptors and co-receptors that are critical for entry into the host cell. HIV-1 entry requires interactions with the main receptor, CD4, and interactions with a GPCR co-receptor, most notably the CXC chemokine receptor, CXCR4 [11–17]. The chemokine CXCL12, also known as stromal-derived factor 1 (SDF-1), is the endogenous ligand of CXCR4. Interestingly, CXCL12/SDF-1 is degraded by dipeptidyl peptidase-4 (CD26/DPPIV). The actions of this enzyme serve to reduce the local concentration of CXCL12/SDF-1 and thereby protect the host cells from viral infection [18,19]. ACE2 and CD26/DPPIV are both proteases with several specific structural similarities. For example, both ACE2 and CD26/DPPIV are attached to cell membranes and can be removed and released into body fluids via a process known as shedding [20,21]. Furthermore, both enzymes are type I transmembrane proteins with a single transmembrane domain, a C-terminal domain facing the cytoplasm, and a large N-terminal extracellular domain that includes the catalytic site.

Glycoprotein 120 kDa (gp120) found on the surface of HIV-1 virions interacts with CD26/DPPIV, which may interact with CXCR4. Among the findings that support our hypothesis, we previously characterized co-modulation of CXCR4 and CD26/DPPIV in human lymphocytes. We also found that the non-catalytic activating function of CD26/DPPIV was altered in the presence of gp120 via a mechanism that was dependent on the expression of both CD4 and CXCR4 [19,22].

Based on these findings, we hypothesized that the ACE2 may have the capacity to interact with receptors that are activated by its substrate, Ang II, and its product, Ang 1-7. Accordingly, this paper aimed at examining the physical and functional interactions of ACE2 with cell surface receptors for Ang II and Ang 1-7. We also performed experiments designed to detect enzyme-receptor complexes in lung tissue, which is the main portal of entry for SARS-CoV-2.

2. Results

2.1. Expression of ACE2 Downregulates AT_1R-Mediated Signaling Induced by Ang II

ACE2 has been identified as the main receptor for SARS coronaviruses. Its substrate, Ang II, is an endogenous agonist that activates the G-protein-coupled receptors (GPCRs) AT_1R and AT_2R. AT_1R couples with the Gq protein; activation by agonists increases the levels of inositol triphosphate and diacylglycerol and mobilizes intracellular calcium. In this first set of experiments, we aimed to determine whether the expression of ACE2 has any impact on AT_1R-mediated signaling. Toward this end, we measured cytoplasmic Ca^{2+} levels in a heterologous expression system using the calmodulin-

derived Ca^{2+} sensor, GCaMP6. Ang II at concentrations of 1 nM to 100 nM was added to HEK-293T cells that expressed both AT1R and GCaMP6. A fluorescent signal with a maximum of 9000 AU at 150 s was detected in response to the two highest concentrations of Ang II (Figure 1A). Interestingly, in a similar experiment targeting HEK-293T cells expressing AT1R and ACE2, a significant decrease in the maximum response was observed (6000 AU signal at the highest concentration of Ang II; Figure 1B). These results suggest that the expression of ACE2 may inhibit AT1R-mediated signaling. The possibility of functional selectivity and Gi coupling was discarded from experiments that evaluated intracellular cAMP levels in the presence or absence of forskolin. While slight increases in cAMP levels were identified in response to micromolar concentrations of Ang II, the expression of ACE2 had no significant impact on these results (Figure 1C).

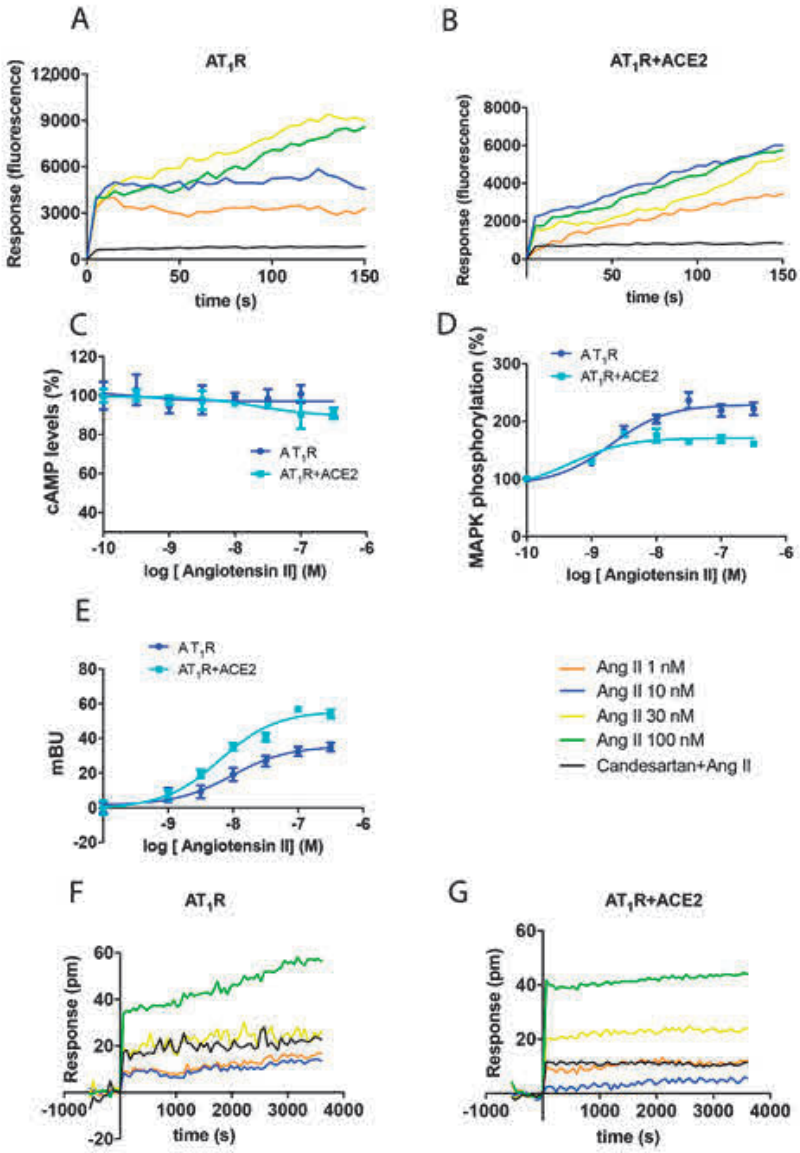

Figure 1. Impact of ACE2 on the functionality of AT1R. HEK-293T cells were transfected with either 0.4 μg AT1R cDNA and 0.2 μg ACE2-HA cDNA (**A**,**B**,**F**,**G**), 0.5 μg AT1R-YFP cDNA, 0.2 μg ACE2-HA cDNA, and 0.5 μg β-arrestin II-RLuc cDNA (**C**), or 0.4 μg AT1R cDNA, 0.2 μg ACE2-HA cDNA, and

0.5 μg cDNA encoding the Ca^{2+} sensor, GCaMP6 (**D**,**E**). After 48 h of incubation, cells were treated with increasing concentrations of the AT_1R agonist, Ang II. Cyclic AMP was measured after 15 min in response to pre-treatment with 0.5 μM forskolin (**A**); as shown, this intervention resulted in approximately 4 nM cAMP, which corresponds to a 240% increase over baseline levels. Results from the evaluation of ERK1/2 phosphorylation (**B**), β-arrestin II recruitment (**C**) Ca^{2+} levels (**D**,**E**), and DMR recordings (**F**,**G**) are presented as dose-response curves. Where indicated, cells were pre-treated with the selective AT_1R receptor antagonist, candesartan (1 μM), before challenge with the receptor agonist. Values shown are the mean ± SEM of 8 independent experiments each performed in triplicate.

Activation of GPCRs results in the engagement of the mitogen-activated protein kinase (MAPK) signaling pathway. As such, we measured extracellular signal-regulated kinase (ERK)1/2 phosphorylation in cells expressing AT_1R and ACE2. While the addition of Ang II to HEK-293T cells expressing AT_1R induced a 125% increase in ERK1/2 phosphorylation over baseline levels, the increase in phosphorylation observed in cells co-expressing AT_1R and ACE2 was limited to 71% (Figure 1D). Similar results were obtained using dynamic mass redistribution (DMR) assays, which is a technique that can be used to measure changes in cytoskeletal structure in response to GPCR activation and the engagement of G-proteins. With this assay, we found that the expression of ACE2 resulted in a 30% decrease in the overall impact of Ang II at AT_1R (Figure 1F,G). Finally, AT_1R-mediated recruitment of β-arrestin was evaluated in cells that co-express β-arrestin II-RLuc and AT_1R-YFP. The specific signal of 37 milli-Bioluminescence Resonance Energy Transfer (BRET) units (mBU) originally detected in cells expressing AT_1R alone increased by 20 mBU in response to ACE2 co-expression (Figure 1E). These results suggest that the expression of ACE2 augments AT_1R-mediated recruitment of β-arrestins.

Taken together, our findings revealed that the expression of ACE2 results in a decrease in AT_1R-mediated signaling in response to Ang II with a concomitant increase in the capacity for β-arrestin recruitment.

2.2. Expression of ACE2 Downregulates AT_2R-Mediated Signaling Induced by Ang II

Signaling assays were performed to assess the impact of ACE2 on AT_2R function. As AT_2R couples with Gi, we first determined intracellular cAMP levels in cells treated with forskolin. Findings shown in Figure 2A reveal that the addition of the selective AT_2R agonist, CGP-42112A (CGP), resulted in a 73% reduction in cAMP levels. This strong effect was attenuated in cells that co-expressed ACE2 (21% reduction). While similar results were obtained in DMR assays (Figure 2F,G), our findings revealed qualitative differences with respect to the engagement of the MAPK signaling pathway. Of note, we found that ERK1/2 phosphorylation following activation of AT_2R was increased from 90% to 232% in response to ACE2 (Figure 2B). These results indicate that ACE2 expression potentiates the link between AT_2R and MAPK signaling.

By contrast, expression of ACE2 had a less profound impact on β-arrestin recruitment via AT_2R when compared to responses mediated by AT_1R. $BRET_{max}$ was 22 mBU in cells expressing AT_2R; this response increased to 29 mBU when ACE2 was also expressed (Figure 2C). As anticipated from findings of AT_2R coupling with Gi and not to Gq, Ang II-mediated activation of this receptor-induced minimal mobilization of intracellular Ca^{2+}. This response was completely abolished in the presence of ACE2 (Figure 2D,E).

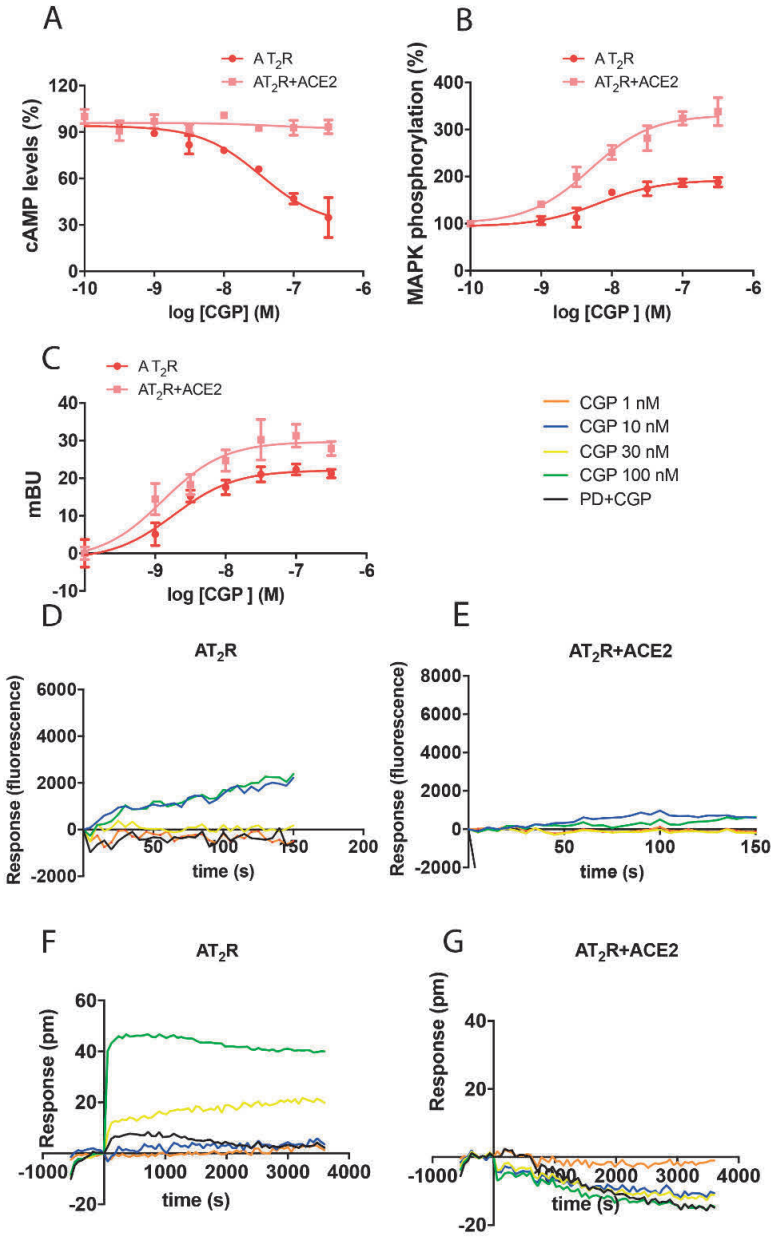

Figure 2. Impact of ACE2 on the functionality of AT2R. HEK-293T cells were transfected with either 0.3 µg AT2R cDNA and 0.2 µg ACE2-HA cDNA(**A**,**B**,**F**,**G**), 0.4 µg AT2R-YFP cDNA, 0.2 µg ACE2-HA cDNA, and 0.5 µg β-arrestin II-RLuc cDNA (**C**), or 0.3 µg AT2R cDNA, 0.2 µg ACE2-HA cDNA, and 0.5 µg cDNA encoding the Ca^{2+}sensor, GCaMP6 (**D**,**E**). After 48 h of incubation, cells were treated with increasing concentrations of the selective AT2R agonist, CGP. Cyclic AMP was measured after 15 min in response to pre-treatment with 0.5 µM forskolin (**A**); see also Legend to Figure 1. Results from the evaluation of ERK1/2 phosphorylation (**B**), β-arrestin II recruitment (**C**), Ca^{2+} levels (**D**,**E**), and DMR recordings (**F**,**G**) are presented as dose-response curves. Where indicated, cells were pre-treated with selective AT2R receptor antagonist, PD123319 (PD; 1 µM), before challenge with the receptor agonist. Values are the mean ± SEM of 8 independent experiments each performed in triplicate.

2.3. Expression of ACE2 Potentiates MasR-Mediated Signaling

Assays analogous to those described in earlier sections were performed to determine the impact of ACE2 on the functionality of MasR. While the recruitment of β-arrestin in response to receptor activation with its ligand, Ang 1-7, was not affected by co-expression of ACE2, expression of ACE2 resulted in the enhancement of all other transduced signals. This was observed in assays targeting cAMP and ERK1/2 phosphorylation and was notably strong with respect to the results of DMR analysis (Figure 3). As such, not only does the catalytic activity of ACE2 generate the endogenous agonist for this receptor, our results reveal that the expression of this enzyme may increase the signaling output from MasR via an enzyme-independent mechanism. We confirmed that MasR activation resulted in no changes in cytoplasmic Ca^{2+} levels, regardless of the presence or absence of ACE2 (Figure 3D,E).

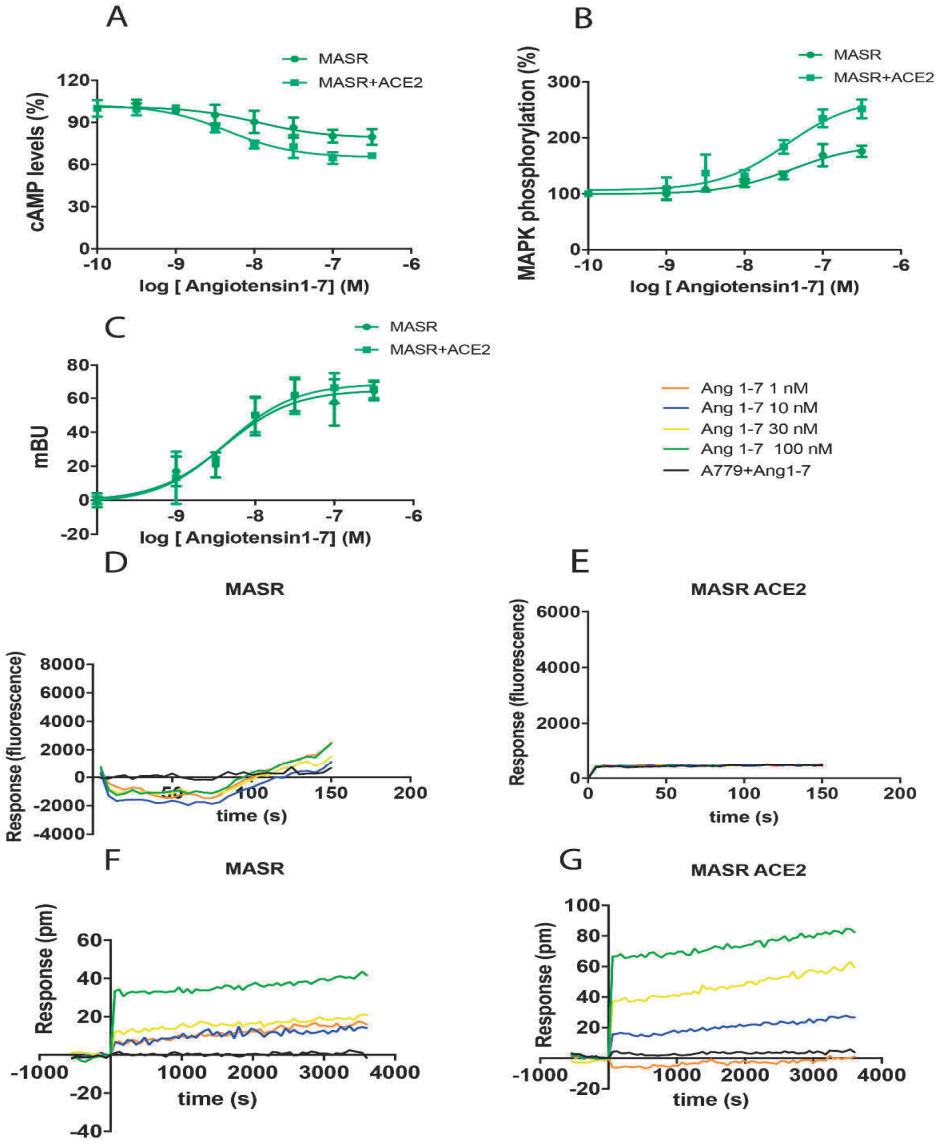

Figure 3. Impact of ACE2 on the functionality of MasR. HEK-293T cells were transfected with 0.5 μg MasR cDNA and 0.2 μg ACE2-HA cDNA (**A**,**B**,**F**,**G**), 0.6 μg MasR-YFP cDNA, 0.2 μg ACE2-HA cDNA, and 0.5 μg encoding β-arrestin II-RLuc cDNA (**C**), or 0.5 μg MasR cDNA, 0.2 μg ACE2-HA cDNA, and 0.5 μg cDNA encoding the Ca^{2+} sensor, GCaMP6 (**D**,**E**). After 48 h of incubation, cells were treated with increasing concentrations of the selective MasR agonist, Ang 1-7. Cyclic AMP was

measured after 15 min in response to pre-treatment with 0.5 μM forskolin (**A**); see also Legend to Figure 1. Results from the evaluation of ERK1/2 phosphorylation (B), β-arrestin II recruitment (**C**), Ca^{2+} levels (**D**,**E**), and DMR recordings (**F**,**G**) are presented as dose-response curves. Where indicated, cells were pre-treated with the selective MasR receptor antagonist, A779 (1 μM), before challenge with the receptor agonist. Values presented are the mean ± SEM of 6 independent experiments each performed in triplicate.

2.4. ACE2 Interacts Directly with AT_1R, AT_2R, and MasR

Naïve HEK-293T cells do not express functionally significant concentrations of RAS components. As such, we hypothesize that outcomes associated with ACE2 expression may be a direct result of receptor-enzyme interactions.

This hypothesis was tested using BRET assays. First, HEK-293T cells were transfected with a constant amount of cDNA encoding AT_1R-RLuc and increasing amounts of cDNA encoding ACE2-eGFP. Findings shown in Figure 4A include a saturable BRET curve which is indicative of direct interactions between AT_1R and ACE2 ($BRET_{max}$ = 120 ± 20 mBU and $BRET_{50}$ = 16 ± 4). Similar assays were performed in cells pretreated for 10 min with Ang II or with the selective AT_1R antagonist, candesartan. While a significant decrease in BRET signal was detected after challenging with the agonist ($BRET_{max}$ = 90 ± 10 mBU and $BRET_{50}$ = 21 ± 5), these parameters did not undergo significant change in response to treatment with a receptor antagonist, candesartan ($BRET_{max}$ = 12 ± 20 mBU and $BRET_{50}$ = 15 ± 5; Figure 4A). These results may be explained by conformational changes that alter the distance between BRET donor and BRET acceptor. Another possibility is internalization, disassembly and recycling in response to agonist challenge. The latter process would lead to reduce the number of AT_1R-ACE2 complexes.

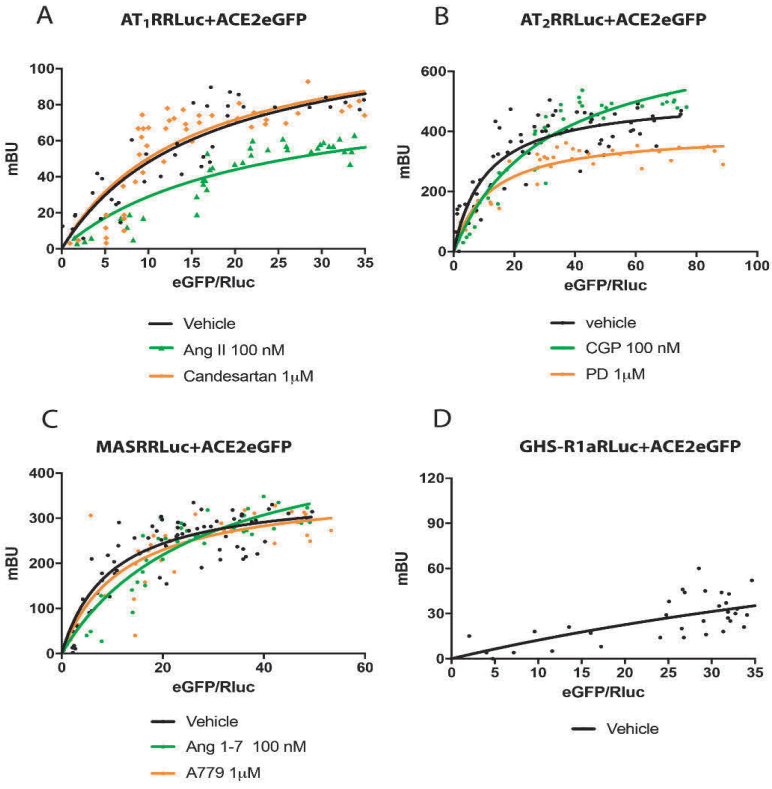

Figure 4. Interactions of RAS receptors and ACE2 as assessed by Bioluminescence Resonance Energy Transfer (BRET) assays. BRET assays were performed in HEK-293T cells transfected with constant amounts of cDNA encoding AT_1R-RLuc (0.5 μg) (**A**), AT_2R-RLuc (0.4 μg) (**B**), MasR-RLuc (0.6 μg) (**C**),

or GHS-R1a-RLuc (0.3 μg; negative control) (**D**) together with increasing amounts of cDNA encoding ACE2-eGFP (0.1 to 1 μg). Cells were treated (red symbols) or not (black symbols) for 25 min with selective antagonists (candesartan for AT_1R, PD123319 for AT_2R or A779 for MasR, both at 1 μM; red symbols) or selective agonists (Ang II for AT_1R, CGP for AT_2R or Ang 1-7 for MasR, all at 100 nM; green symbols). Values correspond to experimental points from 6 independent experiments each performed in quadruplicate. $BRET_{50}$ and $BRET_{max}$ values were calculated by non-linear regression using Prism GraphPad software; specific parameters are as described in the text.

Potential AT_2R-ACE2 interactions were examined in experiments performed in HEK-293T cells transfected with a constant amount of cDNA encoding AT_2R-RLuc and increasing amounts of cDNA encoding ACE2-eGFP. The saturable BRET curve ($BRET_{max}$ = 510 ± 20 mBU and $BRET_{50}$ = 11 ± 2) revealed the formation of AT_2R-ACE2 complexes in the co-transfected HEK-293T cells. However, we observed a significant increase in the height at saturation ($BRET_{max}$ = 750 ± 70 mBU and $BRET_{50}$ = 31 ± 6) in co-transfected cells that were challenged with the AT_2R agonist, CGP (Figure 4B). These results may be explained by conformational changes that reduce the distance between the BRET donor and BRET acceptor. The findings might also be explained by an increase in the number of receptor-enzyme complexes. Challenge with the AT_2R antagonist, PD123319, led to a significant decrease in the BRET signal when compared to results from untreated cells ($BRET_{max}$ = 400 ± 20 mBU and $BRET_{50}$ = 12 ± 2).

Finally, we addressed the possibility of physical interactions between MasR and ACE2. BRET assays confirmed these interactions. However, we observed no responses to treatment with MasR agonists or antagonists (Figure 4C). Parameters defining this interaction were: $BRET_{max}$ = 362 ± 21 mBU and $BRET_{50}$ = 10 ± 2 in the absence of receptor activation, $BRET_{max}$ = 420 ± 60 mBU and $BRET_{50}$ = 16 ± 5 in cells treated with receptor agonist, and $BRET_{max}$ = 370 ± 40 mBU and $BRET_{50}$ = 12 ± 4 in cells treated with receptor antagonist. A non-specific linear signal was obtained in HEK-293T cells that were transfected with the cDNA encoding GHS-R1a-RLuc (negative control) together with increasing amounts of ACE2 (Figure 4D).

2.5. Cell Surface Expression of ACE2 Following Activation of AT_1R and AT_2R

Our findings revealed that ACE2 was capable of functionally interact with RAS receptors. We also discovered that direct interactions between ACE2 and AT_1R and AT_2R underwent a quantitative change in response to receptor activation. As such, our next aim was to assess cell surface expression of ACE2 following RAS receptor activation.

Cell surface expression of ACE2 was first assessed by immunocytochemistry assays targeting HEK-293T cells that express this enzyme together with AT_1R, AT_2R, or MasR. As shown in Figure 5A, ACE2 and the three receptors were all detected at the plasma membrane and were also associated with intracellular structures in the cytoplasm. Dual localization was also observed in cells treated with selective agonists.

Increased green fluorescence documenting ACE2 immunoreactivity in the cytoplasm was detected in AT_1R and ACE2-expressing cells that were treated with Ang II. These results suggested that activation of AT_1R results in decreased expression of ACE2 at the plasma membrane (Figure 5A). By contrast, no significant changes in ACE2 immunoreactivity were detected when cells expressing AT_2R or MasR were treated with their respective receptor agonists.

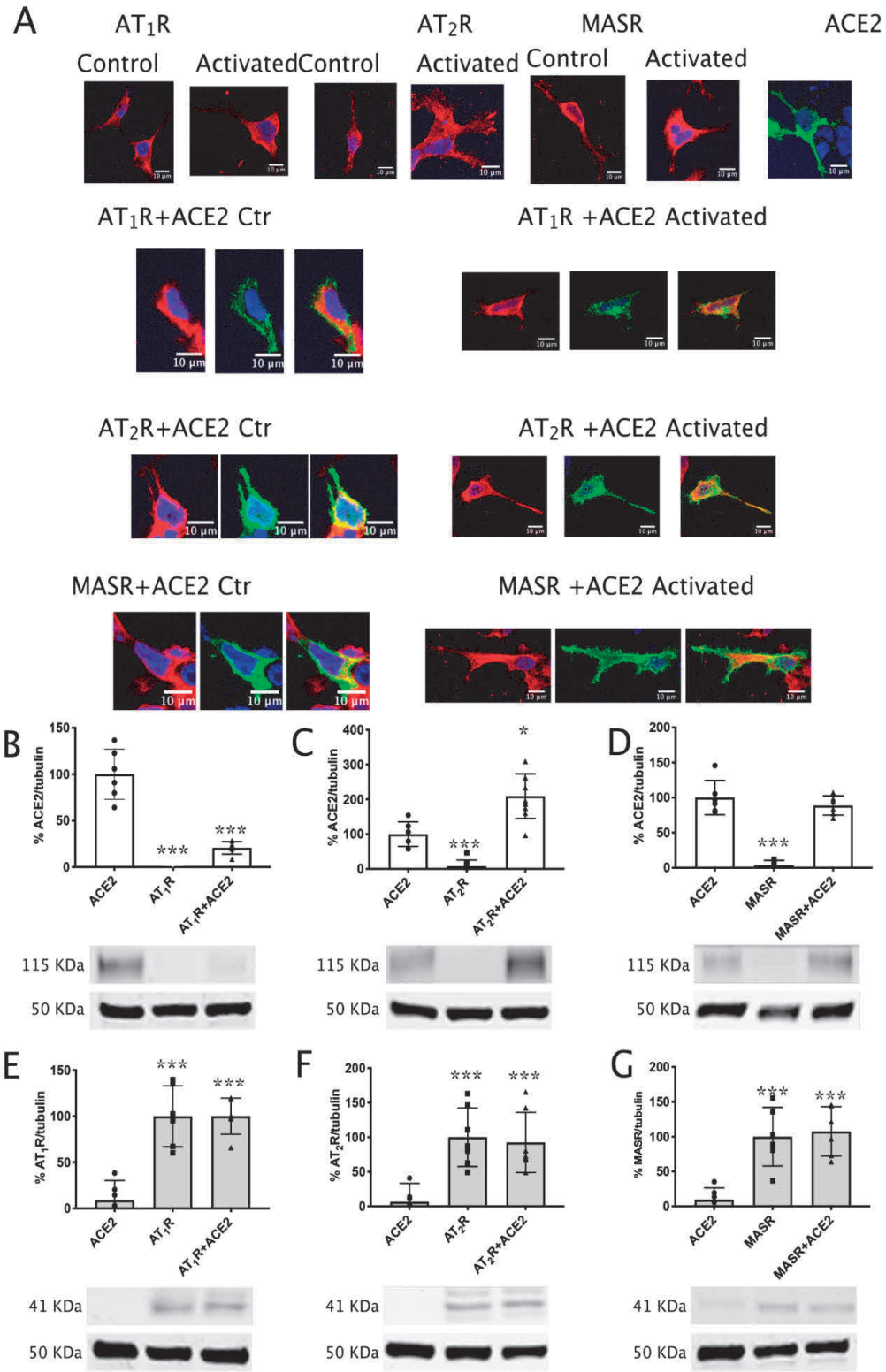

Figure 5. RAS receptors regulate cell surface expression of ACE2. (**A**) Immunocytochemistry assays were performed in HEK-293T cells expressing ACE2-eGFP together with AT1R-RLuc, AT2R-RLuc, or MasR-RLuc and activated with the respective agonists. Cells that expressed each RAS receptor were treated with their respective selective agonist. ACE2-eGFP expression was evaluated quantitatively

via green fluorescence. The Rluc-containing receptors were detected by an anti-RLuc primary antibody and a secondary Cy3-conjugated anti-mouse antibody (red-staining). Colocalization is shown in yellow. Scale bar = 10 μm. (**B–G**) Biotinylation experiments were performed in HEK-293T cells transfected with cDNA encoding AT_1R-RLuc (1 μg; **B**,**E**), AT_2R-RLuc (1 μg; **C**,**F**) or MasR-RLuc (1 μg; **D**,**G**) with or without 0.8 μg of ACE2-HA cDNA. Images from a representative experiment are shown (expansion of the image areas in Figure 5 and position of the MW from this representative experiment appear in Supplementary Figure S1). Immunoreactive bands from 6 independent experiments were quantified. Values presented are the mean ± SD. One-way ANOVA followed by Bonferroni's multiple comparison posthoc tests were used for statistical analysis; * $p < 0.05$, *** $p < 0.001$ vs. ACE2-HA singly-transfected cells.

For improved assessment of cell surface expression, we performed biotinylation experiments using co-transfected cells. The assay conditions used in these experiments permit biotinylation of cell surface proteins only. Immunoblotting was performed on preparations of isolated biotinylated proteins. Fusion proteins containing Rluc or eYFP were used to normalize protein expression; this facilitated comparisons of similar expression levels in experiments performed in cells that expressed ACE2 alone, a receptor, or ACE2 together with a receptor. Using this method, we found that co-expression of ACE2 had no significant impact on the expression of any of the three RAS receptors evaluated (Figure 5B–G).

The results from HEK-293T cells that co-expressed AT_1R-RLuc and ACE2 and were activated with Ang II revealed decreased expression of ACE2-eGFP on Western blots (Figure 5B). When similar assays were performed in cells that co-expressed AT_2R-RLuc and ACE2, a significant increase in the enzyme expression was observed (Figure 5C). However, no differential regulation of ACE2 was observed in HEK-293T cells co-expressing MasR (Figure 5D). The presence of ACE2 had no impact on the expression of AT_1R, AT_2R, or MASR (Figure 5E–G).

Taken together, our results indicate that ligand-mediated activation of AT_1R resulted in diminished cell surface expression of ACE2. By contrast, activation of AT_2R resulted in elevated levels of ACE2. No differential expression of this enzyme was observed in response to activation of MasR.

2.6. Detection of AT_1R-ACE2, AT_2R-ACE2, and MasR-ACE2 Complexes in the Lungs of Adult Mice

Children are less likely to succumb to severe SARS-CoV2 infection; it has been hypothesized that this may be due to comparatively lower levels of ACE2 in lung tissue. Given the findings described above, our next goal was to evaluate ACE2-receptor complexes in the lungs of adult and fetal CD-1 mice. This investigation was approached using sections of fixed tissue and in situ proximity ligation assay (PLA). This technique is instrumental for the detection of complexes formed by two proteins in natural sources.

Using specific antibodies raised against the proteins of interest, we could detect that 14% of cells expressed AT_1R-ACE2 complexes with around 10 red dots/cell-expressing dots (Figure 6A), 11% of cells expressed AT_2R-ACE2 complexes with around 6 red dots/cell-expressing dots (Figure 6B) and that only 8% of cells expressed MasR-ACE2 complexes with around 7 red dots/cell-expressing dots (Figure 6C). These results demonstrate the existence of AT_1R-ACE2, AT_2R-ACE2 and MasR-ACE2 complexes in the adult lung of mice (Figure 6G). Remarkably, no positive signals were observed for any pair of proteins in sections from fetuses (<1% of cells expressed red clusters) (Figure 6D–F,H).

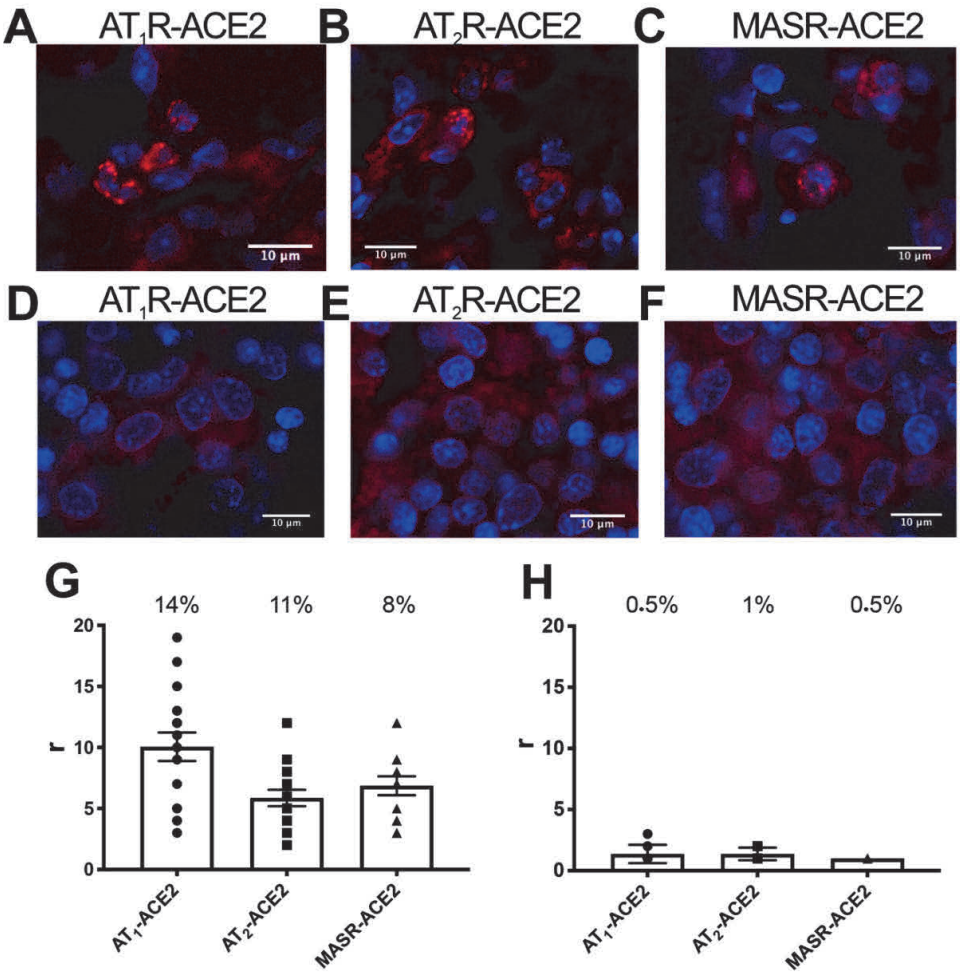

Figure 6. Detection of AT_1R-ACE2, AT_2R-ACE2, and MasR-ACE2 complexes in mouse lung tissue. Proximity Ligation Assays (PLAs) were performed using lung sections of adult (**A**–**C**) or 19-day fetal CD-1 mice (**D**–**F**) as described in the Methods. Cell nuclei were stained with Hoechst (blue). Protein complexes appear as red clusters or dots. Representative images corresponding to stacks of 4 sequential planes are shown. Graphs (**G**,**H**) display the number of clusters and spots in spot-containing cells. Values presented are the mean ± SEM of 5 independent experiments.

3. Discussion

ACE2 on target cells has been identified as a critical receptor for SARS and other coronaviruses [23–26]. However, the mechanisms underlying SARS-CoV-2 entry into cells and the role of ACE2 in facilitating viral infection remain to be clarified. Similar to what has been observed for HIV-1 infection, GPCRs may facilitate viral infection. GPCRs constitute approximately 10% of the human proteome; they are typically expressed on the cell surface and can be internalized via clathrin- or caveolin-dependent mechanisms [27–30]. To the best of our knowledge, there are no published studies that link GCPRs or GPCR internalization mechanisms to the coronavirus life cycle. Of note, peptides derived from SARS, HIV-1 and Ebola virus proteins bind with high affinity to formyl-peptide receptors [30,31]. The physiological role of this GPCR with respect to viral infection is currently unclear.

The chemokine receptor CXCR4 was identified as an HIV-1 co-receptor and mediator of cell entry soon after the identification of this pathogen as the causative agent of AIDS [13,16]. Subsequent studies revealed that CD26/DPPIV interacts with CXCR4 and is targeted by envelope gp120 HIV-1

glycoprotein [19,22,32,33]. HIV-1 entry into target cells involves CXCR4 as well as interactions with CD26/DPPIV and the receptor agonist, CXCL12/SDF-1, which is also a substrate of this enzyme. Potential parallels to mechanisms underlying HIV-1 infection have led us to hypothesize that there is a gap in SARS-related research that will be only fulfilled once GPCRs are considered [34].

As the most straightforward approach toward the identification of GPCRs that may be involved in SARS-CoV-2 infection, we focused on receptors that interact with the ACE2 substrate, Ang II. Toward this end, results of RNA-based interference assays performed in the dorsal vagal complex of the mouse brainstem suggested the existence of interactions between ACE2 and AT_1R [35]. However, the approach used in this study was not designed to address the possibility of direct protein-protein interactions. Similarly, Deshotels et al. [36] performed an important study using both cell transfection and rodent model approaches that revealed Ang II-mediated and AT_1R-dependent regulation of ACE2 expression; the results of co-immunoprecipitation experiments suggested interactions between the two cell surface proteins. This biophysical approach can be used to identify direct interactions; the results revealed that ACE2 may interact with both AT_1R and AT_2R and also with MasR, which is the receptor for Ang 1-7, the product of ACE2-mediated cleavage of Ang II.

Protein-protein interactions occurring at the plasma membrane can modify receptor-mediated signaling responses. As shown here, the expression of ACE2 modulated agonist-induced signaling at all three receptors (i.e., AT_1R, AT_2R, or MasR). Negative modulation of AT_1R or AT_2R-mediated signaling might be expected, given that ACE2 ultimately degrades the endogenous agonist, Ang II. However, the high-affinity CGP agonist used to promote signaling via AT_2R does not undergo significant degradation by ACE2. Equally interesting was the modulation of ACE2 expression observed upon receptor activation. Our results add to findings reported by Bai et al. [37], who described telmisartan-induced downregulation of AT_1R with a concomitant increase in ACE2 activity; treatment of hypertensive rats with this selective AT_1R antagonist rebalanced the RAS system. We found that activation of MasR, the receptor for Ang 1-7, had no significant impact on ACE2 expression. However, activation of the Ang II receptors, AT_1R and AT_2R, led to different outcomes, a finding that is consistent with the opposing physiological roles presumably played by these two receptors.

The loss of cell surface ACE2 in a physiological context could be due to endocytosis or to shedding; the latter phenomenon has been reported for the HIV-1-related peptidase, CD26/DPPIV [20,21]. However, in our experimental conditions, changes in cell surface expression of ACE2 were largely dependent on processes underlying endocytosis and trafficking to the cell surface. This finding is important as it implies that the availability of the SARS receptor might vary depending on the status of the RAS, most notably on the local concentration of Ang II and the relative expression of both AT_1R and AT_2R. As these parameters may vary from cell to cell even under homeostatic conditions, SARS-CoV-2 infection may generate symptoms of varying severity. In other words, the expression of RAS components in a given cell may dictate its susceptibility to SARS-CoV-2 infection and responses that include mild to more severe symptoms of this disease. Our results suggest that cells that express higher levels of AT_2R, especially when activated by Ang II, are more likely to facilitate SARS-CoV-2 attachment due to higher levels of ACE2 expression. Further experiments, preferably those performed with infectious SARS-CoV-2 particles, would be needed to determine whether cells enriched in AT_2R and activated by the endogenous agonist are more susceptible to virion binding, and to assess whether the RAS-related GPCRs complexed with ACE2 promote viral endocytosis.

Severe COVID-19 involves pneumonia and fatal outcomes that often correlate with elevated plasma levels of interleukin-6 (IL-6) and the cytokine storm [38–42]. High levels of IL-6 may be due to its overproduction by activated macrophages as well as by non-immune cells. Of note, bacterial endotoxin has been found to induce the synthesis of IL-6 in osteoblasts [43] and endothelial cells [44]. High levels of ACE2 expression have been detected in the lung which includes an air-exposed interface that is composed of a variety of cells; ACE2 in the human lung is particularly abundant in bronchial transient secretory cells [45,46]. Lung tissue includes both endothelial and epithelial cells that can express nearly all RAS components. Of particular note, ACE2 has been localized at the apical

side of polarized cells [47] where it can facilitate interactions with inhaled virions. As such, our final important objective was to identify ACE2-receptor complexes in the lung. This was made possible by in situ PLA, which is a technique that was specifically developed to detect complexes formed by two membrane proteins [48]. Using this method, we found that ~10% of the cells in adult mouse lung tissue expressed one or more complexed protein pairs, including ACE2/AT_1R, ACE2/AT_2R, and ACE2/MasR. Remarkably, no complexes were detected in mouse fetal lung sections. Given these findings, it is tempting to speculate that the predominance of mild or even asymptomatic infection in children exposed to SARS-CoV-2 might be directly related to the absence of receptor-enzyme complexes that promote viral entry into lung cells. Taken together, our findings suggest that further consideration of ACE2-containing RAS receptor complexes might reveal critical features underlying the mechanism of SARS-CoV-2 infection.

4. Material and Methods

Studies were designed to include groups of equal size and used randomization methods and blinded analysis. Antibody-based immunocytochemical assays were conducted in line with guidelines detailed elsewhere [49,50].

4.1. Reagents

Ang II, CGP, Ang 1-7, candesartan, PD123319, A779, and forskolin were purchased from Sigma-Aldrich (St. Louis, MO, USA).

4.2. Expression Vectors

cDNAs encoding human AT_1R, AT_2R, and MASR were amplified without their stop codons using sense and antisense primers that included either BamHI and HindIII restriction sites (for amplification of AT_1R and AT_2R) or BamHI and EcoRI restriction sites (for amplification of MasR) and subcloned into the pcDNA3.1 expression vector. Amplified fragments were subcloned in-frame with genes encoding the enhanced yellow fluorescent protein (pEYFP-N1; Clontech, Heidelberg, Germany) or Rluc (pRluc-N1; PerkinElmer, Wellesley, MA, USA) at the respective C-termini to produce AT_1R-RLuc, AT_1R-YFP, AT_2R-RLuc, AT_2R-YFP, MAS-RLuc, and MAS-YFP fusion proteins. cDNAs in pcDNA3.1 for ACE2-eGFP (ACE2_OHu20260C_pcDNA3.1(+)-C-eGFP Clone ID: OHu20260C; ORF Clones: Accession No.:NM_021804.3) and for ACE2-HA (ACE2_OHu20260C_pcDNA3.1(+)-N-HA Clone ID:OHu20260C; ORF Clones: Accession No.:NM_021804.3) were purchased from GenScript Biotech (Leiden, The Netherlands).

4.3. Cell Culture and Transient Transfection

HEK-293T cells were grown in Dulbecco's Modified Eagle's Medium (DMEM; Gibco, Paisley, Scotland, UK) supplemented with 2 mM L-glutamine, 100 U/mL penicillin/streptomycin, MEM Non-Essential Amino Acids Solution (1/100) and 5% (*v*/*v*) heat-inactivated fetal bovine serum (FBS) (Invitrogen, Paisley, Scotland, UK). Cells were maintained in a humid atmosphere at 5% CO_2 at 37 °C. Cells were transiently transfected using the polyethylenimine (PEI; Sigma-Aldrich) method as previously described [51].

4.4. Bioluminescence Resonance Energy Transfer (BRET) Assays

HEK-293T cells were transiently transfected with a constant amount of cDNA encoding AT_1R-RLuc, AT_2R-RLuc, MasR-RLuc, or GHS-R1a-Rluc (the latter used as a negative control) together with increasing amounts of cDNA encoding ACE2-eGFP. At 48 h after transfection, cells were adjusted to 20 μg of protein using a Bradford assay kit (Bio-Rad, Munich, Germany) using bovine serum albumin (BSA) for standardization. To quantify protein-eGFP expression, fluorescence was read in a FluoStar Optima Fluorometer (BMG LabTechnologies, Offenburg, Germany) equipped with a high-energy xenon flash lamp and a 10 nm bandwidth excitation filter at 485 nm. For BRET measurements, readings were collected 30 s after the addition of 5 μM coelenterazine H (Molecular Probes, Eugene,

OR, USA) using a Mithras LB 940, which facilitates the integration of signals detected from both the short-wavelength (485 nm) and the long-wavelength filters (510 nm). To quantify protein-RLuc expression, luminescence readings were performed 10 min after the addition of 5 μM coelenterazine H also using a Mithras LB 940. The net BRET is defined as ([long-wavelength emission]/[short-wavelength emission]) minus C_f, with C_f corresponding to the [long-wavelength emission]/[short-wavelength emission] ratio for the donor construct expressed alone in the same experiment. GraphPad Prism software (San Diego, CA, USA) was used to fit the data. BRET is expressed as milli-BRET units (mBU = net BRET × 1000).

4.5. Immunostaining Procedures

HEK-293T cells expressing AT_1R-RLuc, AT_2R-RLuc, or MasR-RLuc in the presence or the absence of ACE2-eGFP were fixed in 4% paraformaldehyde for 15 min and washed twice with phosphate-buffered saline (PBS) containing 20 mM glycine (PBS-glycine). Washed cells were then permeabilized with PBS-glycine containing 0.5% Triton X-100 for 5 min. Fixed and permeabilized cells were treated for 1 h with PBS containing 1% BSA and labeled with primary mouse anti-RLuc antibody (1/100; Millipore, MA, USA) followed by secondary Cy3-conjugated anti-mouse IgG antibody (1/200; Jackson ImmunoResearch, Philadelphia, PA, USA). Samples were washed several times and mounted with 30% Mowiol (Calbiochem/Merck Group, Darmstadt, Germany). Samples were observed using a Zeiss 880 confocal microscope. The signal from eGFP was detected by its green fluorescence and could be distinguished from the red signal observed in response to binding of Cy3-conjugated anti-mouse IgG. Colocalization was identified by yellow fluorescence. The scale bar presented in images measured 10 μm.

4.6. cAMP Determination

HEK-293T cells were transfected with cDNAs encoding AT_1R, AT_2R, or MasR in the presence or the absence of ACE2-HA. Cells were serum-starved in DMEM alone for 2 h before initiating an experiment. Starved cells were detached and suspended in culture medium containing 50 μM of the phosphodiesterase inhibitor, zardaverine (Sigma-Aldrich). Cells were then distributed into 384-well microplates at 2500 cells/well and stimulated for 15 min with increasing concentrations of agonists, including Ang II for AT_1R, CGP for AT_2R, and Ang 1-7 for MasR. Agonists were added at concentrations 0.1 nM to 3 μM or vehicle alone; this was followed by the addition of 0.5 μM forskolin or vehicle alone for an additional 15 min. Readings were performed after a 1 h incubation at 25 °C. Homogeneous time-resolved fluorescence energy transfer (HTRF) measurements were performed using the Lance Ultra cAMP kit (PerkinElmer, Waltham, MA, USA). Fluorescence at 665 nm was analyzed on a PHERAstar Flagship microplate reader equipped with an HTRF optical module (BMG Lab Technologies, Offenburg, Germany).

4.7. ERK Phosphorylation Assays

To determine the extent of ERK1/2 phosphorylation, HEK-293T cells were transfected with cDNAs encoding AT_1R, AT_2R, or MasR in the presence or the absence of ACE2-HA, plated at 40,000 cells/well in transparent Deltalab 96-well microplates, and incubated at 5% CO_2 for 48 h. Cells were serum-starved in DMEM alone for 2–4 h before the start of the experiment. Serum-starved cells were treated for 7 min at 25°C with vehicle or increasing concentrations of agonists (0.1 nM to 3 μM) including Ang II, CGP, or Ang 1-7 for specific receptors as described above. Cells were then washed twice with cold PBS and placed in lysis buffer; cells were lysed for 20 min while undergoing agitation. A 10 μL aliquot of each supernatant was placed in each well of a white ProxiPlate 384-well microplate, and the degree of ERK 1/2 phosphorylation was determined using an AlphaScreen®SureFire® kit (Perkin Elmer) following the instructions of the supplier and using an EnSpire® Multimode Plate Reader (PerkinElmer).

4.8. β-Arrestin 2 Recruitment

Recruitment of β-arrestin was evaluated as previously described [52,53]. Briefly, Bioluminescence Resonance Energy Transfer (BRET) experiments were performed using HEK-293T cells at 48 h after transfection with cDNAs encoding AT_1R-YFP, AT_2R-YFP, or MasR-YFP together with β-arrestin II-Rluc in the presence or the absence of ACE2-HA. Cells (20 μg protein per aliquot) were distributed in 96-well microplates (Corning 3600, white plates with white bottom, Sigma-Aldrich) and were stimulated for 10 min with the indicated agonists, including Ang II, CGP, or Ang 1-7 as described above at concentrations of 0.1 nM to 3 μM before the addition of 5 μM coelenterazine H (Molecular Probes, Eugene, OR). Within 1 min of the addition of coelenterazine H, BRET between β-arrestin II-RLuc and receptor-YFP was determined and quantified. The readings were collected using a Mithras LB 940 (Berthold Technologies, Bad Wildbad, Germany) that facilitates the integration of the signals as described above. To quantify protein-RLuc expression, luminescence readings were performed at 10 min after the addition of 5 μM coelenterazine H.

4.9. Cytoplasmic Ca^{2+} Detection

HEK-293T cells were transfected with the cDNA encoding AT_1R, AT_2R, or MasR together with the Ca^{2+} sensor, GCaMP6 [54] in the presence or the absence of ACE2-HA using the PEI method. At 24 h after transfection, 150,000 cells were plated in each well of a 96-well black, clear-bottom microtiter plate. Cells were then incubated with Mg^{+2}-free Locke's buffer (154 mM NaCl, 5.6 mM KCl, 3.6 mM $NaHCO_3$, 2.3 mM $CaCl_2$, 5.6 mM glucose, and 5 mM HEPES at pH 7.4) supplemented with 10 μM glycine, and pre-treated for 10 min with the selective antagonists, including candesartan (for AT_1R), PD123319 (for AT_2R) and A779 (for MasR), followed by stimulation with increasing concentrations (1 nM to 1 μM) of agonists, including Ang II, CGP, and Ang 1-7 as described above. The fluorescence emission intensity of GCaMP6 was recorded (every 5 s for 150 s, 100 flashes/well) at 515 nm upon excitation at 488 nm on the EnSpire® multimode plate reader.

4.10. Dynamic Mass Redistribution (DMR) Assays

Cell mass redistribution induced upon receptor activation was detected by illuminating the underside of the biosensor with polychromatic light followed by measuring the changes in the wavelength of the reflected monochromatic light. HEK-293T cells expressing AT_1R, AT_2R, or MasR in the presence or the absence of ACE2-HA were seeded in 384-well sensor microplates to 70–80% confluency (approximately 10,000 cells per well). Before the start of the experiment, cells were washed twice with assay buffer (Hank's buffered saline solution [HBSS] with 20 mM HEPES, pH 7.15) followed by a 2 h incubation with assay-buffer containing 0.1% dimethyl sulfoxide (DMSO; 24 °C, 30 μL/well). The sensor plate was then scanned, and a baseline optical signature was recorded for 10 min before adding 10 μL of each of the specific antagonists (candesartan, PD123319, or A779 as described above). Responses were recorded for 30 min; this was followed by the addition of 10 μL of increasing concentrations of the selective agonists (Ang II, CGP, or Ang 1-7) at concentrations from 1 nM to 1 μM; all test compounds were dissolved in assay buffer. Dynamic mass distribution (DMR) responses were monitored for at least 3000 s using an EnSpire® Multimode Plate Reader (PerkinElmer). Results were analyzed using EnSpire Workstation Software v 4.10.

4.11. Immunoblotting

To determine levels of immunoreactive AT_1R, AT_2R, MasR, and ACE2-HA expression in transfected HEK-293T cells, equivalent amounts of cell protein (10 μg) were separated by denaturing 10% sodium dodecyl sulfate (SDS)-polyacrylamide gel electrophoresis (PAGE) and transferred onto polyvinylidene difluoride (PVDF)-fluorescence membranes. Membranes were treated overnight at 4 °C with a mixture of a mouse anti-β-tubulin antibody (1:2000; Sigma-Aldrich), a rabbit anti-ACE2 antibody (1:1000; Cat# ab108252, RRID:AB_10864415, Abcam, Cambridge, UK) and a mouse monoclonal anti-AT_1R antibody (1:1000; Cat# sc-515884, RRID:AB_2801404, Santa Cruz Biotechnology, Dallas, TX, USA), a rabbit monoclonal anti-AT_2R antibody (1:1000; Cat# ab92445,

RRID:AB_10561969, Abcam, Cambridge, UK) and a mouse monoclonal anti-MasR antibody (1:1000; Cat# sc-390453, RRID:AB_2801406, Santa Cruz Biotechnology). Cells were subsequently treated with a mixture of IRDye 800-conjugated anti-mouse antibody (1:10,000; #A9044 from Sigma-Aldrich) and IRDye 680-conjugated anti-rabbit antibody (1:10,000; #926-68071 from LICOR Biosciences, Lincoln, NE, USA) for 2 h at room temperature. Bands were scanned using the Odyssey infrared scanner (LI-COR Biotechnology, Lincoln, NE, USA). Band densities were quantified using the scanner software and receptor level was normalized for differences in loading via normalization to tubulin protein band intensities.

4.12. Biotinylation Experiments

Cell surface proteins were biotinylated as previously described [55,56] using HEK-293T cells that transiently express AT_1R-RLuc, AT_2R-Rluc, or MasR-RLuc in the presence or the absence of ACE2-HA. Before initiation of the experiment, eGFP fluorescence was adjusted to 10,000 fluorescence units and receptor-RLuc to 100,000 bioluminescent units. Briefly, cells were washed three times with borate buffer (10 mM H_3BO_3, pH 8.8 with 150 mM NaCl) and incubated with 50 μg/mL sulfo-NHS-LC-biotin (ThermoFisher Scientific, Halethorpe, MD, USA) in borate buffer for 5 min at room temperature. Cells were then washed three times in borate buffer and again incubated with 50 μg/mL sulfo-NHS-LC-biotin in borate buffer for 10 min at room temperature. This was followed by the addition of 13 mM NH_4Cl for 5 min to quench the remaining biotin. Cells were washed in PBS, disrupted using a polytron (3 strokes at 10 s each), and centrifuged at 16,000× *g* for 30 min. The pellet was solubilized in an ice-cold RIPA buffer (50 mM Tris–HCl, 1% Triton X-100, 0.2% SDS, 100 mM NaCl, 1 mM EDTA, 0.5% sodium deoxycholate) for 30 min and centrifuged at 16,000× *g* for 20 min. The supernatant was incubated with 80 μl streptavidin-agarose beads (Sigma-Aldrich) for 1 h with constant rotation at 4 °C. Beads were washed three times with ice-cold lysis buffer and aspirated to dryness using a 28-gauge needle. Subsequently, 50 μl of SDS–PAGE sample buffer (8 M urea, 2% SDS, 100 mM dithiothreitol, 375 mM Tris, pH 6.8) was added to each sample. Proteins were dissociated by heating to 37 °C for 2 h, resolved by SDS-PAGE (10% gels), and immunoblotted as described above.

4.13. In Situ Proximity Ligation Assays (PLA)

Lungs from adult and 19-day-old fetal CD-1 mice were fixed in 4% paraformaldehyde for 1 day followed by processing with decreasing concentrations of sucrose. Tissue samples were cut in 30 μm-thick sections in a cryostat (Leica CM3050S), mounted on coverslips, and frozen. Frozen tissue samples were washed with PBS containing 20 mM glycine and permeabilized by incubation for 30 min in PBS-glycine containing 0.05% Triton X-100. Tissue sections were incubated for 1 h at 37 °C with blocking solution followed by specific antibodies, including mouse anti-AT_1R (1:100; Cat# sc-515884, RRID:AB_2801404, Santa Cruz Biotechnology), rabbit anti-AT_2R (1:100; Cat# ab92445, RRID:AB_10561969, Abcam), mouse anti-MasR (1:100; Cat# sc-390453, RRID:AB_2801406, Santa Cruz Biotechnology), and rabbit anti-ACE2 (1:100; Cat# ab108252, RRID:AB_10864415, Abcam). These samples were processed using PLA probes that detect rabbit and mouse antibodies (Duolink II PLA probe anti-Rabbit plus and Duolink II PLA probe anti-Mouse minus). Nuclei were stained with Hoechst (1/200; Sigma-Aldrich) and mounted in 30% Mowiol (Calbiochem). Samples were observed using a Zeiss 880 confocal microscope (Leica Microsystems, Mannheim, Germany) equipped with an apochromatic 63X oil-immersion objective (N.A. 1.4), and 405 nm and 561 nm laser lines. For each field of view, a stack of two channels (one per staining) and three to four Z stacks with a step size of 1 μm were acquired. Duolink Image took software was used to identify cells with one or more red spots vs. total cells (cell count determined by the presence of a single blue-stained nucleus). The ratio r was determined as the number of red spots per cell in all red spot-containing cells. This analysis was performed in a blinded fashion (i.e., the observer did not know which sample was undergoing processing and the analyzer did not know whether the results came from adult or fetal mice.

4.14. Validation of Antibody Specificity

Despite the excellent performance of these antibodies in different laboratories [57–60], the specificity of antibodies directed against angiotensin receptors is always subject to question. As such, we performed a series of experiments in which the anti-Ang II receptor antibodies were tested against naïve HEK-293T cells and against cells that express either AT_1R or AT_2R. Signal detected from anti-AT_1R antibody binding was negligible in both naïve and AT_2R-expressing HEK-293T cells. Similarly, the signal detected from anti-AT_2R antibody binding was negligible in both naïve and AT_1R-expressing cells (Supplementary Figure S2). These results are consistent with previous studies that addressed the specificity of antibodies used to detect AT_1Rs in mitochondria [61].

4.15. Data Analysis

Data were obtained from at least five independent experiments and are presented as the mean ± standard error of the mean (SEM). Two-group comparisons were performed using unpaired Student's *t*-tests. Multiple comparisons were performed using one-way ANOVA followed by Bonferroni's post hoc test or two-way ANOVA followed by Tukey's post hoc test. The normality of populations and homogeneity of variances were tested before performing ANOVA. Post hoc tests were run only in the cases in which F achieved $p < 0.05$ and in which there was no significant variance with respect to homogeneity. Statistical analysis was undertaken only when each group size was at least $n = 5$, with n representing the number of independent variables. Technical replicates were not treated as independent variables. Unequal group sizes were due to (a) different sources due to the wide variety of experimental approaches, (b) the need to increase the "n" to ensure data reliability in some of the assays, (c) animal availability, and/or (d) economy of resources as directed by the 3Rs (Replacement, Reduction, and Refinement) rule that governs experimentation with animals. Differences were considered significant when $p \leq 0.05$. Statistical analyses were carried out with GraphPad Prism software version 5 (San Diego, CA, USA; (RRID: SCR_002798)). Outlier tests were not used; all data points (representing the means of technical replicates) were used for analysis. The data and statistical analysis comply with the recommendations detailed elsewhere [49].

4.16. Nomenclature of Targets and Ligands

Key protein targets and ligands in this article are hyperlinked to corresponding entries in http://www.guidetopharmacology.org, the common portal for data from the IUPHAR/BPS Guide to PHARMACOLOGY [62] and are permanently archived in the Concise Guide to PHARMACOLOGY 2019/20 [6].

Supplementary Materials: The following are available online at www.mdpi.com/1422-0067/21/24/9602/s1, Figure S1: Expansion of the image areas in Figure 5 and position of the MW markers corresponding to immunoblots in Figure 5 of the main paper (panels refer to those in Figure 5). Figure S2: Antibody specificity control assays.

Author Contributions: G.N., J.L.L.-G. and R.F. designed and supervised the project. G.N. did all experiments except for those involving proximity ligation assays. A.L. and R.R.-S. helped with the preparation and cell transfection for the signaling assays. A.L. R.R.-S., A.I.R.-P. and I.R.-R. isolated tissue from fetuses and adult mice, performed PLA assays, and analyzed the results in a blinded fashion. R.F. and G.N. actively participated in writing and editing the manuscript. All authors have edited the paper and have received a copy of the final version. All authors have read and agreed to the published version of the manuscript.

Funding: The Molecular Neurobiology Laboratory of the University of Barcelona is considered a research group of excellence by the Regional Catalonian Government (grup consolidat #2017 SGR 1497). This organization does not provide specific funding for personnel, equipment, or reagents nor any payment for services.

Conflicts of Interest: The authors declare no conflict of interest.

Declaration of Transparency and Scientific Rigor: This Declaration acknowledges that this paper adheres to the principles for transparent reporting and scientific rigor for preclinical research as recommended by our Institutions, funding agencies, publishers, and other organizations engaged in supporting research.

References

1. Clarke, N.E.; Turner, A.J. Angiotensin-Converting Enzyme 2: The First Decade. *Int. J. Hypertens.* **2012**, *2012*, 1–12.
2. Wan, Y.; Shang, J.; Graham, R.; Baric, R.S.; Li, F. Receptor Recognition by the Novel Coronavirus from Wuhan: An Analysis Based on Decade-Long Structural Studies of SARS Coronavirus. *J. Virol.* **2020**, *94*.
3. Shang, J.; Ye, G.; Shi, K.; Wan, Y.; Luo, C.; Aihara, H.; Geng, Q.; Auerbach, A.; Li, F. Structural basis of receptor recognition by SARS-CoV-2. *Nature* **2020**, *581*, 221–224.
4. Kuhn, J.H.; Li, W.; Choe, H.; Farzan, M. Angiotensin-converting enzyme 2: A functional receptor for SARS coronavirus. *Cell. Mol. Life Sci.* **2004**, *61*, 2738–2743.
5. Li, W.; Moore, M.J.; Vasllieva, N.; Sui, J.; Wong, S.K.; Berne, M.A.; Somasundaran, M.; Sullivan, J.L.; Luzuriaga, K.; Greeneugh, T.C.; et al. Angiotensin-converting enzyme 2 is a functional receptor for the SARS coronavirus. *Nature* **2003**, *426*, 450–454.
6. Alexander, S.P.; Christopoulos, A.; Davenport, A.P.; Kelly, E.; Mathie, A.; Peters, J.A.; Veale, E.L.; Armstrong, J.F.; Faccenda, E.; Harding, S.D.; et al. The concise guide to pharmacology 2019/20: G protein-coupled receptors. *Br. J. Pharmacol.* **2019**, *176*, S21–S141.
7. Bader, M.; Alenina, N.; Young, D.; Santos, R.A.S.; Touyz, R.M. The meaning of mas. *Hypertension* **2018**, *72*, 1072–1075.
8. Souza, L.L.; Duchene, J.; Todiras, M.; Azevedo, L.C.P.; Costa-Neto, C.M.; Alenina, N.; Santos, R.A.; Bader, M. Receptor mas protects mice against hypothermia and mortality induced by endotoxemia. *Shock* **2014**, *41*, 331–336.
9. Santos, R.A.S.; Simoes e Silva, A.C.; Maric, C.; Silva, D.M.R.; Machado, R.P.; de Buhr, I.; Heringer-Walther, S.; Pinheiro, S.V.B.; Lopes, M.T.; Bader, M.; et al. Angiotensin-(1-7) is an endogenous ligand for the G protein-coupled receptor Mas. *Proc. Natl. Acad. Sci. USA* **2003**, *100*, 8258–8263.
10. Villela, D.; Leonhardt, J.; Patel, N.; Joseph, J.; Kirsch, S.; Hallberg, A.; Unger, T.; Bader, M.; Santos, R.A.; Sumners, C.; et al. Angiotensin type 2 receptor (AT 2 R) and receptor Mas: A complex liaison. *Clin. Sci.* **2015**, *128*, 227–234.
11. Berger, E.A.; Murphy, P.M.; Farber, J.M. CHEMOKINE RECEPTORS AS HIV-1 CORECEPTORS: Roles in Viral Entry, Tropism, and Disease. *Annu. Rev. Immunol.* **1999**, *17*, 657–700.
12. Wang, Q.; Finzi, A.; Sodroski, J. The Conformational States of the HIV-1 Envelope Glycoproteins. *Trends Microbiol.* **2020**.
13. Cammack, N. Human immunodeficiency virus type 1 entry and chemokine receptors: A new therapeutic target. *Antivir. Chem. Chemother.* **1999**, *10*, 53–62.
14. Hoxie, J.A.; Labranche, C.C.; Endres, M.J.; Turner, J.D.; Berson, J.F.; Doms, R.W.; Matthews, T.J. CD4-independent utilization of the CXCR4 chemokine receptor by HIV-1 and HIV-2. In *Journal of Reproductive Immunology*; J Reprod Immunol, 1998; Vol. 41, pp. 197–211.
15. Clapham, P.R.; Reeves, J.D.; Simmons, G.; Dejucq, N.; Hibbitts, S.; McKnight, Á. HIV coreceptors, cell tropism and inhibition by chemokine receptor ligands. In *Molecular Membrane Biology*; Taylor and Francis Ltd.: Abingdon, UK, 1999; Volume 16, pp. 49–55.
16. Choe, H. Chemokine receptors in HIV-1 and SIV infection. *Arch. Pharm. Res.* **1998**, *21*, 634–639.
17. Howard, O.M.Z.; Korte, T.; Tarasova, N.I.; Grimm, M.; Turpin, J.A.; Rice, W.G.; Michejda, C.J.; Blumenthal, R.; Oppenheim, J.J. Small molecule inhibitor of HIV-1 cell fusion blocks chemokine receptor- mediated function. *J. Leukoc. Biol.* **1998**, *64*, 6–13.
18. Shioda, T.; Kato, H.; Ohnishi, Y.; Tashiro, K.; Ikegawa, M.; Nakayama, E.E.; Hu, H.; Kato, A.; Sakai, Y.; Liu, H.; et al. Anti-HIV-1 and chemotactic activities of human stromal cell-derived factor 1α (SDF-1α) and SDF-1β are abolished by CD26/dipeptidyl peptidase IV-mediated cleavage. *Proc. Natl. Acad. Sci. USA* **1998**, *95*, 6331–6336.
19. Herrera, C.; Morimoto, C.; Blanco, J.; Mallol, J.; Arenzana, F.; Lluis, C.; Franco, R. Comodulation of CXCR4 and CD26 in Human Lymphocytes. *J. Biol. Chem.* **2001**, *276*, 19532–19539.
20. Yuzawa, Y.; Brentjens, J.R.; Brett, J.; Caldwell, P.R.; Esposito, C.; Fukatsu, A.; Godman, G.; Stern, D.; Andres, G. Antibody-mediated redistribution and shedding of endothelial antigens in the rabbit. *J. Immunol.* **1993**, *150*, 5633–5646.
21. Yamaguchi, N.; Plant, C.; Biancone, L.; Bachovchin, W.; Mccluskey, R.; Andres, G. In vivo modulation of CD26 (dipeptidyl peptidase IV) in the mouse: Effects of polyreactive and monoreactive antibodies. *Transplantation* **1996**, *62*, 973–985.

22. Blanco, J.; Valenzuela, A.; Herrera, C.; Lluís, C.; Hovanessian, A.G.; Franco, R.; Lluís, C.; Hovanessian, A.G.; Franco, R. The HIV-1 gp120 inhibits the binding of adenosine deaminase to CD26 by a mechanism modulated by CD4 and CXCR4 expression. *FEBS Lett.* **2000**, *477*, 123–128.
23. Yan, R.; Zhang, Y.; Li, Y.; Xia, L.; Zhou, Q. Structure of dimeric full-length human ACE2 in complex with B0AT1. *bioRxiv* **2020**, 2020.02.17.951848.
24. Chen, J.; Subbarao, K. The Immunobiology of SARS. *Annu. Rev. Immunol. Doremalen* **2007**, *25*, 443–472.
25. Wu, K.; Li, W.; Peng, G.; Li, F. Crystal structure of NL63 respiratory coronavirus receptor-binding domain complexed with its human receptor. *Proc. Natl. Acad. Sci. USA* **2009**, *106*, 19970–19974.
26. Kuba, K.; Imai, Y.; Rao, S.; Gao, H.; Guo, F.; Guan, B.; Huan, Y.; Yang, P.; Zhang, Y.; Deng, W.; et al. A crucial role of angiotensin converting enzyme 2 (ACE2) in SARS coronavirus-induced lung injury. *Nat. Med.* **2005**, *11*, 875–879.
27. Escriche, M.; Burgueño, J.; Ciruela, F.; Canela, E.I.; Mallol, J.; Enrich, C.; Lluís, C.; Franco, R. Ligand-induced caveolae-mediated internalization of A1 adenosine receptors: Morphological evidence of endosomal sorting and receptor recycling. *Exp. Cell Res.* **2003**, *285*, 72–90.
28. Ginés, S.; Ciruela, F.; Burgueño, J.; Casadó, V.; Canela, E.I.I.; Mallol, J.; Lluís, C.; Franco, R. Involvement of caveolin in ligand-induced recruitment and internalization of A(1) adenosine receptor and adenosine deaminase in an epithelial cell line. *Mol. Pharmacol.* **2001**, *59*, 1314–1323.
29. Wu, D.-F.; Yang, L.-Q.; Goschke, A.; Stumm, R.; Brandenburg, L.-O.; Liang, Y.-J.; Höllt, V.; Koch, T. Role of receptor internalization in the agonist-induced desensitization of cannabinoid type 1 receptors. *J. Neurochem.* **2008**, *104*, 1132–1143.
30. Mills, J.S. Peptides derived from HIV-1, HIV-2, Ebola virus, SARS coronavirus and coronavirus 229E exhibit high affinity binding to the formyl peptide receptor. *Biochim. Biophys. Acta* **2006**, *1762*, 693–703.
31. Braun, M.C.; Wang, J.M.; Lahey, E.; Rabin, R.L.; Kelsall, B.L. Activation of the formyl peptide receptor by the HIV-derived peptide T-20 suppresses interleukin-12 p70 production by human monocytes. *Blood* **2001**, *97*, 3531–3536.
32. Blanco, J.; Nguyen, C.; Callebaut, C.; Jacotot, E.; Krust, B.; Mazaleyrat, J.-P.; Wakselman, M.; Hovanessian, A.G. Dipeptidyl-peptidase IV-beta. Further characterization and comparison to dipeptidyl-peptidase IV activity of CD26. *Eur. J. Biochem.* **1998**, *256*, 369–378.
33. Valenzuela, A.; Blanco, J.; Callebaut, C.; Jacotot, E.; Lluis, C.; Hovanessian, A.G.; Franco, R. Adenosine Deaminase Binding to Human CD26 Is Inhibited by HIV-1 Envelope Glycoprotein gp120 and Viral Particles. *J. Immunol.* **1997**, *158*.
34. Franco, R.; Rivas-Santisteban, R.; Serrano-Marín, J.; Rodríguez-Pérez, A.; Labandeira-García, J.; Navarro, G. SARS-CoV-2 as a Factor to Disbalance the Renin–Angiotensin System: A Suspect in the Case of Exacerbated IL-6 Production. *J. Immunol.* **2020**, ji2000642.
35. Lin, Z.; Chen, Y.; Zhang, W.; Chen, A.F.; Lin, S.; Morris, M. RNA interference shows interactions between mouse brainstem angiotensin AT1 receptors and angiotensin-converting enzyme 2. *Exp. Physiol.* **2008**, *93*, 676–684.
36. Deshotels, M.R.; Xia, H.; Sriramula, S.; Lazartigues, E.; Filipeanu, C.M. Angiotensin II mediates angiotensin converting enzyme type 2 internalization and degradation through an Angiotensin II type I receptor-dependent mechanism. *Hypertension* **2014**, *64*, 1368–1375.
37. Bai, F.; Pang, X.F.; Zhang, L.H.; Wang, N.P.; McKallip, R.J.; Garner, R.E.; Zhao, Z.Q. Angiotensin II AT1 receptor alters ACE2 activity, eNOS expression and CD44-hyaluronan interaction in rats with hypertension and myocardial fibrosis. *Life Sci.* **2016**, *153*, 141–152.
38. Herold, T.; Jurinovic, V.; Arnreich, C.; Hellmuth, J.C.; Bergwelt-Baildon, M.; Klein, M.; Weinberger, T. Level of IL-6 predicts respiratory failure in hospitalized symptomatic COVID-19 patients. *medRxiv* **2020**, 2020.04.01.20047381.
39. Henry, B.M.; de Oliveira, M.H.S.; Benoit, S.; Plebani, M.; Lippi, G. Hematologic, biochemical and immune biomarker abnormalities associated with severe illness and mortality in coronavirus disease 2019 (COVID-19): A meta-analysis. *Clin. Chem. Lab. Med.* **2020**, *8*, 1021–1028, doi: 10.1515/cclm-2020-0369.
40. Cummings, M.J.; Baldwin, M.R.; Abrams, D.; Jacobson, S.D.; Meyer, B.J.; Balough, E.M.; Aaron, J.G.; Claassen, J.; Rabbani, L.E.; Hastie, J.; et al. Epidemiology, clinical course, and outcomes of critically ill adults with COVID-19 in New York City: A prospective cohort study. *medRxiv* **2020**, doi:10.1016/S0140-6736(20)31189-2.

41. Liu, T.; Zhang, J.; Yang, Y.; Ma, H.; Li, Z.; Zhang, J.; Cheng, J.; Zhang, X.; Zhao, Y.; Xia, Z.; et al. The role of interleukin-6 in monitoring severe case of coronavirus disease 2019. *EMBO Mol. Med.* **2020**, *2*, e12421, doi:10.15252/emmm.202012421.
42. Gong, J.; Dong, H.; Xia, S.Q.; Huang, Y.Z.; Wang, D.; Zhao, Y.; Liu, W.; Tu, S.; Zhang, M.; Wang, Q.; et al. Correlation Analysis Between Disease Severity and Inflammation-related Parameters in Patients with COVID-19 Pneumonia. *medRxiv* **2020**, doi:10.1101/2020.02.25.20025643.
43. Kondo, A.; Koshihara, Y.; Togari, A. Signal Transduction System for Interleukin-6 Synthesis Stimulated by Lipopolysaccharide in Human Osteoblasts. *J. Interf. Cytokine Res.* **2001**, *21*, 943–950.
44. Modat, G.; Dornand, J.; Bernad, N.; Junquero, D.; Mary, A.; Muller, A.; Bonne, C. LPS-stimulated bovine aortic endothelial cells produce IL-1 and IL-6 like activities. *Agents Actions* **1990**, *30*, 403–411.
45. Hamming, I.; Timens, W.; Bulthuis, M.L.C.; Lely, A.T.; Navis, G.J.; van Goor, H. Tissue distribution of ACE2 protein, the functional receptor for SARS coronavirus. A first step in understanding SARS pathogenesis. *J. Pathol.* **2004**, *203*, 631–637.
46. Lukassen, S.; Chua, R.L.; Trefzer, T.; Kahn, N.C.; Schneider, M.A.; Muley, T.; Winter, H.; Meister, M.; Veith, C.; Boots, A.W.; et al. SARS -CoV-2 receptor ACE 2 and TMPRSS 2 are primarily expressed in bronchial transient secretory cells. *EMBO J.* **2020**, *39*, e105114, doi:10.15252/embj.20105114
47. Warner, F.J.; Lew, R.A.; Smith, A.I.; Lambert, D.W.; Hooper, N.M.; Turner, A.J. Angiotensin-converting enzyme 2 (ACE2), but not ACE, is preferentially localized to the apical surface of polarized kidney cells. *J. Biol. Chem.* **2005**, *280*, 39353–39362.
48. Borroto-Escuela, D.O.; Hagman, B.; Woolfenden, M.; Pinton, L.; Jiménez-Beristain, A.; Oflijan, J.; Narvaez, M.; Di Palma, M.; Feltmann, K.; Sartini, S.; et al. In situ proximity ligation assay to study and understand the distribution and balance of GPCR homo- and heteroreceptor complexes in the brain. *Neuromethods* **2016**, *110*, 109–124.
49. Curtis, M.J.; Alexander, S.; Cirino, G.; Docherty, J.R.; George, C.H.; Giembycz, M.A.; Hoyer, D.; Insel, P.A.; Izzo, A.A.; Ji, Y.; et al. A. Experimental design and analysis and their reporting II: Updated and simplified guidance for authors and peer reviewers. *Br. J. Pharmacol.* **2018**, *175*, 987–993.
50. Alexander, S.P.H.; Roberts, R.E.; Broughton, B.R.S.; Sobey, C.G.; George, C.H.; Stanford, S.C.; Cirino, G.; Docherty, J.R.; Giembycz, M.A.; Hoyer, D.; et al. Goals and practicalities of immunoblotting and immunohistochemistry: A guide for submission to the British Journal of Pharmacology. *Br. J. Pharmacol.* **2018**, *175*, 407–411.
51. Navarro, G.; Hradsky, J.; Lluís, C.; Casadó, V.; McCormick, P.J.; Kreutz, M.R.; Mikhaylova, M. NCS-1 associates with adenosine A(2A) receptors and modulates receptor function. *Front. Mol. Neurosci.* **2012**, *5*, 53.
52. Bonaventura, J.; Navarro, G.; Casadó-Anguera, V.; Azdad, K.; Rea, W.; Moreno, E.; Brugarolas, M.; Mallol, J.; Canela, E.I.; Lluís, C.; et al. Allosteric interactions between agonists and antagonists within the adenosine A2A receptor-dopamine D2 receptor heterotetramer. *Proc. Natl. Acad. Sci. USA* **2015**, *112*, E3609–18.
53. Martínez-Pinilla, E.; Rodríguez-Pérez, A.I.I.; Navarro, G.; Aguinaga, D.; Moreno, E.; Lanciego, J.L.L.; Labandeira-García, J.L.L.; Franco, R. Dopamine D2 and angiotensin II type 1 receptors form functional heteromers in rat striatum. *Biochem. Pharmacol.* **2015**, *96*, 131–142.
54. Chen, T.-W.; Wardill, T.J.; Sun, Y.; Pulver, S.R.; Renninger, S.L.; Baohan, A.; Schreiter, E.R.; Kerr, R.A.; Orger, M.B.; Jayaraman, V.; et al. Ultrasensitive fluorescent proteins for imaging neuronal activity. *Nature* **2013**, *499*, 295–300.
55. Ciruela, F.; Soloviev, M.M.; Jeffrey McIlninney, R.A. Co-expression of metabotropic glutamate receptor type 1α with Homer-1a/Vesl-1S increases the cell surface expression of the receptor. *Biochem. J.* **1999**, *341*, 795–803.
56. Canals, M.; Burgueño, J.; Marcellino, D.; Cabello, N.; Canela, E.I.; Mallol, J.; Agnati, L.; Ferré, S.; Bouvier, M.; Fuxe, K.; et al. Homodimerization of adenosine A2A receptors: Qualitative and quantitative assessment by fluorescence and bioluminescence energy transfer. *J. Neurochem.* **2004**, *88*, 726–734.
57. Obermüller, N.; Gentili, M.; Gauer, S.; Gretz, N.; Weigel, M.; Geiger, H.; Gassler, N. Immunohistochemical and mRNA Localization of the Angiotensin II Receptor Subtype 2 (AT2) in Follicular Granulosa Cells of the Rat Ovary. *J. Histochem. Cytochem.* **2004**, *52*, 545–548.
58. Giles, M.E.; Fernley, R.T.; Nakamura, Y.; Moeller, I.; Aldred, G.P.; Ferraro, T.; Penschow, J.D.; McKinley, M.J.; Oldfield, B.J. Characterization of a specific antibody to the rat angiotensin II AT1 receptor. *J. Histochem. Cytochem.* **1999**, *47*, 507–515.

59. Rodriguez-Perez, A.I.; Valenzuela, R.; Villar-Cheda, B.; Guerra, M.J.; Lanciego, J.L.; Labandeira-Garcia, J.L. Estrogen and angiotensin interaction in the substantia nigra. Relevance to postmenopausal Parkinson's disease. *Exp. Neurol.* **2010**, *224*, 517–526.
60. Ruiz-Ortega, M.; Esteban, V.; Suzuki, Y.; Ruperez, M.; Mezzano, S.; Ardiles, L.; Justo, P.; Ortiz, A.; Egido, J. Renal expression of angiotensin type 2 (AT2) receptors during kidney damage. In *Kidney International, Supplement*; Blackwell Publishing Inc.: Malden, MA, USA, 2003; Volume 64.
61. Valenzuela, R.; Costa-Besada, M.A.M.A.; Iglesias-Gonzalez, J.; Perez-Costas, E.; Villar-Cheda, B.; Garrido-Gil, P.; Melendez-Ferro, M.; Soto-Otero, R.; Lanciego, J.L.J.L.; Henrion, D.; et al. Mitochondrial angiotensin receptors in dopaminergic neurons. Role in cell protection and aging-related vulnerability to neurodegeneration. *Cell Death Dis.* **2016**, *7*, e2427.
62. Harding, S.D.; Sharman, J.L.; Faccenda, E.; Southan, C.; Pawson, A.J.; Ireland, S.; Gray, A.J.G.; Bruce, L.; Alexander, S.P.H.; Anderton, S.; et al. The IUPHAR/BPS Guide to Pharmacology in 2018: Updates and expansion to encompass the new guide to immunopharmacology. *Nucleic Acids Res.* **2018**, *46*, D1091–D1106.

3.8 An ACE2/Mas-related receptor MrgE axis in dopaminergic neuron mitochondria.

Rita Valenzuela, Ana I. Rodriguez-Perez, Maria A. Costa-Besada, Araceli Piñeiro, **Rafael Rivas-Santisteban**, Pablo Garrido-Gil, Andrea Lopez-Lopez, Gemma Navarro, Jose L. Lanciego, Rafael Franco, Jose L. Labandeira-Garcia.

Manuscrito publicado en *Redox Biology*.

La enzima convertidora de angiotensina 2 (ACE2), componente clave del sistema renina-angiotensina (RAS), es el receptor de entrada a la célula para el virus SARS-CoV-2. Por este motivo, elucidar los mecanismos moleculares en los que ACE2 se encuentra involucrado es crucial para combatir la enfermedad COVID-19. En el cerebro, concretamente en la región de la *substantia nigra* de rata y mono, hemos detectado que el receptor ACE2, así como los productos de la reacción enzimática que cataliza (Ang 1-7 y alamandina) están altamente concentrados en las mitocondrias y se unen al receptor Mas Related E (MrgE), uno de los receptores del sistema renina-angiotensina alternativo, para producir óxido nítrico (NO). Se ha detectado la expresión del receptor MrgE en neuronas y en glía de la *substantia nigra* y otras regiones cerebrales en roedores y primates. Precisamente en las mitocondrias, se detectó, con el envejecimiento, una disminución de la expresión de ACE2 y MrgE y, en cambio, un aumento en la expresión de NOX4. Estas alteraciones a nivel de expresión del ACE2/MrgE mitocondrial con el envejecimiento pueden jugar un papel importante en la regulación del estrés oxidativo en las neuronas y posiblemente en otras células. También se observó que el tratamiento de células y mitocondrias aisladas con la espícula del virus aumentó el superóxido mitocondrial y disminuyó la actividad de ACE2 mitocondrial, respectivamente. Los resultados presentes sugieren que una desregulación del eje mitocondrial ACE2/MrgE/NO puede desempeñar un papel relevante en los efectos del SARS-CoV-2 a nivel celular.

Redox Biology

An ACE2/Mas-related receptor MrgE axis in dopaminergic neuron mitochondria

--Manuscript Draft--

Manuscript Number:	REDOX-D-21-00386R1
Article Type:	Research Paper
Keywords:	alamandine; Angiotensin 1-7; angiotensin converting enzyme 2; Parkinson; Oxidative Stress; renin-angiotensin system
Corresponding Author:	Jose Labandeira-Garcia University of Santiago de Compostela Santiago de Compostela, Spain
First Author:	Rita Valenzuela
Order of Authors:	Rita Valenzuela
	Ana I Rodriguez-Perez
	Maria A Costa-Besada
	Rafael Rivas-Santisteban
	Pablo Garrido-Gil
	Andrea Lopez-Lopez
	Gemma Navarro
	Jose L Lanciego
	Rafael Franco
	Jose Labandeira-Garcia
Abstract:	ACE2 plays a pivotal role in the balance between the pro-oxidative pro-inflammatory and the anti-oxidative anti-inflammatory arms of the renin-angiotensin system. Furthermore, ACE2 is the entry receptor for SARS-CoV-2. Clarification of ACE2-related mechanisms is crucial for the understanding of COVID-19 and other oxidative stress and inflammation-related processes. In rat and monkey brain, we discovered that the intracellular ACE2 and its products Ang 1-7 and alamandine are highly concentrated in the mitochondria and bind to a new mitochondrial Mas-related receptor MrgE (MrgE) to produce nitric oxide. We found MrgE expressed in neurons and glia of rodents and primates in the substantia nigra and different brain regions. In the mitochondria, ACE2 and MrgE expressions decreased and NOX4 increased with aging. This new ACE2/MrgE/NO axis may play a major role in mitochondrial regulation of oxidative stress in neurons, and possibly other cells. Therefore, dysregulation of the mitochondrial ACE2/MrgE/NO axis may play a major role in neurodegenerative processes of dopaminergic neurons, where mitochondrial dysfunction and oxidative stress play a crucial role. Since ACE2 binds SARS-CoV-2 spike protein, the mitochondrial ACE2/MrgE/NO axis may also play a role in SARS-CoV-2 cellular effects.

High lights

ACE2 products Ang1-7 and alamandine (Ala) highly concentrate in brain mitochondria

Ang1-7 and Ala bind to mitochondrial Mas-related receptor MrgE producing nitric oxide

ACE2/MrgE may play a major role in mitochondrial function and oxidative stress

Clarification of ACE2-related mechanisms is also crucial for understanding COVID-19

Graphical Abstract

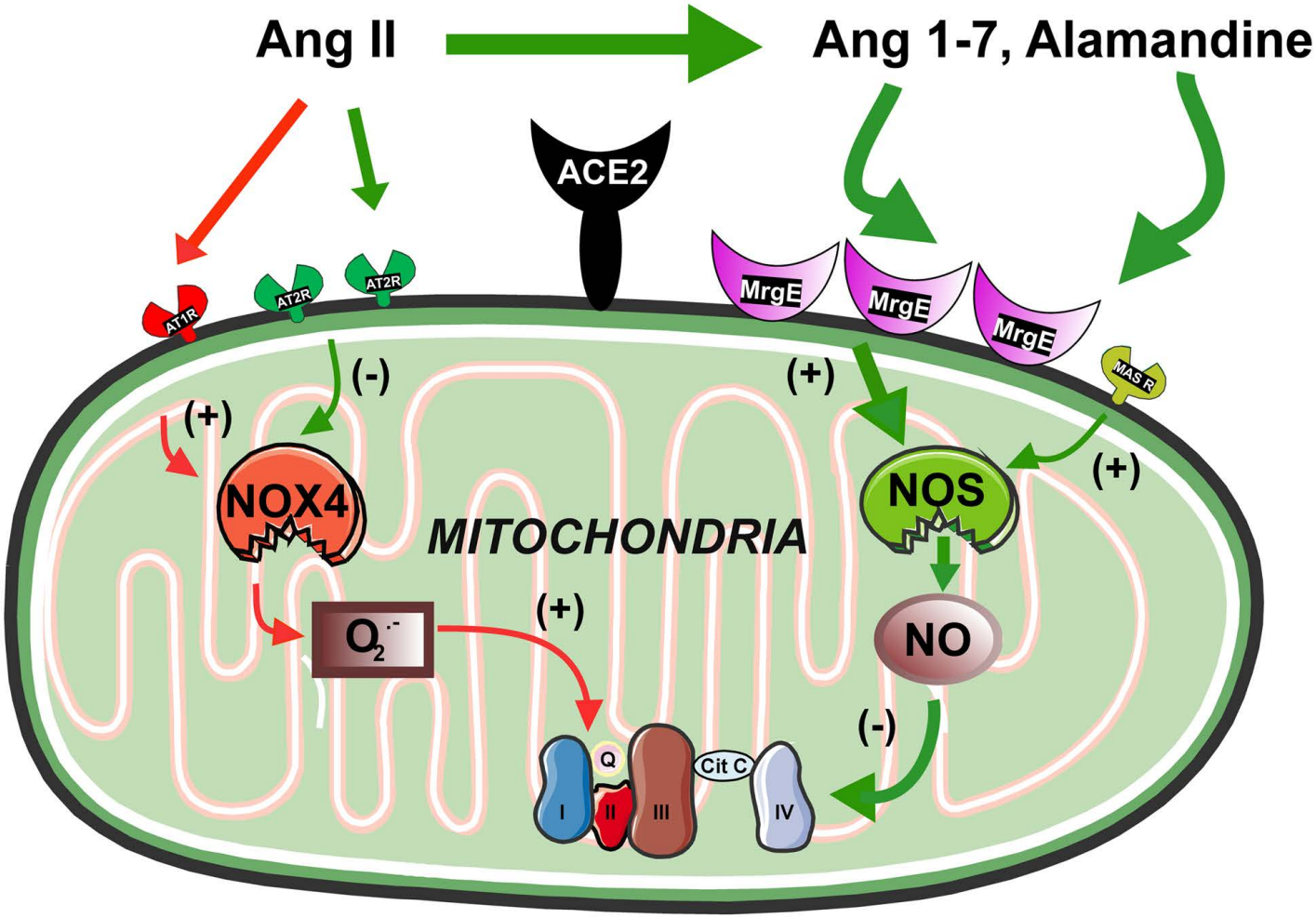

An ACE2/Mas-related receptor MrgE axis in dopaminergic neuron mitochondria.

Rita Valenzuela[1,2], Ana I. Rodriguez-Perez[1,2], Maria A. Costa-Besada[1,3], Rafael Rivas-Santisteban[2,4], Pablo Garrido-Gil[1,2], Andrea Lopez-Lopez[1], Gemma Navarro[2,5], Jose L. Lanciego[2,6], Rafael Franco[2,4], Jose L. Labandeira-Garcia[1,2*]

[1] Cellular and Molecular Neurobiology of Parkinson´s disease, Research Center for Molecular Medicine and Chronic diseases (CIMUS), IDIS, University of Santiago de Compostela, Santiago de Compostela; Spain. [2]Networking Research Center on Neurodegenerative Diseases (CIBERNED), Spain. [3] Cell and Developmental Biology Department, University College London, London, UK. [4]Laboratory of Molecular Neurobiology, Department of Biochemistry and Molecular Biology, Faculty of Biology, University of Barcelona, Barcelona, Spain. [5]Department of Biochemistry and Physiology, Faculty of Pharmacy, University of Barcelona, Barcelona, Spain. [6]Neuroscience Department, Center for Applied Medical Research (CIMA, IdiSNA), University of Navarra, Pamplona, Spain.

***Correspondence:**

Jose L. Labandeira-Garcia M.D., Ph. D., or Rita Valenzuela, Ph.D., Research Center for Molecular Medicine and Chronic diseases (CIMUS), University of Santiago de Compostela, 15706 Santiago de Compostela, Spain. Tel. +34-881815471. E. mail: joseluis.labandeira@usc.es; rita.valenzuela@usc.es

ORCID: 0000-0002-8243-9791

ABSTRACT

ACE2 plays a pivotal role in the balance between the pro-oxidative pro-inflammatory and the anti-oxidative anti-inflammatory arms of the renin-angiotensin system. Furthermore, ACE2 is the entry receptor for SARS-CoV-2. Clarification of ACE2-related mechanisms is crucial for the understanding of COVID-19 and other oxidative stress and inflammation-related processes. In rat and monkey brain, we discovered that the intracellular ACE2 and its products Ang 1-7 and alamandine are highly concentrated in the mitochondria and bind to a new mitochondrial Mas-related receptor MrgE (MrgE) to produce nitric oxide. We found MrgE expressed in neurons and glia of rodents and primates in the substantia nigra and different brain regions. In the mitochondria, ACE2 and MrgE expressions decreased and NOX4 increased with aging. This new ACE2/MrgE/NO axis may play a major role in mitochondrial regulation of oxidative stress in neurons, and possibly other cells. Therefore, dysregulation of the mitochondrial ACE2/MrgE/NO axis may play a major role in neurodegenerative processes of dopaminergic neurons, where mitochondrial dysfunction and oxidative stress play a crucial role. Since ACE2 binds SARS-CoV-2 spike protein, the mitochondrial ACE2/MrgE/NO axis may also play a role in SARS-CoV-2 cellular effects.

Keywords: alamandine; angiotensin 1-7; angiotensin converting enzyme 2; Parkinson; oxidative stress; renin-angiotensin system.

Abbreviations: ACE2, Angiotensin converting enzyme 2; ala, Alamandine; Ang 1-7, Angiotensin 1-7; Ang II, Angiotensin II; AT1, Ang II type 1 receptors; AT2, Ang II type 2 receptors; CD11b, Cluster of differentiation molecule 11b; Ct, Cycle threshold; DIC, differential interference contrast; DMEM, Dulbecco's modified Eagle's medium; D-Pro, D-Proline; FAM-Alamandine, fluorophore-conjugated alamandine FC, frontal cortex; FRET, fluorescence resonance energy transfer; GFAP, Glial fibrillary acidic protein; GPCRs, G-protein–coupled receptors; MasR, Mas receptors; MrgE, Mas-related receptor MRGPR, Mas related receptor family; mRNA, Messenger RNA; MTDR, Mitotracker Deep Red probe; NO, Nitric oxide; NOX4, NADPH oxidase 4; OC, occipital cortex; PB, Phosphate buffer; PD, Parkinson´s disease; RAS, Renin-angiotensin system; SN, substantia nigra; ST, striatum TH, Tyrosine hydroxylase; VDAC, Voltage-dependent anion channel; VM, ventral mesencephalon; WB, Western blot

1. Introduction

The renin-angiotensin system (RAS) was initially considered an endocrine system mainly related to regulation of blood pressure and sodium homeostasis. However, local or paracrine RAS were identified in different tissues and organs, including brain, and intracellular or intracrine RAS have been observed in different cell types [1-4]. At these three levels, RAS shows a prooxidative proinflammatory axis, which is counteracted by an antioxidative anti-inflammatory axis. A number of physiological functions are the result of an adequate equilibrium between both axes, and its disruption is involved in pathological processes. Major components of the prooxidative axis are angiotensin converting enzyme (ACE), which produces angiotensin II (Ang II) that acts on Ang II type 1 receptors (AT1). Major components of the counterregulatory antioxidative arm are Ang II acting on Ang II type 2 receptors (AT2) and, particularly, ACE2, which mainly produces Ang 1-7 that is the endogenous ligand of the Mas receptor (MasR). Previous studies have shown that brain RAS deregulation is involved in neuroinflammation and neurodegeneration, and we have shown the involvement of brain RAS, both at paracrine [5-7] and intracellular/intracrine [8-10] levels, in dopaminergic oxidative stress and neuron degeneration in Parkinson´s disease (PD) models.

Interestingly, it is now known that ACE2, a key component of the antioxidant anti-inflammatory RAS axis, is also the entry receptor used by SARS-CoV-2 to invade cells [11, 12], and a virus-induced dysregulation of the ACE2 and, subsequently, RAS function plays a major role in the inflammatory and fibrotic processes observed in COVID-19 disease in several organs. Although lung lesions are particularly dangerous, other organs are also affected, including brain [13-15]. Possible effects of this type of

viruses on dopaminergic neuron death and PD have also been suggested [16, 17]. Clarification of the role of ACE2, particularly within the cell, is crucial and remains unclear. In dopaminergic neurons, we have previously observed AT1, AT2 and Mas receptors at the mitochondrial level, which modulate the mitochondrial function and oxidative stress [8, 9]. Surprisingly, we observed that intracellular ACE2 was highly concentrated in the mitochondrial fraction as compared with the whole cell homogenate, and mitochondria also had high levels of its product Ang 1-7, suggesting a major role of the mitochondria in ACE2-related intracellular effects. In contrast, the major receptor for Ang 1-7 (i.e. MasR) was at relatively low levels in the mitochondria in comparison with whole cell homogenates [8], suggesting that other receptors mediate the effects of the ACE2/Ang 1-7 on the mitochondrial function. We investigated the Mas related receptor family (MRGPR), which is a group of receptors identified in rodents and humans. Six MRG genes, MrgD, MrgE, MrgF, MrgG, MrgH and Mas1, were observed in rodents, with clear human orthologs [18, 19]. Almost all are considered "orphan" receptors. MrgD subtype is the best known and characterized member, and it was related to the natural MasR ligand, angiotensin 1-7 (Ang 1-7) [20], and to the now considered RAS component alamandine (Ala), a heptapeptide structurally similar to Ang 1-7 [21]. The aim of this study, mainly focused on dopaminergic neurons, was to figure out the mechanism that mediates the effects of the ACE2-induced peptides Ang 1-7 and alamandine in the mitochondria and particularly, major mitochondrial receptors responsible for their effects.

2. Materials and methods

2.1 Experimental design

In previous studies, we found relatively low expression of MasR in the mitochondrial fraction in comparison with mitochondrial ACE2 and Ang 1-7 levels [8].Therefore, in a first set of experiments, we investigated the presence of possible additional unknown receptors which may bind Ang 1-7 in the mitochondria. First, we investigated the expression of major Mas related receptors (i.e. MrgD, MrgE and MrgF) in cell homogenates of substantia nigra compared to nigral MasR and a control tissue with already known levels of Mas related receptors (i.e. testis) using RT quantitative PCR and western blot (WB) analyses. As MrgE was the most abundant Mas related receptor, we isolated mitochondria from the rat nigral region to investigate the possible presence of mitochondrial MrgE using WB for MrgE, mitochondrial marker voltage-dependent anion channel (VDAC) as a marker for mitochondrial fraction, and α-tubulin and GAPDH as markers for cytosol fractions. The specificity of the used ACE2 and MrgE antibodies was assessed in our laboratory by WB analysis of lysates from HEK293 cells transiently transfected with MrgE tagged to fusion tail DDK and ACE2-GFP respectively. Colocalization of MrgE and mitochondrial markers (MTDR) in dopaminergic neurons was confirmed by double immunolabeling and confocal microscopy in cultures of N27 dopaminergic neurons.

Then, we investigated by RT-PCR and WB whether MrgE was the most abundant Mas related receptor only in the SN or was also located in other brain areas (striatum, frontal and occipital cortex). In order to identify the cell types showing MrgE receptors, we used primary mesencephalic cultures and brain sections through the SN, which were analyzed by double immunolabeling for MrgE and the neuronal marker

NeuN, the dopaminergic neuron marker tyrosine hydroxylase (TH), the astrocytic marker glial fibrillary acidic protein (GFAP), and the microglial marker CD11b (complement receptor-3, clone MRC OX42). Finally, major results observed in rats were confirmed in non-human primate (*Macaca fascicularis*) substantia nigra using double immunofluorescence and confocal microscopy for MrgE and different markers of neurons and glial cells, and WB of isolated mitochondria.

A second set of experiments were designed to study functional effects of brain MrgE receptors. First, we performed fluorescence competition binding studies in MrgE- and Mas receptor transfected HEK293 cells to find out the ligands of MrgE receptors. As possible ligands we tested the ACE2-derived products Ang 1-7 (MasR ligand) and Alamandine (MrgD ligand), and also the MrgD ligand ß-Alanine, in the presence/absence of the MrgD blocker D-Proline (D-Pro) or the MasR blocker A-779. Subsequently, cells were incubated with fluorescence labeled alamandine (FAM-alamandine). To verify whether the binding of the ACE2-derived peptides alamandine and/or Ang 1-7 to MrgE produces a functional response in cells, we evaluated levels of nitric oxide (NO) release using live-cell fluorescence time-lapse assays and a DAF-FM Diacetate fluorescent probe in HEK293 cells transfected with MrgE receptor or an empty plasmid as a control. Finally, we investigated the functionality of mitochondrial MrgE receptors. First, we used pure isolated brain mitochondria to exclude any interference of effects of cellular non-mitochondrial receptors. Mitochondrial NO production was detected with a NO fluorometric assay kit. Then, we confirmed MrgE-derived mitochondrial NO production using confocal microscopy and a NO fluorescence probe DAF-FM diacetate in MTDR labelled mitochondria of HEK293 cells transfected with MrgE receptor. We investigated the increase in mitochondrial NO production after treatment with alamandine and/or Ang 1-7. We also observed basal or

constitutive mitochondrial NO production in N27 dopaminergic neurons using colocalization of the NO fluorescence probe DAF-FM diacetate with MTDR labelled mitochondria by confocal microscopy.

In a third set of experiments, we studied possible dysregulation of the mitochondrial MrgE/ACE2 axis by aging. The effect of aging in tissue and mitochondrial MrgE expression was studied using cell homogenates of rat substantia nigra and pure brain isolated mitochondria from young adult (2–3-month old) and aged (18–20-month old) male rats using RT-PCR and WB analysis. In addition, aging related changes in protein expression of mitochondrial ACE2 and the intracellular NADPH form NOX4 were investigated.

2.2 Cell cultures

Mesencephalic primary cultures were obtained by dissecting ventral mesencephalic tissues from rat embryos of 14 days of gestation (E14). After an incubation of 20 min at 37ºC with 0.1% of trypsine, 0.05% of DNase (Sigma), and DMEM (Invitrogen), the tissue was washed and mechanically dissociated in DNase/DMEM. The cell suspension was centrifuged at 50×g for 5 min, and the resulting pellet was resuspended in 0.05% DNase/DMEM. Cells were plated at a density of 1.5 × 105 cells/cm2 onto 35-mm culture dishes (Falcon) previously coated with poly-L-lysine (100 μg/ml; Sigma) and laminin (4 μg/ml; Sigma), and maintained under control conditions (DMEM/HAMS F12/(1:1) containing 10% fetal bovine serum (FBS) in a humidified CO2 incubator (5% CO2; 37 °C) for 8 days in vitro (DIV); the entire culture medium was removed on day 2 and replaced with a fresh culture medium.

The dopaminergic cell line N27 (SCC048, Millipore, MA, USA) was cultured in RPMI 1640 medium supplemented with 10% FBS, 2 mM L-glutamine (Sigma), 100 U/ml penicillin, and 100 μg/ml streptomycin. Human embryonic kidney 293 cells, HEK293 (CRL-11268, ATCC), were cultured in DMEM medium supplemented with 10% FBS, 2 mM L-glutamine (Sigma), 100 U/ml penicillin, and 100 μg/ml streptomycin.

2.3 Animal models

Tissue from SN of young (2–3-month old) and aged (18–20-month old) Sprague-Dawley male rats were used for immunolabeling, WB and RT-PCR. Non-human primate tissue from six adult (4.5–5-year old) male *Macaca fascicularis* was used for confirming major results in rat tissue. Animal handling was conducted in accordance with the Directive 2010/63/EU, European Council Directive 86/609/EEC and the Spanish legislation (RD53/2013). For monkeys, the experimental design was approved by the Ethical Committee for Animal Testing of the University of Navarra (ref: 009-12). Monkeys were captive-bred and supplied by R. C. Hartelust (Leiden, The Netherlands). Rodent experiments were approved by the corresponding committee at the University of Santiago de Compostela. Animals were housed at constant room temperature (RT) (21–22 °C) and 12-h light/dark cycle.

2.4 Isolation of mitochondria from rat and monkey ventral midbrain and cell cultures

Mitochondria from ventral midbrain of rat and monkey were isolated and purified according to the protocol described by Sims and Anderson [22] with few modifications [9]. This protocol was performed to isolate pure mitochondria with minimum contamination by synaptosomes and myelin, and combines differential centrifugation and discontinuous Percoll density gradient centrifugation. Ventral midbrain was removed and rinsed in cold isolation buffer (0.32 M sucrose, 1 mM and 10 mM TRIS; pH 7.4). The tissue was cut into small pieces, transferred to a Dounce homogenizer with 12% Percoll solution, and then homogenized on ice using a loose-fitting and tight-fitting glass pestles. The homogenate was slowly layered on a previously prepared discontinuous Percoll gradient consisting of 26% Percoll layered over 40% Percoll and centrifuged using a fixed-angle rotor at 30 700 × g for 5 min at 4 °C. Three separate bands were produced during centrifugation, and the enriched mitochondrial fraction, which was located at the interface between the 26 and 40% Percoll layers, was carefully taken out with a glass Pasteur pipette. The mitochondrial fraction was diluted with isolation buffer and was centrifuged at 16 700 × g for 10 min at 4 °C. This provided a mitochondrial pellet, which was softly resuspended in the residual supernatant. Finally, the pellet was resuspended in isolation buffer and centrifuged at 7300 × g for 10 min at 4 °C, producing a pellet of pure mitochondria that was used for WB. The same procedure was performed with rat whole-brain tissue to measure mitochondrial NO production.

2.5 Western blot analysis

Isolated mitochondria from rat and monkey ventral midbrain, homogenates from rat different brain regions and rat testicle were lysed in RIPA buffer containing PMSF (Sigma) and protease inhibitor cocktail (Sigma). Tissue lysates were centrifuged and total proteins were quantified using the Pierce BCA Protein Assay Kit (Thermo Scientific). An equal amount of protein lysates were separated on a 10% Bis-Tris polyacrylamide gel and transferred to nitrocellulose membranes. Membranes were incubated overnight at 4ºC with primary antibodies against the MrgE receptor (TA316024; Origene; 1:750), ACE2 (ab108252; Abcam;1:1000) and NOX4 (ab133303; Abcam; 1:800). Membranes were reincubated with loading controls: anti-α-tubulin

(T5168; 1:50.000; Sigma), GAPDH (G9545; 1:25.000; Sigma) and β-actine (A2228; Sigma, 1:10000) as markers of whole homogenate, anti-VDAC/porin (V2139; Sigma; 1:1000) as a marker of mitochondrial fraction. The following horseradish peroxidase (HRP)-conjugated secondary antibodies were used: goat anti-rabbit-HRP and goat anti-mouse-HRP Santa Cruz Biotechnology; 1:2500). Bound antibody was detected with an Immun-Star HRP Chemiluminescent Kit (Bio-Rad; 170-5044) and visualized with a chemiluminescence detection system (Bio-Rad; Molecular Imager ChemiDoc XRS System). The data were then expressed relative to the value obtained for the control to counteract possible variability among batches.

2.6 RNA extraction and real-time quantitative polymerase chain reaction

Total RNA from rat different brain tissues and testicle was extracted with TRIzol (Invitrogen, Paisley, UK) following the manufacturer's protocol. Total RNA (2 µg) was reversed transcribed to complementary DNA (cDNA) using nucleoside triphosphate

containing deoxyribose, random primers and Moloney murine leukaemia virus (M-MLV; Invitrogen, Thermo Fisher Scientific; 200U) reverse transcriptase. Subsequently, the RT-PCR analysis was performed with a QuantStudio 3 platform (Applied Biosystems, Foster City, CA, USA), the EvaGreen qPCR MasterMix (Applied Biological Materials Inc., Vancouver, Canada), and primer sequences indicated below were used to examine the relative levels of Mas, MrgD, MrgE and MrgF receptors. β-Actin was used as a housekeeping gene and was amplified in parallel with the genes of interest. We used the comparative cycle threshold values (cycle threshold (Ct)) method ($2^{-\Delta\Delta Ct}$) to examine the relative messenger RNA (mRNA) expression. A normalized value was obtained by subtracting the Ct of β-actin from the Ct of interest (ΔCt). As it is uncommon to use ΔCt as a relative expression data due to this logarithmic characteristic, the $2^{-\Delta\Delta Ct}$ parameter was used to express the relative expression data. Primer sequences were as follows: for Mas receptors, forward 5′-CTTTGTGGAGAACGGGAT-3′, reverse 5′-GGAGATGTCAGCAATGGA-3′ ; for MrgD, forward 5´-CTGTGACCTGGGTTTACTTT-3´, reverse 5´-CTCAGTAGCCAAATCACCAT-3´; for MrgE, forward 5´-GCCTGATCATGCTGCGGTTC-3´, reverse 5´-AGCAGCAGGTCCAGTAGCAG-3´; for MrgF, forward 5´-CTCTGCGAAGGGAACTCGGA-3´, reverse 5´-GAGTCCAGGCTCCTGTTGGG-3´; and for β-actin, forward 5´-TCGTGCGTGACATTAAAGAG-3´ and reverse 5´-TGCCACAGGATTCCATACC-3´.

2.7 Immunofluorescence labelling

Mesencephalic primary cultures were grown on glass coverslips and co-incubated overnight at 4 °C with different cell markers and a rabbit polyclonal MrgE receptor antibody (LS-C136078, LSBio, 1:100). Different cell types were identified with the corresponding mouse monoclonal antibodies: anti-NeuN (Millipore, 1:500) as neuronal marker, anti-TH (Sigma; 1:5000) as dopaminergic marker, anti-glial fibrillary acidic protein (GFAP, Millipore, 1:500) as astrocyte marker, or anti-CD11b (complement receptor-3, clone MRC OX42, Serotec; 1:100) as microglial marker. Primary antibodies were diluted in DPBS containing 1% BSA and 2% normal donkey serum. Then, the following fluorescent secondary antibodies were incubated for 2 h at RT: Alexa Fluor 568- conjugated donkey anti-rabbit IgG (Molecular Probes; 1:200) or Alexa Fluor 488-conjugated donkey anti-mouse IgG (Molecular Probes; 1:200).

In other experiments, mitochondria from N27 dopaminergic cells were marked with the cell-permeant Mitotracker Deep Red probe (MTDR) (M-22426; InvitroGene; 200nM) for 15 minutes and fixed with 4% paraformaldehyde. After mitochondrial labelling, neurons were incubated with MrgE receptor antibody (LS-C136078, LSBio, 1:100) overnight, followed by the secondary antibody Alexa Fluor 488- conjugated donkey anti-rabbit IgG (Molecular Probes; 1:200). Cell nuclei were marked with the DNA-binding dye Hoechst 33342 (Sigma;10 μg/ml) for 30 min at RT. Finally, mounting was performed with Immumount (Thermo-Shandon).

Rats and monkeys were sacrificed with an overdose of chloral hydrate and transcardially perfused with a cold 4% paraformaldehyde solution in phosphate buffer (PB). Then, brain was removed, cryoprotected and cut into coronal tissue sections (40-μm thick) using a sliding microtome. Tissue sections through the entire SN were processed for double immunofluorescence to identify cells expressing MrgE receptor. The antibody against MrgE receptor was combined with antibodies against tyrosine

hydroxylase (TH) as dopaminergic marker, or glial fibrillary acidic protein (GFAP) as astrocytic marker or cluster of differentiation molecule 11b (CD11b) as microglial marker. Free-floating SN sections were pre-incubated in KPBS-1% BSA with 5% normal donkey serum (Sigma) and 0.05% Triton X-100 (60 min at RT). Tissue sections were then incubated overnight at 4 °C in primary antibodies raised against MrgE receptor (1:100; rabbit polyclonal, LS-C136078, LSBio) and TH (1:1000; mouse monoclonal, T2928, Sigma) or GFAP (1:500; mouse monoclonal; MAB360, Millipore) or rat CD11b (1:50; mouse monoclonal clone OX-42, MCA275, BioRad) or CD11b (1:50; goat polyclonal, Santa Cruz Biotechnology) diluted in KPBS-1% BSA with 5% normal donkey serum. Immunoreactivity was visualized with the following fluorescent secondary antibodies from Molecular Probes (diluted 1:200): Alexa Fluor 568-conjugated donkey anti-rabbit IgG, Alexa Fluor 488-conjugated donkey anti-mouse IgG, and Alexa Fluor 488-conjugated donkey anti-goat IgG. Finally, SN sections were mounted on gelatin-coated slides and coverslipped with Immumount (Thermo-Shandon). Co-localization of markers was confirmed by confocal laser microscopy (AOBS-SP5X; Leica Microsystems Heidelberg GmbH, Mannheim, Germany) performing sequential scan to avoid any potential overlap with the LAS AF software (Leica Microsystems GmbH).

2.8 Transfection of MrgE receptor

HEK293 cells were seeded at a density of 0.4×10^6/well onto 24 well plates with or without glass cover depending on the post-analysis and maintained at 37 °C in a humidified CO2 incubator (5% CO2, 95% air). Cells were transiently transfected with 1

μg of MrgE cDNA (MRGE Myc DDK-tagged, MR216310, Origene) using a commercial transfection reagent, Turbofect (R0533, Thermo Scientific). After a period of 48 h post-transfection, cells were lysed with RIPA and immunoblotted for antibody specificity testing, directly used for in vivo time lapse experiments, or fixed for confocal studies.

For binding studies, HEK293 cells were transiently transfected with the corresponding cDNA using the PEI (PolyEthylenImine, Sigma-Aldrich, St. Louis, MO) method. Briefly, the cDNA diluted in 150 mM NaCl was mixed, 10 min, with PEI (5.5 mM in nitrogen residues) prepared in 150 mM NaCl. cDNA-PEI complexes were transferred to HEK293 cell cultures (6-weel plates) and incubated for 4 hours in a serum-free Dulbecco's modified Eagle's medium (DMEM). Then, the medium was substituted by 10% fetal-calf-serum supplemented DMEM and cells were maintained at 37 ºC in a humid atmosphere of 5% CO2. Experiments were done 48 hours after transfection.

2.9 Specifity of ACE2 and MrgE antibodies and ACE2 activity

The specificity of the MrgE antibody (TA316024, Origene) and ACE2 antibody (ab108252, Abcam) was assessed in our laboratory by WB analysis of lysates from HEK293 cells transiently transfected with MrgE tagged to fusion tail DDK and ACE2-GFP respectively. The specificity was confirmed by the presence of a predominant immunoreactive band in positively transfected lysates, after 48 post-transfection of MrgE receptor (TA316024, Origene; 1:750) or ACE2 enzyme (ab108252, Abcam, 1:1000) and the absence of the fusion tail DDK (TA50011; Origene; 1:1000) band or

mouse monoclonal turboGFP antibody (TA150041; Origene; 1:1000) in negative controls (see Fig. 1 c).

ACE2 activity of the mitochondrial fraction from rat and monkey brain was measured using a commercial ACE2 activity assay kit (AnaSpec, AS-72086) following the manufacturer's specifications. The kit is based on the Mca/Dnp fluorescence resonance energy transfer (FRET) peptide (10 µM). In the FRET peptide, the fluorescence of Mca is quenched by Dnp but a cleavage of the substrate produces a separation into two fragments by the enzyme, so that the fluorescence of Mca is measured at excitation/emission = 330/390 nm using an Infinite M200 multiwell plate reader (TECAN). ACE2 activity was confirmed with the specific ACE2 inhibitor DX600 1 µM, included as a control in the same kit (AnaSpec, AS-72086).

2.10 Fluorescence competition binding studies in MrgE-transfected HEK293 cells

To perform non-radioactive fluorescent ligand binding assays, binding of fluorophore-conjugated alamandine (FAM-alamandine) was tested in control cells and transfected cells expressing Mas-related E (Mrgpre,1 µg cDNA) or Mas (MAS1, 1 µg cDNA) G-protein–coupled receptors (GPCRs). Cells were carefully washed twice with phosphate-buffered saline (PBS, pH 7.4). Then cells were incubated for 10 minutes with the following non-fluorescent compounds: the Mas ligands Ang 1-7 (10 µM) and Alamandine (10 µM), the MrgD ligand ß-Alanine (10 µM), the Mas receptor antagonist A779 (10 µM) or the MrgD antagonist D-Proline (10 µM). Then, cells were incubated with fluorescence labeled alamandine (FAM-alamandine ; 0,1 µM). Incubation was kept

for 1 hour, light-protected and at room temperature. Cells were then washed twice with PBS, detached and distributed in 96-well microplates (black plates with a transparent bottom). Fluorescence measurements were performed by VICTOR Multilabel Plate Reader (PerkinElmer) using a 10 nm bandwidth 495 nm excitation filter and a 10 nm bandwidth 519 nm emission filter. Imaging of FAM-Alamandine fluorophore labeled cells were performed by ZOE Fluorescent Cell Imager (Bio-Rad) inverted microscope equipped with a 20X objective. Brightfield channel uses a ring of multiple green LEDs to avoid chromatic aberration. Green channel for fluorescence images uses a blue LED which is compatible with FAM fluorophore labeled alamandine (excitation and emission wavelength 480/517 nm).

2.11 Live-cell fluorescence time-lapse assays

To determine the production of cellular NO due to activation of MrgE receptors, a DAF-FM Diacetate fluorescent probe (D-23844, ThermoFisher Scientifics) was used in HEK293 cells transfected with MrgE receptor and an empty plasmid as a control. HEK293 cells were seeded in 24-well plate at a density of 3 x 10^4 cells/well, and transfected with MrgE or empty plasmid. Forty-eight hours after transfection, cells were incubated for 30 minutes at RT with the DAF-FM Diacetate probe (5 µM), and washed to remove the excess of probe. Treatments with alamandine (1 µM) or Ang 1-7 (1 µM) were added directly under the microscope, and time-lapse differential interference contrast (DIC) images and fluorescence at 495 and 515 nm (3 fields/well) were captured using a 20X objective at 2 minute intervals for the following 30 minutes. Image capture was achieved automatically, using a Cell Observer instrument (LEICA CTR 7000 HS) equipped with a cell incubation chamber, motorized stage, CCD camera. All operations

were under the control of the Software Leica LAS X. The same conditions of laser intensities/exposure times were used for the entire experiment.

2.12 Mitochondrial nitric oxide production

Mitochondrial nitric oxide (NO) production was detected with a NO fluorometric assay kit (Biovision) in pure isolated mitochondria from rat brain. Total concentrations of nitrates and nitrites have been used as indicators of NO production. Direct quantification of NO is complex due to its brief half-time. An amount of 30 μg of brain isolated mitochondria was incubated for 10 min with MrgD inhibitor, D-Pro (5 μM) and/or 5 min with alamandine (1 μM) to investigate the effect of mitochondrial MrgE receptor activation. Then all nitrates were turned into nitrites by nitrate reductase enzyme. Finally, nitrite reacted with the fluorescent probe DAN (2,3-diaminonaphthalene) and the measurement of nitrite concentration was used as a quantitative measure of NO production. Fluorescence was measured in an Infinite M200 multiwell plate reader (TECAN).

Basal mitochondrial NO production of dopaminergic neurons or MrgE-derived mitochondrial production in MrgE transfected HEK-293T cells were detected by quantifying the NO fluorescence probe DAF-FM Diacetate (InvitroGene, D-23844) in labelled mitochondria. Cells were seeded at 12-well plates (5 x 10^4 cells/well). Then, the DAF-FM probe (5 μM) was incubated for 30 minutes. During the last 20 minutes of loading the NO probe, a mitochondrial marker (Mitotracker deep red, MTDR; 200 nM) was added to the cells for 10 minutes. Then, cells were washed and treated or not treated with alamandine (1μM) or Ang 1-7 (1μM) to assess the NO production. Cells were fixed and co-localization of DAF-FM and MTDR was confirmed by confocal laser

microscopy (AOBS-SP5X; Leica Microsystems Heidelberg GmbH, Mannheim, Germany) performing sequential scan to avoid any potential overlap with the LAS AF software (Leica Microsystems GmbH). Quantification of fluorescence intensity was done with the open source image processing package based on ImageJ software (NIH, Bethesda, MD, USA, rsb.info.nih.gov/ij/).

2.13 Statistical analysis

All statistical analyses were performed using SigmaPlot 11.0 (Systat Software, Inc., CA, USA). All datasets were tested for normality with the Kolmogorov–Smirnov test. If the dataset passed the normality test, parametric tests were used: Student's t test for two group comparisons and one-way ANOVA followed by the Student-Newman-Keuls Method for multiple comparisons. For non-parametric data, two group comparisons were carried out by Mann-Whitney Rank Sum Test and multiple comparisons by Kruskal-Wallis One Way Analysis of Variance on Ranks test followed by Student-Newman-Keuls Method or Dunn's Method were used. Differences were considered statistically significant at $p < 0.05$. No statistical methods were used to predetermine sample sizes, but our sample sizes were similar to those reported previously [7-10, 23].

3. Results

3.1 Discovery of MrgE as a mitochondrial receptor

In previous studies we found relatively low expression of Mas receptors in the mitochondrial fraction in comparison with the whole cell homogenate. However, ACE2

concentration was much higher in mitochondrial fraction than in the whole cell homogenate [8], suggesting a major role of this enzyme in mitochondria. Furthermore, we observed that Ang 1-7 is more abundant than Ang II in pure isolated mitochondria from rat nigral region, suggesting an important role for Ang 1-7 in the mitochondrial function and that it may act not only via mitochondrial Mas receptors but also via additional unknown receptors.

To identify possible mediators of the Ang 1-7 action, first we investigated the expression of major Mas related receptors (MrgD, MrgE and MrgF) in cell homogenates of substantia nigra. Surprisingly, we observed that MrgD mRNA, which is the best-studied Mas related receptor, was practically absent compared to MrgE or MrgF mRNA. As this result was unexpected, we tried several MrgD primers pairs to exclude the possibility of a technical problem. However, a low expression of the transcript for MrgD was consistently found. We observed circa 300 fold more mRNA expression of MrgE and 7 fold in MrgF expression compared to MasR in the SN of the same animals (Fig. 1 a).

Based on these results, we isolated mitochondria from the nigral region in the rat ventral mesencephalon (VM) and investigated the possible presence of MrgE, as an additional mitochondrial receptor that could bind Ang1-7 or other ACE2-derived peptides such as alamandine. In isolated mitochondria, we confirmed the quality of the samples with the use of specific markers such as the voltage-dependent anion channel (VDAC) for the mitochondrial fraction, and the cytosol fraction was confirmed with α tubulin. In isolated mitochondria, we observed a much higher concentration of both ACE2 and MrgE receptors than in the whole cell homogenate (Fig. 1 b).

The specificity of ACE2 and MrgE antibodies was confirmed by WB analysis of HEK293 cells transfected with ACE2-GFP or MrgE-DDK. We observed a predominant

immunoreactive band in transfected cells compared to control non-transfected cells at 48 post-transfection (see below) (Fig. 1 c). In addition, we confirmed the activity of the mitochondrial ACE2 using an activity assay kit (274,6 +/- 23,2 mU/mg). The presence of MrgE at mitochondrial level was confirmed using confocal microscopy. In dopaminergic neuron N27 cell line, we observed co-localization of MrgE immunolabeling with the mitochondrial marker MTDR (Fig. 1 d-g).

3.2 MrgE is the most abundant MRGPR receptor subtype in rat substantia nigra, and it is also expressed in other CNS regions

After observing high levels of MrgE protein in mitochondrial preparations, we further analyzed the expression of major Mas related receptors (i.e. MrgD, MrgE and MrgF) in cell homogenates of substantia nigra (SN) and other areas of the brain. We used rat testis as a positive control tissue, as it is known that it shows a high MrgD expression and low expression of other types of Mas related receptors. We observed that MrgD mRNA was undetectable in SN relative to testis mRNA expression, confirming the specificity of the pair primers used (Fig. 2a). However, MrgE mRNA (Fig. 2b) and protein (Fig. 2e,f) expression were much more abundant in SN than in testis. Gene expression of MrgF subtype was not statistically different between both tissues (Fig. 2c). In addition, we confirmed the presence of MrgE mRNA (Fig. 2d) and protein (Fig. 2g,h) expression in other rat brain areas such as striatum (ST), frontal cortex (FC) and occipital cortex (OC). As in the SN region, MrgD receptors were expressed at very low level in all these brain areas compared to the same amount (µg) of tissue from testis (not shown).

3.3 MrgE is mainly expressed in neurons and at lower levels in glial cells

We then investigated the cell types in which MrgE was present using rat primary mesencephalic cultures (Fig. 3 a-d) and tissue sections from rat substantia nigra (Fig. 3 e-g). Immunolabeling for MrgE receptor was very intense in neurons, colocalizing with the neuronal marker NeuN (Fig. 3 a). Dopaminergic neurons, which were identified with tyrosine hydroxylase (TH), were also intensely immunolabeled for the MrgE receptor (Fig. 3b, e). Astrocytes (i.e. GFAP-positive cells; Fig. 3c, f) and microglia (OX-42 positive cells; Fig. 3d, g), were also immunolabeled for MrgE, although glial cells usually showed less intense immunolabeling. Labeling for MrgE receptor observed by confocal microscopy revealed both plasma membrane and, particularly, intracellular distribution.

3.4 In the nigra of non-human primates, ACE2 and MrgE are also at high levels in the mitochondrial fraction

Major observations in rat tissue were confirmed in non-human primates. As in rats, both ACE2 and MrgE were highly concentrated in the mitochondrial fraction relative to whole cell homogenate (Fig. 4 a, b). We confirmed the presence of ACE2 activity in monkey isolated mitochondria, which was markedly reduced by the ACE2 inhibitor DX600, revealing its functionality (Fig. 4c). In addition, tissue sections through the monkey substantia nigra showed MrgE immunolabeling, which was intense in dopaminergic neurons (i.e. TH-positive cells; Fig. 4d), but was also observed in astrocytes (GFAP-positive cells; Fig. 4e) and microglia (CD11b-positive cells; Fig. 4 f).

3.5 MrgE binds to the ACE2-derived peptides Alamandine and Ang 1-7

We performed fluorescence competition binding studies in MrgE-transfected HEK293 cells to address whether MrgE receptor may be labelled using FAM-conjugated alamandine (FAM-alamandine). In parallel, we also used Mas-R expressing HEK293 cells to test the binding of ligands and blockers to this receptor. In non-transfected HEK293 cells, we did not observe any significant binding of FAM-alamandine, confirming the low MrgE and Mas receptor expression in this cellular model (Fig. 5 a, f, g). However, we observed a significant binding of FAM-alamandine to both MrgE- and Mas-transfected cells. The binding of FAM-alamandine was competed by non-fluorescent alamandine and Ang 1-7 (the natural ligand of MasR), showing that both peptides are able to bind to both receptors. However, the MrgD ligand, β-alanine, only could bind to MrgE-transfected cells but not to Mas-transfected cells (Fig. 5 b, c and h-k)

Once the binding of the ligands was established, we performed binding assays with the MrgD blocker, D-Pro, and the MasR blocker, A-779. We observed that both inhibitors abolished the increase in fluorescence in MrgE- and Mas-transfected cells. This result suggests that D-Pro and A-779 can block the alamandine binding to MrgE and Mas receptors, and therefore their functional effects (Fig. 5 d, e and l, m).

3.6 Alamandine and Angiotensin 1-7 produce an increase in cellular nitric oxide (NO) through MrgE, independently of MasR

Due to the lack of specific ligands for MrgE receptor, we performed live-cell fluorescence time-lapse assays in HEK293 cells transfected with MrgE. To know whether the binding of alamandine and/or Ang 1-7 to MrgE-transfected cells produces functional responses, we evaluated NO release using the fluorescence DAF probe in a time period of 30 min. In the absence of treatment, no fluorescence was observed in control cells (i.e. transfected with the empty plasmid), and a very weak fluorescence was observed in MrgE transfected cells (Fig. 5 n, o and t, u). After 10 min of treatment, we observed an increase in NO-probe fluorescence in alamandine-treated MrgE transfected cells but not in control cells (Fig. 5 p, q and v, x). Moreover, treatment with Ang 1-7 also induced an increase in NO production through MrgE receptors, as revealed by the increase in green fluorescence of DAF probe in MrgE-transfected cells (Fig. 5 y, z) compared to the same treatment in control cells (Fig. 5 r, s). The NO-positive signal was observed during the 30-min measurements, slightly decreasing over the time, confirming the functionality of MrgE receptors independently of other receptors that could bind these ligands, such as MasR.

3.7 MrgE is particularly abundant in the mitochondria and regulates mitochondrial NO production

As mentioned above, we observed that MrgE receptors were enriched in the mitochondrial fraction. Consistent with this, basal NO production of N27 dopaminergic neurons, detected by the NO fluorescence probe DAF-FM, showed a marked colocalization with mitochondrial markers (Fig. 6 a-d). Furthermore, we investigated the functionality of mitochondrial MrgE receptors using isolated mitochondria from rat brain to exclude any interference of effects of cellular non-mitochondrial receptors. As

in cellular assays, treatment of isolated mitochondria with alamandine produced an increase in levels of mitochondrial NO, which was inhibited by pre-incubating the mitochondria with the receptor blocker D-Pro (Fig. 6 e). We confirmed the functional effects of mitochondrial MrgE receptors using confocal microscopy of HEK293 cells transfected with MrgE receptor. We observed an increase in mitochondrial NO production in MrgE-transfected cells after 30 min of alamandine or Ang 1-7 treatment, as shown by the increase in fluorescence of DAF probes in mitochondria identified with MTDR labelling (Fig. 6 f-r). The present results suggest that mitochondrial MrgE receptors modulate NO production at mitochondrial level.

3.8 MrgE expression decreases with aging

In previous studies, we observed a decrease in the expression of components of the protective RAS axis, including AT2 receptors [9, 23], Ang 1-7 and MasR [8] in aged animals relative to young controls. In the present work, we isolated SN from 18-20-month-old rats and from 2-3-month-old rats to investigate the expression of ACE2 and MrgE receptors. We observed that MrgE protein and mRNA expression decreased in substantia nigra from aged rats relative to young rats (Fig. 7 a, b). Aged animals also showed a significant decrease in ACE2 and MrgE levels in the mitochondrial fraction, and a marked increase in NOX4 levels supporting an aging-related shift of the mitochondrial RAS towards the pro-oxidative axis (Fig. 7 c-e).

4. Discussion

In the present study, we discovered that intracellular ACE2 concentrates at high levels in brain mitochondria, and that the MrgE receptor is a major target for the ACE2-related peptides Ang1-7 and alamandine, which induce mitochondrial NO production. Our previous studies in neurons [8, 9] and studies in peripheral cells [24, 25] have shown the presence of receptors related to both pro-oxidative and, more abundantly, antioxidative RAS axes in the mitochondria. While AT1 receptors promote superoxide production via mitochondrial NOX4 activation [9], mitochondrial receptors belonging to the antioxidant axis such as AT2 receptors [9, 24] and MasR [8] modulate respiration and oxidative stress by promoting NO production via mitochondrial NOS. However, mitochondrial levels of Ang 1-7 are much higher (about threefold) than mitochondrial levels of Ang II [8], and in this study we found that mitochondrial MasR are notably less abundant than MrgE receptors. Altogether suggests that the ACE2/Ang 1-7-alamandine/MrgE axis plays a major role in mitochondrial NO generation and modulation of mitochondria-derived oxidative stress, which plays a major role in dopaminergic degeneration and PD.

Consistent with this, we observed that ACE2 and MrgE are decreased in aged animals, which was also observed for other major components of the RAS antioxidative axis such as AT2 [9], Ang 1-7 and MasR [8]. A shift towards the mitochondrial pro-oxidative axis in aged animals is also supported by the present observation of significant increase in NOX4 levels in mitochondria from aged brains. This may contribute to the prooxidative proinflammatory state observed in aged brain and its vulnerability to neurodegeneration, particularly dopaminergic neuron degeneration [26]. In dopaminergic neurons, we have previously shown that the nuclear RAS [10] and the mitochondrial RAS [8, 9] buffer cell oxidative stress, and particularly that derived from the paracrine RAS pro-oxidative activity. However, dysregulation of this compensatory

mechanism during aging or pathological processes may lead to an excess of oxidative stress and neurodegeneration.

It is also important to highlight that ACE2 is the entry receptor of SARS-CoV and SARS-CoV-2 to invade target cells [11, 27]. The effects of SARS-CoV-2 in the brain are still unclear. However, about 36% of Covid-19 patients (45% of severe cases) showed neurological manifestations [28], and a lesion of the brainstem neurons has been suggested to be involved in the respiratory failure in COVID-19 disease [14, 29], as neuronal death has been observed in mice infected with SARS-CoV [30]. Interestingly, high affinity of coronaviruses for basal ganglia and dopaminergic neurons has been suggested [17]. It is usually assumed that COVID-19 infection induces a decrease in levels ACE2 and ACE2 activity at the cell membrane, which results in a decrease in levels of the antioxidative Ang 1-7 and increase in levels of Ang II, leading to a shift towards the prooxidative Ang II/AT1 activity, which results in oxidative stress, inflammation and cell death. The present results open the possibility that a dysregulation of the mitochondrial ACE2/MrgE axis (i.e. the intracellular compensatory antioxidative axis) may also play a role, which should be addressed in future studies specifically designed to clarify this possibility.

Although ACE2 is the entry receptor of SARS-CoV-2, a major anti-inflammatory effect of the ACE2/Ang 1-7 axis has been shown in several organs, and particularly in the lung, which is a major target of SARS-CoV-2 and shows a high expression of ACE2 [31, 32, 33]. These two opposite effects have led to consider ACE2 as a double-edged sword for COVID-19 disease [27, 34]. In recent studies, we have shown that the altered balance between both RAS axes play a major role in effects of virus/viral spike protein in human lung cells, but also in the viral spike protein internalization in cells [35,36]. However, a possible role of the mitochondrial ACE2 in

this process has not yet been investigated by our group or others. Several studies in lung and liver have suggested that NOX4-derived ROS may trigger the pro-inflammatory profibrotic process and that activation of the ACE2/Ang 1-7 axis may counteract this effect [37, 38]. The involvement of NOX4-derived ROS has been shown because the process is blocked by NOX4 inhibitors or NOX4 siRNA, or alamandine or Ang 1-7 [37, 38]. However, cell compartments involved in this NOX4 activation, and particularly the possible involvement of mitochondrial NOX4, have not been addressed. It is normally assumed that binding Ang 1-7 to cell membrane Mas receptors is responsible for the intracellular antioxidative responses. Previous studies have shown that viruses, including SARS-CoV viruses, modulate cell function by modifying mitochondrial processes [39, 40], and that changes in mitochondrial bioenergetics play a major role both in viral replication and early cell responses to viral infection [41]. Several proteins generated from the SARS-CoV viral genome have mitochondrial targeting sequence [40, 42]. Coronavirus spike proteins contain endoplasmic reticulum retrieval signals that can retrieve spike proteins to the endoplasmic reticulum [43, 44]. Viral spike protein may interact with mitochondrial ACE2 via MAMs (mitochondrial associated membrane compartment) [45]. The present findings suggest that a possible role of mitochondrial ACE2 and its main target receptor MrgE should be also investigated in future studies for better comprehension of cell effects SARS-COV-2 in COVID-19.

5. Conclusions

The present study shows for the first time that MrgE receptors are predominantly expressed in mitochondria in the brain, including dopaminergic neurons. Ang 1-7 and alamandine can bind to MrgE receptors to increase NO production, which is known to

counterbalance the increase in ROS at cell and mitochondrial levels. In addition, MrgE receptor expression decreases with aging, which supports the aging-related loss of the protective role of RAS. Overall, the present results suggest that MrgE, and ACE2-derived peptides Ang1-7-and alamandine play a role in mitochondrial regulation of neuronal oxidative stress, which is a major factor involved in dopaminergic neuron degeneration. Dysregulation of the mitochondrial ACE2/Ang 1-7-alamandine axis may also play role in oxidative, inflammatory and fibrotic responses related to the impairment of the ACE2 function such as that observed in COVID-19 disease. The present findings open new avenues for research on these questions.

Declaration of competing interest

The authors have no competing interests to declare.

Acknowledgements

We thank Pilar Aldrey, Iria Novoa and Cristina Gianzo for their technical assistance. Funding: Spanish Ministry of Economy and Competitiveness (RTI2018-098830-B-I00 and RTI2018-094204-B-I00; they include EU FEDER funds). Spanish Ministry of Health (SPI17/00828, RD16/0011/0016 and CIBERNED). Galician Government (XUGA, ED431C 2018/10, ED431G/05). FEDER (Regional European Development Fund)

Authors' contributions

R.V., M.A. C-B and A.L-L. performed cell cultures and in vitro experiments. A.I. R-P and P.G-G performed immunohistochemistry and in vivo experiments with rats. R.R-S, G.N. and R.F. performed binding experiments. P.G.G and J.L. L. performed

experiments with monkey tissue. J.L. L-G and R. V. conceived and supervised the whole study and wrote the manuscript. All authors edited the manuscript.

Data availability

Data are available from the corresponding author upon reasonable request.

References

[1] L.S. Capettini, F. Montecucco, F. Mach, N. Stergiopulos, R.A. Santos, R.F. da Silva, Role of renin-angiotensin system in inflammation, immunity and aging. Curr. Pharm. Des. 18 (2012) 963-970.

[2] X.C. Li, D. Zhu, X. Zheng, J. Zhang, J.L. Zhuo, Intratubular and intracellular renin-angiotensin system in the kidney: a unifying perspective in blood pressure control. Clin. Sci. (Lond) 132 (2018) 1383-1401.

[3] A. da Silva Novaes, R.S. Ribeiro, L.G. Pereira, F.T. Borges, M.A. Boim, Intracrine action of angiotensin II in mesangial cells: subcellular distribution of angiotensin II receptor subtypes AT1 and AT2. Mol. Cell. Biochem. 448(2018) 265-274.

[4] C.E. Evans, J.S. Miners, G. Piva, C.L. Willis, D.M. Heard, E.J. Kidd, M.A. Good, P.G. Kehoe, ACE2 activation protects against cognitive decline and reduces amyloid pathology in the Tg2576 mouse model of Alzheimer's disease. Acta Neuropathol. 139 (2020) 485-502.

[5] J.L. Labandeira-Garcia, P. Garrido-Gil, J. Rodriguez-Pallares, R. Valenzuela, A. Borrajo, A.I. Rodriguez-Perez, Brain renin-angiotensin system and dopaminergic cell vulnerability. Front Neuroanat. 8 (2014) 67.

[6] J.L. Labandeira-Garcia, J. Rodriguez-Pallares, A. Dominguez-Meijide, R. Valenzuela, B. Villar-Cheda, A.I. Rodriguez-Perez, Dopamine-angiotensin interactions in the basal ganglia and their relevance for Parkinson's disease. Mov Disord. 28 (2013) 1337-1342.

[7] A.I. Rodriguez-Perez, D. Sucunza, M.A. Pedrosa, P. Garrido-Gil, J. Kulisevsky, J.L. Lanciego, et al., Angiotensin Type 1 Receptor Antagonists Protect Against

Alpha-Synuclein-Induced Neuroinflammation and Dopaminergic Neuron Death. Neurotherapeutics. 15 (2018) 1063-1081.

[8] M.A. Costa-Besada, R. Valenzuela, P. Garrido-Gil, B. Villar-Cheda, J.A. Parga, J.L. Lanciego, et al., Paracrine and Intracrine Angiotensin 1-7/Mas Receptor Axis in the Substantia Nigra of Rodents, Monkeys, and Humans. Mol Neurobiol. 55 (2018) 5847-67.

[9] R. Valenzuela, M.A. Costa-Besada, J. Iglesias-Gonzalez, E. Perez-Costas, B. Villar-Cheda, P. Garrido-Gil, et al., Mitochondrial angiotensin receptors in dopaminergic neurons. Role in cell protection and aging-related vulnerability to neurodegeneration. Cell Death Dis. 7 (2016) e2427.

[10] B. Villar-Cheda, M.A. Costa-Besada, R. Valenzuela, E. Perez-Costas, M. Melendez-Ferro, J.L. Labandeira-Garcia, The intracellular angiotensin system buffers deleterious effects of the extracellular paracrine system. Cell Death Dis. 8 (2017) e3044.

[11] K. Kuba, Y. Imai, S. Rao, H. Gao, F. Guo, B. Guan, et al., A crucial role of angiotensin converting enzyme 2 (ACE2) in SARS coronavirus-induced lung injury. Nat Med. 11 (2005) 875-879.

[12] R. Yan , Y. Zhang, Y. Li, L. Xia, Y. Guo, Q. Zhou, Structural basis for the recognition of SARS-CoV-2 by full-length human ACE2. Science. 367 (2020) 1444-1448.

[13] A.M. Baig, A. Khaleeq, U. Ali, H. Syeda, Evidence of the COVID-19 Virus Targeting the CNS: Tissue Distribution, Host-Virus Interaction, and Proposed Neurotropic Mechanisms. ACS Chem Neurosci. 11 (2020) 995-998.

[14] Y.C. Li, W.Z. Bai, T. Hashikawa, The neuroinvasive potential of SARS-CoV2 may play a role in the respiratory failure of COVID-19 patients. J Med Virol. 92 (2020) 552-555.

[15] J.M. Saavedra, COVID-19, Angiotensin Receptor Blockers, and the Brain. Cell Mol Neurobiol. 40 (2020) 667-674.

[16] A. Antonini, V. Leta, J. Teo, K.R. Chaudhuri, Outcome of Parkinson's Disease Patients Affected by COVID-19. Mov Disord. 35 (2020) 905-908.

[17] E. Fazzini, J. Fleming, S. Fahn, Cerebrospinal fluid antibodies to coronavirus in patients with Parkinson's disease. Mov Disord. 7 (1992) 153-158.

[18] X. Dong, S. Han, M.J. Zylka, M.I. Simon, D.J. Anderson, A diverse family of GPCRs expressed in specific subsets of nociceptive sensory neurons. Cell. 106 (2001) 619-632.

[19] P.M. Lembo, E. Grazzini, T. Groblewski, D. O'Donnell, M.O. Roy, J. Zhang, et al., Proenkephalin A gene products activate a new family of sensory neuron--specific GPCRs. Nat Neurosci. 5 (2002) 201-209.

[20] A. Tetzner, K. Gebolys, C. Meinert, S. Klein, A. Uhlich, J. Trebicka, et al., G-Protein-Coupled Receptor MrgD Is a Receptor for Angiotensin-(1-7) Involving Adenylyl Cyclase, cAMP, and Phosphokinase A. Hypertension. 68 (2016) 185-194.

[21] R.Q. Lautner, D.C. Villela, R.A. Fraga-Silva, N. Silva, T. Verano-Braga, F. Costa-Fraga, et al., Discovery and characterization of alamandine: a novel component of the renin-angiotensin system. Circ Res. 112 (2013) 1104-1111.

[22] N.R. Sims, M.F. Anderson, Isolation of mitochondria from rat brain using Percoll density gradient centrifugation. Nat Protoc. 3 (2008) 1228-1239.

[23] A.I. Rodriguez-Perez, P. Garrido-Gil, M.A. Pedrosa, M. Garcia-Garrote, R. Valenzuela, G. Navarro, et al., Angiotensin type 2 receptors: Role in aging and neuroinflammation in the substantia nigra. Brain Behav Immun. 87 (2020) 256-271.

[24] P.M. Abadir, D.B. Foster, M. Crow, C.A. Cooke, J.J. Rucker, A. Jain, et al., Identification and characterization of a functional mitochondrial angiotensin system. Proc Natl Acad Sci U S A. 108 (2011) 14849-14854.

[25] B.A. Wilson, M. Nautiyal, T.M. Gwathmey, J.C. Rose, M.C. Chappell, Evidence for a mitochondrial angiotensin-(1-7) system in the kidney. Am J Physiol Renal Physiol. 310 (2016) F637-645.

[26] B. Villar-Cheda, R. Valenzuela, A.I. Rodriguez-Perez, M.J. Guerra, J.L. Labandeira-Garcia, Aging-related changes in the nigral angiotensin system enhances proinflammatory and pro-oxidative markers and 6-OHDA-induced dopaminergic degeneration. Neurobiol Aging. 33 (2012) 204.e1-11.

[27] T. Yan, R. Xiao, G. Lin, Angiotensin-converting enzyme 2 in severe acute respiratory syndrome coronavirus and SARS-CoV-2: A double-edged sword? FASEB J. 34 (2020) 6017-6026.

[28] L. Mao, H. Jin, M. Wang, Y. Hu, S.Chen, Q.He, et al., Neurologic Manifestations of Hospitalized Patients With Coronavirus Disease 2019 in Wuhan, China. JAMA Neurol. 77 (2020) 683-690.

[29] Jr, P.B. McCray, L. Pewe, C. Wohlford-Lenane, M. Hickey, L. Manzel, L. Shi, et al., Lethal infection of K18-hACE2 mice infected with severe acute respiratory syndrome coronavirus. J Virol. 81 (2007) 813-821.

[30] J. Netland, D.K. Meyerholz, S. Moore, M. Cassell, S. Perlman, Severe acute respiratory syndrome coronavirus infection causes neuronal death in the absence of encephalitis in mice transgenic for human ACE2. J Virol. 82 (2008) 7264-7275.

[31] I. Hamming, W. Timens, M.L. Bulthuis, A.T. Lely, G. Navis, H. van Goor, Tissue distribution of ACE2 protein, the functional receptor for SARS coronavirus. A first step in understanding SARS pathogenesis. J Pathol. 203 (2004) 631-637.

[32] H. Zhang, J.M. Penninger, Y. Li, N. Zhong, A.S. Slutsky, Angiotensin-converting enzyme 2 (ACE2) as a SARS-CoV-2 receptor: molecular mechanisms and potential therapeutic target. Intensive Care Med. 46 (2020) 586-590.

[33] N. Klein, F. Gembardt, S. Supe, S.M. Kaestle, H. Nickles, L. Erfinanda, et al., Angiotensin-(1-7) protects from experimental acute lung injury. Crit Care Med. 41 (2013) e334-343.

[34] K. Wang, M. Gheblawi, G.Y. Oudit, Angiotensin Converting Enzyme 2: A Double-Edged Sword. Circulation. 142 (2020) 426–428.

[35] M.A. Pedrosa, R. Valenzuela, P. Garrido-Gil, C.M. Labandeira, G. Navarro, R. Franco, J.L. Labandeira-Garcia, A.I. Rodriguez-Perez, Experimental data using candesartan and captopril indicate no double-edged sword effect in COVID-19. Clin Sci (Lond). 135 (2021) 465-481.

[36] R. Valenzuela, M.A. Pedrosa, P. Garrido-Gil, C.M. Labandeira, G. Navarro, R. Franco, A.I. Rodriguez-Perez, J.L. Labandeira-Garcia, Interactions between ibuprofen, ACE2, renin-angiotensin system and spike protein in the lung. Implications for COVID-19. Clin Transl Med. 11(4) (2021) e371.

[37] Y. Huang, Y. Li, A. Lou, G.Z. Wang, Y. Hu, Y. Zhang, et al., Alamandine attenuates hepatic fibrosis by regulating autophagy induced by NOX4-dependent ROS. Clin Sci (Lond). 134 (2020) 853-869.

[38] Y. Meng, T. Li, G.S. Zhou, Y. Chen, C.H. Yu, M.X. Pang, et al., The angiotensin-converting enzyme 2/angiotensin (1-7)/Mas axis protects against lung fibroblast migration and lung fibrosis by inhibiting the NOX4-derived ROS-mediated RhoA/Rho kinase pathway. Antioxid Redox Signal. 22 (2015) 241-258.

[39] P. Boya, A.L. Pauleau, D. Poncet, R.A. Gonzalez-Polo, N. Zamzami, G. Kroemer, Viral proteins targeting mitochondria: controlling cell death. Biochim Biophys Acta. 1659 (2004) 178-189.

[40] X. Yuan, Y. Shan, Z. Yao, J. Li, Z. Zhao, J. Chen J, et al., Mitochondrial location of severe acute respiratory syndrome coronavirus 3b protein. Mol Cells. 21 (2006) 186-191.

[41] L. Silva da Costa, A.P. Pereira da Silva, A.T. Da Poian, T. El-Bacha, Mitochondrial bioenergetic alterations in mouse neuroblastoma cells infected with Sindbis virus: implications to viral replication and neuronal death. PLoS One. 7 (2012) e33871.

[42] K.K. Singh, G. Chaubey, J.Y. Chen, P. Suravajhala, Decoding SARS-CoV-2 hijacking of host mitochondria in COVID-19 pathogenesis. Am J Physiol Cell Physiol. 319 (2020) C258-267.

[43] E. Lontok, E. Corse, C.E Machamer, Intracellular targeting signals contribute to localization of coronavirus spike proteins near the virus assembly site. J Virol. 78 (2004) 5913-5922.

[44] J. Sadasivan, M. Singh, J.D. Sarma, Cytoplasmic tail of coronavirus spike protein has intracellular targeting signals. J Biosci. 42 (2017) 231-244.

[45] C.D. Williamson, A.M. Colberg-Poley, Access of viral proteins to mitochondria via mitochondria-associated membranes. Rev Med Virol. 19 (2009) 147-164.

Legends

Fig. 1. ACE2 and MrgE receptors in the rat substantia nigra (SN) and cultured dopaminergic neurons. (a) In the SN, MrgE mRNA expression was much higher than Mas receptor and other Mrg receptor expression. (**b)** In isolated mitochondria from the nigral region, ACE2 and MrgE receptors (together with the mitochondrial marker VDAC) were highly concentrated, as compared with the whole cell homogenate (identified by the cytosol marker tubulin). (**c)** The specificity of ACE2 and MrgE antibodies was confirmed by western blot analysis of HEK293 cells transfected with ACE2-GFP or MrgE-DDK, which showed a predominant immunoreactive band compared to control non-transfected cells at 48 h post-transfection. (**d-g)** In dopaminergic N27 cells, MrgE labelling was predominantly cytoplasmatic and colocalized with MTDR-positive mitochondrial labelling. Data are presented as mean ± s.e.m or median (max-min). *$p < 0.05$, Kruskal-Wallis One Way Analysis of Variance on Ranks with Student-Newman-Keuls Method post hoc test (a); Student´s t-test (MrgE) and Mann-Whitney Rank Sum Test (ACE2) (b). Scale bar=25µm. Abbreviations: ACE2, Angiotensin Converting Enzyme 2; H or Wh, whole homogenate; MasR, Mas Receptor; M or Mt, Mitochondrial fraction; MrgE, Mas-related G-protein coupled receptor member E; MrgD, Mas-related G-protein coupled receptor member D; MrgF, Mas-related G-protein coupled receptor member F; MTDR, MitoTracker Deep Red; VDAC, Voltage-dependent anion-selective channel 1.

Fig. 2. Major Mas related receptors (MrgD, MrgE and MrgF) in different brain regions. (**a-h)** Expression of mRNA and protein of major Mas-related receptors in cell homogenates from testis (positive control for MrgD), substantia nigra (SN) and other

areas of the brain (striatum, frontal cortex, occipital cortex; ST, FC, OC). Data are presented as mean ± s.e.m or median (max-min. *$p < 0.05$, Mann-Whitney Rank Sum Test (**a, b, e**); Student´s t-test (**c**); One Way Anova (**d, g**) with Student-Newman-Keuls method post hoc test (**d**). Abbreviations: MrgE, Mas-related G-protein coupled receptor member E; MrgD, Mas-related G-protein coupled receptor member D; MrgF, Mas-related G-protein coupled receptor member F.

Fig. 3. Immunolabeling for MrgE in neurons and glial cells. (a-g) MrgE and Hoechst in different neuronal (NeuN as neuronal marker; TH as dopaminergic marker) and glial (GFAP as astrocytic marker, OX42 as microglial marker) cells in rat primary mesencephalic cultures (**a-d**) and tissue sections from rat substantia nigra (**e-g**). Immunolabeling for MrgE receptor was intense in neurons, and colocalized with NeuN (**a**) and TH (**b, e**). Astrocytes (**c, f**) and microglia (**d, g**) showed less intense immunolabeling. Scale bars: 25 µm (**a-d**); 50 µm (**e-g**). Abbreviations: GFAP, glial fibrillary acidic protein; MrgE, Mas-related G-protein coupled receptor member E; NeuN, Neuronal nuclear antigen; TH, tyrosine hydroxylase.

Fig. 4. ACE2 and MrgE in substantia nigra of non-human primates. (a, b) Protein in western blots from isolated mitochondria showing much higher concentration in the VDAC-positive mitochondrial fraction (Mt) than in the whole cell homogenate (Wh). **c** ACE2 activity in monkey isolated mitochondria, which was significantly reduced by the ACE2 inhibitor DX600. (**d-f)** Confocal microscopy of tissue sections through the monkey substantia nigra showing intense MrgE labelling in dopaminergic neurons (TH-positive cells, **d**) and lower levels of immunolabelling in astrocytes (GFAP-positive cells, **e**) and microglia (CD11b-positive cells, **f**). Data are presented as mean ± s.e.m or

median (max-min). *p< 0.05; Student´s t-test (MrgE) and Mann-Whitney Rank Sum Test (ACE2) (**a);** Student´s t-test (**c**); Scale bars: 50 µm (**d-f**). Abbreviations: ACE2, Angiotensin Converting Enzyme 2; GFAP, glial fibrillary acidic protein; M or Mt, Mitochondrial fraction; H or Wh, whole homogenate; MrgE, Mas-related G-protein coupled receptor member E; TH, tyrosine hydroxylase; VDAC, Voltage-dependent anion-selective channel 1.

Fig. 5. Fluorescence competition binding studies (a-m) and Nitric oxide (NO) release by MrgE activation (n-z). (b, c, h, i) Fluorescence labeled (FAM)-alamandine binds to both MrgE-transfected and Mas-transfected cells. (**a, f, g)** No significant binding was observed in non-transfected control HEK293 cells**.** (**b, c, j, k)** The binding of FAM-alamandine was competed by non-fluorescent alamandine and Ang 1-7, showing that both peptides are able to bind both receptors; the MrgD ligand, β-alanine, only could bind MrgE-transfected cells. (**d, e, l, m)** The MrgD blocker D-Pro, and the MasR blocker A-779 abolished the increase in fluorescence (i.e. alamandine binding) in MrgE- and Mas-transfected cells. (**n, o**, **t, u)** Using a fluorescence DAF probe, NO was not observed in non MrgE transfected controls (i.e. transfected with the empty plasmid; **n, o**) and was very weak in MrgE transfected cells (**t, u**). (**p, q, v, x)** After 10 min of treatment with alamandine MrgE transfected cells (but not control cells) increased NO-probe fluorescence. (**r, s, y, z)** Treatment with Ang 1-7 also produced an increase in NO levels in MrgE-transfected cells compared to control cells. Data are presented as mean ± s.e.m. *p< 0.05. Mann-Whitney Rank Sum Test **(a)**; Kruskal-Wallis One Way Analysis of Variance on Ranks with Dunn's Method post hoc test **(b-e)**. Scale bar: 100 µm (**f-m**) and 90 µm (**n-z**). Abbreviations: Ala, Alamandine; Ang 1-7, Angiotensin 1-7; β-Ala, β-Alanine; D-Pro, D-Proline; DAF-FM, Diaminofluorescein-FM diacetate ;

FAM-alamandine, Fluorescein labelled-alamandine; MrgD, Mas-related G-protein coupled receptor member D; MrgE, Mas-related G-protein coupled receptor member E.

Fig. 6. Mitochondrial nitric oxide (NO) production by MrgE activation. (**a-d)** Basal mitochondrial nitric oxide (NO) colocalizing with the mitochondrial marker MTDR in N27 dopaminergic neurons. € Treatment of rat brain isolated mitochondria with alamandine produced an increase in levels of mitochondrial NO detected by fluorometric assay, which was inhibited by pre-incubating the mitochondria with the receptor blocker D. (**f-r)** The functional effects of mitochondrial MrgE receptors were confirmed using confocal microscopy of HEK293 cells transfected with MrgE receptor. We observed an increase in mitochondrial NO production in MrgE-transfected cells (**f, j-l**) relative to non-transfected cells (**f, g-i**), and particularly 30 min after treatment of transfected cells with alamandine (**f, m-o**), or Ang 1-7 (**f, p-r**). Data are presented as mean ± s.e.m. *p< 0.05. One Way Anova with Student-Newman-Keuls Method post hoc test (**e**); Kruskal-Wallis One Way Analysis of Variance on Ranks with Dunn's Method post hoc test (**f**). Scale bars: 25 µm (**a-d**); 10 µm (**g-r**). Abbreviations: Ala, Alamandine; Ang 1-7, Angiotensin 1-7; DAF-FM: Diaminofluorescein-FM diacetate; D-Pro, D-Proline; MrgE, Mas-related G-protein coupled receptor member E; MTDR, MitoTracker Deep Red.

Fig. 7. Dysregulation of mitochondrial ACE2/MrgE axis by aging. (a, b) MrgE protein and mRNA expression was significantly lower in substantia nigra of aged rats relative to young rats. (**c-e)** In isolated mitochondria, aged rats also showed a significant decrease of ACE2 and MrgE levels relative to young rats, together with a marked increase in mitochondrial NOX4 levels. Data are presented as mean ± s.e.m. *p< 0.05,

Student´s t-test. Abbreviations: ACE2, Angiotensin Converting Enzyme 2; MrgE, Mas-related G-protein coupled receptor member E; NOX4, NADPH oxidase 4; VDAC, Voltage-dependent anion-selective channel 1.

Figure 1

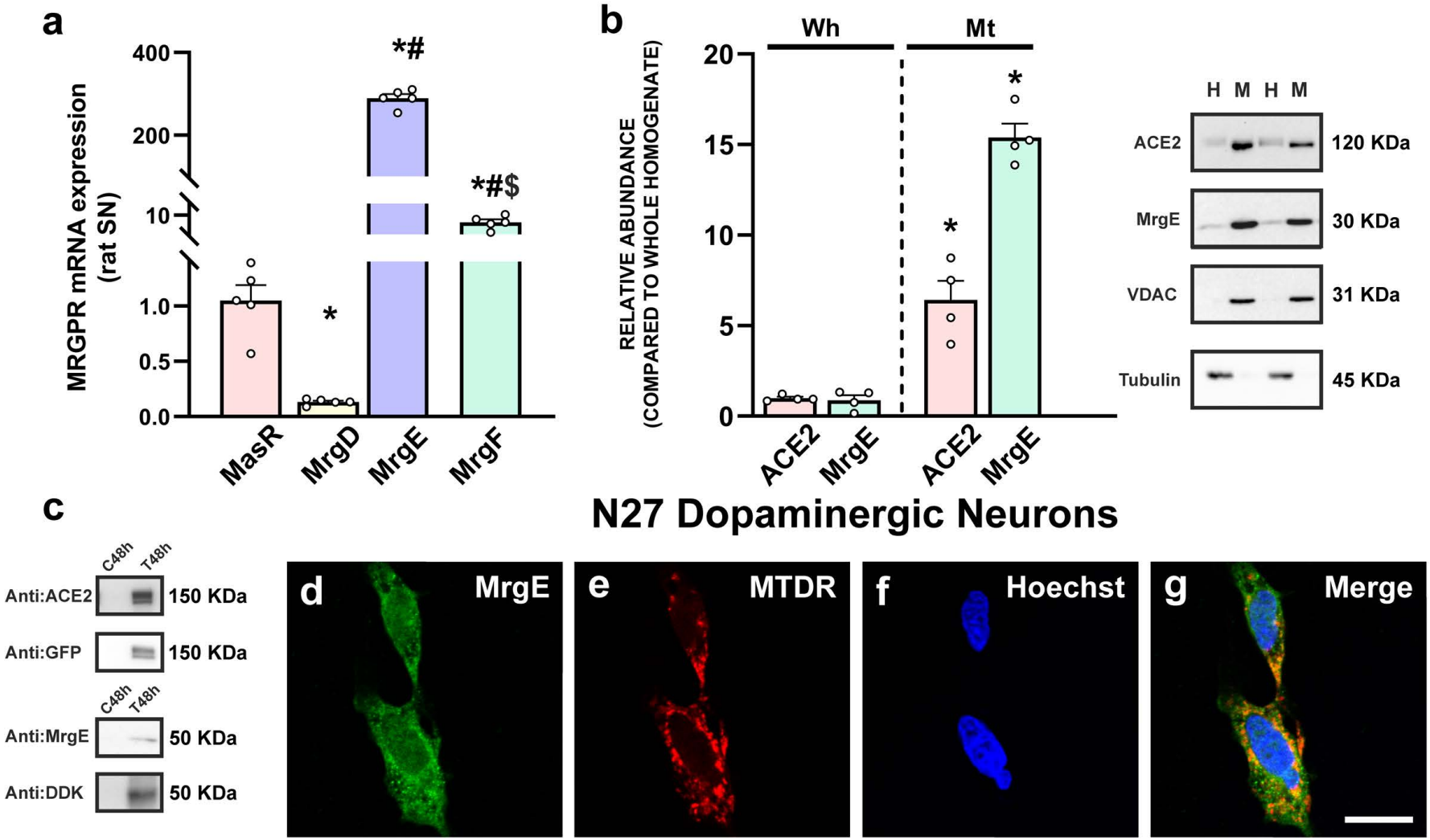
a
MRGPR mRNA expression (rat SN)
400
200
10
1.0
0.5
0.0
*#
*
*#$
MasR
MrgD
MrgE
MrgF
b
RELATIVE ABUNDANCE (COMPARED TO WHOLE HOMOGENATE)
Wh
Mt
20
15
10
5
0
*
*
ACE2
MrgE
ACE2
MrgE
H M H M
ACE2
120 KDa
MrgE
30 KDa
VDAC
31 KDa
Tubulin
45 KDa
c
C48h
T48h
Anti:ACE2
150 KDa
Anti:GFP
150 KDa
C48h
T48h
Anti:MrgE
50 KDa
Anti:DDK
50 KDa
N27 Dopaminergic Neurons
d
MrgE
e
MTDR
f
Hoechst
g
Merge

Figure 2

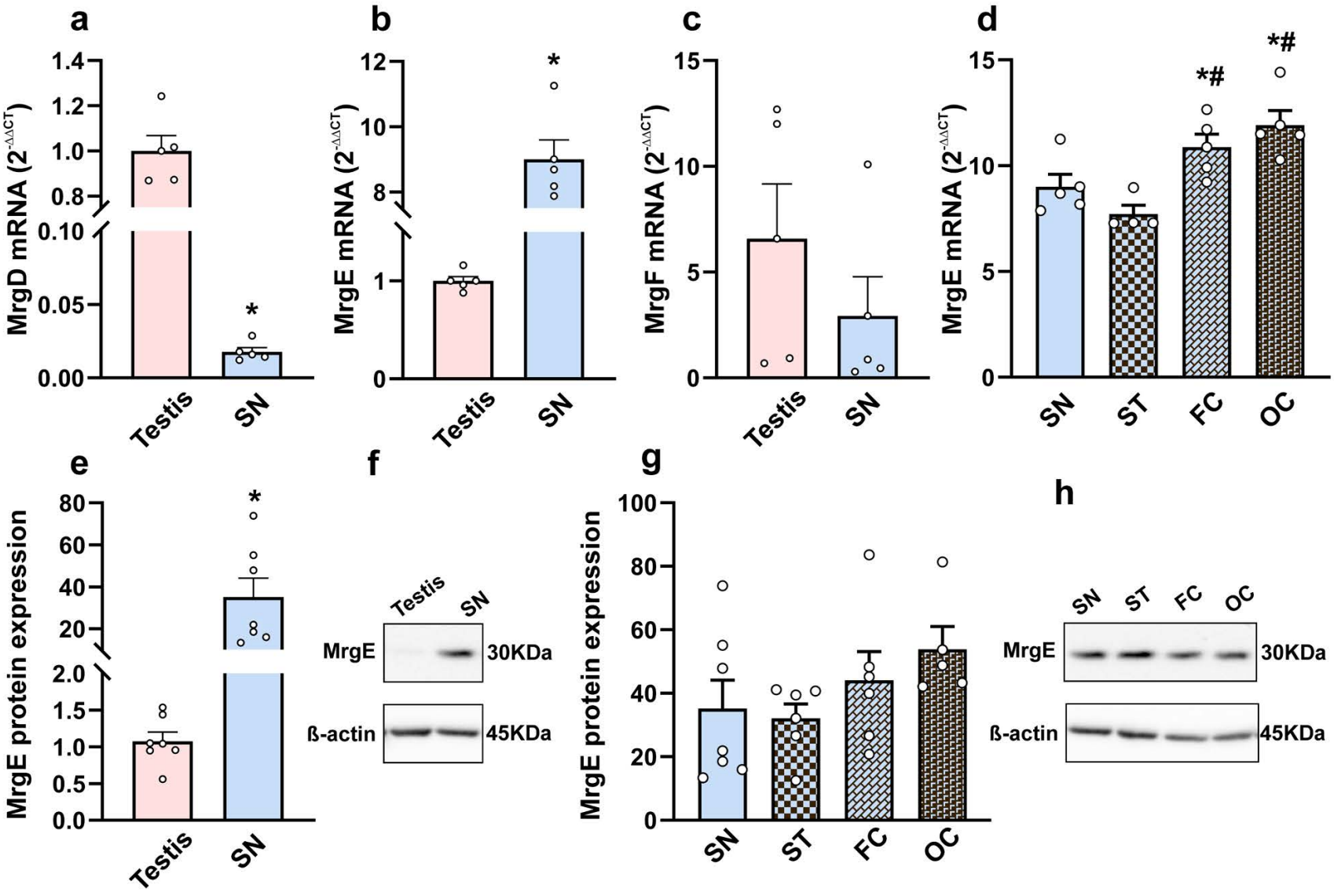
a
b
c
d
e
f
g
h
MrgD mRNA (2^-ΔΔCT)
MrgE mRNA (2^-ΔΔCT)
MrgF mRNA (2^-ΔΔCT)
MrgE mRNA (2^-ΔΔCT)
MrgE protein expression
MrgE protein expression
Testis
SN
ST
FC
OC
MrgE
ß-actin
30KDa
45KDa
*
*#

Figure 3

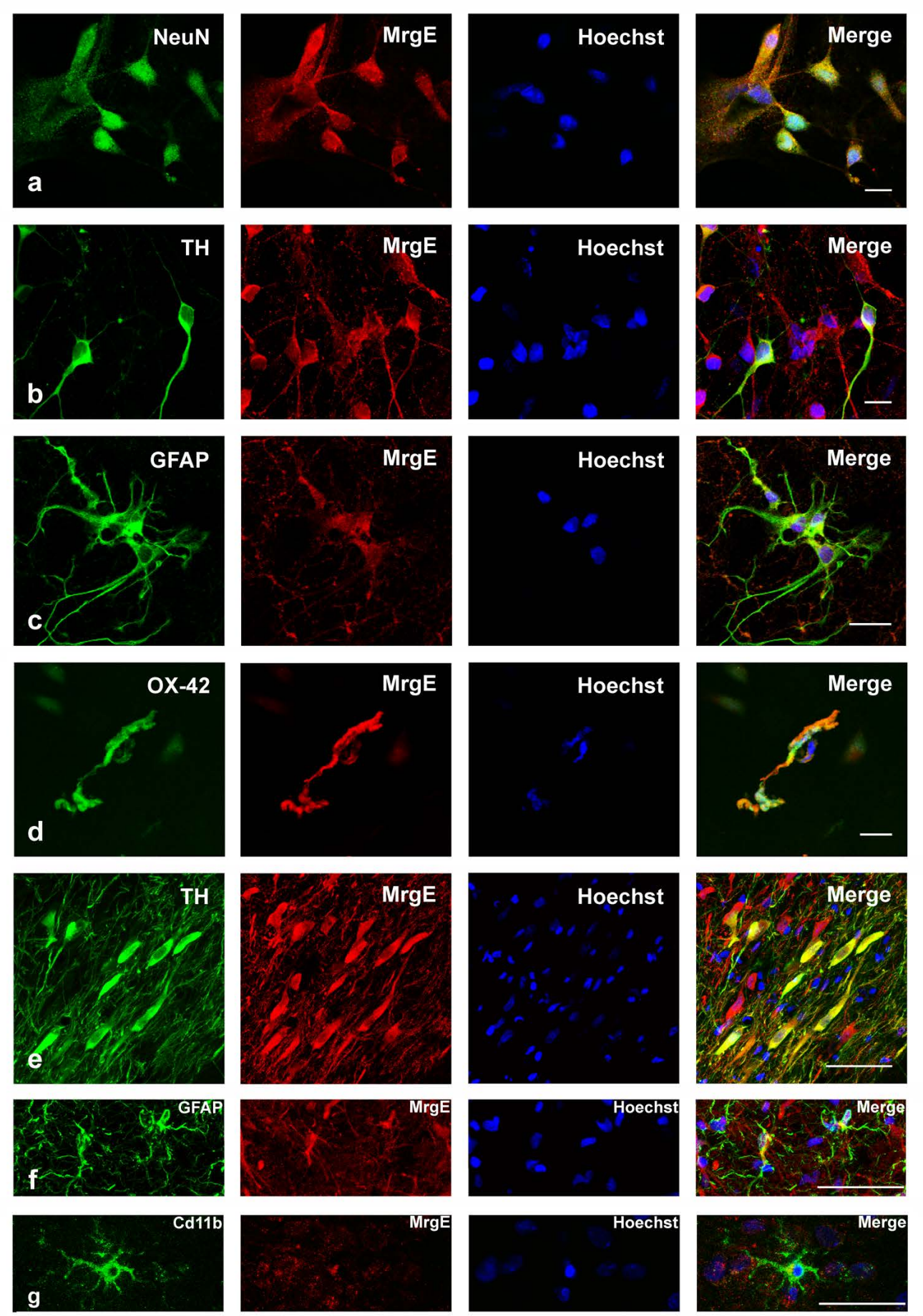
NeuN
MrgE
Hoechst
Merge
a
TH
MrgE
Hoechst
Merge
b
GFAP
MrgE
Hoechst
Merge
c
OX-42
MrgE
Hoechst
Merge
d
TH
MrgE
Hoechst
Merge
e
GFAP
MrgE
Hoechst
Merge
f
Cd11b
MrgE
Hoechst
Merge
g

Figure 4

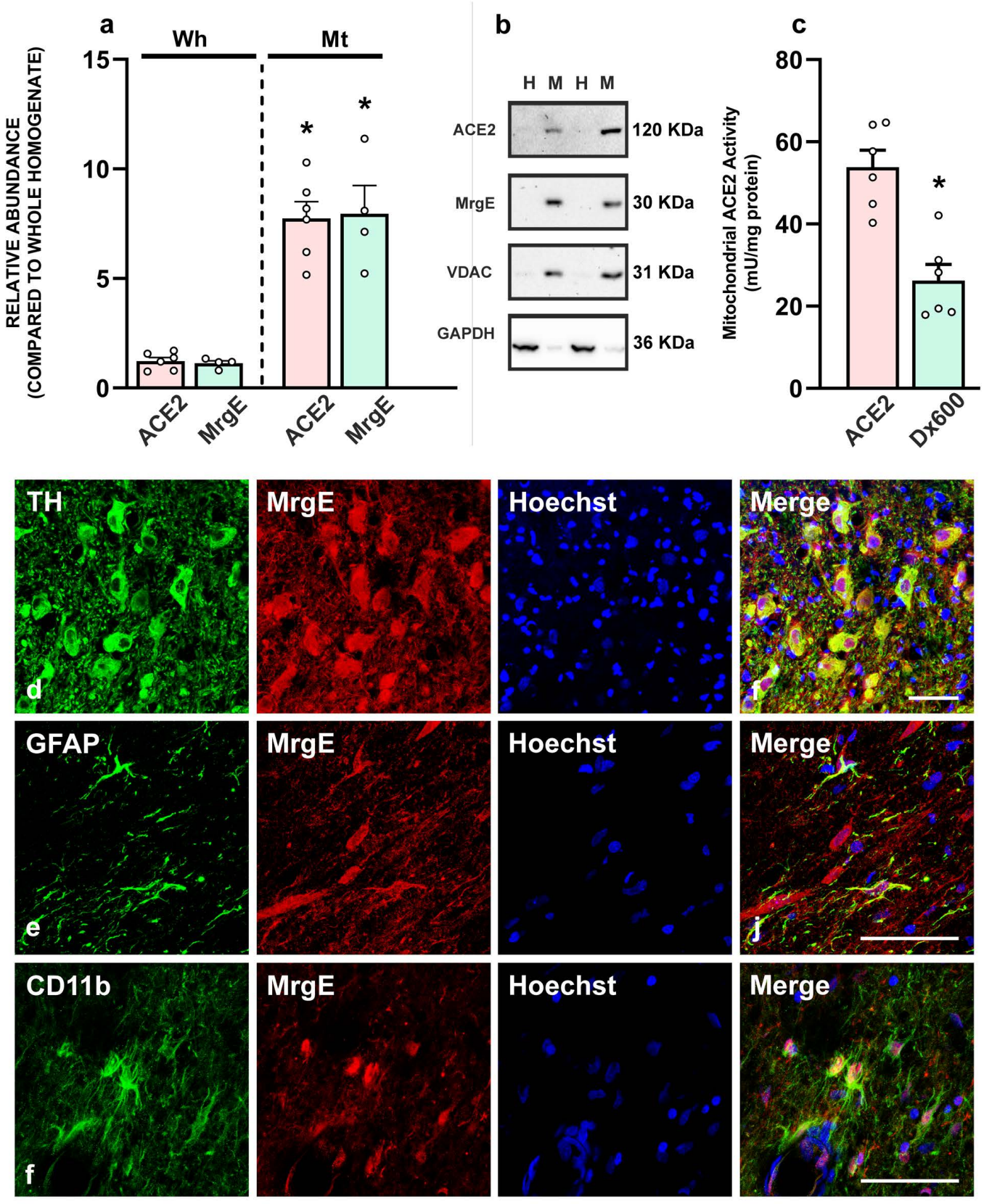
a
Wh
Mt
RELATIVE ABUNDANCE
(COMPARED TO WHOLE HOMOGENATE)
15
10
5
0
*
*
ACE2
MrgE
ACE2
MrgE
b
H M H M
ACE2
120 KDa
MrgE
30 KDa
VDAC
31 KDa
GAPDH
36 KDa
c
Mitochondrial ACE2 Activity
(mU/mg protein)
80
60
40
20
0
*
ACE2
Dx600
TH
MrgE
Hoechst
Merge
d
i
GFAP
MrgE
Hoechst
Merge
e
j
CD11b
MrgE
Hoechst
Merge
f

Figure 5

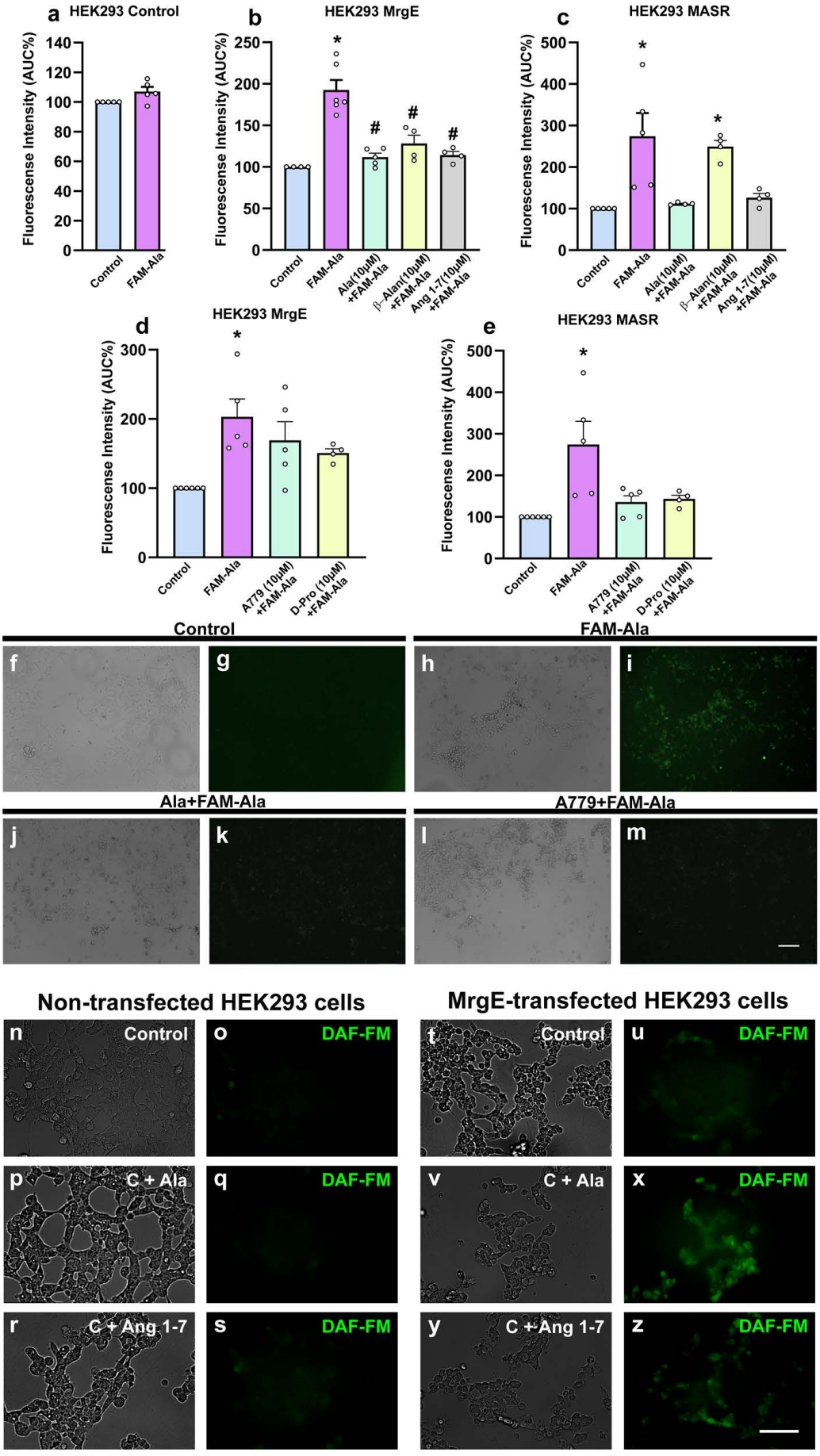
a HEK293 Control
b HEK293 MrgE
c HEK293 MASR
d HEK293 MrgE
e HEK293 MASR
Fluorescense Intensity (AUC%)
Control
FAM-Ala
Ala(10μM) +FAM-Ala
β-Alan(10μM) +FAM-Ala
Ang 1-7(10μM) +FAM-Ala
A779 (10μM) +FAM-Ala
D-Pro (10μM) +FAM-Ala
Control
FAM-Ala
Ala+FAM-Ala
A779+FAM-Ala
Non-transfected HEK293 cells
MrgE-transfected HEK293 cells
Control
DAF-FM
C + Ala
C + Ang 1-7

Figure 6

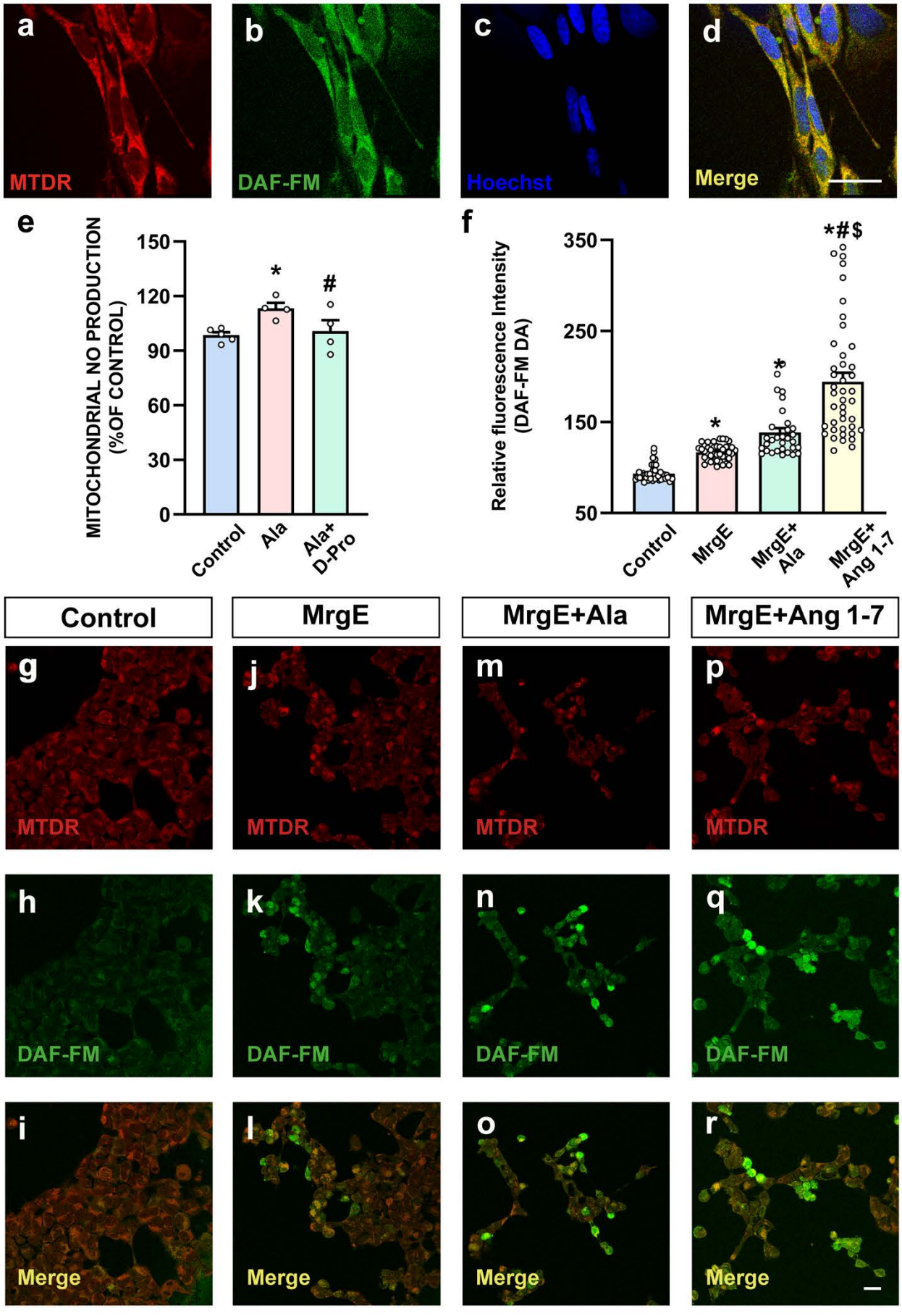
a
MTDR
b
DAF-FM
c
Hoechst
d
Merge
e
MITOCHONDRIAL NO PRODUCTION (%OF CONTROL)
150
120
90
60
30
0
*
#
Control
Ala
Ala+ D-Pro
f
Relative fluorescence Intensity (DAF-FM DA)
350
250
150
50
*
*
*#$
Control
MrgE
MrgE+ Ala
MrgE+ Ang 1-7
Control
MrgE
MrgE+Ala
MrgE+Ang 1-7
g
MTDR
j
MTDR
m
MTDR
p
MTDR
h
DAF-FM
k
DAF-FM
n
DAF-FM
q
DAF-FM
i
Merge
l
Merge
o
Merge
r
Merge

Figure 7

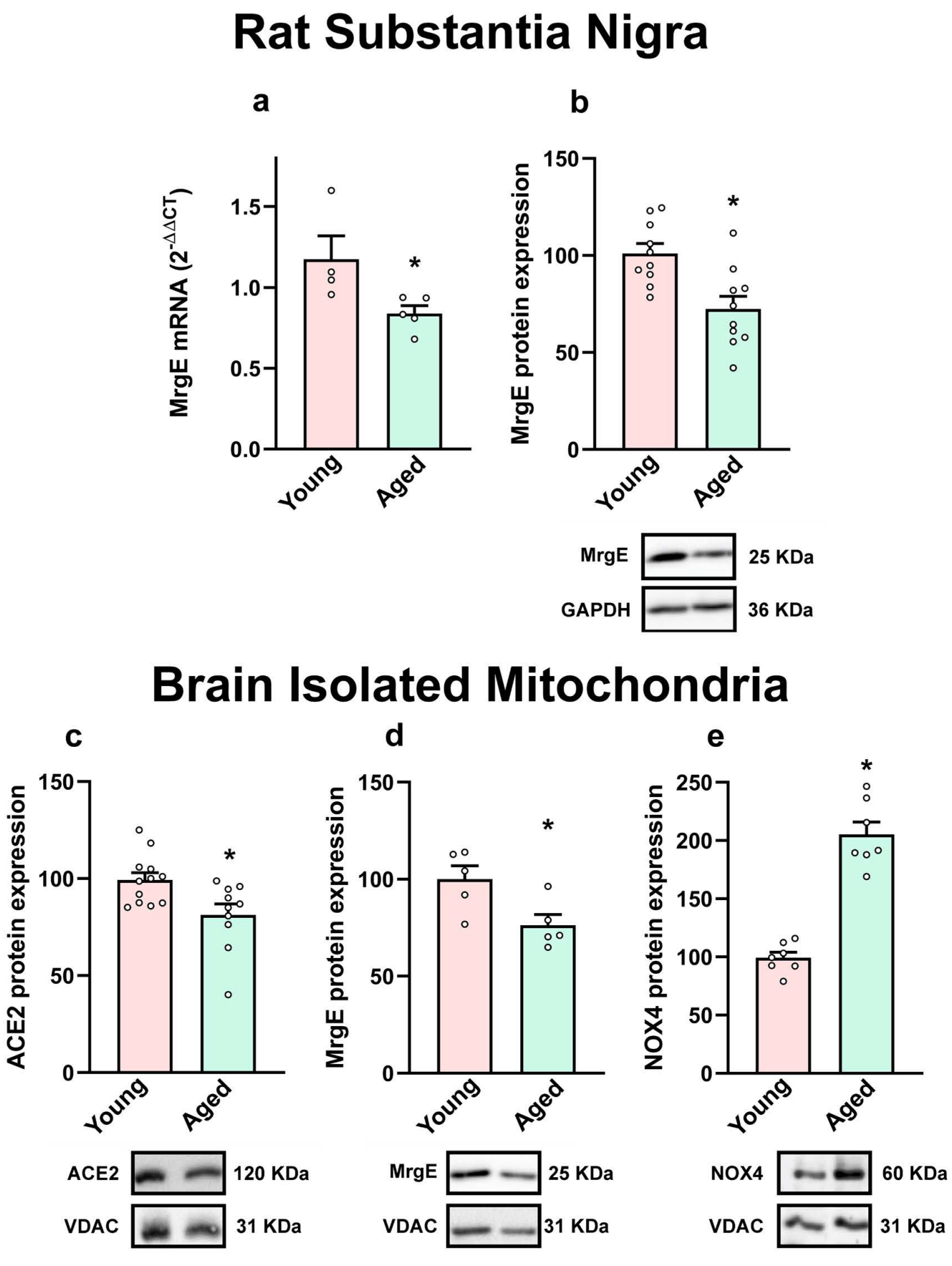
Rat Substantia Nigra
a
b
MrgE mRNA ($2^{-\Delta\Delta CT}$)
1.5
1.0
0.5
0.0
*
Young
Aged
MrgE protein expression
150
100
50
0
*
Young
Aged
MrgE
25 KDa
GAPDH
36 KDa
Brain Isolated Mitochondria
c
d
e
ACE2 protein expression
150
100
50
0
*
Young
Aged
ACE2
120 KDa
VDAC
31 KDa
MrgE protein expression
150
100
50
0
*
Young
Aged
MrgE
25 KDa
VDAC
31 KDa
NOX4 protein expression
250
200
150
100
50
0
*
Young
Aged
NOX4
60 KDa
VDAC
31 KDa

3.9 SARS-CoV-2 as a Factor to Disbalance the Renin-Angiotensin System: A Suspect in the Case of Exacerbated IL-6 Production.

Rafael Franco*, **Rafael Rivas-Santisteban***, Joan Serrano-Marín*, Ana I. Rodríguez-Pérez, José L. Labandeira-García, Gemma Navarro.

Manuscrito publicado en *The Journal of Immunology*, Julio 2020; 205: 1198–1206.

Por lo general, la aparición de fiebre en procesos infecciosos se correlaciona con inflamación, infiltración y con la activación de macrófagos en el órgano afectado y la liberación de citoquinas implicadas en la respuesta inmune. La enzima convertidora de angiotensina 2 (ACE2) se encuentra implicada en la degradación de los péptidos del sistema renina-angiotensina (RAS), principalmente cataliza la conversión de la Ang II a la Ang (1-7). ACE2 se ha descrito como la vía de entrada a la célula del virus SARS-CoV-2. En la COVID-19, la sobreproducción de citoquinas proinflamatorias especialmente la IL-6, indica el papel clave de los macrófagos en esta patología. Al internalizarse el SARS-CoV-2 con ACE2 en la célula, se produce una disminución en la disponibilidad de esta enzima en la superficie celular lo que desencadena en una desregulación entre el péptido angiotensina II que se une a los receptores de angiotensina II tipo 1 (AT_1R) y tipo 2 (AT_2R) y los péptidos Ang (1-7) y alamandina, que activan al protooncogén Mas (MasR) y a los receptores relacionados con Mas (MRGDR). Además de los macrófagos, las células de los distintos tejidos del pulmón expresan componentes del RAS e incluso, algunas células pueden producir IL-6. Comprender como el SARS-CoV-2 desequilibra el RAS a través de ACE2 permitirá prosperar en el diseño de terapias dirigidas para mejorar la patología del COVID-19.

Brief Reviews

The Journal of Immunology

SARS-CoV-2 as a Factor to Disbalance the Renin–Angiotensin System: A Suspect in the Case of Exacerbated IL-6 Production

Rafael Franco,[*,†,1] Rafael Rivas-Santisteban,[*,†,1] Joan Serrano-Marín,[*,1] Ana I. Rodríguez-Pérez,[†,‡] José L. Labandeira-García,[†,‡] and Gemma Navarro[†,§]

Fever in infections correlates with inflammation, macrophage infiltration into the affected organ, macrophage activation, and release of cytokines involved in immune response, hematopoiesis, and homeostatic processes. Angiotensin-converting enzyme 2 (ACE2) is the canonical cell surface receptor for SARS-CoV-2. ACE2 together with angiotensin receptor types 1 and 2 and ACE2 are components of the renin–angiotensin system (RAS). Exacerbated production of cytokines, mainly IL-6, points to macrophages as key to understand differential COVID-19 severity. SARS-CoV-2 may modulate macrophage-mediated inflammation events by altering the balance between angiotensin II, which activates angiotensin receptor types 1 and 2, and angiotensin 1–7 and alamandine, which activate *MAS* proto-oncogene and *MAS*-related D receptors, respectively. In addition to macrophages, lung cells express RAS components; also, some lung cells are able to produce IL-6. Addressing how SARS-CoV-2 unbalances RAS functionality via ACE2 will help design therapies to attenuate a COVID-19–related cytokine storm. *The Journal of Immunology*, 2020, 205: 1198–1206.

A mammalian naive organism exposed to a new pathogen can activate two different branches of the immune system: the innate and the adaptive immunity. The innate immunity is involved in the activation of nonspecific processes such as inflammation, whereas the adaptive immunity is related with Ag-specific processes such as, among other, Ab production or immunological memory. The most serious consequences of COVID-19 infection come from an acute respiratory distress syndrome that is aggravated by exacerbated inflammation (1). Immune cells of the white lineage infiltrate the affected tissue to become macrophages that are subsequently activated to produce and release a variety of cytokines. The plasma levels of one of them, IL-6, directly correlates with COVID-19 severity. Often, the macrophage response is limited and does not aggravate viral infections. However, for unknown reasons, some COVID-19 patients develop the so-called cytokine storm, which correlates with symptom aggravation, and the outcome can be fatal (2–4). Patients (n = 30) in the critical care unit of one of the main hospitals in Barcelona were assessed for plasma/serum levels of four cytokines (IL-6, IL-1β, IL-8, and TNF-α). IL-6 levels led to high interindividual variability, whereas IL-1β levels were within the reference value range. There was not any common trend in IL-8 or TNF-α values, which were either normal or increased. In summary, the most noticeable finding in the cytokine storm was the level of IL-6, which in some patients, may be high enough to lose the dynamic range of measurement (i.e., two orders of magnitude increase or even higher) (Refs. 5, 6, and T. Herold, V. Jurinovic, C. Arnreich, J.C. Hellmuth, M. von Bergwelt-Baildon, M. Klein, and T. Weinberger, manuscript posted on medRxiv, M.J. Cummings, M.R. Baldwin, D. Abrams, S.D. Jacobson, B.J. Meyer, E.M. Balough, J.G. Aaron, J. Claassen, L.E. Rabbani, J. Hastie, B.R. Hochman, J. Salazar-Schicchi, N.H. Yip, D. Brodie, and M.R. O'Donnell, manuscript posted on medRxiv, and J. Gong, H. Dong, S.Q. Xia, Y.Z. Huang, D. Wang, Y. Zhao, W. Liu, S. Tu, M. Zhang, Q. Wang, and F. Lu, manuscript posted on medRxiv). The marked increase in IL-6 levels has prompted the design of a clinical assay using tocilizumab, a monoclonal anti–IL-6 Ab (7, 8). More promising, and already used in COVID-19 patients treated in Spanish hospitals, corticoids may attenuate IL-6 production. It is known that the production of the cytokine is inhibited by glucocorticoids in a wide range of cell types (9). In critical illnesses, the α isoform of the glucocorticoid receptor (or nuclear receptor subfamily 3, group C, member 1 [NR3C1]) arises as a key regulator of homeostatic processes (see Ref. 10 for review).

*Molecular Neurobiology Laboratory, Department of Biochemistry and Molecular Biomedicine, University of Barcelona, 08028 Barcelona, Spain; †Centro de Investigación en Red, Enfermedades Neurodegenerativas, Instituto de Salud Carlos III, 28029 Madrid, Spain; ‡Laboratory of Cellular and Molecular Neurobiology of Parkinson's Disease, Research Center for Molecular Medicine and Chronic Diseases, Department of Morphological Sciences, Santiago de Compostela Health Research Institute, University of Santiago de Compostela, 15782 Santiago de Compostela, Spain; and §Department of Biochemistry and Physiology, Faculty of Pharmacy and Food Science, University of Barcelona, 08028 Barcelona, Spain

[1]R.F., R.R.-S., and J.S.-M. contributed equally.

ORCIDs: 0000-0003-2549-4919 (R.F.); 0000-0002-2078-6819 (R.R.-S.); 0000-0001-9316-0721 (J.S.-M.); 0000-0003-1354-8799 (A.I.R.-P.); 0000-0003-4654-0873 (G.N.).

Received for publication June 1, 2020. Accepted for publication July 1, 2020.

Address correspondence and reprint requests to Dr. Rafael Franco, Universitat de Barcelona, School of Biology, Diagonal 643, Prevosti Building, 08028 Barcelona, Spain. E-mail address: rfranco@ub.edu

Abbreviations used in this article: ACE, angiotensin-converting enzyme; Ang II, angiotensin II; Ang1–7, angiotensin 1–7; AT_1R, Ang II receptor type 1; AT_2R, Ang II receptor type 2; DPPIV, dipeptidyl peptidase IV; GPCR, G-protein–coupled receptor; MasR, Mas receptor; MERS, Middle East respiratory syndrome; Mrgpr, Mas-related GPCR; RAS, renin–angiotensin system; SDF-1, stromal-derived factor 1; STRING, Search Tool for the Retrieval of Interacting Genes/Proteins.

www.jimmunol.org/cgi/doi/10.4049/jimmunol.2000642

The link between the renin–angiotensin system (RAS) and coronaviruses was serendipitously discovered. The angiotensin-converting enzyme (ACE) 2 was identified as the receptor for viruses of the SARS family, SARS-CoV-2 being no exception (11–15). Importantly (see below), ACE2 has peptidase activity; it is one of the newest members of the RAS, which has been widely studied in relationship with the control of blood pressure. Among its components, there are ACE1, which produces angiotensin II (Ang II), and ACE2, which converts Ang II to angiotensin 1–7 (Ang1–7), Ang II receptors (Ang II receptor type 1 [AT_1R] and Ang II receptor type 2 [AT_2R]), and the Ang1–7 receptor. The latter was first identified as a product of an oncogene and because of resemblance to the *mitochondrial assembly* gene from *Saccharomyces cerevisiae* was named as Mas-related proto-oncogene (16). The receptor whose endogenous agonist is Ang1–7 is now known as Mas receptor (MasR). All these angiotensin-related receptors belong to the superfamily of G-protein–coupled receptors (GPRCRs). It should be finally noted that a novel family of receptors has been named as Mas-related GPCRs (Mrgprs) that, interestingly, also respond to Ang1–7 (17–19) but whose endogenous agonist is alamandine, another new RAS member. The relationships between RAS members is shown in Fig. 1.

Peptidases and GPCRs, lessons from HIV-1–related research

The intense multidisciplinary research on HIV-1 infection led to the discovery of one of the main anchoring molecules, the chemokine CXCR4 GPCR, and of other cell surface proteins acting as virus coreceptors. A relevant HIV-1 coreceptor was identified as dipeptidyl peptidase IV (DPPIV), also known as CD26. In human lymphocytes, the link between CXCR4 and CD26 was proven using different approaches (20). Identified in bats but also occurring in primates, CD26 acts as a receptor for Middle East respiratory syndrome (MERS) coronavirus (21, 22). Using the online Search Tool for the Retrieval of Interacting Genes/Proteins (STRING), ACE2 is directly connected with CD26/DPPIV (Fig. 2A). By default, ACE2 is connected to Ang II, which, in turn, is connected to its cognate receptors, AT_1R and AT_2R (Fig. 2A). Interestingly, the appearance of a GPCR related to DPPIV is required to force the system to include chemokine receptors in the search for connections (Fig. 2B). In contrast, with these easy-to-find connections, there are almost no papers linking SARS viruses to GPCRs. In sharp contrast, there are several articles devoted to the link between HIV-1 and GPCRs. This fact probably derives from the exhaustive research on HIV-1 and the AIDS it produces, which was more deadly than coronavirus infections. A physiological substrate of CD26 is the stromal-derived factor 1 (SDF-1), alternatively known as CXCL12, which is the endogenous agonist of the CXCR4 chemokine receptor (Fig. 3). On the one hand, SDF-1 is protective against viral entry into cells, and CD26/DPPIV catalytic activity reduces the concentration of this protective factor (20, 23). On the other hand, CXCR4 is a factor in HIV-1 viral entry (24–30). Unfortunately, SARS-CoV-2 arrived, and no background on GPCRs and the viral proteins and/or viral

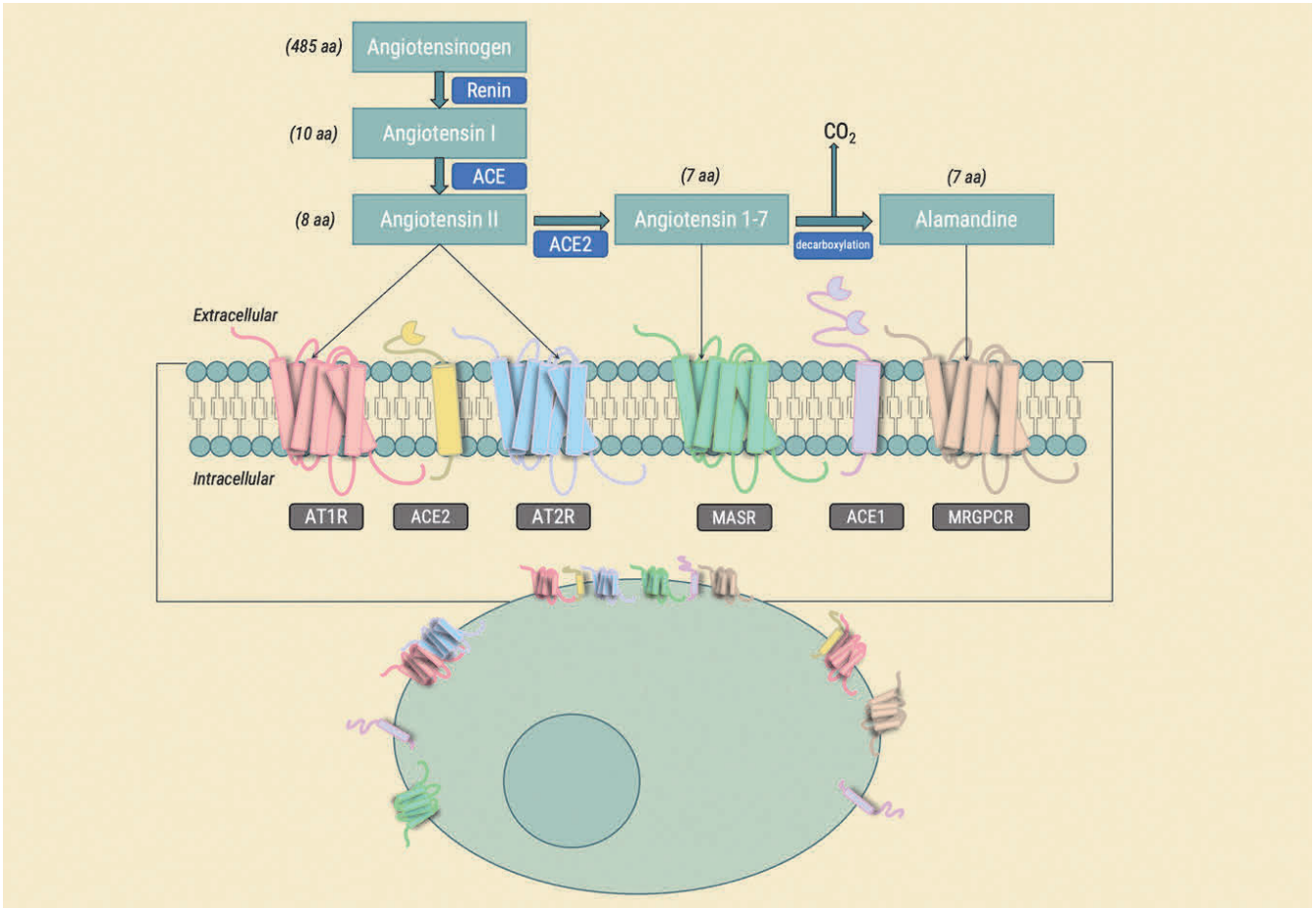

FIGURE 1. Components of RAS.

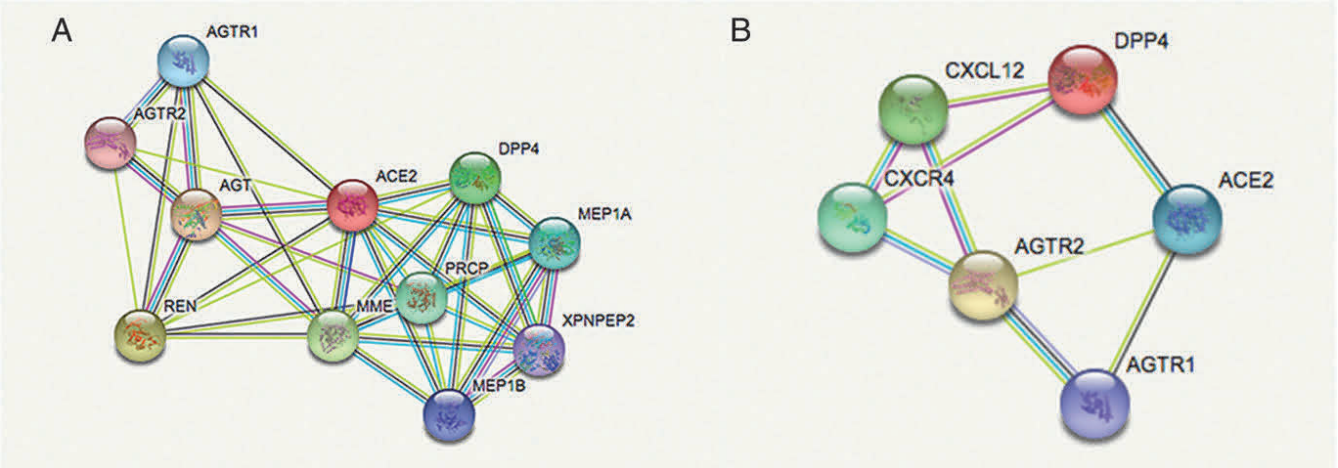

FIGURE 2. Interaction graph analysis for ACE2 and DPPIV/CD26 restricted to human using STRING. (**A**) First shell of interactions between ACE2 and other proteins. (**B**) First shell of interactions between DPPIV (DPP4 in STRING database) and other proteins. Network nodes represent proteins and edges protein–protein associations. The colors of the edges represent different sources of evidence. Known interactions: cyan, from curated databases; magenta, experimentally determined. Predicted interaction: green, gene neighborhood; red, gene fusions; blue, gene co-occurrence. Other: yellow, text mining; black, coexpression; lilac, protein homology. AGT, angiotensinogen; $AGTR_1$, type-1 Ang II receptor; $AGTR_2$, type-2 Ang II receptor; CXCL12, stromal cell-derived factor 1; DPP4, dipeptidyl peptidase 4; MEP1A, meprin A subunit α; MEP1B, meprin A subunit β; MME, neprilysin; PRCP, lysosomal Pro-X carboxypeptidase; REN, renin; XPNPEP2, Xaa-Pro aminopeptidase 2.

entry into the cells exists. Therefore, there is a need to put the focus on the blind point of COVID-19 related research: involved GPCRs, how GPCR functionality is affected by coronaviruses, and whether GPCRs may or not favor SARS entry into cells. Obviously, it is also needed to know how the viral cycle affects the functionality of GPCRs that are directly involved in viral targeting, membrane fusion, and/or viral entrance into cells.

RAS GPCRs, the blind point in SARS research

Extensive research is available related to the receptor of SDF-1, the CXCR4 chemokine receptor, and HIV-1. A search in PubMed on SDF-1 and HIV-1 leads to ~500 articles and 40 reviews, the most recent (review) in May 2020 (31). The number of articles for HIV-1 and CXCR4 are ~8 times higher, and the last review appeared in May 2020 (25). Interestingly, the formyl peptide GPCR binds with high-affinity peptides derived from proteins of HIV-1, SARS, and Ebola viruses (32, 33). However, the physiological and/or pharmacological relevance of such findings reported in 2006 is unclear. With the exception of the results related with the formyl peptide receptor, there are few or no articles devoted to studying links between GPCRs and the SARS family of coronaviruses.

The RAS is widely distributed in the mammalian body, and data in the CNS have provided evidence of a relevant role in immune function modulation. All receptors related to both Ang and Ang1–7 are expressed in microglia and contribute to the regulation of cell activation. There is interest in knowing whether the neurologic alterations observed in some COVID-19 patients are somehow mediated by the RAS system expressed in neurons and/or microglia (34–48). However, our focus in this review is RAS in macrophages, which release IL-6 when activated and also express RAS components. RAS has been for years under scrutiny from assuming that Ang II was proinflammatory and a potential profibrotic agent (49). It

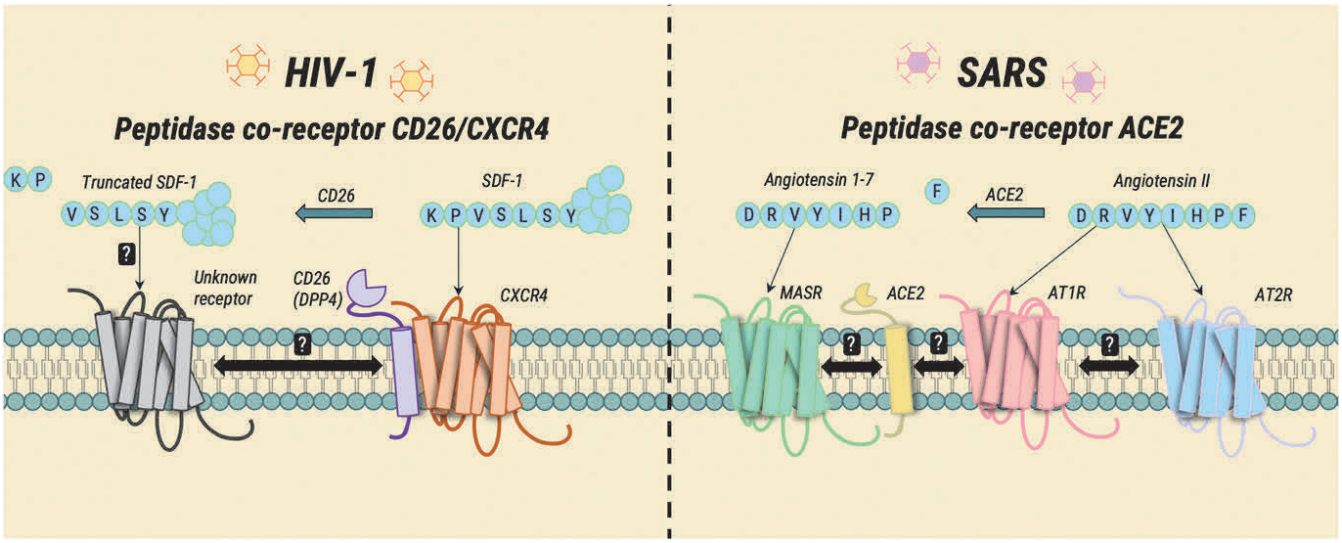

FIGURE 3. Analogies between HIV-1 and SARS receptors and coreceptors Nonconfirmed interactions are represented as a question mark (?).

becomes evident that proinflammation and profibrotic actions depend on an exquisite balance within RAS, whose activity changes depending on the differential cell surface expression of its protein components (enzymes and receptors).

The potential of RAS in IL-6 production and macrophage polarization

Activated macrophages appear in two main phenotypic variants, the proinflammatory or M1 and the anti-inflammatory or M2. From a pharmacological point of view, it is of interest to know how to skew macrophages to the M2 phenotype and whether it is possible that, at some stage of activation, M1 macrophages could be converted into M2 macrophages. Such polarization depends on inhibiting the anti-inflammatory pathway to reinforce the proinflammatory or vice versa. As pointed out in an excellent review in this topic (50), this cross-feedback regulation is due to activation/deactivation of transcription factors: PPARγ, IRF4, and STAT to promote M2 skewing and AP1, NF-κB, STAT1, and IRF5 to promote M1 skewing.

Unlike in renal cells, the RAS Ang1–7-MasR branch has been better characterized in macrophages than the Ang II–AT_1R–AT_2R branch. Although the expression pattern and the role of Ang II receptors in macrophages are not fully elucidated yet, the general idea is that Ang II is proinflammatory and that inhibitors of ACE1 or antagonists of Ang II receptors could be beneficial for patient with inflammatory diseases coursing with inflammation (51). Unfortunately, the system is more complex, as the two Ang II receptors usually have opposite functional activities. The present review complements another review (1) that appeared recently and tackles the issue of whether ACE2 expression is beneficial or not in SARS-CoV-2 infection (52).

In principle, Ang II has opposite effects depending on the receptor that is activated (Fig. 4). Activation of AT_1R by agonists exacerbates inflammation via enhancement of expression of proinflammatory cytokines. In contrast, activation of the AT_2R in macrophages regulates the activity of inducible NO synthase and negatively modulates the production of TNF-α, NF-κB, IL-6, and IL-1β (53, 54). The AT_2R also mediates the production of IL-10 by the activated macrophage (55), thus attenuating the inflammatory response. In physiological scenarios, it is assumed that inflammation occurs with preponderance of AT_1R-mediated signaling but that time passing leads to the downregulation of this receptor and to the upregulation of those RAS receptors whose function is to be anti-inflammatory and/or to mitigate inflammation (Fig. 4, left). There is a variety of ways by which RAS disbalances.

The burden of SARS-CoV-2 infections is much higher in men than in women. In April, it was reported that 2.4 times more men than women died of COVID-19 (56). As the ACE2 gene is in the X chromosome, it is tempting to speculate that gender differences in symptoms and mortality are due to decreased (overall) expression of ACE2 in men. Currently, there are no data to support the benefit of having more or less ACE2 expression. Also, one of the two X chromosomes in women is inactive. Surely 20–30% of genes escape inactivation, and the ACE2 gene seems to be one of them (57), but it is also true that ACE2 expression is greatly affected by sex hormones (58). ACE2 polymorphisms have been described (59), and therefore, males express one protein, whereas females may express two isoforms. If a given isoform represents a higher vulnerability to infection, men would be more

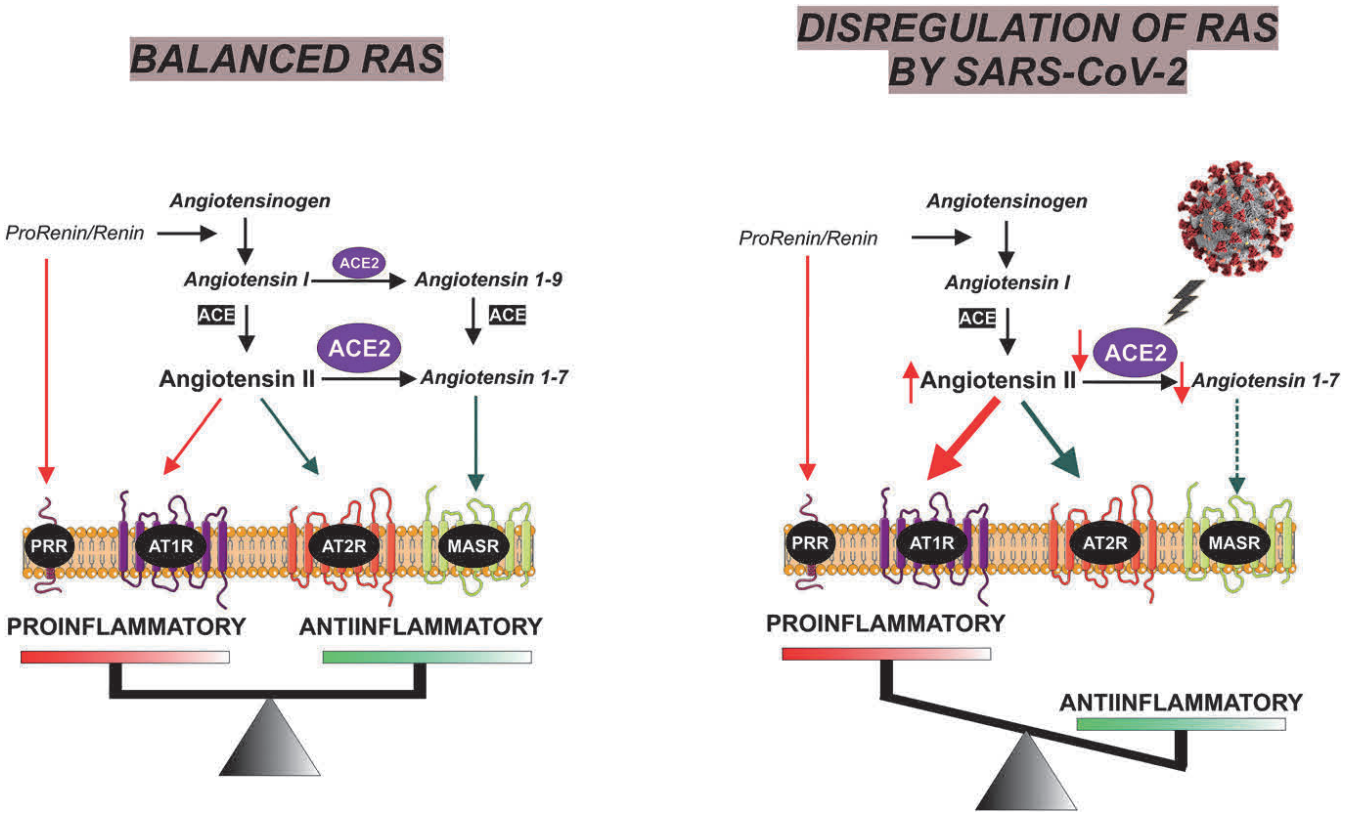

FIGURE 4. Altered ACE2 function because of SARS viral infection leads to proinflammatory outcomes via RAS deregulation. Images produced using Servier Medical Art (http://www.servier.com).

exposed because the second isoform in women could exert a compensatory/protective effect. In summary, ACE2 expression may be different in men and women, but it cannot yet be confirmed that differential expression of equal or polymorphic ACE2 correlates with symptom's severity and with mortality.

A hypothesis based on evidence from SARS research is virus-induced local reduction of ACE2 activity by either reducing its catalytic activity, downregulation, or shedding. In any of those circumstances, Ang II accumulates, Ang1–7 is reduced, and inflammation is prolonged and/or exacerbated (Fig. 4, right).

It is not known whether the two angiotensin receptors interact in macrophages as they do in microglia, where they are upregulated upon activation and where the AT_2R counteracts the proinflammatory effects mediated by the AT_1R (37, 60). Activation of the AT_2R, which is usually upregulated in diseases with inflammatory component, reduces the action of M1 macrophages and, accordingly, the synthesis of TNF-α and IL-6 (61). In summary, more effort is needed to assess the expression of AT_1R and AT_2R in resting and activated macrophages and to define the role of each receptor when macrophages activate in response to different pathogens.

The first evidence linking Ang1–7 to the regulation of cytokine release by LPS-activated macrophages came from studies using ACE2 knockout mice whose macrophages, upon activation, showed altered expression of adhesion molecules and of cytokines (IL-6 included) (62). When ACE2 is overexpressed, there is a marked reduction of Ang II–induced MCP-1 production, which is seemingly mediated by Ang1–7 (63). Those results led us to propose that the Ang1–7-MasR branch of RAS was relevant for regulating macrophage activation (64). The anti-inflammatory action of Ang1–7 was later confirmed in LPS-treated peritoneal macrophages (65) and in a polymicrobial sepsis rat model (66). Very recent results in an endotoxemia rat model show systemic anti-inflammatory action of Ang1–7 that is mediated by the MasR (67).

MasR activation poses a brake in macrophage activation. In fact, genetic ablation of the receptor leads to increased infiltration of macrophages in a variety of tissues and to increased expression of proinflammatory genes (68). Already, in 2012, upregulation of MasR in LPS-treated cells and regulation by Ang1–7 of TNF-α and of IL-6 production by activated macrophages were reported (65). The effect of the most recently identified member of the angiotensin family, alamandine (Fig. 1), and of Ang1–7 depends on the activated macrophage phenotype. In an in vitro model using macrophages activated using different protocols and in subsets of infiltrating lung macrophages isolated after inducing pleurisy in mice, activation of either MasR or Mrgprs is ineffective on resting cells but reduces inflammation because there were fewer cells producing IL-1β and TNF-α (i.e., fewer cells with the M1 proinflammatory phenotype). In contrast, receptor activation by Ang1–7 or alamandine leads to an anti-inflammatory reprograming of activated macrophages (69).

RAS dysregulation in SARS-CoV-2 infection

Based on the involvement of RAS in macrophage biology, alterations induced by SARS-CoV-2 may lead to aberrant macrophage activation. The details of the likely mechanisms operating in macrophages responding to the viral infection are schematized in Fig. 5. First of all, SARS-CoV-2 influences the homeostatic function of its receptor. This issue has not been fully addressed, but even if the SARS-CoV-2 is not affecting peptidase activity, it has been shown that 1) the virus needs ACE2 for entering into cells (70), and 2) there is a coronavirus-induced shedding of ACE2 mediated by transmembrane serine protease 2 (TMPRSS2) and/or disintegrin and metalloproteinase domain-containing protein 17 (ADAM17) (71, 72). About 30 y ago, a selective reduction in cell surface expression of CD26 in cells targeted by HIV-1 was discovered (73). Analogously, ~15 y ago, it was shown that coronavirus infection markedly reduces cell surface ACE2 expression (74, 75).

A decrease in ACE2 in the cell surface leads to RAS disbalance because of an increase in Ang II and a decrease in Ang1–7/alamandine extracellular concentrations. This unbalance of RAS leading to increasing the concentration of the proinflammatory peptide while decreasing the concentration of the anti-inflammatory peptide would exacerbate inflammation and proinflammatory IL production (Fig. 4).

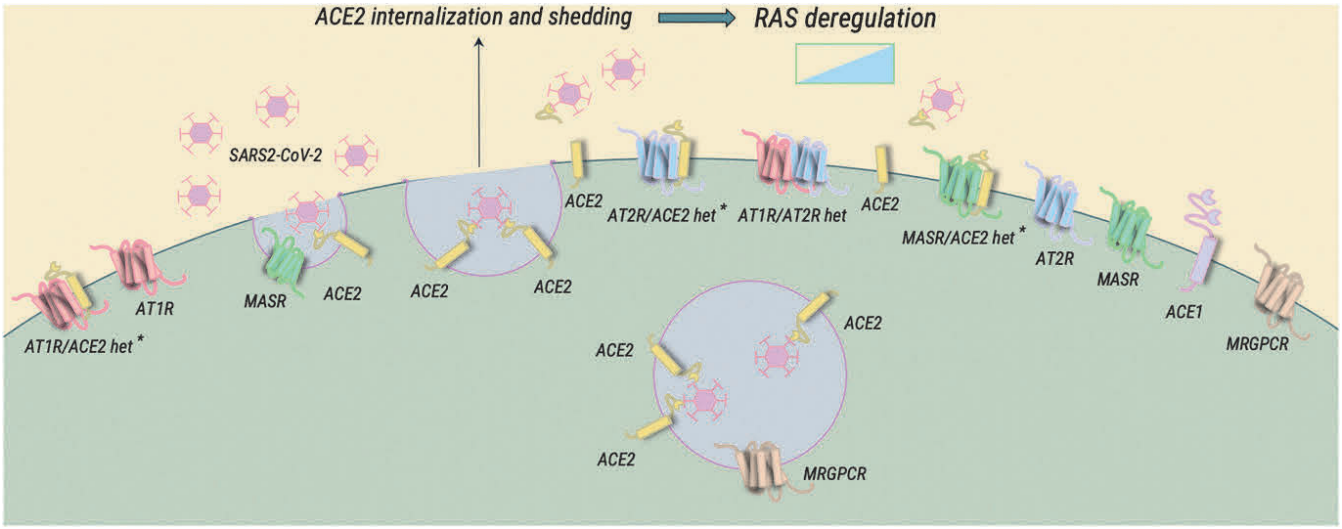

FIGURE 5. Possible scenarios involving RAS under SARS-CoV-2 infection. *1) the potential interaction between ACE2 and the AT_2R or the MasR should be investigated, and 2) there is the possibility of cointernalization of SARS-CoV-2/ACE2 together with ACE2-interacting proteins.

Other scenarios remain speculative, as there are a number of unknowns to fully understand macrophage-associated pathology and propose effective therapies. For instance, it is not known whether ACE2 may interact with the AT_2R, or even with MasR or with Mrgprs. SARS viruses are surrounded by membrane proteins of the host; are ACE2 and angiotensin receptors among them? Downregulation of ACE2 would result in a similar outcome as enzyme inhibition. If the AT_1R is identified as coreceptor, is it disappearing from the cell surface together with ACE2 and/or SARS-CoV-2? This possibility would lead to the preponderance of the action of AT_2R, which, in general terms, is anti-inflammatory; therefore, it is not occurring or only occurs in those patients who do not develop the cytokine storm. Overall, it would be informative to investigate whether ACE2 interacts with other RAS components, thus leading to the possibility that receptors of the RAS are coreceptors for the virus. Also needed is to investigate how the virus itself and/or the spike protein of the virus affect the expression and function of all components of RAS in macrophages and targeted lung cells. As in the case of CD26, ACE2 may have catalytically independent function in those cells; indeed, CD26 in lymphocytes acts as a costimulatory molecule of relevance in immune and endocrine responses (76). In addition, the noncatalytic function of CD26 is altered by HIV-1 viral particles and by the envelope HIV-1 gp120 glycoprotein (77). This action is mechanistically dependent on the expression of the main HIV-1 receptor, CD4, and of CXCR4 (78). Already, in 2008, a role of the C-terminal domain of ACE2 in infections by SARS-CoV was identified (79) but was not investigated further. In summary, it would be important to know how SARS-CoV-2 affects the expression and function of protein RAS components, including the possible heteromers that, hopefully because of COVID-19–related research pressure, may now be discovered (labeled with * in Fig. 5).

Cells other than macrophages are likely involved in aberrant IL-6 production

Inhibiting ACE2 and altering the RAS balance in macrophages surely lead to the increase in proinflammatory cytokines but probably not to the extent of triggering a cytokine storm. Then, other mechanism may operate in cases with serious symptoms, very abnormal IL-6 levels, and increased death risk. It should be noted the title of a recent preprint: "*Level of IL-6 predicts respiratory failure in hospitalized symptomatic COVID-19 patients*" (T. Herold, V. Jurinovic, C. Arnreich, J.C. Hellmuth, M. von Bergwelt-Baildon, M. Klein, and T. Weinberger, manuscript posted on medRxiv). A recent metanalysis confirms that elevated IL-6 is one of the common findings in fatal outcomes (5). It is then reasonable to hypothesize that in the most serious cases, cells of the patient's lungs may be able to release IL-6, thus engaging a harmful, vicious cycle.

The most serious COVID-19 cases course with pneumonia, and ACE2 is heavily expressed in the lung (80). The air-exposed internal surface of the lungs is composed of a variety of cells: ciliated, secretory, pneumocyte, basal, stromal, endothelial, and epithelial. The most abundant (i.e., epithelial and endothelial) are capable of producing IL-6 and express almost every RAS component. ACE2 is expressed in type II pneumocytes and in most respiratory-related epithelial cells, with the notable exception of those in the upper respiratory tract, including nasal and oral mucosa (80). In addition, ACE2 is located in the apical side of polarized cells (81) (i.e., readily available to SARS-CoV-2). How expression of RAS components is affected by SARS-CoV-2 in pneumocytes and lung epithelial or endothelial cells has not been tested yet.

Epithelial cells may produce IL-6. The first article on this issue reported production and secretion of IL-6 by stimulated epithelial cells of the human retinal pigment (82). As demonstrated in a variety of experimental models, endothelial cells may produce IL-6 (83–85). Furthermore, IL-6 and TNF-α produced by macrophages may lead to endothelial dysfunction (86).

From a multicenter validation study in critically ill patients because of sepsis, which also occurs in some COVID-19 patients (87), it is known that markers of endothelium activation are predictive of final outcome and that soluble FLT-1 (sFLT-1) may be a sepsis biomarker (88). The sFLT-1 is a marker of preeclamptic hypertension in which RAS is dysbalanced, and there is an increase in the expression in platelets of the heteromer formed by the AT_1R and the bradykinin B2 receptor (89). Interestingly, the B2 receptor may interact directly with the AT_2R (90). In addition, it has been recently hypothesized that dysregulated bradykinin signaling is behind respiratory complications because of COVID-19 (91), whereas it is known the direct link between bradykinin, platelets, and coagulopathy (92), which is another complication in COVID-19 patients. In fact, some patients not only present a cytokine storm, but signs of disseminated intravascular coagulation, which increased serum levels of fibrin degradation products, such as the D-dimer (93, 94). IL-6 may negatively impact on coagulation control mechanisms (8).

Also known is that human coronavirus spike proteins downregulate ACE2 (95) and that ACE2 expression is protective against lung failure (in a murine model) (74). After COVID-19 infection, sequalae include lung fibrosis that can be mediated by altered RAS. Ang II reportedly upregulates the AT_1R, downregulates the AT_2R (AT_1R/AT_2R ratio going from 0.4 to 1.4), and increases the activity of a profibrotic enzyme, hyaluronidase (96).

Is there a coinfection impacting on IL production by lung cells?

The interindividual response to COVID-19 depends on the viral load, the rate of viral replication, which varies from individual to individual, and the differential expression of the RAS component in the attacked cells (lung cells exposed to the inspired air) and in infiltrating macrophages. However, it cannot be ruled out that opportunistic infections take over and influence disease outcome. Bacterial infection can lead to the production of ILs by cells of the nonimmune system. In fact, bacterial LPS endotoxin can induce IL-6 synthesis by a variety of cells as diverse as osteoblasts (97) and endothelial cells (98). Existing data cannot test the hypothesis that pneumonia is caused by more than one pathogen, but it maintains that possibility. If this were the case, RAS would also have a relevant role.

It should be noted that acute respiratory distress syndrome animal models can be achieved by sepsis induction; therefore, superinfection may be also impacting in the respiratory problems in patients, requiring mechanical ventilation (99). Potential pathogens include, but are not limited to, *Mycoplasma*

and *Chlamydia*, which, in parallel to pneumonia induction, lead to increases in serum of IL-6 levels (100–104), with features such as IL-17–mediated effects that are common in patients infected with MERS-CoV or SARS-CoV viruses (105, 106). Even pneumonia induced by *Escherichia coli* courses with elevated IL-6 concentration in serum, Gram-positive bacteria, leading to lower IL-6 and TNF-α levels than Gram-negative bacteria (107, 108). The very informative report on the findings in interstitial pneumonia versus nonspecific interstitial pneumonia/fibrosis is recommended, which includes the sources of IL-6 upon analysis of lung biopsy specimens (109). The imbalance of RAS in idiopathic pneumonia, the involvement in fibrosis postpneumonia, and the therapeutic possibilities by targeting some of the components are reviewed elsewhere (110).

Conclusions

MERS viruses attach to DPPIV/CD26 peptidase in targeted cells. SARS viruses attach to and alter ACE2 peptidase function with local downregulation and reduction of the catalytic activity, thus altering the Ang II/Ang1–7 and Ang II/alamandine ratios. Such RAS disbalance may lead to serious consequences in cases of inflammation. SARS-CoV-2 not only alters RAS in targeted cells but in macrophages infiltrating the affected tissue(s). The evidence points to a reduction of ACE2 function, by inhibition, downregulation, and/or shedding caused by viral proteins. Further alterations in the function of RAS proteins are likely to occur after coronavirus attack. The link between an altered RAS and cytokine storm and pulmonary fibrosis also needs to be addressed in detail. Such knowledge would likely open new perspectives to combat infection and guide the appropriate management of disease aggravation and of comorbidities.

Disclosures

The authors have no financial conflicts of interest.

References

1. Merad, M., and J. C. Martin. 2020. Pathological inflammation in patients with COVID-19: a key role for monocytes and macrophages. [Published erratum appears in 2020 *Nat. Rev. Immunol.* 20: 448.] *Nat. Rev. Immunol.* 20: 355–362.
2. Chen, J., and K. Subbarao. 2007. The immunobiology of SARS*. *Annu. Rev. Immunol.* 25: 443–472.
3. Chen, N., M. Zhou, X. Dong, J. Qu, F. Gong, Y. Han, Y. Qiu, J. Wang, Y. Liu, Y. Wei, et al. 2020. Epidemiological and clinical characteristics of 99 cases of 2019 novel coronavirus pneumonia in Wuhan, China: a descriptive study. *Lancet* 395: 507–513.
4. Zhou, F., T. Yu, R. Du, G. Fan, Y. Liu, Z. Liu, J. Xiang, Y. Wang, B. Song, X. Gu, et al. 2020. Clinical course and risk factors for mortality of adult inpatients with COVID-19 in Wuhan, China: a retrospective cohort study. [Published erratum appears in 2020 *Lancet* 395: 1038.] *Lancet* 395: 1054–1062.
5. Henry, B. M., M. H. S. de Oliveira, S. Benoit, M. Plebani, and G. Lippi. 2020. Hematologic, biochemical and immune biomarker abnormalities associated with severe illness and mortality in coronavirus disease 2019 (COVID-19): a meta-analysis. *Clin. Chem. Lab. Med.* 58: 1021–1028.
6. Liu, T., J. Zhang, Y. Yang, H. Ma, Z. Li, J. Zhang, J. Cheng, X. Zhang, Y. Zhao, Z. Xia, et al. 2020. The role of interleukin-6 in monitoring severe case of coronavirus disease 2019. *EMBO Mol. Med.* DOI: 10.15252/emmm.202012421.
7. Chen, X., B. Zhao, Y. Qu, Y. Chen, J. Xiong, Y. Feng, D. Men, Q. Huang, Y. Liu, B. Yang, et al. 2020. Detectable serum SARS-CoV-2 viral load (RNAaemia) is closely correlated with drastically elevated interleukin 6 (IL-6) level in critically ill COVID-19 patients. *Clin. Infect. Dis.* DOI: 10.1093/cid/ciaa449.
8. Tanaka, T., M. Narazaki, and T. Kishimoto. 2016. Immunotherapeutic implications of IL-6 blockade for cytokine storm. *Immunotherapy* 8: 959–970.
9. Waage, A., G. Slupphaug, and R. Shalaby. 1990. Glucocorticoids inhibit the production of IL6 from monocytes, endothelial cells and fibroblasts. *Eur. J. Immunol.* 20: 2439–2443.
10. Meduri, G. U., and G. P. Chrousos. 2020. General adaptation in critical illness: glucocorticoid receptor-alpha master regulator of homeostatic corrections. *Front. Endocrinol. (Lausanne)* 11: 161.
11. Clarke, N. E., and A. J. Turner. 2012. Angiotensin-converting enzyme 2: the first decade. *Int. J. Hypertens.* 2012: 307315.
12. Wan, Y., J. Shang, R. Graham, R. S. Baric, and F. Li. 2020. Receptor recognition by the novel coronavirus from Wuhan: an analysis based on decade-long structural studies of SARS coronavirus. *J. Virol.* 94: e00127-20.
13. Shang, J., G. Ye, K. Shi, Y. Wan, C. Luo, H. Aihara, Q. Geng, A. Auerbach, and F. Li. 2020. Structural basis of receptor recognition by SARS-CoV-2. *Nature* 581: 221–224.
14. Kuhn, J. H., W. Li, H. Choe, and M. Farzan. 2004. Angiotensin-converting enzyme 2: a functional receptor for SARS coronavirus. *Cell. Mol. Life Sci.* 61: 2738–2743.
15. Li, W., M. J. Moore, N. Vasilieva, J. Sui, S. K. Wong, M. A. Berne, M. Somasundaran, J. L. Sullivan, K. Luzuriaga, T. C. Greenough, et al. 2003. Angiotensin-converting enzyme 2 is a functional receptor for the SARS coronavirus. *Nature* 426: 450–454.
16. Bader, M., N. Alenina, D. Young, R. A. S. Santos, and R. M. Touyz. 2018. The meaning of mas. *Hypertension* 72: 1072–1075.
17. Souza, L. L., J. Duchene, M. Todiras, L. C. P. Azevedo, C. M. Costa-Neto, N. Alenina, R. A. Santos, and M. Bader. 2014. Receptor MAS protects mice against hypothermia and mortality induced by endotoxemia. *Shock* 41: 331–336.
18. Santos, R. A. S., A. C. Simoes e Silva, C. Maric, D. M. R. Silva, R. P. Machado, I. de Buhr, S. Heringer-Walther, S. V. B. Pinheiro, M. T. Lopes, M. Bader, et al. 2003. Angiotensin-(1-7) is an endogenous ligand for the G protein-coupled receptor Mas. *Proc. Natl. Acad. Sci. USA* 100: 8258–8263.
19. Villela, D., J. Leonhardt, N. Patel, J. Joseph, S. Kirsch, A. Hallberg, T. Unger, M. Bader, R. A. Santos, C. Sumners, and U. M. Steckelings. 2015. Angiotensin type 2 receptor (AT2R) and receptor Mas: a complex liaison. *Clin. Sci. (Lond.)* 128: 227–234.
20. Herrera, C., C. Morimoto, J. Blanco, J. Mallol, F. Arenzana, C. Lluis, and R. Franco. 2001. Comodulation of CXCR4 and CD26 in human lymphocytes. *J. Biol. Chem.* 276: 19532–19539.
21. van Doremalen, N., and V. J. Munster. 2015. Animal models of middle east respiratory syndrome coronavirus infection. *Antiviral Res.* 122: 28–38.
22. Munster, V. J., D. R. Adney, N. van Doremalen, V. R. Brown, K. L. Miazgowicz, S. Milne-Price, T. Bushmaker, R. Rosenke, D. Scott, A. Hawkinson, et al. 2016. Replication and shedding of MERS-CoV in Jamaican fruit bats (Artibeus jamaicensis). *Sci. Rep.* 6: 21878.
23. Shioda, T., H. Kato, Y. Ohnishi, K. Tashiro, M. Ikegawa, E. E. Nakayama, H. Hu, A. Kato, Y. Sakai, H. Liu, et al. 1998. Anti-HIV-1 and chemotactic activities of human stromal cell-derived factor 1alpha (SDF-1alpha) and SDF-1beta are abolished by CD26/dipeptidyl peptidase IV-mediated cleavage. *Proc. Natl. Acad. Sci. USA* 95: 6331–6336.
24. Berger, E. A., P. M. Murphy, and J. M. Farber. 1999. Chemokine receptors as HIV-1 coreceptors: roles in viral entry, tropism, and disease. *Annu. Rev. Immunol.* 17: 657–700.
25. Wang, Q., A. Finzi, and J. Sodroski. 2020. The conformational states of the HIV-1 envelope glycoproteins. *Trends Microbiol.* DOI: 10.1016/j.tim.2020.03.007.
26. Cammack, N. 1999. Human immunodeficiency virus type 1 entry and chemokine receptors: a new therapeutic target. *Antivir. Chem. Chemother.* 10: 53–62.
27. Hoxie, J. A., C. C. LaBranche, M. J. Endres, J. D. Turner, J. F. Berson, R. W. Doms, and T. J. Matthews. 1998. CD4-independent utilization of the CXCR4 chemokine receptor by HIV-1 and HIV-2. *J. Reprod. Immunol.* 41: 197–211.
28. Clapham, P. R., J. D. Reeves, G. Simmons, N. Dejucq, S. Hibbitts, and A. McKnight. 1999. HIV coreceptors, cell tropism and inhibition by chemokine receptor ligands. *Mol. Membr. Biol.* 16: 49–55.
29. Choe, H. 1998. Chemokine receptors in HIV-1 and SIV infection. *Arch. Pharm. Res.* 21: 634–639.
30. Howard, O. M., T. Korte, N. I. Tarasova, M. Grimm, J. A. Turpin, W. G. Rice, C. J. Michejda, R. Blumenthal, and J. J. Oppenheim. 1998. Small molecule inhibitor of HIV-1 cell fusion blocks chemokine receptor-mediated function. *J. Leukoc. Biol.* 64: 6–13.
31. Fang, X., Q. Meng, H. Zhang, B. Liang, S. Zhu, J. Wang, C. Zhang, L. S. Huang, X. Zhang, R. T. Schooley, et al. 2020. Design, synthesis, and biological characterization of a new class of symmetrical polyamine-based small molecule CXCR4 antagonists. *Eur. J. Med. Chem.* 200: 112410.
32. Mills, J. S. 2006. Peptides derived from HIV-1, HIV-2, Ebola virus, SARS coronavirus and coronavirus 229E exhibit high affinity binding to the formyl peptide receptor. *Biochim. Biophys. Acta* 1762: 693–703.
33. Braun, M. C., J. M. Wang, E. Lahey, R. L. Rabin, and B. L. Kelsall. 2001. Activation of the formyl peptide receptor by the HIV-derived peptide T-20 suppresses interleukin-12 p70 production by human monocytes. *Blood* 97: 3531–3536.
34. Labandeira-Garcia, J. L., A. I. Rodríguez-Perez, P. Garrido-Gil, J. Rodriguez-Pallares, J. L. Lanciego, and M. J. Guerra. 2017. Brain renin-angiotensin system and microglial polarization: implications for aging and neurodegeneration. *Front. Aging Neurosci.* 9: 129.
35. Garrido-Gil, P., A. I. Rodriguez-Perez, A. Dominguez-Meijide, M. J. Guerra, and J. L. Labandeira-Garcia. 2018. Bidirectional neural interaction between central dopaminergic and gut lesions in Parkinson's disease models. *Mol. Neurobiol.* 55: 7297–7316.
36. Valenzuela, R., M. A. Costa-Besada, J. Iglesias-Gonzalez, E. Perez-Costas, B. Villar-Cheda, P. Garrido-Gil, M. Melendez-Ferro, R. Soto-Otero, J. L. Lanciego, D. Henrion, et al. 2016. Mitochondrial angiotensin receptors in dopaminergic neurons. Role in cell protection and aging-related vulnerability to neurodegeneration. *Cell Death Dis.* 7: e2427.
37. Rodriguez-Perez, A. I., P. Garrido-Gil, M. A. Pedrosa, M. Garcia-Garrote, R. Valenzuela, G. Navarro, R. Franco, and J. L. Labandeira-Garcia. 2020.

Angiotensin type 2 receptors: role in aging and neuroinflammation in the substantia nigra. *Brain Behav. Immun.* 87: 256–271.
38. Dominguez-Meijide, A., A. I. Rodriguez-Perez, C. Diaz-Ruiz, M. J. Guerra, and J. L. Labandeira-Garcia. 2017. Dopamine modulates astroglial and microglial activity via glial renin-angiotensin system in cultures. *Brain Behav. Immun.* 62: 277–290.
39. Garcia-Garrote, M., A. Perez-Villalba, P. Garrido-Gil, G. Belenguer, J. A. Parga, F. Perez-Sanchez, J. L. Labandeira-Garcia, I. Fariñas, and J. Rodriguez-Pallares. 2019. Interaction between angiotensin type 1, type 2, and Mas receptors to regulate adult neurogenesis in the brain ventricular-subventricular zone. *Cells* 8: 1551.
40. Rivas-Santisteban, R., A. Rodriguez-Perez, A. Muñoz, I. Reyes-Resina, J. Labandeira-García, G. Navarro, and R. Franco. 2020. Angiotensin AT1 and AT2 receptor heteromer expression in the hemilesioned rat model of Parkinson's disease that increases with levodopa-induced dyskinesia. *J. Neuroinflammation.* In press.
41. Valenzuela, R., P. Barroso-Chinea, B. Villar-Cheda, B. Joglar, A. Muñoz, J. L. Lanciego, and J. L. Labandeira-Garcia. 2010. Location of prorenin receptors in primate substantia nigra: effects on dopaminergic cell death. *J. Neuropathol. Exp. Neurol.* 69: 1130–1142.
42. Joglar, B., J. Rodriguez-Pallares, A. I. Rodriguez-Perez, P. Rey, M. J. Guerra, and J. L. Labandeira-Garcia. 2009. The inflammatory response in the MPTP model of Parkinson's disease is mediated by brain angiotensin: relevance to progression of the disease. *J. Neurochem.* 109: 656–669.
43. Rodriguez-Pallares, J., P. Rey, J. A. Parga, A. Muñoz, M. J. Guerra, and J. L. Labandeira-Garcia. 2008. Brain angiotensin enhances dopaminergic cell death via microglial activation and NADPH-derived ROS. *Neurobiol. Dis.* 31: 58–73.
44. Villar-Cheda, B., R. Valenzuela, A. I. Rodriguez-Perez, M. J. Guerra, and J. L. Labandeira-Garcia. 2012. Aging-related changes in the nigral angiotensin system enhances proinflammatory and pro-oxidative markers and 6-OHDA-induced dopaminergic degeneration. *Neurobiol. Aging* DOI: 10.1016/j.neurobiolaging.2010.08.006.
45. Garrido-Gil, P., R. Valenzuela, B. Villar-Cheda, J. L. Lanciego, and J. L. Labandeira-Garcia. 2013. Expression of angiotensinogen and receptors for angiotensin and prorenin in the monkey and human substantia nigra: an intracellular renin-angiotensin system in the nigra. *Brain Struct. Funct.* 218: 373–388.
46. Garrido-Gil, P., A. I. Rodriguez-Perez, P. Fernandez-Rodriguez, J. L. Lanciego, and J. L. Labandeira-Garcia. 2017. Expression of angiotensinogen and receptors for angiotensin and prorenin in the rat and monkey striatal neurons and glial cells. *Brain Struct. Funct.* 222: 2559–2571.
47. Rodriguez-Perez, A. I., D. Sucunza, M. A. Pedrosa, P. Garrido-Gil, J. Kulisevsky, J. L. Lanciego, and J. L. Labandeira-Garcia. 2018. Angiotensin type 1 receptor antagonists protect against alpha-synuclein-induced neuroinflammation and dopaminergic neuron death. *Neurotherapeutics* 15: 1063–1081.
48. Martínez-Pinilla, E., A. I. I. Rodríguez-Pérez, G. Navarro, D. Aguinaga, E. Moreno, J. L. L. Lanciego, J. L. L. Labandeira-García, and R. Franco. 2015. Dopamine D2 and angiotensin II type 1 receptors form functional heteromers in rat striatum. *Biochem. Pharmacol.* 96: 131–142.
49. Benigni, A., P. Cassis, and G. Remuzzi. 2010. Angiotensin II revisited: new roles in inflammation, immunology and aging. *EMBO Mol. Med.* 2: 247–257.
50. Liu, Y.-C., X.-B. Zou, Y.-F. Chai, and Y.-M. Yao. 2014. Macrophage polarization in inflammatory diseases. *Int. J. Biol. Sci.* 10: 520–529.
51. Dagenais, N. J., and F. Jamali. 2005. Protective effects of angiotensin II interruption: evidence for antiinflammatory actions. *Pharmacotherapy* 25: 1213–1229.
52. Banu, N., S. S. Panikar, L. R. Leal, and A. R. Leal. 2020. Protective role of ACE2 and its downregulation in SARS-CoV-2 infection leading to macrophage activation syndrome: therapeutic implications. *Life Sci.* 256: 117905.
53. Isaksson, R., A. Casselbrant, E. Elebring, M. Hallberg, M. Larhed, and L. Fändriks. 2020. Direct stimulation of angiotensin II type 2 receptor reduces nitric oxide production in lipopolysaccharide treated mouse macrophages. *Eur. J. Pharmacol.* 868: 172855.
54. Menk, M., J. A. Graw, C. von Haefen, M. Sifringer, D. Schwaiberger, T. Unger, U. Steckelings, and C. D. Spies. 2015. Stimulation of the angiotensin II AT2 receptor is anti-inflammatory in human lipopolysaccharide-activated monocytic cells. *Inflammation* 38: 1690–1699.
55. Dhande, I., W. Ma, and T. Hussain. 2015. Angiotensin AT2 receptor stimulation is anti-inflammatory in lipopolysaccharide-activated THP-1 macrophages via increased interleukin-10 production. *Hypertens. Res.* 38: 21–29.
56. Jin, J. M., P. Bai, W. He, F. Wu, X. F. Liu, D. M. Han, S. Liu, and J. K. Yang. 2020. Gender differences in patients with COVID-19: focus on severity and mortality. *Front. Public Health* 8: 152.
57. Tukiainen, T., A. C. Villani, A. Yen, M. A. Rivas, J. L. Marshall, R. Satija, M. Aguirre, L. Gauthier, M. Fleharty, A. Kirby, et al; GTEx Consortium; Laboratory, Data Analysis &Coordinating Center (LDACC)—Analysis Working Group; Statistical Methods groups—Analysis Working Group; Enhancing GTEx (eGTEx) groups; NIH Common Fund; NIH/NCI; NIH/NHGRI; NIH/NIMH; NIH/NIDA; Biospecimen Collection Source Site—NDRI; Biospecimen Collection Source Site—RPCI; Biospecimen Core Resource—VARI; Brain Bank Repository—University of Miami Brain Endowment Bank; Leidos Biomedical—Project Management; ELSI Study; Genome Browser Data Integration &Visualization—EBI; Genome Browser Data Integration &Visualization—UCSC Genomics Institute, University of California Santa Cruz. 2017. Landscape of X chromosome inactivation across human tissues. [Published erratum appears in 2018 *Nature* 555: 274.] *Nature* 550: 244–248.
58. Liu, J., H. Ji, W. Zheng, X. Wu, J. J. Zhu, A. P. Arnold, and K. Sandberg. 2010. Sex differences in renal angiotensin converting enzyme 2 (ACE2) activity are 17β-oestradiol-dependent and sex chromosome-independent. *Biol. Sex Differ.* 1: 6.
59. Li, Q., Z. Cao, and P. Rahman. 2020. Genetic variability of human angiotensin-converting enzyme 2 (hACE2) among various ethnic populations. *Mol. Genet. Genomic Med.* DOI: 10.1002/mgg3.1344.
60. Navarro, G., D. Borroto-Escuela, E. Angelats, I. Etayo, I. Reyes-Resina, M. Pulido-Salgado, A. I. Rodríguez-Pérez, E. I. Canela, J. Saura, J. L. Lanciego, et al. 2018. Receptor-heteromer mediated regulation of endocannabinoid signaling in activated microglia. Role of CB_1 and CB_2 receptors and relevance for Alzheimer's disease and levodopa-induced dyskinesia. *Brain Behav. Immun.* 67: 139–151.
61. Sampson, A. K., J. C. Irvine, W. A. Shihata, D. Dragoljevic, N. Lumsden, O. Huet, T. Barnes, T. Unger, U. M. Steckelings, G. L. Jennings, et al. 2016. Compound 21, a selective agonist of angiotensin AT_2 receptors, prevents endothelial inflammation and leukocyte adhesion *in vitro* and *in vivo*. *Br. J. Pharmacol.* 173: 729–740.
62. Thomas, M. C., R. J. Pickering, D. Tsorotes, A. Koitka, K. Sheehy, S. Bernardi, B. Toffoli, T. P. Nguyen-Huu, G. A. Head, Y. Fu, et al. 2010. Genetic Ace2 deficiency accentuates vascular inflammation and atherosclerosis in the ApoE knockout mouse. *Circ. Res.* 107: 888–897.
63. Guo, Y. J., W. H. Li, R. Wu, Q. Xie, and L. Q. Cui. 2008. ACE2 overexpression inhibits angiotensin II-induced monocyte chemoattractant protein-1 expression in macrophages. *Arch. Med. Res.* 39: 149–154.
64. Simões e Silva, A. C., K. D. Silveira, A. J. Ferreira, and M. M. Teixeira. 2013. ACE2, angiotensin-(1-7) and Mas receptor axis in inflammation and fibrosis. *Br. J. Pharmacol.* 169: 477–492.
65. Souza, L. L., and C. M. Costa-Neto. 2012. Angiotensin-(1-7) decreases LPS-induced inflammatory response in macrophages. *J. Cell. Physiol.* 227: 2117–2122.
66. Tsai, H. J., M. H. Liao, C. C. Shih, S. M. Ka, C. M. Tsao, and C. C. Wu. 2018. Angiotensin-(1-7) attenuates organ injury and mortality in rats with polymicrobial sepsis. *Crit. Care* 22: 269.
67. Passaglia, P., F. de Lima Faim, M. E. Batalhão, L. M. Bendhack, J. Antunes-Rodrigues, L. Ulloa, A. Kanashiro, and E. C. Carnio. 2020. Central angiotensin-(1-7) attenuates systemic inflammation via activation of sympathetic signaling in endotoxemic rats. *Brain Behav. Immun.* DOI: 10.1016/j.bbi.2020.04.059.
68. Hammer, A., G. Yang, J. Friedrich, A. Kovacs, D. H. Lee, K. Grave, S. Jörg, N. Alenina, J. Grosch, J. Winkler, et al. 2016. Role of the receptor Mas in macrophage-mediated inflammation in vivo. *Proc. Natl. Acad. Sci. USA* 113: 14109–14114.
69. de Carvalho Santuchi, M., M. F. Dutra, J. P. Vago, K. M. Lima, I. Galvão, F. P. de Souza-Neto, M. Morais E Silva, A. C. Oliveira, F. C. B. de Oliveira, R. Gonçalves, et al. 2019. Angiotensin-(1-7) and alamandine promote anti-inflammatory response in macrophages *in vitro* and *in vivo*. *Mediators Inflamm.* 2019: 2401081.
70. Hoffmann, M., H. Kleine-Weber, S. Schroeder, N. Krüger, T. Herrler, S. Erichsen, T. S. Schiergens, G. Herrler, N. H. Wu, A. Nitsche, et al. 2020. SARS-CoV-2 cell entry depends on ACE2 and TMPRSS2 and is blocked by a clinically proven protease inhibitor. *Cell* 181: 271–280.e8.
71. Lambert, D. W., M. Yarski, F. J. Warner, P. Thornhill, E. T. Parkin, A. I. Smith, N. M. Hooper, and A. J. Turner. 2005. Tumor necrosis factor-α convertase (ADAM17) mediates regulated ectodomain shedding of the severe-acute respiratory syndrome-coronavirus (SARS-CoV) receptor, angiotensin-converting enzyme-2 (ACE2). *J. Biol. Chem.* 280: 30113–30119.
72. Heurich, A., H. Hofmann-Winkler, S. Gierer, T. Liepold, O. Jahn, and S. Pöhlmann. 2014. TMPRSS2 and ADAM17 cleave ACE2 differentially and only proteolysis by TMPRSS2 augments entry driven by the severe acute respiratory syndrome coronavirus spike protein. *J. Virol.* 88: 1293–1307.
73. Blazquez, M. V., J. A. Madueño, R. Gonzalez, R. Jurado, W. W. Bachovchin, J. Peña, and E. Muñoz. 1992. Selective decrease of CD26 expression in T cells from HIV-1-infected individuals. *J. Immunol.* 149: 3073–3077.
74. Imai, Y., K. Kuba, S. Rao, Y. Huan, F. Guo, B. Guan, P. Yang, R. Sarao, T. Wada, H. Leong-Poi, et al. 2005. Angiotensin-converting enzyme 2 protects from severe acute lung failure. *Nature* 436: 112–116.
75. Kuba, K., Y. Imai, T. Ohto-Nakanishi, and J. M. Penninger. 2010. Trilogy of ACE2: a peptidase in the renin-angiotensin system, a SARS receptor, and a partner for amino acid transporters. *Pharmacol. Ther.* 128: 119–128.
76. De Meester, I., S. Korom, J. Van Damme, and S. Scharpé. 1999. CD26, let it cut or cut it down. *Immunol. Today* 20: 367–375.
77. Valenzuela, A., J. Blanco, C. Callebaut, E. Jacotot, C. Lluis, A. G. Hovanessian, and R. Franco. 1997. Adenosine deaminase binding to human CD26 is inhibited by HIV-1 envelope glycoprotein gp120 and viral particles. *J. Immunol.* 158: 3721–3729.
78. Blanco, J., A. Valenzuela, C. Herrera, C. Lluís, A. G. Hovanessian, and R. Franco. 2000. The HIV-1 gp120 inhibits the binding of adenosine deaminase to CD26 by a mechanism modulated by CD4 and CXCR4 expression. *FEBS Lett.* 477: 123–128.
79. Haga, S., N. Yamamoto, C. Nakai-Murakami, Y. Osawa, K. Tokunaga, T. Sata, N. Yamamoto, T. Sasazuki, and Y. Ishizaka. 2008. Modulation of TNF-alpha-converting enzyme by the spike protein of SARS-CoV and ACE2 induces TNF-alpha production and facilitates viral entry. *Proc. Natl. Acad. Sci. USA* 105: 7809–7814.
80. Hamming, I., W. Timens, M. L. C. Bulthuis, A. T. Lely, G. J. Navis, and H. van Goor. 2004. Tissue distribution of ACE2 protein, the functional receptor for SARS coronavirus. A first step in understanding SARS pathogenesis. *J. Pathol.* 203: 631–637.
81. Warner, F. J., R. A. Lew, A. I. Smith, D. W. Lambert, N. M. Hooper, and A. J. Turner. 2005. Angiotensin-converting enzyme 2 (ACE2), but not ACE, is preferentially localized to the apical surface of polarized kidney cells. *J. Biol. Chem.* 280: 39353–39362.

82. Elner, V. M., W. Scales, S. G. Elner, J. Danforth, S. L. Kunkel, and R. M. Strieter. 1992. Interleukin-6 (IL-6) gene expression and secretion by cytokine-stimulated human retinal pigment epithelial cells. *Exp. Eye Res.* 54: 361–368.
83. Lee, Y. W., W. H. Lee, and P. H. Kim. 2010. Oxidative mechanisms of IL-4-induced IL-6 expression in vascular endothelium. *Cytokine* 49: 73–79.
84. Willenberg, H. S., I. Ansurudeen, K. Schebesta, M. Haase, B. Wess, S. Schinner, A. Raffel, M. Schott, and W. A. Scherbaum. 2008. The endothelium secretes interleukin-6 (IL-6) and induces IL-6 and aldosterone generation by adrenocortical cells. *Exp. Clin. Endocrinol. Diabetes* 116(Suppl. 1): S70–S74.
85. Sawa, Y., T. Ueki, M. Hata, K. Iwasawa, E. Tsuruga, H. Kojima, H. Ishikawa, and S. Yoshida. 2008. LPS-induced IL-6, IL-8, VCAM-1, and ICAM-1 expression in human lymphatic endothelium. *J. Histochem. Cytochem.* 56: 97–109.
86. Lee, J., S. Lee, H. Zhang, M. A. Hill, C. Zhang, and Y. Park. 2017. Interaction of IL-6 and TNF-α contributes to endothelial dysfunction in type 2 diabetic mouse hearts. *PLoS One* 12: e0187189.
87. Ren, D., C. Ren, R. Q. Yao, Y. W. Feng, and Y. M. Yao. 2020. Clinical features and development of sepsis in patients infected with SARS-CoV-2: a retrospective analysis of 150 cases outside Wuhan, China. *Intensive Care Med.* DOI: 10.1007/s00134-020-06084-5.
88. Skibsted, S., A. E. Jones, M. A. Puskarich, R. Arnold, R. Sherwin, S. Trzeciak, P. Schuetz, W. C. Aird, and N. I. Shapiro. 2013. Biomarkers of endothelial cell activation in early sepsis. *Shock* 39: 427–432.
89. AbdAlla, S., H. Lother, A. el Massiery, and U. Quitterer. 2001. Increased AT(1) receptor heterodimers in preeclampsia mediate enhanced angiotensin II responsiveness. *Nat. Med.* 7: 1003–1009.
90. Abadir, P. M., A. Periasamy, R. M. Carey, and H. M. Siragy. 2006. Angiotensin II type 2 receptor-bradykinin B_2 receptor functional heterodimerization. *Hypertension* 48: 316–322.
91. Roche, J. A., and R. Roche. 2020. A hypothesized role for dysregulated bradykinin signaling in COVID-19 respiratory complications. *FASEB J.* 34: 7265–7269.
92. Rochaesilva, M. 1964. Chemical mediators of the acute inflammatory reaction. *Ann. N. Y. Acad. Sci.* 116: 899–911.
93. Tang, N., D. Li, X. Wang, and Z. Sun. 2020. Abnormal coagulation parameters are associated with poor prognosis in patients with novel coronavirus pneumonia. *J. Thromb. Haemost.* 18: 844–847.
94. Lillicrap, D. 2020. Disseminated intravascular coagulation in patients with 2019-nCoV pneumonia. *J. Thromb. Haemost.* 18: 786–787.
95. Glowacka, I., S. Bertram, P. Herzog, S. Pfefferle, I. Steffen, M. O. Muench, G. Simmons, H. Hofmann, T. Kuri, F. Weber, et al. 2010. Differential downregulation of ACE2 by the spike proteins of severe acute respiratory syndrome coronavirus and human coronavirus NL63. *J. Virol.* 84: 1198–1205.
96. Bai, F., X. F. Pang, L. H. Zhang, N. P. Wang, R. J. McKallip, R. E. Garner, and Z. Q. Zhao. 2016. Angiotensin II AT1 receptor alters ACE2 activity, eNOS expression and CD44-hyaluronan interaction in rats with hypertension and myocardial fibrosis. *Life Sci.* 153: 141–152.
97. Kondo, A., Y. Koshihara, and A. Togari. 2001. Signal transduction system for interleukin-6 synthesis stimulated by lipopolysaccharide in human osteoblasts. *J. Interferon Cytokine Res.* 21: 943–950.
98. Modat, G., J. Dornand, N. Bernad, D. Junquero, A. Mary, A. Muller, and C. Bonne. 1990. LPS-stimulated bovine aortic endothelial cells produce IL-1 and IL-6 like activities. *Agents Actions* 30: 403–411.
99. Nagase, T., N. Uozumi, S. Ishii, K. Kume, T. Izumi, Y. Ouchi, and T. Shimizu. 2000. Acute lung injury by sepsis and acid aspiration: a key role for cytosolic phospholipase A2. *Nat. Immunol.* 1: 42–46.
100. Qiao, H. M., H. X. Pang, Y. F. Zhang, H. J. Cheng, L. Liu, and J. R. Lu. 2012. Changes of IL-6,IL-10 and TNF-α in children with *Mycoplasma* pneumoniae pneumonia. *J. Clin. Pediatr.* 1: 59–61.
101. Zhang, Y., Y. Zhou, S. Li, D. Yang, X. Wu, and Z. Chen. 2016. The clinical characteristics and predictors of refractory *Mycoplasma* pneumoniae pneumonia in children. *PLoS One* 11: e0156465.
102. Kragsbjerg, P., T. Vikerfors, and H. Holmberg. 1998. Cytokine responses in patients with Pneumonia caused by chlamydia or mycoplasma. *Respiration* 65: 299–303.
103. Kurai, D., K. Nakagaki, H. Wada, T. Saraya, S. Kamiya, Y. Fujioka, K. Nakata, H. Takizawa, and H. Goto. 2013. *Mycoplasma* pneumoniae extract induces an IL-17-associated inflammatory reaction in murine lung: implication for mycoplasmal pneumonia. *Inflammation* 36: 285–293.
104. Zhao, J., W. Zhang, L. Shen, X. Yang, Y. Liu, and Z. Gai. 2017. Association of the ACE, GSTM1, IL-6, NOS3, and CYP1A1 polymorphisms with susceptibility of mycoplasma pneumoniae pneumonia in Chinese children. *Medicine (Baltimore)* 96: e6642.
105. Faure, E., J. Poissy, A. Goffard, C. Fournier, E. Kipnis, M. Titecat, P. Bortolotti, L. Martinez, S. Dubucquoi, R. Dessein, et al. 2014. Distinct immune response in two MERS-CoV-infected patients: can we go from bench to bedside? *PLoS One* 9: e88716.
106. Josset, L., V. D. Menachery, L. E. Gralinski, S. Agnihothram, P. Sova, V. S. Carter, B. L. Yount, R. L. Graham, R. S. Baric, and M. G. Katze. 2013. Cell host response to infection with novel human coronavirus EMC predicts potential antivirals and important differences with SARS coronavirus. *MBio* 4: e00165-13.
107. Kragsbjerg, P., B. Söderquist, H. Holmberg, T. Vikerfors, and D. Danielsson. 1998. Production of tumor necrosis factor-α and interleukin-6 in whole blood stimulated by live Gram-negative and Gram-positive bacteria. *Clin. Microbiol. Infect.* 4: 129–134.
108. Quinton, L. J., M. R. Jones, B. E. Robson, B. T. Simms, J. A. Whitsett, and J. P. Mizgerd. 2008. Alveolar epithelial STAT3, IL-6 family cytokines, and host defense during *Escherichia coli* pneumonia. *Am. J. Respir. Cell Mol. Biol.* 38: 699–706.
109. Park, C. S., S. W. Chung, S. Y. Ki, G. I. Lim, S. T. Uh, Y. H. Kim, D. I. Choi, J. S. Park, D. W. Lee, and M. Kitaichi. 2000. Increased levels of interleukin-6 are associated with lymphocytosis in bronchoalveolar lavage fluids of idiopathic nonspecific interstitial pneumonia. *Am. J. Respir. Crit. Care Med.* 162: 1162–1168.
110. Thannickal, V. J., K. R. Flaherty, F. J. Martinez, and J. P. Lynch, III. 2004. Idiopathic pulmonary fibrosis: emerging concepts on pharmacotherapy. *Expert Opin. Pharmacother.* 5: 1671–1686.

3.10 Experimental and computational analysis of biased agonism on full-length and a C-terminally truncated adenosine A_{2A} receptor.

Gemma Navarro, Ángel Gonzalez, Stefano Campanacci, **Rafael Rivas-Santisteban**, Irene Reyes-Resina, Nil Casajuana-Martin, Arnau Cordomí, Leonardo Pardo y Rafael Franco.

Manuscrito publicado en *Computational and Structural Biotechnology Journal*, Septiembre 2020; 18: 2723-2732.

El agonismo sesgado es la propiedad por la cual algunos compuestos actúan activando de forma diferencial algunas vías de señalización respecto a otras. Este fenómeno adquiere una gran importancia cuando se habla de receptores acoplados a proteína G (GPCRs). Algunas de las señalizaciones mediadas por GPCRs incluyen la activación de proteínas G, la activación de quinasas y la activación de ß-arrestinas. En este artículo caracterizamos la funcionalidad del receptor de adenosina ($A_{2A}R$) con la cola c-terminal completa y la cola c-terminal truncada (que carece de los últimos 40 aminoácidos) en un sistema de expresión heterólogo. El $A_{2A}R$ es un GPCR con gran importancia terapéutica, siendo la diana de un fármaco para el tratamiento de la enfermedad de Parkinson. Se han obtenido datos experimentales de la unión de los ligandos a ambas formas del $A_{2A}R$ y del mismo modo se ha caracterizado la funcionalidad de estos receptores mediante ensayos de determinación de los niveles AMPc intracelular, de determinación de la fosforilación de ERK1/2, de reclutamiento de ß-arrestinas y de la redistribución dinámica de masas. Estos ensayos se efectuaron en presencia de diversos compuestos (los agonistas adenosina, NECA, CGS-21680, PSB-0777 y LUF-5834 y el antagonista específico de $A_{2A}R$, SCH-58261) en células que expresaban $A_{2A}R$ o $A_{2A}{}^{D40}R$. Para el cálculo del agonismo sesgado se ha utilizado como vía de referencia la determinación de los niveles de AMPc y como ligando de referencia, el ligando endógeno adenosina. Se observó que el extremo C-terminal del $A_{2A}R$ es prescindible para el reclutamiento de proteína G y de ß-arrestinas, así como para la activación de la vía de las MAPK. Mediante simulaciones de dinámica molecular sin restricciones se estudiaron las disposiciones estructurales de la cavidad de unión, en presencia de los distintos agonistas utilizados cuya composición estructural y química es diferente.

Computational and Structural Biotechnology Journal 18 (2020) 2723–2732

COMPUTATIONAL AND STRUCTURAL BIOTECHNOLOGY JOURNAL

journal homepage: www.elsevier.com/locate/csbj

Experimental and computational analysis of biased agonism on full-length and a C-terminally truncated adenosine A_{2A} receptor

Gemma Navarro [a,b,1], Angel Gonzalez [c,1], Stefano Campanacci [d,1], Rafael Rivas-Santisteban [a,d], Irene Reyes-Resina [b,d,2], Nil Casajuana-Martin [c], Arnau Cordomí [c], Leonardo Pardo [c,1], Rafael Franco [b,e,1,*]

[a] Dept. Biochemistry and Physiology, Faculty of Pharmacy and Food Science. Universitat de Barcelona. Barcelona, Spain
[b] Centro de Investigación Biomédica en Red sobre Enfermedades Neurodegenerativas. Instituto de Salud Carlos III, Madrid, Spain
[c] Laboratori de Medicina Computacional, Unitat de Bioestadística, Facultat de Medicina, Universitat Autònoma de Barcelona, 08193 Bellaterra, Spain d Faculty of Chemistry, Universitat de Barcelona, Barcelona, Spain
[d] Dept. Biochemistry and Molecular Biomedicine. School of Biology. Universitat de Barcelona. Barcelona. Spain
[e] School of Chemistry. Universitat de Barcelona. Barcelona. Spain

ARTICLE INFO

Article history:
Received 20 May 2020
Received in revised form 15 September 2020
Accepted 16 September 2020
Available online 24 September 2020

Keywords:
G protein coupled receptors
Adenosine A_{2A} receptor
Functional selectivity
G protein binding
β-Arrestin recruitment
Molecular dynamic simulations

ABSTRACT

Biased agonism, the ability of agonists to differentially activate downstream signaling pathways by stabilizing specific receptor conformations, is a key issue for G protein-coupled receptor (GPCR) signaling. The C-terminal domain might influence this functional selectivity of GPCRs as it engages G proteins, GPCR kinases, β-arrestins, and several other proteins. Thus, the aim of this paper is to compare the agonist-dependent selectivity for intracellular pathways in a heterologous system expressing the full-length ($A_{2A}R$) and a C-tail truncated ($A_{2A}^{\Delta 40}R$ lacking the last 40 amino acids) adenosine A_{2A} receptor, a GPCR that is already targeted in Parkinson's disease using a first-in-class drug. Experimental data such as ligand binding, cAMP production, β-arrestin recruitment, ERK1/2 phosphorylation and dynamic mass redistribution assays, which correspond to different aspects of signal transduction, were measured upon the action of structurally diverse compounds (the agonists adenosine, NECA, CGS-21680, PSB-0777 and LUF-5834 and the SCH-58261 antagonist) in cells expressing $A_{2A}R$ and $A_{2A}^{\Delta 40}R$. The results show that taking cAMP levels and the endogenous adenosine agonist as references, the main difference in bias was obtained with PSB-0777 and LUF-5834. The C-terminus is dispensable for both G-protein and β-arrestin recruitment and also for MAPK activation. Unrestrained molecular dynamics simulations, at the μs timescale, were used to understand the structural arrangements of the binding cavity, triggered by these chemically different agonists, facilitating G protein binding with different efficacy.

1. Introduction

Adenosine triphosphate (ATP) is the main energy-transfer molecule and adenosine is one of its main metabolites. Adenosine receptors appeared early in evolution, as sensors of ATP decay, because excess of adenosine correlates with ATP depletion. They are considered as the most ancient within the class A (or rhodopsin-like) G-protein-coupled receptor (GPCR) family. Moreover, phylogenetic studies suggest that adenosine receptors were the first to start diverging [1] from the MECA receptor cluster [2], which is formed by the melanocortin, endothelial differentiation sphingolipid, and cannabinoid receptors. There are four identified mammalian adenosine receptors (humans included) whose cognate heterotrimeric G proteins are G_i (A_1 and A_3) or G_s/G_{olf} (A_{2A} and A_{2B}) [3].

The crystal structure of the A_{2A} receptor ($A_{2A}R$) was one of the first reported for the G-protein-coupled receptor (GPCR) family [4]. Today, there are nearly fifty structures of A_1R and $A_{2A}R$ bound to agonists, antagonists, and/or to G proteins [5]; all of them displaying the common features of class A GPCRs [6]. Unfortunately, the N- and C-terminal domains, which are highly variable in sequence, length, and structure [7], have been removed for crystallization purposes. The long C-terminal domain of $A_{2A}R$ (about 122 amino acids) is known to engage G proteins, GPCR kinases, arrest-

* Corresponding author at: School of Chemistry, University of Barcelona, Diagonal 643, 08028 Barcelona, Spain.
E-mail addresses: rfranco123@gmail.comrfr, anco@ub.edu (R. Franco).
[1] Equal contribution.
[2] Current address: RG Neuroplasticity, Leibniz Institute for Neurobiology, Magdeburg 39118, Germany.

https://doi.org/10.1016/j.csbj.2020.09.028

ins and several other proteins [8,9]. The C-terminus is also responsible for the constitutive activity of the receptor [10], influences the quaternary structure of heteromers [11,12], and is involved in differential intracellular signaling [13].

$A_{2A}R$ offers numerous possibilities for therapeutic applications [14–16]. $A_{2A}R$ antagonists show promise, among others, in Alzheimer's and Parkinson's diseases, attention-deficit hyperactivity disorder, depression, and anxiety. Istradefylline, one of the most studied antagonists, is safe and efficacious in Parkinson and was approved in Japan as *Nouriast*™ and by the US Food and Drug Administration as *Nourianz*™ [17]. $A_{2A}R$ agonists could be used in Niemann Pick type C disease, autism-spectrum disorders, and schizophrenia. Regadenoson, a selective $A_{2A}R$ agonists that is a coronary vasolidator, was approved in the United States as *Lexiscan*™.

These facts open the possibilities for more drug approvals, both agonists and antagonists, related to adenosine receptors. Thus, the aim of this work was double. First, we wanted to analyze the agonist-dependent selectivity for intracellular pathways, known as functional selectivity or biased agonism, using structurally diverse compounds in a heterologous system expressing $A_{2A}R$. Biased agonists might offer attractive therapeutic properties relative to their unbiased counterpart, circumstance that remains to be validated in clinical trials [18]. In fact, adenosine receptor biased agonists could be used for cardioprotection without bradycardia as a serious adverse effect [19,20]. Second, we analyzed in living cells the effect of the C-terminal domain of $A_{2A}R$ in ligand binding and in agonist-induced signaling.

2. Materials and methods

2.1. Reagents

Adenosine, NECA, CGS-21680, PSB-0777, LUF-5834 and SCH-58261 were purchased from Tocris Biosciences (Bristol, UK). HEPES was purchased from SigmaAldrich (St. Louis, MO, US). Stock solutions were prepared in DMSO. Aliquots of these stock solutions were kept frozen at −20 °C until use.

2.2. Cell culture and transient transfection

Human embryonic kidney 293T (HEK-293T) cells were grown in Dulbecco's modified Eagle's medium (DMEM) (Gibco, Paisley, Scotland, UK) supplemented with 2 mM L-glutamine, 1 mM sodium pyruvate, 100 units/ml penicillin/streptomycin, MEM non-essential amino acids solution (1/100) and 5% (v/v) heat inactivated fetal bovine serum (FBS) [all supplements were from Invitrogen, (Paisley, Scotland, UK)]. Cells were incubated in a humid atmosphere of 5% CO_2 at 37 °C. 24 h after seeding in 6-well or 96-well (for ERK phosphorylation assay) plates, cells were transiently transfected with cDNA coding for wild-type $A_{2A}R$ or $A_{2A}^{\Delta 40}R$ (amino acids 372–412 on the C-terminal domain were deleted [21]) with the PEI (PolyEthylenImine, SigmaAldrich) method as previously described [13,22]. Truncation of this part of the C-tail does not remove the proposed phosphorylation codes (PxPxxP/E/D or PxxPxxP/E/D, where P represents phospho-serine or phospho-threonine) for arrestin recruitment [23]. This phosphorylation code starts 33 amino acids after P7.50 of the NPxxY motif in human rhodopsin, whereas truncation of $A_{2A}R$ starts 87 amino acids after P7.50. Cells were incubated for 4 to 5 h with the cDNA of interest, PEI and NaCl in serum-free medium. After that, the serum-free medium was replaced by complete culture medium and cells were incubated for 48 h at 37 °C in 5% CO_2 humid atmosphere. The sequences in the plasmids were those coding for human receptors. It should be noted that within a given experimental session, for instance of determination of cAMP levels, all agonists (plus/minus antagonist when indicated) were tested in the same batch of transfected cells.

2.3. Homogeneous HTRF binding assays

HEK-293T cells growing in 6-well plates were transiently transfected with 1 μg of plasmid encoding for pHALO-tagged human $A_{2A}R$ (pHALO-$A_{2A}R$, Cisbio Bioassays, Codolet, France) or 1 μg of plasmid encoding for pHALO-tagged human $A_{2A}^{\Delta 40}R$ and incubated at 37 °C in a 5% CO_2 humid atmosphere (24 h).

2.4. Covalent labeling of cells expressing pHALO-tagged receptors

48 h post transfection culture medium was removed, cells were washed with PBS and incubated with 100 nM of HALO-Lumi4Tb, a terbium derivative of *O*6-benzylguanine (SSNPTBC, Cisbio Bioassays, Codolet, France) - previously diluted in TagLite Buffer (TLB) (LABMED, Cisbio Bioassays, Codolet, France) for 1 h at 37 °C under 5% CO_2 humid atmosphere. After that, cells were washed with PBS to remove the excess of HALO-Lumi4Tb, detached with Versene (Gibco Life Technologies, Paisley, Scotland, UK), centrifuged at 1,500 rpm for 5 min and resuspended in TLB. Densities of 10,000 cells/well were used to carry out binding assays in white opaque 384-well plates.

2.5. Non-radioactive homogeneous time-resolved FRET-based binding assays

Saturation binding experiments were performed by incubating cells expressing Tb-labeled HALO-$A_{2A}R$ with increasing concentrations of the $A_{2A}R$ antagonist SCH-442416, conjugated to a fluorescent probe developed by Cisbio (red $A_{2A}R$ ligand, purchased from Cisbio Bioassays, Codolet, France). The unspecific signal was obtained by incubating cells expressing Tb-labeled HALO-$A_{2A}R$ with increasing concentrations of red $A_{2A}R$ ligand in the presence of 10 μM unlabeled SCH-58261. Both, fluorescent ligands and unlabeled compounds, were diluted in TLB. 10 μl of labeled cells (10,000 cells/well) were loaded onto 384-well white plates and 5 μl unlabeled SCH-58261 (10 μM final concentration) or TLB were added, followed by the addition of 5 μl of increasing concentrations (0–60 nM range) of red $A_{2A}R$ ligand. Plates were incubated protected from light for 2 h at room temperature before time-resolved fluorescence resonance energy transfer (TR-FRET) signal reading. The specific binding was calculated by subtracting the unspecific binding from the total binding.

For competition binding assays, HEK-293T cells transiently expressing Tb-labeled HALO-$A_{2A}R$, or $A_{2A}^{\Delta 40}R$, were incubated with 20 nM fluorophore-conjugated $A_{2A}R$ ligand, in the presence of increasing concentrations (0–10 μM range) of agonists (or antagonists when indicated). Plates contained 10 μl of labeled cells, and 5 μl of tested compounds or TLB were added prior to the addition of 5 μl of the red $A_{2A}R$ ligand. Plates were then incubated for at least 2 h at room temperature prior to TR-FRET signal detection. Detailed description of the HTRF assay is found elsewhere [24].

2.6. Signal detection and data analysis

Signal was detected using a PHERAstar FS (BMG Lab technologies, Offenburg, Germany) microplate reader equipped with a FRET optic module allowing donor excitation at 337 nm and signal collection at both 665 and 620 nm. A frequency of 10 flashes/well was selected for the xenon flash lamp excitation. The signal was collected at both 665 and 620 nm using the following time-resolved settings: delay, 150 ms; integration time, 500 ms. HTRF ratios were obtained by dividing the acceptor signal (665 nm) by the donor sig-

nal (620 nm) and multiplying this value by 10,000. The 10,000-multiplying factor is used solely for the purpose of easier data handling.

Data were analyzed using Prism 7 software (GraphPad Software, Inc., San Diego, CA), and competition data were fitted by non-linear regression to a one site-fit logIC_{50}, competition curves were -in all cases- monophasic. K_D (dissociation constant) values of the fluorescent ligand were obtained from the specific binding saturation curves. Note that B_{max} values obtained from HTRF saturation curves do not reflect absolute values of receptor binding sites. K_i values were determined from competition binding assays by using the calculated IC_{50} and K_D values and the Cheng-Prusoff equation [25].

2.7. cAMP determination

HEK-293T cells were grown in 6-well plates and transiently transfected with cDNAs for $A_{2A}R$ or for $A_{2A}^{\Delta 40}R$ as described in 2.2. Two hours before initiating the experiment, medium was replaced by serum-free DMEM medium. Then cells were detached, isolated by centrifugation (5 min at 1,500 rpm) and resuspended in DMEM containing 50 μM zardaverine (phosphodiesterase inhibitor) to prevent degradation of cAMP, and 5 mM HEPES (pH 7.4). Cells were placed in white 384-well plates (PerkinElmer) (6,000 cells/well) and incubated with antagonists or vehicle for 15 min before treatment with agonist or vehicle for 15 min. Finally, cAMP-Eu and the fluorescent antibody were added. Readings were performed after one hour incubation at 25 °C. Homogeneous time-resolved fluorescence energy transfer (HTRF) measures were performed using the Lance Ultra cAMP kit (PerkinElmer, Waltham, MA, US). Fluorescence at 665 nm was measured in a PHERAstar Flagship plate reader equipped with an HTRF optical module (BMG Lab technologies, Offenburg, Germany).

2.8. ERK1/2 phosphorylation assays

HEK-293T cells were grown on transparent Biocat Poly-D-Lysine 96-well plates (Deltalab) and kept at the incubator for 24 h. Then cells were transiently transfected with cDNA coding for $A_{2A}R$ or $A_{2A}^{\Delta 40}R$ and incubated for 48 h at 37 °C in a 5% CO_2 humid atmosphere. Supplementary Fig. S1A shows that treatment with CGS-21680 in non-transfected HEK-293T cells is not significantly different to the basal condition. Thus, the expression level of $A_{2A}R$ in non-transfected HEK-293T cells is negligible. 2 h before initiating the experiment, the medium was substituted by serum-free DMEM. Cells were stimulated at 25 °C for 10 min with vehicle or agonists (Supplementary Fig. S1D). ERK phosphorylation was measured at "short" times to detect G-protein mediated signal. After that, cells were washed twice with cold PBS before the addition of lysis buffer (30 μl/well; Perkin Elmer, Waltham, MA, US) and incubated for 15 min at 25 °C on a Heidolph Titramax 100 shaker. 10 μl of each cell lysate was transferred to white ProxiPlate 384-well microplates (PerkinElmer; Waltham, MA, USA). ERK1/2 phosphorylation was determined using AlphaScreen®SureFire® kit (Perkin Elmer, Waltham, MA, US): 5 μl/well of acceptor beads were added. Plates, protected from light, were incubated for 2 h at 25 °C. Finally, 5 μl/well of donor beads were added and plates, protected from light, were incubated for 2 h before analysis. Fluorescence was determined using an EnSpire® Multimode Plate Reader (PerkinElmer, Waltham, MA, USA). The value of reference (100%) was that achieved in the absence of any treatment (basal). The effect of ligands was given in percentage respect to the basal value.

2.9. β-Arrestin 2 recruitment

HEK-293T cells were transiently transfected with 0.625 μg of cDNA coding for β-arrestin 2-Rluc and 2 μg of cDNA coding for A_{2A}-YFP or with 1.5 μg of cDNA coding for β -arrestin 2-Rluc and 4 μg of cDNA coding for $A_{2A}^{\Delta 40}R$-YFP. BRET experiments were performed 48 h after transfection. Cells were detached using HBSS containing 0.1% glucose, centrifuged for 5 min at 3,200 rpm and resuspended in the same buffer. Protein concentration was quantified by using the Bradford assay kit (Bio-Rad, Munich, Germany). Hereafter, YFP fluorescence at 530 nm was quantified in a FluoStar Optima Fluorimeter (BMG Labtechnologies, Offenburg, Germany) to quantify receptor-YFP expression. To measure β -arrestin recruitment, cells (20 μg of protein) were distributed in 96-well microplates (Corning 3600, white plates with white bottom) and were incubated for 10 min with antagonists. Cells were then stimulated with agonists prior to the addition of 5 μM Coelenterazine H (Molecular Probes, Eugene, OR). BRET between β-arrestin 2-Rluc and receptor-YFP was determined and quantified at 5 min after adding coelenterazine H. This time of response was selected from time-response curves (Supplementary Fig. S1C). The readings were collected using a Mithras LB 940 (Berthold Technologies, Bad Wildbad, GE), which allows the integration of the signals detected in the short-wavelength filter (485 nm) and the long wavelength filter (530 nm). To quantify protein-RLuc expression, luminescence readings were also collected 10 min after the addition of 5 μM coelenterazine H.

2.10. Dynamic mass redistribution assays (DMR)

Cell mass redistribution induced upon receptor activation was detected by illuminating with polychromatic light the underside of a biosensor and measuring the changes in the wavelength of the reflected monochromatic light, that is a sensitive function of the index of refraction. The magnitude of the wavelength shift (in picometers) is directly proportional to the amount of mass redistribution. 48 h before the assay, HEK-293T cells were transiently transfected with 2 μg of cDNA coding for $A_{2A}R$ or $A_{2A}^{\Delta 40}R$. HEK-293T cells were seeded in 384-well sensor microplates to obtain 70–80% confluent monolayers constituted by approximately 10,000 cells/well. Prior to the assay, cells were washed twice with assay buffer (HBSS with 20 mM HEPES, pH 7.15 and 1% BSA) (SigmaAldrich, St. Louis, MO, US) and incubated for 2 h with assay-buffer containing 0.1% DMSO (24 °C, 30 μl/well). Hereafter, the sensor plate was scanned, and a baseline optical signature was recorded for 10 min before adding 10 μl of the selective antagonists for 30 min, followed by the addition of 10 μl of the selective agonists; all test compounds were diluted in assay buffer. Then, DMR responses were monitored for at least 5000 s in an EnSpire® Multimode Plate Reader (PerkinElmer, Waltham, MA, USA) by a label-free technology. Results were analyzed using EnSpire Workstation Software v 4.10.

2.11. Calculation of bias factor

Bias factor (bias) was calculated with the following formulas adapted from [26] in which τ represents the agonist efficacy, and K_A the agonist affinity [27].

$$\log bias = \Delta \log \left(\frac{\tau}{K_A}\right)_{j_1} - \Delta \log \left(\frac{\tau}{K_A}\right)_{j_2}$$

$$bias = 10^{\Delta\Delta log\left(\frac{\tau}{K_A}\right)_{j_1 - j_2}}$$

log (τ/K_A) is defined as the transduction coefficient or synonymously as logR, a parameter that can be used to compare agonist activity between different systems. The transduction coefficient is a measure of the ability of a ligand to activate the receptor [28].

The pathway of reference j_1 was cAMP determination for Gs-coupling, whereas the other pathways (ERK1/2 phosphorylation, ß-arrestin 2 recruitment, or DMR) were j_2. τ denotes the maximum value in each response and K_A is the antilogarithm of half maximal effective concentration (EC_{50} if the agonist provides an increase response, IC_{50} if the agonist provides a reduction of the response induced by another reagent).

2.12. Computational methods

Preparation of protein structure and ligand parametrization. Crystal structures of the $A_{2A}R$ in its active intermediate state in complex with the adenosine (PDB id 2YDO), NECA (2YDV) and CGS-21680 (4UHR) agonists, and the crystal structure of $A_{2A}R$ in its inactive state in complex with the ZM241385 antagonist (PDB id 4EIY) were obtained from the Protein Data Bank (rcsb.org). Fusion proteins were removed and stabilizing mutations were mutated to the native sequence using MODELLER v9.12 [29]. Parameters for adenosine, NECA, CGS-21680, PSB-0777, LUF-5834 and SCH-58261 were obtained from the general Amber force field (GAFF) and HF/6-31G*//HF/6-31G*-derived RESP atomic charges calculated with Gaussian09.

Molecular docking. The PSB-0777 and LUF-5834 agonists were docked into the active intermediate state (2YDV) and the SCH-58261 antagonist was docked into the inactive state (4EIY) using the Molecular Operating Environment (MOE) software (Chemical Computing Group Inc., Montreal, Quebec, Canada). One hundred docking solutions per ligand were generated by the triangle matcher algorithm into the active site of the receptor structures. Top-ranking solutions were inspected and conformations in which the central moiety of PSB-0777 and the aminopyridine group of LUF-5834 were located in the same region as the adenine moiety of adenosine and NECA were selected (Supplementary Fig. S2). The binding pose of SCH-58261 was selected in such a manner that the orientation of its pyrazolo-triazolo-pyrimidine central moiety was similar to the bicyclic triazolotrazine core of the highly potent selective antagonist ZM241385 found in the 4EIY structure (Supplementary Fig. S2).

Molecular dynamics (MD) simulations. The complexes of adenosine, NECA, CGS-21680, PSB-0777 and LUF-5834 with the intermediate active structure of $A_{2A}R$ and the complex of SCH-58261 with the inactive structure of $A_{2A}R$ (see above) were embedded in a pre-equilibrated lipid bilayer box containing 1-palmitoyl-2-oleoyl-sn-glycero-3-phosphatidylcholine (POPC), water molecules (TIP3P) and monoatomic Na + and Cl− ions (0.2 M). Assignment of ionization states and hydrogens at physiological pH for the selected structures was conducted with the Protonate3D method [30] as implemented in MOE. D2.50 was deprotonated (negatively charged) for antagonist-bound receptor simulations and protonated (neutral) for agonist-bound receptor simulations [31], whereas H264 was protonated (positively charged) in all simulations [32]. A sodium ion was placed, near the negatively charged D2.50, in the inactive, antagonist-bound, structure of $A_{2A}R$ [33,34]. Molecular systems were subject to a 1000 cycles of energy minimization, followed by 20 ns of gradual relaxation of positional restraints (corresponding to 100, 50, 25 and 10 $kJ.mol^{-1}nm^{-2}$) at protein backbone coordinates before the production phase in order to hydrate the receptor cavities and allow lipids to pack around the protein. After equilibration, unrestrained MD simulation (3 replicas of 1 μs giving a total of 3 μs of sampling time) were produced for each ligand-receptor complex at a constant temperature of 300 K using separate v-rescale thermostats for the receptor, ligands, lipids and solvent molecules. A time step of 2.0 fs was used for the integration of equations of motions. All bonds and angles were kept frozen using the LINCS algorithms. Lennard-Jones interactions were computed using a cutoff of 10 Å, and the electrostatic interactions were treated using PME with the same real-space cutoff under periodic boundary conditions. MD simulations were performed using GROMACS v5.0.7. The AMBER99SB force field as implemented in GROMACS, Berger parameters for POPC lipids, and the GAFF parameters for the ligands (see above) were used for the MD simulations, attending the performance of this protocol on membrane-protein systems [35].

2.13. Statistical analysis

Experimental data was managed and analysed with GraphPad Prism software version 7 (San Diego, CA, USA) or IBM SPSS Statistics version 25.0 (IBM Corp., NY, USA). Unless otherwise stated data are the mean ± S.E.M (n = 5 or higher). P-values lower than 0.05 were considered statistically significant.

3. Results and discussion

3.1. Ligand binding experiments

We studied the binding of the agonists adenosine, NECA and CGS-21680, the partial agonists PSB-0777 and LUF-5834, and the selective antagonist SCH-58261 by homogeneous time-resolved fluorescence (HTRF) experiments, schematized in Fig. 1A, in living HEK-293T cells expressing either wild type (wt) $A_{2A}R$ or a truncated receptor ($A_{2A}^{\Delta 40}R$, lacking the last 40 amino acids of the C-terminal end) tagged with HaloTag on the N-terminus (see 2.3–2.5). First, a saturation curve was performed using a fluorescence-conjugated antagonist (Fig. 1B). The obtained K_D values were 1.7 nM and 1.2 nM for full-length $A_{2A}R$ and $A_{2A}^{\Delta 40}R$, respectively (Table 1). Subsequently, competition assays were performed using 20 nM of the fluorescence-conjugated antagonist and increasing amounts of the ligands (Fig. 1C-1D). The K_i value of each compound was calculated from IC_{50} and K_D values using the Cheng-Prusoff expression [25] (Table 1). The obtained K_i values are in the range of those obtained in radioligand binding assays for isolated membranes from tissues or transfected cells. According to this assay, the K_i values of agonists are in the 13–219 nM range, LUF-5834 being the compound that binds $A_{2A}R$ the strongest and PSB-0777 the weakest. Clearly, removal of the C-terminal domain results in weaker agonist binding to the orthosteric site (a ratio of K_i values in the 1.4–4.4 range, which correspond to binding free energy differences between 0.2 and 0.9 Kcal/mol). On the other hand, removal of the C-terminal domain has a significant impact on the binding of the antagonist SCH-58261 (0.7 nM vs 113.9 nM for full-length $A_{2A}R$ and $A_{2A}^{\Delta 40}R$, respectively; binding free energy difference of 3.0 Kcal/mol).

3.2. Molecular models of agonist binding

The binding of these compounds to $A_{2A}R$ has been extensively studied by site-directed mutagenesis, computer simulations, and supported by the recent crystallographic data of adenosine, NECA and CGS in complex with $A_{2A}R$ (reviewed in [36]). PSB-0777 and LUF-5834 were docked (see 2.12) using, as template, ligands solved in crystal structures with homologous chemical scaffolds (see Supplementary Fig. S2). All molecules but LUF-5834 are structurally related through a common adenosine core. Fig. 2 summarizes the binding modes of all compounds, emphasizing common/different areas of the receptor occupied by each ligand. In order to understand the molecular mechanism of receptor activation (see 3.5),

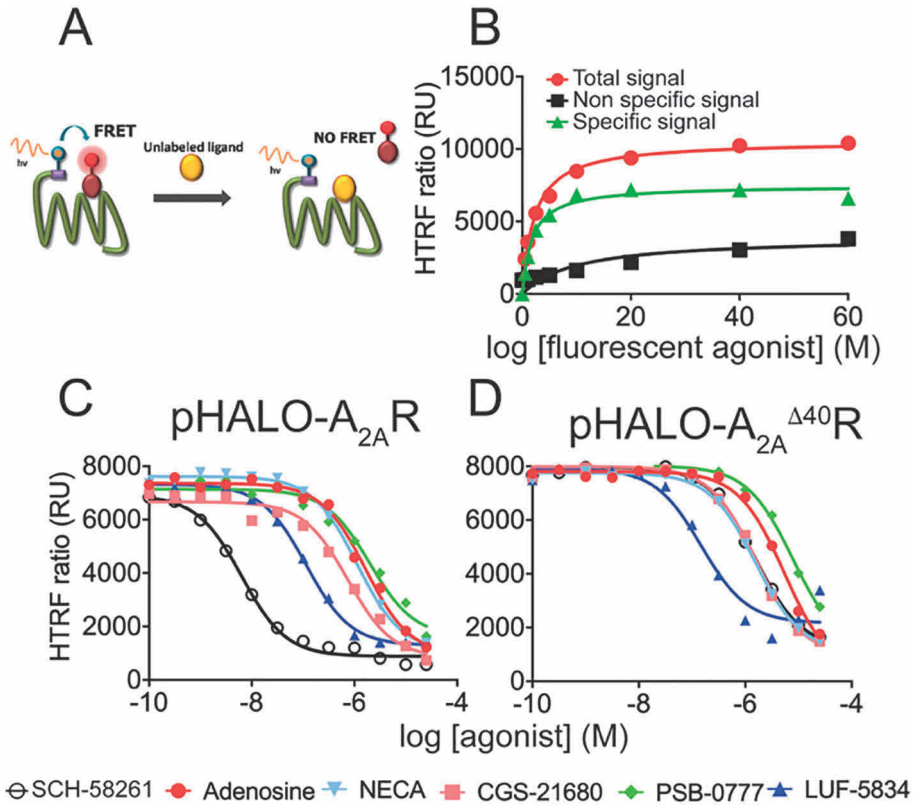

Fig. 1. Competition curves in HTRF-based assays. Panel A: Scheme of the homogeneous binding technology performed in living HEK-293T cells. Panel B. Saturation isotherm of binding of fluorophore-conjugated red $A_{2A}R$ ligand to HEK-293T cells transiently transfected with HALO-$A_{2A}R$ in the absence (red) or presence of 10 μM SCH-58261 (black); specific binding is depicted in green. Panels C-D: Non-radiolabeled HTRF-based competition curves of specific binding of 20 nM fluorophore-conjugated red $A_{2A}R$ ligand in the presence of increasing concentrations of different agonists and of the selective antagonist SCH-58261, in cells expressing $A_{2A}R$ (C) or $A_{2A}^{\Delta 40}R$ (D). Data represent the mean ± SEM of a representative experiment (n = 4). HTRF ratio = (665 nm acceptor signal/620 nm donor signal) × 10,000. (For interpretation of the references to color in this figure legend, the reader is referred to the web version of this article.)

Table 1
IC_{50} and K_i values obtained from competition binding assays in HEK-293T cells expressing wild type $A_{2A}R$ or $A_{2A}^{\Delta 40}R$. Values reported are the mean of three experiments conducted in triplicates fitted to a monophasic competition model.

	$A_{2A}R$		$A_{2A}^{\Delta 40}R$			
	IC_{50} (nM)	K_i (nM)	IC_{50} (nM)	K_i (nM)	$K_i^{\Delta CT}/K_i^{wt}$	$\Delta\Delta G^a$ (kcal/mol)
adenosine	1658	183	4804	531	2.9	0.6
NECA	1118	124	2190	242	2.0	0.4
CGS-21680	746	82.5	1690	187	2.3	0.5
PSB-0777	1984	219	8680	960	4.4	0.9
LUF-5834	115	13	166.0	18	1.4	0.2
SCH-58261	6.3	0.7	1030	114	162.3	3.0

$A_{2A}R$		$A_{2A}^{\Delta 40}R$	
B_{max}	K_D (nM)	B_{max}	K_D (nM)
6959	1.677	9214	1.22

[a]Experimental binding free energy differences between wild type ($A_{2A}R$) and truncated ($A_{2A}^{\Delta 40}R$) receptors, calculated as $\Delta\Delta G = -RT \ln (K_i^{\Delta CT}/K_i^{wt})$ where R is 1.987 cal mol^{-1} K^{-1} and T is the temperature of 298°K (-RT = −0.592 kcal mol^{-1})

we studied by molecular dynamics (MD) simulations (see 2.12) the interactions of crucial ligand moieties to key receptor amino acids in all these regions. Detailed analysis of the simulations shows that these binding modes were stable during the unbiased 1 μs MD simulations (three replicas) as shown by the relatively low movement in root mean-square deviation (rmsd) plots of the receptor and ligand heavy atoms, as well as the conservation of the secondary structure elements of $A_{2A}R$ (Supplementary Figs. S3-S5).

As shown in Fig. 2, three regions (blue, green and yellow rectangles) are invariably occupied by functional groups of all the studied compounds, illustrated by the binding of adenosine in the central panel. The heterocyclic site (blue rectangle) corresponds to the central region and accommodates the adenine moiety of adenosine, NECA, CGS-21680, and PSB-0777, and the aminopyridine group of LUF-5834 through aromatic/hydrophobic interactions with F168, M5.38, M7.35, I7.39 (numbering in Ballesteros and Weinstein scheme [37], except for residues outside helices in which sequence numbers are used) and polar interactions of the exocyclic nitrogen with N6.55 (Supplementary Fig. S3). The second region (green rectangle) accommodates the 5′-hydroxymethyl (adenosine and PSB-0777), N-ethylcarboxamido (NECA and CGS-21680) and hydroxyphenyl group of LUF-5834 (Fig. 2). The 5′-hydroxymethyl group attached to the ribose ring of adenosine and PSB-0777 and the hydroxyphenyl group of LUF-5834 hydrogen bond H6.52 during all the simulation time (Supplementary Fig. S3). NECA and CGS-21680 replace the 5′-hydroxymethyl group by the longer N-ethylcarboxamido group that can directly interact with both H6.52 and T3.36 (Supplementary Fig. S3). Several X-ray structures of $A_{2A}R$ contain crystallized water molecules in the environment of T3.36 and N5.42 [4] that are important for the activity of GPCRs [38,39]. Supplementary Fig. S6 shows that during the MD simulations adenosine, PSB-0777 and LUF-5834 maintain this water bridge, whereas NECA and CGS-21680 cannot because the N-ethylcarboxamido group interacts with T3.36. Finally, the third region (yellow rectangle) is occupied by the ribose moiety of adenosine derivatives and by the carbonitrile substituent of LUF-5834. Most important interactions in this site imply the formation of

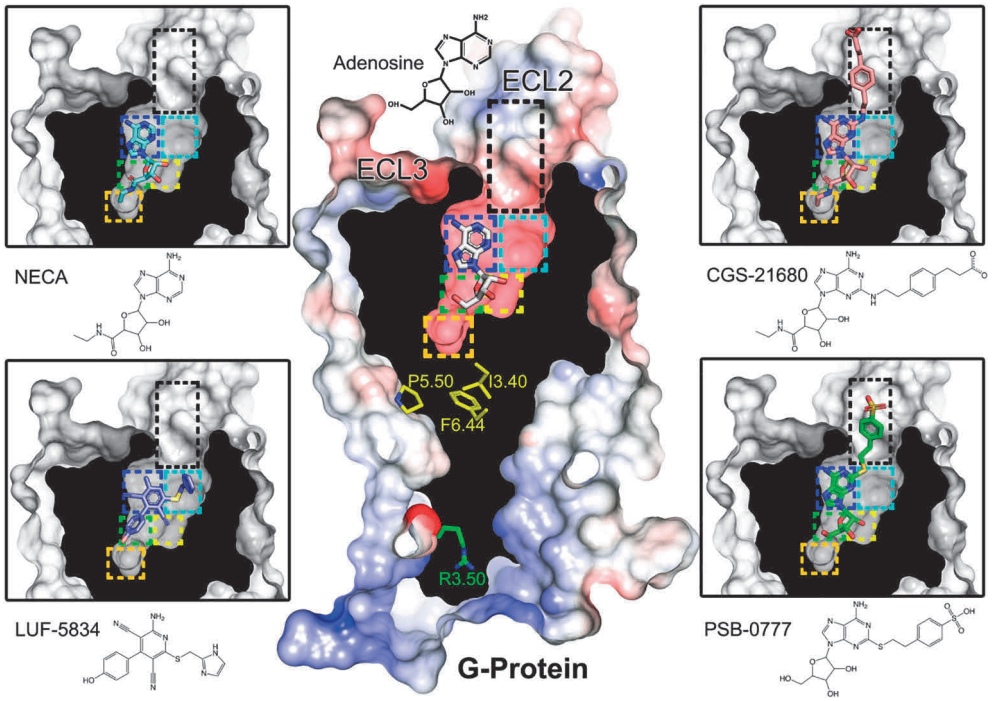

Fig. 2. Ligand-receptor complexes. Cross-section through the $A_{2A}R$, highlighting the agonists adenosine (white sticks), NECA (cyan), CGS-21680 (pink), PSB-0777 (green) and LUF-5834 (blue) occupying the binding site. Color rectangles highlight regions of the orthosteric binding cavity that are occupied by functional groups of the studied agonists (see 3.2). The PIF motif (in yellow) located below the orthosteric binding cavity, and the side chain of the highly conserved R3.50 (in green) of the DRY motif near the G protein binding site are highlighted. (For interpretation of the references to color in this figure legend, the reader is referred to the web version of this article.)

hydrogen bonds from the hydroxyl groups at positions C2 and C3 of the ribose moiety of adenosine derivatives with the S7.42 and H7.43 residues.

Three additional regions are occupied by the ligands (orange, cyan and black in Fig. 2). The ethyl group of the N-ethylcarboxamido moiety of NECA and CGS-21680 extends deep into the binding pocket (orange), forming hydrophobic interactions with C5.46 (Supplementary Fig. S3). These interactions between aliphatic chains and sulfur-containing amino acids have been shown to be of high energy [40]. The long substituents of CGS-21680 and PSB-0777 expand toward the extracellular loops through a cavity within TMs 1, 2 and 7 (black rectangle), which has been shown to influence G protein and β-arrestin signaling in other GPCRs [41,42]. The negatively charged SO_3^- group of PSB-0777 interacts with His264 in ECL3, whereas the longer chain of CGS-21680 permits the negatively charged COO^- to form an ionic interaction with K153 in ECL2 (Supplementary Fig. S7). Finally, the imidazole substituent of LUF-5834 interacts with residues Y1.35, A2.61, I2.64, S2.65, and I7.39 in the sideward region of the binding cavity (cyan rectangle). This binding orientation of LUF-5834 has been previously proposed using mutagenesis studies [43]. This region is generally occupied by inverse agonists and, thus, we believe contributes to the low activity of LUF-5834 regarding the rest of the agonists.

3.3. Agonist-induced signaling responses

Next, we measured four functional read-outs that correspond to different steps of the signaling pathways in cells expressing full-length $A_{2A}R$ or $A_{2A}^{\Delta 40}R$: cAMP production, β-arrestin recruitment, ERK1/2 phosphorylation, and dynamic mass redistribution (DMR) assays (Fig. 3 and Table 2). Immediately following receptor activation, cAMP levels increase as the result of adenylyl cyclase activation by Gs. Next, receptor phosphorylation by G protein kinases triggers β-arrestin recruitment. Later, ERK signaling is regulated by G protein or/and β-arrestin. DMR accounts for events that occur much later in the signaling pathway such as protein trafficking, rearrangement of cytoskeleton and adhesion or morphological changes. The amount of transfected cDNA for $A_{2A}R$ and $A_{2A}^{\Delta 40}R$ was adjusted to obtain similar receptor expression levels (Supplementary Fig. S1B). β-arrestin recruitment and ERK1/2 phosphorylation were analyzed by time response curves (Supplementary Figs. S1C-S1D). In our cAMP assay conditions, adenosine, NECA, and CGS-21680 behaved as full agonists, whereas PSB-0777 and LUF-5834 were partial agonists on full-length $A_{2A}R$. The effect was specific for all agonists as shown by the blockade of cAMP production using the selective receptor antagonist SCH-58261 (Supplementary Fig. S8). β-arrestin recruitment assays showed that PSB-0777 and NECA are more efficient in recruitment than adenosine and CGS-21680. Remarkably, LUF-5834, which is a partial agonist in the cAMP assay, is as efficient as CGS-21680 and adenosine in β-arrestin recruitment. pERK1/2 dose–response curves follow similar patterns as cAMP curves, with the exceptions of PSB-0777 that behaves as a full agonist, and LUF-5834 that is a very weak partial agonist. DMR responses were all very similar with PSB-0777 providing a slightly larger signal at higher concentrations.

In agreement with previous reports [10], removal the last 40 amino acids of the C-terminus in the $A_{2A}^{\Delta 40}R$ construct caused a right-shift of the cAMP dose–response curves (a ratio of EC_{50} values in the 2.2–9.8 range, similar to the range of K_i ratios) with almost no change in E_{max} for all agonists, with the exception of LUF-5834 whose effect became almost negligible in the truncated form of the receptor (Fig. 3 and Table 2). C-terminal truncation provides a small decrease in β-arrestin recruitment with no changes in E_{max} rank order relative to full-length $A_{2A}R$. pERK1/2 dose–response curves of $A_{2A}^{\Delta 40}R$ were very similar to full-length $A_{2A}R$ except that pEC_{50} increased for the truncated receptor, which goes against the general trend, and the potency of NECA and PSB-0777 became close to that of adenosine and CGS-21680. Finally, DMR read-outs of $A_{2A}^{\Delta 40}R$ were almost negligible for NECA and adenosine while we could observe a higher signal for PSB-0777 compared to that of the other compounds in $A_{2A}R$ and $A_{2A}^{\Delta 40}R$.

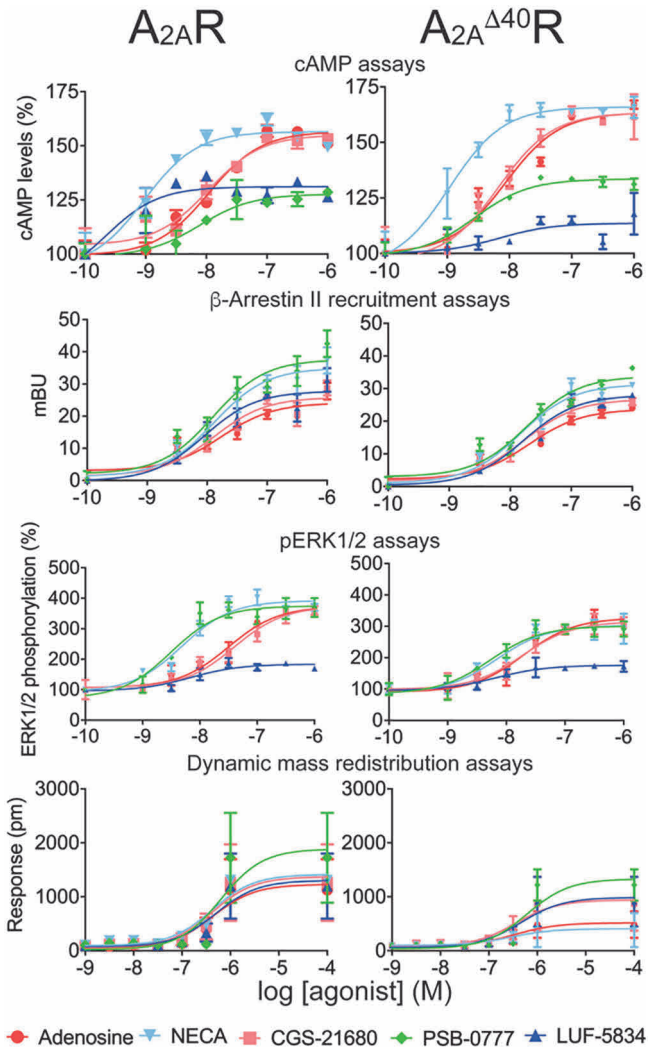

Fig. 3. Signaling in cells expressing either $A_{2A}R$ or $A_{2A}^{\Delta 40}R$. Dose response curves on 0.5 μM forskolin-induced cAMP levels, on ß-arrestin recruitment, on ERK1/2 phosphorylation, and on dynamic mass redistribution (DMR). Data (n = 12, each in triplicates) for cAMP are given in percentage (100% represents the forskolin effect). Data (n = 10, each in triplicates) for BRET assays, used to determine β-arrestin recruitment, are given in milliBRET Units (mBU). Data (n = 6, each in triplicates) for ERK1/2 phosphorylation are expressed as % with respect to basal levels. DMR tracings are representing the picometer (pm)-shifts of reflected light wavelengths over time upon ligand treatment.

3.4. Addressing biased agonism

Bias factors were calculated taking as reference the effect of adenosine, the endogenous compound, and the Gs-mediated signal, i.e. cAMP response elicited by adenosine (see *2.8*). Bias factors for CGS-21680, PSB-0777, LUF-5834 and NECA agonists in cAMP, β-arrestin recruitment, ERK1/2 phosphorylation and DMR signaling responses are summarized in the radar plot of Fig. 4. Adenosine and CGS-21680 are balanced agonists with similar bias factors for the four pathways, whereas NECA has small factors for DMR and β-arrestin recruitment and LUF-5834 has small factors for all responses other than cAMP. By contrast, PSB-0777 has a higher bias for the pERK1/2 response. Truncation of the C-terminus makes LUF-5834 and PSB-0777 more balanced. In fact, LUF-5834 acquires the largest bias factors for β-arrestin recruitment, ERK1/2 phosphorylation and DMR. By contrast, NECA keeps the small factors for β-arrestin recruitment and DMR. Overall the results are consistent with the C-terminus being dispensable for both G-protein and arrestin recruitment and also for MAPK activation (ERK1/2 phosphorylation and DMR), with only minor differences in signaling compared to full-length $A_{2A}R$.

3.5. Molecular mechanisms of agonist-induced receptor activation

The first step to understand the mechanisms of agonist-induced receptor activation, was to compare by MD simulations the trajectories of amino acids at positions 3.40, 5.50, and 6.44 (Fig. 5), which have been named as the "P-I-F" motif [44], the "transmission switch" [45], the "triad core" [46] or the connector region [6], in the presence of the agonists adenosine, NECA, CGS-21680, PSB-0777 and LUF-5834 and the antagonist SCH-58261. These residues, located below the ligand binding cavity and above the G protein or arrestin binding cavity (see Fig. 2), adopt different positions upon binding of agonists or antagonists [47,48], and we have been using them to predict the effect of the ligand on the conformational state of the receptor [49–51]. Clearly, the agonist-bound, active-like complexes are characterized relative to the antagonist-bound, inactive-like, complex by the proposed inward movement of TM5 at the highly conserved P5.50, rotation of TM3 due to a steric clash with the bulky I3.40, and an outward movement of F6.44 in TM6 (Fig. 5). Unfortunately, these movements are similar for full and partial agonists and cannot be used to explain the different agonist pharmacological profiles.

Thus, in order to understand the structural arrangements of the binding cavity, triggered by these chemically different agonists, facilitating G protein binding or β-arrestin recruitment with different efficacy, we studied the trajectories of a selected group of 34 amino acids either located above (in the ligand binding cavity) and below (in the G protein or arrestin binding cavity) the "transmission switch" amino acids in the presence of agonists and the antagonist (see Supplementary Table S1). In the bivariate correlation analysis, dependent variables are E_{max} values measured in cAMP production and β-arrestin recruitment, whereas independent variables are the movement of the chosen amino acid in the agonist-bound, active-like complexes relative to the antagonist-bound, inactive-like complex. This is measured as the distance

Table 2
pEC_{50} and E_{max} values obtained in HEK-293T cells expressing wild type $A_{2A}R$ or truncated $A_{2A}^{\Delta 40}R$ for cAMP production, β-arrestin II recruitment, ERK1/2 phosphorylation and dynamic mass redistribution (DMR) response (Fig. 3).

	cAMP assays				β -arrestin assays				pERK1/2 assays				DMR assays			
	$A_{2A}R$		$A_{2A}^{\Delta 40}R$		$A_{2A}R$		$A_{2A}^{\Delta 40}R$		$A_{2A}R$		$A_{2A}^{\Delta 40}R$		$A_{2A}R$		$A_{2A}^{\Delta 40}R$	
	pEC_{50}	E_{max}	pEC_{50}	E_{max}	pEC_{50}	E_{max}	pEC_{50}	E_{max}	pEC_{50}	E_{max}	pEC_{50}	E_{max}	pEC_{50}	E_{max}	pEC_{50}	E_{max}
Adenosine	8.0	156.6	8.1	163.5	7.8	24.1	7.7	23.7	7.5	373.0	7.7	326.9	6.4	1231	6.4	517.8
NECA	9.0	156.6	9.0	166.0	7.9	34.9	7.8	31.3	8.3	392.1	8.2	302.6	6.4	1416	6.5	407.9
CGS-21680	8.0	155.1	8.2	163.4	7.9	25.9	7.8	26.8	7.4	373.5	7.7	315.2	6.4	1374	6.4	941.5
PSB-0777	8.1	127.7	8.6	133.5	7.9	37.6	7.7	33.8	8.5	374.7	8.3	300.7	6.2	1887	6.2	1332
LUF-5834	9.7	131.1	8.2	113.6	8.0	27.8	7.8	28.0	8.2	183.9	8.2	175.8	6.3	1306	6.3	988.6

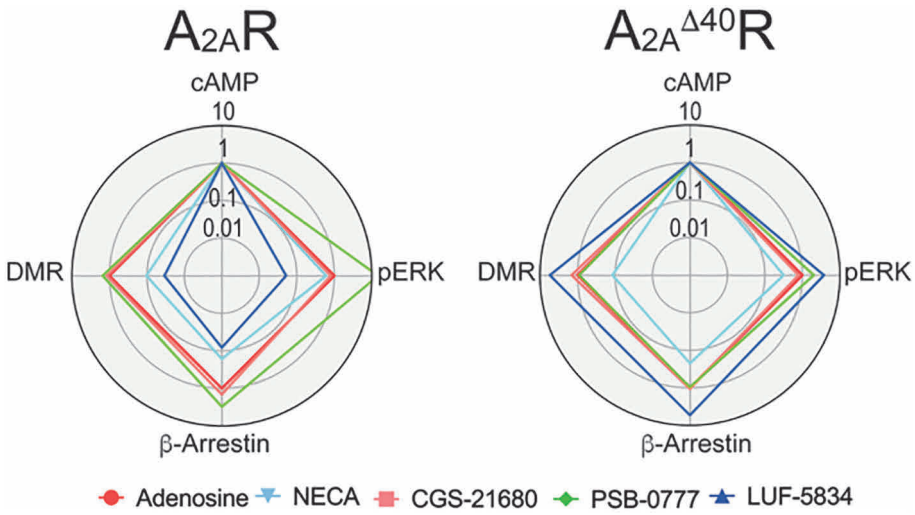

Fig. 4. Radar plot representation of bias factors. Plots show the bias factors of the different compounds in the different functional outcomes in cells expressing $A_{2A}R$ or $A_{2A}^{\Delta 40}R$. Adenosine and the Gs-cAMP signaling pathway were used as reference for calculations.

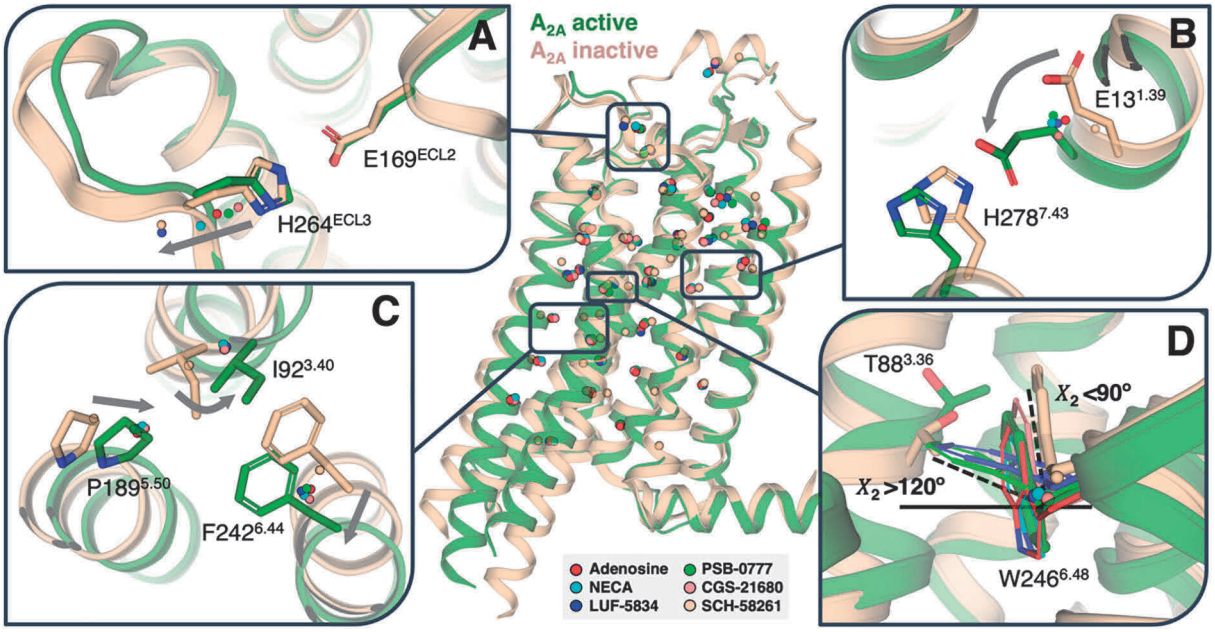

Fig. 5. Receptor side-chain movements in response to agonists. Plot of the centroids (calculated from 100 snapshots) of the C_β atoms of a selected group of 34 amino acids (Table S1) located above (in the ligand binding cavity) and below (in the G protein or β-arrestin binding cavity) the "transmission switch" amino acids obtained during 1 μs of MD simulations of $A_{2A}R$ in the presence of the agonists adenosine, NECA, CGS-21680, PSB-0777 and LUF-5834 and a selective antagonist SCH-58261. The distances between the centroids of the agonist-bound conformations and the centroid of the antagonist-bound conformation were statistically correlated with E_{max} values measured in cAMP production and β-arrestin recruitment (Table S1). (A) Movement of the salt bridge between $E169^{ECL2}$ and $H264^{ECL3}$ that is proposed to govern the residence time of ligands. (B) Movement of $E13^{1.39}$, and the nearby $H278^{7.43}$, that correlates with β-arrestin recruitment. (C) The proposed mechanism of receptor activation at the "transmission switch" amino acids (inward movement of TM 5, an anticlockwise rotation of TM 3, and an outward movement of TM 6, see arrows) is observed but similar for full and partial agonists. (D) Movement of $T88^{3.36}$ and $W246^{6.48}$ that correlate with cAMP production (Supplementary Fig. S9).

between the centroid (calculated from 100 snapshots obtained during 1 μs of unbiased MD simulations) of the C_β positions of the chosen amino acids of $A_{2A}R$ bound to agonists and the centroid of $A_{2A}R$ bound to the antagonist. No deviations from normality (Shapiro-Wilk test) are observed in all variables, thus, correlation analyses were performed using a Pearson test for continuous, normally distributed variables.

Although ligand efficacy is a function of multiple factors, we found a clear statistically significant correlation between E_{max} in cAMP assays and the movement of the side chains of T3.36 ($p = 0.033$) and W6.48 ($p = 0.015$) above the "transmission switch" and Y5.58 ($p = 0.039$) below the "transmission switch" (Supplementary Table S1). Y5.58 is a key amino acid in the process of receptor activation as it stabilizes the extended conformation of R3.50 in the active state [52]. Positions 3.36 and 6.48 have been described as conformational toggle or trigger switches involved in the initial agonist-induced receptor activation in other GPCRs such as cannabinoid CB_1R [53,54], serotonin $5HT_4R$ [55], melanocorin MC4R [56], $mGlu_2R$ [57], or $A_{2A}R$ [58]. With the aim of understanding at the molecular level the different activation trends among agonists, we explored the amount of time, in the MD simulations, the side chains of T3.36 and W6.48 spend in the *gauche*

+ (*g+*, χ_1 = -60°), *gauche-* (*g-*, χ_1 = 60°) or *trans* (*t*, χ_1 = 180°) conformations (see Supplementary Fig. S9). Clearly, the antagonist-bound structure favors the *g+/g+* conformations of T3.36 and W6.48, whereas full agonists adenosine, NECA, and CGS-21680 favor the *g-/g+* conformations. Notably, partial agonists PSB-0777 and LUF-5834 cannot achieve these *g-/g+* conformations as frequently as full agonists. In this respect, it should be noted that Thr residues in this *g-* conformation are capable of hydrogen bonding the backbone carbonyl in the previous turn of the helix, which is known to trigger a local opening of the helix [59] that might be necessary for receptor activation. Importantly, the T3.36A mutation impedes signaling [43,60] and the W6.48A mutation has significant deleterious effects on receptor function [43].

In the case of E_{max} in β-arrestin recruitment, we found a statistically significant correlation only with the movement of the side chain of E1.39 (p = 0.014) above the "transmission switch" (Supplementary Table S1). Because E1.39 and H7.43 might form an ionic interaction we calculated the distance between these side chains in the presence of the different agonists. However, we have not observed a statistically significant correlation between this distance and E_{max} in β-arrestin recruitment.

4. Conclusion

The agonist-dependent selectivity for intracellular pathways of $A_{2A}R$ has been studied using, in synergy, molecular modeling tools and pharmacological assays. This combination of expertise has permitted to understand the structural arrangements of the binding cavity, triggered by chemically different agonists, facilitating G protein binding with different efficacy. The mechanism of agonist-induced β-arrestin recruitment seems more difficult to rationalize. First, different ligands stimulation might induce distinct patterns of receptor phosphorylation, which direct specific β-arrestin conformations and functional outcomes [61–63]. Second, there is increasing evidence that biased signaling could also be a consequence of binding kinetics [64–66]. In particular, a relation between residence time of ligands with biased signaling in both A_1R and $A_{2A}R$ [67,68] that is governed by a salt bridge between $E169^{ECL2}$ and $H264^{ECL3}$ in $A_{2A}R$ (Fig. 5A) [69,70] has been shown. Finally, the last 40 amino acids of the C-terminal end of $A_{2A}R$ receptor are dispensable for both G-protein and arrestin recruitment and also for MAPK activation (ERK1/2 phosphorylation and DMR).

5. Notes

Authors declare no conflict of interest.

Funding

This work was partially supported by grants from the Spanish Ministry of Economy and Competitiveness (BFU2015-64405-R, SAF2017-84117-R, RTI2018-094204-B-I00 and PID2019-109240RB-I00; they may include FEDER funds), the Alzheimer's Association (AARFD-17-503612) and by a grant from Fundació la Marató de TV3 (201413-30).

CRediT authorship contribution statement

Gemma Navarro: Conceptualization, Validation, Supervision, Project administration, Resources, Writing - original draft, Funding acquisition. **Angel Gonzalez:** Validation, Supervision, Project administration, Resources. **Stefano Campanacci:** Investigation. **Rafael Rivas-Santisteban:** Investigation. **Irene Reyes-Resina:** Investigation. **Nil Casajuana-Martin:** Investigation. **Arnau Cordomí:** Investigation, Validation, Supervision. **Leonardo Pardo:** Conceptualization, Validation, Project administration, Resources, Writing - original draft, Funding acquisition. **Rafael Franco:** Conceptualization, Validation, Project administration, Resources, Writing - original draft, Funding acquisition.

Appendix A. Supplementary data

Supplementary data to this article can be found online at https://doi.org/10.1016/j.csbj.2020.09.028.

References

[1] Mickael ME, Rajput A, Steyn J, Wiemerslage L, Burglin T. An optimised phylogenetic method sheds more light on the main branching events of rhodopsin-like superfamily. Comp Biochem Physiol Part D Genomics Proteomics 2016;20:85–94.
[2] Fredriksson R, Lagerstrom MC, Lundin LG, Schioth HB. The g-protein-coupled receptors in the human genome form five main families. Phylogenetic analysis, paralogon groups, and fingerprints. Mol Pharmacol 2003;63:1256–72.
[3] Fredholm BB, IJzerman AP, Jacobson KA, Linden J, Muller CE. International Union of Basic and Clinical Pharmacology. LXXXI. Nomenclature and classification of adenosine receptors–an update. Pharmacol Rev 2011;63:1–34.
[4] Jaakola VP, Griffith MT, Hanson MA, Cherezov V, Chien EY, Lane JR, et al. The 2.6 angstrom crystal structure of a human A2A adenosine receptor bound to an antagonist. Science 2008;322:1211–7.
[5] Pandy-Szekeres G, Munk C, Tsonkov TM, Mordalski S, Harpsoe K, Hauser AS, et al. GPCRdb in 2018: adding GPCR structure models and ligands. Nucleic Acids Res 2018;46:D440–6.
[6] Weis WI, Kobilka BK. The molecular basis of G protein-coupled receptor activation. Annu Rev Biochem 2018;87:897–919.
[7] Gonzalez A, Cordomí A, Caltabiano G, Campillo M, Pardo L. Impact of helix irregularities on sequence alignment and homology modelling of G protein-coupled receptors. ChemBioChem 2012;13:1393–9.
[8] Ciruela F, Canela L, Burgueno J, Soriguera A, Cabello N, Canela EI, et al. Heptaspanning membrane receptors and cytoskeletal/scaffolding proteins: focus on adenosine, dopamine, and metabotropic glutamate receptor function. J Mol Neurosci 2005;26:277–92.
[9] Keuerleber S, Gsandtner I, Freissmuth M. From cradle to twilight: the carboxyl terminus directs the fate of the A(2A)-adenosine receptor. Biochim Biophys Acta 2011;1808:1350–7.
[10] Klinger M, Kuhn M, Just H, Stefan E, Palmer T, Freissmuth M, et al. Removal of the carboxy terminus of the A2A-adenosine receptor blunts constitutive activity: differential effect on cAMP accumulation and MAP kinase stimulation. Naunyn Schmiedebergs Arch Pharmacol 2002;366:287–98.
[11] Navarro G, Ferre S, Cordomi A, Moreno E, Mallol J, Casado V, et al. Interactions between intracellular domains as key determinants of the quaternary structure and function of receptor heteromers. J Biol Chem 2010;285:27346–59.
[12] Kofalvi A, Moreno E, Cordomi A, Cai NS, Fernandez-Duenas V, Ferreira SG, et al. Control of glutamate release by complexes of adenosine and cannabinoid receptors. BMC Biol 2020;18:9.
[13] Navarro G, Cordomi A, Brugarolas M, Moreno E, Aguinaga D, Perez-Benito L, et al. Cross-communication between Gi and Gs in a G-protein-coupled receptor heterotetramer guided by a receptor C-terminal domain. BMC Biol 2018;16:24.
[14] de Lera Ruiz M, Lim YH, Zheng J. Adenosine A2A receptor as a drug discovery target. J Med Chem 2014;57:3623–50.
[15] Gutierrez-de-Teran H, Sallander J, Sotelo E. Structure-based rational design of adenosine receptor ligands. Curr Top Med Chem 2017;17:40–58.
[16] Domenici MR, Ferrante A, Martire A, Chiodi V, Pepponi R, Tebano MT, et al. Adenosine A2A receptor as potential therapeutic target in neuropsychiatric disorders. Pharmacol Res 2019;147:104338.
[17] Dungo R, Deeks ED. Istradefylline: first global approval. Drugs 2013;73:875–82.
[18] Wisler JW, Rockman HA, Lefkowitz RJ. Biased G protein-coupled receptor signaling: changing the paradigm of drug discovery. Circulation 2018;137:2315–7.
[19] Valant C, May LT, Aurelio L, Chuo CH, White PJ, Baltos JA, et al. Separation of on-target efficacy from adverse effects through rational design of a bitopic adenosine receptor agonist. PNAS 2014;111:4614–9.
[20] Smith JS, Lefkowitz RJ, Rajagopal S. Biased signalling: from simple switches to allosteric microprocessors. Nat Rev Drug Discov 2018;17:243–60.
[21] Burgueno J, Blake DJ, Benson MA, Tinsley CL, Esapa CT, Canela EI, et al. The adenosine A2A receptor interacts with the actin-binding protein alpha-actinin. J Biol Chem 2003;278:37545–52.
[22] Medrano M, Aguinaga D, Reyes-Resina I, Canela EI, Mallol J, Navarro G, et al. Orexin A/hypocretin modulates leptin receptor-mediated signaling by allosteric modulations mediated by the ghrelin GHS-R1A receptor in hypothalamic neurons. Mol Neurobiol 2018;55:4718–30.

[23] Zhou XE, He Y, de Waal PW, Gao X, Kang Y, Van Eps N, et al. Identification of phosphorylation codes for arrestin recruitment by G protein-coupled receptors. Cell 2017;170(457–469):e13.
[24] Martinez-Pinilla E, Rabal O, Reyes-Resina I, Zamarbide M, Navarro G, Sanchez-Arias JA, et al. Two affinity sites of the cannabinoid subtype 2 receptor identified by a novel homogeneous binding assay. J Pharmacol Exp Ther 2016;358:580–7.
[25] Cheng YC, Prusoff WH. Relationship between the inhibition constant (Ki) and the concentration of inhibitor which causes 50 per cent inhibition (IC50) of an enzymatic reaction. Biochem Pharmacol 1973;22:3099–108.
[26] Rajagopal S, Ahn S, Rominger DH, Gowen-MacDonald W, Lam CM, Dewire SM, et al. Quantifying ligand bias at seven-transmembrane receptors. Mol Pharmacol 2011;80:367–77.
[27] Black JW, Leff P. Operational models of pharmacological agonism. Proc R Soc Lond B 1983;220:141–62.
[28] Kenakin T, Christopoulos A. Measurements of ligand bias and functional affinity. Nat Rev Drug Discov 2013;12:483.
[29] Webb B, Sali A. Comparative Protein Structure Modeling Using MODELLER. Curr Protoc Bioinform 2014;47. 5 6 1-32.
[30] Labute P. Protonate3D: assignment of ionization states and hydrogen coordinates to macromolecular structures. Proteins 2009;75:187–205.
[31] Rodriguez-Espigares I, Torrens-Fontanals M, Tiemann JKS, Aranda-Garcia D, Ramirez-Anguita JM, Stepniewski TM, et al. GPCRmd uncovers the dynamics of the 3D-GPCRome. Nat Methods 2020;17:777–87.
[32] Massink A, Gutierrez-de-Teran H, Lenselink EB, Ortiz Zacarias NV, Xia L, Heitman LH. Sodium ion binding pocket mutations and adenosine A2A receptor function. Mol Pharmacol 2015;87:305–13.
[33] Liu W, Chun E, Thompson AA, Chubukov P, Xu F, Katritch V, et al. Structural basis for allosteric regulation of GPCRs by sodium ions. Science 2012;337:232–6.
[34] Gutierrez-de-Teran H, Massink A, Rodriguez D, Liu W, Han GW, Joseph JS, et al. The role of a sodium ion binding site in the allosteric modulation of the A(2A) adenosine G protein-coupled receptor. Structure 2013;21:2175–85.
[35] Cordomi A, Caltabiano G, Pardo L. Membrane protein simulations using AMBER force field and berger lipid parameters. J Chem Theory Comput 2012;8:948–58.
[36] Jespers W, Schiedel AC, Heitman LH, Cooke RM, Kleene L, van Westen GJP, et al. Structural mapping of adenosine receptor mutations: ligand binding and signaling mechanisms. Trends Pharmacol Sci 2018;39:75–89.
[37] Ballesteros JA, Weinstein H. Integrated methods for the construction of three dimensional models and computational probing of structure-function relations in G-protein coupled receptors. Methods Neurosci 1995;25:366–428.
[38] Pardo L, Deupi X, Dolker N, Lopez-Rodriguez ML, Campillo M. The role of internal water molecules in the structure and function of the rhodopsin family of G protein-coupled receptors. ChemBioChem 2007;8:19–24.
[39] Venkatakrishnan AJ, Ma AK, Fonseca R, Latorraca NR, Kelly B, Betz RM, et al. Diverse GPCRs exhibit conserved water networks for stabilization and activation. Proc Natl Acad Sci USA 2019.
[40] Gomez-Tamayo JC, Cordomi A, Olivella M, Mayol E, Fourmy D, Pardo L. Analysis of the interactions of sulfur-containing amino acids in membrane proteins. Protein Sci 2016;25:1517–24.
[41] Liu JJ, Horst R, Katritch V, Stevens RC, Wuthrich K. Biased signaling pathways in beta2-adrenergic receptor characterized by 19F-NMR. Science 2012;335:1106–10.
[42] McCorvy JD, Butler KV, Kelly B, Rechsteiner K, Karpiak J, Betz RM, et al. Structure-inspired design of beta-arrestin-biased ligands for aminergic GPCRs. Nat Chem Biol 2018;14:126–34.
[43] Lane JR, Klein Herenbrink C, van Westen GJ, Spoorendonk JA, Hoffmann C, IJzerman AP. A novel nonribose agonist, LUF5834, engages residues that are distinct from those of adenosine-like ligands to activate the adenosine A(2a) receptor. Mol Pharmacol 2012;81:475–87.
[44] Wacker D, Wang C, Katritch V, Han GW, Huang XP, Vardy E, et al. Structural Features for Functional Selectivity at Serotonin Receptors. Science 2013;340:615–9.
[45] Venkatakrishnan AJ, Deupi X, Lebon G, Tate CG, Schertler GF, Babu MM. Molecular signatures of G-protein-coupled receptors. Nature 2013;494:185–94.
[46] Huang W, Manglik A, Venkatakrishnan AJ, Laeremans T, Feinberg EN, Sanborn AL, et al. Structural insights into micro-opioid receptor activation. Nature 2015;524:315–21.
[47] Sansuk K, Deupi X, Torrecillas IR, Jongejan A, Nijmeijer S, Bakker RA, et al. A structural insight into the reorientation of transmembrane domains 3 and 5 during family A G protein-coupled receptor activation. Mol Pharmacol 2011;79:262–9.
[48] Rasmussen SG, Choi HJ, Fung JJ, Pardon E, Casarosa P, Chae PS, et al. Structure of a nanobody-stabilized active state of the beta(2) adrenoceptor. Nature 2011;469:175–80.
[49] Troupiotis-Tsailaki A, Zachmann J, Gonzalez-Gil I, Gonzalez A, Ortega-Gutierrez S, Lopez-Rodriguez ML, et al. Ligand chain length drives activation of lipid G protein-coupled receptors. Sci Rep 2017;7:2020.
[50] Izquierdo C, Gomez-Tamayo JC, Nebel JC, Pardo L, Gonzalez A. Identifying human diamine sensors for death related putrescine and cadaverine molecules. PLoS Comput Biol 2018;14:e1005945.
[51] Llinas Del Torrent C, Casajuana-Martin N, Pardo L, Tresadern G, Perez-Benito L. Mechanisms underlying allosteric molecular switches of metabotropic glutamate receptor 5. J Chem Inf Model 2019;59:2456–66.
[52] Park JH, Scheerer P, Hofmann KP, Choe HW, Ernst OP. Crystal structure of the ligand-free G-protein-coupled receptor opsin. Nature 2008;454:183–7.
[53] McAllister SD, Hurst DP, Barnett-Norris J, Lynch D, Reggio PH, Abood ME. Structural mimicry in class A G protein-coupled receptor rotamer toggle switches: the importance of the F3.36(201)/W6.48(357) interaction in cannabinoid CB1 receptor activation. J Biol Chem 2004;279:48024–37.
[54] Krishna Kumar K, Shalev-Benami M, Robertson MJ, Hu H, Banister SD, Hollingsworth SA, et al. Structure of a signaling cannabinoid receptor 1-G protein complex. Cell 2019;176(448–458):e12.
[55] Pellissier LP, Sallander J, Campillo M, Gaven F, Queffeulou E, Pillot M, et al. Conformational toggle switches implicated in basal constitutive and agonist-induced activated states of 5-hydroxytryptamine-4 receptors. Mol Pharmacol 2009;75:982–90.
[56] Ersoy BA, Pardo L, Zhang S, Thompson DA, Millhauser G, Govaerts C, et al. Mechanism of N-terminal modulation of activity at the melanocortin-4 receptor GPCR. Nat Chem Biol 2012;8:725–30.
[57] Perez-Benito L, Doornbos MLJ, Cordomi A, Peeters L, Lavreysen H, Pardo L, et al. Molecular switches of allosteric modulation of the metabotropic glutamate 2 receptor. Structure 2017;25(1153–1162):e4.
[58] Rodriguez D, Pineiro A, Gutierrez-de-Teran H. Molecular dynamics simulations reveal insights into key structural elements of adenosine receptors. Biochemistry 2011;50:4194–208.
[59] Deupi X, Olivella M, Sanz A, Dolker N, Campillo M, Pardo L. Influence of the g-conformation of Ser and Thr on the structure of transmembrane helices. J Struct Biol 2010;169:116–23.
[60] Bertheleme N, Singh S, Dowell SJ, Hubbard J, Byrne B. Loss of constitutive activity is correlated with increased thermostability of the human adenosine A2A receptor. Br J Pharmacol 2013;169:988–98.
[61] Nobles KN, Xiao K, Ahn S, Shukla AK, Lam CM, Rajagopal S, et al. Distinct phosphorylation sites on the beta(2)-adrenergic receptor establish a barcode that encodes differential functions of beta-arrestin. Sci Signal 2011;4:ra51.
[62] Yang F, Yu X, Liu C, Qu CX, Gong Z, Liu HD, et al. Phospho-selective mechanisms of arrestin conformations and functions revealed by unnatural amino acid incorporation and (19)F-NMR. Nat Commun 2015;6:8202.
[63] Yang Z, Yang F, Zhang D, Liu Z, Lin A, Liu C, et al. Phosphorylation of G protein-coupled receptors: from the barcode hypothesis to the flute model. Mol Pharmacol 2017;92:201–10.
[64] Klein Herenbrink C, Sykes DA, Donthamsetti P, Canals M, Coudrat T, Shonberg J, et al. The role of kinetic context in apparent biased agonism at GPCRs. Nat Commun 2016;7:10842.
[65] Grundmann M, Kostenis E. Temporal bias: time-encoded dynamic GPCR signaling. Trends Pharmacol Sci 2017;38:1110–24.
[66] Jensen DD, Lieu T, Halls ML, Veldhuis NA, Imlach WL, Mai QN, et al. Neurokinin 1 receptor signaling in endosomes mediates sustained nociception and is a viable therapeutic target for prolonged pain relief. Sci Transl Med 2017;9.
[67] Guo D, Mulder-Krieger T, Ijzerman AP, Heitman LH. Functional efficacy of adenosine A(2)A receptor agonists is positively correlated to their receptor residence time. Br J Pharmacol 2012;166:1846–59.
[68] Yun Y, Chen J, Liu R, Chen W, Liu C, Wang R, et al. Long residence time adenosine A1 receptor agonists produce sustained wash-resistant antilipolytic effect in rat adipocytes. Biochem Pharmacol 2019;164:45–52.
[69] Segala E, Guo D, Cheng RK, Bortolato A, Deflorian F, Dore AS, et al. Controlling the dissociation of ligands from the adenosine A2A receptor through modulation of salt bridge strength. J Med Chem 2016;59:6470–9.
[70] Guo D, Pan AC, Dror RO, Mocking T, Liu R, Heitman LH, et al. Molecular basis of ligand dissociation from the adenosine A2A receptor. Mol Pharmacol 2016;89:485–91.

3.11 Adenosine A_{2A} Receptor Antagonists Affects NMDA Glutamate Receptor Function. Potential to Address Neurodegeneration in Alzheimer's Disease.

Rafael Franco, **Rafael Rivas-Santisteban**, Mireia Casanovas, Alejandro Lillo, Carlos A Saura, Gemma Navarro.

Manuscrito publicado en *Cells*, Marzo 2020; 9: 1075.

El receptor ionotrópico de glutamato N-metil d-aspartato (NMDAR) es una de las principales dianas terapéuticas para combatir la enfermedad de Alzheimer (AD), ya que la hiperactivación de los NMDAR extrasinápticos se ha descrito como uno de los mecanismos moleculares implicados en la aparición de la AD. El objetivo principal de nuestra investigación fue determinar si el receptor de adenosina A_{2A} ($A_{2A}R$), que también es una diana clave para combatir la neurodegeneración, puede alterar la señalización mediada por el NMDAR. Nuestros resultados mediante la técnica de transferencia de energía resonante por bioluminiscencia (BRET) confirman la interacción específica entre los receptores NMDA y A_{2A}. Mediante los ensayos de ligación por proximidad (PLA) detectamos un aumento en la expresión del heterómero $A_{2A}R$-NMDAR en microglía activada en comparación a la microglía control, este hecho también se observó en cultivos primarios de microglía de ratones $APP_{Sw,Ind}$. También se efectuaron ensayos de PLA en neuronas, donde se observó una menor formación de los complejos heteroméricos $A_{2A}R$-NMDAR respecto a los ensayos en células gliales. Los ensayos de caracterización funcional revelaron un efecto de antagonismo cruzado en el heterómero de receptores A_{2A}-NMDA. Así, el uso de un antagonista específico para $A_{2A}R$ podría ser útil como terapia preventiva de la hiperactivación del NMDAR. En conclusión, el uso de antagonistas de $A_{2A}R$, como el fármaco Istradefylline, ya aprobado para el tratamiento de la enfermedad de Parkinson, tienen un gran potencial para el tratamiento de la AD.

cells

MDPI

Article

Adenosine A_{2A} Receptor Antagonists Affects NMDA Glutamate Receptor Function. Potential to Address Neurodegeneration in Alzheimer's Disease

Rafael Franco [1,2,*], Rafael Rivas-Santisteban [1,2], Mireia Casanovas [1,2], Alejandro Lillo [3], Carlos A. Saura [2,4] and Gemma Navarro [2,3,*]

1 Departament de Bioquímica i Biomedicina Molecular, Universitat de Barcelona, 08028 Barcelona, Spain; rrivasbioq@gmail.com (R.R.-S.); mcasanfe8@gmail.com (M.C.)
2 Centro de Investigación Biomédica en Red sobre Enfermedades Neurodegenerativas, Instituto de Salud Carlos III, Valderrebollo, 5, 28031 Madrid, Spain; carlos.saura@uab.cat
3 Departament of Biochemistry and Physiology, Faculty of Pharmacy and Food Science, Universitat de Barcelona, 08028 Barcelona, Spain; alilloma55@gmail.com
4 Institut de Neurociències, Department de Bioquímica i Biologia Molecular, Universitat Autònoma de Barcelona, Bellaterra, 08193 Barcelona, Spain
* Correspondence: rfranco123@gmail.com (R.F.); g.navarro@ub.edu (G.N.)

Received: 27 March 2020; Accepted: 19 April 2020; Published: 26 April 2020

Abstract: (1) Background. *N*-methyl D-aspartate (NMDA) ionotropic glutamate receptor (NMDAR), which is one of the main targets to combat Alzheimer's disease (AD), is expressed in both neurons and glial cells. The aim of this paper was to assess whether the adenosine A_{2A} receptor (A_{2A}R), which is a target in neurodegeneration, may affect NMDAR functionality. (2) Methods. Immuno-histo/cytochemical, biophysical, biochemical and signaling assays were performed in a heterologous cell expression system and in primary cultures of neurons and microglia (resting and activated) from control and the $APP_{Sw,Ind}$ transgenic mice. (3) Results. On the one hand, NMDA and A_{2A} receptors were able to physically interact forming complexes, mainly in microglia. Furthermore, the amount of complexes was markedly enhanced in activated microglia. On the other hand, the interaction resulted in a novel functional entity that displayed a cross-antagonism, that could be useful to prevent the exacerbation of NMDAR function by using A_{2A}R antagonists. Interestingly, the amount of complexes was markedly higher in the hippocampal cells from the $APP_{Sw,Ind}$ than from the control mice. In neurons, the number of complexes was lesser, probably due to NMDAR not interacting with the A_{2A}R. However, the activation of the A_{2A}R receptors resulted in higher NMDAR functionality in neurons, probably by indirect mechanisms. (4) Conclusions. A_{2A}R antagonists such as istradefylline, which is already approved for Parkinson's disease (Nouriast® in Japan and Nourianz® in the US), have potential to afford neuroprotection in AD in a synergistic-like fashion. i.e., via both neurons and microglia.

Keywords: G-protein-coupled receptors; functional selectivity; microglia; neuroprotection; cognition; signaling

1. Introduction

Alzheimer's disease (AD) is characterized by two pathological hallmarks, amyloid plaques composed of β-amyloid peptides and neurofibrillary tangles composed of hyperphosphorylated tau protein. Patients are currently treated with two drug types: *N*-methyl D-aspartate ionotropic glutamate receptor (NMDAR) modulators and acetylcholinesterase inhibitors. An anti-AD approved drug acting on NMDAR, memantine (marketed in many Countries as Namenda®), is a negative

allosteric modulator acting as a low-affinity open channel blocker. The drug was developed to find a weak negative modulator as both strong or weak NMDAR activities are noxious [1–3]. Unfortunately, the efficacy of current drugs is low and none prevent the disease progression [4]. It is well established that AD correlates with NMDAR functional alterations that cannot be addressed by drugs acting in the orthosteric center; in fact, NMDAR-related drugs used in AD patients are allosteric modulators of the receptor.

Adenosine is an autacoid, i.e., a hormone-like locally acting molecule, that exerts metabolic and regulatory functions in almost any tissue and cell type of the mammalian body. In the brain, it is one of the main neuromodulators acting via four G-protein-coupled receptors (GPCRs): A_1, A_{2A}, A_{2B} and A_3. The adenosine A_{2A} receptor ($A_{2A}R$), a G_s-coupled GPCR, is heavily expressed in the motor control brain areas [5] but is also expressed in other CNS regions [5]. Remarkably, an antagonist of the receptor, istradefylline, has been recently approved as a first-in-class drug for the treatment of Parkinson's disease [6–8] (Nouriast® in Japan and Nourianz® in the US). Apart from combating motor symptoms and/or minimizing the side effect of anti-parkinsonian medication, $A_{2A}R$ antagonists may be neuroprotective. Mechanisms of neuroprotection are based in in vitro and in vivo pharmacological studies. Pioneering work using adenosine itself led to a review entitled "Cerebral Protection by Adenosine" [9]. Based on data using brain ischemia-reperfusion models, it was already evident that adenosine could achieve the same neuroprotective effects as NMDAR blockers. The data came from studies focused on neurons, and the molecular mechanisms, including the type of adenosine receptor, were not known. As pointed out below, NMDAR are expressed in glia where adenosine receptors are also expressed. It is noteworthy that the $A_{2A}R$ is upregulated in activated microglia [10].

More recent studies conducted to explore the therapeutic possibilities to combat AD have used different assays with genetic ablation or a pharmacological blockade of the adenosine A_{2A} receptor, resulting in neuroprotection in different models. Briefly, taking into account the most recent reports, the expression of the A_{2A} receptor is altered even in peripheral blood cells from patients with AD or vascular dementia [11]. In addition, deletion of the receptor was beneficial in a tauopathy mouse model [12] and $A_{2A}R$ antagonists were protective in both the APPswe/PS1dE9 [13] and the triple 3×Tg-AD transgenic AD models [14]. Finally it should be noted that the early synaptic events seemed mediated by the $A_{2A}R$ in the 3×Tg-AD transgenic AD mouse model [15].

Based on the extensive background, the aim of this paper was to investigate whether the activation of the $A_{2A}R$ may regulate NMDAR function in both neurons and microglia cells. Although NMDAR function is instrumental for neurotransmission, senescent neurons have little resources to prevent death and rely on the support provided by glial cells. Among them, microglia are of interest since $A_{2A}R$ expression is enhanced in activated microglia where the NMDAR is also expressed [16–19]. Our results suggested that $A_{2A}R$ antagonists may provide neuroprotection via the modulation of NMDAR functionality.

2. Materials and Methods

2.1. Reagents

Lipopolysaccharide (LPS) and interferon-γ (IFN-γ) were purchased from Sigma Aldrich (St Louis, MO, USA); receptor ligands were purchased from Tocris Bioscience (Bristol, UK). Agonists were: *N*-methyl D-aspartate (NMDA) 4-[2-[[6-Amino-9-(*N*-ethyl-β-D-ribofuranuronamidosyl)-9*H*-purin-2-yl]amino]ethyl]benzenepropanoic acid hydrochloride (CGS-21680). Antagonists were: (*5S*,*10R*)-(+)-5-Methyl-10,11-dihydro-5*H*-dibenzo [a,d]cyclohepten-5,10-imine maleate (MK-801) and 2-(2-Furanyl)-7-(2-phenylethyl)-7*H*-pyrazolo[4,3-e] [1,2,4]triazolo[1,5-c]pyrimidin-5-amine (SCH-58261).

2.2. Fusion Proteins

To create A_{2A}R-*Renilla* luciferase (RLuc and A_{2A}R-yellow fluorescent protein (YFP) fusion molecules, the human version of adenosine A_{2A}R cDNA lacking the stop codon, was obtained by PCR and subcloned to a *Renilla* luciferase (RLuc)-containing vector (p*RLuc*; PerkinElmer, Wellesley, MA, USA) and a yellow fluorescent protein (YFP)-containing vector (pEYEP-N1; Clontech, Heidelberg, Germany) using sense and antisense primers harboring unique restriction sites for HindIII and BamHI. A similar approach was used to generate the cDNAs for GluN1-RLuc and caldendrin-YFP fusion proteins.

2.3. APP Transgenic Mouse Model of Alzheimer's Disease (AD)

$APP_{Sw,Ind}$ transgenic mice (line J9; C57BL/6 background), expressing human APP695 harboring the familial AD-linked Swedish (K670N/M671L) and Indiana (V717F) mutations under the PDGFβ promoter, were obtained by crossing $APP_{Sw,Ind}$ to non-transgenic (WT) mice [20]. Animals come from a colony established by co-author Carlos A. Saura in the Autonomous Barcelona University; animals came directly from the laboratory who developed the transgenic animal after signing the *ad hoc* Transfer Agreement.

2.4. Cell Culture and Transfection

HEK-293T human embryonic kidney cells from the American Type Culture Collection (ATCC) were grown in Dulbecco's modified Eagle's medium (DMEM) (Gibco, Paisley, Scotland, UK) supplemented with 2 mM L-glutamine, 100 U/mL penicillin/streptomycin, MEM Non-Essential Amino Acids Solution (1/100) and 5% (*v*/*v*) heat inactivated fetal bovine serum (FBS) (Gibco, Paisley, Scotland, UK). The cells were maintained in a humid atmosphere of 5% CO_2 at 37 °C. The cells were transiently transfected using Polyethylenimine (PEI, Sigma Aldrich, St. Louis, MO, USA) as previously described [21].

To prepare mice primary microglial cultures (C57BL/6 wild type or transgenic mice), the brain was removed at postnatal days 2 to 4. The microglial cells were isolated as described in [22] and grown in a DMEM medium supplemented with 2 mM L-glutamine, 100 U/mL penicillin/streptomycin, and 5% (*v*/*v*) heat inactivated FBS. For neuronal primary cultures, the hippocampus from mouse embryos (E19) was removed and the neurons were isolated as described by Hradsky et al., 2013 [23]. Cells were grown in a neurobasal medium supplemented with 2 mM L-glutamine, 100 U/mL penicillin/streptomycin, supplement (2% *v*/*v*) with B27 (Gibco). For cAMP assays, cells were grown on 6-well plates at a density of 500,000 cells/well, for ERK 1/2 phosphorylation assays, cells were placed in 96-well plates at a density of 50,000 cells/well; for proximity ligation assay cells were placed in 12-well plates with coverslips. Cell counting was assessed using trypan blue and a countless II FL automated cell counter (Thermo Fisher Scientific, Waltham, MA, USA). Experiments were carried out 15 days later and the medium was replaced every 5–7 days. The animal handling and protocols were conducted in accordance with the European Council Directive 2010/63/UE as well as in keeping with the current Spanish legislation (RD53/2013). The ethics committee of the two institutions (University of Barcelona and Autonomous University of Barcelona) were in charge of law implementation.

2.5. Immunocytochemistry

The transfected HEK-293T cells or primary microglial culture cells seeded in coverslips were fixed in 4% paraformaldehyde for 15 min and washed twice with phosphate-buffered saline (PBS) containing 20 mM glycine, before permeabilization with PBS-glycine containing 0.2% Triton X-100 (5 min incubation for the HEK-293T cells and 15 min for the microglial culture cells). The HEK-293T cells were treated for 1 h with PBS containing 1% bovine serum albumin (BSA), labeled with mouse monoclonal anti-RLuc antibody (1/100; mAB4400, EMD Millipore, Darmstadt, Germany) and subsequently treated with Cy3 anti-mouse (1/200; 715-166-150, Jackson ImmunoResearch (red)) immunoglobulin G (IgG) (1 h each). Microglial cells were treated for 1 h with PBS containing 1% BSA and labelled with a mouse

anti-iNOS (1/100; NOS2 (C-11): sc-7271; SCB) antibody, a mouse monoclonal anti-arginase I (1/100; 610708; BD Biosciences, San Jose, CA, USA) antibody or a rabbit polyclonal anti-Ki-67 (1/100; ab15580; Abcam, Cambridge, UK) antibody, and subsequently treated with a Cy3-conjugated anti-rabbit (1/200; 711-165-152; Jackson ImmunoResearch (red), West Grove, PA, USA) or anti-mouse (1/200; 715-166-150; Jackson ImmunoResearch (red), West Grove, PA, USA) IgG secondary antibodies (1 h each). The nuclei were stained with Hoechst (1/100; Sigma Aldrich, St. Louis, MO, USA). The samples were washed several times and mounted with 30% Mowiol (Calbiochem, San Diego, CA, USA). The images were obtained in a Leica SP2 confocal microscope (Leica Microsystems). The instrument was equipped with an apochromatic 63X oil-immersion objective (N.A. 1.4), and 488 nm and 561 nm laser lines.

2.6. Bioluminescence Resonance Energy Transfer (BRET) Assays

For the BRET assays, the HEK-293T cells were transiently co-transfected with a constant amount of cDNAs encoding for GluN1-RLuc and GluN2 and with increasing amounts of cDNAs corresponding to A_{2A}R-YFP or caldendrin-YFP. Forty-eight hours post-transfection, the cell suspension was adjusted to 20 μg of protein using a Bradford assay kit (Bio-Rad, Munich, Germany) and BSA for standardization. To quantify the protein-YFP expression, fluorescence was read in a Mithras LB 940 (Berthold Technologies, Bad Wildbad, Germany) equipped with a high-energy xenon flash lamp, using a 10 nm bandwidth excitation filter at 485 nm reading. For BRET and BRET with bimolecular complementation (BiFLC) measurements, the readings were collected 1 min after the addition of 5 μM coelenterazine H (Molecular Probes, Eugene, OR, USA) using a Mithras LB 940, which allowed the integration of the signals detected in the short-wavelength filter at 485 nm and the long-wavelength filter at 530 nm. To quantify the protein-RLuc expression, luminescence readings were performed 10 min after the 5 μM coelenterazine H addition using a Mithras LB 940. The net BRET was defined as ((long-wavelength emission)/(short-wavelength emission)) − C_f, where C_f corresponds to ((long-wavelength emission)/(short-wavelength emission)) for the donor construct expressed alone in the same experiment. The GraphPad Prism software (San Diego, CA, USA) was used to fit the data. BRET is expressed as milli BRET units, mBU (net BRET × 1000).

2.7. Cyclic Adenylic Acid (cAMP) Determination

Two hours before initiating the experiment, culture medium for HEK-293T-transfected or primary neuronal or glial cells was exchanged by serum-starved DMEM medium. Then, the cells were detached, resuspended in a growing medium containing 50 μM zardaverine (Tocris Bioscience, Bristol, UK) and plated in 384-well microplates (2500 cells/well), pretreated (15 min) with the corresponding antagonists (SCH-58261 for A_{2A}R and MK-801 for NMDAR) or vehicle and stimulated with agonists (CGS-21680 for A_{2A}R and NMDA for NMDAR) (15 min) before adding 0.5 μM forskolin or vehicle (15 min). The readings were performed after a 1 h incubation (room temperature). Homogeneous time-resolved fluorescence energy transfer (HTRF) measures were performed using the Lance Ultra cAMP kit (PerkinElmer, Waltham, MA, USA). Fluorescence at 665 nm was analyzed on a PHERAstar Flagship microplate reader equipped with an HTRF optical module (BMG Lab technologies, Offenburg, Germany).

2.8. Extracellular Signal-Regulated Kinase (ERK) Phosphorylation Determination

To determine the ERK1/2 phosphorylation, 40,000 HEK-293T cells/well, 50,000 microglia cells/well or 50,000 neurons/well were plated in transparent 96-well microplates and kept in the incubator for 48 h (HEK-293T cells) or 12 days (microglia and neuronal culture cells). Two to four h before initiating the experiment, the medium was substituted for a serum-starved DMEM medium. Then, the cells were pre-treated at room temperature for 10 min with the specific antagonists (SCH-58261 for A_{2A}R and MK-801 for NMDAR) or vehicle in a serum-starved DMEM medium and stimulated for an additional 10 min with the specific agonists (CGS-21680 for A_{2A}R and *N*-methyl D-aspartate (NMDA) for NMDAR) or vehicle. The cells were then washed twice with cold PBS before the addition of a lysis buffer (20 min treatment in constant agitation). Subsequently, 10 μL of each supernatant was

placed in white ProxiPlate 384-well microplates and the ERK 1/2 phosphorylation was determined using the AlphaScreen®SureFire® kit (Perkin Elmer, Waltham, MA, USA) following the instructions of the supplier and using an EnSpire® Multimode Plate Reader (PerkinElmer, Waltham, MA, USA).

2.9. Assessment of Dynamic Mass Redistribution (DMR)

The cell mass redistribution induced upon receptor activation was detected by illuminating the underside of a biosensor with a polychromatic light and measuring the changes in the wavelength of the reflected monochromatic light that was a sensitive function of the index of refraction. The magnitude of this wavelength shift (in picometers) was directly proportional to the amount of DMR. HEK-293T cells and neuronal and microglial primary cultures were seeded in 384-well sensor microplates to obtain 70–80% confluent monolayers constituted of approximately 10,000 cells per well. Prior to the assay, the cells were washed twice and incubated for 2 h with assay buffer (Hank's balanced salt solution (HBSS) with 20 mM 4-(2-hydroxyethyl)-1-piperazineethanesulfonic acid (HEPES) buffer, pH 7.15) containing 0.1% DMSO (24 °C, 30 µL/well). Hereafter, the sensor plate was scanned and a baseline optical signature was recorded for 10 min before adding the 10 µL of the specific antagonists (SCH-58261 for A_{2A}R and MK-801 for NMDAR), that were recoded for 30 min followed by the addition of 10 µL of the specific agonists (CGS-21680 for A_{2A}R and NMDA for NMDAR); all the test compounds were dissolved in the assay buffer. The cell signaling signature was determined using an EnSpire® Multimode Plate Reader (PerkinElmer, Waltham, MA, USA) by a label-free technology. The results were analyzed using the EnSpire Workstation Software v 4.10.

2.10. Determination of Cytoplasmic Calcium Ion Level Increase

HEK-293T cells were transfected with the cDNAs for human A_{2A}R, for GCaMP6 calcium sensor, and/or for both the GluN1 and GluN2 subunits of the NMDAR [24]. Forty-eight hours after transfection, 150,000 HEK-293T cells/well were plated in 96-well black, clear bottom microtiter plates and were incubated with Mg^{2+}-free Locke's buffer (154 mM NaCl, 5.6 mM KCl, 3.6 mM $NaHCO_3$, 2.3 mM $CaCl_2$, 5.6 mM glucose and 5 mM HEPES, pH 7.4) supplemented with 10 µM glycine. The cells were treated with the specific antagonists (SCH-58261 for A_{2A}R and MK-801 for NMDAR) for 10 min, followed by the addition of the receptor agonists, CGS-21680 for A_{2A}R and NMDA for NMDAR, just a few seconds before the readings. The fluorescence emission intensity of the GCaMP6 was recorded at 515 nm upon excitation at 488 nm on the EnSpire® Multimode Plate Reader (PerkinElmer, Waltham, MA, USA) for 225 s every 5 s.

2.11. In Situ Proximity Ligation Assay (PLA)

PLA was performed with reagents from Sigma Aldrich and following the protocols of the supplier. In brief, microglial and neuronal primary cells grown on glass coverslips were fixed in 4% paraformaldehyde for 15 min, washed with PBS containing 20 mM glycine to quench the aldehyde groups, and permeabilized with the same buffer containing 0.05% Triton X-100 (15 min). After 1 h incubation at 37 °C with blocking solution, the cells were treated with specific antibodies against A_{2A} or NMDA receptors: mouse monoclonal anti-A_{2A}R (1/100, Millipore, Darmstadt, Germany) or rabbit polyclonal anti-GluN1 antibody (1/200, Millipore). The cells were processed using the PLA probes detecting mouse and rabbit antibodies (Duolink II PLA probe anti-rabbit plus and Duolink PLA probe anti-mouse minus; Sigma Aldrich) and were prepared with Hoechst (1/200; Sigma Aldrich, St. Louis, MO, USA) using a mounting medium. The images were obtained in a Leica SP2 confocal microscope (Leica Microsystems, Mannheim, Germany). For each field of view a stack of two channels (one per staining) and 3 to 4 Z stacks with a step size of 1 µm were acquired. The quantification of the cells containing one or more red spots versus the total cells (blue nucleus), and in cells containing spots, the ratio r (number of red spots/cell), were determined by the Duolink Image tool software (Sigma Aldrich, St. Louis, MO, USA).

2.12. Statistical Analysis

The data in the graphs are the mean ± SEM (n = 5, at least). The GraphPad Prism software version 7 (San Diego, CA, USA) was used for the data fitting and statistical analysis. The Kolmogorov-Smirnov test with the correction of Lilliefors was used to evaluate the normal distribution and the Levene test was used to evaluate the homogeneity of variance. A one-way ANOVA followed by the post-hoc Bonferroni's test were used when comparing multiple values. When a pair of values were compared, the Student's t test was used. Significant differences were considered when the p value was < 0.05.

3. Results

3.1. NMDA Receptors May Directly Interact with Adenosine A_{2A} Receptors

N-methyl-D-aspartate receptor (NMDAR) activation regulates synaptic plasticity and neuronal survival. However, an increase in the NMDAR activity is associated to excitotoxicity and cell death and this is the main reason it is targeted by one of the existing anti-AD drugs. On the other hand, adenosine is a neuromodulator and one of the main mediators is the A_{2A} receptor ($A_{2A}R$), which is expressed in both CNS neurons and glial cells. To address a potential interaction between the two receptors, we first performed immunocytochemical assays in a heterologous expression system. HEK-293T cells were transfected with cDNAs for $A_{2A}R$-RLuc or for GluN1 fused to RLuc and the GluN2B subunit of NMDAR (transfection of the two subunits was necessary for reconstituting a functional NMDA receptor). The membrane and cytoplasmic expression of both: A_{2A} and NMDA receptors was observed (Figure 1A). Then, colocalization was addressed in cells transfected with the cDNAs for $A_{2A}R$-YFP and for GluN1-RLuc and GluN2B subunits. The degree of colocalization was significant (Figure 1B) but while it demonstrated expression in the same compartment(s), it did not allow the discovery of direct protein–protein interaction. Accordingly, the A_{2A}-NMDA receptor interaction was assayed by bioluminescence resonance energy transfer (BRET) using HEK-293T cells expressing a reconstituted NMDAR fused to RLuc and increasing amounts of $A_{2A}R$-YFP. The saturable BRET curve indicated a specific interaction between the A_{2A} and the NMDA receptors ($BRET_{max}$ 141 ± 14 and $BRET_{50}$ 155 ± 22). As a negative control, the $A_{2A}R$ was substituted by the calcium sensor protein, caldendrin, and the result was a linear relationship that was indicative of unspecificity (Figure 1C). In summary $A_{2A}R$ may interact with NMDAR but not with caldendrin in living transiently transfected HEK-293T cells.

3.2. Functional Properties of A_{2A}-NMDA Receptor Heteromer Complex

Adenosine $A_{2A}R$ couple to G_s proteins, activating adenylate cyclase and increasing cAMP intracellular levels. In preliminary assays, we demonstrated that cytosolic cAMP levels increased when HEK-293T cells expressing $A_{2A}R$ were treated with the selective ligand, CGS-21680 (Supplementary Figure S1A). Furthermore, this effect was specific, because it was blocked by pre-treatment with the selective antagonist SCH-58261. Neither NMDA, nor a NMDAR antagonist, MK-801, induced any effect (Supplementary Figure S1A). Similar results were obtained in extracellular signal-regulated kinase (ERK) phosphorylation and label-free dynamic mass redistribution (DMR) assays (Supplementary Figure S1B,C). As expected, cytosolic calcium did not increase upon $A_{2A}R$ stimulation (Supplementary Figure S1A–D) but it did increase when HEK-293T cells were transfected with reconstituted NMDAR and treated with NMDA (Supplementary Figure S1A–H). Whereas the stimulation with NMDA did not alter the cytosolic cAMP levels (Supplementary Figure S1A–E), it induced MAPK phosphorylation and modified the DMR outputs. Although the effects were specific and blocked by a selective NMDAR antagonist, MK-801 (Supplementary Figure S1F,G), they were not altered by either a selective $A_{2A}R$ agonist, CGS-21680, or a selective $A_{2A}R$ antagonist, SCH-58261.

Once receptor-mediated signaling was characterized in the cells expressing $A_{2A}R$ or NMDAR receptors, cross-modulation was assayed in the co-transfected HEK-293T cells in which the cAMP levels, MAPK phosphorylation, label-free DMR and the calcium release signals were analyzed. Remarkably, the cAMP data revealed that the signal obtained after the $A_{2A}R$ stimulation was blocked by both $A_{2A}R$

and NMDAR antagonists (Figure 2A). Such a property is known as cross-antagonism and would be useful to identify A_{2A}-NMDA receptor complexes in natural sources. In fact, cross-antagonism is considered a heteromer print [25,26]. Coactivation of the A_{2A} and NMDA receptors led to a decrease in the CGS-21680-induced effect, indicating that the NMDAR activation impacted on adenosine A_{2A}R signaling. In the MAPK phosphorylation assays, the activation of both A_{2A} and NMDA receptors were able to activate the MAPK pathway. In addition, whereas the A_{2A}R-mediated signaling was smaller when the two receptors were co-expressed, the NMDAR-mediated signaling was stronger. This result indicated a possible potentiation of A_{2A}R over the NMDAR signaling when forming the A_{2A}-NMDA receptor complexes. However, the coactivation of both receptors did not result in an additive effect. It is noteworthy that any signal was counteracted by either the NMDAR or A_{2A}R selective antagonists, i.e., cross-antagonism was also detected. (Figure 2B). DMR data were similar to those found in cAMP and MAPK assays. The A_{2A}R- and NMDAR-agonist-induced signals were blocked by both the NMDAR and A_{2A}R selective antagonists, while the coactivation of both receptors produced a stronger signal than that of the NMDA but smaller than that of the A_{2A}R agonist. Finally, in terms of calcium mobilization, the coactivation of both receptors produced a similar effect to that induced by the NMDAR stimulation but interestingly, the NMDA effect was blocked by both NMDA and A_{2A} receptor antagonists (A_{2A} receptor agonists did not yet induce cytosolic calcium increases) (Figure 2D). The results may be explained by i) the A_{2A}R expression increasing the NMDAR function and ii) the NMDAR activation blocking adenosine A_{2A}R signaling and iii) a cross-antagonism due to inter-protomer allosteric communication within the A_{2A}R and NMDAR heteromer.

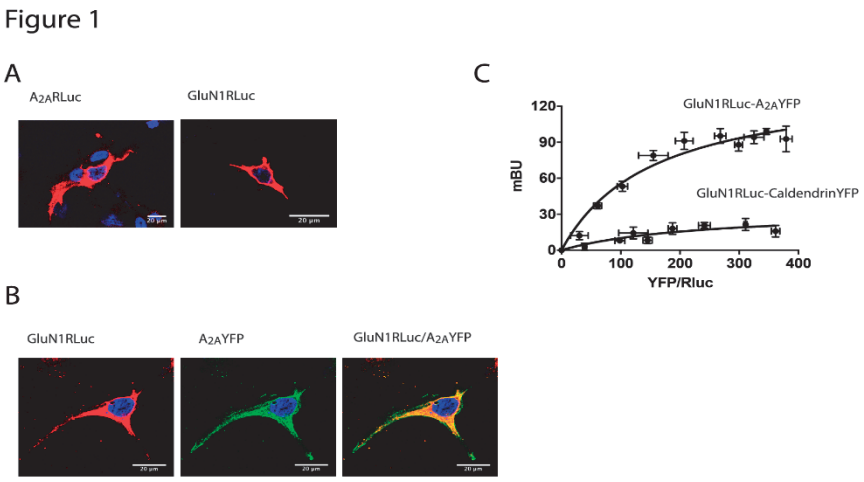

Figure 1. The *N*-methyl D-aspartate (NMDA) and the adenosine A_{2A} receptors interact to form heteromeric complexes. In (**A**,**B**), HEK-293T cells were transfected with 0.5 μg cDNA corresponding to the A_{2A} receptor (A_{2A}R)-*Renilla* luciferase (RLuc) (**A left**) or 0.5 μg cDNA corresponding to the GluN1-RLuc in the presence of 0.3 μg cDNA corresponding to GluN2 (**A right**) or co-transfected with 0.4 μg cDNA for A_{2A}R-yellow fluorescent protein (YFP) and 0.4 μg cDNA corresponding to the GluN1-RLuc in the presence of 0.25 μg cDNA corresponding to the GluN2 (**B**). Confocal microscopy images are shown. The receptors fused to RLuc were identified by immunocytochemistry (red) and the proteins fused to YFP were identified by its own fluorescence (green). Colocalization is shown in yellow in the merge image. Scale bar: 20 μm. In (**C**), the bioluminescence resonance energy transfer (BRET) saturation experiments were performed in HEK-293T cells transfected with 0.3 μg of cDNA corresponding to the GluN1-RLuc, 0.2 μg of cDNA corresponding to the GluN2 and increasing amounts of cDNA corresponding to A_{2A}R-YFP (0.1 μg to 0.5 μg) or caldendrin-YFP (0.1 μg to 0.7 μg) as a negative control. The relative amount of BRET is given as a function of 1000× the ratio between the fluorescence of the acceptor (YFP) and the luciferase activity of the donor (RLuc). BRET is expressed as milli BRET units (mBU) and is given as the mean ± SEM of 6 different experiments grouped as a function of the amount of BRET acceptor.

Figure 2

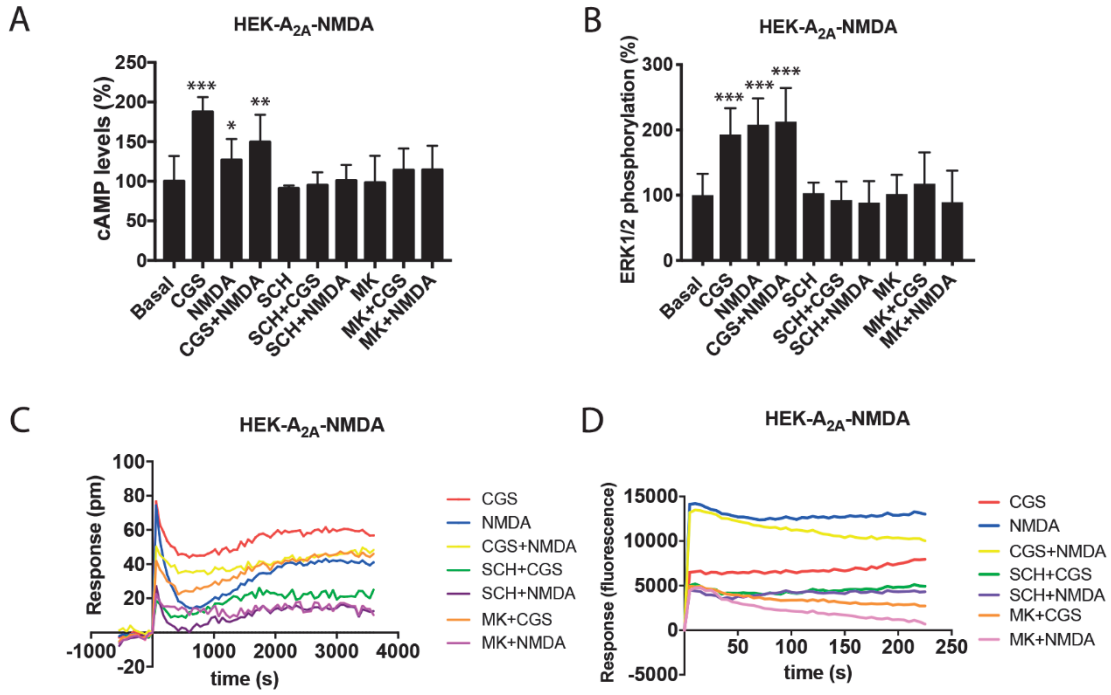

Figure 2. Functional characterization of the A_{2A}-NMDA receptor heteromer in HEK-293T cells. In (**A**) to (**D**), HEK-293T cells expressing $A_{2A}R$ (0.5 µg of cDNA), GluN1 (0.5 µg of cDNA) and GluN2 (0.5 µg of cDNA) (**A**–**C**) or expressing $A_{2A}R$ (0.5 µg of cDNA), GluN1 (0.5 µg of cDNA), GluN2 (0.5 µg of cDNA) and 6GCaMP calcium sensor (0.75 µg of cDNA) (**D**) were pre-incubated or not with 1 µM of the $A_{2A}R$ antagonist SCH-58261 (SCH) or with 1 µM of the NMDA antagonist, MK-801 (MK), followed by treatment with 100 nM of the $A_{2A}R$ agonist CGS-21680 (CGS), 15 µM of NMDA or both, and the cAMP levels (**A**), extracellular signal-regulated (ERK) 1/2 phosphorylation (**B**), representative traces of dynamic mass redistribution (DMR) (**C**) and the representative traces of intracellular Ca^{2+} responses over time (**D**) were determined. Values are the mean ± SEM of 10 to 12 different experiments. ERK 1/2 phosphorylation levels and cAMP increases are expressed as percentage over basal. A one-way ANOVA followed by a Bonferroni multiple comparison post-hoc test showed a significant effect over 100% (* $p < 0.05$, ** $p < 0.01$, *** $p < 0.001$).

3.3. *A_{2A}-NMDA Receptor Heteromer Complex Expression in Resting and Activated Microglia*

Due to the renowned interest in glial cells as targets to combat neurodegenerative diseases and due to the expression of both receptors in these cells, we next analyzed the A_{2A}-NMDA receptor complex expression in the microglial primary cultures from wild type mice. Interestingly, the proximity ligation assay (PLA) showed 23% of cells with clusters of receptor complexes depicted as red dots (two red dots per cell) (Figure 3A,B). Moreover, when the microglia was activated using LPS and IFN-γ, the $A_{2A}R$-NMDAR heteromer expression was markedly enhanced, with 92% of cells showing red dots and an eight-fold increase in dots/cell (16 dots in activated cells versus two in resting cells) (Figure 3A,B). Similar assays were performed in hippocampal neuronal primary cultures; 28% of neurons showed red dots. Overall, these results showed that the A_{2A}-NMDA receptor complexes may play a relevant role in activated microglia cells.

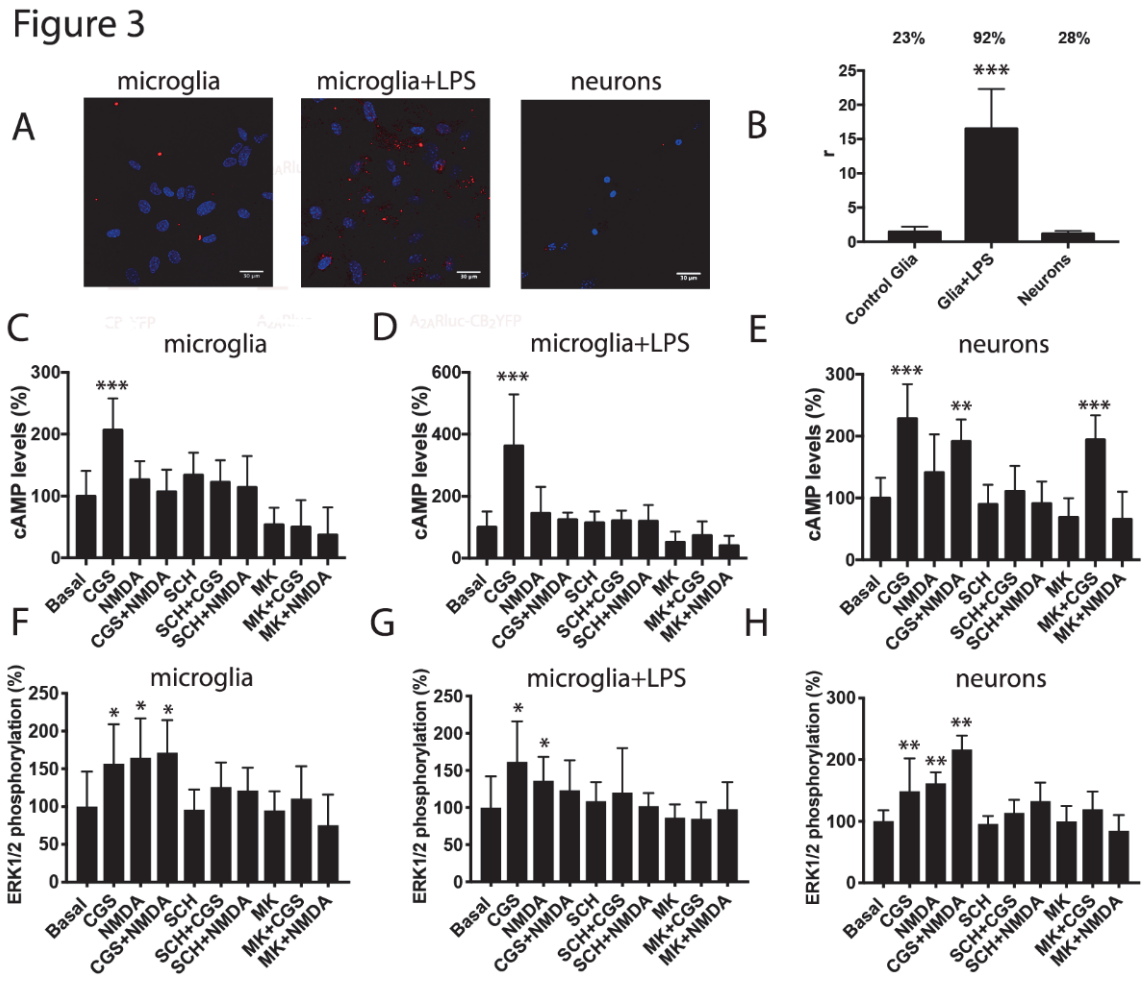

Figure 3. Expression and functionality of the A_{2A} and NMDA receptors heteromers in the microglial and neuronal primary cultures. Panels (**A**,**B**). The proximity ligation assay (PLA) was performed in mice microglial primary cultures treated or not with 1 μM lipopolysaccharide (LPS) and 200 U/mL interferon-γ (IFN-γ) to activate the microglia and in the mice hippocampal primary cultures of neurons using the primary antibodies specific for the A_{2A} and NMDA receptors. In all cases, the cell nuclei were stained with Hoechst (blue). The confocal microscopy images are shown (superimposed sections) in which heteromers appear as red clusters (in neurons or microglia). Scale bars = 30 μm. The bar graph (**B**) shows the number of the red dots/cell (r) and the numbers above the bars indicate the percentage of cells presenting red dots. Values are the mean ± SEM (n = 8). A one-way ANOVA followed by Bonferroni's multiple comparison post-hoc test were used for statistical analysis (*** $p < 0.001$, versus control -resting- microglia). Panels (**C**–**H**) display the microglial primary cultures treated (**D**,**G**) or not (**C**,**F**) with 1 μM LPS and 200 U/mL IFN-γ and the mice hippocampal primary cultures of the neurons (**E**,**H**) that were pre-incubated or not with 1 μM of the A_{2A}R antagonist SCH-58261 (SCH) or with 1 μM of the NMDAR antagonist MK-801 (MK) followed by treatment with 100 nM of the A_{2A}R agonist CGS-21680 (CGS), 15 μM NMDA or both, and the cAMP levels (**C**–**E**) and ERK 1/2 phosphorylation signal (**F**–**H**) were determined. The values are the mean ± SEM of 10 to 12 different experiments. The ERK 1/2 phosphorylation levels and cAMP increases were expressed as a percentage over basal. A one-way ANOVA followed by a Bonferroni multiple comparison post-hoc test showed a significant effect over 100% (* $p < 0.05$, ** $p < 0.01$, *** $p < 0.001$).

The functional cross-talk was assayed by the analysis of the cAMP intracellular levels in the microglia cells and in neurons. In both, the resting and the activated microglia, only the activation of the A_{2A}R results in cAMP responses, that were reverted by the A_{2A}R antagonist and by the NMDAR antagonist. We observed similar results in neurons but without cross-antagonism, probably reflecting

that not all NMDA receptors were interacting with the $A_{2A}R$ (Figure 3C–E). The activation of either the NMDAR or the $A_{2A}R$ resulted in the MAPK pathway activation. Interestingly, coactivation led to a small non additive effect only in microglia cultures, once more supporting the idea that not all NMDA receptors in neurons were interacting with the $A_{2A}R$. However, cross-antagonism was detected in both the microglial and neuronal cells (Figure 3F–H).

3.4. A_{2A}R-NMDAR Heteromer Expression is Elevated in Primary Microglia from $APP_{Sw/Ind}$ Mice

Alzheimer's disease (AD) is one of the most prevalent neurodegenerative diseases worldwide; the causes are unknown and current drugs have little efficacy. NMDAR function is enhanced in the initial stages of AD, thus leading to altered intracellular calcium handling and the gradual loss of synaptic function [27,28]. In addition, $A_{2A}R$ expression markedly increases in neurodegenerative diseases with an inflammatory component. Accordingly, we moved to assess the expression of $A_{2A}R$-NMDAR heteromers in a transgenic AD mouse model.

We first analyzed the expression of A_{2A}-NMDA receptor complexes in the primary cultures of microglia and neurons from the hippocampus of $APP_{Sw,Ind}$ mice. The hippocampal microglia and neuronal primary cultures were obtained from two-day-old pups or 19-day-old fetuses, respectively, and were independently cultured. PLA data analysis was blindly done before knowing the genotyping results. Remarkably, whereas 29% of the cultured microglia from the controls animals showed red dots, the percentage of cells from transgenic animals was 75% (three dots/cell in control versus six dots/cell in transgenic) (Figure 4A,B). The same assay type in neurons led to a low percentage of cells expressing receptor clusters (11% in control and 16% in transgenic) (Figure 4A,B). These results suggested that microglia cells were resting in control animals and activated in AD-mice.

After determining the occurrence of A_{2A}-NMDA receptor complexes in microglia primary cultures, we moved to characterize the activated microglia phenotype in the $APP_{Sw,Ind}$ mice model. When microglia cells are activated, they can evolve showing different characteristics, with two opposite phenotypes: M1 microglia inducing a pro-inflammatory state and cytotoxic effects and M2 microglia inducing an anti-inflammatory state and neuroprotective effects. Then, the microglia primary cultures of the control and $APP_{Sw,Ind}$ mice models were prepared and analyzed by immunocytochemistry. Through the analysis, an important increase in inducible nitric oxide synthase (iNOS) a marker of the M1 phenotype, was observed in microglia from $APP_{Sw,Ind}$ mice compared to controls (Figure 4C,D). Moreover, fluorescence signal quantitation indicated an important increase in arginase-1 (Arg-1), a marker of the M2 phenotype, in $APP_{Sw,Ind}$ –derived microglia (Figure 4C,D). These results indicated an important increase in both M1 and M2 microglia in the AD-mice model. Interestingly, when the same assay was repeated by pretreating the $APP_{Sw,Ind}$-derived cultures for one week with the $A_{2A}R$ antagonist SCH-58261, a significant decrease in iNOS and a small but significant increase in Arg-1 fluorescence were observed, indicating that $A_{2A}R$ antagonists skew activated microglia towards the neuroprotective M2 phenotype.

Then, no alteration in microglia proliferation marker was observed upon analysis of the Ki-67 fluorescence signal in the $APP_{Sw,Ind}$ mice models treated or not with SCH-58261 and control (WT) animals (Figure 4C,D).

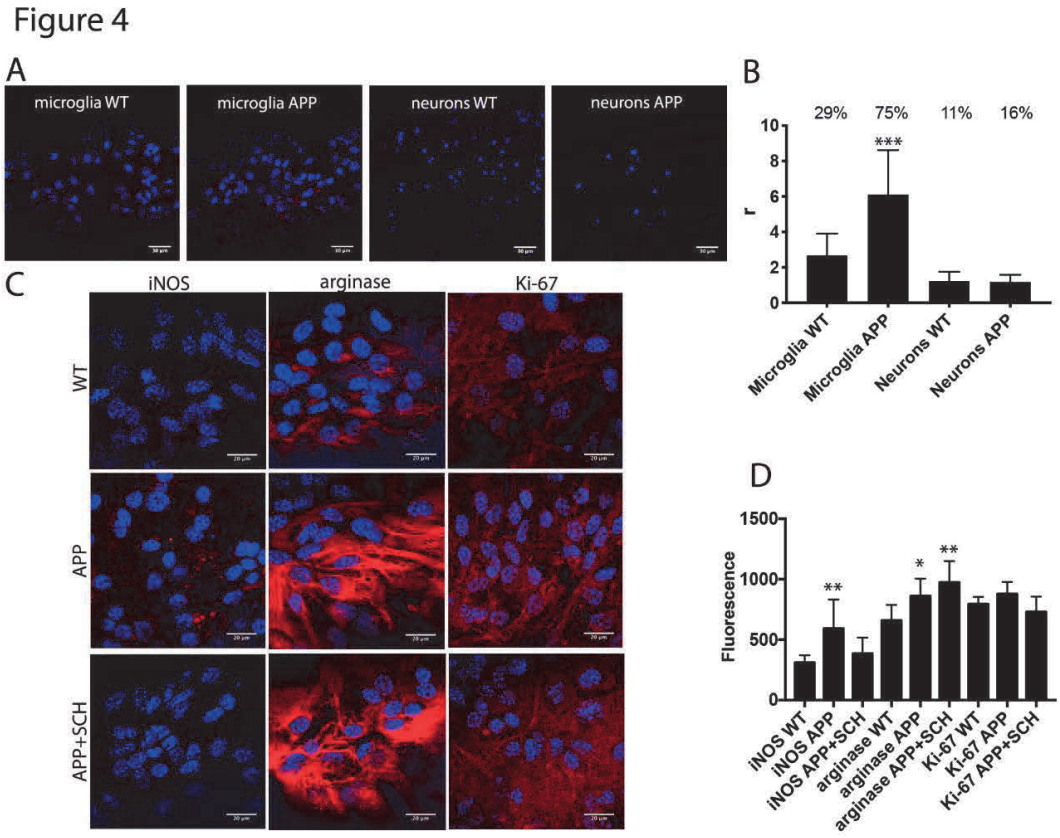

Figure 4. Microglial markers in primary cultures from $APP_{Sw,Ind}$ mice. In (**A,B**), proximity ligation assays (PLAs) were performed in microglial and in the hippocampus neuronal primary cultures of control (WT) and $APP_{Sw,Ind}$ mice using primary antibodies specific for A_{2A} and NMDA receptors. In all cases, the cell nuclei were stained with Hoechst (blue). The confocal microscopy images are shown (superimposed sections) in which the heteromers appear as red clusters (in neurons or microglia). Scale bars = 30 μm (neurons and microglia). The bar graph (**B**) shows the number of red dots/cell (r) and the numbers above the bars indicate the percentage of cells presenting red dots. Values are the mean ± SEM (n = 6). A one-way ANOVA followed by Bonferroni's multiple comparison post-hoc test were used for statistical analysis (*** $p < 0.001$, versus WT -control-). In (**C**,**D**), immunocytochemical assays were performed in the primary cultures of microglia $APP_{Sw,Ind}$ mice or control (WT) animals pretreated or not for one week with the $A_{2A}R$ antagonist SCH-58261. The staining was performed using the antibodies that detected either arginase-1 marker, the antiproliferation cell protein Ki-67 or nitric oxide synthase and a Cy3-conjugated secondary antibody (red). The fluorescence was quantified in all the panels using the Fiji program and normalization by cell number. Representative images in all conditions are shown in (**C**). A one-way ANOVA followed by Bonferroni's multiple comparison post-hoc test were used for statistical analysis (* $p < 0.05$, ** $p < 0.01$; versus WT).

3.5. $A_{2A}R$ Activation Negatively Modulates NMDA Receptor Signaling in Microglia but it Increases NMDAR Signaling in Neurons from $APP_{Sw,Ind}$ Mice

To analyze the adenosine regulatory effects over NMDAR functionality in the AD model, primary cultures of microglia and neurons were prepared from the hippocampus of $APP_{Sw,Ind}$ mice and control animals. Intracellular cAMP levels, ERK1/2 phosphorylation and DMR were determined upon receptor activation and coactivation.

On the one hand, $A_{2A}R$ activation led to an increase in cAMP levels in the neurons and microglia from control and transgenic animals. As expected, NMDA did not modify cAMP levels but counteracted the action of $A_{2A}R$ agonists. In addition, the selective NMDAR antagonist reverted the effect of CGS-21680 (cross-antagonism) (Figure 5A–D). The MAPK pathway activation was similar

in microglia from control and transgenic animals, with a similar effect in the individual activation or the coactivation of receptors. In these cells, bidirectional cross-antagonism was found (Figure 5E,F). In neurons coactivation led to a more robust effect than individual treatments. We found a partial cross-antagonism that fits with the hypothesis that, in neurons, not all NMDAR are directly interacting with the $A_{2A}R$ (Figure 5G,H). DMR recordings in glial cells were only obtained upon $A_{2A}R$ activation with NMDA being ineffective and with a lack or a small cross-antagonism. A relevant finding was underscored using neurons, because those from the control animals were much less responsive to CGS-21680 than those from the transgenic animals. Moreover, NMDA also induced a robust response in the cells from transgenic animals; however, coactivation did not lead to synergism or additive effects (Figure 5I–L).

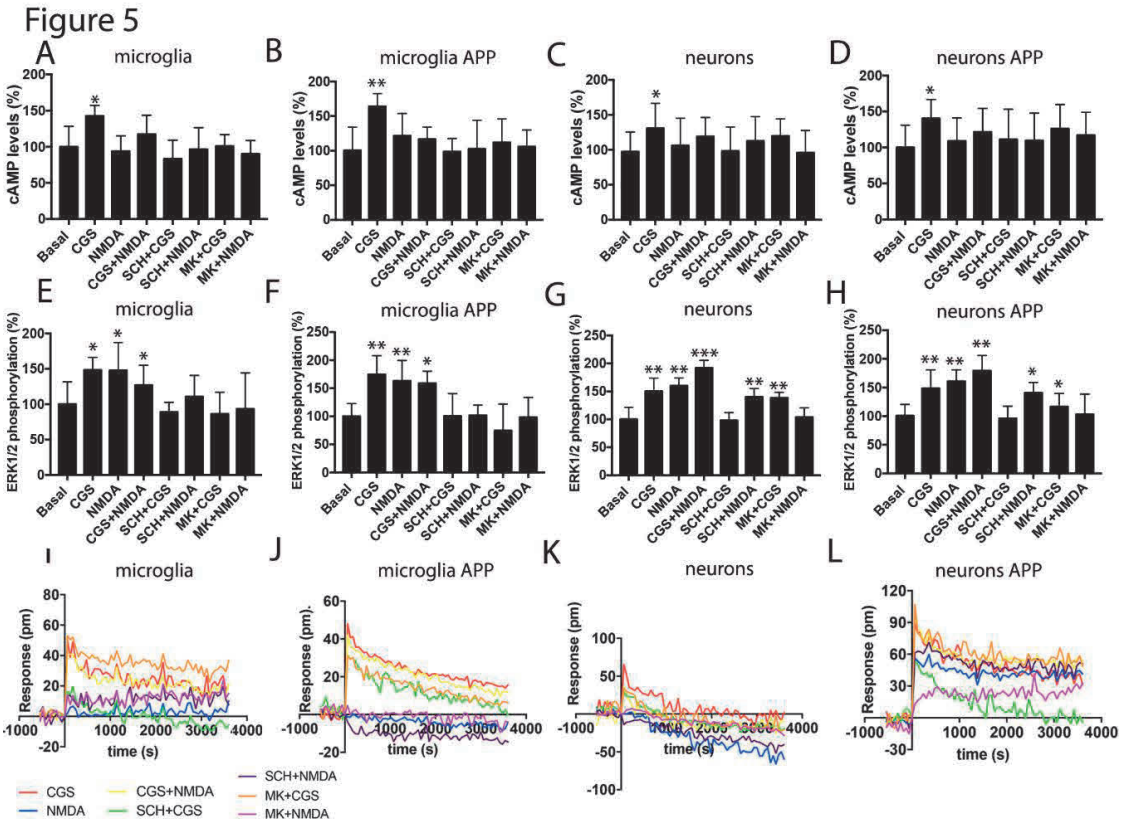

Figure 5. Functionality of the A_{2A}-NMDA receptor heteromer in the $APP_{Sw,Ind}$ mice model of Alzheimer's disease(AD). In (**A**–**L**), the microglial and neuronal primary cultures from the hippocampus of the WT and $APP_{Sw,Ind}$ mice (**E**,**H**) were pre-incubated with vehicle, 1 μM of the $A_{2A}R$ antagonist SCH-58261 (SCH) or 1 μM of the NMDAR antagonist, MK-801 (MK), followed by treatment with 100 nM of the $A_{2A}R$ agonist CGS-21680 (CGS), 15 μM NMDA or both, and the cAMP levels (**A**–**D**), ERK 1/2 phosphorylation signal (**E**–**H**) and the representative traces of dynamic mass redistribution (DMR) over time (**I**–**L**) were determined. Values are the mean ± SEM of 10 to 12 different experiments. ERK 1/2 phosphorylation levels and cAMP increases are expressed as percentage over basal. A one-way ANOVA followed by a Bonferroni multiple comparison post-hoc test showed a significant effect over basal (* $p < 0.05$, ** $p < 0.01$, *** $p < 0.001$).

4. Discussion

Adenosine A_1 and A_{2A} receptors have deserved attention as potential targets to prevent neurodegeneration [29]. NMDA-induced preconditioning studies have led to controversial results on the usefulness of agonists or antagonists of the A_1 receptors to afford neuroprotection (see [30] and references therein). In contrast, there is a consensus on the safety and the neuroprotective potential of the A_{2A} receptor antagonists. Pharmacological studies in parkinsonian models, the dopamine/adenosine

antagonism and the use of knock-out mice reinforced the view that targeting the $A_{2A}R$ in striatal neurons could be useful in the therapy of Parkinson's disease [31–36]. All the experimental effort plus drug discovery programs in pharmaceutical companies have led to the approval of istradefylline, a selective $A_{2A}R$ antagonist, for the therapy of Parkinson's disease in Japan and the US [6–8].

Evidence on the possibility of targeting $A_{2A}R$ for combating dementia-related neurodegeneration has come from different sides and is consistent in both cell and animal models. Early synaptic deficits in the APP/PS1 mouse model of Alzheimer's disease involved neuronal adenosine $A_{2A}R$ [37]. Electrophysiological studies in CA1 pyramidal neurons showed that the activation of those adenosine receptors enhanced chemically evoked NMDAR currents [38]. In an early β-amyloid-based AD model, adenosine production from ATP release was detrimental for cognition but not in the knock-out $A_{2A}R$ mouse [39]. Classically, the $A_{2A}R$ in neurons has been the focus in AD-related research. Another recent example is the involvement of the neuronal receptor in the memory deficits and synaptic loss in a tauopathy mouse model. Previously, it was demonstrated that receptor gene deletion was neuroprotective in the tauopathy model [12,40]. Remarkably, the A_{2A} receptor has a relevant function in activated microglia, which was found surrounding the pathological hallmarks of AD [41,42]. The activation of microglial $A_{2A}R$ enhances the production of proinflammatory mediators [43]. These results fit with the finding that the blockade of the microglial receptor reduces neuroinflammation and more importantly, may lead to an improvement of cognitive impairment [44]. Cunha and collaborators have compiled in different reviews the potential of targeting $A_{2A}R$ in both neurons and microglia to combat cognition and/or neurodegeneration in Alzheimer's disease and other age-related dementias [45,46]. Coincidentally, it is well accepted that the most consumed adenosine receptor antagonists, caffeine in coffee and theophylline in tea, do protect against suffering from Alzheimer's disease [47].

Our results show that further to the blockade of classical signaling mediated G_s-coupled GPCRs, $A_{2A}R$ antagonists have the potential to combat AD by impacting one of the most relevant pathophysiological molecular mechanisms, namely modulation of NMDAR function. The early studies showing neuroprotection via adenosine impacting on NMDA-mediated effects [9] were never attributed to a direct interaction between adenosine and NMDA receptors. We here identified A_{2A}-NMDA receptor complexes with particular properties. Unlike GPCRs that are prone to form complexes containing two different receptors, few examples of direct interactions between metabotropic (GPCR) and ionotropic receptors have been reported, probably due to lack of ad hoc assays. Interestingly, the cross-antagonism here detected for the $A_{2A}R$-NMDAR couple was often found in GPCR-GPCR complexes; when cross antagonism is actually detected, GPCR-GPCR heteromer formation is suspected [25,26,48]. As further discussed below, the impairment of NMDAR function by $A_{2A}R$ antagonists is an attractive possibility to afford neuroprotection in AD.

The assessment of receptor complex expression led to various relevant findings. On the one hand, the expression in activated microglia was markedly higher than in resting microglia. Moreover, the expression in the microglia from the $APP_{Sw,Ind}$ was higher than that in the microglia from the control mice. These results agree with a different phenotype of microglia in these transgenic AD models and reinforces the hypothesis that microglia from the $APP_{Sw,Ind}$ protect neurons as the cognitive impairment only appears several months after birth [49]. On the other hand, complexes were also expressed in hippocampal neurons although the expression was similar in transgenic and control mice. By combining the expression data with the signaling results, it seems that the amount of $A_{2A}R$-NMDAR interactions was comparatively higher in the microglia than in neurons and that there were a significant number of NMDAR in hippocampal neurons that were not interacting with the $A_{2A}R$. The latter does not imply a lack of functional $A_{2A}R$-NMDAR interactions but that both direct allosteric modulations within the macromolecular complex as well as indirect interactions, i.e., via cross-talk between second messengers, like Ca^{2+}, impacting on the cAMP-PKA pathway.

As pointed out in the introduction, we undertook this investigation to find indirect ways to modulate the overactivity of the NMDAR. At least in part, neuronal death in AD (and in other

neurodegenerative diseases) is due to excitotoxicity, i.e., by excess of glutamate that in turn results in the exacerbation of NMAR functionality [50]. Unfortunately, full blockade of the NMDAR is not feasible as it is fundamental for neural cell viability, while the current NMDAR allosteric modulators are not showing significant efficacy in either AD patients nor neuroprotection. Hence, current attempts to prevent neuronal death in AD should target either neurons, which are already altered, or glial cells surrounding "suffering" neurons. In our opinion, the results in this paper plus the literature data on neuroprotection by targeting the $A_{2A}R$ (see [29,51] for review) reinforces the hypothesis that $A_{2A}R$ antagonists could modulate glutamatergic action in AD and afford neuroprotection.

Supplementary Materials: The following are available online at http://www.mdpi.com/2073-4409/9/5/1075/s1, Figure S1: Functional signaling of A_{2A} and NMDA receptors in HEK-293T cells.

Author Contributions: Conceptualization, R.F. and G.N.; data curation, G.N.; formal analysis, G.N.; funding acquisition, R.F., C.A.S. and G.N.; investigation, R.R.-S., M.C. and A.L.; resources, C.A.S.; supervision, R.F., C.A.S. and G.N.; writing—original draft, R.F. and G.N.; writing—review and editing, R.R.-S., M.C., A.L. and C.A.S. All authors have read and agreed to the published version of the manuscript.

Funding: This work was partially supported by the AARFD-17-503612 grant from the US Alzheimer's Association and by grants from the Spanish Ministry of Economy and Competitiveness (BFU2015-64405-R, SAF2016-80027-R, SAF2017-84117-R, and PID2019-109240RB-I00 and RTI2018-094204-B-I00; they may include FEDER funds).

Conflicts of Interest: Authors declare no conflict of interest.

References

1. Lipton, S. Pathologically-Activated Therapeutics for Neuroprotection: Mechanism of NMDA Receptor Block by Memantine and S-Nitrosylation. *Curr. Drug Targets* **2007**, *8*, 261–632. [CrossRef] [PubMed]
2. Lipton, S.A. Paradigm shift in neuroprotection by NMDA receptor blockade: Memantine and beyond. *Nat. Rev. Drug Discov.* **2006**, *5*, 160–170. [CrossRef] [PubMed]
3. Parsons, C.G.; Stöffler, A.; Danysz, W. Memantine: A NMDA receptor antagonist that improves memory by restoration of homeostasis in the glutamatergic system-too little activation is bad, too much is even worse. *Neuropharmacology* **2007**, *53*, 699–723. [CrossRef]
4. Kisby, B.; Jarrell, J.T.; Agar, M.E.; Cohen, D.S.; Rosin, E.R.; Cahill, C.M.; Rogers, J.T.; Huang, X. Alzheimer's Disease and Its Potential Alternative Therapeutics. *J. Alzheimer's Dis. Park.* **2019**, *9*, 477. [CrossRef]
5. Rosin, D.L.; Robeva, A.; Woodard, R.L.; Guyenet, P.G.; Linden, J. Immunohistochemical Localization of Adenosine A 2A Receptors in the Rat Central Nervous System. *J. Comp. Neurol.* **1998**, *401*, 163–186. [CrossRef]
6. Kondo, T.; Mizuno, Y. Japanese Istradefylline Study Group A long-term study of istradefylline safety and efficacy in patients with Parkinson disease. *Clin. Neuropharmacol.* **2015**, *38*, 41–46. [CrossRef]
7. Saki, M.; Yamada, K.; Koshimura, E.; Sasaki, K.; Kanda, T. In vitro pharmacological profile of the A2A receptor antagonist istradefylline. *Naunyn. Schmiedebergs. Arch. Pharmacol.* **2013**, *386*, 963–972. [CrossRef]
8. Mizuno, Y.; Kondo, T. Adenosine A2A receptor antagonist istradefylline reduces daily OFF time in Parkinson's disease. *Mov. Disord.* **2013**, *28*, 1138–1141. [CrossRef]
9. Schubert, P.; Kreutzberg, G.W. Cerebral protection by adenosine. *Acta Neurochir. Suppl.* **1993**, *57*, 80–88.
10. Franco, R.; Reyes-Resina, I.; Aguinaga, D.; Lillo, A.; Jiménez, J.; Raïch, I.; Borroto-Escuela, D.O.; Ferreiro-Vera, C.; Canela, E.I.; Sánchez de Medina, V.; et al. Potentiation of cannabinoid signaling in microglia by adenosine A2A receptor antagonists. *Glia* **2019**, *67*, 2410–2423. [CrossRef]
11. Gussago, C.; Arosio, B.; Casati, M.; Ferri, E.; Gualandris, F.; Tedone, E.; Nicolini, P.; Rossi, P.D.; Abbate, C.; Mari, D. Different adenosine A2A receptor expression in peripheral cells from elderly patients with vascular dementia and Alzheimer's disease. *J. Alzheimer's Dis.* **2014**, *40*, 45–49. [CrossRef] [PubMed]
12. Laurent, C.; Burnouf, S.; Ferry, B.; Batalha, V.L.; Coelho, J.E.; Baqi, Y.; Malik, E.; Mariciniak, E.; Parrot, S.; Van Der Jeugd, A.; et al. A2A adenosine receptor deletion is protective in a mouse model of Tauopathy. *Mol. Psychiatry* **2016**, *21*, 97–107. [CrossRef] [PubMed]
13. Faivre, E.; Coelho, J.E.; Zornbach, K.; Malik, E.; Baqi, Y.; Schneider, M.; Cellai, L.; Carvalho, K.; Sebda, S.; Figeac, M.; et al. Beneficial Effect of a Selective Adenosine A2A Receptor Antagonist in the APPswe/PS1dE9 Mouse Model of Alzheimer's Disease. *Front. Mol. Neurosci.* **2018**, *11*, 235. [CrossRef] [PubMed]

14. Temido-Ferreira, M.; Ferreira, D.G.; Batalha, V.L.; Marques-Morgado, I.; Coelho, J.E.; Pereira, P.; Gomes, R.; Pinto, A.; Carvalho, S.; Canas, P.M.; et al. Age-related shift in LTD is dependent on neuronal adenosine A2A receptors interplay with mGluR5 and NMDA receptors. *Mol. Psychiatry* **2018**, 1–25. [CrossRef]
15. Silva, A.C.; Lemos, C.; Gonçalves, F.Q.; Pliássova, A.V.; Machado, N.J.; Silva, H.B.; Canas, P.M.; Cunha, R.A.; Lopes, J.P.; Agostinho, P. Blockade of adenosine A2A receptors recovers early deficits of memory and plasticity in the triple transgenic mouse model of Alzheimer's disease. *Neurobiol. Dis.* **2018**, *117*, 72–81. [CrossRef]
16. Streit, W.J.; Kreutzberg, G.W. Lectin binding by resting and reactive microglia. *J. Neurocytol.* **1987**, *16*, 249–260. [CrossRef]
17. Streit, W.J. Microglia and neuroprotection: Implications for Alzheimer's disease. *Brain Res. Brain Res. Rev.* **2005**, *48*, 234–239. [CrossRef]
18. Wendt, S.; Wogram, E.; Korvers, L.; Kettenmann, H. Experimental cortical spreading depression induces NMDA receptor dependent potassium currents in microglia. *J. Neurosci.* **2016**, *36*, 6165–6174. [CrossRef]
19. Wu, Q.; Zhao, Y.; Chen, X.; Zhu, M.; Miao, C. Propofol attenuates BV2 microglia inflammation via NMDA receptor inhibition. *Can. J. Physiol. Pharmacol.* **2018**, *96*, 241–248. [CrossRef]
20. Mucke, L.; Masliah, E.; Yu, G.Q.; Mallory, M.; Rockenstein, E.M.; Tatsuno, G.; Hu, K.; Kholodenko, D.; Johnson-Wood, K.; McConlogue, L. High-level neuronal expression of abeta 1-42 in wild-type human amyloid protein precursor transgenic mice: Synaptotoxicity without plaque formation. *J. Neurosci.* **2000**, *20*, 4050–4058. [CrossRef]
21. Martínez-Pinilla, E.; Rodríguez-Pérez, A.I.I.; Navarro, G.; Aguinaga, D.; Moreno, E.; Lanciego, J.L.L.; Labandeira-García, J.L.L.; Franco, R. Dopamine D2 and angiotensin II type 1 receptors form functional heteromers in rat striatum. *Biochem. Pharmacol.* **2015**, *96*, 131–142. [CrossRef]
22. Newell, E.; Exo, J.; Verrier, J.; Jackson, T.; Gillespie, D.; Janesko-Feldman, K.; Kochanek, P.; Jackson, E. 2′,3′-cAMP, 3′-AMP, 2′-AMP and adenosine inhibit TNF-α and CXCL10 production from activated primary murine microglia via A2A receptors. *Brain Res.* **2015**, *1594*, 27–35. [CrossRef] [PubMed]
23. Hradsky, J.; Mikhaylova, M.; Karpova, A.; Kreutz, M.R.; Zuschratter, W. Super-resolution microscopy of the neuronal calcium-binding proteins Calneuron-1 and Caldendrin. *Methods Mol. Biol.* **2013**, *963*, 147–169. [PubMed]
24. Chen, T.-W.; Wardill, T.J.; Sun, Y.; Pulver, S.R.; Renninger, S.L.; Baohan, A.; Schreiter, E.R.; Kerr, R.A.; Orger, M.B.; Jayaraman, V.; et al. Ultrasensitive fluorescent proteins for imaging neuronal activity. *Nature* **2013**, *499*, 295–300. [CrossRef] [PubMed]
25. Ferré, S.; Baler, R.; Bouvier, M.; Caron, M.G.; Devi, L.A.; Durroux, T.; Fuxe, K.; George, S.R.; Javitch, J.A.; Lohse, M.J.; et al. Building a new conceptual framework for receptor heteromers. *Nat. Chem. Biol.* **2009**, *5*, 131–134. [CrossRef]
26. Franco, R.; Martínez-Pinilla, E.; Lanciego, J.L.; Navarro, G. Basic Pharmacological and Structural Evidence for Class A G-Protein-Coupled Receptor Heteromerization. *Front. Pharmacol.* **2016**, *7*, 76. [CrossRef]
27. Paoletti, P.; Bellone, C.; Zhou, Q. NMDA receptor subunit diversity: Impact on receptor properties, synaptic plasticity and disease. *Nat. Rev. Neurosci.* **2013**, *14*, 383–400. [CrossRef] [PubMed]
28. Kodis, E.J.; Choi, S.; Swanson, E.; Ferreira, G.; Bloom, G.S. N-methyl-D-aspartate receptor–mediated calcium influx connects amyloid-β oligomers to ectopic neuronal cell cycle reentry in Alzheimer's disease. *Alzheimer's Dement.* **2018**, *14*, 1302–1312. [CrossRef]
29. Stockwell, J.; Jakova, E.; Cayabyab, F.S. Adenosine A1 and A2A Receptors in the Brain: Current Research and Their Role in Neurodegeneration. *Molecules* **2017**, *22*, 676. [CrossRef]
30. Constantino, L.C.; Pamplona, F.A.; Matheus, F.C.; Ludka, F.K.; Gomez-Soler, M.; Ciruela, F.; Boeck, C.R.; Prediger, R.D.; Tasca, C.I. Adenosine A1 receptor activation modulates N-methyl-d-aspartate (NMDA) preconditioning phenotype in the brain. *Behav. Brain Res.* **2015**, *282*, 103–110. [CrossRef]
31. Gui, L.; Duan, W.; Tian, H.; Li, C.; Zhu, J.; Chen, J.F.; Zheng, J. Adenosine A2Areceptor deficiency reduces striatal glutamate outflow and attenuates brain injury induced by transient focal cerebral ischemia in mice. *Brain Res.* **2009**, *1297*, 185–193. [CrossRef] [PubMed]
32. Schwarzschild, M.A.; Chen, J.-F.; Ascherio, A. Caffeinated clues and the promise of adenosine A(2A) antagonists in PD. *Neurology* **2002**, *58*, 1154–1160. [CrossRef] [PubMed]
33. Chen, J.-F. Adenosine receptor control of cognition in normal and disease. *Int. Rev. Neurobiol.* **2014**, *119*, 257–307. [PubMed]

34. Chen, J.-F.; Sonsalla, P.K.; Pedata, F.; Melani, A.; Domenici, M.R.; Popoli, P.; Geiger, J.; Lopes, L.V.; de Mendonça, A. Adenosine A2A receptors and brain injury: Broad spectrum of neuroprotection, multifaceted actions and "fine tuning" modulation. *Prog. Neurobiol.* **2007**, *83*, 310–331. [CrossRef]
35. Fuxe, K.; Ferré, S.; Canals, M.; Torvinen, M.; Terasmaa, A.; Marcellino, D.; Goldberg, S.R.; Staines, W.; Jacobsen, K.X.; Lluis, C.; et al. Adenosine A_{2A} and Dopamine D_2 Heteromeric Receptor Complexes and Their Function. *J. Mol. Neurosci.* **2005**, *26*, 209–220. [CrossRef]
36. Fuxe, K.; Ferré, S.; Genedani, S.; Franco, R.; Agnati, L.F. Adenosine receptor-dopamine receptor interactions in the basal ganglia and their relevance for brain function. *Physiol. Behav.* **2007**, *92*, 210–217. [CrossRef]
37. Da Silva, S.V.; Haberl, M.G.; Zhang, P.; Bethge, P.; Lemos, C.; Gonçalves, N.; Gorlewicz, A.; Malezieux, M.; Gonçalves, F.Q.; Grosjean, N.; et al. Early synaptic deficits in the APP/PS1 mouse model of Alzheimer's disease involve neuronal adenosine A2A receptors. *Nat. Commun.* **2016**, *7*, 11915. [CrossRef]
38. Mouro, F.M.; Rombo, D.M.; Dias, R.B.; Ribeiro, J.A.; Sebastião, A.M. Adenosine A2A receptors facilitate synaptic NMDA currents in CA1 pyramidal neurons. *Br. J. Pharmacol.* **2018**, *175*, 4386–4397. [CrossRef]
39. Gonçalves, F.Q.; Lopes, J.P.; Silva, H.B.; Lemos, C.; Silva, A.C.; Gonçalves, N.; Tomé, Â.R.; Ferreira, S.G.; Canas, P.M.; Rial, D.; et al. Synaptic and memory dysfunction in a β-amyloid model of early Alzheimer's disease depends on increased formation of ATP-derived extracellular adenosine. *Neurobiol. Dis.* **2019**, *132*. [CrossRef]
40. Carvalho, K.; Faivre, E.; Pietrowski, M.J.; Marques, X.; Gomez-Murcia, V.; Deleau, A.; Huin, V.; Hansen, J.N.; Kozlov, S.; Danis, C.; et al. Exacerbation of C1q dysregulation, synaptic loss and memory deficits in tau pathology linked to neuronal adenosine A2A receptor. *Brain* **2019**, *142*, 3636–3654. [CrossRef]
41. Angulo, E.; Casadó, V.; Mallol, J.; Canela, E.I.; Viñals, F.; Ferrer, I.; Lluis, C.; Franco, R. A1 adenosine receptors accumulate in neurodegenerative structures in Alzheimer disease and mediate both amyloid precursor protein processing and tau phosphorylation and translocation. *Brain Pathol.* **2003**, *13*, 440–451. [CrossRef] [PubMed]
42. Catafau, A.; Bullich, S. Non-Amyloid PET Imaging Biomarkers for Neurodegeneration: Focus on Tau, Alpha-Synuclein and Neuroinflammation. *Curr. Alzheimer Res.* **2016**, *14*, 169–177. [CrossRef] [PubMed]
43. Saura, J.; Angulo, E.; Ejarque, A.; Casado, V.; Tusell, J.M.; Moratalla, R.; Chen, J.-F.F.; Schwarzschild, M.A.; Lluis, C.; Franco, R.; et al. Adenosine A2A receptor stimulation potentiates nitric oxide release by activated microglia. *J. Neurochem.* **2005**, *95*, 919–929. [CrossRef]
44. Rebola, N.; Simões, A.P.; Canas, P.M.; Tomé, A.R.; Andrade, G.M.; Barry, C.E.; Agostinho, P.M.; Lynch, M.A.; Cunha, R.A. Adenosine A2A receptors control neuroinflammation and consequent hippocampal neuronal dysfunction. *J. Neurochem.* **2011**, *117*, 100–111. [CrossRef]
45. Cunha, R.A. *How Does Adenosine Control Neuronal Dysfunction and Neurodegeneration?* Blackwell Publishing Ltd.: Hoboken, NJ, USA, 2016; Volume 139, pp. 1019–1055.
46. Santiago, A.R.; Baptista, F.I.; Santos, P.F.; Cristóvão, G.; Ambrósio, A.F.; Cunha, R.A.; Gomes, C.A.; Pintor, J. Role of microglia adenosine A2A receptors in retinal and brain neurodegenerative diseases. *Mediat. Inflamm.* **2014**, *2014*, 465694. [CrossRef]
47. Eskelinen, M.H.; Kivipelto, M. Caffeine as a protective factor in dementia and Alzheimer's disease. *J. Alzheimer's Dis.* **2010**, *20*, S167–S174. [CrossRef]
48. Franco, R.; Aguinaga, D.; Jiménez, J.; Lillo, J.; Martínez-Pinilla, E.; Navarro, G. Biased receptor functionality versus biased agonism in G-protein-coupled receptors. *Biomol. Concepts* **2018**, *9*, 143–154. [CrossRef]
49. Navarro, G.; Borroto-Escuela, D.; Angelats, E.; Etayo, I.; Reyes-Resina, I.; Pulido-Salgado, M.; Rodríguez-Pérez, A.; Canela, E.; Saura, J.; Lanciego, J.L.; et al. Receptor-heteromer mediated regulation of endocannabinoid signaling in activated microglia. Role of CB1 and CB2 receptors and relevance for Alzheimer's disease and levodopa-induced dyskinesia. *Brain. Behav. Immun.* **2018**, *67*, 139–151. [CrossRef]
50. Lewerenz, J.; Maher, P. Chronic glutamate toxicity in neurodegenerative diseases-What is the evidence? *Front. Neurosci.* **2015**, *9*, 469. [CrossRef]
51. Lopes, L.V.; Sebastião, A.M.; Ribeiro, J.A. Adenosine and related drugs in brain diseases: Present and future in clinical trials. *Curr. Top. Med. Chem.* **2011**, *11*, 1087–1101. [CrossRef]

3.12 N-Methyl-D-Aspartate (NMDA) and cannabinoid CB_2 receptors form functional complexes in neural cells. Insights into the therapeutic potential of NMDA receptors in neurons and microglia.

Rafael Rivas-Santisteban, Alejandro Lillo, Jaume Lillo, Anna Del-Ser, Carles Saura, Rafael Franco*, Gemma Navarro*.

Manuscrito enviado para su consideración en *Brain, Behavior and Immunity*.

El receptor de cannabinoides tipo 2 (CB_2R) es un componente clave en la señalización del sistema endocannabinoide, cuya funcionalidad se ha descrito con propiedades antiinflamatoria y neuroprotectoras. Por otra parte, el receptor de N-metil-D-aspartato (NMDAR) es una diana de gran interés para mejorar la fisiopatología de la enfermedad de Alzheimer (AD). El objetivo de nuestro estudio es detectar la formación de estructuras heteroméricas formadas por el NMDAR y el CB_2R, y observar como se comportan funcionalmente estos complejos. Nuestros ensayos mediante transferencia de energía resonante por bioluminiscencia (BRET) en un modelo heterólogo de expresión confirmó la formación de complejos NMDAR-CB_2R. Mediante ensayos de ligación por proximidad (PLA) detectamos un incremento significativo del heterómero de receptores NMDA-CB_2 en cultivos de neuronas de hipocampo y microglía de ratón modelo de la AD ($APP_{Sw/Ind}$) respecto a los ratones control. Se caracterizó el complejo NMDAR-CB_2R mediante ensayos de determinación de los niveles de AMPc, calcio intracelular, determinación de las ERKs1/2 fosforiladas y de redistribución dinámica de masas (DMR). De manera interesante, se observó un cross-talk negativo al producirse la coactivación de ambos receptores con sus agonistas específicos. En conclusión, la activación de CB_2R de forma específica, a la vez que atenúa la señalización mediada por NMDAR, puede suponer un tratamiento con gran potencial en pacientes con la AD, mejorando su calidad de vida.

N-Methyl-D-Aspartate (NMDA) and cannabinoid CB_2 receptors form functional complexes in neural cells. Insights into the therapeutic potential of neuronal and microglial NMDA receptors.

Rafael Rivas-Santisteban[1,2], Alejandro Lillo[3,4], Jaume Lillo[1,2], Joan-Biel Rebassa[4], Joan S. Contestí[4], Anna del Ser-Badía[3,5], Carlos A. Saura[3,5], Rafael Franco[1,2,6*], Gemma Navarro[1,3,4*]

Affiliations:

[1] Centro de Investigación Biomédica en Red Enfermedades Neurodegenerativas (CiberNed), National Institute of Health Carlos iii. Madrid. Spain.

[2] Departament de Bioquímica i Biomedicina Molecular, Universitat de Barcelona, 08028 Barcelona, Spain

[3] Institut de Neurociències, Department de Bioquímica i Biologia Molecular, Universitat Autònoma de Barcelona, Bellaterra, 08193 Barcelona, Spain

[4] Department of Biochemistry and Physiology, Faculty of Pharmacy and Food Science, University of Barcelona, Barcelona, Spain

[5] Centro de Investigación Biomédica en Red sobre Enfermedades Neurodegenerativas, Instituto de Salud Carlos III, Valderrebollo, 5, 28031 Madrid, Spain; carlos.saura@uab.cat

[6] School of Chemistry. University of Barcelona, Barcelona, Spain.

***Corresponding authors:**

Rafael Franco (rfranco123@gmail.com; rfranco@ub.edu)
School of Biology. Universitat de Barcelona.
Diagonal 643. Prevosti Building.
Barcelona 08028. Spain
Tel +34 934021208

Gemma Navarro (g.navarro@ub.edu)
School of Pharmacy. Universitat de Barcelona
Joan XXIII, 29-31
Barcelona 08028. Spain
Tel +34 934034500

Summary

Cannabinoid CB_2 receptors, which are target of neuroprotection and N-Methyl-D-Aspartate (NMDA) ionotropic glutamate receptors, which are key in mediating excitatory neurotransmission, are expressed in both neurons and glia. As NMDA receptors are target of current medication in Alzheimer's disease patients and with the aim of finding neuromodulators of their actions that could provide benefits in dementia, we hypothesized that cannabinoids could modulate NMDA function. In a heterologous system we identified CB_2-NMDAcomplexes with a particular heteromer print consisting of impairment by cannabinoids of NMDA receptor function. The print was detected in activated primary microglia treated with lipopolysaccharide and interferon-γ. CB_2R activation blunted NMDA receptor-mediated signaling in primary hippocampal neurons from $APP_{Sw/Ind}$ mice, a Alzheimer's disease model. Furthermore, imaging studies showed that primary cells (microglia or neurons) from $APP_{Sw/Ind}$ mice displayed a marked overexpression of macromolecular CB_2-NMDA receptor complexes thus becoming a tool to modulate excessive glutamate input using cannabinoids.

Keywords
Alzheimer's disease, neuroprotection, G-protein-coupled receptors, excitotoxicity,

Introduction

Alzheimer's disease (AD) is the most common neurodegenerative disorder affecting more than 46 million people worldwide. The prediction is that the number of affected individuals will grow due to aging population. This pathology first described by Alois Alzheimer is characterized by a serious cognitive deficit and behavioral abnormalities (Alzheimer, 1911). Pathological hallmarks are the presence of ß-amyloid (Aß) deposits (extracellular plaques) and of hyperphosphorylated tau protein aggregates (intracellular neurofibrillary tangles) (Ulm et al., 2021). At the molecular level, several characteristics have been reported, among others, an increase in oxidative stress and defective mitochondrial dynamics (Bhatia and Sharma, 2021). To this day, no truly effective treatment has been developed. In addition to the approved drugs, cholinesterase inhibitors and NMDA receptor modulators (see below), multiple strategies have been proposed over the years (see (Ettcheto et al., 2020)).

The most affected neurons are located in the ascending cholinergic system whose somas are situated in Meinert's basal nucleus, thereafter, neurodegeneration in hippocampal, amygdala and neocortex areas, leads to the pathological AD features (Arendt et al., 1986; Doucette et al., 1986; Etienne et al., 1986). The main excitatory neurotransmitter glutamate, is crucial for the physiological state of the brain. Excitatory glutamatergic neurotransmission is required for neuronal survival and synaptic plasticity; however, aberrant activity promotes excitotoxicity and cell death (Wang et al., 2017; Wang and Reddy, 2017). Ionotropic ligand-gated glutamate receptors are the main mediators of glutamate action in the CNS. In addition, glutamate can activate the so-called metabotropic receptors that are not channels but G protein-coupled receptors (GPCRs). Three ionotropic glutamate receptors have been discovered, namely kainate, α-amino-3-hydroxy-5-methyl-4-isoxazolepropionic acid (AMPA) and N-methyl-D-aspartate (NMDA) receptors. The N-methyl-D-aspartate (NMDA) receptor plays an important role in neuronal plasticity and learning mechanisms. Memantine a drug approved for AD therapy (Lipton, 2007, 2006) targets NMDA receptors, which are multimers composed of different subunits whose consensual nomenclature is: GluN1, GluN2A, GluN2B, GluN2C, GluN2D, GluN3A and GluN3B (Alexander et al., 2019). A combination of these subunits leads to different tetrameric functional NMDA receptors (NMDARs). Moreover, the combination of different subunits leads to NMDARs with different functional and pharmacological properties. Activation of synaptic NMDARs has been reported to control synaptic plasticity and stimulate cell survival, while activation of extrasynaptic NMDARs promotes cell death and thus contributes to the etiology of AD. The limited effect of memantine in AD is likely due to an allosteric effect on extrasynaptic NMDARs (Stazi and Wirths, 2021; Wang et al., 2017; Wang and Reddy, 2017).

Endocannabinoids in the CNS, act as retrograde neuromodulators, i.e. they are released from the membrane of a postsynaptic neuron and act on receptors in the presynaptic neuron. However, cannabinoid receptors are widely expressed in the CNS, not only in neurons but in astrocytes, microglia and oligodendrocytes. There are two cannabinoid receptors, CB_1 and CB_2, that belong to the superfamily of GPCRs. CB_1 is considered the most abundant GPCR in the CNS and is expressed in many different neuronal types. The expression of the CB_2 receptor (CB_2R) is restricted to some neuronal populations, e.g. in the globus pallidus (J.L. Lanciego et al., 2011) or the cerebellum (Ashton et al., 2006), but is expressed in other neural cell types (Chung et al., 2016; Navarro et al., 2016; Pazos et al., 2013; Reyes-Resina et al., 2018; Stella, 2010; Wu et al., 2013). GPCRs may interact

to form homo and heterodimers which for many of the receptors in the superfamily constitute the real functional units (Borroto-Escuela et al., 2014; Ferré et al., 2009). Heteromers have different functionality than homomers, and different heterodimers have different signaling properties thus adding diversity to the action of neurotransmitters/neuromodulators that is mediated by GPCRs. CB_1 and CB_2 receptors may form functional heteromers that are heavily expressed in the neurons of the globus pallidus (Callén et al., 2012; José L Lanciego et al., 2011; Sierra et al., 2015) and that have a relevant function in activated microglia (Callén et al., 2012; Navarro et al., 2018). CB_2R and CB_1-CB_2 receptor heteromers are considered to exert neuroprotective actions (Cilia, 2018; Fernández-López et al., 2007; Micale et al., 2007; Rodríguez-Cueto et al., 2018; Sánchez and García-Merino, 2012); they have been proposed as targets to delay progression of Parkinson's disease (Navarro et al., 2018).

The NMDA receptor plays a central role in the CNS excitatory neurotransmission, being also a therapeutic target to combat AD. Receptor function deregulation is, at least in part, responsible for the progression of the disease. In this regard it would be interesting to discover membrane proteins capable of interacting with NMDA receptors, and being able to modulate their function to slow the onset of symptoms and the progressive neurodegeneration. In relation to neurodegenerative diseases, cannabinoid receptors appear as modulators of both neurotransmission and neuroinflammation. The aim of this study was to investigate whether the NMDA and the cannabinoid CB_2 receptors interact functionally in neurons and microglia in physiological conditions and in pathological AD models.

Results

N-methyl-D-aspartate receptors (NMDARs) interact with the cannabinoid CB_2 receptor in a heterologous expression system.

The NMDA receptor plays a central role in excitatory neurotransmission, being also a therapeutic target to combat AD. Receptor function deregulation is, at least in part, responsible for the progression of the disease. In this regard, it would be interesting to discover membrane proteins capable of interacting with NMDA receptors, and being able to modulate their functionality. We considered that cannabinoid CB_2 receptors (CB_2R) could be candidates for receptor-receptor interaction. Accordingly, HEK-293T cells were transfected with the cDNAs for CB_2R fused to YFP, for the GluN1 NMDAR subunit fused to RLuc and for the GluN2B subunit. Expression of these two protomers, GluN1 and GluN2B, leads to the assembly of a tetrameric structure, which is required for NMDA receptor functionality. Immunocytochemical assays showed that CB_2R-YFP, detected by YFP's own fluorescence, was expressed at the plasma membrane and also intracellularly (Fig. 1A). Qualitatively, similar expression was detected for the NMDA-RLuc receptor by using a specific anti-RLuc antibody (Fig. 1B). Moreover, a high level of colocalization between the two receptors was observed in the plasma membrane and in intracellular organelles (yellow in Fig. 1C). The results are suggestive of possible direct interactions. To demonstrate the hypothesis of a physical interaction between CB_2 and NMDA receptors, HEK-293T cells were transfected with a constant amount of cDNA for GluN1-RLuc and for GluN2B and increasing amounts of cDNA for CB_2R-YFP. The saturable curve obtained in Bioluminescence Energy Transfer (BRET) experiments was consistent with a physical interacting between CB_2R and GluN1 and the formation of CB_2-NMDA

receptor complexes (Fig. 1D, E). When HEK-293T cells were transfected with a constant amount of GluN1-RLuc and increasing amounts of the ghrelin receptor 1a fused to YFP (GHS-R1a-YFP), the linear relationship between the BRET donor/acceptor ratio indicated a lack of interaction of these two proteins (negative control; Fig. 1E red).

CB_2R activation impairs signaling via the NMDA receptor expressed in HEK-293T cells

In HEK-293T cells only expressing GluN1 and GluN2B subunits, intracellular cAMP levels were increased upon treatment with either NMDA or MK-801, a NMDAR selective antagonist (Fig. 2A). As Gi is the cognate protein coupled to the CB_2R, activation of the receptor leads to adenylate cyclase activity inhibition and decrease of intracellular cAMP levels. Such canonical functionality was confirmed in HEK-293T cells expressing CB_2R treated with forskolin and, afterwards, with a selective CB_2R agonist, JWH-133. The decrease in forskolin-induced cAMP levels was mediated by the cannabinoid receptor as it was completely counteracted by the pretreatment with a selective antagonist, SR 144528 (Fig. 2B). In HEK-293T cells expressing GluN1, GluN2B and CB_2R, CB_2R activation produced a significant decrease in forskolin induced cAMP levels, that was counteracted by the activation of the NMDAR (Fig. 2C). This phenomenon is usually described as negative cross-talk and can serve as a print/pattern to identify CB_2-NMDA receptor complexes in natural sources. The small decrease upon NMDAR activation was not significant. The CB_2R antagonist, SR-144528, blocked CB_2R activation while the NMDAR antagonist produced no effect (Fig. 2C).

Next, we determined MAPK pathway activation by means of ERK1/2 phosphorylation assays. It should be noted that both NMDAR and CB_2R activation leads to engagement of the MAPK pathway. Then, in HEK-293T cells expressing GluN1 and GluN2B, NMDA activation induced an effect that was counteracted by MK-801 pretreatment (Fig. 2D); analogously, in HEK-293T expressing the CB_2R, JWH-133 produced a significant effect that disappeared by the pretreatment with SR-144528 (Fig. 2E). In cells coexpressing the two receptors, NMDA induced a circa 2-fold increase in ERK1/2 phosphorylation; in contrast, CB_2R activation led to a non-significant response. Furthermore, coactivation with both agonists impeded the link of the CB_2-NMDA receptor complex to the MAPK pathway (Fig. 2F). Finally, antagonist pre-treatment did not lead to cross-antagonism, i.e. the antagonist of one receptor did not block the effect of the agonist of the partner receptor in the heteromer.

Activation of NMDA by glutamate results in the opening of the ligand-gated ion channel to allow calcium influx. In HEK-293T cells expressing ~~the~~ NMDAR the increase in cytoplasmic calcium caused by NMDA was inhibited in cells pretreated with the antagonist MK-801 (Fig. 3A). As expected, JWH-133 did not produce any calcium signal in HEK-293T cells expressing the CB_2R (Fig. 3B). However, this CB_2R agonist blocked NMDA-induced effect in HEK-293T cells coexpressing NMDAR and CB_2R, thus showing a negative cross-talk. In addition, the CB_2R antagonist, SR-144528, potentiated the NMDA-induced effect. These results indicate that, when forming complexes with CB_2Rs, NMDA receptor activation is restrained by CB_2R (activation) unless CB_2R is blocked by its antagonist (Fig. 3C).

Finally, the label-free technique Dynamic Mass Redistribution (DMR) that underscores ligand-induced changes due to multiple pathways and cellular events was applied (Ellen

E code 2011). First, in cells expressing CB_2R or NMDAR redistribution of mass occurred upon agonist treatment (Fig. 3D,E); the effects were partially inhibited by pretreatment with selective antagonists. In cotransfected cells, it was demonstrated that coactivation induced no additive effect, while the CB_2R antagonist, SR-144528, potentiated NMDA activation (Fig. 3F).

To sum up, heteromers constituted by the two receptors (CB_2-NMDA-Hets) show a negative crosstalk that may disappear when the partner receptor is blocked by an antagonist. It should be noted that the blockade of CB_2R markedly potentiates the ligand-gated ionotropic action subsequent to NMDAR activation.

CB_2R activation blocks NMDA signaling in activated microglia

The cannabinoid receptor CB_2R is upregulated in activated microglia likely having a neuroprotective role. Then, to evaluate the possible role of the CB_2R in regulating NMDAR function, mouse primary microglia were activated (48 h) with 1 μM LPS and 200 U/ml IFN-γ, or vehicle, and treated with receptor ligands. Treatment of non-activated cells with the CB_2R agonist, JWH-133, did not produce any significant decrease of forskolin-induced cAMP levels. This is likely due to the low CB_2R expression levels in resting microglia. In contrast, in activated microglial cell cultures, in which the CB_2R is upregulated, JWH-133 treatment induced a significant decrease of forskolin-induced cAMP levels, that was completely blocked by the CB_2R antagonist, SR144528, but not by NMDAR antagonist, MK-801. However, no effect was found when the two agonists were added together, i.e. a negative cross-talk was detected (Fig. 4B). These results were similar to those observed in transfected HEK-293T cells.

In resting cells the effect on MAPK pathway activation of either JWH-133 or NMDA was not significant (Fig. 4C). In activated microglia, the significant effect of both CB_2R and NMDAR agonists on increasing ERK1/2 phosphorylation was, however, significantly decreased when the two agonists were added together (Fig. 4D). Pretreatment with the NMDAR antagonist, MK-801, did not block the effect of JWH-133, whereas the CB_2R antagonist, SR-144528, slightly decreased the NMDAR-mediated effect. These results are consistent with the occurrence of CB_2-NMDA-Hets in activated microglia in which CB_2R activation exerts a negative regulation over the NMDAR link to the MAPK pathway.

Differential levels of CB_2-NMDA-Hets in neurons and microglia from $APP_{Sw/Ind}$ mice

Finally, we investigated the levels and cross-talk of CB_2R/NMDAR complexes in primary hippocampal neurons of control and $APP_{Sw/Ind}$ transgenic mice. First, the expression of CB_2-NMDAR-Hets was determined by *in situ* PLA (see Methods). Compared with control mice, CB_2-NMDA-Hets expression was circa two-fold higher in primary neurons and circa 2.6 fold higher in microglia from $APP_{Sw/Ind}$ mice (Fig. 5A-D). These results demonstrate that CB_2R-NMDA receptor complexes are aberrantly increased in both neurons and microglia of $APP_{Sw/Ind}$ mice.

CB_2R activation blocks NMDAR-mediated signaling in primary hippocampal neurons from $APP_{Sw/Ind}$ mice

After describing the functional characterization of the newly identified CB_2-NMDA receptor complex in microglia, we moved to primary cultures of neurons from mice

hippocampus. Intracellular cAMP levels were determined in primary neurons treated with forskolin and with selective receptor agonists. Whereas CB_2R activation produced a significant 30% decrease of forskolin-induced cAMP levels, NMDA did not generate any significant effect but counteracted the activation of the cannabinoid receptor (Fig. 5G). Thus, the negative cross-talk observed in transfected HEK-293T cells was also noticeable in primary neurons, thus suggesting the occurrence of functional CB_2-NMDA-Hets in hippocampal neurons. A similar phenomenon was also observed upon analysis of MAPK pathway activation: JWH-133 and NMDA induced ERK1/2 phosphorylation, which was undetectable in cells simultaneously treated with the two agonists (Fig. 5I). In addition, as observed in HEK-293T cells, pretreatment with the CB_2R selective antagonist blocked the JWH-133-induced signal while exerted no significant effect on NMDAR activation. Reciprocally, the NMDAR antagonist reverted the effect of NMDA but not that due to JWH-133. Finally, similar results were obtained in DMR label-free assays (Fig. 5K), i.e. NMDA receptor activation blocked CB_2R function and vice versa. Moreover, as observed in transfected HEK-293T cells, SR144528 pretreatment potentiated the NMDAR action.

Finally, we investigated the expression and cross-talk of cannabinoid CB_2 and NMDA receptors in primary neurons from control and $APP_{Sw/Ind}$ mice. Interestingly, it was observed that CB_2R activity was potentiated in $APP_{Sw/Ind}$ neurons, and contrary to control mice, it was not blocked by cotreatment with NMDA (see Fig. 5H). Upon analysis of MAPK pathway activation, JWH-133 and NMDA induced ERK1/2 phosphorylation, which was undetectable in cells simultaneously treated with the two agonists (Fig. 5J). Remarkably, the pretreatment with the CB_2R selective antagonist blocked the NMDAR-mediated effect in samples from control animals, and with more potency than in $APP_{Sw/Ind}$ neurons. This cross-antagonism was found in the opposite direction, i.e. the antagonist of the NMDAR completely blocked the JWH-133 effect. Finally, in Dynamic Mass Redistribution assays a negative cross-talk was identifiable when the two agonists were added together. This phenomenon, which was observed in neurons from both control and $APP_{Sw/Ind}$ mice (Fig. 5L), indicate that NMDAR activation blocks CB_2R function and vice versa.

Discussion

Ionotropic glutamate receptors are essential for the proper functioning of the mammalian central nervous system. The NMDA receptor is key to many aspects of glutamate-mediated actions in the nervous system, for excitatory neurotransmission, but also for development and neurogenesis. However, a dark side is related to excitotoxicity due to excessive levels of extracellular glutamate and the subsequent accumulation of toxic levels of ions in the cytoplasm of neurons. In this sense, it was hypothesized that NMDA would be a target of neurodegenerative diseases since, in fact, among the few existing drugs to combat AD, a negative allosteric NMDAR modulator, Memantine^R, was approved several years ago. Although the main interest has logically focused on neurons, NMDARs are expressed in glial cells, where they play a critical role in maintaining brain homeostasis. This work was based on the hypothesis that the action of NMDAR could be regulated by cannabinoid receptors and we focused on neurons and microglia, whose activation phenotype affects the progression of AD.

Although the different GPCRs tend to form dimers and oligomers, it was assumed that the multimeric structure of ionotropic receptors prevented the addition of more proteins to form macromolecular complexes with particular physiological properties. In fact, few

examples of direct interactions between ionotropic receptors and GPCRs have been reported. We had previously demonstrated the interaction of a GPCR, which is a target for neuroprotection, the adenosine A_{2A} receptor, and NMDAR. This complex appears to have a relevant role in activated microglia where these complexes, which are expressed in the microglia of WT animals, are markedly upregulated in cells of AD transgenic mice (Franco et al., 2020).

In this report we first addressed the possibility of a direct interaction between CB_2R and NMDAR, and the results were positive, that is, these two receptors can form complexes that alter the effect exerted by NMDA or CB_2R agonists. This finding is remarkable and confirms that GPCRs that are relevant to maintaining a correct neuroprotective balance (the adenosine A_{2A} receptor is a significant example ((Franco et al., 2020))) can interact with ionotropic receptors. Although CB_2R is less abundant in neurons than the cannabinoid CB_1 receptor, it can be found in neurons in different brain regions, and here we were able to find CB_2-NMDA-Hets in primary hippocampal neurons (Fig. 5). In microglia, heteromers were present but at a lower level at resting than in activated cells; this is likely due to the increase in CB_2R, whose expression in resting conditions was quite low.

In the heterologous expression system the most noticeable property of the CB_2-NMDA-Hets was the negative cross-talk, namely simultaneous treatment with the two agonists led to absence of response in either the Gi/adenylate cyclase/cAMP pathway or the MAPK pathway. Because CB_2R agonists could not, in the heteromeric context, significantly phosphorylate ERK1/2, the blocking effect appears to be direct, that is, due to intra-CB_2-NMDA-Het allosteric interactions and conformational changes upon binding of cannabinoids to the CB_2R. Perhaps the most noticeable effect was the reduction by CB_2R agonists of the ionotropic function of the NMDAR. The cross-antagonism found in complexes formed by two GPCRs was not found in HEK-293T cells expressing CB_2 and NMDA receptors. This contrast with the $A_{2A}R$-NMDAR couple properties whose structure allows detecting cross-antagonism when GPCR-GPCR heteromer formation is suspected (Ferré et al., 2009; Franco et al., 2018a, 2016).

Importantly, CB_2-NMDA-Hets were also detected in hippocampal neurons, although the glutamate/cannabinoid relationships are more complex. In WT animals, the finding related to Gi-coupled actions of the CB_2R were similar to those found in the heterologous cells, basically there was a negative cross-talk. However, this cross-talk was not found in cells from the $APP_{Sw/Ind}$ transgenic mice. On the one hand, these finding show that hippocampal neurons from WT and transgenic mice are different, already, in early steps of CNS development; the AD-like phenotype takes months to be detectable. On the other hand, the results may indicate a lack of complexes in neurons from the AD mouse model. The cross-antagonism detected in samples from those mice, i.e. the antagonist of one receptor blunted the link to the MAPK pathway and vice versa, shows that CB_2-NMDA-Hets are present. Thus the most reasonable hypothesis is that different populations of receptors coexist and that the CB_2-NMDA-Het is one of them. This hypothesis could explain why NMDA does not affect the JWH-133 effect on cAMP levels; perhaps Gi-coupled to CB_2R are not interacting with NMDARs in neurons from transgenic animal or the CB_2-NMDA-Het is not well coupled to the Gi. Remarkably, the negative cross-talk in the link to the MAPK pathway occurs in both neurons from WT and from $APP_{Sw/Ind}$ animals. The presence of complexes was confirmed by PLA, which furthermore showed

that the expression of the CB_2-NMDA-Het increases in both microglia and neurons from the transgenic mice (compared with levels in WT mice).

NMDAR is a target to combat AD. However, drugs that directly affect its function are not effective in the medium/long term (Lipton, 2006). Finding GPCRs that can interact and modulate NMDAR-mediated function holds promise for innovative treatments targeting neurons, microglia, or both. In the case of $A_{2A}R$, impairment of NMDAR function by $A_{2A}R$ antagonists is an attractive possibility. In the present study, cannabinoids could provide equivalent benefits by significantly reducing the effect of agonists that activate NMDAR. With the exception of Δ^9-tetrahydrocannabinol (THC), which produces CB_1R-mediated psychotropic effects, most of the natural cannabinoids studied so far are generally safe. Additionally, there is an increased interest in cannabinoids as potential drugs to combat a variety of diseases (Alvarez et al., 2008; Fernández-Ruiz et al., 2013; van der Stelt and Di Marzo, 2005).

A deleterious factor in neurodegenerative diseases, including AD, is excitotoxicity, that is, the aberrant increase in cytoplasmic Ca^{2+} levels after excessive stimulation of NMDAR by extracellular glutamate (Lewerenz and Maher, 2015). Since allosteric modulators that act directly on NMDAR do not provide much help to AD patients, an interacting GPCR-mediated allosteric modulation is an attractive possibility to explore further. In the case of CB_2R, its complex pharmacology can be an added value to find the best way to regulate the NMDAR function. In fact, cannabinoids show multiple modes of binding and biased signaling due to the wormhole-like structure of their orthosteric site and due to the existence of various non-orthosteric binding sites. Multiple modes of cannabinoid binding to CB_2R lead to specific receptor conformations underlying functional selectivity (biased agonism) (Navarro et al., 2020) and, ultimately, differentially regulating NMDAR function. As an example, we have designed bitopic ligands that bind to an exosite located at the entrance of the structure that connects the orthosteric site with the lipid bilayer (Morales et al., 2020). These findings constitute a selective advantage since the expression of CB_2-NMDA-Het increases in neurons and microglia of $APPS_{w/Ind}$ transgenic mice.

Materials and Methods

Reagents

Lipopolysaccharide (LPS), interferon-γ (IFN-γ), JWH-133 (JWH) and SR-144528 (SR) were purchased from Sigma-Aldrich (St Louis, MO, USA). N-methyl-D-aspartate (NMDA), MK-801 (MK) and forskolin (FK) were purchased from Tocris (Bristol, UK). Tau and p-Tau proteins were kindly provided by Prof. J. Avila (CBM, UAM-CSIC, Madrid, Spain). Detailed descriptions of the elaboration and processing of proteins can be found elsewhere (Pérez et al., 2002; Tarutani et al., 2016)

HEK-293T cells and primary cultures

Human embryonic kidney (HEK-293T) cells were grown in Dulbecco's modified Eagle's medium (DMEM) (Gibco) supplemented with 2 mM L-glutamine, 100 µg/ml sodium pyruvate, 100 U/ml penicillin/streptomycin, MEM non-Essential Amino Acids Solution (1/100) and 5% (v/v) heat inactivated Fetal Bovine Serum (FBS) (all supplements were from Invitrogen, Paisley, Scotland, UK). Cells were maintained at 37 ºC in a humid atmosphere of 5% CO_2.

To prepare mice striatal primary microglial cells, brain was removed from C57BL/6 mice of 2–4 days of age. Microglial cells were isolated as described in (Newell et al., 2015). Briefly, striatum tissue was dissected, carefully stripped of its meninges and digested with 0.25% trypsin for 20 min at 37 ºC. Trypsinization was stopped by washing the tissue. Cells were brought to a cell suspension by passage through 0.9 mm and 0.5 mm nails followed by passage through a 100 µm pore mesh. Glial cells were resuspended in medium and seeded at a density of 1 x 10^6 cells/ml in 6-well plates for cyclic adenylic acid (cAMP) assays, in 12-well plates with coverslips for in situ proximity ligation assays (PLA) and in 96-well plates for mitogen-activated protein kinase (MAPK) activation experiments. Cultures were grown in DMEM medium supplemented with 2 mM L-glutamine, 100 U/ml penicillin/streptomycin, MEM non-Essential amino acids preparation (1/100) and 5% (v/v) heat inactivated Fetal Bovine Serum (FBS) (Invitrogen, Paisley, Scotland, UK) and maintained at 37ºC in humidified 5% CO_2 atmosphere and, unless otherwise stated, medium was replaced once a week.

For culturing primary neurons, the striatum from mouse embryos (E19) was removed and the neurons were isolated as described by Hradsky et al., 2013 (Hradsky et al., 2013) and plated at a density of circa 120,000 cells/cm^2. Cells were grown in a neurobasal medium supplemented with 2 mM L-glutamine, 100 U/mL penicillin/streptomycin, and 2% (v/v) B27 supplement (Gibco) in a 6-, 12- or 96-well plate for 12 days. Cultures were maintained at 37ºC in a humidified 5% CO_2 atmosphere and medium was replaced every 4–5 days.

Immunodetection of specific markers (Neu N for neurons and CD-11b for microglia) showed that neuronal preparations contained >98% neurons and microglia preparations contained, at least, 98% microglial cells (Franco et al., 2018b).

$APP_{Sw/Ind}$ Transgenic Mice

$APP_{Sw/Ind}$ transgenic mice (line J9; C57BL/6 background) expressing human APP695 harboring the FAD-linked Swedish (K670N/M671L) and Indiana (V717F) mutations under the platelet derived growth factor subunit B (PDGFB) promoter were obtained by crossing $APPS_{w/Ind}$ to nontransgenic (control) mice (Mucke et al., 2000). Control and $APP_{w;Ind}$ embryos (E16.5) were genotyped individually, and hippocampus/cortex dissected and prepared for microglia and neuron primary cultures as described elsewhere (Franco et al., 2018b; Navarro et al., 2018). All experimental procedures were conducted according to the approved protocols from the Animal and Human Ethical Committee of the Universitat Autònoma de Barcelona (CEEAH 2895) and Generalitat de Catalunya (10571) following the experimental European Union guidelines and regulations (2010/63/EU)

Fusion proteins

Human cDNAs for the GluN1 NMDA receptor subunit, for the CB_2 receptor and for the ghrelin GHS1a receptor, all cloned into pcDNA3.1 were amplified without their stop

codons using sense and antisense primers harboring either BamHI and HindIII restriction sites to amplify GluN1, BamHI and KpnI restriction sites to amplify CB_2 receptor or EcoRI and KpnI restriction sites to amplify GHS1a receptor. Amplified fragments were then subcloned to be in frame with an enhanced yellow fluorescent protein (pEYFP-N1; Clontech, Heidelberg, Germany) or a RLuc (pRLuc-N1; PerkinElmer, Wellesley, MA) on the C-terminal end of the receptor to produce GluN1-RLuc, CB_2R-YFP and GHSR1a-YFP fusion proteins.

Cell transfection

HEK-293T cells were transiently transfected with the corresponding cDNA by the PEI (PolyEthylenImine, Sigma-Aldrich) method. Briefly, the corresponding cDNA diluted in 150 mM NaCl was mixed with PEI (5.5 mM in nitrogen residues) also prepared in 150 mM NaCl for 10 min. The cDNA-PEI complexes were transferred to HEK-293T cells and were incubated for 4 hours in a serum-starved medium. Then, the medium was replaced by fresh supplemented culture medium and cells were maintained at 37 ºC in a humid atmosphere of 5% CO_2. 48 hours after transfection, cells were washed, detached, and resuspended in the assay buffer.

Immunocytochemistry

HEK-293T cells were seeded on glass coverslips in 12-well plates. 24 hours after, cells were transfected with CB_2-YFP cDNA (1 µg), GluN1-RLuc cDNA (1 µg) and GluN2B cDNA (0.75 µg). 48 h after, cells were fixed in 4% paraformaldehyde for 15 min and washed twice with PBS containing 20 mM glycine before permeabilization with PBS-glycine containing 0.2% Triton X-100 (5 min incubation). Cells were blocked during 1 hour with PBS containing 1% bovine serum albumin. HEK-293T cells were labeled with a mouse anti-RLuc antibody (1/100; Millipore, Darmstadt, Germany) and subsequently treated with Cy3-conjugated anti-mouse (1/200; Jackson ImmunoResearch (red)) antibody (1 hour each). The CB_2R-YFP expression was detected by the YFP's own fluorescence. Nuclei were stained with Hoechst (1/100 from stock 1 mg/mL; SigmaAldrich). Samples were washed several times and mounted with 30% Mowiol (Calbiochem).

Images were obtained in a Zeiss LSM 880 confocal microscope (ZEISS, Germany) with the 40X and 63X oil objectives.

Bioluminescence resonance energy transfer (BRET) assay

For BRET assay, HEK-293T cells were transiently cotransfected with a constant amount of cDNA encoding for GluN1-RLuc (0.25 µg) and GluN2B (0.15 µg) and with increasing amounts of cDNA corresponding to CB_2R-YFP (0.25 to 1.25 µg). As negative control, HEK-293T cells were transiently cotransfected with a constant amount of cDNA encoding for GluN1-RLuc (0.25 µg) and GluN2B (0.15 µg) and with increasing amounts of cDNA corresponding to GHSR1a-YFP (0.25 to 1.5 µg). To control the cell number, sample protein concentration was determined using a Bradford assay kit (Bio-Rad, Munich, Germany) using bovine serum albumin (BSA) dilutions as standards. To

quantify fluorescent proteins, cells (20 µg of total protein) were distributed in 96-well microplates (black plates with a transparent bottom) and fluorescence was read in a Fluostar Optima Fluorimeter (BMG Labtech, Offenburg, Germany) equipped with a high-energy xenon flash lamp, using a 10 nm bandwidth excitation filter at 485 nm. For BRET measurements, the equivalent of 20 µg of total protein cell suspension was distributed in 96-well white microplates with white bottom (Corning 3600, Corning, NY). BRET was determined one minute after adding coelenterazine H (Molecular Probes, Eugene, OR), using a Mithras LB 940 plate reader (Berthold Technologies, DLReady, Germany), which allows the integration of the signals detected in the short-wavelength filter at 485 nm and the long-wavelength filter at 530 nm. To quantify GluN1-RLuc expression, luminescence readings were obtained 10 min after the addition of 5 µM coelenterazine H. MilliBRET units (mBU) are defined as:

$$\mathrm{mBU} = \left[\frac{\lambda_{530}(\mathrm{long-wavelength\ emission})}{\lambda_{485}(\mathrm{short-wavelength\ emission})} - \mathrm{C_f}\right] x\ 1000$$

where C_f corresponds to [(long-wavelength emission)/(short-wavelength emission)] for the RLuc construct expressed alone in the same experiment.

cAMP level determination

The analysis of cAMP levels was performed in HEK-293T cells cotransfected with the cDNA for two subunits of the NMDA receptor, GluN1 (1 µg) and GluN2B (0.75 µg) or/and/or the cDNA for the CB_2R (1 µg). Similar assays were also performed in primary microglia and primary neurons prepared from wild type mice or the transgenic $APP_{Sw/Ind}$ AD mice model. In the case of microglia cells were first activated using 1 µM LPS and 200 U/mL IFN-γ (48 hours). 2 hours before the experiment the medium was substituted by serum-starved DMEM medium. Cells growing in medium containing 50 µM zardaverine were distributed in 384-well microplates (2,000 HEK-293T cells or 4,000 hippocampal neurons or microglial cells per well) followed by the stimulation with the NMDA and/or CB_2R agonists (NMDA (15 µM) and/or JWH-133 (100 nM)) for 15 min before adding 0.5 µM forskolin or vehicle for an additional 15 min period. When indicated cells were pre-treated (15 min) with the NMDA or CB_2R antagonists, respectively, MK-801 (1 µM) or SR-144528 (1 µM). Homogeneous time-resolved fluorescence energy transfer (HTRF) measures were performed using the Lance Ultra cAMP kit (PerkinElmer). Fluorescence at 665 nm was analyzed on a PHERAstar Flagship microplate reader equipped with an HTRF optical module (BMG Labtech). A standard curve for cAMP was obtained in each experiment.

MAP kinase pathway activation is measured by ERK1/2 phosphorylation

Hippocampal neurons, microglial cells or HEK-293T cells cotransfected with the cDNA for the protomers of the NMDA receptor, GluN1 (1 µg) and GluN2B (0.75 µg), and/or with the cDNA for CB_2R (1 µg) were plated in transparent Deltalab 96-well microplates. Primary microglial cells were activated by incubating cells with 1 µM LPS and 200 U/mL IFN-γ during 48 hours. Two hours before the experiment, the medium was substituted by

serum-starved DMEM medium. Cells were treated or not for 10 min with the selective antagonists (MK-801 (1 µM) or SR-144528 (1 µM)) followed by 7 min treatment with the selective agonists (NMDA (15 µM) and/or JWH-133 (100 nM)). Cells were then washed twice with cold PBS before the addition of lysis buffer (15 min treatment). 10 µL of each supernatant were placed in white ProxiPlate 384-well microplates and ERK1/2 phosphorylation were determined using an AlphaScreen®SureFire® kit (Perkin Elmer) following the instructions of the supplier and using an EnSpire® Multimode Plate Reader (PerkinElmer).

Detection of cytoplasmic calcium levels

HEK-293T cells were cotransfected with the cDNA for the protomers of the NMDA receptor channel GluN1 (1 µg) and GluN2B (0.75 µg), with thee cDNA for CB_2R (1 µg) and with the cDNA for the GCaMP6 calcium sensor (1 µg) (Chen et al., 2013) by the use of PEI method (Section "Cell Transfection"). 48 hours after transfection, HEK-293T cells plated in 6-well black, clear bottom plates, were incubated with Mg^{2+}-free Locke's buffer (154 mM NaCl, 5.6 mM KCl, 3.6 mM $NaHCO_3$, 2.3 mM $CaCl_2$, 5.6 mM glucose, 5 mM HEPES, 10 µM glycine, pH 7.4). On line recordings were performed right after addition of agonists. When indicated cells were pre-treated with receptor antagonists for 10 min. Fluorescence emission intensity due to complexes GCaMP6 was recorded at 515 nm upon excitation at 488 nm on the EnSpire® Multimode Plate Reader for 150 s every 5 s at 100 flashes per well.

Dynamic Mass-Redistribution (DMR) label free assays

Cell signaling was explored using an EnSpire® Multimode Plate Reader (PerkinElmer) by a label-free technology. Cellular cytoskeleton redistribution induced upon receptor activation was detected by illuminating the underside of the plate with polychromatic light and measured as changes in wavelength of the reflected monochromatic light. The magnitude of this wavelength shift (in picometers) is directly proportional to the amount of DMR. To determine the label free-DMR signal, 10,000 HEK-293T cells cotransfected with cDNAs for the protomers of the NMDA receptor channel, GluN1 (1 µg) and GluN2B (0.75 µg) and/or with the cDNA for the CB_2R (1 µg). Similar assays were performed using 10,000 primary neurons from wild type or transgenic $APP_{Sw/Ind}$ mice. Transparent 384-well fibronectin coated microplates were used until obtaining 70-80% confluent monolayers (kept in the incubator for 24 h). Previous to the assay, cells were washed twice with assay buffer (HBSS with 20 mM HEPES, pH 7.15, 0.1% DMSO) and incubated in the reader with assay-buffer for 2 hours at 24°C. Hereafter, the sensor plate was scanned and a baseline optical signature was recorded for 10 minutes before adding 10 µL of selective agonists (NMDA (15 µM) and/or JWH-133 (100 nM)) also dissolved in assay buffer. When indicated cells were pre-treated with antagonists (MK-801 (1 µM) or SR-144528 (1 µM); 10 µL in volume). Real time DMR responses by the were monitored for a minimum of 3600 s.

Proximity Ligation Assay (PLA)

Detection in natural sources of clusters formed by the NMDA and CB_2 receptors was addressed in primary hippocampal microglia and hippocampal neurons of wild type mice

or the transgenic $APP_{Sw/Ind}$ mice model. Cells grown on glass coverslips, were fixed in 4% paraformaldehyde for 15 min, washed twice with PBS containing 20 mM glycine to quench the aldehyde groups, permeabilized with the same buffer containing 0.05% Triton X-100 between 5 to 15 min and washed with PBS. After 1 hour incubation at 37°C with the blocking solution in a pre-heated humidity chamber, samples were incubated overnight at 4ºC with a mixture of a rabbit monoclonal anti-GluN1 antibody (1/100, ab52177, Abcam, Cambridge, UK) and a mouse monoclonal anti-CB_2R antibody (1/100, sc-293188, Santa Cruz Biotechnology, Texas, USA). Nuclei were stained with Hoechst (1/100 from 1 mg/mL stock; SigmaAldrich). The antibodies were validated following the method in the technical brochure of the vendor with fairly similar results. Cells were further processed using the PLA probes detecting primary antibodies (Duolink In Situ PLA probe Anti-Mouse plus and Duolink In Situ PLA probe Anti-Rabbit minus) (1/5 v:v for 1-hour at 37ºC). Ligation and amplification were done as indicated by the supplier (SigmaAldrich) and cells were mounted using the mounting medium Mowiol (30%) (Calbiochem). To detect red dots corresponding to CB_2-NMDA-Hets, samples were observed in a Zeiss LSM 880 confocal microscope (ZEISS, Germany) equipped with an apochromatic 63X oil-immersion objective, and a 405 nm and 561 nm laser lines. For each field of view a stack of two channels (one per staining) and 3 Z-planes with a step size of 1 μm were acquired. The Andy's algorithm, a specific ImageJ macro for reproducible and high-throughput quantification of the total PLA foci dots and total nuclei, was used for data analysis (Law et al., 2017).

Statistical analysis

The data in graphs are the mean ± SEM (at least n=5). GraphPad Prism 9 software (San Diego, CA, USA) was used for data fitting and statistical analysis. One-way ANOVA followed by *post-hoc* Bonferroni's test were used when comparing multiple values. When a pair of values were compared, the Student's t test was used. Significant differences were considered when the p value was <0.05.

Acknowledgements

Not applicable

Funding

This work was partially supported by the AARFD-17-503612 grant (to GN) from the US Alzheimer's Association, and by grants SAF2017-84117-R (to GN), PID2019-106615RB-100 (to CAS) and RTI2018-094204-B-I00 (to RF) from the Spanish Ministerio de Ciencia, Innovación y Universidades (MCIU; or equivalent) and Spanish Agencia Estatal de Investigación (AEI); they include UE FEDER funds. The research group of the University of Barcelona is considered of excellence (grup consolidat #2017 SGR 1497) by the Regional Catalonian Government, which does not provide any specific funding for reagents or for payment of services or Open Access fees).

Figure legends

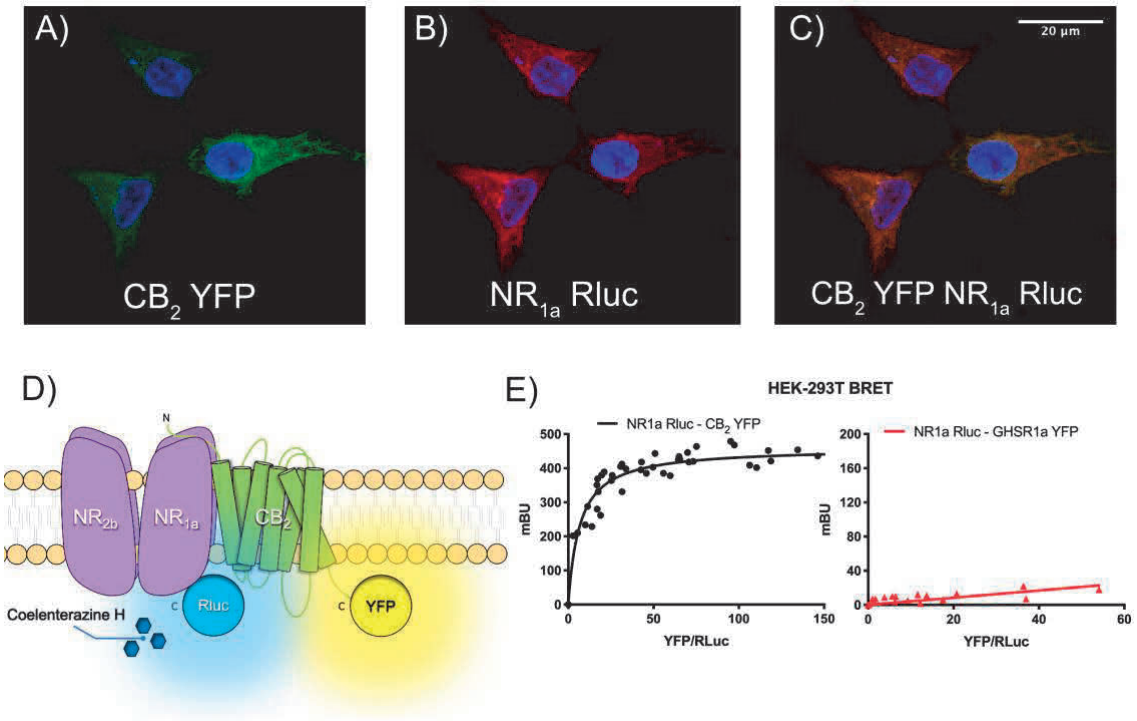

Figure 1. The NMDA receptor interacts with the cannabinoid CB_2 receptor in a heterologous expression system. Panels A-C: Immunocytochemistry performed in HEK-293T cells expressing CB_2-YFP (A) (1 µg cDNA), that was detected by its own yellow fluorescence (green), and GluN1-Rluc receptor (1 µg cDNA) (B), that was detected by a mouse monoclonal anti-Rluc antibody and a secondary Cy3-conjugated anti-mouse IgG antibody (red). Colocalization is shown in yellow (C). Cell nuclei were stained with Hoechst (blue). Images are taken near the bottom of the cell, i.e. it mainly includes the membrane in contact with the glass of the plate. Scale bar: 20 µm. Panel D: Schematic representation of BRET assay: the occurrence of energy transfer depends on the distance between the BRET donor (Rluc) and the BRET acceptor (YFP). Panel E: BRET assays were performed in HEK-293T cells transfected with a constant amount of cDNAs for GluN1-Rluc (0.25 µg), GluN2B (0.15 µg) and increasing amounts of cDNA for CB_2R-YFP (0.25 to 1.25 µg) (black) or (as negative control) GHSR1aR-YFP (0.25 to 1.25 µg) (red). Values are the mean ± S.E.M. of 8 independent experiments performed in duplicates.

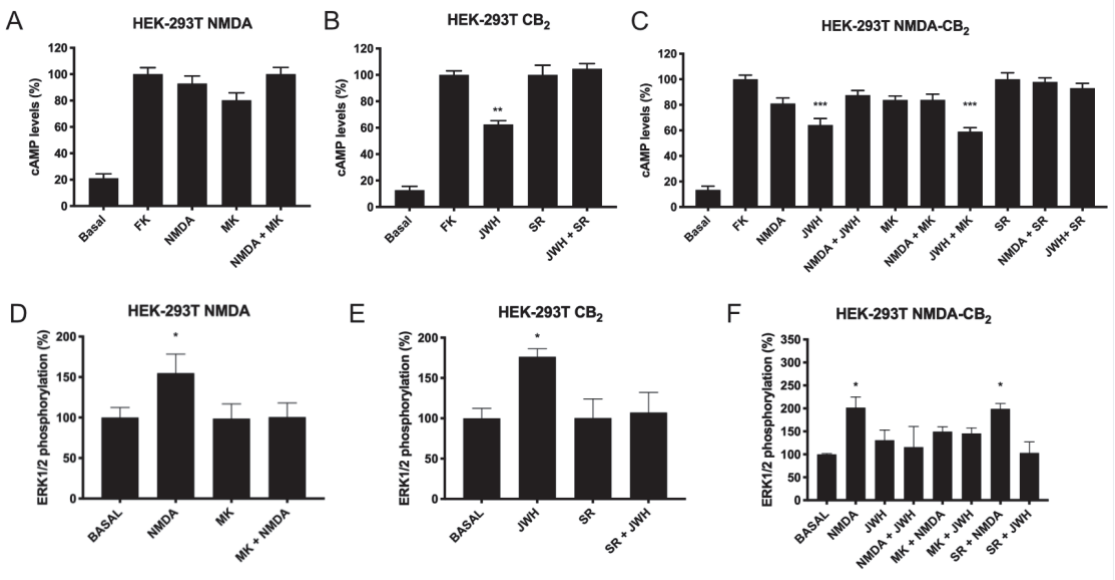

Figure 2. Signaling in HEK-293T cells expressing NMDA-CB_2R heteromers. HEK-293T cells transfected with the cDNAs for two protomers of the NMDA receptor: GluN1 (1 μg) and GluN2B (0.75 μg) and/or with the cDNA for the CB_2R (1 μg), were treated with selective agonists (15 μM NMDA for NMDAR and/or 100 nM JWH-133 for CB_2R). When indicated cells were pretreated with selective receptor antagonists (1 μM MK-801 for NMDA or 1 μM SR-144528 for CB_2R). Panels A-C: Intracellular cAMP levels were determined by TR-FRET as described in Methods. As G_i coupling was assessed, decreases in cAMP levels were determined in cells previously treated with 0.5 μM forskolin (15 min). Values are the mean ± S.E.M. of 6 independent experiments performed in triplicates. In cAMP one-way ANOVA followed by Bonferroni's multiple comparison *post hoc* test were used for statistical analysis (*$p < 0.05$, **$p < 0.01$, ***$p < 0.001$ versus forskolin treatment). Panels D-F: ERK1/2 phosphorylation was analyzed using an AlphaScreen®SureFire® kit (Perkin Elmer). Values are the mean ± S.E.M. of 5 independent experiments performed in triplicates. One-way ANOVA followed by Bonferroni's multiple comparison *post hoc* test were used for statistical analysis (*$p < 0.05$, **$p < 0.01$, ***$p < 0.001$ versus vehicle treatment).

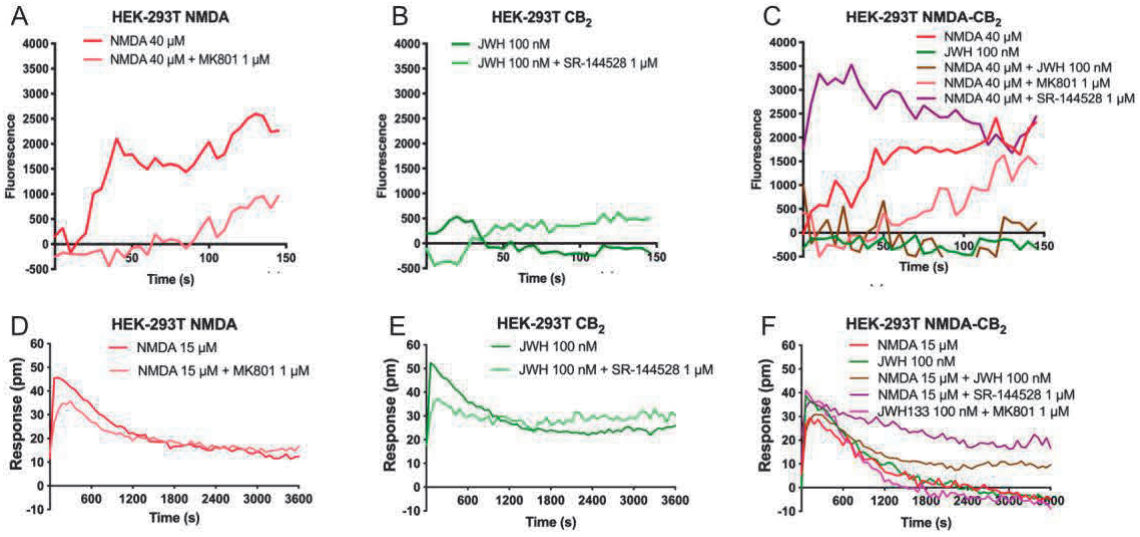

Figure 3. DMR and intracellular calcium mobilization in HEK-293T cells expressing NMDA-CB_2R heteromers. HEK-293T cells were transfected with the cDNAs for two protomers of the NMDA receptor: GluN1 (1 μg) and GluN2B (0.75 μg) and/or with the cDNA for the CB_2R (1 μg); for

calcium assays cells were also transfected with the cDNA for the engineered calcium sensor, 6GCaMP (1 μg) (D-F). Receptors were activated using selective agonists (40 μM NMDA (for calcium detection assays) or 15 μM NDMA (for DMR assays) for NMDAR and/or 100 nM JWH-133 for CB_2R). When indicated cells were pretreated with selective receptor antagonists (1 μM MK-801 for NMDA or 1 μM SR-144528 for CB_2R). Real-time calcium-induced fluorescence or DMR readings were collected. Values in each figure are from a representative experiment out of 5 independently performed.

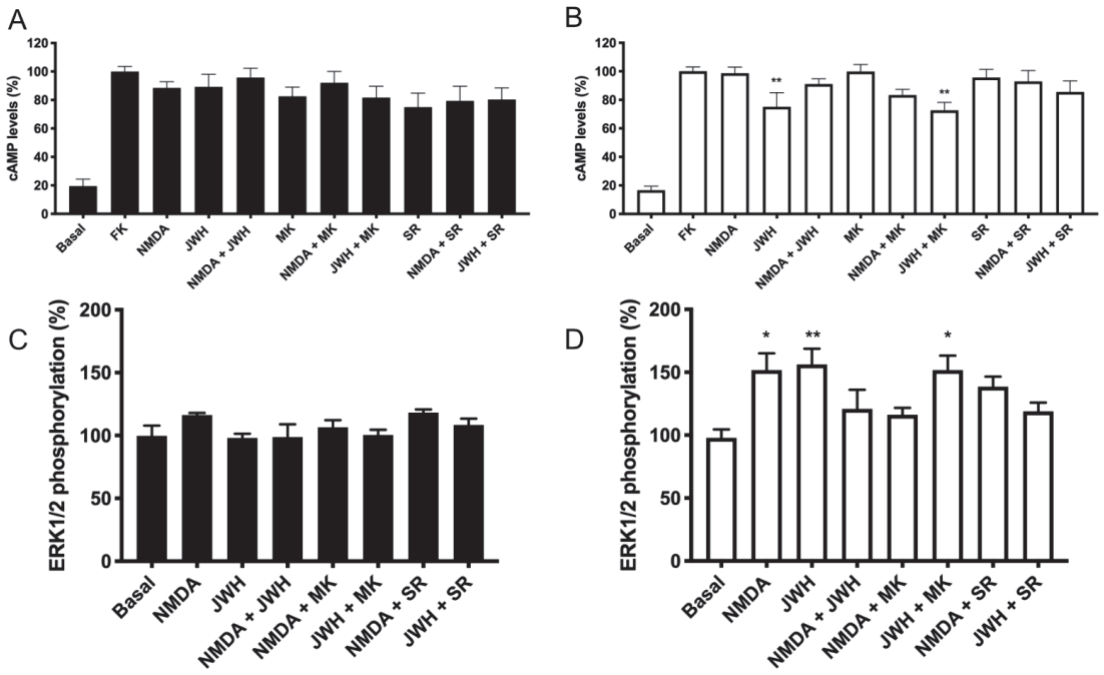

Figure 4. Signaling in primary microglia activated with LPS and IFN-γ. Primary microglial cells were incubated for 48 h in the absence (black bars) or in the presence (white bars) of 1 μM LPS and 200 U/mL IFN-γ. Cells were treated with selective agonists (15 μM NMDA for NMDA channel, and/or 100 nM JWH-133 for CB_2R) and cAMP levels and MAPK pathway activation were determined. As G_i coupling was assessed, decreases in cAMP levels were determined in cells previously treated with 0.5 μM forskolin (15 min). When indicated cells were pretreated with selective receptor antagonists (1 μM MK-801 for NMDA or 1 μM SR-144528 for CB_2R). Values are the mean ± S.E.M. of 5 independent experiments performed in triplicates. One-way ANOVA followed by Bonferroni's multiple comparison *post hoc* test were used for statistical analysis (*$p < 0.05$, **$p < 0.01$, ***$p < 0.001$ versus forskolin treatment in cAMP determinations or versus vehicle treatment (basal) in ERK phosphorylation assays).

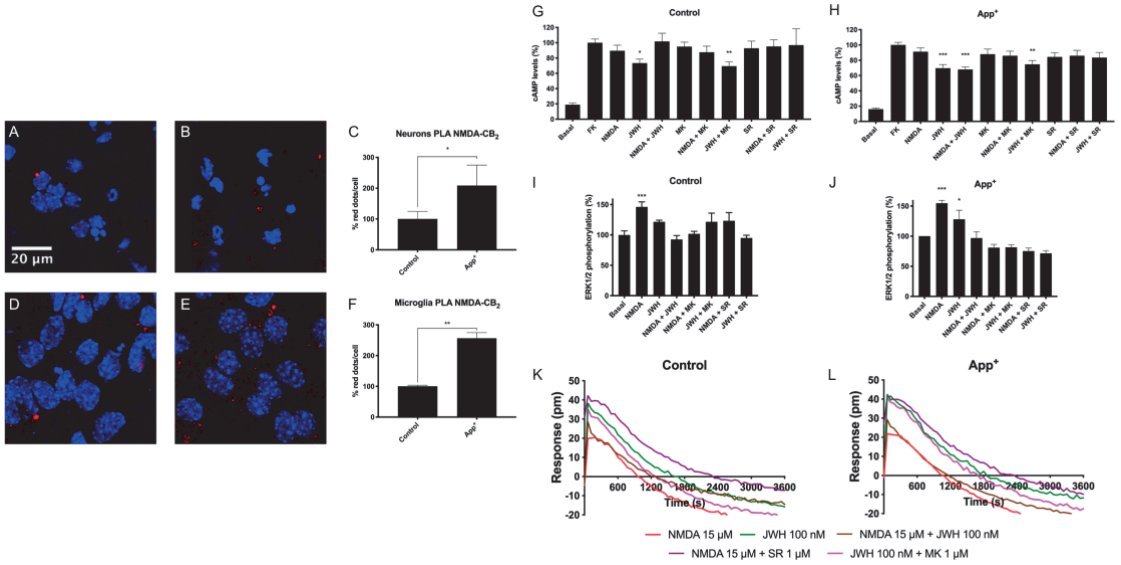

Figure 5. NMDA-CB_2R heteromer levels and functionality in $APP_{Sw/Ind}$ neurons. Panels A-F: Expression of NMDA-CB_2R heteromers in mouse primary neurons (A-B) and microglia (D-E) of wild type (A, D) and $APP_{Sw/Ind}$ transgenic mice (B, E) as determined by PLA (see Methods) using specific primary antibodies against the GluN1 subunit and against the CB_2R receptor. Confocal microscopy images (stacks of 3 consecutive panels) show heteroreceptor complexes as red clusters over Hoechst-stained nuclei (blue). Five independent experiments were performed using, for each condition, 5 preparations per session. Bar graphs show the amount of red dots/cell in $APP_{Sw/Ind}$ mice and control animals (*$p < 0.05$, **$p < 0.01$; Student's t test versus the control condition). Panels G-L: Primary neurons from control and $APP_{Sw/Ind}$ mice were treated with selective agonists (15 µM NMDA for NMDA channel, and/or 100 nM JWH-133 for CB_2R) and cAMP levels (G-H), ERK1/2 phosphorylation (Panel I-J) and DMR (K-L) assays were determined. When indicated cells were pretreated with selective receptor antagonists (1 µM MK-801 for NMDA or 1 µM SR-144528 for CB_2R). Values are the mean ± S.E.M. of 5 independent experiments performed in triplicates. One-way ANOVA followed by Bonferroni's multiple comparison *post hoc* test were used for statistical analysis (*$p < 0.05$, **$p < 0.01$, ***$p < 0.001$ versus forskolin treatment in cAMP determinations or versus vehicle treatment (basal) in ERK phosphorylation assays).

References

Alexander, S.P.H., Mathie, A., Peters, J.A., Veale, E.L., Striessnig, J., Kelly, E., Armstrong, J.F., Faccenda, E., Harding, S.D., Pawson, A.J., Sharman, J.L., Southan, C., Davies, J.A., Aldrich, R.W., Becirovic, E., Biel, M., Catterall, W.A., Conner, A.C., Davies, P., Delling, M., Di Virgilio, F., Falzoni, S., George, C., Goldstein, S.A., Grissmer, S., Ha, K., Hammelmann, V., Hanukoglu, I., Jarvis, M., Jensen, A.A., Kaczmarek, L.K., Kellenberger, S., Kennedy, C., King, B., Lynch, J.W., Perez-Reyes, E., Plant, L.D., Rash, L.D., Ren, D., Sivilotti, L.G., Smart, T.G., Snutch, T.P., Tian, J., Van den Eynde, C., Vriens, J., Wei, A.D., Winn, B.T., Wulff, H., Xu, H., Yue, L., Zhang, X., Zhu, M., 2019. The concise guide to pharmacology 2019/20: Ion channels. Br. J. Pharmacol. 176, S142–S228. https://doi.org/10.1111/bph.14749

Alvarez, F.J., Lafuente, H., Rey-Santano, M.C., Mielgo, V.E., Gastiasoro, E., Rueda, M., Pertwee, R.G., Castillo, A.I., Romero, J., Martínez-Orgado, J., 2008. Neuroprotective effects of the nonpsychoactive cannabinoid cannabidiol in hypoxic-ischemic newborn piglets. Pediatr. Res. 64, 653–658. https://doi.org/10.1203/PDR.0b013e318186e5dd

Alzheimer, A., 1911. Über eigenartige Krankheitsfälle des späteren Alters. Gesamte Neurol Psychiatr. 4, 385.

Arendt, T., Zveuintshva, H.G., Lkontovich, T.A., 1986. Dendritic changes in the basal nucleus of meynert and in the diagonal band nucleus in Alzheimer's disease-A quantitative Golgi investigation. Neuroscience 19. https://doi.org/10.1016/0306-4522(86)90141-7

Ashton, J.C., Friberg, D., Darlington, C.L., Smith, P.F., 2006. Expression of the cannabinoid CB2 receptor in the rat cerebellum: an immunohistochemical study. Neurosci. Lett. 396, 113–6. https://doi.org/10.1016/j.neulet.2005.11.038

Bhatia, V., Sharma, S., 2021. Role of mitochondrial dysfunction, oxidative stress and autophagy in progression of Alzheimer's disease. J. Neurol. Sci. https://doi.org/10.1016/j.jns.2020.117253

Borroto-Escuela, D.O., Brito, I., Romero-Fernandez, W., Di Palma, M., Oflijan, J., Skieterska, K., Duchou, J., Van Craenenbroeck, K., Suárez-Boomgaard, D., Rivera, A., Guidolin, D., Agnati, L.F., Fuxe, K., 2014. The G protein-coupled receptor heterodimer network (GPCR-HetNet) and its hub components. Int. J. Mol. Sci. 15, 8570–8590. https://doi.org/10.3390/ijms15058570

Callén, L., Moreno, E., Barroso-Chinea, P., Moreno-Delgado, D., Cortés, A., Mallol, J., Casadó, V., Lanciego, J.L., Franco, R., Lluis, C., Canela, E.I., McCormick, P.J., 2012. Cannabinoid receptors CB1 and CB2 form functional heteromers in brain. J. Biol. Chem. 287, 20851–65. https://doi.org/10.1074/jbc.M111.335273

Chen, T.-W., Wardill, T.J., Sun, Y., Pulver, S.R., Renninger, S.L., Baohan, A., Schreiter, E.R., Kerr, R.A., Orger, M.B., Jayaraman, V., Looger, L.L., Svoboda, K., Kim, D.S., 2013. Ultrasensitive fluorescent proteins for imaging neuronal activity. Nature 499, 295–300. https://doi.org/10.1038/nature12354

Chung, Y.C., Shin, W.-H.H., Baek, J.Y., Cho, E.J., Baik, H.H., Kim, S.R., Won, S.-Y.Y., Jin, B.K., 2016. CB2 receptor activation prevents glial-derived neurotoxic mediator production, BBB leakage and peripheral immune cell infiltration and rescues dopamine neurons in the MPTP model of Parkinson's disease. Exp. Mol. Med. 48, e205. https://doi.org/10.1038/emm.2015.100

Cilia, R., 2018. Molecular Imaging of the Cannabinoid System in Idiopathic Parkinson's Disease, in: International Review of Neurobiology. pp. 305–345. https://doi.org/10.1016/bs.irn.2018.08.004

Doucette, R., Fisman, M., Hachinski, V.C., Mersky, H., 1986. Cell Loss from the Nucleus Basalis of Meynert in Alzheimer's Disease. Can. J. Neurol. Sci. / J. Can. des Sci. Neurol. 13, 435–440. https://doi.org/10.1017/S0317167100037070

Etienne, P., Robitaille, Y., Wood, P., Gauthier, S., Nair, N.P.V., Quirion, R., 1986. Nucleus basalis neuronal loss, neuritic plaques and choline acetyltransferase activity in advanced Alzheimer's disease. Neuroscience 19, 1279–1291. https://doi.org/10.1016/0306-4522(86)90142-9

Ettcheto, M., Busquets, O., Espinosa-Jiménez, T., Verdaguer, E., Auladell, C., Camins, A., 2020. A Chronological Review of Potential Disease-Modifying Therapeutic Strategies for Alzheimer's Disease. Curr. Pharm. Des. 26, 1286–1299. https://doi.org/10.2174/1381612826666200211121416

Fernández-López, D., Pazos, M.R., Tolón, R.M., Moro, M.A., Romero, J., Lizasoain, I., Martínez-Orgado, J., 2007. The cannabinoid agonist WIN55212 reduces brain damage in an in vivo model of hypoxic-ischemic encephalopathy in newborn rats. Pediatr. Res. 62, 255–60. https://doi.org/10.1203/PDR.0b013e318123fbb8

Fernández-Ruiz, J., Sagredo, O., Pazos, M.R., García, C., Pertwee, R., Mechoulam, R., Martínez-Orgado, J., 2013. Cannabidiol for neurodegenerative disorders: important new clinical applications for this phytocannabinoid? Br. J. Clin. Pharmacol. 75, 323–333. https://doi.org/10.1111/j.1365-2125.2012.04341.x

Ferré, S., Baler, R., Bouvier, M., Caron, M.G.M.G., Devi, L.A.L.A., Durroux, T., Fuxe, K., George, S.R.S.R.S.R., Javitch, J.A.J.A.J. a, Lohse, M.J.M.J., Mackie, K., Milligan, G., Pfleger, K.D.G.K.D.G.G., Pin, J.P.J.-P.J.-P., Volkow, N.D.N.D., Waldhoer, M., Woods, A.S.A.S., Franco, R., 2009. Building a new conceptual framework for receptor heteromers. Nat. Chem. Biol. 5, 131–134. https://doi.org/10.1038/nchembio0309-131

Franco, R., Aguinaga, D., Jiménez, J., Lillo, J., Martínez-Pinilla, E., Navarro, G., 2018a. Biased receptor functionality versus biased agonism in G-protein-coupled receptors. Biomol. Concepts 9, 143–154. https://doi.org/10.1515/bmc-2018-0013

Franco, R., Aguinaga, D., Reyes, I., Canela, E.I., Lillo, J., Tarutani, A., Hasegawa, M., Del Ser-Badia, A., del Rio, J.A., Kreutz, M.R., Saura, C.A., Navarro, G., 2018b. N-Methyl-D-Aspartate Receptor Link to the MAP Kinase Pathway in Cortical and Hippocampal Neurons and Microglia Is Dependent on Calcium Sensors and Is Blocked by α-Synuclein, Tau, and Phospho-Tau in Non-transgenic and Transgenic APPSw,Ind Mice. Front. Mol. Neurosci. 11, 273. https://doi.org/10.3389/fnmol.2018.00273

Franco, R., Martínez-Pinilla, E., Lanciego, J.L.J.L.J.L.J.L., Navarro, G., 2016. Basic Pharmacological and Structural Evidence for Class A G-Protein-Coupled Receptor Heteromerization. Front. Pharmacol. 7:76. https://doi.org/10.3389/fphar.2016.00076

Franco, R., Rivas-Santisteban, R., Casanovas, M., Lillo, A., Saura, C.A., Navarro, G., 2020. Adenosine A2A Receptor Antagonists Affects NMDA Glutamate Receptor Function. Potential to Address Neurodegeneration in Alzheimer's Disease. Cells 9, 1075. https://doi.org/10.3390/cells9051075

Hradsky, J., Mikhaylova, M., Karpova, A., Kreutz, M.R., Zuschratter, W., 2013. Super-resolution microscopy of the neuronal calcium-binding proteins Calneuron-1 and Caldendrin. Methods Mol. Biol. 963, 147–69. https://doi.org/10.1007/978-1-62703-230-8_10

Lanciego, J.L., Barroso-Chinea, P., Rico, A.J., Conte-Perales, L., Callén, L., Roda, E., Gómez-Bautista, V., López, I.P., Lluis, C., Labandeira-García, J.L., Franco, R., 2011. Expression of the mRNA coding the cannabinoid receptor 2 in the pallidal

complex of Macaca fascicularis. J. Psychopharmacol. 25. https://doi.org/10.1177/0269881110367732
Lanciego, José L, Barroso-Chinea, P., Rico, A.J., Conte-Perales, L., Callén, L., Roda, E., Gómez-Bautista, V., López, I.P., Lluis, C., Labandeira-García, J.L., Franco, R., 2011. Expression of the mRNA coding the cannabinoid receptor 2 in the pallidal complex of Macaca fascicularis. J. Psychopharmacol. 25, 97–104. https://doi.org/10.1177/0269881110367732
Law, A.M.K., Yin, J.X.M., Castillo, L., Young, A.I.J., Piggin, C., Rogers, S., Caldon, C.E., Burgess, A., Millar, E.K.A., O'Toole, S.A., Gallego-Ortega, D., Ormandy, C.J., Oakes, S.R., 2017. Andy's Algorithms: new automated digital image analysis pipelines for FIJI. Sci. Rep. 7, 15717. https://doi.org/10.1038/s41598-017-15885-6
Lewerenz, J., Maher, P., 2015. Chronic glutamate toxicity in neurodegenerative diseases-What is the evidence? Front. Neurosci. https://doi.org/10.3389/fnins.2015.00469
Lipton, S., 2007. Pathologically-Activated Therapeutics for Neuroprotection: Mechanism of NMDA Receptor Block by Memantine and S-Nitrosylation. Curr. Drug Targets 8, 621–632. https://doi.org/10.2174/138945007780618472
Lipton, S.A., 2006. Paradigm shift in neuroprotection by NMDA receptor blockade: Memantine and beyond. Nat. Rev. Drug Discov. https://doi.org/10.1038/nrd1958
Micale, V., Mazzola, C., Drago, F., 2007. Endocannabinoids and neurodegenerative diseases. Pharmacol. Res. 56, 382–92. https://doi.org/10.1016/j.phrs.2007.09.008
Morales, P., Navarro, G., Gómez-Autet, M., Redondo, L., Fernández-Ruiz, J., Pérez-Benito, L., Cordomí, A., Pardo, L., Franco, R., Jagerovic, N., 2020. Discovery of Homobivalent Bitopic Ligands of the Cannabinoid CB2 Receptor**. Chem. - A Eur. J. 26, 15839–15842. https://doi.org/10.1002/chem.202003389
Mucke, L., Masliah, E., Yu, G.Q., Mallory, M., Rockenstein, E.M., Tatsuno, G., Hu, K., Kholodenko, D., Johnson-Wood, K., McConlogue, L., 2000. High-level neuronal expression of abeta 1-42 in wild-type human amyloid protein precursor transgenic mice: synaptotoxicity without plaque formation. J. Neurosci. 20, 4050–8. https://doi.org/20/11/4050 [pii]
Navarro, G., Borroto-Escuela, D., Angelats, E., Etayo, I., Reyes-Resina, I., Pulido-Salgado, M., Rodríguez-Pérez, A., Canela, E., Saura, J., Lanciego, J.L., Labandeira-García, J.L., Saura, C.A., Fuxe, K., Franco, R., 2018. Receptor-heteromer mediated regulation of endocannabinoid signaling in activated microglia. Role of CB1 and CB2 receptors and relevance for Alzheimer's disease and levodopa-induced dyskinesia. Brain. Behav. Immun. 67, 139–151. https://doi.org/10.1016/j.bbi.2017.08.015
Navarro, G., Morales, P., Rodríguez-Cueto, C., Fernández-Ruiz, J., Jagerovic, N., Franco, R., 2016. Targeting Cannabinoid CB2 Receptors in the Central Nervous System. Medicinal Chemistry Approaches with Focus on Neurodegenerative Disorders. Front. Neurosci. 10. https://doi.org/10.3389/fnins.2016.00406
Navarro, G., Varani, K., Lillo, A., Vincenzi, F., Rivas-Santisteban, R., Raïch, I., Reyes-Resina, I., Ferreiro-Vera, C., Borea, P.A., Sánchez de Medina, V., Nadal, X., Franco, R., 2020. Pharmacological data of cannabidiol- and cannabigerol-type phytocannabinoids acting on cannabinoid CB1, CB2 and CB1/CB2 heteromer receptors. Pharmacol. Res. 159, 104940. https://doi.org/10.1016/j.phrs.2020.104940
Newell, E., Exo, J., Verrier, J., Jackson, T., Gillespie, D., K Janesko-Feldman, Kochanek, P., Jackson, E., 2015. 2',3'-cAMP, 3'-AMP, 2'-AMP and adenosine inhibit TNF-α and CXCL10 production from activated primary murine microglia

via A2A receptors. Brain Res. 1594, 27–35. https://doi.org/doi: 10.1016/j.brainres.2014.10.059
Pazos, M.R.R., Mohammed, N., Lafuente, H., Santos, M., Martínez-Pinilla, E., Moreno, E., Valdizan, E., Romero, J., Pazos, A., Franco, R., Hillard, C.J.C.J., Alvarez, F.J.F.J., Martínez-Orgado, J., 2013. Mechanisms of cannabidiol neuroprotection in hypoxic-ischemic newborn pigs: Role of 5HT1A and CB2 receptors. Neuropharmacology 71, 282–291. https://doi.org/10.1016/j.neuropharm.2013.03.027
Pérez, M., Valpuesta, J.M., Medina, M., Montejo de Garcini, E., Avila, J., 2002. Polymerization of τ into Filaments in the Presence of Heparin: The Minimal Sequence Required for τ - τ Interaction. J. Neurochem. 67, 1183–1190. https://doi.org/10.1046/j.1471-4159.1996.67031183.x
Reyes-Resina, I., Navarro, G., Aguinaga, D., Canela, E.I., Schoeder, C.T., Załuski, M., Kieć-Kononowicz, K., Saura, C.A., Müller, C.E., Franco, R., 2018. Molecular and functional interaction between GPR18 and cannabinoid CB2G-protein-coupled receptors. Relevance in neurodegenerative diseases. Biochem. Pharmacol. In the Press. https://doi.org/10.1016/j.bcp.2018.06.001
Rodríguez-Cueto, C., Santos-García, I., García-Toscano, L., Espejo-Porras, F., Bellido, Ml., Fernández-Ruiz, J., Muñoz, E., de Lago, E., 2018. Neuroprotective effects of the cannabigerol quinone derivative VCE-003.2 in SOD1G93A transgenic mice, an experimental model of amyotrophic lateral sclerosis. Biochem. Pharmacol. 157, 217–226. https://doi.org/10.1016/j.bcp.2018.07.049
Sánchez, A.J., García-Merino, A., 2012. Neuroprotective agents: Cannabinoids. Clin. Immunol. 142, 57–67. https://doi.org/10.1016/j.clim.2011.02.010
Sierra, S., Luquin, N., Rico, A.J., Gómez-Bautista, V., Roda, E., Dopeso-Reyes, I.G., Vázquez, A., Martínez-Pinilla, E., Labandeira-García, J.L., Franco, R., Lanciego, J.L., 2015. Detection of cannabinoid receptors CB1 and CB2 within basal ganglia output neurons in macaques: changes following experimental parkinsonism. Brain Struct. Funct. 220, 2721–38. https://doi.org/10.1007/s00429-014-0823-8
Stazi, M., Wirths, O., 2021. Chronic Memantine Treatment Ameliorates Behavioral Deficits, Neuron Loss, and Impaired Neurogenesis in a Model of Alzheimer's Disease. Mol. Neurobiol. 58, 204–216. https://doi.org/10.1007/s12035-020-02120-z
Stella, N., 2010. Cannabinoid and cannabinoid-like receptors in microglia, astrocytes, and astrocytomas. Glia 58, 1017–1030. https://doi.org/10.1002/glia.20983
Tarutani, A., Suzuki, G., Shimozawa, A., Nonaka, T., Akiyama, H., Hisanaga, S.I., Hasegawa, M., 2016. The effect of fragmented pathogenic α-synuclein seeds on prion-like propagation. J. Biol. Chem. 291, 18675–18688. https://doi.org/10.1074/jbc.M116.734707
Ulm, B.S., Borchelt, D.R., Moore, B.D., 2021. Remodeling Alzheimer-amyloidosis models by seeding. Mol. Neurodegener. 16, 8. https://doi.org/10.1186/s13024-021-00429-4
van der Stelt, M., Di Marzo, V., 2005. Cannabinoid receptors and their role in neuroprotection. Neuromolecular Med. 7, 37–50. https://doi.org/10.1385/NMM:7:1-2:037
Wang, Q., Li, W.-X., Dai, S.-X., Guo, Y.-C., Han, F.-F., Zheng, J.-J., Li, G.-H., Huang, J.-F., 2017. Meta-Analysis of Parkinson's Disease and Alzheimer's Disease Revealed Commonly Impaired Pathways and Dysregulation of NRF2-Dependent Genes. J. Alzheimers. Dis. 56, 1525–1539. https://doi.org/10.3233/JAD-161032
Wang, R., Reddy, P.H., 2017. Role of Glutamate and NMDA Receptors in Alzheimer's

Disease. J. Alzheimer's Dis. 57, 1041–1048. https://doi.org/10.3233/JAD-160763
Wu, J., Bie, B., Yang, H., Xu, J.J., Brown, D.L., Naguib, M., 2013. Activation of the CB2 receptor system reverses amyloid-induced memory deficiency. Neurobiol. Aging 34, 791–804. https://doi.org/10.1016/j.neurobiolaging.2012.06.011

RESUMEN DE RESULTADOS Y DISCUSIÓN

4. Resumen de resultados y discusión

Desde hace varios años la señalización mediada a través de GPCRs y de sus agrupaciones oligoméricas, que constituyen nuevas unidades funcionales, tiene un papel protagonista como diana farmacológica de múltiples patologías, incluidas las enfermedades neurodegenerativas.

La acción de los receptores GPCR puede ser modulada de diferentes maneras dependiendo del contexto celular. La señalización mediada por GPCRs no sólo depende de la proteína G acoplada, sino de otras moléculas capaces de interactuar con el receptor y/o con la maquinaria de señalización (Brady and Limbird 2002).

El agonismo sesgado, uno de los enfoques recientes y más prometedores para el descubrimiento de fármacos, es especialmente relevante para los receptores cannabinoides, cuyo desarrollo farmacológico se ve obstaculizado tanto por la naturaleza hidrofóbica de los agonistas como por la estructura particular de los receptores, resuelta para el CB_1R (Hua et al. 2016, 2017) y para el CB_2R (Li et al. 2019).

El estudio del *apartado 3.1* se centró, en primer lugar, en comparar en un modelo heterólogo de expresión el agonismo sesgado de una batería de compuestos cannabinoides sobre los receptores CB_1 y CB_2 utilizando como referencia un agonista sintético (la ACEA para células que únicamente expresaban el CB_1R o el heterómero de receptores CB_1-CB_2, y el JWH-133 como referencia para células que expresaban únicamente el CB_2R). Se demostró que todos los agonistas utilizados excepto el Δ^9-THC, mostraban un agonismo sesgado más marcado para el CB_1R que para el CB_2R. Los resultados obtenidos relativos al Δ^9-THC fueron inesperados, por un lado, el sesgo en CB_1R fue similar al de otro compuesto psicoactivo, el CP-55940. Y, por otro lado, la acción del Δ^9-THC en CB_2R se encuentra claramente sesgada hacia la fosforilación de ERK1/2, el reclutamiento de β-arrestina y la redistribución dinámica de masas (DMR). Curiosamente, esta tendencia en las células que expresan CB_2R se correlaciona con un aparente fracaso en el acoplamiento a $G\alpha_i$ cuando el receptor es activado por el Δ^9-THC. Hay controversia en torno a la acción del Δ^9-THC en CB_2R, en algunos estudios señaliza a través de $G\alpha_i$ (Felder et al. 1995; Iwamura et al. 2001) mientras que en otros estudios, y en línea con nuestros resultados, el Δ^9-THC no se acopla a $G\alpha_i$ a través de CB_2R (Slipetz et al. 1995). En ellos se demuestra que el Δ^9-THC a concentraciones entre 10 nM y 1 μM no fue capaz de inhibir los niveles de AMPc inducidos por la forskolina en células COS-7 y CHO transfectadas con CB_2R (Bayewitch et al. 1995). Las posibilidades para explicar las discrepancias son, entre otras, i) la señalización acoplada a $G\alpha_i$ podría deberse a que el Δ^9-THC actúa sobre el CB_1R y no sobre el CB_2R, ii) hay otro receptor que responde al Δ^9-THC a través de $G\alpha_i$ o iii) las altas concentraciones utilizadas (por ejemplo, 10-50 μM (Jeon et al. 1996)) están proporcionando efectos inespecíficos que resultan en la disminución de los niveles de AMPc inducidos por la forskolina. Los estudios de caracterización funcional realizados en paralelo demostraron que el acoplamiento a la proteína $G\alpha_i$ no se produce en el caso del CB_2R pero sí en el caso del CB_1R, es decir, el Δ^9-THC se comporta en el CB_1R como un potente agonista completo capaz de disminuir los niveles de AMPc inducidos por la forskolina.

La modulación alostérica sesgada, es decir, el agonismo sesgado en presencia de un modulador alostérico del CB_1R fue estudiado en el estudio de (Khajehali et al. 2015). Sus resultados demostraron que el modulador Org27569 bloqueó principalmente los efectos mediados por $G\alpha_i$. En cambio, Org27569 no afectó a la fosforilación de ERK inducida por algunos de los agonistas de CB_1R. Del mismo modo en nuestros estudios en los *apartados 3.1 y 3.2* analizamos el efecto modulador de los fitocannabinoides CBD y CBG sobre los receptores CB_1 y CB_2. Los resultados obtenidos destacan el importante papel del CBD y del CBG en la regulación de la señalización de los cannabinoides. Estudios recientes han demostrado que el CBD afecta a la señalización mediada por el CB_1R (Laprairie et al. 2015) y el CB_2R (Martínez-Pinilla et al. 2017), probablemente mediante la unión a un sitio alostérico. A partir de los datos de estos dos trabajos, se deduce que el sitio alostérico de los receptores CB_1 y CB_2 tienen una localización diferente.

Es atractivo especular que el CBD puede estar afectando a los receptores CB_1, CB_2 y eventualmente a otros GPCRs al interactuar con las interfaces lípidicas del receptor. Esta hipótesis podría explicar el cúmulo de efectos reportados para el CBD; aunque en todos los casos, la unión al sitio ortostérico ocurre a concentraciones micromolares, es decir, demasiado elevadas para ser de relevancia fisiológica. Hay que tener en cuenta que la concentración de CBD utilizada en esta Tesis doctoral donde se observan resultados significativos fue de 100 nM.

Sorprendentemente, nuestros hallazgos demuestran que la selectividad funcional inducida por los agonistas (Δ^9-THC, PM224, Anandamida y CP55940) se reduce cuando los receptores cannabinoides forman complejos heteroméricos. Los resultados sugieren que el complejo heteroreceptor se encuentra estrechamente acoplado a la maquinaria de señalización, con menos posibilidades de señalización sesgada. De hecho, en las células que expresan el heterómero de receptores CB_1-CB_2, el Δ^9-THC tampoco puede modificar significativamente los niveles de AMPc inducidos por la forskolina. En conjunto, estos resultados son importantes, ya que demuestran que existe un vínculo directo entre la señalización mediada por $G\alpha_i$ y la activación de las MAPK (Goldsmith and Dhanasekaran 2007), que puede ser comprometida por el Δ^9-THC actuando sobre el CB_1R pero no sobre el CB_2R o sobre los complejos heterómeros CB_1R-CB_2R. También fue relevante el hallazgo de una mayor funcionalidad cuando las células que coexpresaban los dos receptores fueron pretratadas con el CBD. Este resultado puede explicar algunos de los datos controvertidos sobre si el fitocannabinoide interactúa o no con los receptores cannabinoides. Podemos concluir que la acción inducida por el CBD puede ser consecuencia de la unión a un sitio alostérico en ambos receptores, como se sugiere en los dos trabajos mencionados (Laprairie et al. 2015; Martínez-Pinilla et al. 2017). El efecto del CBD sobre las acciones de la anandamida en ambos receptores cannabinoides fue particularmente notable, potenciando el reclutamiento de ß-arrestinas.

En definitiva, el descubrimiento de fármacos cannabinoides puede aprovechar la modulación de la selectividad funcional por parte del CBD y del CBG.

Por otra parte, y de forma similar a nuestro trabajo anterior, el objetivo principal del estudio del *apartado 3.2* era abordar comparativamente la farmacología del CBG y sus efectos sobre los receptores CB_1 y CB_2, y sobre el heterómero de receptores CB_1-CB_2. Se efectuaron experimentos de unión mediante ensayos basados en ligandos radiomarcados y no radiomarcados en el CB_2R que indican que el CBG actúa como un ligando agonista parcial competitivo. Teniendo en cuenta nuestros resultados, la hipótesis más razonable es pensar que el CBG se une al centro ortostérico del CB_2R. Cabe señalar que las diferencias en la afinidad encontradas según el tipo de ensayo pueden deberse al hecho de que la unión obtenida mediante fluorescencia homogénea resuelta en el tiempo (HTRF) se realiza en células vivas, mientras que los ensayos de unión por radioligando se realizan en membranas aisladas. Por otra parte, los resultados obtenidos de la unión del CBG al CB_1R tienen una interpretación más compleja. La Ki obtenida para la unión al CB_1R utilizando el [3H]-CP-55940 se encuentra en el rango micromolar, como ocurrió con los datos de la unión del radioligando al CB_2R. Sin embargo, el CBG no pudo competir con la unión del [3H]-WIN-55,212-2 al CB_1R. Teniendo en cuenta que los sitios de reconocimiento para el CP-55940 y el WIN-55,212-2 no son idénticos en el CB_1R, una posibilidad es que el CBG se una al centro ortostérico pero mostrando parámetros de unión de equilibrio diferentes dependiendo del radioligando. En otras palabras, el CBG fue capaz de distinguir entre dos subregiones del centro ortostérico en el CB_1R. En consecuencia, el CBG podría actuar sobre el CB_1R (pero no sobre el CB_2R) como modulador no competitivo alostérico, como se ha descrito para el CBD (Laprairie et al. 2015). Hay que considerar que la afinidad de un compuesto puede variar en función del contexto del receptor, por las limitaciones de la membrana, la heteromerización o la interacción con las proteínas G, entre otras causas.

En las células HEK-293T que expresaban el CB_1R, la señalización mediada por el CBG está sesgada hacia la vía mediada por $G\alpha_i$. Esto concuerda con nuestro hallazgo de un efecto significativo en ensayos de DMR; ya que es frecuente que las señales de DMR se correlacionen con la alteración en

los niveles de AMPc en el caso de los receptores acoplados a proteínas $G\alpha_i$ y $G\alpha_s$ (Grundmann and Kostenis 2015a, 2015b; Hamamoto, Kobayashi, and Saito 2015). Tomando en conjunto todos los resultados, se puede concluir que una acción alostérica del CBG sobre el CB_1R no explicaría por qué es capaz de promover la señalización mediada por $G\alpha_i$.

Por otra parte, los datos de los ensayos funcionales mediados por CB_2R fueron más fáciles de interpretar. En primer lugar, la eficacia del CBG fue menor en comparación con los agonistas sintéticos selectivos y los endocannabinoides. Además, el CBG produjo un agonismo sesgado, con un efecto pequeño sobre los niveles de AMPc y bastante marcado en la fosforilación de ERK1/2 y el reclutamiento de β-arrestinas. Por lo tanto, el CBG actuó como un agonista parcial y, como tal, fue capaz de reducir los efectos inducidos por otros agonistas cannabinoides. Obteniendo resultados similares tanto a una concentración de 1 μM como a 100 nM.

Debido a la compleja farmacología de los cannabinoides, los ensayos funcionales de determinación de AMPc intracelular, detección de fosforilación de ERK1/2, reclutamiento de ß-arrestinas y ensayos de la DMR se llevaron a cabo para investigar si el CBG pudiera estar ejerciendo una acción moduladora sobre el heterómero CB_1R-CB_2R. En esta Tesis se ha descrito la complejidad de la interacción CB_1R-CB_2R, mientras que en el estudio de (Callén et al. 2012) mostraron una interacción cruzada negativa en un sistema de expresión heterólogo, la interacción alostérica en el complejo CB_1R-CB_2R se convierte en un efecto sinérgico cuando los cultivos primarios de microglía son activados (tratada con LPS y IFN-γ) y en cultivos primarios de microglía de un modelo transgénico de la enfermedad de Alzheimer (Gemma Navarro, Borroto-Escuela, et al. 2018). Los experimentos de dosis respuesta realizados en nuestro estudio mostraron que el tratamiento con el CBG en ausencia de cualquier otro agonista, condujo a efectos aditivos/sinérgicos sobre el AMPc y en ensayos de la DMR. Por el contrario, en la fosforilación de ERK y el reclutamiento de β-arrestina, encontramos el cross-talk negativo ya descrito para este heterómero cuando se utilizan agonistas completos para activar los receptores (Callén et al. 2012). Estos resultados sugieren que el agonismo parcial en el CB_2R está regulado por la presencia del CB_1R. Teniendo en cuenta los resultados obtenidos, el CBG modula significativamente la acción endocannabinoide mediada por CB_2R o CB_1R-CB_2R, mientras que los efectos son débiles en las células que expresan únicamente CB_1R.

En conclusión, los resultados presentados en este estudio revelan que el fitocannabinoide no psicotrópico CBG puede ejercer acciones beneficiosas con potencial terapéutico a través de los receptores cannabinoides.

Se ha demostrado que algunos compuestos cannabinoides pueden unirse y activar la funcionalidad del receptor GPR55 (Moriconi et al. 2010). La regulación que ejerce sobre los receptores CB_1 y CB_2 puede ser clave para el desarrollo de nuevas estrategias terapéuticas. Es por ello por lo que en nuestra investigación en los *apartados 3.3 y 3.4* nos centramos en analizar la expresión de los complejos heteroméricos CB_1-GPR55 y CB_2-GPR55 en distintas regiones cerebrales en un modelo animal de primate.

El mapeo de los receptores ionotrópicos y metabotrópicos en el SNC fue uno de los logros fundamentales para conocer las bases moleculares que rigen los neurotransmisores y los circuitos cerebrales. Del mismo modo, el mapeo de los receptores dopaminérgicos y las neuronas productoras de dopamina permitió proponer un primer modelo de control motor, constituido básicamente por neuronas dopaminérgicas en la *substantia nigra*, las vías de los ganglios basales (BG) y las neuronas de salida del BG que se proyectan al tálamo (Wooten et al. 1997). La información de entrada (procedente principalmente de las proyecciones glutamatérgicas corticoestriatales y tálamo-estriatales) se procesa a nivel del cuerpo estriado a través de las neuronas espinosas medianas (MSN) gabaérgicas y las interneuronas estriatales (Chang and Kita 1992; Kaneko et al. 1993; Kita, Kosaka, and Heizmann 1990).

El modelo más sencillo de control motor considera dos vías estriatales, conocidas como la vía directa y la vía indirecta. La primera contiene neuronas que expresan receptores de dopamina D_1 y se proyectan "directamente" a la división interna del globo pálido (GPi), y la segunda contiene neuronas que expresan receptores de dopamina D_2 y se proyectan "indirectamente" a la división externa del globo pálido (GPe). El modelo también fue cuestionado por el descubrimiento de neuronas de proyección que contienen tanto receptores D_1 como D_2 y que pueden interactuar para formar heterómeros D_1-D_2 en roedores y primates (Hasbi et al. 2009; Perreault et al. 2016; Rico et al. 2017). Como cabría esperar, el circuito de control motor del BG es más complejo en los primates que en los roedores. En los seres humanos, la desregulación de todo el sistema por la falta de producción de dopamina, debido a la muerte progresiva de las neuronas dopaminérgicas nigroestriatales, da lugar a la aparición de los síntomas motores cardinales que caracterizan típicamente a la enfermedad de Parkinson (PD).

La evidencia acumulada durante las últimas dos décadas usando modelos animales de PD sostuvo el potencial terapéutico de los cannabinoides como fármacos para combatir los síntomas de la PD y para retrasar la progresión de la enfermedad (Fernández-Ruiz, Moro, and Martínez-Orgado 2015; Sagredo et al. 2007) ya que los compuestos cannabinoides se dirigen al CB_1R y regulan la función del GPR55 y, además, estos dos GPCRs pueden interactuar para formar nuevas unidades funcionales.

Mediante ensayos de PLA se abordó la expresión del heterómero CB_1R-GPR55 en los diferentes tipos neuronales existentes en el estriado del primate no humano, un animal experimental muy valioso para el estudio de la PD. Es necesario considerar que se requiere un mayor esfuerzo de investigación para determinar los posibles cambios, si los hay, en los niveles de expresión del heterómero CB_1R-GPR55 en animales parkinsonianos (con o sin disquinesia inducida por el tratamiento con la levodopa). Nuestros resultados muestran que el heterómero CB_1R-GPR55 se expresa en todos los tipos de células neuronales, excepto en las interneuronas colinérgicas ($ChAT^+$). La presencia del heterómero CB_1R-GPR55 en las neuronas de proyección marcadas con dextrano amina biotinilada (BDA) indica que se expresan en las MSN que proyectan al GPi y/o al GPe. Puntualizar que en las neuronas de proyección, el heterómero CB_1R-GPR55 se encontró en el soma de la célula, y no en las dendritas. Las interneuronas estriatales positivas para la parvalbúmina (PV), la calretinina (CR) y la óxido nítrico sintasa (nNOS) también expresaban el heterómero CB_1R-GPR55. La mayor expresión de este heterómero se encontró en las interneuronas PV^+, seguidas de las interneuronas CR^+ y luego de las interneuronas $nNOS^+$.

La expresión generalizada del CB_1R era de esperar, ya que se considera el GPCR con mayor presencia en las neuronas del SNC. Sin embargo, los hallazgos sobre el receptor GPR55 son muy novedosos, ya que no se había descrito previamente su mapeo a nivel individual. Curiosamente, se identificó el heterómero CB_1R-GPR55 tanto en la superficie celular neuronal como en localizaciones intracelulares. Aunque existen muy pocos estudios que demuestren la presencia de GPCRs en localizaciones distintas a la superficie celular, el CB_1R ha sido identificado en las mitocondrias, donde regula el metabolismo energético (Bénard et al. 2012; Gutiérrez-Rodríguez et al. 2018; Hebert-Chatelain et al. 2014; Melser et al. 2017). Aunque es necesario seguir investigando y mejorando las técnicas que permitan describir la localización subcelular de los complejos heteroméricos de receptores, la localización intracelular del heterómero CB_1R-GPR55 sugiere un papel funcional independiente del control mediado por el receptor cannabinoide de liberación de neurotransmisores en los terminales de los axones.

Continuando con lo estudiado en las investigaciones del *apartado 3.3 y 3.4* nos planteamos detectar si en el parkinsonismo se produce una alteración de la expresión de los heterómeros CB_1R -GPR55 y/o CB_2R-GPR55.

Mediante ensayos de PLA obtuvimos unos resultados que muestran que la expresión de ambos heterómeros fue significativamente mayor en el modelo primate tratado con el 1-metil-4-fenil1,2,3,6-tetrahidropiridina (MPTP), para la inducción de la PD, en todos los núcleos analizados (caudado,

putamen y accumbens). En este modelo de PD se ha descrito el aumento de la expresión estriatal de forma similar para otros heterómeros formados por los receptores de dopamina D_1, histamina H_3 y NMDA (Rodríguez-Ruiz et al. 2017). También es interesante la disminución detectada de ambos heterómeros cuando los animales parkinsonianos se vuelven discinéticos tras el tratamiento crónico con levodopa; una alteración similar se ha demostrado para los complejos heteroméricos de $A_{2A}R/D_2R/CB_1R$ (Armentero et al. 2011; Pinna et al. 2014). Por el contrario, también hay publicaciones que han reportado un aumento en la expresión de ciertos heterómeros en modelos de PD que presentan discinesias, como por ejemplo el heterómero de receptores de dopamina D_1-D_3 en macacos discinéticos (Fuxe et al. 2015; Marcellino et al. 2008).

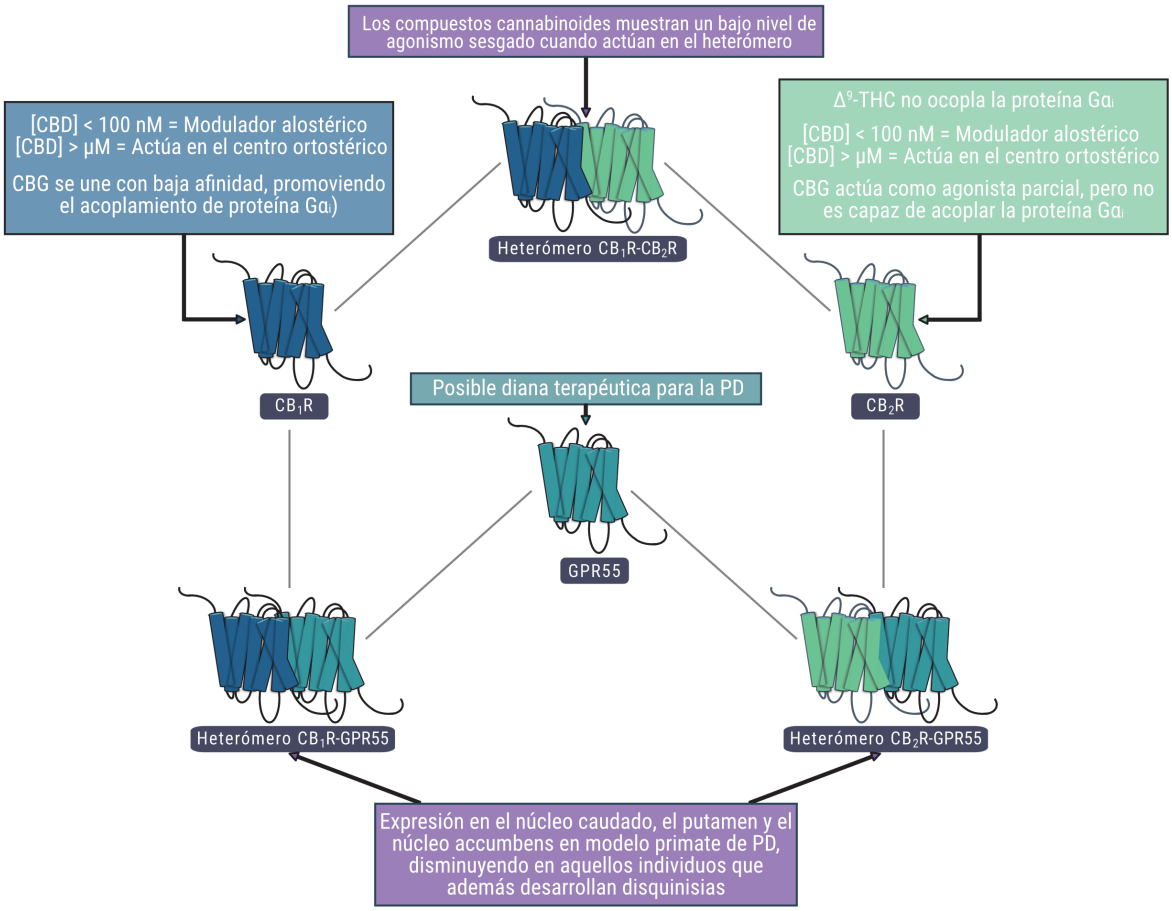

Figura 21. Resumen gráfico: los receptores cannabinoides como posible diana terapéutica.

Para el desarrollo de fármacos, el CB_1R se consideró en primer lugar como mejor alternativa que el CB_2R, debido a su mayor expresión en las neuronas. Sin embargo, los potenciales efectos psicotrópicos de los fármacos que actúan sobre el CB_1R junto al incremento en los niveles de expresión del receptor CB_2 en procesos inflamatorios, han llevado a centrar más la atención en el receptor CB_2 como diana terapéutica. Nuestros resultados indicaron que, para contrarrestar el aumento de la expresión del receptor asociado a la PD, la intervención más adecuada sería el uso de antagonistas del CB_1R y/o del GPR55. Mientras que el GPR55 ha sido poco abordado en el descubrimiento de fármacos, los graves efectos secundarios del rimonabant, un antagonista del CB_1R, llevaron a los organismos reguladores a retirar del mercado este fármaco contra la obesidad (Christensen et al. 2007). Por otra parte, las miradas se centraron en CB_2R basándose, principalmente, en su beneficiosa capacidad para regular la microglía hacia un fenotipo antiinflamatorio M2 (Navarro et al. 2016; Palomo-Garo et al. 2016; Price et al. 2009). En este sentido, pueden ser de gran utilidad los agonistas de CB_2R y los moduladores alostéricos como el cannabidiol, un fitocannabinoide muy seguro (Fernández-Ruiz et al. 2011; Gemma Navarro, Reyes-Resina, et al.

2018; Pertwee 2012). A día de hoy, en lo que respecta al GPR55, es importante señalar que la afinidad, la potencia y la selectividad de los fitocannabinoides y cannabinoides sintéticos son inconsistentes entre los estudios publicados. El GPR55 muestra las características más singulares, ya que parece actuar principalmente a través de la familia de proteínas $G\alpha_{12/13}$ y RhoA (Ryberg et al. 2007), pero también puede acoplarse a otras proteínas G (Waldeck-Weiermair et al. 2008). Utilizando diferentes ensayos homogéneos, (Anavi-Goffer et al. 2012) publicaron que ciertos cannabinoides pueden tanto activar el GPR55 como atenuar la fosforilación de ERK1/2 mediada por lisofosfatidilinositol (LPI), concluyendo que "los ligandos cannabinoides tienen una interacción compleja con el sistema de señalización LPI/GPR55" (Anavi-Goffer et al. 2012). Por ello, es necesario un mayor esfuerzo experimental para descifrar la forma más conveniente de abordar al GPR55 como diana terapéutica, es decir, comprobar que compuestos se unen con mayor eficacia al mismo, como afectan a su señalización y, finalmente, si su uso terapéutico es realmente eficaz y seguro.

La variada farmacología a menudo reportada para CB_1R y CB_2R, y de manera aún más extrema para GPR55, hace que estos receptores sean excelentes candidatos para demostrar que la heteromerización influye en la farmacología y el acoplamiento a las distintas vías de señalización. En concreto, nuestros resultados abren nuevas perspectivas para abordar un nuevo tratamiento, no dopaminérgico, para los pacientes con la PD.

Los avances en el conocimiento del RAS periférico han sido fundamentales para desarrollar una terapia exitosa para combatir la hipertensión. Por otra parte, el entendimiento del RAS en el SNC es todavía limitado, pero con claras implicaciones en la neurotransmisión dopaminérgica. Este hecho ofrece a la señalización mediada por los receptores del RAS, con un gran potencial terapéutico contra la PD. Así, en las investigaciones realizadas en los *apartados 3.5 y 3.6* se describen las posibles interacciones entre los receptores del RAS AT_1, AT_2 y MasR, y se descifran las propiedades funcionales de las unidades resultantes de las interacciones receptor-receptor. Los ensayos realizados muestran comportamientos diferenciales en función de la vía de señalización y de las interacciones entre receptores.

Las alteraciones del equilibrio del RAS al envejecer afectan a casi cualquier proceso fisiológico. El RAS es clave en la regulación de procesos homeostáticos tanto en la periferia, como en los riñones y los pulmones; como en el SNC, en el cerebro. El desequilibrio del RAS al envejecer se considera una oportunidad para intervenir utilizando ligandos de los receptores del RAS para combatir diferentes enfermedades. Se ha descrito como el desbalance del RAS, estrictamente regulado en condiciones normosaludables, supone la aparición progresiva de enfermedades como la hipertensión (Sun et al. 2015) o la nefropatía diabética (Rubio-Ruíz et al. 2014). Además, el RAS se desregula en las enfermedades de Parkinson (PD) y Alzheimer (AD), siendo las enfermedades neurodegenerativas más frecuentes relacionadas con el envejecimiento del SNC (Hornykiewicz 2006; Oertel 1995; Rocca 1994).

Uno de los valores añadidos de cualquier terapia basada en el RAS y dirigida a la PD es la seguridad de los antagonistas de los receptores de angiotensina que se han utilizado durante décadas en pacientes hipertensos. En contraposición, una dificultad es el hecho de que no todos los fármacos son capaces de atravesar la barrera hematoencefálica. Se sugiere que los antagonistas ya utilizados en la hipertensión y capaces de atravesar la barrera hematoencefálica también podrían ser utilizados para la terapia de la PD (Kirik, Winkler, and Björklund 2001). Sin embargo, quedan incógnitas por resolver sobre los beneficios concretos que estos antagonistas pueden aportar para paliar los síntomas de la PD, como evitar las discinesias inducidas por la levodopa (L-DOPA) y/o retrasar la progresión de la enfermedad.

En primer lugar, se ha descrito que los efectos globales de la señalización mediada por los receptores AT_1 y AT_2 son opuestos. En varios tejidos, la hiperactividad del receptor AT_1 se ha relacionado con cambios proinflamatorios relacionados con el envejecimiento (Villar-Cheda et al. 2014). Por el contrario, la señalización mediada por AT_2R se ha reportado con propiedades antiinflamatorias (Bhat

et al. 2019). Se han propuesto diferentes mecanismos para explicar los efectos contrarios a los mediados por los receptores AT_1 que desencadena la activación de los receptores AT_2 (Padia and Carey 2013; Patel and Hussain 2018). Aunque la cuestión es compleja, la expresión de AT_2R en el cerebro aumenta en procesos inflamatorios por lo que tiene un papel relevante de este receptor en la regulación de la neuroinflamación, gracias a su potente función antiinflamatoria. En nuestros experimentos realizados con microglía estriatal activada (tratada con LPS y IFN-γ) la señalización mediada por las MAP quinasas se ve suprimida mediante el tratamiento combinado con agonistas de los receptores AT_1 y AT_2.

Los receptores AT_1, AT_2 (Porrello et al. 2011) y Mas del RAS (Rabie et al. 2020), se encuentran expresados en los ganglios basales del estriado cerebral. Precisamente, el cuerpo estriado es la zona cerebral que sufre un mayor deterioro en la PD. En este sentido, en esta Tesis doctoral hemos focalizado el estudio del RAS hacia la búsqueda de nuevas estrategias para combatir esta enfermedad.

Por una parte, en nuestros estudios demostramos mediante ensayos de PLA en un modelo de rata, la expresión del heterómero AT_1R-AT_2R en células estriatales y su regulación al alza correlacionada con la aparición de la PD y con el tratamiento posterior con la L-DOPA, el agente terapéutico más extendido en la PD (Hornykiewicz 2017). Del mismo modo, en nuestros resultados observamos que los niveles de expresión de los heterómeros que contienen MasR (AT_1R-MasR y AT_2R-MasR), también se ve incrementada en células estriatales del modelo animal de la PD en comparación a los animales control y, aún de forma más acusada, en animales tratados con L-DOPA. El marcado aumento de los heterómeros AT_1R-MasR en los animales discinéticos abre nuevas vías terapéuticas para combatir este conocido efecto secundario de la medicación antiparkinsoniana. Es una evidencia que existe una alteración en la expresión de los heterómeros que contienen receptores de dopamina en la PD, bien en una o en diferentes etapas de la enfermedad. Por lo general, la expresión de estos heterómeros (por ejemplo D_1R-D_3R) en la discinesia es menor que en los animales con PD tratados con L-DOPA pero que no presentan discinesias. Estos resultados son relevantes debido al potencial rol de los antagonistas de la angiotensina tanto para mejorar los síntomas de la PD como para minimizar las discinesias inducidas por la L-DOPA.

La estrategia para mejorar la fisiopatología de la PD y detener en cierta medida la progresión de la enfermedad es retrasar la muerte del aproximadamente 30% de las neuronas dopaminérgicas nigroestriatales que quedan en el momento del diagnóstico de la PD. La microglía en lo que se refiere a la neuroinflamación, es clave para preservar las neuronas de la muerte. La señalización mediada por AT_1R es potenciadora del fenotipo proinflamatorio de la microglía, por lo que el bloqueo de los receptores AT_1 se ha propuesto con el objetivo de reducir la neuroinflamación crónica (Jarrott and Williams 2016; Joglar et al. 2009) como la que ocurre en la PD. Hay consenso entre la comunidad científica que describe la activación de los receptores AT_1 como perjudicial, por ejemplo, la hiperactivación de AT_1R supone un aumento de la pérdida neuronal mediada por la microglía en el estado epiléptico inducido en ratas (Sun et al. 2015). Por otra parte, la activación de los receptores AT_2 y Mas (Labandeira-Garcia et al. 2017) atenúa la activación de la microglía proinflamatoria, siendo por ello estos receptores beneficiosos para disminuir procesos inflamatorios exacerbados. Un ejemplo de estas propiedades antiinflamatorias mediadas por los receptores AT_2 y Mas se describe en un modelo de roedor de encefalomielitis autoinmune (Valero-Esquitino et al. 2015). El informe (Bennion et al. 2017) demuestra que la activación del receptor AT_2 en las neuronas y las células gliales proporciona una neuroprotección a largo plazo en el ictus, tanto por mecanismos directos como indirectos. Del mismo modo, las terapias relacionadas con la activación del MasR para retrasar la progresión de la PD deberían considerar los componentes del RAS en la microglía, con el objetivo final de atenuar la inflamación o sesgar la microglía hacia el fenotipo neuroprotector y antiinflamatorio M2 (Franco and Fernández-Suárez 2015).

Uno de los hallazgos relevantes en nuestro trabajo es la incapacidad del AT_2R para disminuir los niveles intracelulares de AMPc en las neuronas estriatales cuando se tratan con un agonista selectivo

(CGP-42112a). Sin embargo, y de manera notable, el receptor AT_2 se volvió funcional en presencia de candesartán, el antagonista selectivo del AT_1R. Por lo tanto, el tratamiento con antagonistas del AT_1R en las neuronas estriatales puede conseguir dos efectos beneficiosos, que consisten en reprimir las señalización perjudicial mediada por el AT_1R y permitir al AT_2R recuperar su funcionalidad, con los beneficios asociados a su activación. Este fenómeno se debe a las interacciones proteína-proteína entre los receptores del heterómero AT_1R-AT_2R, donde el receptor AT_1 actúa bloqueando la señalización de AT_2 cuando están formando complejo y, al unirse el antagonista de AT_1R se produce el desbloqueo de la funcionalidad mediada por AT_2R (Hinz et al. 2018). Por otro lado, el receptor AT_2 en la microglía, forma parte de los heterómeros AT_1R-AT_2R y AT_2R-MasR, constituyendo una diana prometedora para la PD debido a su elevada expresión en animales modelo de Parkinson y, incluidos aquellos que presentan las disquinesias inducidas por la L-DOPA. Otros estudios también avalan como la manipulación farmacológica de los componentes del RAS presenta un potencial terapéutico en la PD (Labandeira-Garcia et al. 2017).

Una característica novedosa que observamos en nuestros resultados, y que también se puede explicar por la interacción entre receptores, es que el antagonista de MasR fue capaz de aumentar el pico de liberación de calcio inducido por el agonista de AT_1R (Franco et al. 2007, 2018). En contraposición, en los resultados obtenidos en las células HEK-293T transfectadas y en la microglía activada, no se observa un antagonismo cruzado entre los receptores AT_1 y AT_2 sobre MasR en las neuronas estriatales. Sorprendentemente, la expresión de los heterómeros AT_1R-MasR y AT_2R-MasR en la microglía activada está vinculada a la activación de la vía MAPK con un cross-talk negativo y un antagonismo cruzado. En la microglía se detectó una señalización diferencial cuando se comparó la funcionalidad de los heterómeros AT_1R-AT_2R con los AT_1R-MasR o con los AT_2R-MasR, puesto que los heterómeros que expresan MasR muestran un antagonismo cruzado que no se encuentra en AT_1R-AT_2R. Esto dato es prometedor desde el punto de vista terapéutico, porque si existiera el antagonismo cruzado en el heterómero AT_1R-AT_2R, conduciría a un callejón sin salida en términos de neuroprotección; debido a las acciones contrarias que promueven ambos receptores de angiotensina (Rivas-Santisteban et al. 2020).

Como en cualquier estudio centrado en una enfermedad neurodegenerativa, la base experimental conlleva una serie de limitaciones. Entre ellas, en nuestros estudios extrapolamos el comportamiento de células "adultas" al obtenido en nuestros experimentos con las células de cultivos primarios de ratones recién nacidos o fetos. Aunque se trata de un procedimiento habitual, es necesario tener este dato en consideración. Otra limitación de nuestros estudios es la variedad de tipos de células neurales, ya que la funcionalidad del receptor en respuesta a un determinado ligando puede variar de una célula a otra (Franco et al. 2018) e incluso entre los diferentes estadios de una misma enfermedad.

En conclusión, por una parte y de forma sorprendente, podemos afirmar que en los heterómeros AT_1R-AT_2R el antagonista de AT_1R libera el freno de la activación del receptor AT_2 favoreciendo así un efecto de neuroprotección. Por otra, y como se observa en los resultados expuestos, aparece un incremento significativo del heterómero AT_1R-MasR y del heterómero AT_2R-MasR en ratas modelo de PD, tratadas o no con L-DOPA. Finalmente, también se ha demostrado que el receptor Mas ejerce una modulación significativa sobre la señalización de los receptores AT_1 y AT_2. Todo ello, y a pesar de que se requiere de una mayor investigación al respecto, convierte a estos receptores del RAS en una buena diana terapéutica para el desarrollo de una terapia farmacológica con posibilidades de mejorar la calidad de vida de los enfermos de Parkinson.

Si consideramos el sistema renina-angiotensina como diana terapéutica, no podemos obviar el papel clave que juegan las enzimas convertidoras de angiotensinas (ACE1 y ACE2), puesto que pueden interactuar con los receptores del RAS y pueden modular de manera directa la concentración local de agonistas de los receptores RAS. Por ello nos planteamos en el estudio del *apartado 3.7* investigar los posibles complejos formados entre la enzima ACE2 y los receptores del RAS AT_1, AT_2 y Mas,

detectando como estos complejos pueden modular la expresión a nivel de membrana y la funcionalidad de dichos receptores.

La ACE2 ha sido identificada como un componente crítico para el proceso infectivo del SARS y otros coronavirus (Chen and Subbarao 2007; Kuba et al. 2005). Recientemente, esta enzima está cobrando una gran importancia entre la comunidad científica debido a actuar como puerta de entrada a la célula para el virus SARS-CoV-2, causante de la enfermedad COVID-19. Siendo, por ello, un componente clave en el proceso de infección (Yan et al. 2020).

Como el enfoque más directo para la identificación de GPCRs que pueden estar involucrados en la infección de SARS-CoV-2, nos centramos en los receptores del RAS que unen el sustrato de ACE2, el péptido Ang II. En la investigación de (Deshotels et al. 2014) se demostró que la expresión de ACE2 era regulada por la presencia de Ang II y dependiente de los niveles de expresión de AT_1R tanto en células transfectadas como en un modelo de roedor. Además, los resultados de los experimentos de co-inmunoprecipitación sugirieron la existencia de una interacción directa entre las dos proteínas de la superficie celular (ACE2 y AT_1R). Nuestros resultados revelaron que la ACE2 puede interactuar tanto con el AT_1R como con el AT_2R y también con el MasR, que es el receptor de la Ang (1-7), el producto de la degradación de la Ang II mediada por la ACE2.

De manera interesante, detectamos como la expresión de ACE2 modula la señalización inducida por agonistas en AT_1R, AT_2R y MasR. Podría esperarse una modulación negativa de la señalización mediada por el AT_1R, dado que la ACE2 degrada en última instancia el agonista endógeno, la Ang II, pero en nuestros resultados obtuvimos una disminución más acusada de los niveles de AMPc y del reclutamiento de ß-arrestinas cuando el AT_1R es activado en presencia de la ACE2. Sin embargo, el agonista CGP-42112a utilizado para promover la señalización a través del AT_2R no sufre una degradación por parte de la ACE2. Así, podemos concluir que la activación de los receptores AT_1R y AT_2R en células que también expresaban ACE2, induce resultados diferentes, un hallazgo que es consistente con las funciones fisiológicas opuestas que desempeñan estos dos receptores. No obstante, encontramos que la expresión de ACE2 en células que también expresaban el MasR, no tuvo un impacto significativo en la señalización de MasR.

La expresión diferencial de los componentes del RAS en una célula determinada puede establecer su susceptibilidad a la infección por el SARS-CoV-2 y la aparición de una sintomatología leve a otra más grave del COVID-19. Nuestros resultados sugieren que las células que expresan niveles más altos de AT_2R son más propensas a facilitar la adhesión del SARS-CoV-2 debido a la correlación con niveles más altos de expresión de ACE2. Serían necesarios más experimentos, preferiblemente los realizados con partículas infecciosas de SARS-CoV-2, para determinar si las células enriquecidas en AT_2R y activadas por el agonista endógeno son más susceptibles a la unión del SARS-CoV-2, y para evaluar si los GPCRs relacionados con RAS y que forman complejos con ACE2 promueven la endocitosis viral.

Se han detectado altos niveles de expresión de ACE2 en el pulmón, que incluye una interfaz expuesta al aire; la ACE2 en el pulmón humano es particularmente abundante en las células secretoras transitorias bronquiales (Hamming et al. 2004; Lukassen et al. 2020). El tejido pulmonar incluye tanto células endoteliales como epiteliales, que pueden expresar casi todos los componentes del RAS. Por lo tanto, el último propósito del artículo del *apartado 3.7* consiste en identificar los complejos ACE2-receptor del RAS en el pulmón y detectar la posible variación en su expresión en la etapa adulta. Estos estudios se desarrollaron mediante ensayos de PLA que nos permitieron encontrar como el aproximado 10% de las células del tejido pulmonar de ratones adultos expresaban uno o más pares de los heterómeros ACE2-AT_1R, ACE2-AT_2R y/o ACE2/MasR. Sorprendentemente, no se detectaron estos complejos heteroméricos en secciones de pulmón de ratón fetal. Teniendo en cuenta estos hallazgos, es tentador especular que el predominio de la infección leve o incluso asintomática en los niños expuestos al SARS-CoV-2 podría estar directamente relacionada con la ausencia de complejos receptor-enzima que promueven la entrada viral en las células pulmonares. En conjunto, nuestros

hallazgos sugieren que un mayor estudio de los complejos de receptores del RAS que contienen ACE2 podría revelar características críticas que subyacen al mecanismo de la infección por SARS-CoV-2.

En el estudio del *apartado 3.8* extendimos nuestra investigación sobre el RAS a unos receptores que hoy en día siguen planteando muchas incógnitas, la familia de los receptores relacionados con MasR (Mas-related receptors). Descubrimos que la ACE2 intracelular se concentra en altos niveles en las mitocondrias cerebrales, y que el receptor Mas-related E (MrgE) es una diana importante para los péptidos Ang1-7 y alamandina, induciendo la producción de óxido nítrico (NO) mitocondrial. Además, los resultados sugieren que el eje mitocondrial ACE2/MrgE puede ser una nueva diana terapéutica para la COVID-19, ya que modula las funciones bioenergéticas mitocondriales, que suelen estar implicadas en la supervivencia y replicación de los virus.

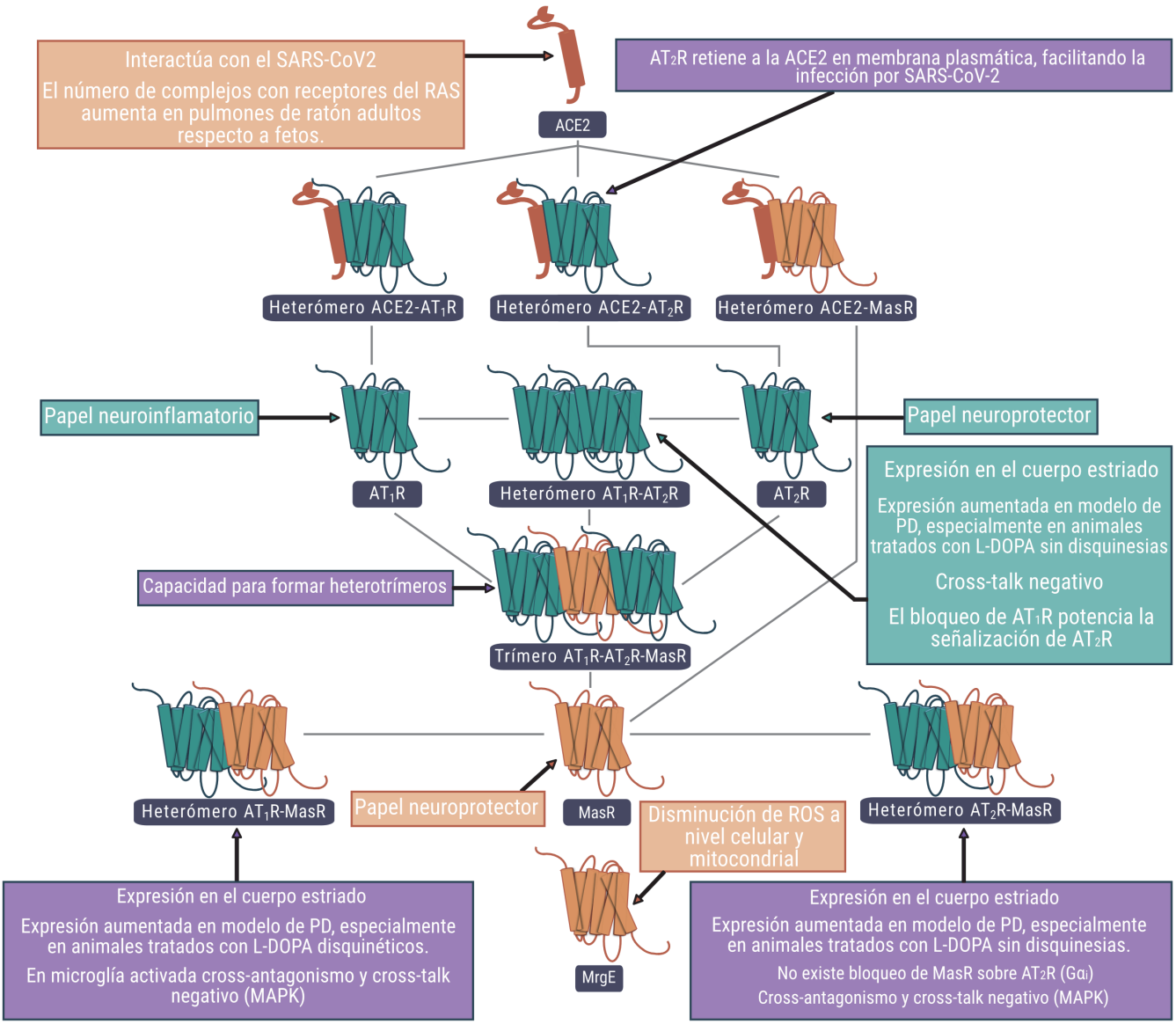

Figura 22. Resumen gráfico: implicación del sistema RAS en la infección por SARS-CoV-2 y en la patología del Parkinson.

Los receptores del RAS también se expresan en las mitocondrias. En estos orgánulos el AT_1R promueve la producción de superóxido a través de la activación de NOX4 mitocondrial, mientras los receptores AT_2 (Abadir et al. 2011; Valenzuela et al. 2016) y MasR (Costa-Besada et al. 2018), tienen un papel antioxidante, promoviendo la producción de NO a través de la NOS mitocondrial. Hay que

tener en cuenta que la disponibilidad mitocondrial de la Ang (1-7) es aproximadamente tres veces superior a la de la Ang II (Costa-Besada et al. 2018). Sin embargo, según nuestros resultados encontramos que los MasR mitocondriales son notablemente menos abundantes que los receptores MrgE. Todo ello apunta a que el eje ACE2/Ang (1-7)/alamandina/MrgE juega un papel importante en la generación de NO mitocondrial y en la modulación del estrés oxidativo derivado de las mitocondrias, al menos a nivel neuronal. Los resultados obtenidos nos indican que el eje pro-oxidativo mitocondrial es el predominante en los animales envejecidos, aumentando la susceptibilidad a la neurodegeneración y a la muerte neuronal (Villar-Cheda et al. 2012).

La infección por SARS-CoV-2 induce una desregulación perjudicial del RAS, en la que se produce una disminución de los niveles de ACE2 en la membrana celular y por tanto de su actividad enzimática (Kuba et al. 2005), dando lugar a una disminución de los niveles de la Ang (1-7) antioxidante y a un aumento de los niveles de la Ang II, lo que conduce a un cambio hacia la actividad prooxidativa de la vía Ang II/AT_1R, que da lugar a estrés oxidativo, inflamación y muerte celular. Los resultados obtenidos sugieren que una desregulación del eje mitocondrial ACE2/MrgE (es decir, el eje antioxidante compensatorio intracelular) también puede desempeñar un papel importante.

Normalmente se asume que la unión de la Ang 1-7 a los receptores Mas de la membrana celular es responsable de las respuestas antioxidantes intracelulares. En esta Tesis doctoral se ha visto que el tratamiento de células SH-SY5Y humanas con la espícula del SARS-CoV-2 (proteína S) induce un aumento de los niveles mitocondriales de superóxido. Para confirmar que la proteína S del SARS-CoV-2 puede actuar sobre el eje ACE2/MrgE mitocondrial, tratamos mitocondrias aisladas con la proteína S y observamos una disminución significativa de los niveles de actividad de la ACE2 mitocondrial. Estudios anteriores habían demostrado que los virus, incluido el SARS-CoV, modulan la función celular modificando los procesos mitocondriales (Boya et al. 2004; Yuan et al. 2006), y que los cambios en la bioenergética mitocondrial desempeñan un papel importante tanto en la replicación viral como en las primeras respuestas celulares a la infección viral (Silva da Costa et al. 2012).

En conclusión, nuestros resultados demuestran i) la expresión de los receptores MrgE en las mitocondrias del cerebro, y en las neuronas dopaminérgicas en particular, ii.) que la Ang (1-7) y la alamandina pueden unirse a los receptores MrgE para aumentar la producción de NO, que se sabe que contrarresta el aumento de ROS a nivel celular y mitocondrial. iii) La proteína S del SARS-CoV-2 puede afectar al eje mitocondrial ACE2/MrgE, provocando una desregulación del RAS y una disfunción mitocondrial. Así podemos concluir que la desregulación del eje mitocondrial ACE2/Ang (1-7)-alamandina puede desempeñar un papel importante en las respuestas oxidativas e inflamatorias relacionadas con el deterioro de la función de ACE2, como el observado en la enfermedad COVID-19.

Tal y como recopilamos en nuestro artículo del *apartado 3.9*, los casos de COVID-19 grave conllevan una neumonía y resultados fatales que a menudo se correlacionan con niveles plasmáticos elevados de interleucina-6 (IL-6) y una tormenta de citoquinas (Zhao et al. 2017). Los niveles elevados de IL-6 pueden deberse a una sobreproducción por parte de los macrófagos activados, así como de las células no inmunes. Curiosamente y, al igual que se ha observado en la infección por el VIH-1, los GPCRs pueden facilitar la infección viral. El receptor de quimioquinas CXCR4 fue identificado como correceptor del VIH-1 y como mediador de la entrada celular poco después de la identificación de este patógeno como agente causante del SIDA (Herrera et al. 2001). Estudios posteriores revelaron que la dipeptidil peptidasa-4 (CD26 o DPPIV) interactúa con el CXCR4 y es el objetivo de la glicoproteína de la envoltura del VIH-1 (gp120) (Aliyari Serej et al. 2017). La entrada del VIH-1 en las células diana implica a CXCR4, así como las interacciones con CD26/DPPIV y el agonista del receptor, CXCL12/SDF-1, que también es un sustrato de la enzima CD26/DPPIV. Los posibles paralelismos del transcurso infectivo del SARS-CoV-2 con los mecanismos de la infección por el VIH-1 nos han llevado a plantear como los GPCR también podrían participar activamente en el proceso de infección e internalización a la célula de los virus.

Continuando con la búsqueda de dianas terapéuticas para el tratamiento de enfermedades neurodegenerativas, seleccionamos al receptor A_{2A} como objetivo de nuestras investigaciones debido a su alta expresión en el cerebro, por la seguridad reportada por diversas investigaciones de antagonistas que actúan sobre dicho receptor, así como por su alto potencial para prevenir la neurodegeneración (Stockwell, Jakova, and Cayabyab 2017). De hecho, la aprobación de la istradefilina, un antagonista selectivo de $A_{2A}R$, para la terapia contra la enfermedad de Parkinson es un hecho en Japón y en los Estados Unidos (Kondo and Mizuno 2015; Mizuno and Kondo 2013). En el estudio del *apartado 3.10* nos enfocamos en descubrir si la cola c-terminal del receptor A_{2A}, inusualmente larga, juega un papel relevante en su funcionalidad. Otros estudios describen la implicación de esta cola en el bloqueo de la funcionalidad del A_1R (Ferre et al. 2008) y del D_2R (Ferré et al. 2016) cuando forman un complejo heteromérico con $A_{2A}R$.

En primer lugar, seleccionamos una batería de moléculas con diferentes estructuras capaces de unirse al $A_{2A}R$. Mediante simulaciones de dinámica molecular (MD) determinamos que todos los compuestos ensayados se unían de forma estable al receptor. Al profundizar en la unión del ligando al receptor, se observó una clara tendencia en nuestros resultados, dónde la eliminación de los últimos 40 aminoácidos del dominio C-terminal ($A_{2A}^{\Delta 40}R$) resultó en una unión más débil tanto de los agonistas al sitio ortostérico como del antagonista SCH-58261.

A nivel de señalización, en nuestras condiciones de ensayo de determinación del AMPc intracelular, la adenosina, la NECA y el CGS-21680 se comportan como agonistas completos, mientras que el PSB-0777 y el LUF-5834 únicamente como agonistas parciales del $A_{2A}R$. Los ensayos de reclutamiento de ß-arrestinas demostraron que el PSB-0777 y la NECA son más eficientes en el reclutamiento que la propia adenosina y el CGS-21680. Sorprendentemente, LUF-5834, que es un agonista parcial a nivel de acoplamiento de proteína $G\alpha_s$ en el ensayo de AMPc, es tan eficiente como el CGS-21680 y la adenosina en el reclutamiento de ß-arrestinas. Las curvas dosis-respuesta de pERK1/2 siguen patrones similares a las curvas de AMPc, con las excepciones del PSB-0777 que se comporta como un agonista completo, y el LUF-5834 que actúa como un débil agonista parcial. Nuestros resultados, en concordancia con informes anteriores (Klinger et al. 2002), muestran que la señalización mediada por la forma truncada $A_{2A}^{\Delta 40}R$ no causó una alteración en el efecto máximo de los agonistas ensayados en las dosis-respuesta de AMPc, con la excepción del LUF5834 cuyo efecto se convirtió en prácticamente insignificativo en la forma truncada del receptor. El truncamiento del extremo C-terminal proporcionó también una disminución del reclutamiento de ß-arrestinas en comparación con el $A_{2A}R$ de longitud completa. Para terminar, puntualizar que las curvas dosis-respuesta de pERK1/2 del $A_{2A}^{\Delta 40}R$ fueron muy similares a las del $A_{2A}R$ de longitud completa.

Debido a la gran relevancia farmacológica que esconde el conocimiento de la vía de señalización preferencial de un determinado compuesto, para minimizar al máximo sus efectos secundarios indeseados (Michel and Charlton 2018), se calculó la selectividad funcional de cada uno de los compuestos para cada una de las vías estudiadas, tomando como referencia la adenosina, el compuesto endógeno, y como vía de señalización principal la mediada por la proteína $G\alpha_s$, es decir, el incremento del AMPc intracelular.

El análisis realizado demuestra que la adenosina y el CGS-21680 son agonistas equilibrados con "*bias factor*" similares para las cuatro vías ensayadas, mientras que la NECA tiene factores pequeños para el reclutamiento ß-arrestinas y la DMR y el LUF-5834 tiene factores pequeños para todas las respuestas exceptuando la modulación de los niveles de AMPc intracelulares. Por el contrario, el PSB-0777 tiene un mayor sesgo para la respuesta a pERK1/2. El truncamiento del extremo C-terminal hace que LUF-5834 y PSB-0777 se encuentren más equilibrados. De hecho, el LUF-5834 adquiere los mayores factores de sesgo para el reclutamiento de ß-arrestinas, la fosforilación de ERK1/2 y la DMR. Por el contrario, NECA mantiene los factores pequeños para el reclutamiento de ß-arrestinas y la DMR. En general, los resultados son consistentes con que el extremo C-terminal es prescindible tanto para el reclutamiento de la proteína G y las ß-arrestinas como para la activación de las MAPK

(fosforilación de ERK1/2) y la DMR, con sólo pequeñas diferencias en la señalización en comparación con el A_{2A}R de longitud completa.

El diferente comportamiento detectado en el reclutamiento de ß-arrestinas inducido por agonistas puede deberse a una inducción alternativa en los patrones de fosforilación del receptor, que dirigen conformaciones específicas de la ß-arrestina (Yang et al. 2015, 2017). Por otra parte, hay evidencias de que la señalización sesgada podría ser también una consecuencia de la cinética de unión (Grundmann and Kostenis 2017).

Como hemos visto, existe un consenso sobre la seguridad y el potencial neuroprotector de los antagonistas de los receptores A_{2A}. Los estudios farmacológicos en modelos parkinsonianos, el antagonismo dopamina/adenosina y el uso de ratones knock-out reforzaron la opinión de que dirigirse al A_{2A}R en las neuronas estriatales podría ser útil en la terapia de la enfermedad de Parkinson (Fuxe et al. 2005, 2007; Gui et al. 2009). Además, este receptor también podría ser la llave para mejorar la fisiopatología de otras enfermedades neurodegenerativas, como la enfermedad de Alzheimer (AD), existiendo estudios que vinculan los primeros déficits sinápticos en el modelo de ratón de la AD con el receptor A_{2A} neuronal (Viana da Silva et al. 2016). Además, estudios electrofisiológicos en neuronas piramidales CA1 mostraron que la activación de esos receptores de adenosina potenciaba las corrientes del NMDAR (Mouro et al. 2018). También se ha reportado la función relevante del receptor A_{2A} en la microglía activada, característica en la AD (Angulo et al. 2006), donde la activación del A_{2A}R microglial aumenta la producción de mediadores proinflamatorios (Saura et al. 2005). Estos resultados coinciden con el hallazgo de que el bloqueo del A_{2A}R microglial reduce la neuroinflamación y, lo que es más importante, puede conducir a una mejora del deterioro cognitivo (Rebola et al. 2011). De hecho, está bien aceptado que los antagonistas del receptor de adenosina más consumidos, la cafeína presente en el café y la teofilina en el té, protegen contra la aparición de la AD (Eskelinen and Kivipelto 2010). En base a estos antecedentes, nos propusimos en nuestro estudio del *apartado 3.11* determinar la posible interacción entre los receptores A_{2A} y NMDA, siendo la desregulación funcional de este último uno de los mecanismos moleculares clave en la aparición de la AD.

Aunque los diferentes GPCRs tienden a formar dímeros y oligómeros, se suponía que la estructura multimérica de los receptores ionotrópicos impedía la adición de más proteínas para formar complejos macromoleculares con propiedades fisiológicas particulares. De hecho, se han descrito pocos ejemplos de interacciones directas entre receptores ionotrópicos y GPCRs. Sin embargo, nuestros resultados muestran que, además del bloqueo de la señalización clásica del receptor A_{2A} mediada por el acoplamiento a proteína $G\alpha_s$, el antagonista de A_{2A}R tiene el potencial de combatir la AD incidiendo en la modulación de la función de los NMDAR, cuando se encuentran formando el complejo heteromérico A_{2A}R-NMDAR. Los primeros estudios que mostraban el efecto neuroprotector inducido por la adenosina sobre el NMDAR (Rudolphi et al. 1992) nunca se atribuyeron a una interacción directa entre la adenosina y los receptores ionotrópicos. Si es cierto que al menos en parte, la muerte neuronal en la AD, y en otras enfermedades neurodegenerativas, se debe a la excitotoxicidad, es decir, al exceso de glutamato que, a su vez, provoca la hiperactivación de la funcionalidad del NMDAR (Lewerenz and Maher 2015). En nuestro estudio, identificamos por primera vez complejos de receptores A_{2A}-NMDA con propiedades particulares. De forma interesante, se detectó un fenómeno de antagonismo cruzado, habitual en complejos heteroméricos GPCR-GPCR (Franco et al. 2016), donde los antagonistas de A_{2A}R bloquean la sobreactivación de NMDAR.

La evaluación de la expresión del complejo A_{2A}R-NMDAR condujo a varios hallazgos relevantes. Por un lado, la expresión en la microglía activada era notablemente mayor que en la microglía en reposo. Por otra parte, la expresión en la microglía de los ratones $APP_{Sw,Ind}$ fue mayor que la de la microglía de los ratones de control. Estos resultados refuerzan la hipótesis de que la microglía de ratones $APP_{Sw,Ind}$ protege a las neuronas, ya que el deterioro cognitivo sólo aparece varios meses después del nacimiento (G Navarro et al. 2018). Por otro lado, los complejos también se expresaron en las neuronas del hipocampo, aunque la expresión fue similar en los ratones transgénicos y en los control,

por lo que habría un número significativo del NMDAR en las neuronas del hipocampo que no interactúa con el $A_{2A}R$, que se encuentra sobreexpresado en las neuronas de animales $APP_{Sw,Ind}$.

Aunque el interés principal de nuestro estudio se ha centrado en las neuronas, los NMDAR, como hemos descrito, también se expresan en las células gliales, donde desempeñan un papel fundamental en el mantenimiento de la homeostasis cerebral. Para continuar profundizando en nuestras investigaciones para intentar buscar moduladores de la funcionalidad del NMDAR decidimos estudiar la posible interacción entre NMDAR y CB_2R en nuestro estudio del *apartado 3.12*. El papel neuroprotector y antiinflamatorio del receptor CB_2 hoy día está fuera de toda duda (van der Stelt and Di Marzo 2005), esto nos llevo a pensar que potenciar su funcionalidad podría mejorar la fisiopatología de la AD, ya que se expresa en las neuronas y células de microgliales del SNC.

En nuestra investigación reportamos por primera vez la interacción específica entre CB_2R y NMDAR, es decir, la capacidad de estos dos receptores de formar complejos heteroméricos. Aunque el CB_2R es menos abundante en las neuronas que el receptor CB_1, puede encontrarse en neuronas de diferentes regiones del cerebro, de hecho, detectamos heterómeros CB_2R-NMDAR en cultivos primarios de neuronas del hipocampo. En la microglía, los heterómeros se detectaron pero a un nivel de expresión más bajo en los cultivos en reposo en comparación con las células activadas; esto se debe, probablemente, al aumento de la expresión del CB_2R en condiciones de neuroinflamación.

En el sistema de expresión heteróloga, la propiedad más notable del heterómero CB_2R-NMDAR fue el cross-talk negativo, es decir, el tratamiento simultáneo con los dos agonistas condujo a la ausencia de respuesta en la vía mediada por el acoplamiento de $G\alpha_i$ y en la fosforilación de las MAPK. Dado que los agonistas del CB_2R no pudieron, en el contexto heteromérico, fosforilar significativamente las ERK1/2, el efecto de bloqueo parece ser directo, es decir, debido a las interacciones alostéricas entre los receptores y a los cambios conformacionales al unirse los cannabinoides al CB_2R. Quizás el efecto más notable fue la reducción por parte de los agonistas del CB_2R de la función ionotrópica del NMDAR. El antagonismo cruzado encontrado en los complejos formados por dos GPCRs no se encontró en las células HEK-293T que expresaban los receptores CB_2 y NMDA. Este resultado contrasta con las propiedades que encontramos en la pareja $A_{2A}R$-NMDAR, cuya estructura permite detectar el antagonismo cruzado entre ambos protómeros.

En los heterómeros CB_2R-NMDAR presentes en las neuronas de los animales WT, se detectó un cross-talk negativo similar al observado en cultivos heterólogos. Sin embargo, este cross-talk no se encontró en las células de los ratones transgénicos $APP_{Sw/Ind}$. Por un lado, estos resultados muestran que las neuronas del hipocampo de los ratones WT y transgénicos son diferentes ya en las primeras etapas del desarrollo del SNC; el fenotipo similar al de la AD tarda meses en ser detectable. El antagonismo cruzado detectado en las muestras de estos ratones a nivel de fosforilación de MAPK demuestra que los heterómeros CB_2R-NMDAR se encuentran presentes. Así, la hipótesis más razonable consiste en que coexisten diferentes poblaciones de los receptores y que los heterómeros CB_2R-NMDAR son una de ellas. Esta hipótesis podría explicar por qué el NMDA no afecta al efecto inducido por el JWH-133 sobre los niveles de AMPc; quizás los CB_2R acoplados a $G\alpha_i$ no están interactuando con los NMDARs en las neuronas del animal transgénico. Sorprendentemente, el cross-talk negativo en el enlace con la vía de las MAPK se produce tanto en las neuronas de animales WT como en las de $APP_{Sw/Ind}$. Por otra parte, la presencia de complejos CB_2R-NMDAR fue confirmada por ensayos de PLA, que además mostró un aumento significativo tanto en la microglía como en las neuronas de los ratones transgénicos, en comparación con los niveles detectados en los ratones WT.

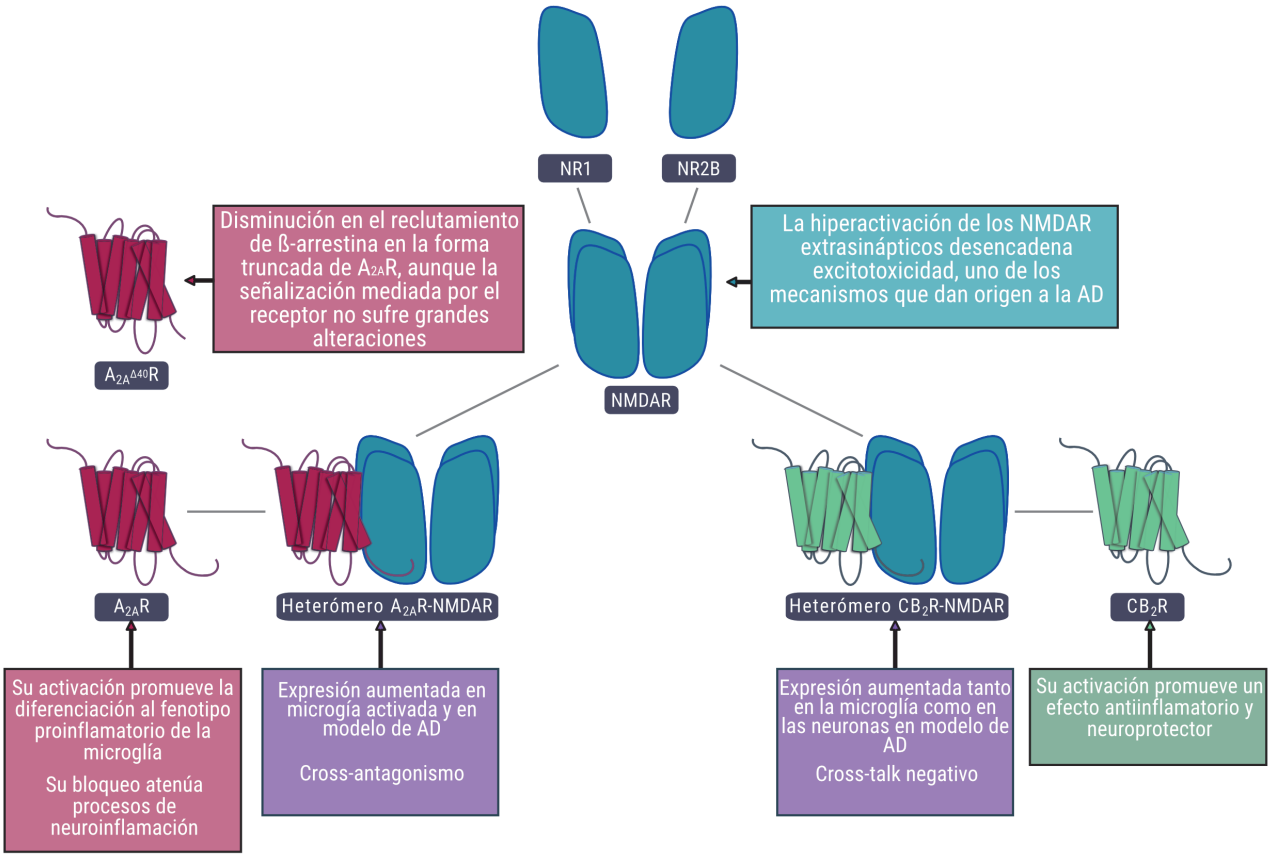

Figura 23. Resumen gráfico: implicación de los complejos heteroméricos A_{2A}R-NMDAR y CB_2R-NMDAR en la patología del Alzheimer.

Desgraciadamente abordar una estrategia terapéutica, aunque es factible, también es una tarea compleja, esto es debido a que un bloqueo total del NMDAR no sería viable al ser fundamental para la viabilidad de las células neuronales. Por otra parte, los moduladores alostéricos del NMDAR actuales no están mostrando una eficacia significativa ni en los pacientes con AD ni en la neuroprotección (Ahmed, Haider, and Ametamey 2020) dado que los moduladores alostéricos que actúan directamente sobre el NMDAR no proporcionan mucha ayuda a los pacientes con AD. Así, una modulación alostérica mediada por un GPCR que interactúe directamente con el NMDAR es una posibilidad atractiva.

En conclusión, los intentos actuales de prevenir la muerte neuronal en la AD deberían focalizarse en regular únicamente aquellos receptores de NMDA que se comportan de forma aberrante. En definitiva, los resultados de nuestro trabajo sugieren que la disminución en la funcionalidad de los NMDAR por parte de los antagonistas de los A_{2A}R es una posibilidad atractiva para promover un efecto neuroprotector en la AD. Por otra parte, la capacidad de CB_2R de regular negativamente la señalización mediada por NMDAR, así como el incremento en la expresión del heterómero de receptores NMDA-CB_2 en modelo de ratón de Alzheimer abre la posibilidad de utilizar compuestos cannabinoides naturales, generalmente seguros, para promover los efectos beneficiosos mediados por CB_2R para mejorar la fisiopatología de la AD.

Teniendo en cuenta los resultados obtenidos y presentados en esta Tesis doctoral se puede concluir el gran potencial terapéutico, actual y futuro, que poseen los GPCRs en el tratamiento de las enfermedades neurodegenerativas ya sea utilizando aproximaciones directas que potencien los efectos beneficiosos que promueven, como el AT_2R, o bien aproximaciones indirectas que busquen modular la acción de otros receptores clave, como el bloqueo de A_{2A}R o CB_2R sobre la señalización perjudicial de NMDAR.

CONCLUSIONES

5. Conclusiones

1. El CBD modula negativamente la funcionalidad de los receptores CB_1 y CB_2 a concentraciones del rango nanomolar mediante su unión al sitio alostérico de los receptores cannabinoides. A concentraciones del rango micromolar es capaz de unirse al sitio ortostérico y activar estos receptores.

2. El CBG tiene baja afinidad por el CB_1R, nuestros resultados sugieren una modulación negativa de la señalización de este receptor mediante su unión al sitio alostérico. Por otra parte, el CBG actúa como agonista parcial en el CB_2R, exhibiendo un comportamiento sesgado con capacidad para promover la fosforilación de ERK1/2 y el reclutamiento de β-arrestinas.

3. Se ha detectado un aumento en la expresión de los heterómeros CB_1R-GPR55 y CB_2R-GPR55 en modelo de primate de la enfermedad de Parkinson, disminuyendo su expresión en aquellos individuos que presentan discinesias.

4. Se ha demostrado la interacción específica entre los receptores AT_1 y AT_2. Se observa un cross-talk negativo al coactivar ambos receptores con Ang II y CGP-42112a. Además, el bloqueo de AT_1R con candesartan produce una potenciación en la señalización mediada por la activación de AT_2R. En cultivos primarios de microglía activada se observa una mayor activación de AT_1R y de AT_2R en comparación a la microglía en reposo. Se ha detectado un incremento de la expresión del heterómero AT_1R-AT_2R en el modelo animal de enfermedad de Parkinson que no mostraba discinesias.

5. Se ha demostrado la interacción de los receptores AT_1 y Mas y de los receptores AT_2 y Mas. Se observa un fenómeno de cross-talk negativo en ambos complejos. Además, se detectó el fenómeno de cross-antagonismo unidireccional en el complejo heteromérico AT_1R-MasR pero no el heterómero AT_2R-MasR. Se ha demostrado la interacción heterotrimérica AT_1R-AT_2R-MasR mediante ensayos de BRET y SRET. Se ha observado una mayor expresión de los heterómeros AT_1R-MasR y AT_2R-MasR en el grupo lesionado modelo animal de enfermedad de Parkinson en comparación con el grupo control.

6. Se han demostrado las interacciones ACE2-AT_1R, ACE2-AT_2R y ACE2-MasR. Además, la expresión de ACE2 moduló la señalización inducida por agonistas en AT_1R, atenuándola a nivel global, y en AT_2R, atenuando la señalización mediada por $G\alpha_i$ y en DMR pero potenciando la fosforilación de ERK1/2, sin embargo, no pareció afectar a la funcionalidad de MasR. La activación de AT_1R resulta en una disminución de la expresión en membrana de la enzima ACE2, mientras que la activación de AT_2R incrementa la expresión de ACE2. La expresión de complejos ACE2-receptor del RAS es mayor en tejido pulmonar adulto en comparación con el mismo tejido fetal.

7. Se ha detectado la expresión de MrgE en mitocondrias procedentes de homogenados celulares de cerebro de rata. El MrgE, cuyos niveles de expresión en la mitocondria disminuyen con la edad, tiene un claro papel antioxidante mediante la producción de óxido nítrico.

8. Se ha establecido que la forma trucada del extremo c-terminal del receptor A_{2A} ($A_{2A}^{\Delta 40}R$) supone una unión más débil tanto de agonistas como antagonista al receptor, aunque no supone un impedimento para la señalización mediante el acoplamiento de proteína G o para el reclutamiento de ß-arrestinas.

9. Se ha demostrado la interacción entre los receptores A_{2A}, CB_2R y NMDA, formando los heterómeros $A_{2A}R$-NMDAR y CB_2R-NMDAR que constituyen nuevas unidades funcionales. Mientras que el complejo $A_{2A}R$-NMDAR muestra un cross-antagonismo bidireccional, el heterómero CB_2R-NMDAR se caracteriza por un fenómeno de cross-talk negativo. La expresión de los heterómeros $A_{2A}R$-NMDAR y CB_2R-NMDAR aumenta significativamente en el modelo de Alzheimer $App_{Sw/ind}$ en comparación con los animales control.

REFERENCIAS

Aarsland, D., K. Brønnick, U. Ehrt, P. P. De Deyn, S. Tekin, M. Emre, and J. L. Cummings. 2007. "Neuropsychiatric Symptoms in Patients with Parkinson's Disease and Dementia: Frequency, Profile and Associated Care Giver Stress." Journal of Neurology, Neurosurgery and Psychiatry 78(1):36–42. doi: 10.1136/jnnp.2005.083113.

Abadir, P. M., D. B. Foster, M. Crow, C. A. Cooke, J. J. Rucker, A. Jain, B. J. Smith, T. N. Burks, R. D. Cohn, N. S. Fedarko, R. M. Carey, B. O'Rourke, and J. D. Walston. 2011. "Identification and Characterization of a Functional Mitochondrial Angiotensin System." Proceedings of the National Academy of Sciences 108(36):14849–54. doi: 10.1073/pnas.1101507108.

Abadir, Peter M., Ammasi Periasamy, Robert M. Carey, and Helmy M. Siragy. 2006. "Angiotensin II Type 2 Receptor-Bradykinin B2 Receptor Functional Heterodimerization." Hypertension 48(2):316–22. doi: 10.1161/01.HYP.0000228997.88162.a8.

AbdAlla, Said, Heinz Lother, Ahmed M. Abdel-tawab, and Ursula Quitterer. 2001. "The Angiotensin II AT2 Receptor Is an AT1 Receptor Antagonist." Journal of Biological Chemistry 276(43):39721–26. doi: 10.1074/jbc.M105253200.

AbdAlla, Said, Heinz Lother, Adel el Massiery, and Ursula Quitterer. 2001. "Increased AT1 Receptor Heterodimers in Preeclampsia Mediate Enhanced Angiotensin II Responsiveness." Nature Medicine 7(9):1003–9. doi: 10.1038/nm0901-1003.

AbdAlla, Said, Heinz Lother, Ahmed El Missiry, Pavel Sergeev, Andreas Langer, Yasser El Faramawy, and Ursula Quitterer. 2009. "Dominant Negative AT2 Receptor Oligomers Induce G-Protein Arrest and Symptoms of Neurodegeneration." Journal of Biological Chemistry 284(10):6566–74. doi: 10.1074/jbc.M808277200.

Abood, Mary E., Kara E. Ditto, Melissa A. Noel, Vincent M. Showalter, and Tao Qing. 1997. "Isolation and Expression of a Mouse CB1 Cannabinoid Receptor Gene. Comparison of Binding Properties with Those of Native CB1 Receptors in Mouse Brain and N18TG2 Neuroblastoma Cells." Biochemical Pharmacology 53(2):207–14. doi: 10.1016/S0006-2952(96)00727-7.

Aggarwal, S. K. 2016. "Use of Cannabinoids in Cancer Care: Palliative Care." Current Oncology 23(March):S33–36. doi: 10.3747/co.23.2962.

Ahmed, Hazem, Ahmed Haider, and Simon M. Ametamey. 2020. "N -Methyl-D-Aspartate (NMDA) Receptor Modulators: A Patent Review (2015-Present)." Expert Opinion on Therapeutic Patents 30(10):743–67. doi: 10.1080/13543776.2020.1811234.

Ahmed, Heba A., and Tauheed Ishrat. 2020. "The Brain AT2R—a Potential Target for Therapy in Alzheimer's Disease and Vascular Cognitive Impairment: A Comprehensive Review of Clinical and Experimental Therapeutics." Molecular Neurobiology 57(8):3458–84. doi: 10.1007/s12035-020-01964-9.

Al-Attraqchi, Omar H. A., Mahesh Attimarad, Katharigatta N. Venugopala, Anroop Nair, and Noor H. A. Al-Attraqchi. 2019. "Adenosine A2A Receptor as a Potential Drug Target - Current Status and Future Perspectives." Current Pharmaceutical Design 25(25):2716–40. doi: 10.2174/1381612825666190716113444.

Al-Zoubi, Rufaida, Paula Morales, and Patricia H. Reggio. 2019. "Structural Insights into Cb1 Receptor Biased Signaling." International Journal of Molecular Sciences 20(8). doi: 10.3390/ijms20081837.

Alberti, Thaís Barbosa, Wagner Luiz Ramos Barbosa, José Luiz Fernandes Vieira, Nádia Rezende Barbosa Raposo, and Rafael Cypriano Dutra. 2017. "(−)-β-Caryophyllene, a CB2 Receptor-Selective Phytocannabinoid, Suppresses Motor Paralysis and Neuroinflammation in a Murine Model of Multiple Sclerosis." International Journal of Molecular Sciences 18(4):1–14. doi: 10.3390/ijms18040691.

Alenina, Natalia, Tatjana Baranova, Eugene Smirnow, Michael Bader, Andrea Lippoldt, Eugene Patkin, and Thomas Walther. 2002. "Cell Type-Specific Expression of the Mas Proto-Oncogene in Testis." Journal of Histochemistry and Cytochemistry 50(5):691–95. doi: 10.1177/002215540205000510.

Alenina, Natalia, Ping Xu, Brit Rentzsch, Eugene L. Patkin, and Michael Bader. 2008. "Genetically Altered Animal Models for Mas and Angiotensin-(1-7)." Experimental Physiology 93(5):528–37.

doi: 10.1113/expphysiol.2007.040345.

Alexander, Stephen P. H., Jacqui Cooper, John Shine, and Stephen J. Hill. 1996. "Characterization of the Human Brain Putative A(2B) Adenosine Receptor Expressed in Chinese Hamster Ovary (CHO.A(2B4)) Cells." British Journal of Pharmacology 119(6):1286–90. doi: 10.1111/j.1476-5381.1996.tb16035.x.

Alhouayek, Mireille, Julien Masquelier, and Giulio G. Muccioli. 2018. "Lysophosphatidylinositols, from Cell Membrane Constituents to GPR55 Ligands." Trends in Pharmacological Sciences 39(6):586–604. doi: 10.1016/j.tips.2018.02.011.

Aliyari Serej, Zeynab, Abbas Ebrahimi Kalan, Ahmad Mehdipour, and Hojjatollah Nozad Charoudeh. 2017. "Regulation and Roles of CD26/DPPIV in Hematopoiesis and Diseases." Biomedicine & Pharmacotherapy 91:88–94. doi: 10.1016/j.biopha.2017.04.074.

Alzheimer's Association Report. 2019. "2019 Alzheimer's Disease Facts and Figures." Alzheimer's & Dementia 15(3):321–87. doi: 10.1016/j.jalz.2019.01.010.

Ambühl, Philipp, Dominik Felix, and Mahesh C. Khosla. 1994. "[7-D-ALA]-Angiotensin-(1-7): Selective Antagonism of Angiotensin-(1-7) in the Rat Paraventricular Nucleus." Brain Research Bulletin 35(4):289–91. doi: 10.1016/0361-9230(94)90103-1.

Amin M.R., and Ali DW. 2019. "Pharmacology of Medical Cannabis." Advances in Experimental Medicine and Biology 1162:151–65.

An, Dongchen, Steve Peigneur, Louise Antonia Hendrickx, and Jan Tytgat. 2020. "Targeting Cannabinoid Receptors: Current Status and Prospects of Natural Products." International Journal of Molecular Sciences 21(14):1–33. doi: 10.3390/ijms21145064.

Anavi-Goffer, Sharon, Gemma Baillie, Andrew J. Irving, Jürg Gertsch, Iain R. Greig, Roger G. Pertwee, and Ruth A. Ross. 2012a. "Modulation of L-α-Lysophosphatidylinositol/GPR55 Mitogen-Activated Protein Kinase (MAPK) Signaling by Cannabinoids*." Journal of Biological Chemistry 287(1):91–104. doi: 10.1074/jbc.M111.296020.

Anavi-Goffer, Sharon, Gemma Baillie, Andrew J. Irving, Jürg Gertsch, Iain R. Greig, Roger G. Pertwee, and Ruth A. Ross. 2012b. "Modulation of L-α-Lysophosphatidylinositol/GPR55 Mitogen-Activated Protein Kinase (MAPK) Signaling by Cannabinoids." Journal of Biological Chemistry 287(1):91–104. doi: 10.1074/jbc.M111.296020.

Anderson, Roy M., Christoforos Hadjichrysanthou, Stephanie Evans, and Mei Mei Wong. 2017. "Why Do so Many Clinical Trials of Therapies for Alzheimer's Disease Fail?" The Lancet 390(10110):2327–29. doi: 10.1016/S0140-6736(17)32399-1.

Angulo, Ester, Vicent Casadó, Josefa Mallol, Enric I. Canela, Francesc Viñals, Isidre Ferrer, Carmen Lluis, and Rafael Franco. 2006. "A1 Adenosine Receptors Accumulate in Neurodegenerative Structures in Alzheimer's Disease and Mediate Both Amyloid Precursor Protein Processing and Tau Phosphorylation and Translocation." Brain Pathology 13(4):440–51. doi: 10.1111/j.1750-3639.2003.tb00475.x.

Apostu, Dragos, Ondine Lucaciu, Alexandru Mester, Horea Benea, Daniel Oltean-Dan, Florin Onisor, Mihaela Baciut, and Simion Bran. 2019. "Cannabinoids and Bone Regeneration." Drug Metabolism Reviews 51(1):65–75. doi: 10.1080/03602532.2019.1574303.

Aquino, Camila Catherine, and Susan H. Fox. 2015. "Clinical Spectrum of Levodopa-Induced Complications." Movement Disorders 30(1):80–89. doi: 10.1002/mds.26125.

Armentero, Marie Therese, Annalisa Pinna, Sergi Ferré, José Luis Lanciego, Christa E. Müller, and Rafael Franco. 2011. "Past, Present and Future of A2A Adenosine Receptor Antagonists in the Therapy of Parkinson's Disease." Pharmacology & Therapeutics 132(3):280–99. doi: 10.1016/j.pharmthera.2011.07.004.

Aso, Ester, and Isidro Ferrer. 2016. "CB2 Cannabinoid Receptor As Potential Target against Alzheimer's Disease." Frontiers in Neuroscience 10(May):1–10. doi: 10.3389/fnins.2016.00243.

Aso, Ester, Salvador Juvés, Rafael Maldonado, and Isidro Ferrer. 2013. "CB2 Cannabinoid Receptor Agonist Ameliorates Alzheimer-like Phenotype in AβPP/PS1 Mice." Journal of Alzheimer's Disease 35(4):847–58. doi: 10.3233/JAD-130137.

Awad, Alaa S., Liping Huang, Hong Ye, Elizabeth Thu Anh Duong, W. Kline Bolton, Joel Linden, and

Mark D. Okusa. 2006. "Adenosine A2A Receptor Activation Attenuates Inflammation and Injury in Diabetic Nephropathy." American Journal of Physiology - Renal Physiology 290(4):828–37. doi: 10.1152/ajprenal.00310.2005.

Azam, Shofiul, Md. Ezazul Haque, Md. Jakaria, Dong-Kug Choi, Song-Hee Jo, In-Su Kim, and Dong-Kug Choi. 2020. "G-Protein-Coupled Receptors in CNS : A Potential Neurodegenerative Disorders and Associated." Cells 9:506.

Bacart, Johan, Caroline Corbel, Ralf Jockers, Stéphane Bach, and Cyril Couturier. 2008. "The BRET Technology and Its Application to Screening Assays." Biotechnology Journal 3(3):311–24. doi: 10.1002/biot.200700222.

Bader, Michael, Natalia Alenina, Miguel A. Andrade-Navarro, and Robson A. Santos. 2014. "Mas and Its Related G Protein–Coupled Receptors, Mrgprs." Pharmacological Reviews 66(4):1080–1105. doi: 10.1124/pr.113.008136.

Bagyinszky, Eva, Min Ju Kang, Jungmin Pyun, Vo Van Giau, Seong Soo A. An, and Sang Yun Kim. 2019. "Early-Onset Alzheimer's Disease Patient with Prion (PRNP) p.Val180ile Mutation." Neuropsychiatric Disease and Treatment 15:2003–13. doi: 10.2147/NDT.S215277.

Balenga, N. A., E. Martínez-Pinilla, J. Kargl, R. Schröder, M. Peinhaupt, W. Platzer, Z. Bálint, M. Zamarbide, I. G. Dopeso-Reyes, A. Ricobaraza, J. M. Pérez-Ortiz, E. Kostenis, M. Waldhoer, A. Heinemann, and R. Franco. 2014. "Heteromerization of GPR55 and Cannabinoid CB2 Receptors Modulates Signalling." British Journal of Pharmacology 171(23):5387–5406. doi: 10.1111/bph.12850.

Bara-Jimenez, W., A. Sherzai, T. Dimitrova, A. Favit, F. Bibbiani, M. Gillespie, M. J. Morris, M. M. Mouradian, and T. N. Chase. 2003. "Adenosine A2A Receptor Antagonist Treatment of Parkinson's Disease." Neurology 61(3):293–96. doi: 10.1212/01.WNL.0000073136.00548.D4.

Barber, Melissa N., Donella B. Sampey, and Robert E. Widdop. 1999. "AT2 Receptor Stimulation Enhances Antihypertensive Effect of AT1 Receptor Antagonist in Hypertensive Rats." Hypertension 34(5):1112–16. doi: 10.1161/01.HYP.34.5.1112.

Barreto, Carlos A. V., Salete J. Baptista, António José Preto, Pedro Matos-Filipe, Joana Mourão, Rita Melo, and Irina Moreira. 2020. "Prediction and Targeting of GPCR Oligomer Interfaces." Progress in Molecular Biology and Translational Science 169:105–49. doi: 10.1016/bs.pmbts.2019.11.007.

Bayer, Thomas A. 2015. "Proteinopathies, a Core Concept for Understanding and Ultimately Treating Degenerative Disorders?" European Neuropsychopharmacology 25(5):713–24. doi: 10.1016/j.euroneuro.2013.03.007.

Bayewitch, Michael, Tomer Avidor-Reiss, Rivka Levy, Jacob Barg, Raphael Mechoulam, and Zvi Vogel. 1995. "The Peripheral Cannabinoid Receptor: Adenylate Cyclase Inhibition and G Protein Coupling." FEBS Letters 375(1–2):143–47. doi: 10.1016/0014-5793(95)01207-U.

Bedford, Juliet, Delia Enria, Johan Giesecke, David L. Heymann, Chikwe Ihekweazu, Gary Kobinger, H. Clifford Lane, Ziad Memish, Myoung don Oh, Amadou Alpha Sall, Anne Schuchat, Kumnuan Ungchusak, and Lothar H. Wieler. 2020. "COVID-19: Towards Controlling of a Pandemic." The Lancet 395(10229):1015–18. doi: 10.1016/S0140-6736(20)30673-5.

Bellini, Giulia, Anna Grandone, Marco Torella, Emanuele Miraglia Del Giudice, Bruno Nobili, Laura Perrone, Sabatino Maione, and Francesca Rossi. 2015. "The Cannabinoid Receptor 2 Q63R Variant Modulates the Relationship between Childhood Obesity and Age at Menarche." PLoS ONE 10(10):1–7. doi: 10.1371/journal.pone.0140142.

Belvisi, Daniele, Roberta Pellicciari, Andrea Fabbrini, Matteo Costanzo, Sara Pietracupa, Maria De Lucia, Nicola Modugno, Francesca Magrinelli, Carlo Dallocchio, Tommaso Ercoli, Claudio Terravecchia, Alessandra Nicoletti, Paolo Solla, Giovanni Fabbrini, Michele Tinazzi, Alfredo Berardelli, and Giovanni Defazio. 2020. Risk Factors of Parkinson Disease: Simultaneous Assessment, Interactions, and Etiologic Subtypes. Vol. 95.

Bénard, Giovanni, Federico Massa, Nagore Puente, Joana Lourenço, Luigi Bellocchio, Edgar Soria-Gómez, Isabel Matias, Anna Delamarre, Mathilde Metna-Laurent, Astrid Cannich, Etienne Hebert-Chatelain, Christophe Mulle, Silvia Ortega-Gutiérrez, Mar Martín-Fontecha, Matthias

Klugmann, Stephan Guggenhuber, Beat Lutz, Jürg Gertsch, Francis Chaouloff, María Luz López-Rodríguez, Pedro Grandes, Rodrigue Rossignol, and Giovanni Marsicano. 2012. "Mitochondrial CB1 Receptors Regulate Neuronal Energy Metabolism." Nature Neuroscience 15(4):558–64. doi: 10.1038/nn.3053.

Benarroch, Eduardo E. 2018. "Glutamatergic Synaptic Plasticity and Dysfunction in Alzheimer Disease: Emerging Mechanisms." Neurology 91(3):125–32. doi: 10.1212/WNL.0000000000005807.

Benicky, Julius, Enrique Sánchez-Lemus, Masaru Honda, Tao Pang, Martina Orecna, Juan Wang, Yan Leng, De Maw Chuang, and Juan M. Saavedra. 2011. "Angiotensin II AT1 Receptor Blockade Ameliorates Brain Inflammation." Neuropsychopharmacology 36(4):857–70. doi: 10.1038/npp.2010.225.

Bennion, Douglas M., Jacob D. Isenberg, Allison T. Harmel, Kelly DeMars, Alex N. Dang, Chad H. Jones, Megan E. Pignataro, Justin T. Graham, U. Muscha Steckelings, Jon C. Alexander, Marcelo Febo, Eric G. Krause, Annette D. de Kloet, Eduardo Candelario-Jalil, and Colin Sumners. 2017. "Post-Stroke Angiotensin II Type 2 Receptor Activation Provides Long-Term Neuroprotection in Aged Rats" edited by T. V. Arumugam. PLOS ONE 12(7):e0180738. doi: 10.1371/journal.pone.0180738.

Betarbet, Ranjita, Todd B. Sherer, Donato a Di, and J. Timothy Greenamyre. 2002. "Mechanistic Approaches to Parkinson's Disease." Biomedical Research 30322.

Bhat, Shahnawaz Ali, Anika Sood, Rakesh Shukla, and Kashif Hanif. 2019. "AT2R Activation Prevents Microglia Pro-Inflammatory Activation in a NOX-Dependent Manner: Inhibition of PKC Activation and P47 Phox Phosphorylation by PP2A." Molecular Neurobiology 56(4):3005–23. doi: 10.1007/s12035-018-1272-9.

Bischof, Gérard N., Michael Ewers, Nicolai Franzmeier, Michel J. Grothe, Merle Hoenig, Ece Kocagoncu, Julia Neitzel, James B. Rowe, Antonio Strafella, Alexander Drzezga, and Thilo van Eimeren. 2019. "Connectomics and Molecular Imaging in Neurodegeneration." European Journal of Nuclear Medicine and Molecular Imaging 46(13):2819–30. doi: 10.1007/s00259-019-04394-5.

Bitker, Laurent, and Louise M. Burrell. 2019. "Classic and Nonclassic Renin-Angiotensin Systems in the Critically Ill." Critical Care Clinics 35(2):213–27. doi: 10.1016/j.ccc.2018.11.002.

Boison, Detlev. 2013. "Adenosine Kinase: Exploitation for Therapeutic Gain." Pharmacological Reviews 65(3):906–43. doi: 10.1124/pr.112.006361.

Borroto-Escuela, Dasiel O., Ismel Brito, Wilber Romero-Fernandez, Michael Di Palma, Julia Oflijan, Kamila Skieterska, Jolien Duchou, Kathleen Van Craenenbroeck, Diana Suárez-Boomgaard, Alicia Rivera, Diego Guidolin, Luigi F. Agnati, and Kjell Fuxe. 2014. "The G Protein-Coupled Receptor Heterodimer Network (GPCR-HetNet) and Its Hub Components." International Journal of Molecular Sciences 15(5):8570–90. doi: 10.3390/ijms15058570.

Borroto-Escuela, Dasiel O., David Rodriguez, Wilber Romero-Fernandez, Jon Kapla, Mariama Jaiteh, Anirudh Ranganathan, Tzvetana Lazarova, Kjell Fuxe, and Jens Carlsson. 2018. "Mapping the Interface of a GPCR Dimer: A Structural Model of the A2A Adenosine and D2 Dopamine Receptor Heteromer." Frontiers in Pharmacology 9(AUG):1–16. doi: 10.3389/fphar.2018.00829.

Boschmann, Michael, Stefan Engeli, Frauke Adams, Gabriele Franke, Friedrich C. Luft, Arya M. Sharma, and Jens Jordan. 2006. "Influences of AT1 Receptor Blockade on Tissue Metabolism in Obese Men." American Journal of Physiology - Regulatory Integrative and Comparative Physiology 290(1):219–23. doi: 10.1152/ajpregu.00341.2005.

Bottari, Serge P., Verdon Taylor, Isabelle N. King, Yvonne Bogdal, Steven Whitebread, and Marc de Gasparo. 1991. "Angiotensin II AT2 Receptors Do Not Interact with Guanine Nucleotide Binding Proteins." European Journal of Pharmacology: Molecular Pharmacology 207(2):157–63. doi: 10.1016/0922-4106(91)90091-U.

Boya, Patricia, Anne-Laure Pauleau, Delphine Poncet, Rosa-Ana Gonzalez-Polo, Naoufal Zamzami, and Guido Kroemer. 2004. "Viral Proteins Targeting Mitochondria: Controlling Cell Death." Biochimica et Biophysica Acta (BBA) - Bioenergetics 1659(2–3):178–89. doi:

10.1016/j.bbabio.2004.08.007.

Brady, Ashley E., and Lee E. Limbird. 2002. "G Protein-Coupled Receptor Interacting Proteins: Emerging Roles in Localization and Signal Transduction." Cellular Signalling 14(4):297–309. doi: 10.1016/S0898-6568(01)00239-X.

Burack, M. A., J. Hartlein, H. P. Flores, L. Taylor-Reinwald, J. S. Perlmutter, and N. J. Cairns. 2010. "In Vivo Amyloid Imaging in Autopsy-Confirmed Parkinson Disease with Dementia." Neurology 74(1):77–84. doi: 10.1212/WNL.0b013e3181c7da8e.

Burch, J., C. McKenna, S. Palmer, G. Norman, J. Glanville, M. Sculpher, and N. Woolacott. 2009. "Rimonabant for the Treatment of Overweight and Obese People." Health Technology Assessment (Winchester, England) 13 Suppl 3:13–22. doi: 10.3310/hta13suppl3/03.

Burnstock, G. 2007. "Purine and Pyrimidine Receptors." Cellular and Molecular Life Sciences 64(12):1471–83. doi: 10.1007/s00018-007-6497-0.

Burrell, Louise M., Colin I. Johnston, Christos Tikellis, and Mark E. Cooper. 2004. "ACE2, a New Regulator of the Renin-Angiotensin System." Trends in Endocrinology and Metabolism 15(4):166–69. doi: 10.1016/j.tem.2004.03.001.

Burstein, Ethan S., Thomas R. Ott, Michele Feddock, Jian Nong Ma, Steve Fuhs, Steven Wong, Hans H. Schiffer, Mark R. Brann, and Norman R. Nash. 2006. "Characterization of the Mas-Related Gene Family: Structural and Functional Conservation of Human and Rhesus MrgX Receptors." British Journal of Pharmacology 147(1):73–82. doi: 10.1038/sj.bjp.0706448.

Cahill, Thomas J., Alex R. B. Thomsen, Jeffrey T. Tarrasch, Bianca Plouffe, Anthony H. Nguyen, Fan Yang, Li Yin Huang, Alem W. Kahsai, Daniel L. Bassoni, Bryant J. Gavino, Jane E. Lamerdin, Sarah Triest, Arun K. Shukla, Benjamin Berger, John Little, Albert Antar, Adi Blanc, Chang Xiu Qu, Xin Chen, Kouki Kawakami, Asuka Inoue, Junken Aoki, Jan Steyaert, Jin Peng Sun, Michel Bouvier, Georgios Skiniotis, and Robert J. Lefkowitz. 2017. "Distinct Conformations of GPCR-β-Arrestin Complexes Mediate Desensitization, Signaling, and Endocytosis." Proceedings of the National Academy of Sciences of the United States of America 114(10):2562–67. doi: 10.1073/pnas.1701529114.

Callén, Lucía, Estefanía Moreno, Pedro Barroso-Chinea, David Moreno-Delgado, Antoni Cortés, Josefa Mallol, Vicent Casadó, José Luis Lanciego, Rafael Franco, Carmen Lluis, Enric I. Canela, and Peter J. McCormick. 2012a. "Cannabinoid Receptors CB1 and CB2 Form Functional Heteromers in Brain." Journal of Biological Chemistry 287(25):20851–65. doi: 10.1074/jbc.M111.335273.

Callén, Lucía, Estefanía Moreno, Pedro Barroso-Chinea, David Moreno-Delgado, Antoni Cortés, Josefa Mallol, Vicent Casadó, José Luis Lanciego, Rafael Franco, Carmen Lluis, Enric I. Canela, and Peter J. McCormick. 2012b. "Cannabinoid Receptors CB1 and CB2 Form Functional Heteromers in Brain." Journal of Biological Chemistry 287(25):20851–65. doi: 10.1074/jbc.M111.335273.

Cameron, Brent, and Gary E. Landreth. 2010. "Inflammation, Microglia, and Alzheimer's Disease." Neurobiology of Disease 37(3):503–9. doi: 10.1016/j.nbd.2009.10.006.

Canals, Meritxell, Javier Burgueño, Daniel Marcellino, Núria Cabello, Enric I. Canela, Josefa Mallol, Luigi Agnati, Sergi Ferré, Michel Bouvier, Kjell Fuxe, Francisco Ciruela, Carmen Lluis, and Rafael Franco. 2004. "Homodimerization of Adenosine A2A Receptors: Qualitative and Quantitative Assessment by Fluorescence and Bioluminescence Energy Transfer." Journal of Neurochemistry 88(3):726–34. doi: 10.1046/j.1471-4159.2003.02200.x.

Canals, Meritxell, Laura Jenkins, Elaine Kellett, and Graeme Milligan. 2006. "Up-Regulation of the Angiotensin II Type 1 Receptor by the MAS Proto-Oncogene Is Due to Constitutive Activation of Gq/G11 by MAS." Journal of Biological Chemistry 281(24):16757–67. doi: 10.1074/jbc.M601121200.

Capuron, Lucile, and Andrew H. Miller. 2011. "Immune System to Brain Signaling: Neuropsychopharmacological Implications." Pharmacology and Therapeutics 130(2):226–38. doi: 10.1016/j.pharmthera.2011.01.014.

Carai, Mauro A. M., Giancarlo Colombo, Paola Maccioni, and Gian Luigi Gessa. 2006. "Efficacy of Rimonabant and Other Cannabinoid CB1 Receptor Antagonists in Reducing Food Intake and Body Weight: Preclinical and Clinical Data." CNS Drug Reviews 12(2):91–99. doi:

10.1111/j.1527-3458.2006.00091.x.
Carey, Robert M. 2017. "AT2 Receptors: Potential Therapeutic Targets for Hypertension." American Journal of Hypertension 30(4):339–47. doi: 10.1093/ajh/hpw121.
Carpenter, Byron, and Guillaume Lebon. 2017. "Human Adenosine A2A Receptor: Molecular Mechanism of Ligand Binding and Activation." Frontiers in Pharmacology 8(DEC):1–15. doi: 10.3389/fphar.2017.00898.
Carriba, Paulina, Gemma Navarro, Francisco Ciruela, Sergi Ferré, Vicent Casadó, Luigi Agnati, Antoni Cortés, Josefa Mallol, Kjell Fuxe, Enric I. Canela, Carmen Lluís, and Rafael Franco. 2008. "Detection of Heteromerization of More than Two Proteins by Sequential BRET-FRET." Nature Methods 5(8):727–33. doi: 10.1038/nmeth.1229.
Carriba, Paulina, Oskar Ortiz, Kshitij Patkar, Zuzana Justinova, Jessica Stroik, Andrea Themann, Christa Müller, Anima S. Woods, Bruce T. Hope, Francisco Ciruela, Vicent Casadó, Enric I. Canela, Carme Lluis, Steven R. Goldberg, Rosario Moratalla, Rafael Franco, and Sergi Ferré. 2007. "Striatal Adenosine A2A and Cannabinoid CB1 Receptors Form Functional Heteromeric Complexes That Mediate the Motor Effects of Cannabinoids." Neuropsychopharmacology 32(11):2249–59. doi: 10.1038/sj.npp.1301375.
Casetta, I., F. Vincenzi, D. Bencivelli, C. Corciulo, M. Gentile, E. Granieri, P. A. Borea, and K. Varani. 2014. "A2A Adenosine Receptors and Parkinson's Disease Severity." Acta Neurologica Scandinavica 129(4):276–81. doi: 10.1111/ane.12181.
Castillo, Pablo E., Thomas J. Younts, Andrés E. Chávez, and Yuki Hashimotodani. 2012. "Endocannabinoid Signaling and Synaptic Function." Neuron 76(1):70–81. doi: 10.1016/j.neuron.2012.09.020.
Chakraborty, Hirak, and Amitabha Chattopadhyay. 2015. "Excitements and Challenges in GPCR Oligomerization: Molecular Insight from FRET." ACS Chemical Neuroscience 6(1):199–206. doi: 10.1021/cn500231d.
Chan, H. C. Stephe., Yi Li, Thamani Dahoun, Horst Vogel, and Shuguang Yuan. 2019. "New Binding Sites, New Opportunities for GPCR Drug Discovery." Trends in Biochemical Sciences 44(4):312–30. doi: 10.1016/j.tibs.2018.11.011.
Chan, Kui K., Danielle Dorosky, Preeti Sharma, Shawn A. Abbasi, John M. Dye, David M. Kranz, Andrew S. Herbert, and Erik Procko. 2020. "Engineering Human ACE2 to Optimize Binding to the Spike Protein of SARS Coronavirus 2." Science 369(6508):1261–65. doi: 10.1126/SCIENCE.ABC0870.
Chang, H. T., and H. Kita. 1992. "Interneurons in the Rat Striatum: Relationships between Parvalbumin Neurons and Cholinergic Neurons." Brain Research 574(1–2):307–11. doi: 10.1016/0006-8993(92)90830-3.
Chappell, Mark C., K. Bridget Brosnihan, Debra I. Diz, and Carlos M. Ferrario. 1989. "Identification of Angiotensin-(1-7) in Rat Brain." The Journal of Biological Chemistry 264(28):16518–23.
Che, Tao, Susruta Majumdar, Saheem A. Zaidi, Pauline Ondachi, John D. Mccorvy, Sheng Wang, Philip D. Mosier, Rajendra Uprety, Eyal Vardy, Brian E. Krumm, Gye Won, Ming-yue Lee, Els Pardon, Jan Steyaert, Xi-ping Huang, T. Ryan, Vadim Cherezov, Vsevolod Katritch, Daniel Wacker, and L. Bryan. 2018. "Stucture of Active State of Kappa Opioid Receptor." 172:55–67. doi: 10.1016/j.cell.2017.12.011.Structure.
Chemistry, Basic. 2007. "Dizocilpine." 1–4.
Chen, Jun, and Kanta Subbarao. 2007. "The Immunobiology of SARS." Annual Review of Immunology 25(1):443–72. doi: 10.1146/annurev.immunol.25.022106.141706.
Chiti, Fabrizio, Martino Calamai, Niccolò Taddei, Massimo Stefani, Giampietro Ramponi, and Christopher M. Dobson. 2002. "Studies of the Aggregation of Mutant Proteins in Vitro Provide Insights into the Genetics of Amyloid Diseases." Proceedings of the National Academy of Sciences of the United States of America 99(SUPPL. 4):16419–26. doi: 10.1073/pnas.212527999.
Chiu, A. T., James W. Ryan, John M. Stewart, and F. E. Dorer. 1976. "Formation of Angiotensin III by Angiotensin-Converting Enzyme." Biochemical Journal 155(1):189–92. doi: 10.1042/bj1550189.

Christensen, Robin, Pernelle Kruse Kristensen, Else Marie Bartels, Henning Bliddal, and Arne Astrup. 2007. "Efficacy and Safety of the Weight-Loss Drug Rimonabant: A Meta-Analysis of Randomised Trials." The Lancet 370(9600):1706–13. doi: 10.1016/S0140-6736(07)61721-8.

Citron, Martin. 2010. "Alzheimer's Disease: Strategies for Disease Modification." Nature Reviews Drug Discovery 9(5):387–98. doi: 10.1038/nrd2896.

Congreve, Miles, Chris de Graaf, Nigel A. Swain, and Christopher G. Tate. 2020. "Impact of GPCR Structures on Drug Discovery." Cell 181(1):81–91. doi: 10.1016/j.cell.2020.03.003.

Connolly, Alexandre, Brian J. Holleran, Élie Simard, Jean Patrice Baillargeon, Pierre Lavigne, and Richard Leduc. 2019. "Interplay between Intracellular Loop 1 and Helix VIII of the Angiotensin II Type 2 Receptor Controls Its Activation." Biochemical Pharmacology 168(May):330–38. doi: 10.1016/j.bcp.2019.07.018.

Costa-Besada, Maria A., Rita Valenzuela, Pablo Garrido-Gil, Begoña Villar-Cheda, Juan A. Parga, Jose L. Lanciego, and Jose L. Labandeira-Garcia. 2018. "Paracrine and Intracrine Angiotensin 1-7/Mas Receptor Axis in the Substantia Nigra of Rodents, Monkeys, and Humans." Molecular Neurobiology 55(7):5847–67. doi: 10.1007/s12035-017-0805-y.

Costenla, Ana Rita, Rodrigo A. Cunha, and Alexandre De Mendonça. 2010. "Caffeine, Adenosine Receptors, and Synaptic Plasticity." Journal of Alzheimer's Disease 20(SUPPL.1). doi: 10.3233/JAD-2010-091384.

Cottrell, G. S. 2013. "Roles of Proteolysis in Regulation of GPCR Function." British Journal of Pharmacology 168(3):576–90. doi: 10.1111/j.1476-5381.2012.02234.x.

Craig Venter, J., M. D. Adams, E. W. Myers, P. W. Li, R. J. Mural, G. G. Sutton, H. O. Smith, M. Yandell, C. A. Evans, R. A. Holt, J. D. Gocayne, P. Amanatides, R. M. Ballew, D. H. Huson, J. R. Wortman, Q. Zhang, C. D. Kodira, X. H. Zheng, L. Chen, M. Skupski, G. Subramanian, P. D. Thomas, J. Zhang, G. L. Gabor Miklos, C. Nelson, S. Broder, A. G. Clark, J. Nadeau, V. A. McKusick, N. Zinder, A. J. Levine, R. J. Roberts, M. Simon, C. Slayman, M. Hunkapiller, R. Bolanos, A. Delcher, I. Dew, D. Fasulo, M. Flanigan, L. Florea, A. Halpern, S. Hannenhalli, S. Kravitz, S. Levy, C. Mobarry, K. Reinert, K. Remington, J. Abu-Threideh, E. Beasley, K. Biddick, V. Bonazzi, R. Brandon, M. Cargill, I. Chandramouliswaran, R. Charlab, K. Chaturvedi, Z. Deng, V. di Francesco, P. Dunn, K. Eilbeck, C. Evangelista, A. E. Gabrielian, W. Gan, W. Ge, F. Gong, Z. Gu, P. Guan, T. J. Heiman, M. E. Higgins, R. R. Ji, Z. Ke, K. A. Ketchum, Z. Lai, Y. Lei, Z. Li, J. Li, Y. Liang, X. Lin, F. Lu, G. V. Merkulov, N. Milshina, H. M. Moore, A. K. Naik, V. A. Narayan, B. Neelam, D. Nusskern, D. B. Rusch, S. Salzberg, W. Shao, B. Shue, J. Sun, Z. Yuan Wang, A. Wang, X. Wang, J. Wang, M. H. Wei, R. Wides, C. Xiao, C. Yan, A. Yao, J. Ye, M. Zhan, W. Zhang, H. Zhang, Q. Zhao, L. Zheng, F. Zhong, W. Zhong, S. C. Zhu, S. Zhao, D. Gilbert, S. Baumhueter, G. Spier, C. Carter, A. Cravchik, T. Woodage, F. Ali, H. An, A. Awe, D. Baldwin, H. Baden, M. Barnstead, I. Barrow, K. Beeson, D. Busam, A. Carver, A. Center, M. Lai Cheng, L. Curry, S. Danaher, L. Davenport, R. Desilets, S. Dietz, K. Dodson, L. Doup, S. Ferriera, N. Garg, A. Gluecksmann, B. Hart, J. Haynes, C. Haynes, C. Heiner, S. Hladun, D. Hostin, J. Houck, T. Howland, C. Ibegwam, J. Johnson, F. Kalush, L. Kline, S. Koduru, A. Love, F. Mann, D. May, S. McCawley, T. McIntosh, I. McMullen, M. Moy, L. Moy, B. Murphy, K. Nelson, C. Pfannkoch, E. Pratts, V. Puri, H. Qureshi, M. Reardon, R. Rodriguez, Yu H. Rogers, D. Romblad, B. Ruhfel, R. Scott, C. Sitter, M. Smallwood, E. Stewart, R. Strong, E. Suh, R. Thomas, N. Ni Tint, S. Tse, C. Vech, G. Wang, J. Wetter, S. Williams, M. Williams, S. Windsor, E. Winn-Deen, K. Wolfe, J. Zaveri, K. Zaveri, J. F. Abril, R. Guigo, M. J. Campbell, K. V. Sjolander, B. Karlak, A. Kejariwal, H. Mi, B. Lazareva, T. Hatton, A. Narechania, K. Diemer, A. Muruganujan, N. Guo, S. Sato, V. Bafna, S. Istrail, R. Lippert, R. Schwartz, B. Walenz, S. Yooseph, D. Allen, A. Basu, J. Baxendale, L. Blick, M. Caminha, J. Carnes-Stine, P. Caulk, Y. H. Chiang, M. Coyne, C. Dahlke, A. Deslattes Mays, M. Dombroski, M. Donnelly, D. Ely, S. Esparham, C. Fosler, H. Gire, S. Glanowski, K. Glasser, A. Glodek, M. Gorokhov, K. Graham, B. Gropman, M. Harris, J. Heil, S. Henderson, J. Hoover, D. Jennings, C. Jordan, J. Jordan, J. Kasha, L. Kagan, C. Kraft, A. Levitsky, M. Lewis, X. Liu, J. Lopez, D. Ma, W. Majoros, J. McDaniel, S. Murphy, M. Newman, T. Nguyen, N. Nguyen, M. Nodell, S. Pan, J. Peck, M. Peterson, W. Rowe, R. Sanders, J. Scott, M. Simpson, T. Smith, A. Sprague, T. Stockwell, R. Turner, E. Venter, M. Wang, M. Wen, D. Wu, M.

Wu, A. Xia, A. Zandieh, and X. Zhu. 2001. "The Sequence of the Human Genome." Science 291(5507):1304–51. doi: 10.1126/science.1058040.

Cull-Candy, Stuart G., and Daniel N. Leszkiewicz. 2004. "Role of Distinct NMDA Receptor Subtypes at Central Synapses." Science's STKE : Signal Transduction Knowledge Environment 2004(255). doi: 10.1126/stke.2552004re16.

Danyel, Leon A., Patrick Schmerler, Ludovit Paulis, Thomas Unger, and U. Muscha Steckelings. 2013. "Impact of AT2-Receptor Stimulation on Vascular Biology, Kidney Function, and Blood Pressure." Integrated Blood Pressure Control 6:153–61. doi: 10.2147/IBPC.S34425.

Dawson, T. M. 2006. "Parkin and Defective Ubiquitination in Parkinson's Disease." Journal of Neural Transmission, Supplement (70):209–13. doi: 10.1007/978-3-211-45295-0_32.

Dawson, Ted M., Todd E. Golde, and Clotilde Lagier-Tourenne. 2018. "Animal Models of Neurodegenerative Diseases." Nature Neuroscience 21(10):1370–79. doi: 10.1038/s41593-018-0236-8.

Deshotels, Matthew R., Huijing Xia, Srinivas Sriramula, Eric Lazartigues, and Catalin M. Filipeanu. 2014. "Angiotensin II Mediates Angiotensin Converting Enzyme Type 2 Internalization and Degradation Through an Angiotensin II Type I Receptor–Dependent Mechanism." Hypertension 64(6):1368–75. doi: 10.1161/HYPERTENSIONAHA.114.03743.

Devost, Dominic, Rory Sleno, Darlaine Pé Trin, Alice Zhang, Yuji Shinjo, Rakan Okde, Junken Aoki, Asuka Inoue, and Terence E. Hébert. 2017. "Conformational Profiling of the AT1 Angiotensin II Receptor Reflects Biased Agonism, G Protein Coupling, and Cellular Context." Journal of Biological Chemistry 292(13):5443–56. doi: 10.1074/jbc.M116.763854.

Dittus, Jason, Shannon Cooper, Gerald Obermeir, and Lakshmidevi Pulakat. 1999. "Role of the Third Intracellular Loop of the Angiotensin II Receptor Subtype AT2 in Ligand-Receptor Interaction." FEBS Letters 445(1):23–26. doi: 10.1016/S0014-5793(99)00085-X.

Domenici, Maria Rosaria, Antonella Ferrante, Alberto Martire, Valentina Chiodi, Rita Pepponi, Maria Teresa Tebano, and Patrizia Popoli. 2019. "Adenosine A2A Receptor as Potential Therapeutic Target in Neuropsychiatric Disorders." Pharmacological Research 147(June):104338. doi: 10.1016/j.phrs.2019.104338.

Dong, Xinzhong, Sang kyou Han, Mark J. Zylka, Melvin I. Simon, and David J. Anderson. 2001. "A Diverse Family of GPCRs Expressed in Specific Subsets of Nociceptive Sensory Neurons." Cell 106(5):619–32. doi: 10.1016/S0092-8674(01)00483-4.

Donoghue, Mary, Frank Hsieh, Elizabeth Baronas, Kevin Godbout, Michael Gosselin, Nancy Stagliano, Michael Donovan, Betty Woolf, Keith Robison, Raju Jeyaseelan, Roger E. Breitbart, and Susan Acton. 2000. "A Novel Angiotensin-Converting Enzyme – Related to Angiotensin 1-9." Circ Res 87:e1–9.

Dore, Kim, Ivar S. Stein, Jennifer A. Brock, Pablo E. Castillo, Karen Zito, and P. Jesper Sjöström. 2017. "Unconventional NMDA Receptor Signaling." Journal of Neuroscience 37(45):10800–807. doi: 10.1523/JNEUROSCI.1825-17.2017.

Drury, A. N., and A. Szent-Györgyi. 1929. "The Physiological Activity of Adenine Compounds with Especial Reference to Their Action upon the Mammalian Heart." The Journal of Physiology 68(3):213–37. doi: 10.1113/jphysiol.1929.sp002608.

Dugger, Brittany N., and Dennis W. Dickson. 2017. "Pathology of Neurodegenerative Diseases." Cold Spring Harbor Perspectives in Biology 9(7). doi: 10.1101/cshperspect.a028035.

Duke, Lisa M., Roger G. Evans, and Robert E. Widdop. 2005. "AT2 Receptors Contribute to Acute Blood Pressure-Lowering and Vasodilator Effects of AT1 Receptor Antagonism in Conscious Normotensive but Not Hypertensive Rats." American Journal of Physiology - Heart and Circulatory Physiology 288(5 57-5):2289–97. doi: 10.1152/ajpheart.01096.2004.

Dyer, Adam H., Claire Murphy, Brian Lawlor, and Sean P. Kennelly. 2020. "Social Networks in Mild-to-Moderate Alzheimer Disease: Longitudinal Relationships with Dementia Severity, Cognitive Function, and Adverse Events." Aging and Mental Health 0(0):1–7. doi: 10.1080/13607863.2020.1745146.

Eddy, Matthew T., Ming Yue Lee, Zhan Guo Gao, Kate L. White, Tatiana Didenko, Reto Horst, Martin

Audet, Pawel Stanczak, Kyle M. McClary, Gye Won Han, Kenneth A. Jacobson, Raymond C. Stevens, and Kurt Wüthrich. 2018. "Allosteric Coupling of Drug Binding and Intracellular Signaling in the A2A Adenosine Receptor." Cell 172(1–2):68-80.e12. doi: 10.1016/j.cell.2017.12.004.

Elbegdorj, Orgil, Richard B. Westkaemper, and Yan Zhang. 2013. "A Homology Modeling Study toward the Understanding of Three-Dimensional Structure and Putative Pharmacological Profile of the G-Protein Coupled Receptor GPR55." Journal of Molecular Graphics and Modelling 39(5):50–60. doi: 10.1016/j.jmgm.2012.10.005.

Eskelinen, Marjo H., and Miia Kivipelto. 2010. "Caffeine as a Protective Factor in Dementia and Alzheimer's Disease" edited by R. A. Cunha and A. de Mendonça. Journal of Alzheimer's Disease 20(s1):S167–74. doi: 10.3233/JAD-2010-1404.

Etelvino, Gisele Maia, Antônio Augusto Bastos Peluso, and Robson Augusto Souza Santos. 2014. "New Components of the Renin-Angiotensin System: Alamandine and the Mas-Related G Protein-Coupled Receptor D." Current Hypertension Reports 16(6):10–15. doi: 10.1007/s11906-014-0433-0.

Farag, S., and O. Kayser. 2017. Chapter 1 - The Cannabis Plant: Botanical Aspects. Elsevier Inc.

Faron-Górecka, Agata, Marta Szlachta, Magdalena Kolasa, Joanna Solich, Andrzej Górecki, Maciej Kuśmider, Dariusz Żurawek, and Marta Dziedzicka-Wasylewska. 2019. "Understanding GPCR Dimerization." Methods in Cell Biology 149:155–78. doi: 10.1016/bs.mcb.2018.08.005.

Felder, C. C., K. E. Joyce, E. M. Briley, J. Mansouri, K. Mackie, O. Blond, Y. Lai, A. L. Ma, and R. L. Mitchell. 1995. "Comparison of the Pharmacology and Signal Transduction of the Human Cannabinoid CB1 and CB2 Receptors." Molecular Pharmacology 48(3):443–50.

Ferguson, Stephen S. G., Larry S. Barak, Jie Zhang, and Marc G. Caron. 1996. "G-Protein-Coupled Receptor Regulation: Role of G-Protein-Coupled Receptor Kinases and Arrestins." Canadian Journal of Physiology and Pharmacology 74(10):1095–1110. doi: 10.1139/y96-124.

Fernández-Ruiz, Javier. 2019. "The Biomedical Challenge of Neurodegenerative Disorders: An Opportunity for Cannabinoid-Based Therapies to Improve on the Poor Current Therapeutic Outcomes." British Journal of Pharmacology 176(10):1370–83. doi: 10.1111/bph.14382.

Fernández-Ruiz, Javier, Miguel Moreno-Martet, Carmen Rodríguez-Cueto, Cristina Palomo-Garo, María Gómez-Cañas, Sara Valdeolivas, Carmen Guaza, Julián Romero, Manuel Guzmán, Raphael Mechoulam, and José A. Ramos. 2011. "Prospects for Cannabinoid Therapies in Basal Ganglia Disorders." British Journal of Pharmacology 163(7):1365–78. doi: 10.1111/j.1476-5381.2011.01365.x.

Fernández-Ruiz, Javier, María A. Moro, and José Martínez-Orgado. 2015. "Cannabinoids in Neurodegenerative Disorders and Stroke/Brain Trauma: From Preclinical Models to Clinical Applications." Neurotherapeutics 12(4):793–806. doi: 10.1007/s13311-015-0381-7.

Ferrão, Fernanda M., Luiza H. D. Cardoso, Heather A. Drummond, Xiao C. Li, Jia L. Zhuo, Dayene S. Gomes, Lucienne S. Lara, Adalberto Vieyra, and Jennifer Lowe. 2017. "Luminal ANG II Is Internalized as a Complex with AT1R/AT2R Heterodimers to Target Endoplasmic Reticulum in LLC-PK1 Cells." American Journal of Physiology - Renal Physiology 313(2):F440–49. doi: 10.1152/ajprenal.00261.2016.

Ferrario, Carlos M. 2011. "ACE2: More of Ang-(1–7) or Less Ang II?" Current Opinion in Nephrology and Hypertension 20(1):1–6. doi: 10.1097/MNH.0b013e3283406f57.

Ferre, S., C. Quiroz, A. Woods, R. Cunha, P. Popoli, F. Ciruela, C. Lluis, R. Franco, K. Azdad, and S. Schiffmann. 2008. "An Update on Adenosine A2A-Dopamine D2 Receptor Interactions: Implications for the Function of G Protein-Coupled Receptors." Current Pharmaceutical Design 14(15):1468–74. doi: 10.2174/138161208784480108.

Ferré, Sergi. 2015. "The GPCR Heterotetramer: Challenging Classical Pharmacology." Trends in Pharmacological Sciences 36(3):145–52. doi: 10.1016/j.tips.2015.01.002.

Ferré, Sergi, Jordi Bonaventura, Dardo Tomasi, Gemma Navarro, Estefanía Moreno, Antonio Cortés, Carme Lluís, Vicent Casadó, and Nora D. Volkow. 2016. "Allosteric Mechanisms within the Adenosine A2A-Dopamine D2 Receptor Heterotetramer." Neuropharmacology 104:154–60. doi:

10.1016/j.neuropharm.2015.05.028.
Ferré, Sergi, and Francisco Ciruela. 2019. "Functional and Neuroprotective Role of Striatal Adenosine A2A Receptor Heterotetramers." Journal of Caffeine and Adenosine Research 9(3):89–97. doi: 10.1089/caff.2019.0008.
Ferre, Sergi, Francisco Ciruela, Janusz Borycz, Marcello Solinas, Davide Quarta, Katerina Antoniou, Cesar Quiroz, Zuzana Justinova, Carme Lluis, Rafael Franco, and Steven R. Goldberg. 2008a. "Adenosine A1-A2A Receptor Heteromers: New Targets for Caffeine in the Brain." Frontiers in Bioscience 13(6):2391–99. doi: 10.2741/2852.
Ferre, Sergi, Francisco Ciruela, Janusz Borycz, Marcello Solinas, Davide Quarta, Katerina Antoniou, Cesar Quiroz, Zuzana Justinova, Carme Lluis, Rafael Franco, and Steven R. Goldberg. 2008b. "Adenosine A1-A2A Receptor Heteromers: New Targets for Caffeine in the Brain." Frontiers in Bioscience 13(6):2391–99. doi: 10.2741/2852.
Ferré, Sergi, Francisco Ciruela, Meritxell Canals, Daniel Marcellino, Javier Burgueno, Vicent Casadó, Joëlle Hillion, Maria Torvinen, Francesca Fanelli, Piero De Benedetti, Steven R. Goldberg, Michel Bouvier, Kjell Fuxe, Luigi F. Agnati, Carme Lluis, Rafael Franco, and Amina Woods. 2004. "Adenosine A2A-Dopamine D2 Receptor-Receptor Heteromers. Targets for Neuro-Psychiatric Disorders." Parkinsonism and Related Disorders 10(5):265–71. doi: 10.1016/j.parkreldis.2004.02.014.
Ferré, Sergi, César Quiroz, Marco Orru, Xavier Guitart, Gemma Navarro, Antonio Cortés, Vicent Casadó, Enric I. Canela, Carme Lluis, and Rafael Franco. 2011. "Adenosine A(2A) Receptors and A(2A) Receptor Heteromers as Key Players in Striatal Function." Frontiers in Neuroanatomy 5(June):36. doi: 10.3389/fnana.2011.00036.
Flores-Soto, M. E., V. Chaparro-Huerta, M. Escoto-Delgadillo, E. Vazquez-Valls, R. E. González-Castañeda, and C. Beas-Zarate. 2012. "Estructura y Función de Las Subunidades Del Receptor a Glutamato Tipo NMDA." Neurologia 27(5):301–10. doi: 10.1016/j.nrl.2011.10.014.
Floris, Matteo, Davide Sabbadin, Ricardo Medda, Alessandro Bulfone, and Stefano Moro. 2012. "Adenosiland: Walking through Adenosine Receptors Landscape." European Journal of Medicinal Chemistry 58:248–57. doi: 10.1016/j.ejmech.2012.10.022.
Forman, Mark S., John Q. Trojanowski, and Virginia M. Y. Lee. 2004. "Neurodegenerative Diseases: A Decade of Discoveries Paves the Way for Therapeutic Breakthroughs." Nature Medicine 10(10):1055–63. doi: 10.1038/nm1113.
Forrester, Steven J., George W. Booz, Curt D. Sigmund, Thomas M. Coffman, Tatsuo Kawai, Victor Rizzo, Rosario Scalia, and Satoru Eguchi. 2018. "Angiotensin II Signal Transduction: An Update on Mechanisms of Physiology and Pathophysiology." Physiological Reviews 98(3):1627–1738. doi: 10.1152/physrev.00038.2017.
Franco, R., C. Lluis, E. I. Canela, J. Mallol, L. Agnati, V. Casadó, F. Ciruela, S. Ferré, and K. Fuxe. 2007. "Receptor-Receptor Interactions Involving Adenosine A1 or Dopamine D1 Receptors and Accessory Proteins." Journal of Neural Transmission 114(1):93–104. doi: 10.1007/s00702-006-0566-7.
Franco, Rafael, David Aguinaga, Jasmina Jiménez, Jaume Lillo, Eva Martínez-Pinilla, and Gemma Navarro. 2018a. "Biased Receptor Functionality versus Biased Agonism in G-Protein-Coupled Receptors." Biomolecular Concepts 9(1):143–54. doi: 10.1515/bmc-2018-0013.
Franco, Rafael, David Aguinaga, Jasmina Jiménez, Jaume Lillo, Eva Martínez-Pinilla, and Gemma Navarro. 2018b. "Biased Receptor Functionality versus Biased Agonism in G-Protein-Coupled Receptors." Biomolecular Concepts 9(1):143–54. doi: 10.1515/bmc-2018-0013.
Franco, Rafael, Vicent Casadó, Antoni Cortés, Carla Ferrada, Josefa Mallol, Amina Woods, Carme Lluis, Enric I. Canela, and Sergi Ferré. 2007. "Basic Concepts in G-Protein-Coupled Receptor Homo- and Heterodimerization." The Scientific World JOURNAL 7:48–57. doi: 10.1100/tsw.2007.197.
Franco, Rafael, and Diana Fernández-Suárez. 2015. "Alternatively Activated Microglia and Macrophages in the Central Nervous System." Progress in Neurobiology 131:65–86. doi: 10.1016/j.pneurobio.2015.05.003.

Franco, Rafael, Eva Martínez-Pinilla, J. L. José L. J. L. Jose Luis Lanciego, and Gemma Navarro. 2016. "Basic Pharmacological and Structural Evidence for Class A G-Protein-Coupled Receptor Heteromerization." Frontiers in Pharmacology 7:76. doi: 10.3389/fphar.2016.00076.

Franco, Rafael, Eva Martínez-Pinilla, Ana Ricobaraza, and Peter J. McCormick. 2013. "Challenges in the Development of Heteromer-GPCR-Based Drugs." Progress in Molecular Biology and Translational Science 117:143–62. doi: 10.1016/B978-0-12-386931-9.00006-4.

Franco, Rafael, and Gemma Navarro. 2018. "Adenosine A2A Receptor Antagonists in Neurodegenerative Diseases: Huge Potential and Huge Challenges." Frontiers in Psychiatry 9(MAR):1–5. doi: 10.3389/fpsyt.2018.00068.

Franco, Rafael, Rafael Rivas-Santisteban, Irene Reyes-Resina, Mireia Casanovas, Catalina Pérez-Olives, Carlos Ferreiro-Vera, Gemma Navarro, Verónica Sánchez de Medina, and Xavier Nadal. 2020. "Pharmacological Potential of Varinic-, Minor-, and Acidic Phytocannabinoids." Pharmacological Research 158(February):104801. doi: 10.1016/j.phrs.2020.104801.

Fredholm, Bertil B., Giulia Arslan, Linda Halldner, Björn Kull, Gunnar Schulte, and Wyeth Wasserman. 2000. "Structure and Function of Adenosine Receptors and Their Genes." Naunyn-Schmiedeberg's Archives of Pharmacology 362(4–5):364–74. doi: 10.1007/s002100000313.

Fredholm, Bertil B., Yijuang Chern, Rafael Franco, and Michail Sitkovsky. 2007. "Aspects of the General Biology of Adenosine A2A Signaling." Progress in Neurobiology 83(5):263–76. doi: 10.1016/j.pneurobio.2007.07.005.

Fredholm, Bertil B., and Per Svenningsson. 2020. "Why Target Brain Adenosine Receptors? A Historical Perspective." Parkinsonism and Related Disorders 80(S1):S3–6. doi: 10.1016/j.parkreldis.2020.09.027.

Fredholm, Bertil, Rodrigo Cunha, and Per Svenningsson. 2005. "Pharmacology of Adenosine A2A Receptors and Therapeutic Applications." Current Topics in Medicinal Chemistry 3(4):413–26. doi: 10.2174/1568026033392200.

Fried, Nathan T., Melanie B. Elliott, and Michael L. Oshinsky. 2017. "The Role of Adenosine Signaling in Headache: A Review." Brain Sciences 7(3). doi: 10.3390/brainsci7030030.

Frisoni, G. B., M. P. Laakso, A. Beltramello, C. Geroldi, A. Bianchetti, H. Soininen, and M. Trabucchi. 1999. "Hippocampal and Entorhinal Cortex Atrophy in Frontotemporal Dementia and Alzheimer's Disease." Neurology 52(1):91–100. doi: 10.1212/wnl.52.1.91.

Fuxe, K., D. O. Borroto-Escuela, D. Marcellino, W. Romero-Fernandez, M. Frankowska, D. Guidolin, M. Filip, L. Ferraro, A. S. Woods, A. Tarakanov, F. Ciruela, L. F. Agnati, and S. Tanganelli. 2012. "GPCR Heteromers and Their Allosteric Receptor-Receptor Interactions." Current Medicinal Chemistry 19(3):356–63. doi: 10.2174/092986712803414259.

Fuxe, Kjell, Sergi Ferré, Meritxell Canals, Maria Torvinen, Anton Terasmaa, Daniel Marcellino, Steven R. Goldberg, William Staines, Kirsten X. Jacobsen, Carmen Lluis, Amina S. Woods, Luigi F. Agnati, and Rafael Franco. 2005. "Adenosine A2A and Dopamine D2 Heteromeric Receptor Complexes and Their Function." Journal of Molecular Neuroscience 26(2–3):209–20. doi: 10.1385/JMN:26:2-3:209.

Fuxe, Kjell, Sergi Ferré, Susanna Genedani, Rafael Franco, and Luigi F. Agnati. 2007. "Adenosine Receptor–Dopamine Receptor Interactions in the Basal Ganglia and Their Relevance for Brain Function." Physiology & Behavior 92(1–2):210–17. doi: 10.1016/j.physbeh.2007.05.034.

Fuxe, Kjell, Diego Guidolin, Luigi F. Agnati, and Dasiel O. Borroto-Escuela. 2015. "Dopamine Heteroreceptor Complexes as Therapeutic Targets in Parkinson's Disease." Expert Opinion on Therapeutic Targets 19(3):377–98. doi: 10.1517/14728222.2014.981529.

Fyhrquist, F., and O. Saijonmaa. 2008. "Renin-Angiotensin System Revisited." Journal of Internal Medicine 264(3):224–36. doi: 10.1111/j.1365-2796.2008.01981.x.

Gao, Hui Ming, and Jau Shyong Hong. 2008. "Why Neurodegenerative Diseases Are Progressive: Uncontrolled Inflammation Drives Disease Progression." Trends in Immunology 29(8):357–65. doi: 10.1016/j.it.2008.05.002.

Garcez, Michelle Lima, Adriani Paganini Damiani, Robson Pacheco, Lucas Rodrigues, Larissa Letieli de Abreu, Márcio Correa Alves, Vanessa Moraes de Andrade, and Carina Rodrigues Boeck. 2019.

"Caffeine Neuroprotection Decreases A2A Adenosine Receptor Content in Aged Mice." Neurochemical Research 44(4):787–95. doi: 10.1007/s11064-018-02710-3.

García-Nafría, Javier, Yang Lee, Xiaochen Bai, Byron Carpenter, and Christopher G. Tate. 2018. "Cryo-EM Structure of the Adenosine A2A Receptor Coupled to an Engineered Heterotrimeric G Protein." BioRxiv 1–19. doi: 10.1101/267674.

Garland, Stephen L. 2013. "Are GPCRs Still a Source of New Targets?" Journal of Biomolecular Screening (9):947–66. doi: 10.1177/1087057113498418.

Georgieva, Teodora, Savitha Devanathan, Dagmar Stropova, Chad K. Park, Zdzislaw Salamon, Gordon Tollin, Victor J. Hruby, William R. Roeske, Henry I. Yamamura, and Eva Varga. 2008. "Unique Agonist-Bound Cannabinoid CB1 Receptor Conformations Indicate Agonist Specificity in Signaling." European Journal of Pharmacology 581(1–2):19–29. doi: 10.1016/j.ejphar.2007.11.053.

Ghiringhelli, Franois, Mélanie Bruchard, Fanny Chalmin, and Cédric Rébé. 2012. "Production of Adenosine by Ectonucleotidases: A Key Factor in Tumor Immunoescape." Journal of Biomedicine and Biotechnology 2012. doi: 10.1155/2012/473712.

Gironacci, Mariela M., Hugo P. Adamo, Gerardo Corradi, Robson A. Santos, Pablo Ortiz, and Oscar A. Carretero. 2011. "Angiotensin (1-7) Induces Mas Receptor Internalization." Hypertension 58(2):176–81. doi: 10.1161/HYPERTENSIONAHA.111.173344.

Goetz, Christopher G. 2011. "The History of Parkinson's Disease: Early Clinical Descriptions and Neurological Therapies." Cold Spring Harbor Perspectives in Medicine 1(1):1–16. doi: 10.1101/cshperspect.a008862.

Goldsmith, Z. G., and D. N. Dhanasekaran. 2007. "G Protein Regulation of MAPK Networks." Oncogene 26(22):3122–42. doi: 10.1038/sj.onc.1210407.

Gomes, Catarina V., Manuella P. Kaster, Angelo R. Tomé, Paula M. Agostinho, and Rodrigo A. Cunha. 2011. "Adenosine Receptors and Brain Diseases: Neuroprotection and Neurodegeneration." Biochimica et Biophysica Acta - Biomembranes 1808(5):1380–99. doi: 10.1016/j.bbamem.2010.12.001.

Gomperts, S. N., D. M. Rentz, E. Moran, J. A. Becker, J. J. Locascio, W. E. Klunk, C. A. Mathis, D. R. Elmaleh, T. Shoup, A. J. Fischman, B. T. Hyman, J. H. Growdon, and K. A. Johnson. 2008. "Imaging Amyloid Deposition in Lewy Body Diseases." Neurology 71(12):903–10. doi: 10.1212/01.wnl.0000326146.60732.d6.

Gonçalves, Anderson Ricardo Roman, Clarice Kazue Fujihara, Ana Lúcia Mattar, Denise Maria Avancini Costa Malheiros, Irene De Lourdes Noronha, Gilberto De Nucci, and Roberto Zatz. 2004. "Renal Expression of COX-2, ANG II, and AT1 Receptor in Remnant Kidney: Strong Renoprotection by Therapy with Losartan and a Nonsteroidal Anti-Inflammatory." American Journal of Physiology - Renal Physiology 286(5 55-5). doi: 10.1152/ajprenal.00238.2003.

Gosselin, Mylène J., Patrice C. Leclerc, Mannix Auger-Messier, Gaétan Guillemette, Emanuel Escher, and Richard Leduc. 2000. "Molecular Cloning of a Ferret Angiotensin II AT1 Receptor Reveals the Importance of Position 163 for Losartan Binding." Biochimica et Biophysica Acta - Molecular Cell Research 1497(1):94–102. doi: 10.1016/S0167-4889(00)00046-X.

Gough, Nancy R. 2016. "Focus Issue: New Insights in GPCR to G Protein Signaling." Science Signaling 9(423):1–3. doi: 10.1126/scisignal.aaf7642.

Graeber, M. B. 1998. "The Case Described by Alois Alzheimer in 1911." 111–22.

Green, Dustin P. 2021. "The Role of Mrgprs in Pain." Neuroscience Letters 744(January):135544. doi: 10.1016/j.neulet.2020.135544.

Greenamyre, J. Timoth., Gillian MacKenzie, Tsung-I. Peng, and Stacy E. Stephans. 1999. "Mitochondrial Dysfunction in Parkinson's Disease" edited by G. C. Brown, D. G. Nicholls, and C. E. Cooper. Biochemical Society Symposia 66(2):85–97. doi: 10.1042/bss0660085.

Grenz, Almut, Dirk Homann, and Holger K. Eltzschig. 2011. "Extracellular Adenosine: A Safety Signal That Dampens Hypoxia-Induced Inflammation during Ischemia." Antioxidants and Redox Signaling 15(8):2221–34. doi: 10.1089/ars.2010.3665.

Grisanti, Laurel A., Sarah M. Schumacher, Douglas G. Tilley, and Walter J. Koch. 2018. "Designer

Approaches for G Protein–Coupled Receptor Modulation for Cardiovascular Disease." JACC: Basic to Translational Science 3(4):550–62. doi: 10.1016/j.jacbts.2017.12.002.
Grundmann, Manuel, and Evi Kostenis. 2015a. "Holistic Methods for the Analysis of CNMP Effects." Pp. 339–57 in.
Grundmann, Manuel, and Evi Kostenis. 2015b. "Label-Free Biosensor Assays in GPCR Screening." Pp. 199–213 in.
Grundmann, Manuel, and Evi Kostenis. 2017. "Temporal Bias: Time-Encoded Dynamic GPCR Signaling." Trends in Pharmacological Sciences 38(12):1110–24. doi: 10.1016/j.tips.2017.09.004.
Gui, Li, Wei Duan, Hong Tian, Chuanming Li, Jie Zhu, Jiang-Fan Chen, and Jian Zheng. 2009. "Adenosine A2A Receptor Deficiency Reduces Striatal Glutamate Outflow and Attenuates Brain Injury Induced by Transient Focal Cerebral Ischemia in Mice." Brain Research 1297:185–93. doi: 10.1016/j.brainres.2009.08.050.
Guieu, Régis, Jean-Claude Deharo, Baptiste Maille, Lia Crotti, Ermino Torresani, Michele Brignole, and Gianfranco Parati. 2020. "Adenosine and the Cardiovascular System: The Good and the Bad." Journal of Clinical Medicine 9(5):1366. doi: 10.3390/jcm9051366.
Gundry, Jaimee, Rachel Glenn, Priya Alagesan, and Sudarshan Rajagopal. 2017. "A Practical Guide to Approaching Biased Agonism at G Protein Coupled Receptors." Frontiers in Neuroscience 11(JAN):1–6. doi: 10.3389/fnins.2017.00017.
Gupta, Manveen K., Maradumane L. Mohan, and Sathyamangla V. Naga Prasad. 2018. G Protein-Coupled Receptor Resensitization Paradigms. Vol. 339. 1st ed. Elsevier Inc.
Gurevich, Vsevolod V., and Eugenia V. Gurevich. 2020. "Biased GPCR Signaling: Possible Mechanisms and Inherent Limitations." Pharmacology and Therapeutics 211:107540. doi: 10.1016/j.pharmthera.2020.107540.
Gutiérrez-Rodríguez, Ana, Itziar Bonilla-Del Río, Nagore Puente, Sonia M. Gómez-Urquijo, Christine J. Fontaine, Jon Egaña-Huguet, Izaskun Elezgarai, Sabine Ruehle, Beat Lutz, Laurie M. Robin, Edgar Soria-Gómez, Luigi Bellocchio, Jalindar D. Padwal, Mario van der Stelt, Juan Mendizabal-Zubiaga, Leire Reguero, Almudena Ramos, Inmaculada Gerrikagoitia, Giovanni Marsicano, and Pedro Grandes. 2018. "Localization of the Cannabinoid Type-1 Receptor in Subcellular Astrocyte Compartments of Mutant Mouse Hippocampus." Glia 66(7):1417–31. doi: 10.1002/glia.23314.
Habib, Ashraf S., M. B. B. Ch, M. Sc, Harold Minkowitz, and Timothy Osborn. 2008. "Trial of Intravenous Adenosine for Perioperative Analgesia." Anesthesiology 109(6):1085–91.
Hamamoto, Akie, Yuki Kobayashi, and Yumiko Saito. 2015. "Identification of Amino Acids That Are Selectively Involved in Gi/o Activation by Rat Melanin-Concentrating Hormone Receptor 1." Cellular Signalling 27(4):818–27. doi: 10.1016/j.cellsig.2015.01.008.
Hamming, I., W. Timens, MLC Bulthuis, AT Lely, GJ Navis, and H. van Goor. 2004. "Tissue Distribution of ACE2 Protein, the Functional Receptor for SARS Coronavirus. A First Step in Understanding SARS Pathogenesis." The Journal of Pathology 203(2):631–37. doi: 10.1002/path.1570.
Handa, Rajash K., Carlos M. Ferrario, and Jack W. Strandhoy. 1996. "Renal Actions of Angiotensin-(1-7): In Vivo and in Vitro Studies." American Journal of Physiology 270(1 PART 2):141–47. doi: 10.1152/ajprenal.1996.270.1.f141.
Hanlon, Katherine E., and Todd W. Vanderah. 2010. "Constitutive Activity at the Cannabinoid CB1 Receptor and Behavioral Responses." Pp. 3–30 in Physiology & behavior. Vol. 176.
Hanuš, Lumír Ondřej. 2009. "Pharmacological and Therapeutic Secrets of Plant and Brain (Endo)Cannabinoids." Medicinal Research Reviews 29(2):213–71. doi: 10.1002/med.20135.
Harrison, Charlotte, and K. Ravi Acharya. 2014. "ACE for All – a Molecular Perspective." Journal of Cell Communication and Signaling 8(3):195–210. doi: 10.1007/s12079-014-0236-8.
Hartmann, Christian J., Sabine Fliegen, Stefan J. Groiss, Lars Wojtecki, and Alfons Schnitzler. 2019. "An Update on Best Practice of Deep Brain Stimulation in Parkinson's Disease." Therapeutic Advances in Neurological Disorders 12:1–20. doi: 10.1177/1756286419838096.
Hasbi, Ahmed, Theresa Fan, Mohammad Alijaniaram, Tuan Nguyen, Melissa L. Perreault, Brian F. O'Dowd, and Susan R. George. 2009. "Calcium Signaling Cascade Links Dopamine D1–D2

Receptor Heteromer to Striatal BDNF Production and Neuronal Growth." Proceedings of the National Academy of Sciences 106(50):21377–82. doi: 10.1073/pnas.0903676106.

Haskó, György, Luca Antonioli, and Bruce N. Cronstein. 2018. "Adenosine Metabolism, Immunity and Joint Health." Biochemical Pharmacology 151(February):307–13. doi: 10.1016/j.bcp.2018.02.002.

Haskó, György, and Bruce N. Cronstein. 2004. "Adenosine: An Endogenous Regulator of Innate Immunity." Trends in Immunology 25(1):33–39. doi: 10.1016/j.it.2003.11.003.

Haspula, Dhanush, and Michelle A. Clark. 2020. "Cannabinoid Receptors: An Update on Cell Signaling, Pathophysiological Roles and Therapeutic Opportunities in Neurological, Cardiovascular, and Inflammatory Diseases." International Journal of Molecular Sciences 21(20):1–65. doi: 10.3390/ijms21207693.

Hayashida, Wataru, Masatsugu Horiuchi, and Victor J. Dzau. 1996. "Intracellular Third Loop Domain of Angiotensin II Type-2 Receptor: Role in Mediating Signal Transduction and Cellular Function." Journal of Biological Chemistry 271(36):21985–92. doi: 10.1074/jbc.271.36.21985.

Head, Brian P., Hemal H. Patel, and Paul A. Insel. 2014. "Interaction of Membrane/Lipid Rafts with the Cytoskeleton: Impact on Signaling and Function." Biochimica et Biophysica Acta (BBA) - Biomembranes 1838(2):532–45. doi: 10.1016/j.bbamem.2013.07.018.

Headrick, John P., Kevin J. Ashton, Roselyn B. Rose'Meyer, and Jason N. Peart. 2013. "Cardiovascular Adenosine Receptors: Expression, Actions and Interactions." Pharmacology and Therapeutics 140(1):92–111. doi: 10.1016/j.pharmthera.2013.06.002.

Hebert-Chatelain, Etienne, Leire Reguero, Nagore Puente, Beat Lutz, Francis Chaouloff, Rodrigue Rossignol, Pier-Vincenzo Piazza, Giovanni Benard, Pedro Grandes, and Giovanni Marsicano. 2014. "Cannabinoid Control of Brain Bioenergetics: Exploring the Subcellular Localization of the CB1 Receptor." Molecular Metabolism 3(4):495–504. doi: 10.1016/j.molmet.2014.03.007.

Heisters, Daiga. 2011. "Parkinson's: Symptoms, Treatments and Research." British Journal of Nursing 20(9):548–54. doi: 10.12968/bjon.2011.20.9.548.

Henrion, Daniel, Nathalie Kubis, and Bernard I. Lévy. 2001. "Physiological and Pathophysiological Functions of the AT2 Subtype Receptor of Angiotensin II from Large Arteries to the Microcirculation." Hypertension 38(5):1150–57. doi: 10.1161/hy1101.096109.

Herrera, Carolina, Chikao Morimoto, Julià Blanco, Josefa Mallol, Fernando Arenzana, Carmen Lluis, and Rafael Franco. 2001. "Comodulation of CXCR4 and CD26 in Human Lymphocytes." Journal of Biological Chemistry 276(22):19532–39. doi: 10.1074/jbc.M004586200.

Higuchi, Sadaharu, Haruhiko Ohtsu, Hiroyuki Suzuki, Heigoro Shirai, Gerald D. Frank, and Satoru Eguchi. 2007. "Angiotensin II Signal Transduction through the AT1 Receptor: Novel Insights into Mechanisms and Pathophysiology." Clinical Science 112(7–8):417–28. doi: 10.1042/CS20060342.

Hill, Jeremy D., Viviana Zuluaga-Ramirez, Sachin Gajghate, Malika Winfield, Uma Sriram, Slava Rom, and Yuri Persidsky. 2019. "Activation of GPR55 Induces Neuroprotection of Hippocampal Neurogenesis and Immune Responses of Neural Stem Cells Following Chronic, Systemic Inflammation." Brain, Behavior, and Immunity 76(215):165–81. doi: 10.1016/j.bbi.2018.11.017.

Hinz, Sonja, Gemma Navarro, Dasiel Borroto-Escuela, Benjamin F. Seibt, Christoph Ammon, Elisabetta De Filippo, Azeem Danish, Svenja K. Lacher, Barbora Červinková, Muhammad Rafehi, Kjell Fuxe, Anke C. Schiedel, Rafael Franco, and Christa E. Müller. 2018. "Adenosine A2A Receptor Ligand Recognition and Signaling Is Blocked by A2B Receptors." Oncotarget 9(17):13593–611. doi: 10.18632/oncotarget.24423.

Hinz, Sonja, Gemma Navarro, Dasiel Borroto-Escuela, Benjamin F. Seibt, York-Christoph Ammon, Elisabetta de Filippo, Azeem Danish, Svenja K. Lacher, Barbora Červinková, Muhammad Rafehi, Kjell Fuxe, Anke C. Schiedel, Rafael Franco, and Christa E. Müller. 2018. "Adenosine A2A Receptor Ligand Recognition and Signaling Is Blocked by A2B Receptors." Oncotarget 9(17):13593–611. doi: 10.18632/oncotarget.24423.

Hisahara, Shin, and Shun Shimohama. 2011. "Dopamine Receptors and Parkinson's Disease." International Journal of Medicinal Chemistry 2011:1–16. doi: 10.1155/2011/403039.

Hoe, Kwang Lae, Ines Armando, Gustavo Baiardi, Taduru Sreenath, Ashok Kulkarni, Alfredo Martínez, and Juan M. Saavedra. 2003. "Molecular Cloning, Characterization, and Distribution of the Gerbil Angiotensin II AT2 Receptor." American Journal of Physiology - Regulatory Integrative and Comparative Physiology 285(6 54-6):1373–83. doi: 10.1152/ajpregu.00008.2003.

Horiuchi, Masatsugu, Meiko Hamai, Tai Xing Cui, Masaru Iwai, and Yasuhiko Minokoshi. 1999. "Cross Talk between Angiotensin II Type 1 and Type 2 Receptors: Cellular Mechanism of Angiotensin Type 2 Receptor-Mediated Cell Growth Inhibition." Hypertension Research - Clinical and Experimental 22(2):67–74. doi: 10.1291/hypres.22.67.

Hornykiewicz, O. 2006. "The Discovery of Dopamine Deficiency in the Parkinsonian Brain." Journal of Neural Transmission. Supplementum (70):9–15. doi: 10.1007/978-3-211-45295-0_3.

Hornykiewicz, Oleh. 2017. "L-DOPA." Journal of Parkinson's Disease 7(s1):S3–10. doi: 10.3233/JPD-179004.

Hou, Yujun, Xiuli Dan, Mansi Babbar, Yong Wei, Steen G. Hasselbalch, Deborah L. Croteau, and Vilhelm A. Bohr. 2019. "Ageing as a Risk Factor for Neurodegenerative Disease." Nature Reviews Neurology 15(10):565–81. doi: 10.1038/s41582-019-0244-7.

Howlett, Allyn C., and Mary E. Abood. 2017. "CB 1 and CB 2 Receptor Pharmacology." Pp. 169–206 in Physiology & behavior. Vol. 176.

Hryhorowicz, Szymon, Marta Kaczmarek-Ryś, Angelika Andrzejewska, Klaudia Staszak, Magdalena Hryhorowicz, Aleksandra Korcz, and Ryszard Słomski. 2019. "Allosteric Modulation of Cannabinoid Receptor 1— Current Challenges and Future Opportunities." International Journal of Molecular Sciences 20(23):1–19. doi: 10.3390/ijms20235874.

Hu, G., G. Ren, and Y. Shi. 2011. "The Putative Cannabinoid Receptor GPR55 Promotes Cancer Cell Proliferation." Oncogene 30(2):139–41. doi: 10.1038/onc.2010.502.

Hua, Tian, Kiran Vemuri, Spyros P. Nikas, Robert B. Laprairie, Yiran Wu, Lu Qu, Mengchen Pu, Anisha Korde, Shan Jiang, Jo-Hao Ho, Gye Won Han, Kang Ding, Xuanxuan Li, Haiguang Liu, Michael A. Hanson, Suwen Zhao, Laura M. Bohn, Alexandros Makriyannis, Raymond C. Stevens, and Zhi-Jie Liu. 2017. "Crystal Structures of Agonist-Bound Human Cannabinoid Receptor CB1." Nature 547(7664):468–71. doi: 10.1038/nature23272.

Hua, Tian, Kiran Vemuri, Mengchen Pu, Lu Qu, Gye Won Han, Yiran Wu, Suwen Zhao, Wenqing Shui, Shanshan Li, Anisha Korde, Robert B. Laprairie, Edward L. Stahl, Jo-Hao Ho, Nikolai Zvonok, Han Zhou, Irina Kufareva, Beili Wu, Qiang Zhao, Michael A. Hanson, Laura M. Bohn, Alexandros Makriyannis, Raymond C. Stevens, and Zhi-Jie Liu. 2016. "Crystal Structure of the Human Cannabinoid Receptor CB1." Cell 167(3):750-762.e14. doi: 10.1016/j.cell.2016.10.004.

Huang, Yunhong, Nicholas Todd, and Amantha Thathiah. 2017. "The Role of GPCRs in Neurodegenerative Diseases: Avenues for Therapeutic Intervention." Current Opinion in Pharmacology 32:96–110. doi: 10.1016/j.coph.2017.02.001.

Imbernon, Monica, Lauren Whyte, Adenis Diaz-Arteaga, Wendy R. Russell, Natalia R. Moreno, María J. Vazquez, Carmen R. Gonzalez, Alberto Díaz-Ruiz, Miguel Lopez, Maria M. Malagón, Ruth A. Ross, Carlos Dieguez, and Ruben Nogueiras. 2014. "Regulation of GPR55 in Rat White Adipose Tissue and Serum LPI by Nutritional Status, Gestation, Gender and Pituitary Factors." Molecular and Cellular Endocrinology 383(1–2):159–69. doi: 10.1016/j.mce.2013.12.011.

Ingraham, Nicholas E., Abdo G. Barakat, Ronald Reilkoff, Tamara Bezdicek, Timothy Schacker, Jeffrey G. Chipman, Christopher J. Tignanelli, and Michael A. Puskarich. 2020. "Understanding the Renin-Angiotensin-Aldosterone-SARS-CoV Axis: A Comprehensive Review." European Respiratory Journal 56(1). doi: 10.1183/13993003.00912-2020.

Insel, Paul A., Krishna Sriram, Matthew W. Gorr, Shu Z. Wiley, Alexander Michkov, Cristina Salmerón, and Amy M. Chinn. 2019. "GPCRomics: An Approach to Discover GPCR Drug Targets." Trends in Pharmacological Sciences 40(6):378–87. doi: 10.1016/j.tips.2019.04.001.

Iqbal, K., F. Liu, C. X. Gong, and I. Grundke-Iqbal. 2010. "Tau in Alzheimer Disease and Related Tauopathies." Current Alzheimer Research 7(8):656–64. doi: 10.2174/156720510793611592.

Ishiguro, H., S. Iwasaki, L. Teasenfitz, S. Higuchi, Y. Horiuchi, T. Saito, T. Arinami, and E. S. Onaivi. 2007. "Involvement of Cannabinoid CB2 Receptor in Alcohol Preference in Mice and Alcoholism

in Humans." Pharmacogenomics Journal 7(6):380–85. doi: 10.1038/sj.tpj.6500431.
Iwai, Masaru, and Masatsugu Horiuchi. 2009. "Devil and Angel in the Renin-Angiotensin System: ACE-Angiotensin II-AT1 Receptor Axis vs. ACE2-Angiotensin-(1-7)-Mas Receptor Axis." Hypertension Research 32(7):533–36. doi: 10.1038/hr.2009.74.
Iwamura, H., H. Suzuki, Y. Ueda, T. Kaya, and T. Inaba. 2001. "In Vitro and in Vivo Pharmacological Characterization of JTE-907, a Novel Selective Ligand for Cannabinoid CB2 Receptor." The Journal of Pharmacology and Experimental Therapeutics 296(2):420–25.
Jacobson, Kenneth A. 2009. "Introduction to Adenosine Receptors as Therapeutic Targets." Pp. 1–24 in Bone. Vol. 23.
Jacobson, Kenneth A., Ramachandran Balasubramanian, Francesca Deflorian, and Zhan Guo Gao. 2012. "G Protein-Coupled Adenosine (P1) and P2Y Receptors: Ligand Design and Receptor Interactions." Purinergic Signalling 8(3):419–36. doi: 10.1007/s11302-012-9294-7.
Jacobson, Kenneth A., and Zhan Guo Gao. 2006. "Adenosine Receptors as Therapeutic Targets." Nature Reviews Drug Discovery 5(3):247–64. doi: 10.1038/nrd1983.
Jacobson, Kenneth A., Zhan Guo Gao, Pierre Matricon, Matthew T. Eddy, and Jens Carlsson. 2020. "Adenosine A2A Receptor Antagonists: From Caffeine to Selective Non-Xanthines." British Journal of Pharmacology 0–1. doi: 10.1111/bph.15103.
Jacobson, Kenneth A., Luigino Antonio Giancotti, Filomena Lauro, Fatma Mufti, and Daniela Salvemini. 2020. "Treatment of Chronic Neuropathic Pain: Purine Receptor Modulation." Pain 161(7):1425–41. doi: 10.1097/j.pain.0000000000001857.
Jarrott, Bevyn, and Spencer J. Williams. 2016. "Chronic Brain Inflammation: The Neurochemical Basis for Drugs to Reduce Inflammation." Neurochemical Research 41(3):523–33. doi: 10.1007/s11064-015-1661-7.
Jastrzebska, Beata. 2015. "Rhodopsin: Methods and Protocols." Rhodopsin: Methods and Protocols 1–410. doi: 10.1007/978-1-4939-2330-4.
Javed, Hayate, Sheikh Azimullah, M. Emdadul Haque, and Shreesh K. Ojha. 2016. "Cannabinoid Type 2 (CB2) Receptors Activation Protects against Oxidative Stress and Neuroinflammation Associated Dopaminergic Neurodegeneration in Rotenone Model of Parkinson's Disease." Frontiers in Neuroscience 10(AUG):1–14. doi: 10.3389/fnins.2016.00321.
Jeon, Y. J., K. H. Yang, J. T. Pulaski, and N. E. Kaminski. 1996. "Attenuation of Inducible Nitric Oxide Synthase Gene Expression by Delta 9-Tetrahydrocannabinol Is Mediated through the Inhibition of Nuclear Factor- Kappa B/Rel Activation." Molecular Pharmacology 50(2):334–41.
Jiang, Xuliang, David Fischer, Xiaoyan Chen, Sean D. McKenna, Heli Liu, Venkataraman Sriraman, Henry N. Yu, Andreas Goutopoulos, Steve Arkinstall, and Xiaolin He. 2014. "Evidence for Follicle-Stimulating Hormone Receptor as a Functional Trimer." Journal of Biological Chemistry 289(20):14273–82. doi: 10.1074/jbc.M114.549592.
Joglar, Belen, Jannette Rodriguez-Pallares, Ana Isabel Rodriguez-Perez, Pablo Rey, Maria Jose Guerra, and Jose Luis Labandeira-Garcia. 2009. "The Inflammatory Response in the MPTP Model of Parkinson's Disease Is Mediated by Brain Angiotensin: Relevance to Progression of the Disease." Journal of Neurochemistry 109(2):656–69. doi: 10.1111/j.1471-4159.2009.05999.x.
Jones, Emma S., Antony Vinh, Claudia A. McCarthy, Tracey A. Gaspari, and Robert E. Widdop. 2008. "AT2 Receptors: Functional Relevance in Cardiovascular Disease." Pharmacology and Therapeutics 120(3):292–316. doi: 10.1016/j.pharmthera.2008.08.009.
Jucker, Mathias, and Lary C. Walker. 2013. "Self-Propagation of Pathogenic Protein Aggregates in Neurodegenerative Diseases." Nature 501(7465):45–51. doi: 10.1038/nature12481.
Juillerat-Jeanneret, Lucienne. 2020. "The Other Angiotensin II Receptor: AT2R as a Therapeutic Target." Journal of Medicinal Chemistry 63(5):1978–95. doi: 10.1021/acs.jmedchem.9b01780.
Kalaria, Raj. 2002. "Similarities between Alzheimer's Disease and Vascular Dementia." Journal of the Neurological Sciences 203–204:29–34. doi: 10.1016/S0022-510X(02)00256-3.
Kamel, Ahmed S., Noha F. Abdelkader, Sahar S. Abd El-Rahman, Marwan Emara, Hala F. Zaki, and Mahmoud M. Khattab. 2018. "Stimulation of ACE2/ANG(1–7)/Mas Axis by Diminazene

Ameliorates Alzheimer's Disease in the D-Galactose-Ovariectomized Rat Model: Role of PI3K/Akt Pathway." Molecular Neurobiology 55(10):8188–8202. doi: 10.1007/s12035-018-0966-3.

Kaneko, Takeshi, Ryuichi Shigemoto, Shigetada Nakanishi, and Noboru Mizuno. 1993. "Substance P Receptor-Immunoreactive Neurons in the Rat Neostriatum Are Segregated into Somatostatinergic and Cholinergic Aspiny Neurons." Brain Research 631(2):297–303. doi: 10.1016/0006-8993(93)91548-7.

Kang, Yanyong, Oleg Kuybeda, Parker W. De Waal, Somnath Mukherjee, Ned Van Eps, Przemyslaw Dutka, X. Edward Zhou, Alberto Bartesaghi, Satchal Erramilli, Takefumi Morizumi, Xin Gu, Yanting Yin, Ping Liu, Yi Jiang, Xing Meng, Gongpu Zhao, Karsten Melcher, Oliver P. Ernst, Anthony A. Kossiakoff, Sriram Subramaniam, and H. Eric Xu. 2018. "Cryo-EM Structure of Human Rhodopsin Bound to an Inhibitory G Protein." Nature 558(7711):553–58. doi: 10.1038/s41586-018-0215-y.

Kanno, Takeshi, Akinobu Gotoh, Yumiko Fujita, Takashi Nakano, and Tomoyuki Nishizaki. 2012. "A 3 Adenosine Receptor Mediates Apoptosis in 5637 Human Bladder Cancer Cells by G q Protein/PKC-Dependent AIF Upregulation." Cellular Physiology and Biochemistry 30(5):1159–68. doi: 10.1159/000343306.

Kapur, Ankur, Pingwei Zhao, Haleli Sharir, Yushi Bai, Marc G. Caron, Larry S. Barak, and Mary E. Abood. 2009. "Atypical Responsiveness of the Orphan Receptor GPR55 to Cannabinoid Ligands." Journal of Biological Chemistry 284(43):29817–27. doi: 10.1074/jbc.M109.050187.

Kargl, J., L. Andersen, C. Hasenöhrl, D. Feuersinger, A. Stančic, A. Fauland, C. Magnes, A. El-Heliebi, S. Lax, S. Uranitsch, J. Haybaeck, A. Heinemann, and R. Schicho. 2016. "GPR55 Promotes Migration and Adhesion of Colon Cancer Cells Indicating a Role in Metastasis." British Journal of Pharmacology 173(1):142–54. doi: 10.1111/bph.13345.

Kargl, Julia, Nariman Balenga, Gerald P. Parzmair, Andrew J. Brown, Akos Heinemann, and Maria Waldhoer. 2012. "The Cannabinoid Receptor CB1 Modulates the Signaling Properties of the Lysophosphatidylinositol Receptor GPR55." Journal of Biological Chemistry 287(53):44234–48. doi: 10.1074/jbc.M112.364109.

Karila, Laurent, Amine Benyamina, Lisa Blecha, Olivier Cottencin, and Joël Billieux. 2016. "The Synthetic Cannabinoids Phenomenon." Current Pharmaceutical Design 22(42):6420–25. doi: 10.2174/1381612822666160919093450.

Kaschina, Elena, Pawel Namsolleck, and Thomas Unger. 2017. "AT2 Receptors in Cardiovascular and Renal Diseases." Pharmacological Research 125:39–47. doi: 10.1016/j.phrs.2017.07.008.

Kaschina, Elena, and Thomas Unger. 2003. "Angiotensin AT1/AT2 Receptors: Regulation, Signalling and Function." Blood Pressure 12(2):70–88. doi: 10.1080/08037050310001057.

Kaushik, Susmita, and Ana Maria Cuervo. 2015. "Proteostasis and Aging." Nature Medicine 21(12):1406–15. doi: 10.1038/nm.4001.

Kawai, Tatsuo, Steven J. Forrester, Shannon O'Brien, Ariele Baggett, Victor Rizzo, and Satoru Eguchi. 2017. "AT1 Receptor Signaling Pathways in the Cardiovascular System." Pharmacological Research 125(1):4–13. doi: 10.1016/j.phrs.2017.05.008.

Kenakin, T. 1995. "Agonist-Receptor Efficacy II: Agonist Trafficking of Receptor Signals." Trends in Pharmacological Sciences 16(7):232–38. doi: 10.1016/S0165-6147(00)89032-X.

Khajehali, Elham, Daniel T. Malone, Michelle Glass, Patrick M. Sexton, Arthur Christopoulos, and Katie Leach. 2015. "Biased Agonism and Biased Allosteric Modulation at the CB1 Cannabinoid Receptor." Molecular Pharmacology 88(2):368–79. doi: 10.1124/mol.115.099192.

Khurana, Leepakshi, Ken Mackie, Daniele Piomelli, and Debra A. Kendall. 2017. "Modulation of CB1 Cannabinoid Receptor by Allosteric Ligands: Pharmacology and Therapeutic Opportunities." Neuropharmacology 124(1):3–12. doi: 10.1016/j.neuropharm.2017.05.018.

Kilpeläinen, Tommi, Ulrika H. Julku, Reinis Svarcbahs, and Timo T. Myöhänen. 2019. "Behavioural and Dopaminergic Changes in Double Mutated Human A30P*A53T Alpha-Synuclein Transgenic Mouse Model of Parkinson´s Disease." Scientific Reports 9(1):1–13. doi: 10.1038/s41598-019-54034-z.

Kirik, Deniz, Christian Winkler, and Anders Björklund. 2001. "Growth and Functional Efficacy of Intrastriatal Nigral Transplants Depend on the Extent of Nigrostriatal Degeneration." The Journal of Neuroscience 21(8):2889–96. doi: 10.1523/JNEUROSCI.21-08-02889.2001.

Kita, H., T. Kosaka, and C. W. Heizmann. 1990. "Parvalbumin-Immunoreactive Neurons in the Rat Neostriatum: A Light and Electron Microscopic Study." Brain Research 536(1–2):1–15. doi: 10.1016/0006-8993(90)90002-S.

Kitada, Tohru, Shuichi Asakawa, Nobutaka Hattori, Hiroto Matsumine, Yasuhiro Yamamura, Shinsei Minoshima, Masayuki Yokochi, Yoshikuni Mizuno, and Nobuyoshi Shimizu. 1998. "Mutations in the Parkin Gene Cause Autosomal Recessive Juvenile Parkinsonism." Nature 392(6676):605–8. doi: 10.1038/33416.

Kittana, Naim. 2018. "Angiotensin-Converting Enzyme 2–Angiotensin 1-7/1-9 System: Novel Promising Targets for Heart Failure Treatment." Fundamental and Clinical Pharmacology 32(1):14–25. doi: 10.1111/fcp.12318.

Kivipelto, Miia, Francesca Mangialasche, and Tiia Ngandu. 2018. "Lifestyle Interventions to Prevent Cognitive Impairment, Dementia and Alzheimer Disease." Nature Reviews Neurology 14(11):653–66. doi: 10.1038/s41582-018-0070-3.

Klinger, Markus, Mandy Kuhn, Herwig Just, Eduard Stefan, Timothy Palmer, Michael Freissmuth, and Christian Nanoff. 2002. "Removal of the Carboxy Terminus of the A2A -Adenosine Receptor Blunts Constitutive Activity: Differential Effect on CAMP Accumulation and MAP Kinase Stimulation." Naunyn-Schmiedeberg's Archives of Pharmacology 366(4):287–98. doi: 10.1007/s00210-002-0617-z.

Koehl, Antoine, Hongli Hu, Dan Feng, Bingfa Sun, Yan Zhang, Michael J. Robertson, Matthew Chu, Tong Sun Kobilka, Toon Laermans, Jan Steyaert, Jeffrey Tarrasch, Somnath Dutta, Rasmus Fonseca, William I. Weis, Jesper M. Mathiesen, Georgios Skiniotis, and Brian K. Kobilka. 2019. "Structural Insights into the Activation of Metabotropic Glutamate Receptors." Nature 566(7742):79–84. doi: 10.1038/s41586-019-0881-4.

Köhr, Georg. 2006. "NMDA Receptor Function: Subunit Composition versus Spatial Distribution." Cell and Tissue Research 326(2):439–46. doi: 10.1007/s00441-006-0273-6.

Kondo, Tomoyoshi, and Yoshikuni Mizuno. 2015. "A Long-Term Study of Istradefylline Safety and Efficacy in Patients with Parkinson Disease." Clinical Neuropharmacology 38(2):41–46. doi: 10.1097/WNF.0000000000000073.

Kong, Yanying, Qiuju Peng, Nan Lv, Jin Yuan, Zhirong Deng, Xiaolin Liang, Si Chen, and Laiyou Wang. 2020. "Paeoniflorin Exerts Neuroprotective Effects in a Transgenic Mouse Model of Alzheimer's Disease via Activation of Adenosine A1 Receptor." Neuroscience Letters 730(April):135016. doi: 10.1016/j.neulet.2020.135016.

Kraybill, M. L., E. B. Larson, D. W. Tsuang, L. Teri, W. C. McCormick, J. D. Bowen, W. A. Kukull, J. B. Leverenz, and M. M. Cherrier. 2005. "Cognitive Differences in Dementia Patients with Autopsy-Verified AD, Lewy Body Pathology, or Both." Neurology 64(12):2069–73. doi: 10.1212/01.WNL.0000165987.89198.65.

Kuba, Keiji, Yumiko Imai, Shuan Rao, Hong Gao, Feng Guo, Bin Guan, Yi Huan, Peng Yang, Yanli Zhang, Wei Deng, Linlin Bao, Binlin Zhang, Guang Liu, Zhong Wang, Mark Chappell, Yanxin Liu, Dexian Zheng, Andreas Leibbrandt, Teiji Wada, Arthur S. Slutsky, Depei Liu, Chuan Qin, Chengyu Jiang, and Josef M. Penninger. 2005. "A Crucial Role of Angiotensin Converting Enzyme 2 (ACE2) in SARS Coronavirus–Induced Lung Injury." Nature Medicine 11(8):875–79. doi: 10.1038/nm1267.

Kumar, A., E. Koss, D. Metzler, A. Moore, and R. P. Friedland. 1988. "Behavioral Symptomatology in Dementia of the Alzheimer Type." Alzheimer Disease and Associated Disorders 2(4):363–65. doi: 10.1097/00002093-198802040-00005.

Kumar, Anil, Arti Singh, and Ekavali. 2015. "A Review on Alzheimer's Disease Pathophysiology and Its Management: An Update." Pharmacological Reports 67(2):195–203. doi: 10.1016/j.pharep.2014.09.004.

Kumar, Sathish, Nasrollah Rezaei-Ghaleh, Dick Terwel, Dietmar R. Thal, Mélisande Richard, Michael Hoch, Jessica M. Mc Donald, Ullrich Wüllner, Konstantin Glebov, Michael T. Heneka, Dominic M.

Walsh, Markus Zweckstetter, and Jochen Walter. 2011. "Extracellular Phosphorylation of the Amyloid β 2-Peptide Promotes Formation of Toxic Aggregates during the Pathogenesis of Alzheimer's Disease." EMBO Journal 30(11):2255–65. doi: 10.1038/emboj.2011.138.

Kunos, George, and Douglas Osei-Hyiaman. 2008. "Endocannabinoids and Liver Disease. IV. Endocannabinoid Involvement in Obesity and Hepatic Steatosis." American Journal of Physiology - Gastrointestinal and Liver Physiology 294(5):1101–4. doi: 10.1152/ajpgi.00057.2008.

Labandeira-Garcia, Jose L., Ana I. Rodríguez-Perez, Pablo Garrido-Gil, Jannette Rodriguez-Pallares, Jose L. Lanciego, and Maria J. Guerra. 2017. "Brain Renin-Angiotensin System and Microglial Polarization: Implications for Aging and Neurodegeneration." Frontiers in Aging Neuroscience 9. doi: 10.3389/fnagi.2017.00129.

Lanznaster, Débora, Caio M. Massari, Vendula Marková, Tereza Šimková, Romain Duroux, Kenneth A. Jacobson, Víctor Fernández-Dueñas, Carla I. Tasca, and Francisco Ciruela. 2019. "Adenosine A1-A2A Receptor-Receptor Interaction: Contribution to Guanosine-Mediated Effects." Cells 8(12). doi: 10.3390/cells8121630.

Laprairie, R. B., A. M. Bagher, M. E. M. Kelly, and E. M. Denovan-Wright. 2015. "Cannabidiol Is a Negative Allosteric Modulator of the Cannabinoid CB1 Receptor." British Journal of Pharmacology 172(20):4790–4805. doi: 10.1111/bph.13250.

Latt, Mark Dominic, Simon Lewis, Olfat Zekry, and Victor S. C. Fung. 2019. "Factors to Consider in the Selection of Dopamine Agonists for Older Persons with Parkinson's Disease." Drugs and Aging 36(3):189–202. doi: 10.1007/s40266-018-0629-0.

Lauckner, Jane E., Jill B. Jensen, Huei Ying Chen, Hui Chen Lu, Bertil Hille, and Ken Mackie. 2008. "GPR55 Is a Cannabinoid Receptor That Increases Intracellular Calcium and Inhibits M Current." Proceedings of the National Academy of Sciences of the United States of America 105(7):2699–2704. doi: 10.1073/pnas.0711278105.

Lautner, Roberto Queiroga, Daniel C. Villela, Rodrigo A. Fraga-Silva, Neiva Silva, Thiago Verano-Braga, Fabiana Costa-Fraga, Joachim Jankowski, Vera Jankowski, Frederico Sousa, Andreia Alzamora, Everton Soares, Claudiane Barbosa, Frank Kjeldsen, Aline Oliveira, Janaina Braga, Silvia Savergnini, Gisele Maia, Antonio Bastos Peluso, Danielle Passos-Silva, Anderson Ferreira, Fabiana Alves, Almir Martins, Mohan Raizada, Renata Paula, Daisy Motta-Santos, Friederike Kemplin, Adriano Pimenta, Natalia Alenina, Ruben Sinisterra, Michael Bader, Maria Jose Campagnole-Santos, and Robson A. S. Santos. 2013. "Discovery and Characterization of Alamandine: A Novel Component of the Renin-Angiotensin System." Circulation Research 112(8):1104–11. doi: 10.1161/CIRCRESAHA.113.301077.

Lebon, Guillaume, Patricia C. Edwards, Andrew G. W. Leslie, and Christopher G. Tate. 2015. "Molecular Determinants of CGS21680 Binding to the Human Adenosine A2A Receptor." Molecular Pharmacology 87(6):907–15. doi: 10.1124/mol.114.097360.

Lebon, Guillaume, Tony Warne, and Christopher G. Tate. 2012. "Agonist-Bound Structures of G Protein-Coupled Receptors." Current Opinion in Structural Biology 22(4):482–90. doi: 10.1016/j.sbi.2012.03.007.

Lee, Ming Chak, Ka Ka Ting, Seray Adams, Bruce J. Brew, Roger Chung, and Gilles J. Guillemin. 2010. "Characterisation of the Expression of NMDA Receptors in Human Astrocytes." PLoS ONE 5(11):1–11. doi: 10.1371/journal.pone.0014123.

de Lera Ruiz, Manuel, Yeon-Hee Lim, and Junying Zheng. 2014. "Adenosine A2A Receptor as a Drug Discovery Target." Journal of Medicinal Chemistry 57(9):3623–50. doi: 10.1021/jm4011669.

Lewerenz, Jan, and Pamela Maher. 2015. "Chronic Glutamate Toxicity in Neurodegenerative Diseases-What Is the Evidence?" Frontiers in Neuroscience 9(DEC).

Lewitt, Peter A. 2015. "Levodopa Therapy for Parkinson's Disease: Pharmacokinetics and Pharmacodynamics." Movement Disorders 30(1):64–72. doi: 10.1002/mds.26082.

Li, Edmond C. K., Balraj S. Heran, and James M. Wright. 2014. "Angiotensin Converting Enzyme (ACE) Inhibitors versus Angiotensin Receptor Blockers for Primary Hypertension." Cochrane Database of Systematic Reviews 2017(12). doi: 10.1002/14651858.CD009096.pub2.

Li, Ping, Mark C. Chappell, Carlos M. Ferrario, and K. Bridget Brosnihan. 1997. "Angiotensin-(1-7) Augments Bradykinin-Induced Vasodilation by Competing with ACE and Releasing Nitric Oxide." Hypertension 29(1 II):394–400. doi: 10.1161/01.hyp.29.1.394.

Li, Xiaoting, Tian Hua, Kiran Vemuri, Jo-Hao Ho, Yiran Wu, Lijie Wu, Petr Popov, Othman Benchama, Nikolai Zvonok, K'ara Locke, Lu Qu, Gye Won Han, Malliga R. Iyer, Resat Cinar, Nathan J. Coffey, Jingjing Wang, Meng Wu, Vsevolod Katritch, Suwen Zhao, George Kunos, Laura M. Bohn, Alexandros Makriyannis, Raymond C. Stevens, and Zhi-Jie Liu. 2019. "Crystal Structure of the Human Cannabinoid Receptor CB2." Cell 176(3):459-467.e13. doi: 10.1016/j.cell.2018.12.011.

Liao, Wang, and Jianping Wu. 2020. "The ACE2/Ang (1–7)/MasR Axis as an Emerging Target for Antihypertensive Peptides." Critical Reviews in Food Science and Nutrition 0(0):1–15. doi: 10.1080/10408398.2020.1781049.

Lillo, Alejandro, Eva Martínez-Pinilla, Irene Reyes-Resina, Gemma Navarro, and Rafael Franco. 2020. "Adenosine A2A and A3 Receptors Are Able to Interact with Each Other. A Further Piece in the Puzzle of Adenosine Receptor-Mediated Signaling." International Journal of Molecular Sciences 21(14):5070. doi: 10.3390/ijms21145070.

Limanaqi, Fiona, Francesca Biagioni, Stefano Gambardella, Pietro Familiari, Alessandro Frati, and Francesco Fornai. 2020. "Promiscuous Roles of Autophagy and Proteasome in Neurodegenerative Proteinopathies." International Journal of Molecular Sciences 21(8):1–31. doi: 10.3390/ijms21083028.

Lin, Wenwei, and Taosheng Chen. 2018. "Using TR-FRET to Investigate Protein–Protein Interactions: A Case Study of PXR-Coregulator Interaction." Advances in Protein Chemistry and Structural Biology 110:31–63. doi: 10.1016/bs.apcsb.2017.06.001.

Lindau, M., O. Almkvist, J. Kushi, K. Boone, S. E. Johansson, L. O. Wahlund, J. L. Cummings, and Bruce L. Miller. 2000. "First Symptoms - Frontotemporal Dementia versus Alzheimer's Disease." Dementia and Geriatric Cognitive Disorders 11(5):286–93. doi: 10.1159/000017251.

Linden, Joel. 1994. "Cloned Adenosine A3 Receptors: Pharmacological Properties, Species Differences and Receptor Functions." Trends in Pharmacological Sciences 15(8):298–306. doi: 10.1016/0165-6147(94)90011-6.

Liotta, Giuseppe, Helena Canhao, Fabian Cenko, Rita Cutini, Ercole Vellone, Maddalena Illario, Przemyslaw Kardas, Andrea Poscia, Rute Dinis Sousa, Leonardo Palombi, and Maria Cristina Marazzi. 2018. "Active Ageing in Europe: Adding Healthy Life to Years." Frontiers in Medicine 5(April):8–11. doi: 10.3389/fmed.2018.00123.

Lipton, Richard B., Hans Christoph Diener, Matthew S. Robbins, Sandy Yacoub Garas, and Ketu Patel. 2017. "Caffeine in the Management of Patients with Headache." Journal of Headache and Pain 18(1). doi: 10.1186/s10194-017-0806-2.

Liu, Chun Hua, Zheng Gong, Zong Lai Liang, Zhi Xin Liu, Fan Yang, Yu Jing Sun, Ming Liang Ma, Yi Jing Wang, Chao Ran Ji, Yu Hong Wang, Mei Jie Wang, Fu Ai Cui, Amy Lin, Wen Shuai Zheng, Dong Fang He, Chang Xiu Qu, Peng Xiao, Chuan Yong Liu, Alex R. B. Thomsen, Thomas Joseph Cahill, Alem W. Kahsai, Fan Yi, Kun Hong Xiao, Tian Xue, Zhuan Zhou, Xiao Yu, and Jin Peng Sun. 2017. "Arrestin-Biased AT1R Agonism Induces Acute Catecholamine Secretion through TRPC3 Coupling." Nature Communications 8:1–17. doi: 10.1038/ncomms14335.

Liu, Jinping, Lirong Chang, Yizhi Song, Hui Li, and Yan Wu. 2019. "The Role of NMDA Receptors in Alzheimer's Disease." Frontiers in Neuroscience 13(FEB):1–22. doi: 10.3389/fnins.2019.00043.

Liu, Qingyun, Xiao Ming Guan, William J. Martin, Terrence P. McDonald, Michelle K. Clements, Qingping Jiang, Zhizhen Zeng, Marlene Jacobson, David L. Williams, Hong Yu, Douglas Bomford, David Figueroa, John Mallee, Ruiping Wang, Jilly Evans, Robert Gould, and Christopher P. Austin. 2001. "Identification and Characterization of Novel Mammalian Neuropeptide FF-like Peptides That Attenuate Morphine-Induced Antinociception." Journal of Biological Chemistry 276(40):36961–69. doi: 10.1074/jbc.M105308200.

Lu, D., and D. E. Potter. 2017. "Cannabinoids and the Cannabinoid Receptors: An Overview." Handbook of Cannabis and Related Pathologies: Biology, Pharmacology, Diagnosis, and Treatment 553–63. doi: 10.1016/B978-0-12-800756-3.00068-5.

Lu, Hong, Lisa A. Cassis, Craig W. Vande. Kooi, and Alan Daugherty. 2016. "Structure and Functions of Angiotensinogen." Hypertension Research 39(7):492–500. doi: 10.1038/hr.2016.17.

Lücking, Christoph B., Alexandra Dürr, Vincenzo Bonifati, Jenny Vaughan, Giuseppe De Michele, Thomas Gasser, Biswadjiet S. Harhangi, Giuseppe Meco, Patrice Denèfle, Nicholas W. Wood, Yves Agid, D. Nicholl, M. M. B. Breteler, B. A. Oostra, M. De Mari, R. Marconi, A. Filla, A. M. Bonnet, E. Broussolle, P. Pollak, O. Rascol, M. Rosier, Arnould Arnould, and Alexis Brice. 2000. "Association between Early-Onset Parkinson's Disease and Mutations in the Parkin Gene." New England Journal of Medicine 342(21):1560–67. doi: 10.1056/NEJM200005253422103.

Lukassen, Soeren, Robert Lorenz Chua, Timo Trefzer, Nicolas C. Kahn, Marc A. Schneider, Thomas Muley, Hauke Winter, Michael Meister, Carmen Veith, Agnes W. Boots, Bianca P. Hennig, Michael Kreuter, Christian Conrad, and Roland Eils. 2020. "SARS -CoV-2 Receptor ACE 2 and TMPRSS 2 Are Primarily Expressed in Bronchial Transient Secretory Cells." The EMBO Journal 39(10). doi: 10.15252/embj.20105114.

Luttrell, Louis M. 2008. "Reviews in Molecular Biology and Biotechnology: Transmembrane Signaling by G Protein-Coupled Receptors." Molecular Biotechnology 39(3):239–64. doi: 10.1007/s12033-008-9031-1.

Lutz, Beat, Giovanni Marsicano, Rafael Maldonado, and Cecilia J. Hillard. 2015. "The Endocannabinoid System in Guarding against Fear, Anxiety and Stress." Nature Reviews Neuroscience 16(12):705–18. doi: 10.1038/nrn4036.

Malfitano, Anna Maria, Sreemanti Basu, Katarzyna Maresz, Maurizio Bifulco, and Bonnie N. Dittel. 2014. "What We Know and Do Not Know about the Cannabinoid Receptor 2 (CB2)." Seminars in Immunology 26(5):369–79. doi: 10.1016/j.smim.2014.04.002.

Mandelkow, E. 1999. "The Tangled Tale of Tau." Nature 402(6762):588–89. doi: 10.1038/45095.

Mandelkow, Eva Maria, and Eckhard Mandelkow. 2012. "Biochemistry and Cell Biology of Tau Protein in Neurofibrillary Degeneration." Cold Spring Harbor Perspectives in Medicine 2(7):1–26. doi: 10.1101/cshperspect.a006247.

Manglik, Aashish, and Andrew C. Kruse. 2017. "Structural Basis for G Protein-Coupled Receptor Activation." Biochemistry 56(42):5628–34. doi: 10.1021/acs.biochem.7b00747.

Marcellino, Daniel, Sergi Ferré, Vicent Casadó, Antonio Cortés, Bernard Le Foll, Carmen Mazzola, Filippo Drago, Oliver Saur, Holger Stark, Aroa Soriano, Chanel Barnes, Steven R. Goldberg, Carme Lluis, Kjell Fuxe, and Rafael Franco. 2008. "Identification of Dopamine D1–D3 Receptor Heteromers." Journal of Biological Chemistry 283(38):26016–25. doi: 10.1074/jbc.M710349200.

Marcu, Jahan, Linda Console-Bram, and Mary E. Abood. 2013. "Current Cannabinoid Receptor Nomenclature and Pharmacological Principles." Endocannabinoid Regulation of Monoamines in Psychiatric and Neurological Disorders 25–54. doi: 10.1007/978-1-4614-7940-6_3.

Marinissen, Maria Julia, and J. Silvio Gutkind. 2001. "G-Protein-Coupled Receptors and Signaling Networks: Emerging Paradigms." Trends in Pharmacological Sciences 22(7):368–76. doi: 10.1016/S0165-6147(00)01678-3.

Márquez-Gómez, Ricardo, Meridith T. Robins, Citlaly Gutiérrez-Rodelo, Juan Manuel Arias, Jesús Alberto Olivares-Reyes, Richard M. van Rijn, and José Antonio Arias-Montaño. 2018. "Functional Histamine H3 and Adenosine A2A Receptor Heteromers in Recombinant Cells and Rat Striatum." Pharmacological Research 129:515–25. doi: 10.1016/j.phrs.2017.11.036.

Martínez-Pinilla, Eva, Katia Varani, Irene Reyes-Resina, Edgar Angelats, Fabrizio Vincenzi, Carlos Ferreiro-Vera, Julen Oyarzabal, Enric I. Canela, José L. Lanciego, Xavier Nadal, Gemma Navarro, Pier Andrea Borea, and Rafael Franco. 2017. "Binding and Signaling Studies Disclose a Potential Allosteric Site for Cannabidiol in Cannabinoid CB2 Receptors." Frontiers in Pharmacology 8. doi: 10.3389/fphar.2017.00744.

Martinotti, Giovanni, Rita Santacroce, Duccio Papanti, Yasmine Elgharably, Mariya Prilutskaya, and Ornella Corazza. 2017. "Synthetic Cannabinoids: Psychopharmacology, Clinical Aspects, Psychotic Onset." CNS & Neurological Disorders Drug Targets 16(5):567–75. doi: 10.2174/1871527316666170413101839.

Martire, Alberto, Catia Lambertucci, Rita Pepponi, Antonella Ferrante, Nicholas Benati, Michela Buccioni, Diego Dal Ben, Gabriella Marucci, Karl Norbert Klotz, Rosaria Volpini, and Patrizia Popoli. 2019. "Neuroprotective Potential of Adenosine A 1 Receptor Partial Agonists in Experimental Models of Cerebral Ischemia." Journal of Neurochemistry 149(2):211–30. doi: 10.1111/jnc.14660.

Matavelli, Luis C., and Helmy M. Siragy. 2015. "AT2 Receptor Activities and Pathophysiological Implications." Journal of Cardiovascular Pharmacology 65(3):226–32. doi: 10.1097/FJC.0000000000000208.

Matsuda, Lisa A., Stephen J. Lolait, Michael J. Brownstein, Alice C. Young, and Tom I. Bonner. 1990. "Structure of a Cannabinoid Receptor and Functional Expression of the Cloned CDNA." Nature 346(6284):561–64. doi: 10.1038/346561a0.

Mattsson-Carlgren, Niklas, Sebastian Palmqvist, Kaj Blennow, and Oskar Hansson. 2020. "Increasing the Reproducibility of Fluid Biomarker Studies in Neurodegenerative Studies." Nature Communications 11(1):1–11. doi: 10.1038/s41467-020-19957-6.

Mawuenyega, Kwasi G., Wendy Sigurdson, Vitaliy Ovod, Ling Munsell, Tom Kasten, John C. Morris, Kevin E. Yarasheski, and Randall J. Bateman. 2010. "Decreased Clearance of CNS β-Amyloid in Alzheimer's Disease." Science 330(6012):1774. doi: 10.1126/science.1197623.

McCarthy, Claudia A., Antony Vinh, Jennifer K. Callaway, and Robert E. Widdop. 2009. "Angiotensin AT2 Receptor Stimulation Causes Neuroprotection in a Conscious Rat Model of Stroke." Stroke 40(4):1482–89. doi: 10.1161/STROKEAHA.108.531509.

McCudden, C. R., M. D. Hains, R. J. Kimple, D. P. Siderovski, and F. S. Willard. 2005. "G-Protein Signaling: Back to the Future." Cellular and Molecular Life Sciences 62(5):551–77. doi: 10.1007/s00018-004-4462-3.

McKinney, Clare A., Caroline Fattah, Christopher M. Loughrey, Graeme Milligan, and Stuart A. Nicklin. 2014. "Angiotensin-(1-7) and Angiotensin-(1-9): Function in Cardiac and Vascular Remodelling." Clinical Science 126(12):815–27. doi: 10.1042/CS20130436.

Meixiong, James, and Xinzhong Dong. 2017. "Mas-Related G Protein-Coupled Receptors and the Biology of Itch Sensation." Annual Review of Genetics 51:103–21. doi: 10.1146/annurev-genet-120116-024723.

Melser, Su, Antonio C. Pagano Zottola, Roman Serrat, Nagore Puente, Pedro Grandes, Giovanni Marsicano, and Etienne Hebert-Chatelain. 2017. "Functional Analysis of Mitochondrial CB1 Cannabinoid Receptors (MtCB1) in the Brain." Pp. 143–74 in.

Meng, Fan, Guo xi Xie, Derek Chalmers, Caurnel Morgan, Stanley J. Watson, and Huda Akil. 1994. "Cloning and Expression of the A2a Adenosine Receptor from Guinea Pig Brain." Neurochemical Research 19(5):613–21. doi: 10.1007/BF00971338.

Merighi, Stefania, Stefania Gessi, and Pier Andrea Borea. 2018. "Adenosine Receptors: Structure, Distribution, and Signal Transduction." Receptors 34:33–57. doi: 10.1007/978-3-319-90808-3_3.

Miao, Yinglong, Apurba Bhattarai, Anh T. N. Nguyen, Arthur Christopoulos, and Lauren T. May. 2018. "Structural Basis for Binding of Allosteric Drug Leads in the Adenosine A1 Receptor." Scientific Reports 8(1):1–13. doi: 10.1038/s41598-018-35266-x.

Michel, Martin C., Hans R. Brunner, Carolyn Foster, and Yong Huo. 2016. "Angiotensin II Type 1 Receptor Antagonists in Animal Models of Vascular, Cardiac, Metabolic and Renal Disease." Pharmacology and Therapeutics 164:1–81. doi: 10.1016/j.pharmthera.2016.03.019.

Michel, Martin C., and Steven J. Charlton. 2018. "Biased Agonism in Drug Discovery-Is It Too Soon to Choose a Path?" Molecular Pharmacology 93(4):259–65. doi: 10.1124/mol.117.110890.

Miller, William E., Daniel A. Houtz, Christopher D. Nelson, P. E. Kolattukudy, and Robert J. Lefkowitz. 2003. "G-Protein-Coupled Receptor (GPCR) Kinase Phosphorylation and β-Arrestin Recruitment Regulate the Constitutive Signaling Activity of the Human Cytomegalovirus US28 GPCR." Journal of Biological Chemistry 278(24):21663–71. doi: 10.1074/jbc.M303219200.

Mizuno, Yoshikuni, and Tomoyoshi Kondo. 2013. "Adenosine A2A Receptor Antagonist Istradefylline Reduces Daily OFF Time in Parkinson's Disease." Movement Disorders 28(8):1138–41. doi:

10.1002/mds.25418.
Moeller, I., A. M. Allen, S. Y. Chai, J. Zhuo, and F. A. O. Mendelsohn. 1998. "Bioactive Angiotensin Peptides." Journal of Human Hypertension 12(5):289–93. doi: 10.1038/sj.jhh.1000640.
Mogi, Masaki, Masaru Iwai, and Masatsugu Horiuchi. 2009. "New Insights into the Regulation of Angiotensin Receptors." Current Opinion in Nephrology and Hypertension 18(2):138–43. doi: 10.1097/MNH.0b013e328324f5fa.
Mogi, Masaki, Jun Iwanami, and Masatsugu Horiuchi. 2012. "Roles of Brain Angiotensin II in Cognitive Function and Dementia." International Journal of Hypertension 2012. doi: 10.1155/2012/169649.
Mohan, Maradumane L., Neelakantan T. Vasudevan, Manveen K. Gupta, E. Elizabeth, Sathyamangla V. Naga Prasad, and Cleveland Clinic Foundation. 2015. "Balancing Act of Receptor Function." Current Molecular Pharmacology.
Moreau, Jean Luc, and Gerda Huber. 1999. "Central Adenosine A(2A) Receptors: An Overview." Brain Research Reviews 31(1):65–82. doi: 10.1016/S0165-0173(99)00059-4.
Moreira, Fabrício A., and José Alexandre S. Crippa. 2009. "The Psychiatric Side-Effects of Rimonabant." Revista Brasileira de Psiquiatria 31(2):145–53. doi: 10.1590/S1516-44462009000200012.
Morgan, J. M., D. G. McCormack, M. J. D. Griffiths, C. J. Morgan, P. J. Barnes, and T. W. Evans. 1991. "Adenosine as a Vasodilator in Primary Pulmonary Hypertension." Circulation 84(3):1145–49. doi: 10.1161/01.CIR.84.3.1145.
Moriconi, A., I. Cerbara, M. Maccarrone, and A. Topai. 2010. "GPR55: Current Knowledge and Future Perspectives of a Purported 'Type-3' Cannabinoid Receptor." Current Medicinal Chemistry 17(14):1411–29. doi: 10.2174/092986710790980069.
Mouro, Francisco M., Diogo M. Rombo, Raquel B. Dias, Joaquim A. Ribeiro, and Ana M. Sebastião. 2018. "Adenosine A2A Receptors Facilitate Synaptic NMDA Currents in CA1 Pyramidal Neurons." British Journal of Pharmacology 175(23):4386–97. doi: 10.1111/bph.14497.
Muangpaisan, Weerasak, Aju Mathews, Hiroyuki Hori, and David Seidel. 2011. "A Systematic Review of the Worldwide Prevalence and Incidence of Parkinson's Disease." Journal of the Medical Association of Thailand 94(6):749–55.
Mundell, Stuart, and Eamonn Kelly. 2011. "Adenosine Receptor Desensitization and Trafficking." Biochimica et Biophysica Acta - Biomembranes 1808(5):1319–28. doi: 10.1016/j.bbamem.2010.06.007.
Muñoz, Marina C., Jorge F. Giani, and Fernando P. Dominici. 2010. "Angiotensin-(1-7) Stimulates the Phosphorylation of Akt in Rat Extracardiac Tissues in Vivo via Receptor Mas." Regulatory Peptides 161(1–3):1–7. doi: 10.1016/j.regpep.2010.02.001.
Munro, Sean, Kerrie L. Thomas, and Muna Abu-Shaar. 1993. "Molecular Characterization of a Peripheral Receptor for Cannabinoids." Nature 365(6441):61–65. doi: 10.1038/365061a0.
Murphy, T. J., R. Wayne Alexander, Kathy K. Griendling, Marschall S. Runge, and Kenneth E. Bernstein. 1991. "Isolation of a CDNA Encoding the Vascular Type-1 Angiotensin II Receptor." Nature 351(6323):233–36. doi: 10.1038/351233a0.
Mustafa, Sanam, Heng B. See, Ruth M. Seeber, Stephen P. Armstrong, Carl W. White, Sabatino Ventura, Mohammed Akli Ayoub, and Kevin D. G. Pfleger. 2012. "Identification and Profiling of Novel α 1A-Adrenoceptor-CXC Chemokine Receptor 2 Heteromer." Journal of Biological Chemistry 287(16):12952–65. doi: 10.1074/jbc.M111.322834.
N. Bohinc, Brittany, and Diane Gesty-Palmer. 2012. "β-Arrestin-Biased Agonism at the Parathyroid Hormone Receptor Uncouples Bone Formation from Bone Resorption." Endocrine, Metabolic & Immune Disorders - Drug Targets 11(2):112–19. doi: 10.2174/187153011795564151.
Nakajima, Masatoshi, Howard G. Hutchinson, Masahiko Fujinaga, Wataru Hayashida, Ryuichi Morishita, Lunan Zhang, Masatsugu Horiuchi, Richard E. Pratt, and Victor J. Dzau. 1995. "The Angiotensin II Type 2 (AT2) Receptor Antagonizes the Growth Effects of the AT1 Receptor: Gain-of-Function Study Using Gene Transfer." Proceedings of the National Academy of Sciences of

the United States of America 92(23):10663–67. doi: 10.1073/pnas.92.23.10663.
Navarrete, Marta, and Alfonso Araque. 2008. "Endocannabinoids Mediate Neuron-Astrocyte Communication." Neuron 57(6):883–93. doi: 10.1016/j.neuron.2008.01.029.
Navarro, G, D. Borroto-Escuela, E. Angelats, I. Etayo, I. Reyes-Resina, M. Pulido-Salgado, AI. Rodríguez-Pérez, EI. Canela, Josep Saura, José Luis Lanciego, José Luis Labandeira-García, Carlos A. Saura, Kjell Fuxe, and Rafael Franco. 2018. "Receptor-Heteromer Mediated Regulation of Endocannabinoid Signaling in Activated Microglia. Role of CB1 and CB2 Receptors and Relevance for Alzheimer's Disease and Levodopa-Induced Dyskinesia." Brain, Behavior, and Immunity 67:139–51. doi: 10.1016/j.bbi.2017.08.015.
Navarro, Gemma, Dasiel Borroto-Escuela, Edgar Angelats, Íñigo Etayo, Irene Reyes-Resina, Marta Pulido-Salgado, Ana I. Rodríguez-Pérez, Enric I. Canela, Josep Saura, José Luis Lanciego, José Luis Labandeira-García, Carlos A. Saura, Kjell Fuxe, and Rafael Franco. 2018. "Receptor-Heteromer Mediated Regulation of Endocannabinoid Signaling in Activated Microglia. Role of CB1 and CB2 Receptors and Relevance for Alzheimer's Disease and Levodopa-Induced Dyskinesia." Brain, Behavior, and Immunity 67:139–51. doi: 10.1016/j.bbi.2017.08.015.
Navarro, Gemma, Paula Morales, Carmen Rodríguez-Cueto, Javier Fernández-Ruiz, Nadine Jagerovic, and Rafael Franco. 2016. "Targeting Cannabinoid CB2 Receptors in the Central Nervous System. Medicinal Chemistry Approaches with Focus on Neurodegenerative Disorders." Frontiers in Neuroscience 10. doi: 10.3389/fnins.2016.00406.
Navarro, Gemma, Irene Reyes-Resina, Rafael Rivas-Santisteban, Verónica Sánchez de Medina, Paula Morales, Salvatore Casano, Carlos Ferreiro-Vera, Alejandro Lillo, David Aguinaga, Nadine Jagerovic, Xavier Nadal, and Rafael Franco. 2018a. "Cannabidiol Skews Biased Agonism at Cannabinoid CB1 and CB2 Receptors with Smaller Effect in CB1-CB2 Heteroreceptor Complexes." Biochemical Pharmacology 157:148–58. doi: 10.1016/j.bcp.2018.08.046.
Navarro, Gemma, Irene Reyes-Resina, Rafael Rivas-Santisteban, Verónica Sánchez de Medina, Paula Morales, Salvatore Casano, Carlos Ferreiro-Vera, Alejandro Lillo, David Aguinaga, Nadine Jagerovic, Xavier Nadal, and Rafael Franco. 2018b. "Cannabidiol Skews Biased Agonism at Cannabinoid CB1 and CB2 Receptors with Smaller Effect in CB1-CB2 Heteroreceptor Complexes." Biochemical Pharmacology 157:148–58. doi: 10.1016/j.bcp.2018.08.046.
Navarro, Gemma, Katia Varani, Irene Reyes-Resina, Verónica Sánchez de Medina, Rafael Rivas-Santisteban, Carolina Sánchez Carnerero Callado, Fabrizio Vincenzi, Salvatore Casano, Carlos Ferreiro-Vera, Enric I. Canela, Pier Andrea Borea, Xavier Nadal, and Rafael Franco. 2018. "Cannabigerol Action at Cannabinoid CB1 and CB2 Receptors and at CB1-CB2 Heteroreceptor Complexes." Frontiers in Pharmacology 9(JUN). doi: 10.3389/fphar.2018.00632.
Nehme, Ali, Fouad A. Zouein, Zeinab Deris Zayeri, and Kazem Zibara. 2019. "An Update on the Tissue Renin Angiotensin System and Its Role in Physiology and Pathology." Journal of Cardiovascular Development and Disease 6(2):14. doi: 10.3390/jcdd6020014.
Neubig, Richard R., Michael Spedding, Terry Kenakin, and Arthur Christopoulos. 2003. "International Union of Pharmacology Committee on Receptor Nomenclature and Drug Classification. XXXVIII. Update on Terms and Symbols in Quantitative Pharmacology." Pharmacological Reviews 55(4):597–606. doi: 10.1124/pr.55.4.4.
Niu, H., I. Álvarez-Álvarez, F. Guillén-Grima, and I. Aguinaga-Ontoso. 2017. "Prevalencia e Incidencia de La Enfermedad de Alzheimer En Europa: Metaanálisis." Neurologia 32(8):523–32. doi: 10.1016/j.nrl.2016.02.016.
Nong, Yi, Yue Qiao Huang, William Ju, Lorraine V. Kalia, Gholamreza Ahmadian, Yu Tian Wang, and Michael W. Salter. 2003. "Glycine Binding Primes NMDA Receptor Internalization." Nature 422(6929):302–7. doi: 10.1038/nature01497.
Ocaranza, Maria Paz, Sergio Lavandero, Jorge E. Jalil, Jaqueline Moya, Melissa Pinto, Ulises Novoa, Felipe Apablaza, Leticia González, Carol Hernández, Manuel Varas, René López, Iván Godoy, Hugo Verdejo, and Mario Chiong. 2010. "Angiotensin-(1-9) Regulates Cardiac Hypertrophy in Vivo and in Vitro." Journal of Hypertension 28(5):1054–64. doi: 10.1097/HJH.0b013e328335d291.

Oertel, W. H. 1995. "Parkinson's Disease: Epidemiology, (Differential) Diagnosis, Therapy, Relation to Dementia." Arzneimittel-Forschung 45(3A):386–89.

Ohtsu, Haruhiko, Hiroyuki Suzuki, Hidekatsu Nakashima, Sudhir Dhobale, Gerald D. Frank, Evangeline D. Motley, and Satoru Eguchi. 2006. "Angiotensin II Signal Transduction through Small GTP-Binding Proteins: Mechanism and Significance in Vascular Smooth Muscle Cells." Hypertension 48(4):534–40. doi: 10.1161/01.HYP.0000237975.90870.eb.

De Oliveira, Paulo A., James A. R. Dalton, Marc López-Cano, Adrià Ricarte, Xavier Morató, Filipe C. Matheus, Andréia S. Cunha, Christa E. Müller, Reinaldo N. Takahashi, Víctor Fernández-Dueñas, Jesús Giraldo, Rui D. Prediger, and Francisco Ciruela. 2017. "Angiotensin II Type 1/Adenosine A 2A Receptor Oligomers: A Novel Target for Tardive Dyskinesia." Scientific Reports 7(1):1–12. doi: 10.1038/s41598-017-02037-z.

Oliveros, A., C. H. Cho, A. Cui, S. Choi, D. Lindberg, D. Hinton, M. H. Jang, and D. S. Choi. 2017. "Adenosine A2A Receptor and ERK-Driven Impulsivity Potentiates Hippocampal Neuroblast Proliferation." Translational Psychiatry 7(4). doi: 10.1038/tp.2017.64.

Onaran, H. Ongun, Caterina Ambrosio, Özlem Ugur, Erzsebet Madaras Koncz, Maria Cristina Grò, Vanessa Vezzi, Sudarshan Rajagopal, and Tommaso Costa. 2017. "Systematic Errors in Detecting Biased Agonism: Analysis of Current Methods and Development of a New Model-Free Approach." Scientific Reports 7(November 2016):1–17. doi: 10.1038/srep44247.

Orihuela, Ruben, Christopher A. McPherson, and Gaylia Jean Harry. 2016. "Microglial M1/M2 Polarization and Metabolic States." British Journal of Pharmacology 173(4):649–65. doi: 10.1111/bph.13139.

Pacher, Pál, Sándor Bátkai, and George Kunos. 2006. "The Endocannabinoid System as an Emerging Target of Pharmacotherapy." Pharmacological Reviews 58(3):389–462. doi: 10.1124/pr.58.3.2.

Padia, Shetal H, and Robert M. Carey. 2013. "AT2 Receptors: Beneficial Counter-Regulatory Role in Cardiovascular and Renal Function." Pflugers Archiv : European Journal of Physiology 465(1):99–110. doi: 10.1007/s00424-012-1146-3.

Padia, Shetal H., and Robert M. Carey. 2013. "AT2 Receptors: Beneficial Counter-Regulatory Role in Cardiovascular and Renal Function." Pflügers Archiv - European Journal of Physiology 465(1):99–110. doi: 10.1007/s00424-012-1146-3.

Palczewski, K., T. Kumasaka, T. Hori, C. A. Behnke, H. Motoshima, B. A. Fox, I. Le Trong, D. C. Teller, T. Okada, R. E. Stenkamp, M. Yamamoto, and M. Miyano. 2000. "Crystal Structure of Rhodopsin: A G Protein-Coupled Receptor." Science 289(5480):739–45. doi: 10.1126/science.289.5480.739.

Palmer, K., A. K. Berger, R. Monastero, B. Winblad, L. Bäckman, and L. Fratiglioni. 2007. "Predictors of Progression from Mild Cognitive Impairment to Alzheimer Disease." Neurology 68(19):1596–1602. doi: 10.1212/01.wnl.0000260968.92345.3f.

Palmer, T. M., and G. L. Stiles. 1995. "Adenosine Receptors." Neuropharmacology 34(7):683–94. doi: 10.1016/0028-3908(95)00044-7.

Palomo-Garo, Cristina, Yolanda Gómez-Gálvez, Concepción García, and Javier Fernández-Ruiz. 2016. "Targeting the Cannabinoid CB2 Receptor to Attenuate the Progression of Motor Deficits in LRRK2-Transgenic Mice." Pharmacological Research 110:181–92. doi: 10.1016/j.phrs.2016.04.004.

Papadia, Sofia, and Giles E. Hardingham. 2007. "The Dichotomy of NMDA Receptor Signaling." Neuroscientist 13(6):572–79. doi: 10.1177/1073858407305833.

Parker, Linda A., Erin M. Rock, and Cheryl L. Limebeer. 2011. "Regulation of Nausea and Vomiting by Cannabinoids." British Journal of Pharmacology 163(7):1411–22. doi: 10.1111/j.1476-5381.2010.01176.x.

Parlar, Ali, Seyfullah Oktay Arslan, Muhammed Fatih Doğan, Saliha Ayşenur Çam, Alper Yalçin, Ebru Elibol, Mehmet Kaya Özer, Fatih Üçkardeş, and Halil Kara. 2018. "The Exogenous Administration of CB2 Specific Agonist, GW405833, Inhibits Inflammation by Reducing Cytokine Production and Oxidative Stress." Experimental and Therapeutic Medicine 16(6):4900–4908. doi: 10.3892/etm.2018.6753.

Pastor-Anglada, Marçal, and Sandra Pérez-Torras. 2018. "Who Is Who in Adenosine Transport." Frontiers in Pharmacology 9(JUN):1–10. doi: 10.3389/fphar.2018.00627.

Patel, Sanket, and Tahir Hussain. 2018. "Dimerization of AT2 and Mas Receptors in Control of Blood Pressure." Current Hypertension Reports 20(5):41. doi: 10.1007/s11906-018-0845-3.

Paul, Martin, Ali Poyan Mehr, and Reinhold Kreutz. 2006. "Physiology of Local Renin-Angiotensin Systems." Physiological Reviews 86(3):747–803. doi: 10.1152/physrev.00036.2005.

Paz Ocaranza, Maria, Jaime A. Riquelme, Lorena García, Jorge E. Jalil, Mario Chiong, Robson A. S. Santos, and Sergio Lavandero. 2020. "Counter-Regulatory Renin–Angiotensin System in Cardiovascular Disease." Nature Reviews Cardiology 17(2):116–29. doi: 10.1038/s41569-019-0244-8.

Perreault, Melissa L., Ahmed Hasbi, Maurice Y. F. Shen, Theresa Fan, Gemma Navarro, Paul J. Fletcher, Rafael Franco, José L. Lanciego, and Susan R. George. 2016. "Disruption of a Dopamine Receptor Complex Amplifies the Actions of Cocaine." European Neuropsychopharmacology 26(9):1366–77. doi: 10.1016/j.euroneuro.2016.07.008.

Pertwee, R. G. 2007. "GPR55: A New Member of the Cannabinoid Receptor Clan?" British Journal of Pharmacology 152(7):984–86. doi: 10.1038/sj.bjp.0707464.

Pertwee, Roger G. 2006. "Cannabinoid Pharmacology: The First 66 Years." British Journal of Pharmacology 147(SUPPL. 1). doi: 10.1038/sj.bjp.0706406.

Pertwee, Roger G. 2012. "Targeting the Endocannabinoid System with Cannabinoid Receptor Agonists: Pharmacological Strategies and Therapeutic Possibilities." Philosophical Transactions of the Royal Society B: Biological Sciences 367(1607):3353–63. doi: 10.1098/rstb.2011.0381.

Peterfreund, Robert A., Mia MacCollin, James Gusella, and J. Stephen Fink. 1996. "Characterization and Expression of the Human A2a Adenosine Receptor Gene." Journal of Neurochemistry 66(1):362–68. doi: 10.1046/j.1471-4159.1996.66010362.x.

Petralia, R. S., Y. X. Wang, F. Hua, Z. Yi, A. Zhou, L. Ge, F. A. Stephenson, and R. J. Wenthold. 2010. "Organization of NMDA Receptors at Extrasynaptic Locations." Neuroscience 167(1):68–87. doi: 10.1016/j.neuroscience.2010.01.022.

Pin, Jean Philippe, Julie Kniazeff, Laurent Prézeau, Jiang Feng Liu, and Philippe Rondard. 2019. "GPCR Interaction as a Possible Way for Allosteric Control between Receptors." Molecular and Cellular Endocrinology 486(February):89–95. doi: 10.1016/j.mce.2019.02.019.

Pinna, Annalisa, Jordi Bonaventura, Daniel Farré, Marta Sánchez, Nicola Simola, Josefa Mallol, Carme Lluís, Giulia Costa, Younis Baqi, Christa E. Müller, Antoni Cortés, Peter McCormick, Enric I. Canela, Eva Martínez-Pinilla, José L. Lanciego, Vicent Casadó, Marie-Therese Armentero, and Rafael Franco. 2014. "L-DOPA Disrupts Adenosine A2A–Cannabinoid CB1–Dopamine D2 Receptor Heteromer Cross-Talk in the Striatum of Hemiparkinsonian Rats: Biochemical and Behavioral Studies." Experimental Neurology 253:180–91. doi: 10.1016/j.expneurol.2013.12.021.

Pitt, Bertram. 1997. "ACE Inhibitors in Heart Failure: Prospects and Limitations." Cardiovascular Drugs and Therapy 11(SUPPL. 1):285–90. doi: 10.1023/A:1007795915009.

Porrello, Enzo R., Lea M. D. Delbridge, and Walter G. Thomas. 2009. "Molecular Endocrinology Laboratory, Baker Heart Research Institute, Prahran, Victoria 3004, Australia, Physiology, University of Melbourne, Parkville, Victoria 3010, Australia 2 Department Of." Vascular 2:958–72.

Porrello, Enzo R., Kevin D. G. Pfleger, Ruth M. Seeber, Hongwei Qian, Cristina Oro, Fe Abogadie, Lea M. D. Delbridge, and Walter G. Thomas. 2011. "Heteromerization of Angiotensin Receptors Changes Trafficking and Arrestin Recruitment Profiles." Cellular Signalling 23(11):1767–76. doi: 10.1016/j.cellsig.2011.06.011.

Price, David A., Alex A. Martinez, Alexandre Seillier, Wouter Koek, Yolanda Acosta, Elizabeth Fernandez, Randy Strong, Beat Lutz, Giovanni Marsicano, James L. Roberts, and Andrea Giuffrida. 2009. "WIN55,212-2, a Cannabinoid Receptor Agonist, Protects against Nigrostriatal Cell Loss in the 1-Methyl-4-Phenyl-1,2,3,6-Tetrahydropyridine Mouse Model of Parkinson's

Disease." European Journal of Neuroscience 29(11):2177–86. doi: 10.1111/j.1460-9568.2009.06764.x.

Proietto, J., A. Rissanen, J. B. Harp, N. Erondu, Q. Yu, S. Suryawanshi, M. E. Jones, A. O. Johnson-Levonas, S. B. Heymsfield, K. D. Kaufman, and J. M. Amatruda. 2010. "A Clinical Trial Assessing the Safety and Efficacy of the CB1R Inverse Agonist Taranabant in Obese and Overweight Patients: Low-Dose Study." International Journal of Obesity 34(8):1243–54. doi: 10.1038/ijo.2010.38.

Qin, Yongwei, Xiaolei Sun, Xiaoyi Shao, Chun Cheng, Jinrong Feng, Wei Sun, Delin Gu, Wei Liu, Feifan Xu, and Yinong Duan. 2015. "Macrophage-Microglia Networks Drive M1 Microglia Polarization After Mycobacterium Infection." Inflammation 38(4):1609–16. doi: 10.1007/s10753-015-0136-y.

Rabie, Mostafa A., Mai A. Abd El Fattah, Noha N. Nassar, Dalaal M. Abdallah, and Hanan S. El-Abhar. 2020. "Correlation between Angiotensin 1–7-Mediated Mas Receptor Expression with Motor Improvement, Activated STAT3/SOCS3 Cascade, and Suppressed HMGB-1/RAGE/NF-KB Signaling in 6-Hydroxydopamine Hemiparkinsonian Rats." Biochemical Pharmacology 171:113681. doi: 10.1016/j.bcp.2019.113681.

Rabie, Mostafa A., Mai A. Abd El Fattah, Noha N. Nassar, Hanan S. El-Abhar, and Dalaal M. Abdallah. 2018. "Angiotensin 1-7 Ameliorates 6-Hydroxydopamine Lesions in Hemiparkinsonian Rats through Activation of MAS Receptor/PI3K/Akt/BDNF Pathway and Inhibition of Angiotensin II Type-1 Receptor/NF-KB Axis." Biochemical Pharmacology 151:126–34. doi: 10.1016/j.bcp.2018.01.047.

Rebola, Nelson, Ana Patrícia Simões, Paula M. Canas, Angelo R. Tomé, Geanne M. Andrade, Claire E. Barry, Paula M. Agostinho, Marina A. Lynch, and Rodrigo A. Cunha. 2011. "Adenosine A2A Receptors Control Neuroinflammation and Consequent Hippocampal Neuronal Dysfunction." Journal of Neurochemistry 117(1):100–111. doi: 10.1111/j.1471-4159.2011.07178.x.

Reggio, Patricia Hodapp, and Derek M. Shore. 2015. "The Therapeutic Potential of Orphan GPCRs, GPR35 and GPR55." Frontiers in Pharmacology 6(MAR):1–22. doi: 10.3389/fphar.2015.00069.

Reis, Rosana I., Marie D. Nogueira, Ana Lucia Campanha-Rodrigues, Larissa Miranda Pereira, Maria Claudina C. Andrade, Lucas T. Parreiras-e-Silva, Claudio M. Costa-Neto, Renato Arruda Mortara, and Dulce E. Casarini. 2018. "The Binding of Captopril to Angiotensin I-Converting Enzyme Triggers Activation of Signaling Pathways." American Journal of Physiology - Cell Physiology 315(3):C367–79. doi: 10.1152/ajpcell.00012.2016.

Rico, Alberto J., Iria G. Dopeso-Reyes, Eva Martínez-Pinilla, Diego Sucunza, Diego Pignataro, Elvira Roda, David Marín-Ramos, José L. Labandeira-García, Susan R. George, Rafael Franco, and José L. Lanciego. 2017. "Neurochemical Evidence Supporting Dopamine D1–D2 Receptor Heteromers in the Striatum of the Long-Tailed Macaque: Changes Following Dopaminergic Manipulation." Brain Structure and Function 222(4):1767–84. doi: 10.1007/s00429-016-1306-x.

Rios, C. D., B. A. Jordan, I. Gomes, and L. A. Devi. 2001. "G-Protein-Coupled Receptor Dimerization: Modulation of Receptor Function." Pharmacology and Therapeutics 92(2–3):71–87. doi: 10.1016/S0163-7258(01)00160-7.

Rivas-Santisteban, Rafael, Ana I. Rodriguez-Perez, Ana Muñoz, Irene Reyes-Resina, José Luis Labandeira-García, Gemma Navarro, and Rafael Franco. 2020. "Angiotensin AT1and AT2receptor Heteromer Expression in the Hemilesioned Rat Model of Parkinson's Disease That Increases with Levodopa-Induced Dyskinesia." Journal of Neuroinflammation 17(1):1–16. doi: 10.1186/s12974-020-01908-z.

Rizzi, Liara, Idiane Rosset, and Matheus Roriz-Cruz. 2014. "Global Epidemiology of Dementia: Alzheimer's and Vascular Types." BioMed Research International 2014(Figure 1). doi: 10.1155/2014/908915.

Robinson, Dean M., and Gillian M. Keating. 2006. "Memantine." Drugs 66(11):1515–34. doi: 10.2165/00003495-200666110-00015.

Rocca, W. A. 1994. "Frequency, Distribution, and Risk Factors for Alzheimer's Disease." The Nursing Clinics of North America 29(1):101–11.

Roche, Michelle, and David P. Finn. 2010. "Brain CB2 Receptors: Implications for Neuropsychiatric Disorders." Pharmaceuticals 3(8):2517–33. doi: 10.3390/ph3082517.

Rodriguez-Perez, Ana I., Pablo Garrido-Gil, Maria A. Pedrosa, Maria Garcia-Garrote, Rita Valenzuela, Gemma Navarro, Rafael Franco, and Jose L. Labandeira-Garcia. 2020. "Angiotensin Type 2 Receptors: Role in Aging and Neuroinflammation in the Substantia Nigra." Brain, Behavior, and Immunity 87(December):256–71. doi: 10.1016/j.bbi.2019.12.011.

Rodríguez-Romo, Roxana, Kenia Benítez, Jonatan Barrera-Chimal, Rosalba Pérez-Villalva, Arturo Gómez, Diana Aguilar-León, Jesús F. Rangel-Santiago, Sara Huerta, Gerardo Gamba, Norma Uribe, and Norma A. Bobadilla. 2016. "AT1 Receptor Antagonism before Ischemia Prevents the Transition of Acute Kidney Injury to Chronic Kidney Disease." Kidney International 89(2):363–73. doi: 10.1038/ki.2015.320.

Rodríguez-Ruiz, Mar, Estefanía Moreno, David Moreno-Delgado, Gemma Navarro, Josefa Mallol, Antonio Cortés, Carme Lluís, Enric I. Canela, Vicent Casadó, Peter J. McCormick, and Rafael Franco. 2017. "Heteroreceptor Complexes Formed by Dopamine D1, Histamine H3, and N-Methyl-D-Aspartate Glutamate Receptors as Targets to Prevent Neuronal Death in Alzheimer's Disease." Molecular Neurobiology 54(6):4537–50. doi: 10.1007/s12035-016-9995-y.

Romero-Sánchez, Héctor Alonso, Liliana Mendieta, Amaya Montserat Austrich-Olivares, Gabriela Garza-Mouriño, Marcela Benitez-Diaz Mirón, Arrigo Coen, and Beatriz Godínez-Chaparro. 2020. "Unilateral Lesion of the Nigroestriatal Pathway with 6-OHDA Induced Allodynia and Hyperalgesia Reverted by Pramipexol in Rats." European Journal of Pharmacology 869:172814. doi: 10.1016/j.ejphar.2019.172814.

Rominger, David H., Conrad L. Cowan, William Gowen-Macdonald, and Jonathan D. Violin. 2014. "Biased Ligands: Pathway Validation for Novel GPCR Therapeutics." Current Opinion in Pharmacology 16(1):108–15. doi: 10.1016/j.coph.2014.04.002.

Ronca, Richard D., Alyssa M. Myers, Doina Ganea, Ronald F. Tuma, Ellen A. Walker, and Sara Jane Ward. 2015. "A Selective Cannabinoid CB2 Agonist Attenuates Damage and Improves Memory Retention Following Stroke in Mice." Life Sciences 138(215):72–77. doi: 10.1016/j.lfs.2015.05.005.

Ros-Ruiz, Silvia, Pedro Aranda-Lara, Juan C. Fernández, M. Dolores Martínez-Esteban, Cristina Jironda, Pilar Hidalgo, and Domingo Hernández-Marrero. 2012. "High Doses of Irbesartan Offer Long-Term Kidney Protection in Cases of Established Diabetic Nephropathy." Nefrologia : Publicacion Oficial de La Sociedad Espanola Nefrologia 32(2):187–96. doi: 10.3265/Nefrologia.pre2011.Nov.10962.

Ross, Christopher A., and Michelle A. Poirier. 2004. "Protein Aggregation and Neurodegenerative Disease." Nature Medicine 10(7):S10. doi: 10.1038/nm1066.

Ross, E. M., A. C. Howlett, and A. G. Gilman. 1979. "Identification and Partial Characterization of Some Components of Hormone-Stimulated Adenylate Cyclase." Progress in Clinical and Biological Research Vol. 31:735–49.

Rossi, Francesca, Silvia Mancusi, Giulia Bellini, Domenico Roberti, Francesca Punzo, Simona Vetrella, Sofia Maria Rosaria Matarese, Bruno Nobili, Sabatino Maione, and Silverio Perrotta. 2011. "CNR2 Functional Variant (Q63R) Influences Childhood Immune Thrombocytopenic Purpura." Haematologica 96(12):1883–85. doi: 10.3324/haematol.2011.045732.

Rozenfeld, Raphael, Achla Gupta, Khatuna Gagnidze, Maribel P. Lim, Ivone Gomes, Dinah Lee-Ramos, Natalia Nieto, and Lakshmi A. Devi. 2011. "AT1R-CB_1R Heteromerization Reveals a New Mechanism for the Pathogenic Properties of Angiotensin II." The EMBO Journal 30(12):2350–63. doi: 10.1038/emboj.2011.139.

Rubio-Ruíz, M. E., L. Del Valle-Mondragón, V. Castrejón-Tellez, E. Carreón-Torres, E. Díaz-Díaz, and V. Guarner-Lans. 2014. "Angiotensin II and 1-7 during Aging in Metabolic Syndrome Rats. Expression of AT1, AT2 and Mas Receptors in Abdominal White Adipose Tissue." Peptides 57:101–8. doi: 10.1016/j.peptides.2014.04.021.

Rudolphi, K. A., P. Schubert, F. E. Parkinson, and B. B. Fredholm. 1992. "Neuroprotective Role of Adenosine in Cerebral Ischaemia." Trends in Pharmacological Sciences 13(12):439–45. doi:

10.1016/0165-6147(92)90141-r.

Russo, Margherita, Vincenzo Dattola, Anna Lisa Logiudice, Rosella Ciurleo, Edoardo Sessa, Rosaria De Luca, Placido Bramanti, Alessia Bramanti, Antonino Naro, and Rocco Salvatore Calabr. 2017. "The Role of Sativex in Robotic Rehabilitation in Individuals with Multiple Sclerosis Rationale, Study Design, and Methodology." Medicine (United States) 96(46):4–8. doi: 10.1097/MD.0000000000008826.

Ryberg, E., N. Larsson, S. Sjögren, S. Hjorth, N. O. Hermansson, J. Leonova, T. Elebring, K. Nilsson, T. Drmota, and P. J. Greasley. 2007. "The Orphan Receptor GPR55 Is a Novel Cannabinoid Receptor." British Journal of Pharmacology 152(7):1092–1101. doi: 10.1038/sj.bjp.0707460.

Ryberg, E, N. Larsson, S. Sjögren, S. Hjorth, N. O. Hermansson, J. Leonova, T. Elebring, K. Nilsson, T. Drmota, and P. J. Greasley. 2007. "The Orphan Receptor GPR55 Is a Novel Cannabinoid Receptor." British Journal of Pharmacology 152(7):1092–1101. doi: 10.1038/sj.bjp.0707460.

Rydning, Siri L., Paul H. Backe, Mirta M. L. Sousa, Zafar Iqbal, Ane Marte Øye, Ying Sheng, Mingyi Yang, Xiaolin Lin, Geir Slupphaug, Tonje H. Nordenmark, Magnus D. Vigeland, Magnar Bjørås, Chantal M. Tallaksen, and Kaja K. Selmer. 2017. "Novel UCHL1 Mutations Reveal New Insights into Ubiquitin Processing." Human Molecular Genetics 26(6):1031–40. doi: 10.1093/hmg/ddw391.

Saavedra, Juan M. 2012a. "Angiotensin II AT1 Receptor Blockers Ameliorate Inflammatory Stress: A Beneficial Effect for the Treatment of Brain Disorders." Cellular and Molecular Neurobiology 32(5):667–81. doi: 10.1007/s10571-011-9754-6.

Saavedra, Juan M. 2012b. "Angiotensin II AT1 Receptor Blockers as Treatments for Inflammatory Brain Disorders." Clinical Science 123(10):567–90. doi: 10.1042/CS20120078.

Sagredo, Onintza, Moisés García-Arencibia, Eva de Lago, Simone Finetti, Alessandra Decio, and Javier Fernández-Ruiz. 2007. "Cannabinoids and Neuroprotection in Basal Ganglia Disorders." Molecular Neurobiology 36(1):82–91. doi: 10.1007/s12035-007-0004-3.

Saliba, Soraya Wilke, Hannah Jauch, Brahim Gargouri, Albrecht Keil, Thomas Hurrle, Nicole Volz, Florian Mohr, Mario Van Der Stelt, Stefan Bräse, and Bernd L. Fiebich. 2018. "Anti-Neuroinflammatory Effects of GPR55 Antagonists in LPS-Activated Primary Microglial Cells." Journal of Neuroinflammation 15(1):1–13. doi: 10.1186/s12974-018-1362-7.

Sampaio, Walkyria Oliveira, Robson Augusto Souza Dos Santos, Raphael Faria-Silva, Leonor Tapias Da Mata Machado, Ernesto L. Schiffrin, and Rhian M. Touyz. 2007. "Angiotensin-(1-7) through Receptor Mas Mediates Endothelial Nitric Oxide Synthase Activation via Akt-Dependent Pathways." Hypertension 49(1):185–92. doi: 10.1161/01.HYP.0000251865.35728.2f.

Sanchez-Lemus, Enrique, Yuki Murakami, Ignacio M. Larrayoz-Roldan, Armen J. Moughamian, Jaroslav Pavel, Tsuyoshi Nishioku, and Juan M. Saavedra. 2008. "Angiotensin II At1 Receptor Blockade Decreases Lipopolysaccharide-Induced Inflammation in the Rat Adrenal Gland." Endocrinology 149(10):5177–88. doi: 10.1210/en.2008-0242.

Santos-Lozano, Alejandro, Helios Pareja-Galeano, Fabian Sanchis-Gomar, Miguel Quindós-Rubial, Carmen Fiuza-Luces, Carlos Cristi-Montero, Enzo Emanuele, Nuria Garatachea, and Alejandro Lucia. 2016. "Physical Activity and Alzheimer Disease: A Protective Association." Mayo Clinic Proceedings 91(8):999–1020. doi: 10.1016/j.mayocp.2016.04.024.

Santos, Rita, Oleg Ursu, Anna Gaulton, A. Patrícia Bento, Ramesh S. Donadi, Cristian G. Bologa, Anneli Karlsson, Bissan Al-Lazikani, Anne Hersey, Tudor I. Oprea, and John P. Overington. 2016. "A Comprehensive Map of Molecular Drug Targets." Nature Reviews Drug Discovery 16(1):19–34. doi: 10.1038/nrd.2016.230.

Santos, Robson A. S., Maria J. Campagnole-santos, and P. Andrade. 2000. "Angiotensin-(1–7): An Update." 91:45–62.

Santos, Robson A. S., Anderson J. Ferreira, Sérgio V. B. Pinheiro, Walkyria O. Sampaio, Rhian Touyz, and Maria José Campagnole-Santos. 2005. "Angiotensin-(1-7) and Its Receptor as a Potential Targets for New Cardiovascular Drugs." Expert Opinion on Investigational Drugs 14(8):1019–31. doi: 10.1517/13543784.14.8.1019.

Sarlus, Heela, Michael T. Heneka, Heela Sarlus, and Michael T. Heneka. 2017. "Microglia in

Alzheimer's Disease Microglia in Alzheimer ' s Disease." 127(9):3240–49.
Sas-Strózik, Agnieszka, Magdalena Krajewska, and Miroslaw Banasik. 2020. "The Significance of Angiotensin II Type 1 Receptor (AT1 Receptor) in Renal Transplant Injury." Advances in Clinical and Experimental Medicine 29(5):629–33. doi: 10.17219/acem/121510.
Sasaki, Katsutoshi, Yoshiaki Yamano, Smriti Bardhan, Naoharu Iwai, John J. Murray, Mamoru Hasegawa, Yuzuru Matsudat, and Tadashi Lnagami. 1991. "Cloning and Expression of a Complementary DNA Encoding a Bovine Adrenal Angiotensin II Type-1 Receptor." Nature 351(6323):230–33. doi: 10.1038/351230a0.
Saura, Josep, Ester Angulo, Aroa Ejarque, Vicent Casado, Josep M. Tusell, Rosario Moratalla, Jiang-Fan Chen, Michael A. Schwarzschild, Carme Lluis, Rafael Franco, and Joan Serratosa. 2005. "Adenosine A2A Receptor Stimulation Potentiates Nitric Oxide Release by Activated Microglia." Journal of Neurochemistry 95(4):919–29. doi: 10.1111/j.1471-4159.2005.03395.x.
Savica, Rodolfo, Brandon R. Grossardt, Walter A. Rocca, and James H. Bower. 2018. "Parkinson Disease with and without Dementia: A Prevalence Study and Future Projections." Movement Disorders 33(4):537–43. doi: 10.1002/mds.27277.
Sawzdargo, Marek, Tuan Nguyen, Dennis K. Lee, Kevin R. Lynch, Regina Cheng, Henry H. Q. Heng, Susan R. George, and Brian F. O'Dowd. 1999. "Identification and Cloning of Three Novel Human G Protein-Coupled Receptor Genes GPR52, ΨGPR53 and GPR55: GPR55 Is Extensively Expressed in Human Brain." Molecular Brain Research 64(2):193–98. doi: 10.1016/S0169-328X(98)00277-0.
Schicho, Rudolf, and Martin Storr. 2012. "A Potential Role for GPR55 in Gastrointestinal Functions." Current Opinion in Pharmacology 12(6):653–58. doi: 10.1016/j.coph.2012.09.009.
Schimrigk, Sebastian, Martin Marziniak, Christine Neubauer, Eva Maria Kugler, Gudrun Werner, and Dimitri Abramov-Sommariva. 2017. "Dronabinol Is a Safe Long-Term Treatment Option for Neuropathic Pain Patients." European Neurology 78(5–6):320–29. doi: 10.1159/000481089.
Schmidt, André P., Diogo R. Lara, and Diogo O. Souza. 2007. "Proposal of a Guanine-Based Purinergic System in the Mammalian Central Nervous System." Pharmacology and Therapeutics 116(3):401–16. doi: 10.1016/j.pharmthera.2007.07.004.
Schwitzer, Thomas, Raymund Schwan, Karine Angioi-Duprez, Anne Giersch, and Vincent Laprevote. 2016. "The Endocannabinoid System in the Retina: From Physiology to Practical and Therapeutic Applications." Neural Plasticity 2016. doi: 10.1155/2016/2916732.
Scroll, Please, and Down For. 2010. "Journal of the History of the Neurosciences: Basic and Clinical Perspectives." (April 2012):37–41.
Setó-Salvia, Núria, Jordi Clarimón, Javier Pagonabarraga, Berta Pascual-Sedano, Antonia Campolongo, Onofre Combarros, Jose Ignacio Mateo, Daniel Regaña, Merce Martínez-Corral, Marta Marquié, Daniel Alcolea, Marc Suárez-Calvet, Laura Molina-Porcel, Oriol Dols, Teresa Gómez-Isla, Rafael Blesa, Alberto Lleó, and Jaime Kulisevsky. 2011. "Dementia Risk in Parkinson Disease." Archives of Neurology 68(3):140–49. doi: 10.1001/archneurol.2011.17.
Shah, Maliha, and Ana M. Catafau. 2014. "Molecular Imaging Insights into Neurodegeneration: Focus on Tau PET Radiotracers." Journal of Nuclear Medicine 55(6):871–74. doi: 10.2967/jnumed.113.136069.
Shao, Yi Ming, Xiaohua Ma, Priyankar Paira, Aaron Tan, Deron Raymond Herr, Kah Leong Lim, Chee Hoe Ng, Gopalakrishnan Venkatesan, Karl Norbert Klotz, Stephanie Federico, Giampiero Spalluto, Siew Lee Cheong, Yu Zong Chen, and Giorgia Pastorin. 2018. "Discovery of Indolylpiperazinylpyrimidines with Dual-Target Profiles at Adenosine A2A and Dopamine D2 Receptors for Parkinson's Disease Treatment." PLoS ONE 13(1):1–27. doi: 10.1371/journal.pone.0188212.
Shao, Zhenhua, Jie Yin, Karen Chapman, Magdalena Grzemska, Lindsay Clark, Junmei Wang, and Daniel M. Rosenbaum. 2016. "High-Resolution Crystal Structure of the Human CB1 Cannabinoid Receptor." Nature 540(7634):602–6. doi: 10.1038/nature20613.
Shemesh, Ronen, Amir Toporik, Zurit Levine, Iris Hecht, Galit Rotman, Assaf Wool, Dvir Dahary, Eyal Gofer, Yossef Kliger, Michal Ayalon Soffer, Avi Rosenberg, Dani Eshel, and Yossi Cohen. 2008.

"Discovery and Validation of Novel Peptide Agonists for G-Protein-Coupled Receptors." Journal of Biological Chemistry 283(50):34643–49. doi: 10.1074/jbc.M805181200.

Shen, Hai-Ying, and Jiang-Fan Chen. 2009. "Adenosine A2A Receptors in Psychopharmacology: Modulators of Behavior, Mood and Cognition." Current Neuropharmacology 7(3):195–206. doi: 10.2174/157015909789152191.

Shen, Zhiwei, Jianfeng Lei, Xueyuan Li, Zhanjing Wang, Xinjie Bao, and Renzhi Wang. 2018. "Multifaceted Assessment of the APP/PS1 Mouse Model for Alzheimer's Disease: Applying MRS, DTI, and ASL." Brain Research 1698:114–20. doi: 10.1016/j.brainres.2018.08.001.

Shimada, Ichio, Takumi Ueda, Yutaka Kofuku, Matthew T. Eddy, and Kurt Wüthrich. 2019. "GPCR Drug Discovery: Integrating Solution NMR Data with Crystal and Cryo-EM Structures." Nature Reviews Drug Discovery 18(1):59–82. doi: 10.1038/nrd.2018.180.

Shinohara, Tokuyuki, Masataka Harada, Kazuhiro Ogi, Minoru Maruyama, Ryo Fujii, Hideyuki Tanaka, Shoji Fukusumi, Hidetoshi Komatsu, Masaki Hosoya, Yuko Noguchi, Takuya Watanabe, Takeo Moriya, Yasuaki Itoh, and Shuji Hinuma. 2004. "Identification of a G Protein-Coupled Receptor Specifically Responsive to β-Alanine." Journal of Biological Chemistry 279(22):23559–64. doi: 10.1074/jbc.M314240200.

Shpakov, A. O. 2013. "Heterotrimeric G Proteins." Brenner's Encyclopedia of Genetics: Second Edition (April 2016):454–56. doi: 10.1016/B978-0-12-374984-0.00706-3.

Shryock, John C., Stephen Snowdy, Pier Giovanni Baraldi, Barbara Cacciari, Giampiero Spalluto, Angela Monopoli, Ennio Ongini, Stephen P. Baker, and Luiz Belardinelli. 1998. "A(2A)-Adenosine Receptor Reserve for Coronary Vasodilation." Circulation 98(7):711–18. doi: 10.1161/01.CIR.98.7.711.

Silva da Costa, Leandro, Ana Paula Pereira da Silva, Andrea T. Da Poian, and Tatiana El-Bacha. 2012. "Mitochondrial Bioenergetic Alterations in Mouse Neuroblastoma Cells Infected with Sindbis Virus: Implications to Viral Replication and Neuronal Death" edited by V. Saks. PLoS ONE 7(4):e33871. doi: 10.1371/journal.pone.0033871.

Simcocks, Anna C., Lannie O'Keefe, Kayte A. Jenkin, Michael L. Mathai, Deanne H. Hryciw, and Andrew J. McAinch. 2014. "A Potential Role for GPR55 in the Regulation of Energy Homeostasis." Drug Discovery Today 19(8):1145–51. doi: 10.1016/j.drudis.2013.12.005.

Simrén, Joel, Nicholas J. Ashton, Kaj Blennow, and Henrik Zetterberg. 2020. "An Update on Fluid Biomarkers for Neurodegenerative Diseases: Recent Success and Challenges Ahead." Current Opinion in Neurobiology 61:29–39. doi: 10.1016/j.conb.2019.11.019.

Singh, Lovedeep, Ritu Kulshrestha, Nirmal Singh, and Amteshwar Singh Jaggi. 2018. "Mechanisms Involved in Adenosine Pharmacological Preconditioning-Induced Cardioprotection." Korean Journal of Physiology and Pharmacology 22(3):225–34. doi: 10.4196/kjpp.2018.22.3.225.

Singh, Nagendra S., Michel Bernier, and Irving W. Wainer. 2016. "Selective GPR55 Antagonism Reduces Chemoresistance in Cancer Cells." Pharmacological Research 111(3):757–66. doi: 10.1016/j.phrs.2016.07.013.

Śledziński, Paweł, Joanna Zeyland, Ryszard Słomski, and Agnieszka Nowak. 2018. "The Current State and Future Perspectives of Cannabinoids in Cancer Biology." Cancer Medicine 7(3):765–75. doi: 10.1002/cam4.1312.

Slipetz, D. M., G. P. O'Neill, L. Favreau, C. Dufresne, M. Gallant, Y. Gareau, D. Guay, M. Labelle, and K. M. Metters. 1995. "Activation of the Human Peripheral Cannabinoid Receptor Results in Inhibition of Adenylyl Cyclase." Molecular Pharmacology 48(2):352–61.

Snyder, S. H. 1985. "Adenosine as a Neuromodulator." Annual Review of Neuroscience VOL. 8:103–24. doi: 10.1146/annurev.neuro.8.1.103.

Southan, Christopher. 2016. "Retrieving GPCR Data from Public Databases." Current Opinion in Pharmacology 30:38–43. doi: 10.1016/j.coph.2016.07.002.

Southern, Craig, Jennifer M. Cook, Zaynab Neetoo-Isseljee, Debra L. Taylor, Catherine A. Kettleborough, Andy Merritt, Daniel L. Bassoni, William J. Raab, Elizabeth Quinn, Tom S. Wehrman, Anthony P. Davenport, Andrew J. Brown, Andrew Green, Mark J. Wigglesworth, and Steve Rees. 2013. "Screening β-Arrestin Recruitment for the Identification of Natural Ligands

for Orphan G-Protein-Coupled Receptors." Journal of Biomolecular Screening 18(5):599–609. doi: 10.1177/1087057113475480.

Sparks, Matthew A., Steven D. Crowley, Susan B. Gurley, Maria Mirotsou, and Thomas M. Coffman. 2014. "Classical Renin-Angiotensin System in Kidney Physiology." Pp. 1201–28 in Comprehensive Physiology. Vol. 23. Hoboken, NJ, USA: John Wiley & Sons, Inc.

Spillantini, Maria Grazia, Marie Luise Schmidt, Virginia M. Y. Lee, John Q. Trojanowski, Ross Jakes, and Michel Goedert. 1997. "α-Synuclein in Lewy Bodies." Nature 388(6645):839–40. doi: 10.1038/42166.

Spires-Jones, Tara L., Johannes Attems, and Dietmar Rudolf Thal. 2017. "Interactions of Pathological Proteins in Neurodegenerative Diseases." Acta Neuropathologica 134(2):187–205. doi: 10.1007/s00401-017-1709-7.

Stadel, Rebecca, Kwang H. Ahn, and Debra A. Kendall. 2011. "The Cannabinoid Type-1 Receptor Carboxyl-Terminus, More than Just a Tail." Journal of Neurochemistry 117(1):1–18. doi: 10.1111/j.1471-4159.2011.07186.x.

Stahl, Stephen M. 2018. "New Hope for Alzheimer's Dementia as Prospects for Disease Modification Fade: Symptomatic Treatments for Agitation and Psychosis." CNS Spectrums 23(5):291–97. doi: 10.1017/S1092852918001360.

Steele, Haley R., and Liang Han. 2020. "The Signaling Pathway and Polymorphisms of Mrgprs." Neuroscience Letters 744(September 2020):135562. doi: 10.1016/j.neulet.2020.135562.

van der Stelt, Mario, and Vincenzo Di Marzo. 2005. "Cannabinoid Receptors and Their Role in Neuroprotection." Neuromolecular Medicine 7(1–2):37–50. doi: 10.1385/NMM:7:1-2:037.

Stephenson, Jodie, Erik Nutma, Paul van der Valk, and Sandra Amor. 2018. "Inflammation in CNS Neurodegenerative Diseases." Immunology 154(2):204–19. doi: 10.1111/imm.12922.

Stockwell, Jocelyn, Elisabet Jakova, and Francisco S. Cayabyab. 2017. "Adenosine A1 and A2A Receptors in the Brain: Current Research and Their Role in Neurodegeneration." Molecules 22(4):676. doi: 10.3390/molecules22040676.

Stoker, Thomas B., Kelli M. Torsney, and Roger A. Barker. 2018. "Emerging Treatment Approaches for Parkinson's Disease." Frontiers in Neuroscience 12(OCT):1–10. doi: 10.3389/fnins.2018.00693.

Strotmann, Rainer, Kristin Schröck, Iris Böselt, Claudia Stäubert, Andreas Russ, and Torsten Schöneberg. 2011. "Evolution of GPCR: Change and Continuity." Molecular and Cellular Endocrinology 331(2):170–78. doi: 10.1016/j.mce.2010.07.012.

Sun, Hong, HaiQin Wu, Xin Yu, GuiLian Zhang, Ru Zhang, ShuQin Zhan, HuQing Wang, Ning Bu, XiaoLing Ma, and YongNan Li. 2015. "Angiotensin II and Its Receptor in Activated Microglia Enhanced Neuronal Loss and Cognitive Impairment Following Pilocarpine-Induced Status Epilepticus." Molecular and Cellular Neuroscience 65:58–67. doi: 10.1016/j.mcn.2015.02.014.

Sun, Xiaofei, Monica Cappelletti, Yingju Li, Christopher L. Karp, Senad Divanovic, and Sudhansu K. Dey. 2014. "Cnr2 Deficiency Confers Resistance to Inflammation- Induced Preterm Birth in Mice." Endocrinology 155(10):4006–14. doi: 10.1210/en.2014-1387.

Suzuki, Nobuchika, Nicole Hajicek, and Tohru Kozasa. 2009. "Regulation and Physiological Functions of G12/13-Mediated Signaling Pathways." NeuroSignals 17(1):55–70. doi: 10.1159/000186690.

Sveinbjornsdottir, Sigurlaug. 2016. "The Clinical Symptoms of Parkinson's Disease." Journal of Neurochemistry 318–24. doi: 10.1111/jnc.13691.

Takezako, Takanobu, Hamiyet Unal, Sadashiva S. Karnik, and Koichi Node. 2017. "Current Topics in Angiotensin II Type 1 Receptor Research: Focus on Inverse Agonism, Receptor Dimerization and Biased Agonism." Pharmacological Research 123:40–50. doi: 10.1016/j.phrs.2017.06.013.

Tan, Jeanne M. M., Esther S. P. Wong, and Kah Leong Lim. 2009. "Protein Misfolding and Aggregation in Parkinson's Disease." Antioxidants and Redox Signaling 11(9):2119–34. doi: 10.1089/ars.2009.2490.

Tetzner, Anja, Kinga Gebolys, Christian Meinert, Sabine Klein, Anja Uhlich, Jonel Trebicka, Óscar Villacañas, and Thomas Walther. 2016. "G-Protein-Coupled Receptor MrgD Is a Receptor for Angiotensin-(1-7) Involving Adenylyl Cyclase, CAMP, and Phosphokinase A." Hypertension 68(1):185–94. doi: 10.1161/HYPERTENSIONAHA.116.07572.

Tha, Kyi Kyi, Yasunobu Okuma, Hiroyuki Miyazaki, Toshihiko Murayama, Takashi Uehara, Rieko Hatakeyama, Yuka Hayashi, and Yasuyuki Nomura. 2000. "Changes in Expressions of Proinflammatory Cytokines IL-1β, TNF-α and IL-6 in the Brain of Senescence Accelerated Mouse (SAM) P8." Brain Research 885(1):25–31. doi: 10.1016/S0006-8993(00)02883-3.

Thibaudeau, Tiffany A., Raymond T. Anderson, and David M. Smith. 2018. "A Common Mechanism of Proteasome Impairment by Neurodegenerative Disease-Associated Oligomers." Nature Communications 9(1). doi: 10.1038/s41467-018-03509-0.

Tigerstedt, Robert, and P. Q. Bergman. 1898. "Niere Und Kreislauf 1." Skandinavisches Archiv Für Physiologie 8(1):223–71. doi: 10.1111/j.1748-1716.1898.tb00272.x.

Tirupula, Kalyan C., Russell Desnoyer, Robert C. Speth, and Sadashiva S. Karnik. 2014. "Atypical Signaling and Functional Desensitization Response of MAS Receptor to Peptide Ligands." PLoS ONE. doi: 10.1371/journal.pone.0103520.

Tsuzuki, Satoshi, Toshihiro Ichiki, Hiroshi Nakakubo, Yutaka Kitami, Deng Fu Guo, Heigoro Shirai, and Tadashi Inagami. 1994. "Molecular Cloning and Expression of the Gene Encoding Human Angiotensin II Type 2 Receptor." Biochemical and Biophysical Research Communications 200(3):1449–54.

Tudurí, Eva, Monica Imbernon, Rene Javier Hernández-Bautista, Marta Tojo, Johan Fernø, Carlos Diéguez, and Rubén Nogueiras. 2017. "Gpr55: A New Promising Target for Metabolism?" Journal of Molecular Endocrinology 58(3):R191–202. doi: 10.1530/JME-16-0253.

Turcotte, Caroline, Marie Renée Blanchet, Michel Laviolette, and Nicolas Flamand. 2016. "The CB2 Receptor and Its Role as a Regulator of Inflammation." Cellular and Molecular Life Sciences 73(23):4449–70. doi: 10.1007/s00018-016-2300-4.

Turner, Sarah E., Claire M. Williams, Leslie Iversen, and Benjamin J. Whalley. 2017. Molecular Pharmacology of Phytocannabinoids. Vol. 103.

Valenzano, Kenneth J., Laykea Tafesse, Gary Lee, James E. Harrison, Jamie M. Boulet, Susan L. Gottshall, Lilly Mark, Michelle S. Pearson, Wendy Miller, Shen Shan, Leyana Rabadi, Yakov Rotshteyn, Suzanne M. Chaffer, Paul I. Turchin, David A. Elsemore, Mathew Toth, Lee Koetzner, and Garth T. Whiteside. 2005. "Pharmacological and Pharmacokinetic Characterization of the Cannabinoid Receptor 2 Agonist, GW405833, Utilizing Rodent Models of Acute and Chronic Pain, Anxiety, Ataxia and Catalepsy." Neuropharmacology 48(5):658–72. doi: 10.1016/j.neuropharm.2004.12.008.

Valenzuela, Rita, Maria A. Costa-Besada, Javier Iglesias-Gonzalez, Emma Perez-Costas, Begoña Villar-Cheda, Pablo Garrido-Gil, Miguel Melendez-Ferro, Ramon Soto-Otero, Jose L. Lanciego, Daniel Henrion, Rafael Franco, and Jose L. Labandeira-Garcia. 2016. "Mitochondrial Angiotensin Receptors in Dopaminergic Neurons. Role in Cell Protection and Aging-Related Vulnerability to Neurodegeneration." Cell Death & Disease 7(10):e2427–e2427. doi: 10.1038/cddis.2016.327.

Valero-Esquitino, Verónica, Kristin Lucht, Pawel Namsolleck, Florianne Monnet-Tschudi, Tobias Stubbe, Franziska Lucht, Meng Liu, Friederike Ebner, Christine Brandt, Leon A. Danyel, Daniel C. Villela, Ludovit Paulis, Christa Thoene-Reineke, Björn Dahlöf, Anders Hallberg, Thomas Unger, Colin Sumners, and U. Muscha Steckelings. 2015. "Direct Angiotensin Type 2 Receptor (AT2R) Stimulation Attenuates T-Cell and Microglia Activation and Prevents Demyelination in Experimental Autoimmune Encephalomyelitis in Mice." Clinical Science 128(2):95–109. doi: 10.1042/CS20130601.

Vecchio, Elizabeth A., Paul J. White, and Lauren T. May. 2019. "The Adenosine A2B G Protein-Coupled Receptor: Recent Advances and Therapeutic Implications." Pharmacology and Therapeutics 198:20–33. doi: 10.1016/j.pharmthera.2019.01.003.

Verkhratsky, Alexei, and Frank Kirchhoff. 2007. "NMDA Receptors in Glia." Neuroscientist 13(1):28–37. doi: 10.1177/1073858406294270.

Viana da Silva, Silvia, Matthias Georg Haberl, Pei Zhang, Philipp Bethge, Cristina Lemos, Nélio Gonçalves, Adam Gorlewicz, Meryl Malezieux, Francisco Q. Gonçalves, Noëlle Grosjean, Christophe Blanchet, Andreas Frick, U. Valentin Nägerl, Rodrigo A. Cunha, and Christophe Mulle. 2016. "Early Synaptic Deficits in the APP/PS1 Mouse Model of Alzheimer's Disease Involve

Neuronal Adenosine A2A Receptors." Nature Communications 7(1):11915. doi: 10.1038/ncomms11915.

Villar-Cheda, Begoña, Antonio Dominguez-Meijide, Rita Valenzuela, Noelia Granado, Rosario Moratalla, and Jose L. Labandeira-Garcia. 2014. "Aging-Related Dysregulation of Dopamine and Angiotensin Receptor Interaction." Neurobiology of Aging 35(7):1726–38. doi: 10.1016/j.neurobiolaging.2014.01.017.

Villar-Cheda, Begoña, Rita Valenzuela, Ana I. Rodriguez-Perez, Maria J. Guerra, and Jose L. Labandeira-Garcia. 2012. "Aging-Related Changes in the Nigral Angiotensin System Enhances Proinflammatory and pro-Oxidative Markers and 6-OHDA-Induced Dopaminergic Degeneration." Neurobiology of Aging 33(1):204.e1-204.e11. doi: 10.1016/j.neurobiolaging.2010.08.006.

Villar, Van Anthony M., Santiago Cuevas, Xiaoxu Zheng, and Pedro A. Jose. 2016. Localization and Signaling of GPCRs in Lipid Rafts. Vol. 132. Elsevier Ltd.

Villela, Daniel C., Danielle G. Passos-Silva, and Robson A. S. Santos. 2014. "Alamandine: A New Member of the Angiotensin Family." Current Opinion in Nephrology and Hypertension 23(2):130–34.

Villela, Daniel, Julia Leonhardt, Neal Patel, Jason Joseph, Sebastian Kirsch, Anders Hallberg, Thomas Unger, Michael Bader, Robson A. Santos, Colin Sumners, and U. Muscha Steckelings. 2015. "Angiotensin Type 2 Receptor (AT 2 R) and Receptor Mas: A Complex Liaison." Clinical Science 128(4):227–34. doi: 10.1042/CS20130515.

Vincenzi, Fabrizio, Annalisa Ravani, Silvia Pasquini, Stefania Merighi, Stefania Gessi, Romeo Romagnoli, Pier Giovanni Baraldi, Pier Andrea Borea, and Katia Varani. 2016. "Positive Allosteric Modulation of A1 Adenosine Receptors as a Novel and Promising Therapeutic Strategy for Anxiety." Neuropharmacology 111:283–92. doi: 10.1016/j.neuropharm.2016.09.015.

Wackenfors, Angelica, Emil Pantev, Malin Emilson, Lars Edvinsson, and Malin Malmsjö. 2004. "Angiotensin II Receptor MRNA Expression and Vasoconstriction in Human Coronary Arteries: Effects of Heart Failure and Age." Basic and Clinical Pharmacology and Toxicology 95(6):266–72. doi: 10.1111/j.1742-7843.2004.t01-1-pto950504.x.

Waldeck-Weiermair, Markus, Cristina Zoratti, Karin Osibow, Nariman Balenga, Edith Goessnitzer, Maria Waldhoer, Roland Malli, and Wolfgang F. Graier. 2008. "Integrin Clustering Enables Anandamide-Induced Ca2+ Signaling in Endothelial Cells via GPR55 by Protection against CB1-Receptor-Triggered Repression." Journal of Cell Science 121(10):1704–17. doi: 10.1242/jcs.020958.

Wallinder, Charlotta, Christian Sköld, Sara Sundholm, Marie-Odile Guimond, Samir Yahiaoui, Gunnar Lindeberg, Nicole Gallo-Payet, Mathias Hallberg, and Mathias Alterman. 2019. " High Affinity Rigidified AT 2 Receptor Ligands with Indane Scaffolds ." MedChemComm 10(12):2146–60. doi: 10.1039/c9md00402e.

Wang, D., T. Chen, X. Zhou, R. Couture, and Y. Hong. 2013. "Activation of Mas Oncogene-Related Gene (Mrg) C Receptors Enhances Morphine-Induced Analgesia through Modulation of Coupling of μ-Opioid Receptor to Gi-Protein in Rat Spinal Dorsal Horn." Neuroscience 253:455–64. doi: 10.1016/j.neuroscience.2013.08.069.

Wang, Jingjing, Tian Hua, and Zhi Jie Liu. 2020. "Structural Features of Activated GPCR Signaling Complexes." Current Opinion in Structural Biology 63:82–89. doi: 10.1016/j.sbi.2020.04.008.

Wang, Jun, Ben J. Gu, Colin L. Masters, and Yan Jiang Wang. 2017. "A Systemic View of Alzheimer Disease - Insights from Amyloid-β Metabolism beyond the Brain." Nature Reviews Neurology 13(10):612–23. doi: 10.1038/nrneurol.2017.111.

Wang, Rui, and P. Hemachandra Reddy. 2017. "Role of Glutamate and NMDA Receptors in Alzheimer's Disease." Journal of Alzheimer's Disease 57(4):1041–48. doi: 10.3233/JAD-160763.

Wang, Wen Ying, Meng Shan Tan, Jin Tai Yu, and Lan Tan. 2015. "Role of Pro-Inflammatory Cytokines Released from Microglia in Alzheimer's Disease." Annals of Translational Medicine 3(10):1–15. doi: 10.3978/j.issn.2305-5839.2015.03.49.

Wang, Yan, Mark Del Borgo, Huey W. Lee, Dhaniel Baraldi, Baydaa Hirmiz, Tracey A. Gaspari, Kate M. Denton, Marie Isabel Aguilar, Chrishan S. Samuel, and Robert E. Widdop. 2017. "Anti-Fibrotic

Potential of AT2 Receptor Agonists." Frontiers in Pharmacology 8(AUG):1–7. doi: 10.3389/fphar.2017.00564.

Weibrecht, Irene, Karl Johan Leuchowius, Carl Magnus Clausson, Tim Conze, Malin Jarvius, W. Mathias Howell, Masood Kamali-Moghaddam, and Ola Söderberg. 2010. "Proximity Ligation Assays: A Recent Addition to the Proteomics Toolbox." Expert Review of Proteomics 7(3):401–9. doi: 10.1586/epr.10.10.

Whitebread, Steven E., Verdon Taylor, Serge P. Bottari, Bruno Kamber, and Marc de Gasparo. 1991. "Radioiodinated CGP 42111A: A Novel High Affinity and Highly Selective Ligand for the Characterization of Angiotensin AT2 Receptors." Biochemical and Biophysical Research Communications 181(3):1365–71. doi: 10.1016/0006-291X(91)92089-3.

Whyte, Lauren S., Erik Ryberg, Natalie A. Sims, Susan A. Ridge, Ken Mackie, Peter J. Greasley, Ruth A. Ross, and Michael J. Rogers. 2009. "The Putative Cannabinoid Receptor GPR55 Affects Osteoclast Function in Vitro and Bone Mass in Vivo." Proceedings of the National Academy of Sciences of the United States of America 106(38):16511–16. doi: 10.1073/pnas.0902743106.

Wilson, R. I., and R. A. Nicoll. 2001. "Endogenous Cannabinoids Mediate Retrograde Signalling at Hippocampal Synapses." Nature 410(6828):588–92. doi: 10.1038/35069076.

Wise, Alan, Michael Sheehan, Stephen Rees, Melanie Lee, and Graeme Milligan. 1999. "Comparative Analysis of the Efficacy of A1 Adenosine Receptor Activation of G(i/o)α G Proteins Following Coexpression of Receptor and G Protein and Expression of A1 Adenosine Receptor-G(i/o)α Fusion Proteins." Biochemistry 38(8):2272–78. doi: 10.1021/bi982054f.

Wisler, James W., Kunhong Xiao, Alex R. B. Thomsen, and Robert J. Lefkowitz. 2014. "Recent Developments in Biased Agonism." Current Opinion in Cell Biology 27(1):18–24. doi: 10.1016/j.ceb.2013.10.008.

Woodhams, Stephen G., Victoria Chapman, David P. Finn, Andrea G. Hohmann, and Volker Neugebauer. 2017. "The Cannabinoid System and Pain." Neuropharmacology 124(1):105–20. doi: 10.1016/j.neuropharm.2017.06.015.

Wooten, G. Frederick, Lillian J. Currie, James P. Bennett, Madaline B. Harrison, Joel M. Trugman, and W. Davis Parker. 1997. "Maternal Inheritance in Parkinson's Disease." Annals of Neurology 41(2):265–68. doi: 10.1002/ana.410410218.

Wouters, Elise, Lakshmi Vasudevan, René A. J. Crans, Deepak K. Saini, and Christophe P. Stove. 2019. "Luminescence- and Fluorescence-Based Complementation Assays to Screen for Gpcr Oligomerization: Current State of the Art." International Journal of Molecular Sciences 20(12):1–35. doi: 10.3390/ijms20122958.

Wright, John W., Leen H. Kawas, and Joseph W. Harding. 2013. "A Role for the Brain RAS in Alzheimer's and Parkinson's Diseases." Frontiers in Endocrinology 4(October):1–12. doi: 10.3389/fendo.2013.00158.

Wu, Congqing, Hong Lu, Lisa A. Cassis, and Alan Daugherty. 2011. "Molecular and Pathophysiological Features of Angiotensinogen: A Mini Review." American Chinese Journal of Medicine and Science 4(4):183. doi: doi:10.1002/cphy.c130040.

Xie, Fan Meng Guo xi, Derek Chalmers, Caurnel Morgan, Stanley J. Watson, and Huda Akil. 1994. "Cloning and Characterization of a Pharmacologically Distinct A1 Adenosine Receptor from Guinea Pig Brain." Molecular Brain Research 26(1–2):143–55. doi: 10.1016/0169-328X(94)90085-X.

Xie, Weilin, Oi Wan Wan, and Kenny K. K. Chung. 2010. "New Insights into the Role of Mitochondrial Dysfunction and Protein Aggregation in Parkinson's Disease." Biochimica et Biophysica Acta - Molecular Basis of Disease 1802(11):935–41. doi: 10.1016/j.bbadis.2010.07.014.

Xiong, Nian, Xi Long, Jing Xiong, Min Jia, Chunnuan Chen, Jinsha Huang, Devina Ghoorah, Xiangquan Kong, Zhicheng Lin, and Tao Wang. 2012. "Mitochondrial Complex I Inhibitor Rotenone-Induced Toxicity and Its Potential Mechanisms in Parkinson's Disease Models." Critical Reviews in Toxicology 42(7):613–32. doi: 10.3109/10408444.2012.680431.

Xu, Fei, Huixian Wu, Vsevolod Katritch, Gye Won Han, Kenneth A. Jacobson, Zhan Guo Gao, Vadim Cherezov, and Raymond C. Stevens. 2011. "Structure of an Agonist-Bound Human A2A

Adenosine Receptor." Science 332(6027):322–27. doi: 10.1126/science.1202793.
Xu, Ping, Srinivas Sriramula, and Eric Lazartigues. 2011. "ACE2/ANG-(1-7)/Mas Pathway in the Brain: The Axis of Good." American Journal of Physiology - Regulatory Integrative and Comparative Physiology 300(4):804–17. doi: 10.1152/ajpregu.00222.2010.
Xu, Yueming, Yuxia Wang, Yang Wang, Kaiwen Liu, Yao Peng, Deqiang Yao, Houchao Tao, Haiguang Liu, and Gaojie Song. 2019. "Mutagenesis Facilitated Crystallization of GLP-1R." IUCrJ 6:996–1006. doi: 10.1107/S2052252519013496.
Y.Y. Szeto, Jennifer, and Simon J.G. Lewis. 2016. "Current Treatment Options for Alzheimer's Disease and Parkinson's Disease Dementia." Current Neuropharmacology 14(4):326–38. doi: 10.2174/1570159x14666151208112754.
Yan, Renhong, Yuanyuan Zhang, Yaning Li, Lu Xia, Yingying Guo, and Qiang Zhou. 2020. "Structural Basis for the Recognition of SARS-CoV-2 by Full-Length Human ACE2." Science 367(6485):1444–48. doi: 10.1126/science.abb2762.
Yang, Fan, Xiao Yu, Chuan Liu, Chang-Xiu Qu, Zheng Gong, Hong-Da Liu, Fa-Hui Li, Hong-Mei Wang, Dong-Fang He, Fan Yi, Chen Song, Chang-Lin Tian, Kun-Hong Xiao, Jiang-Yun Wang, and Jin-Peng Sun. 2015. "Phospho-Selective Mechanisms of Arrestin Conformations and Functions Revealed by Unnatural Amino Acid Incorporation and 19F-NMR." Nature Communications 6(1):8202. doi: 10.1038/ncomms9202.
Yang, Longhe, Yanting Li, Jie Ren, Chenggang Zhu, Jin Fu, Donghai Lin, and Yan Qiu. 2014. "Celastrol Attenuates Inflammatory and Neuropathic Pain Mediated by Cannabinoid Receptor Type 2." International Journal of Molecular Sciences 15(8):13637–48. doi: 10.3390/ijms150813637.
Yang, Tianxin, and Chuanming Xu. 2017. "Physiology and Pathophysiology of the Intrarenal Renin-Angiotensin System: An Update." Journal of the American Society of Nephrology 28(4):1040–49. doi: 10.1681/ASN.2016070734.
Yang, Zhao, Fan Yang, Daolai Zhang, Zhixin Liu, Amy Lin, Chuan Liu, Peng Xiao, Xiao Yu, and Jin-Peng Sun. 2017. "Phosphorylation of G Protein-Coupled Receptors: From the Barcode Hypothesis to the Flute Model." Molecular Pharmacology 92(3):201–10. doi: 10.1124/mol.116.107839.
Yeliseev, Alexei. 2019. "Expression and Preparation of a G-Protein-Coupled Cannabinoid Receptor CB 2 for NMR Structural Studies." Current Protocols in Protein Science 96(1):139–48. doi: 10.1002/cpps.83.
Yeliseev, Alexei, and Klaus Gawrisch. 2017. "Expression and NMR Structural Studies of Isotopically Labeled Cannabinoid Receptor Type II." Pp. 387–403 in Physiology & behavior. Vol. 176.
Yoon, Hye Eun, Eun Nim Kim, Min Young Kim, Ji Hee Lim, In Ae Jang, Tae Hyun Ban, Seok Joon Shin, Cheol Whee Park, Yoon Sik Chang, and Bum Soon Choi. 2016. "Age-Associated Changes in the Vascular Renin-Angiotensin System in Mice." Oxidative Medicine and Cellular Longevity 2016. doi: 10.1155/2016/6731093.
Yoshioka, Kazuaki, Osamu Saitoh, and Hiroyasu Nakata. 2001. "Heteromeric Association Creates a P2Y-like Adenosine Receptor." Proceedings of the National Academy of Sciences of the United States of America 98(13):7617–22. doi: 10.1073/pnas.121587098.
Young, Brent M., Elaine Nguyen, Matthew A. J. Chedrawe, Jan K. Rainey, and Denis J. Dupré. 2017. "Differential Contribution of Transmembrane Domains IV, V, VI, and VII to Human Angiotensin II Type 1 Receptor Homomer Formation." Journal of Biological Chemistry 292(8):3341–50. doi: 10.1074/jbc.M116.750380.
Young, Dallan, K. O'Neill, T. Jessell, and Michael Wigler. 1988. "Characterization of the Rat Mas Oncogene and Its High-Level Expression in the Hippocampus and Cerebral Cortex of Rat Brain." Proceedings of the National Academy of Sciences 85(14):5339–42. doi: 10.1073/pnas.85.14.5339.
Young, Dallan, Gayle Waitches, Carmen Birchmeier, Ottavio Fasano, and Michael Wigler. 1986. "Isolation and Characterization of a New Cellular Oncogene Encoding a Protein with Multiple Potential Transmembrane Domains." Cell 45(5):711–19. doi: 10.1016/0092-8674(86)90785-3.
Yuan, Xiaoling, Yajun Shan, Zhenyu Yao, Jianyong Li, Zhenhu Zhao, Jiapei Chen, and Yuwen Cong. 2006. "Mitochondrial Location of Severe Acute Respiratory Syndrome Coronavirus 3b Protein."

Molecules and Cells 21(2):186–91. doi: 16682811.

Zahra, Walia, Sachchida Nand Rai, Hareram Birla, Saumitra Sen Singh, Hagera Dilnashin, Aaina Singh Rathore, and Surya Pratap Singh. 2020. "The Global Economic Impact of Neurodegenerative Diseases: Opportunities and Challenges." Pp. 333–45 in Bioeconomy for Sustainable Development. Vol. 14. Singapore: Springer Singapore.

Zetterberg, Henrik. 2017. "Applying Fluid Biomarkers to Alzheimer's Disease." American Journal of Physiology - Cell Physiology 313(1):C3–10. doi: 10.1152/ajpcell.00007.2017.

Zhang, Jiandong, and Steven D. Crowley. 2013. "The Role of Type 1 Angiotensin Receptors on T Lymphocytes in Cardiovascular and Renal Diseases." Current Hypertension Reports 15(1):39–46. doi: 10.1007/s11906-012-0318-z.

Zhang, Lin, Noël Taylor, Yuhong Xie, Roger Ford, Jeremy Johnson, Janet E. Paulsen, and Brian Bates. 2005. "Cloning and Expression of MRG Receptors in Macaque, Mouse, and Human." Molecular Brain Research 133(2):187–97. doi: 10.1016/j.molbrainres.2004.10.007.

Zhang, Weiwei, Bin Jiao, Tingting Xiao, Chuzheng Pan, Xixi Liu, Lin Zhou, Beisha Tang, and Lu Shen. 2016. "Mutational Analysis of PRNP in Alzheimer's Disease and Frontotemporal Dementia in China." Scientific Reports 6(September):1–7. doi: 10.1038/srep38435.

Zhang, Yan, Dilip K. Deb, Juan Kong, Gang Ning, Yurong Wang, George Li, Yunzi Chen, Zhongyi Zhang, Stephen Strugnell, Yves Sabbagh, Cynthia Arbeeny, and Yan Chun Li. 2009. "Long-Term Therapeutic Effect of Vitamin D Analog Doxercalciferol on Diabetic Nephropathy: Strong Synergism with AT1 Receptor Antagonist." American Journal of Physiology - Renal Physiology 297(3). doi: 10.1152/ajprenal.00247.2009.

Zhang, Zhongyi, Yan Zhang, Gang Ning, Dilip K. Deb, Juan Kong, and Chun Li Yan. 2008. "Combination Therapy with AT1 Blocker and Vitamin D Analog Markedly Ameliorates Diabetic Nephropathy: Blockade of Compensatory Renin Increase." Proceedings of the National Academy of Sciences of the United States of America 105(41):15896–901. doi: 10.1073/pnas.0803751105.

Zhao, Jie, Wen Zhang, Li Shen, Xiaomeng Yang, Yi Liu, and Zhongtao Gai. 2017. "Association of the ACE, GSTM1, IL-6, NOS3, and CYP1A1 Polymorphisms with Susceptibility of Mycoplasma Pneumoniae Pneumonia in Chinese Children." Medicine 96(15):e6642. doi: 10.1097/MD.0000000000006642.

Zheng, Jiyue, Xiaohu Zhang, and Xuechu Zhen. 2018. "Development of Adenosine A2A Receptor Antagonists for the Treatment of Parkinson's Disease: A Recent Update and Challenge." ACS Chemical Neuroscience. doi: 10.1021/acschemneuro.8b00313.

Zhou, Qun Yong, L. I. Chuanyu, Mark E. Olah, Robert A. Johnson, Gary L. Stiles, and Olivier Civelli. 1992. "Molecular Cloning and Characterization of an Adenosine Receptor: The A3 Adenosine Receptor." Proceedings of the National Academy of Sciences of the United States of America 89(16):7432–36. doi: 10.1073/pnas.89.16.7432.

Zhou, X. Edward, Karsten Melcher, and H. Eric Xu. 2017. "Understanding the GPCR Biased Signaling through G Protein and Arrestin Complex Structures." Current Opinion in Structural Biology 45:150–59. doi: 10.1016/j.sbi.2017.05.004.

Zhuo, Jialong, Christine Maric, Peter J. Harris, Daine Alcorn, and Frederick A. O. Mendelsohn. 1997. "Localization and Functional Properties of Angiotensin II AT1 Receptors in the Kidney: Focus on Renomedullary Interstitial Cells." Hypertension Research 20(4):233–50. doi: 10.1291/hypres.20.233.

Zrenner, Rita, Mark Stitt, Uwe Sonnewald, and Ralf Boldt. 2006. "Pyrimidine and Purine Biosynthesis and Degradation in Plants." Annual Review of Plant Biology 57:805–36. doi: 10.1146/annurev.arplant.57.032905.105421.

Zylka, Mark J. 2011. "Pain-Relieving Prospects for Adenosine Receptors and Ectonucleotidases." Trends in Molecular Medicine 17(4):188–96. doi: 10.1016/j.molmed.2010.12.006.

afael i as antiste an

Universidad de Barcelona
Departamento de Bioquímica y Biomedicina Molecular
Grupo de Neurobiologia Molecular

Barcelona, 2021